Berichte des Meteorologischen Instituts

der Albert-Ludwigs-Universität Freiburg

Nr. 19

Helmut Mayer and Dirk Schindler (Eds.)

Proceedings of the

2nd International Conference

Wind Effects on Trees

Albert-Ludwigs-University of Freiburg, Germany

13-16 October 2009

Freiburg, October 2009

ISSN 1435-618X

Self-publishing company of the Meteorological Institute, Albert-Ludwigs-University of Freiburg, Germany

Print:	Printing office of the Albert-Ludwigs-University of Freiburg
Editor:	Prof. Dr. Helmut Mayer
	Meteorological Institute, Albert-Ludwigs-University of Freiburg
	Werthmannstr. 10, D-79085 Freiburg, Germany
	Tel.: +49/761/203-3590; Fax: +49/761/203-3586
	e-mail: meteo@meteo.uni-freiburg.de
Documentation:	Ber. Meteor. Inst. Univ. Freiburg Nr. 19, 2009, 339 pp.

Editorial

Storm damages in forests cause economic losses and encourage various consequential damages in forests. Changes of intensity, frequency and seasonal distribution of storms and gales may challenge stability advantages of deciduous trees (leafless in winter), increase the risks of conifers' farming as well as require a revision of established silvicultural strategies and long-term productive times.

Against this background, a pronounced interest exists in forestry and forest science to update previous strategies to reduce the storm risk of forests taking into account modern results of different investigations (e.g. experiments, numerical simulations, statistical analyses).

Similar to preceding international conferences on the impact of storms on single trees, clump of trees and forest stands, e.g.

- International Conference "Wind Effects on Trees", 16-18 September 2003, University of Karlsruhe, Germany,
- International Conference "Wind and Trees", 5-9 August 2007, University of British Columbia, Vancouver, Canada,

the 2nd International Conference "Wind Effects on Trees", which is hosted from 13-16 October 2009 by the Meteorological Institute, Albert-Ludwigs-University of Freiburg, Germany, in collaboration with the Forest Research Institute Baden-Wuerttemberg, Freiburg, Germany, and the IUFRO Section 8.01.11, will provide an excellent opportunity to present and discuss new developments, approaches and methodologies in the context of wind and tree interactions.

The oral and poster presentations at the auditorium of the Albert-Ludwigs-University of Freiburg were subdivided into the fields: wind climatology, air flow at forest edges, air flow around trees, aerodynamic interaction between wind and trees, storm impacts and risk modelling, mechanics of trees under wind loading, failure criteria of trees, ecological dynamics and strong winds, ecological dynamics following windthrow, silviculture, tree level management and harvest design to reduce wind damage, and post storm damage responses.

The organisers of this conference would like to express their thanks to the approximately 100 participants from over 25 countries. They are indebted to the authors of oral and poster presentations, the session chairs as well as the scientific and local organising committee.

In its present form, the proceedings volume contains extended abstracts of more than 80% of the presentations. The authors have the sole responsibility for the contents of their extended abstracts.

Helmut Mayer and Dirk Schindler (Eds.)

Contents

About the influence of the windward edge structure on the flow characteristics at forest edges

Cornelia Frank, Bodo Ruck, Michael Tischmacher

Institute for Hydromechanics, University of Karlsruhe, Germany

Abstract

Experimental investigations in an atmospheric boundary layer wind tunnel were carried out in order to study the influence of the windward edge structure on the flow characteristics at the canopy top. Two different types of forest edges were used. The inclination angle was varied three times for both edge types and all inclined edges were combined with both dense and sparse forest stands. In addition, a configuration was investigated where the airflow in the trunk space of the dense forest was blocked completely by the windward arrangement of an impermeable wall.

1. Introduction

The amount of storm damage in forest stands depends on numerous parameters such as topography, stand density, canopy roughness, tree species, forest edge structure and soil parameters. A detailed knowledge of the relations between these various influencing parameters and the flow field is necessary to work out silvicultural strategies for the reduction of the storm damage risk and to assess the storm damage vulnerability of forest stands.

2. Methods

The experimental study has been carried out in the closed, 29 m long atmospheric boundary layer wind tunnel of the Laboratory of Building- and Environmental Aerodynamics at the Institute for Hydromechanics at the University of Karlsruhe. The characteristics of the simulated neutrally stratified atmospheric boundary layer, generated in the wind tunnel by means of vortex generators and roughness elements, are already described in Frank and Ruck (2007). The boundary layer is typical for suburban terrain and forest areas respectively.

The velocity measurements were accomplished by means of a two-component laser Doppler anemometer (2D-LDA) system. At every measuring point, about 26 600 data points were sampled in coincidence mode with a sampling frequency of 500 Hz. Hence, one point measurement took 53 s.

Canopy model

Forest arrangements with inclined windward stand edges of different structure were investigated in the scale 1:200. Two different types of edges were used: single tree edges (Figs. 1b-d) and abstracted edges, made of highly porous foam (Figs. 1e-g). Fig. 1a shows the dense forest with vertical edge and open trunk space. The inclination angle TW was varied three times for both edge types and all inclined edges were combined with both the dense stand (BD100) and the sparse stand (BD25), where every 2^{nd} to 4^{th} row was removed (see also Frank and Ruck, 2009). The used foam material is characterised by a very uniform, open-celled structure and is specified by 10 p.p.i (i.e. 10 pores

per inch, cell size = ca. 2.5 mm) and a pore volume fraction of 97 %. The pressure loss coefficient of this foam amounts to $k_{r,M} \approx 300\ m^{-1}$ in model scale (corresponding to $k_{r,N} = 1.5\ m^{-1}$ in full scale). The height of the foam edges amounts to 11 cm at the windward stand edge, thus, the edge is slightly lower than the mean stand height H = 11.5 cm. The single tree edges consist of individual trees arranged at distances of 2 cm x 2 cm (what corresponds to the tree distance of the dense stand (BD 100)). The structure of the single tree edges is less uniform, but more natural and slightly sparser than that of the foam edges. In addition, a configuration was investigated where the airflow in the trunk space of the dense forest was blocked completely by the windward arrangement of an impermeable wall (Fig. 1h).

The approach flow takes place perpendicular to the stand edge. The origin of the used x,z-coordinate system is located on the wind tunnel floor at the windward side of the actual stand (i.e. at the leeward side of the upstream forest edges) with the x-axis in horizontal streamwise direction and the z-axis in upward oriented vertical direction (Fig. 1h).

In order to detect the flow phenomena near the canopy top, measurements were carried out at a height z/H = 1.13 with a high spatial resolution between 1 cm = 0.087·H (2 m in nature) near the windward edge and 5 cm = 0.435·H (10 m) near the leeward edge.

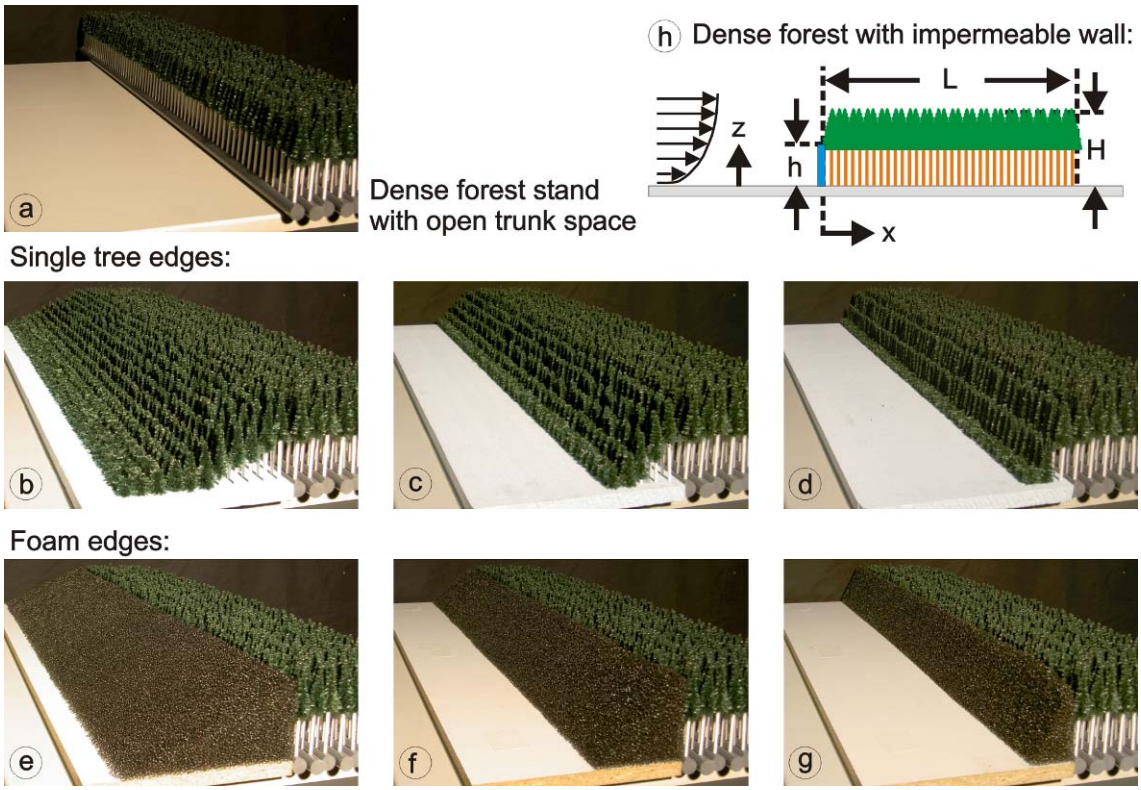

Fig. 1: Photos of the investigated forest edges: dense stand (BD100 = 600 trees/ha) a) with open trunk space (TW = 90°), b-d) with single tree edges [b) TW = 27°, c) TW = 45°, d) TW = 63°], e-f) with foam edges [e) TW = 27°, f) TW = 45°, g) TW = 63°]. h) sketch of the dense forest with impermeable wall and nomenclature used

3. Results

In this chapter, the streamwise variability of the wind loads near the canopy top (z/H = 1.13) is described. The mean wind load is proportional to the square of the mean horizontal velocity; the maximum wind load is proportional to the square of the sum of the mean horizontal velocity and the product of a gust weighting factor and the standard deviation of the mean horizontal velocity. The gust weighting factor was assumed to be 3.5. The wind loads are normalised by the wind load in the undisturbed approach flow at the same height. Furthermore, the ratio of maximum to mean wind load at z/H = 1.13 is also shown.

3.1 Edge structure impact for sparse forest stands

For the sparse forest stands, no clear dependency of the mean and maximum wind loads on the inclination angle was observed, neither for the foam nor the single tree edges, see Fig. 2. The differences between the curves are all in all quite small and, thus, lie probably in the range of the measuring accuracy.

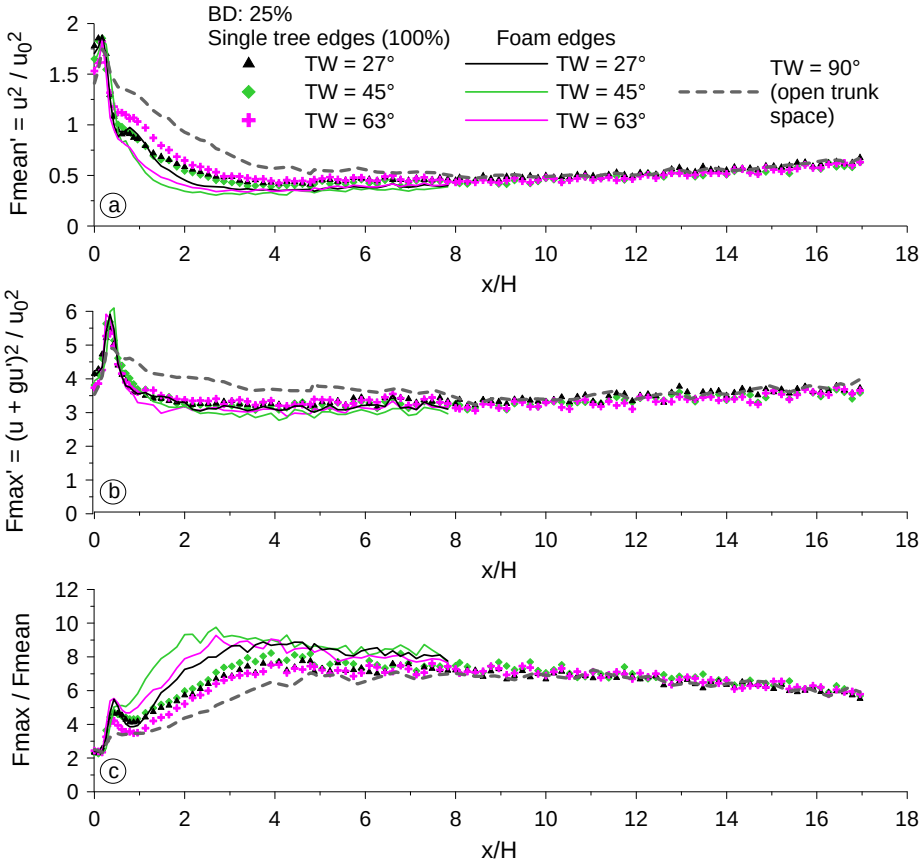

Fig. 2: Streamwise variability of wind loads near the canopy top (z/H = 1.13) above sparse forest stands (BD25) with different edges: a) normalised mean wind loads Fmean', b) normalised maximum wind loads Fmax', c) ratio of maximum to mean wind loads Fmax/Fmean; the variability above the sparse stand with open trunk space is also depicted (u_0 = 5.4 m/s)

For 1 < x/H < 4, the mean wind loads are smaller for the foam edges than for the single tree edges, whereas no significant differences were observed for the maximum wind loads. Consequently, the Fmax/Fmean-ratio is higher in this area for the stands with foam edges. The latter agrees by trend with the observations above dense forest stands.

A comparison of the sparse stand with open trunk space and the arrangements with inclined edges shows, that for 0.5 < x/H < 8 the wind loads above the forests with inclined edges are clearly smaller. The lowest Fmax/Fmean-ratios occur above the sparse forest with open trunk space.

3.2 Edge structure impact for dense forest stands

Dense forest with inclined edges

With increasing inclination angle both the mean and the maximum wind loads near the canopy top above dense stands with single tree edges decrease slightly and the Fmax/Fmean-ratio increases slightly, see Fig. 3. (For the foam edges, such clear trends were observed only between the shallow and the two steeper edges).

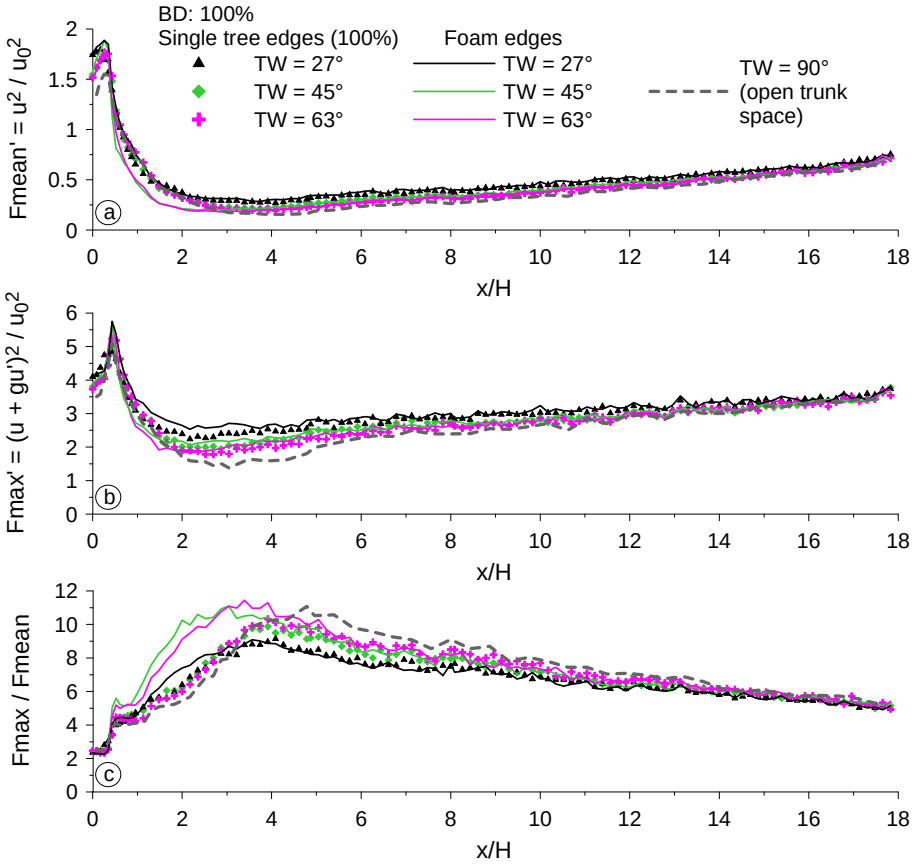

Fig. 3: Streamwise variability of wind loads near the canopy top (z/H = 1.13) above dense forest stands (BD100) with different inclined edges: a) mean wind loads, b) maximum wind loads, c) ratio of maximum to mean wind loads; the variability above the dense stand with open trunk space is also depicted (u_0 = 5.4 m/s)

The lowest wind loads occur for x/H > 2 above the dense forest with open trunk space. In comparison to the single tree edges, the maximum Fmax/Fmean-ratio moves towards the edge for the foam edges. The maximum Fmax/Fmean-ratio above the stands with the two steep foam edges is comparable to that observed above the dense stand with open trunk space and it is slightly higher than that above the stands with steep single tree edges. Near the windward stand edge (x/H < 4) the highest Fmax/Fmean-ratios occur above the forests with steep foam edges and further downstream above the dense forest with open trunk space. The lowest Fmax/Fmean-ratios appear above the dense stand with shallow single tree edge (TW = 27°).

Dense forest with impermeable wall

The impacts of an impermeable wall, being arranged windward of the dense stand and impeding the inflow of air in the trunk space, on the wind loads are shown in Fig. 4. In comparison to the dense stand with open trunk space, both mean and maximum wind loads increase. The Fmax/Fmean-ratio increases near the windward edge (x/H < 4) and decreases slightly further downstream. The impacts of the wall are comparable by trend to the implications of the foam edges, being characterized by a high density.

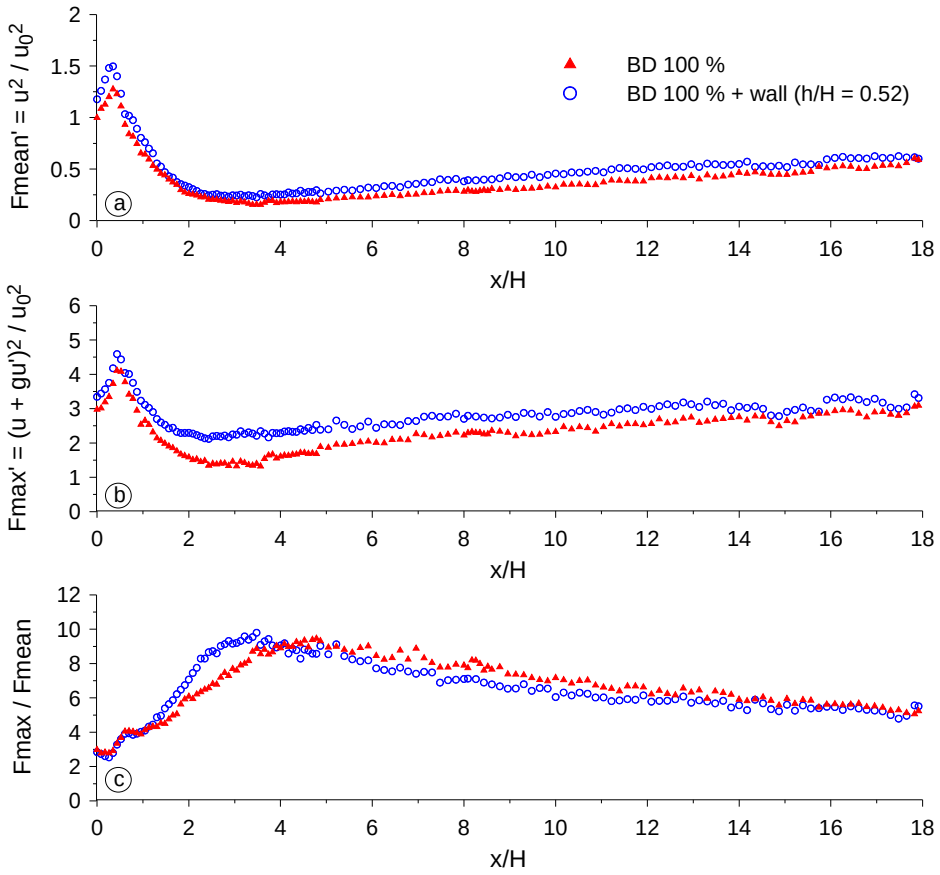

Fig. 4: Streamwise variability of wind loads near the canopy top (z/H = 1.13) above the dense forest stand (BD100) with windward arranged, impermeable wall (at x/H = 0): a) mean wind loads, b) maximum wind loads, c) ratio of maximum to mean wind loads; the variability above the dense stand without wall is also depicted (u_0 = 5.4 m/s)

3.3 Comparison of edge structure impact for sparse and dense forest stands

The arrangement of identical edges windward of sparse and dense forests results in an assimilation of the wind load curves (Figs. 2 and 3). The quite strong dependency of the mean and maximum wind loads on the stand density observed above the windward stand half for the forests with open trunk space diminishes due to the presence of the inclined edges. In general, the inclination angle seems to have a slightly higher influence for the dense stands than for the sparse stands as the curves of both edge types scatter stronger above the dense stands. Leeward of the denser foam edges, the differences between the curves of the sparse and dense forests are slightly smaller than leeward of the sparser single tree edges.

4. Conclusions

The results show that the windward edge structure affects the flow phenomena near the canopy top predominantly above the windward stand half, thus, its impact is locally restricted. This observation agrees with those of Dupont and Brunet (2008) and Gardiner and Stacey (1996). The similar trends observed above dense forests with impermeable wall and inclined edges suggest that the (total) density of the edge (and thus the amount of volume flux through the edge) is primarily responsible for the curve progression near the canopy top.

Acknowledgement

These investigations were performed within the project ‘Improving the storm stability of forest stands’ which is part of the RESTER-network (‘Strategies for the reduction of the storm damage risk for forests’) within the research program ‘Challenge climate change’. The authors would like to thank the Ministry for the Environment of the German federal state Baden-Württemberg for the financial support of this project.

References

Dupont, S., Brunet, Y., 2008: Impact of forest edge shape on tree stability: a large-eddy simulation study. Forestry 81, 299-316.

Frank, C., Ruck, B., 2007: Windkanalstudie zur Strömung in Waldlichtungen. Proc. 15. Fachtagung "Lasermethoden in der Strömungsmesstechnik", Rostock, 9.1-9.9.

Frank, C., Ruck, B., 2009: About the influence of the stand density on the flow characteristics at forest edges. Ber. Meteor. Inst. Univ. Freiburg No. 19, 15-21.

Gardiner, B., Stacey, G., 1996: Designing forest edges to improve wind stability. Forestry Commission, Technical Paper 16. 8 p.

Authors’ address:

Dr. Cornelia Frank (frank@ifh.uni-karlsruhe.de)
Prof. Dr. Bodo Ruck (ruck@uka.de)
Dipl.-Math. Michael Tischmacher (tischmacher@ifh.uni-karlsruhe.de)
Laboratory of Building- and Environmental Aerodynamics, Institute for Hydromechanics,
University of Karlsruhe, Kaiserstr. 12, D-76128 Karlsruhe, Germany

About the influence of the stand density on the flow characteristics at forest edges

Cornelia Frank, Bodo Ruck

Institute for Hydromechanics, University of Karlsruhe, Germany

Abstract

The paper presents experimental wind tunnel investigations in order to demonstrate the influence of the stand density on the flow characteristics at the canopy top near forest edges. The density of homogeneous forest stands was varied three times by removing whole rows of the originally dense model forest. In addition, staggered forest configurations were studied, consisting of sparse and dense forest areas of varied length.

1. Introduction

Aerodynamically, forest edges are highly permeable steps (length of inner and outer forest edges in Germany: 700.000 km), which interact with the atmospheric boundary layer flow. It is known, that the amount of storm damage in forest stands depends on numerous parameters such as topography, stand density, canopy roughness, tree species, forest edge structure and soil parameters. However, it is not clear, how the stand density alters the flow field situation at the canopy near forest edges in detail. It is believed that the stand density has an impact on the storm damage risk. Thus, to contribute to the assessment of the storm damage vulnerability of forest stands, detailed flow field investigations at the canopy near forest edges are needed.

2. Methods

The experimental set-up is the same as in Frank et al. (2009).

The density of the homogeneous forest stands was varied three times by removing whole rows of the originally dense model forest (see Fig. 1 and Table 1). In addition, staggered forest arrangements were investigated, consisting of sparse and dense forest areas of varied length, see Fig. 2. According to their spatial composition in stream-wise direction, these arrangements can be further sub-divided into two types: “Sparse - Dense” and “Dense - Sparse”. For each type, four different length ratios L/H were studied, where H = 23 m is the stand height in full scale. All forests are characterised by vertical edges (inclination angle TW = 90°) and an open trunk space.

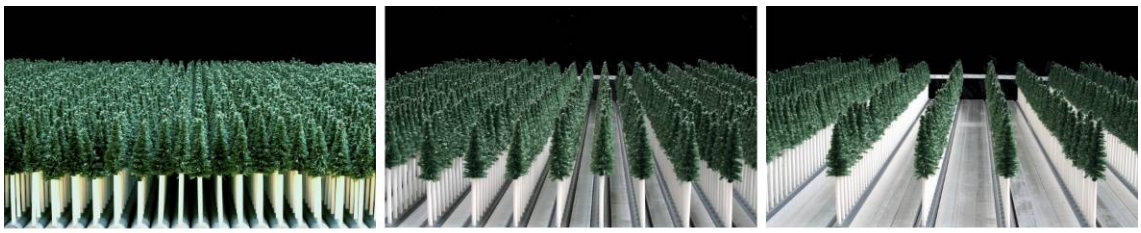

Dense forest: 600 trees/ha (BD100) | Medium dense forest: 300 trees/ha (BD50) | Sparse forest: 150 trees/ha (BD25)

Fig. 1: Photos of the investigated homogeneous forest stands of varied stand density

Table 1: Homogeneous forest stands: outline of tests (ax = spacing between the trees in stream-wise direction, ay = spacing between the trees in lateral direction (perpendicular to the approach flow), Lw = length of the forest = distance between first and last tree row, H = mean stand height = 23 m, *stand density based on the ground area of the reference configuration)

	Stand density BD*			ax/H	ay/H	Lw/H
	[%]	Model	Nature			
		[trees/m²]	[trees/ha]	[-]	[-]	[-]
Reference	100	2400	600	0.18	0.17	17.9
Every 2nd row removed	50	1200	300	0.35		17.3
Every 2nd to 4th row removed	25	600	150	0.70		17.0

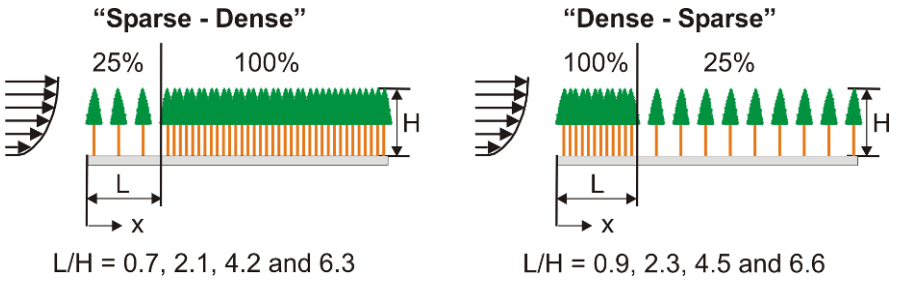

Fig. 2: Sketch of the staggered forest arrangements of varied length L (100% = 600 trees/ha, 25% = 150 trees/ha, H = 23 m)

3. Results

In this chapter, the streamwise variability of the wind loads near the canopy top (z/H = 1.13) is described. The mean wind load is proportional to the square of the mean horizontal velocity; the maximum wind load is proportional to the square of the sum of the mean horizontal velocity and the product of a gust weighting factor and the standard deviation of the mean horizontal velocity. The gust weighting factor was assumed to be 3.5. The wind loads are normalised by the wind load in the undisturbed approach flow at the same height. Furthermore, the ratio of maximum to mean wind load at z/H = 1.13 is also shown.

3.1 Homogeneous forest stands

Fig. 3 shows the streamwise variability of the wind loads above homogeneous forest stands of varied stand density at a height z/H = 1.13. Above the windward stand half both the mean and the maximum wind loads clearly increase with decreasing stand density, whereas the Fmax/Fmean-ratio decreases. Above the leeward stand half the maximum wind load increases slightly due to an increase of the turbulent kinetic energy, whereas the differences at the mean wind loads are relatively small in this area. The highest values of mean and maximum wind loads are observed near the windward stand edge, the highest Fmax/Fmean-ratios occur at x/H ≈ 5.

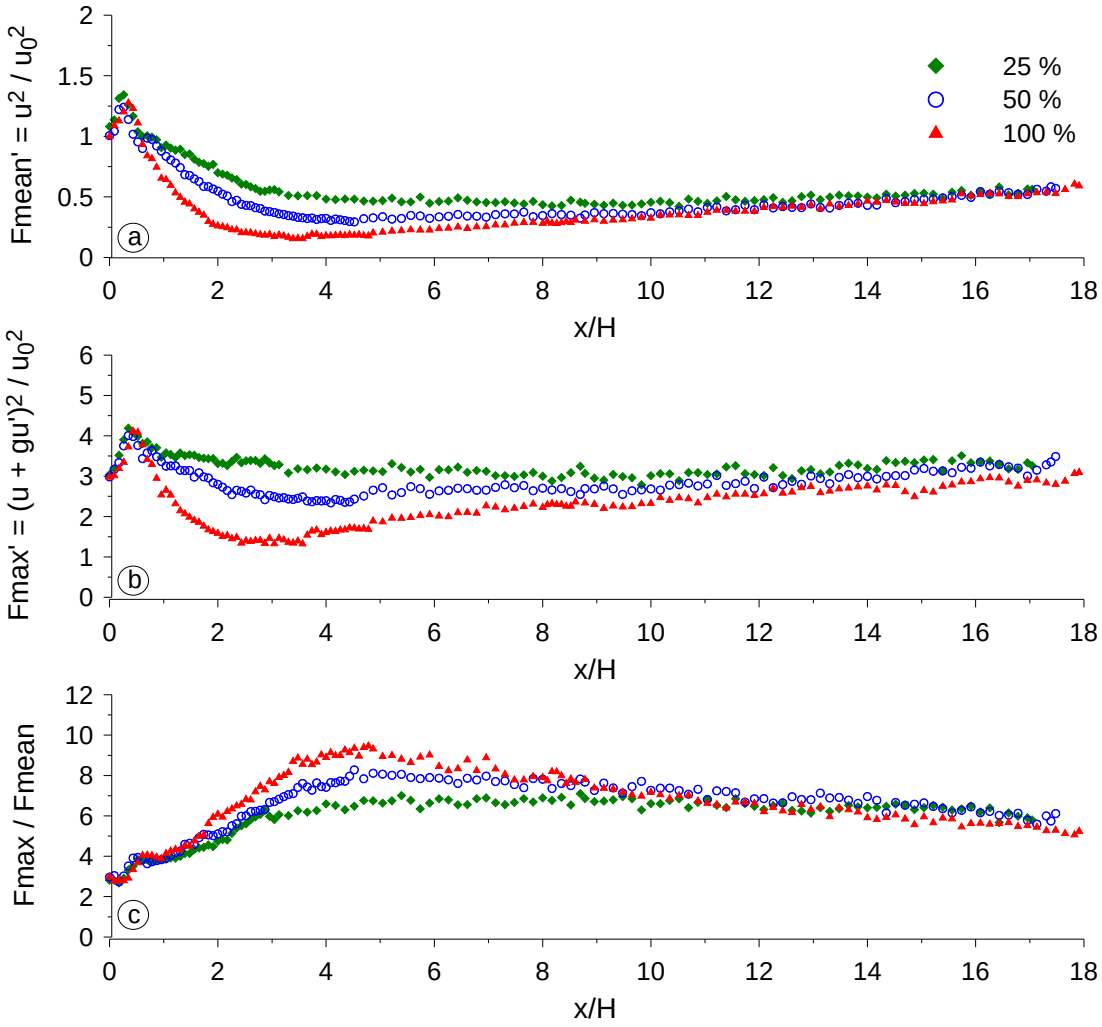

Fig. 3: Streamwise variability of wind loads near the canopy top (z/H = 1.13) above homogeneous forest stands of varied stand density: a) normalised mean wind loads Fmean', b) normalised maximum wind loads Fmax', c) ratio of maximum to mean wind loads Fmax/Fmean (u_0 = 5.4 m/s)

3.2 Staggered forest arrangements

Type "Sparse - Dense"

In Fig. 4 the streamwise variability of the wind loads above staggered forest arrangements of the type „Sparse - Dense" (with stand densities BD = 25/100 %) and additionally above the homogeneous forest stands of comparable stand densities is depicted. The vertical lines mark the transitions from sparse to dense forest area, that is, the position of the inner stand edges. The curves of the staggered arrangements are embedded by the curves of the homogeneous forest stands. If the windward arranged sparse forest area is short (L = 0.7H) the curves resemble yet those above the homogeneous dense stand, however, in the near-edge area up to x/H ≈ 4 the wind loads are slightly higher. For the configurations with longer sparse forest areas (L ≥ 2.1H), the curves of the staggered arrangements are nearly identical near the windward forest edge to the curves of the homogeneous sparse stand and they are comparable from a certain distance downstream

of the inner stand edge to the curves of the homogeneous dense stand. The wind loads adjust to the varied stand density in an area between about 1-2H upstream and 4-5H downstream of the inner stand edges. With increasing length of the windward arranged sparse forest area, the minima of both the mean and the maximum wind loads increase and the maximum of the Fmax/Fmean-ratio decreases.

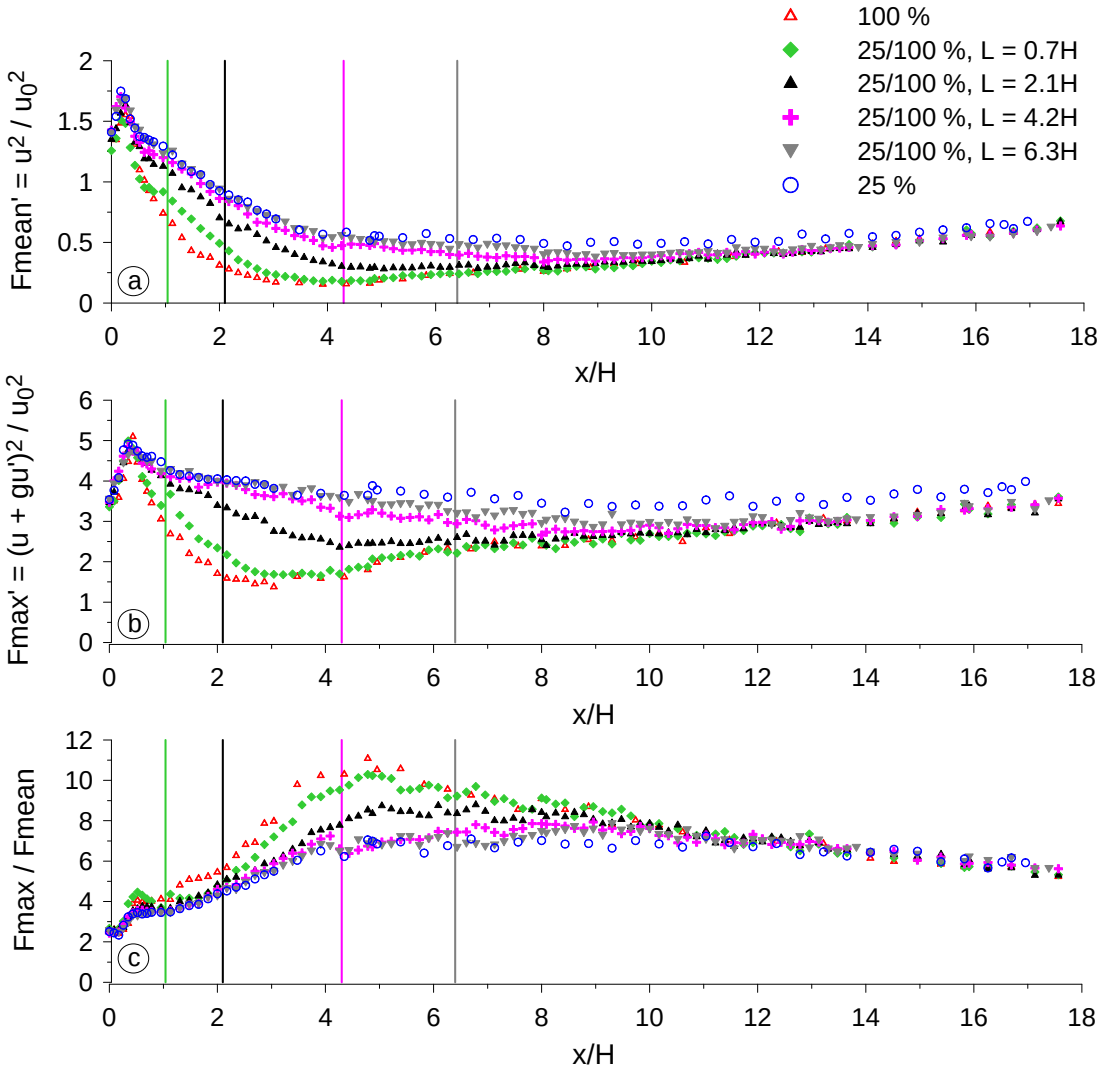

Fig. 4: Streamwise variability of wind loads near the canopy top (z/H = 1.13) above staggered forest stands (BD25 – BD100) of varied length: a) normalised mean wind loads Fmean', b) normalised maximum wind loads Fmax', c) ratio of maximum to mean wind loads Fmax/Fmean; the variability above the homogeneous stands of corresponding stand densities is also depicted (u_0=5.4 m/s)

Type "Dense - Sparse"

Fig. 5 shows that the curves of the staggered arrangements of the type "Dense - Sparse" are likewise embedded by those of the both homogeneous stands. The curves of the staggered arrangements are close to the windward forest edge nearly identical to those of the homogeneous dense stand. When the windward arranged dense forest area is

short (L/H = 0.9) a clear increase of the wind loads is observed downstream of the inner stand edge in comparison to the homogeneous dense stand; for L/H = 2.3 only a slight increase occurs. For longer dense forest areas (L/H = 4.5 and 6.6) the wind load distributions along the whole forest length are similar to those of the homogeneous dense forest. The area in which the wind loads adjust to the varied stand density is all in all longer for the staggered arrangements of the type "Dense – Sparse" than for the "Sparse – Dense"-configurations.

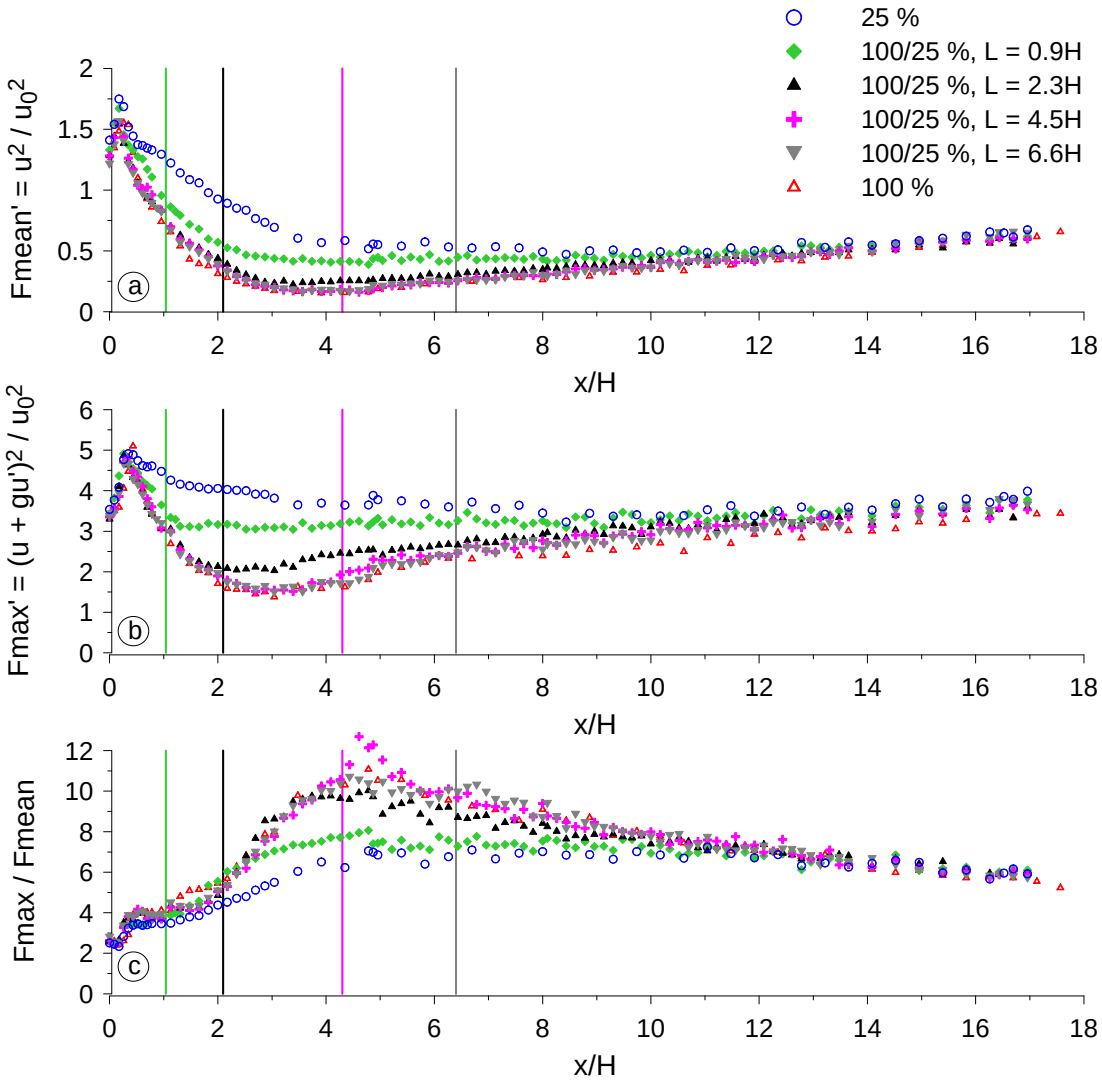

Fig. 5: Streamwise variability of wind loads near the canopy top (z/H = 1.13) above staggered forest stands (BD100 – BD25) of varied length: a) normalised mean wind loads Fmean', b) normalised maximum wind loads Fmax', c) ratio of maximum to mean wind loads Fmax/Fmean; The variability above the homogeneous stands of corresponding stand densities is also shown (u_0=5.4 m/s)

4. Discussion

Gardiner and Stacey (1996) measured mean and extreme stem bending moments along 15 m high Sitka model forests of varied stand density and also determined a gust factor describing the ratio of extreme to mean stem bending moment. Even if their model forests are denser and smaller than ours, a comparison of the different quantities shows a good agreement by trend. Only near the windward forest edge (x/H < 1) the behaviour of the wind load curves near the canopy top is contrary, what can be attributed to the fact that bending moments are integral quantities describing the change of wind loads over the whole stand height and that in the near-edge area the wind loads at z < H still contribute significantly to the resultant bending moment.

Gardiner and Stacey (1996) as well as Dupont and Brunet (2008) carried out studies about the influence of forest edge structure on the amount of the applying bending moments and found out that upstream sparse forest areas being 2H long result in a bending moment reduction in the near-edge area of the dense stand. Our measurements confirm their results by trend, see Fig. 6, however, our results also show that further downstream (at a higher distance to the inner stand edge) the wind loads will increase.

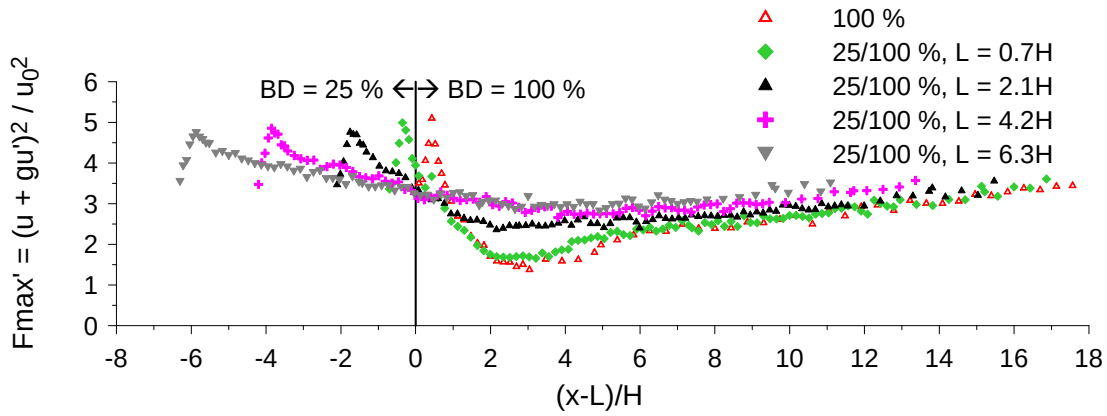

Fig. 6: Streamwise variability of the maximum wind load near the canopy top (z/H = 1.13) above staggered forest stands (BD25 – BD100) of varied length

Acknowledgement

These investigations were performed within the project 'Improving the storm stability of forest stands' which is part of the RESTER-network ('Strategies for the reduction of the storm damage risk for forests') within the research program 'Challenge climate change'. The authors would like to thank the Ministry for the Environment of the German federal state Baden-Württemberg for the financial support of this project.

References

Frank, C., Ruck, B., Tischmacher, M., 2009: About the influence of the windward edge structure on the flow characteristics at forest edges. Ber. Meteor. Inst. Univ. Freiburg No. 19, 9-14.

Dupont, S., Brunet, Y., 2008: Impact of forest edge shape on tree stability: a large-eddy simulation study. Forestry 81, 299-316.

Gardiner, B., Stacey, G., 1996: Designing forest edges to improve wind stability. Forestry Commission, Technical Paper 16. 8 p.

Authors' address:

Dr. Cornelia Frank (frank@ifh.uni-karlsruhe.de)
Prof. Dr. Bodo Ruck (ruck@uka.de)
Laboratory of Building- and Environmental Aerodynamics, Institute for Hydromechanics
University of Karlsruhe
Kaiserstr. 12, D-76128 Karlsruhe, Germany

Modeling wind fields in tall canopies - towards better momentum distribution using 3D vegetation scans in high resolution

Ronald Queck[1], Anne Bienert[2], Stefan Harmansa[1]

[1]Institute of Hydrology and Meteorology, Dresden University of Technology, Germany
[2]Institute of Photogrammetry and Remote Sensing, Dresden University of Technology, Germany

Abstract

DFG priority program MetStröm was launched with the focus to improve methods for modeling atmospheric processes. The aim of the subproject TurbEFA is to describe the inhomogeneity of turbulent exchange processes in and over a real forest canopy. A crucial step is the use of more detailed information about vegetation structure. A method is presented how to record vegetation structure and make this information applicable for model use and deriving turbulence parameters as well.

1. Introduction

The momentum distribution in forests is dominated by inhomogeneities like step changes in stand height and forest clearings. Therefore the application of turbulence closure models to describe the wind fields in tall canopies is limited by the parameterization of plant architecture. The relationship between wind speed, drag coefficient and plant area distribution was experimentally investigated in a mixed conifer forests in the lower ranges of the Osterzgebirge on the basis of a dense 3D representation obtained from terrestrial laser scanner data. An evaluation of the results will be done by application of a Reynolds Average Navier-Stokes (RANS) model. The aim of the study is to contribute to the solution of the following questions. Which quantities influence the drag beside the plant area density (keywords: streamlining, stability)? What is the "source area" for the turbulence measured at a certain point? What shape has the relationship between the effective drag coefficient and the Laser derived Voxel Space LVS?

2. Study area and data recording

The Anchor Station Tharandter Wald ASTW participates in the CarboEurope Integrated Project CEIP and is located in the eastern part of a large forested area (60 km^2), about 25 km southwest of Dresden (50°57'49''N, 13°34'01''E, 380 m a.s.l., see Fig. 1 for surroundings). Most of the common features of the site are described by Feigenwinter et al. (2004) and Grünwald and Bernhofer (2007).

The stand with dominating spruce was established in 1887. The species of the main canopy are composed of 87 % coniferous evergreen (72 % Picea abies, 15 % Pinus sylvestris) and 13 % deciduous (10 % Larix decidua, 1 % Betula spec. and 2 % others). The tree density is 477 trees ha^{-1}, the single side leaf area index is 6.7 m^2/m^2 and the mean canopy height around the permanent tower (HM) is 30 m. The mean breast height diameter is 33 cm. The ground is mainly covered with young Fagus sylvatica (20 %)

and Deschampsia flexuosa (50 %). The investigated wind sectors cover a 50 m x 90 m clearing, called „Wildacker“, approximately 100 m west of the permanent tower.

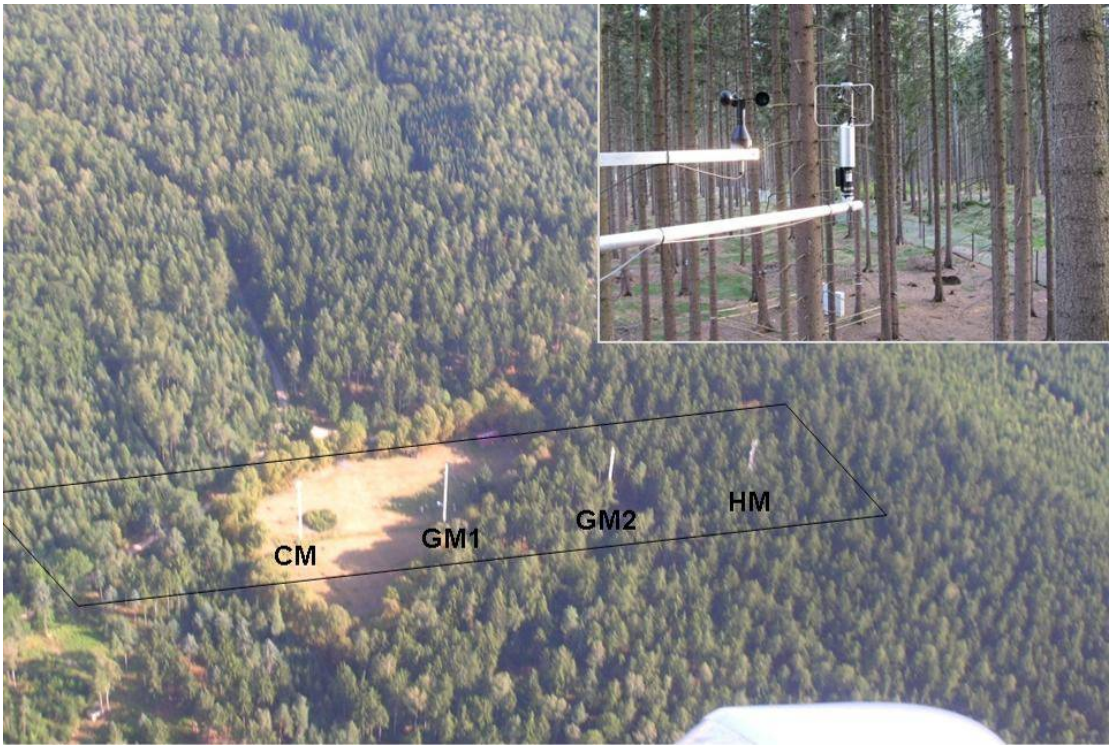

Fig. 1: Aerial photo with towers (shot by W. Junkermann, 31 July 2008) and the outlined model domain: HM indicates the permanent scaffolding tower (height 42 m), GM1 and GM2 are temporarily build scaffolding towers (40 m) as well as CM an telescope tower (30 m)

3. Meteorological measurements

From May 2008 to May 2009 intensive turbulence measurements took place on a transect over the forest clearing. In total 25 measurement points on 4 towers (heights: 30m, 40m, 40m, 42m) including five at ground level position (2 m), are used to record the turbulent flow. The ultrasonic anemometer (R.M. Young Meteorological Instruments, MI, US) were mounted on booms in a distance of 2-3 m to the scaffolding towers. All raw data (measured at 20 Hz) were logged simultaneously and in post processing combined to statistics for several time intervals.

$$\rho \frac{d\overline{u'w'}}{dz} = -\rho C_D(z) PAD(z) u^2(z) \qquad \text{Eq. 1}$$

Profiles of the drag coefficient C_D are defined by the equilibrium between the vertical change of drag force (left hand site of Eq. 1) and the rate of horizontal momentum transfer (right hand side of Eq. 1). The product of the drag coefficient and the plant area density $C_D(z)PAD(z)$ is then obtainable by wind measurements (see Fig. 2)

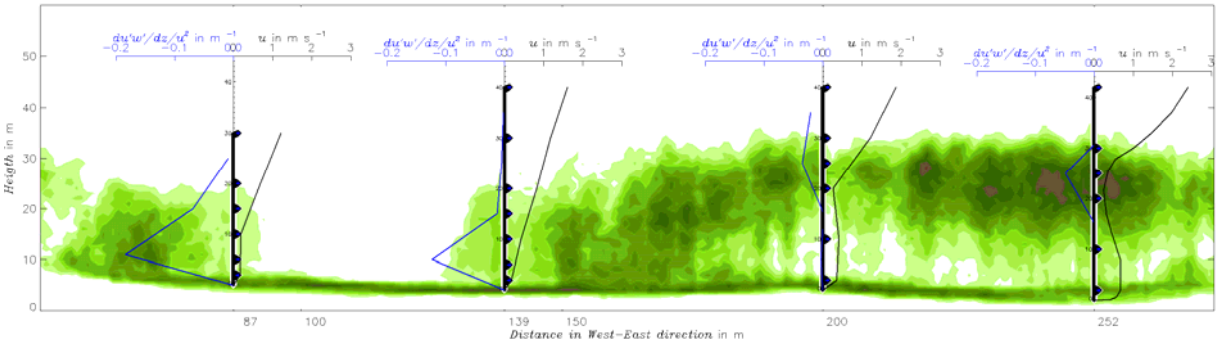

Fig. 2: „Vegetation“ (green): 2D Laser Voxel Space LVS derived by averaging the y-dimension (depth) of the 3D LVS; black charts: mean measured wind speed; blue charts: change of drag force per horizontal momentum

4. Terrestrial laser scanning (TLS)

Terrestrial laser scanning is a fast developing new 3D measurement technique and depicts an efficient method to record accurate 3D models of the vegetation. The forest stands around the clearing (500 m x 120 m) were scanned with a Riegl LMS-Z 420i and a Faro LSHE880 laser scanner (Fig. 3). In total, scans from 13 different ground positions and from the top of the main tower (height: 40m) were taken. The scans were merged into a single 3D representation of the stand by using tie points. Finally, the stand is described with approximately 50 million accurately measured surface points.

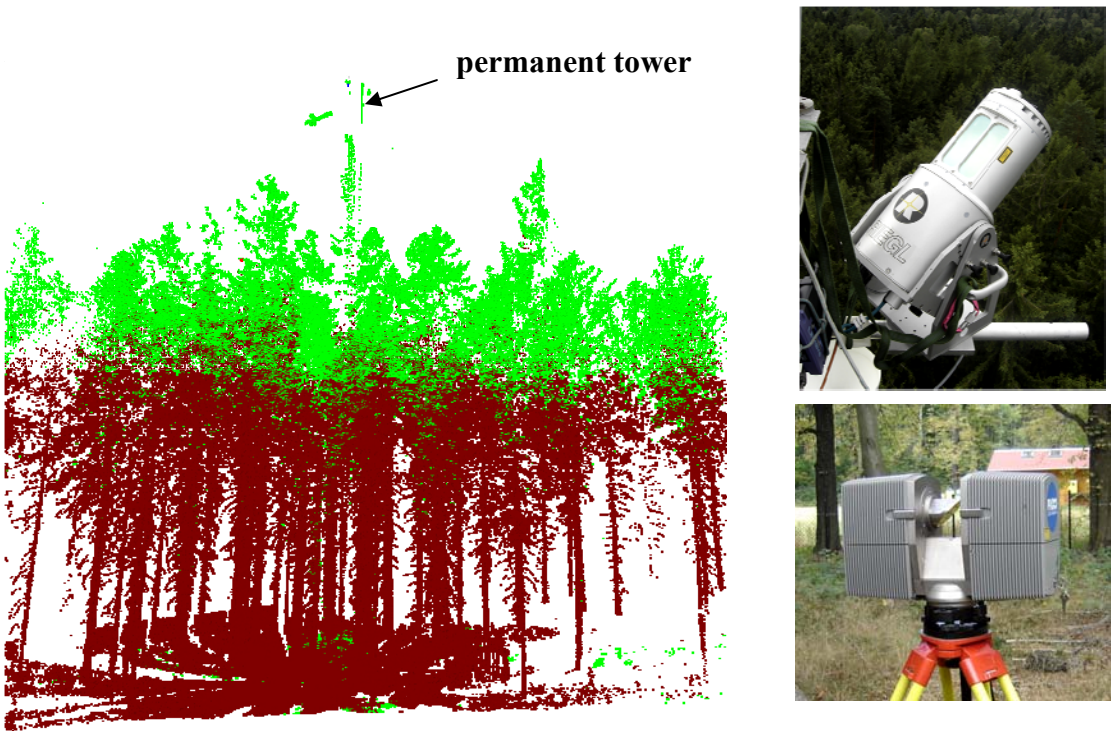

Fig. 3: Laser scanner point cloud recorded from ground (brown points) and main tower (green points) (thinned for printing purposes); Riegl LMS Z-420i mounted on the permanent tower (top right) and Faro LSHE880 (bottom right) laser scanners

5. Analysis of the TLS data

The detection of trees was performed automatically in three different horizontal layers of the 3D point cloud by an approach, which is described in detail by Bienert et al. (2007). A square structure element (size: s) is moved over the slice in X/Y projection and searches for point clusters. An object will be separated into two objects if the distance between one point and the nearest one is bigger than s/2. To classify the objects as trees, a circle fitting with all points of an object was done.

After tree detection, the average tree distances in the transect were calculated. The horizontal distances of a tree to its nearest neighbours were calculated by applying a Delaunay triangulation, which can be seen in Fig. 4. Finally the average tree distance is defined as the mean value of all determined distances.

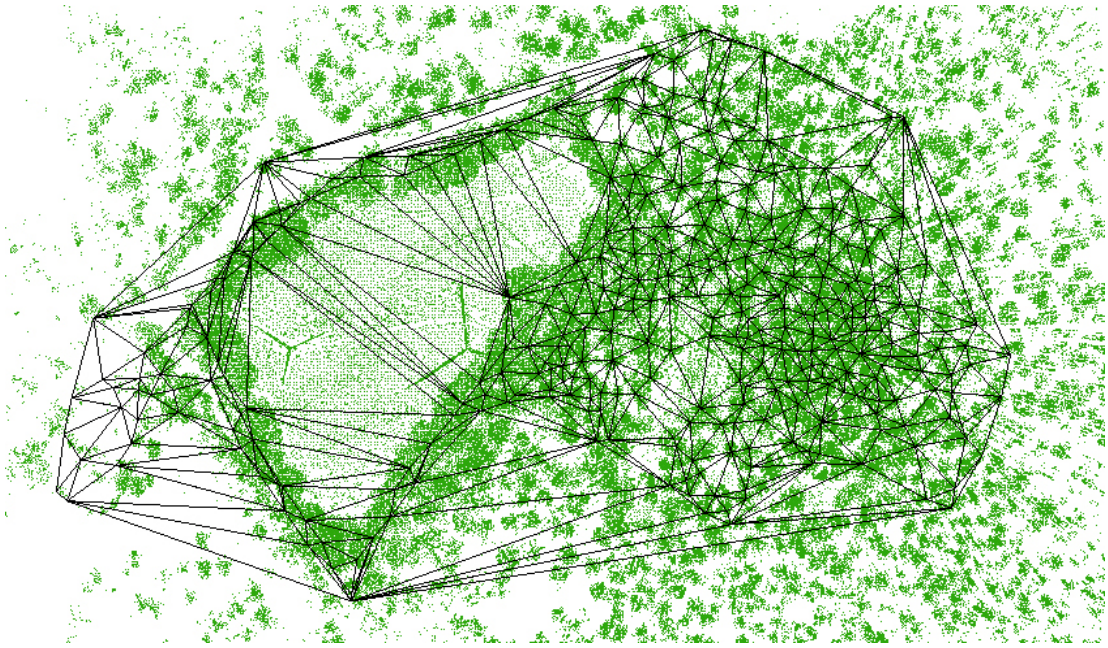

Fig. 4: Delaunay triangulation of the detected tree positions

The 3D point cloud of a selected tree group was transformed into a 3D voxel space (3D LVS). A voxel space is defined as a space with adjacent cubes aligned along three coordinate axes. In our case, we choose voxel size of 1 m. Depending on the scan position a laser pulse penetrates different voxels before hitting the surface. Objects behind another object are not detected, and scan shadows occur. For each voxel, depending on the scan position:

- the total hit of points on a surface (N_{Hit}),
- the number of measurements which penetrate the voxel and result in hits behind the voxel (N_{Miss}) and
- the number of potential hits (N_{Shadow}) which result in hits in front of the voxel in case of occlusions (caused by e.g. stems, ground vegetation and crowns)

are counted.

In case of a clear view to the voxel, without occlusions (N_{Shadow} = 0) and penetrations (N_{Miss} =0), N_{max} defines the maximum point count of hits (N_{max} = N_{Hit}). By using these values, a normalised point density P_i of each voxel and scan position is calculated. Because of different scan positions *i*, a voxel could include laser measurements of different views). To take these different positions into account, a weighting function w_i is used to determine the reflection probability $P_{Reflection}$ (Eq. 2) with values between 0 and 1. A similar method was presented from Aschoff et al. (2006). $P_{Reflection}$ as the normalised point density of each voxel represents the plant area density PAD.

$$P_{\text{Reflection}} = \frac{P_i \cdot w_i + P_{i+1} \cdot w_{i+1} + \ldots + P_n \cdot w_n}{w_i + w_{i+1} + \ldots + w_n} \qquad \text{(Eq. 2)}$$

with $N_{\max} = N_{Hit} + N_{Miss} + N_{Shadow}$ $\quad P_i = \frac{N_{Hit} + N_{Miss}}{N_{\max}}$ $\quad w_i = \frac{N_{Hit}}{N_{\max}}$

where

$P_{Reflection}$	reflection probability of a voxel
P_i	normalised point density of a voxel per scan position
w_i	weighting function of a voxel per scan position
i…n	scan position, n = total number of scan positions

6. Implementation in flow model

In flow models the influence of vegetation on momentum is usually considered by implementation of a friction term ($c_d \cdot PAD \cdot \overline{u} \cdot \vec{u}_i$) in the momentum equations. Therefore high resoluted vegetation scans are a prerequisite for more detailed modelled flow fields inside the canopy. Using simple geometric calculations (superposition of different grids) the scanned *PAD* distribution can be transformed in *PAD* profiles of the spatial model domain resolution. For use in a 2D model averaged *PAD* profiles were calculated over a range of 30 m perpendicular to the transect line. A first result of horizontal wind speeds along the transect can be seen in Fig. 5, which were calculated by a non hydrostatic RANS model for the stationary case. For the turbulence model a 1.5 order closure was used.

7. Conclusions and future work

Thus the derived measure for the PAD, the spatial arrangement of points inside the voxel and the drag coefficients calculated from turbulence measurements will be used to derive a functional relationship for the friction term in numerical models.

Future Work will deal with the improvement of the voxel data analysis by determining additional voxel information. The application of morphological operations (dilatation and erosion) in 3D voxel space could give some more information for shaded and therefore empty voxels without points inside. Also the direction of the principal axes and some texture parameters such as variance and homogeneity of a voxel will allow a more

reliable classification between the different vegetation elements like stem, branch and leaf.

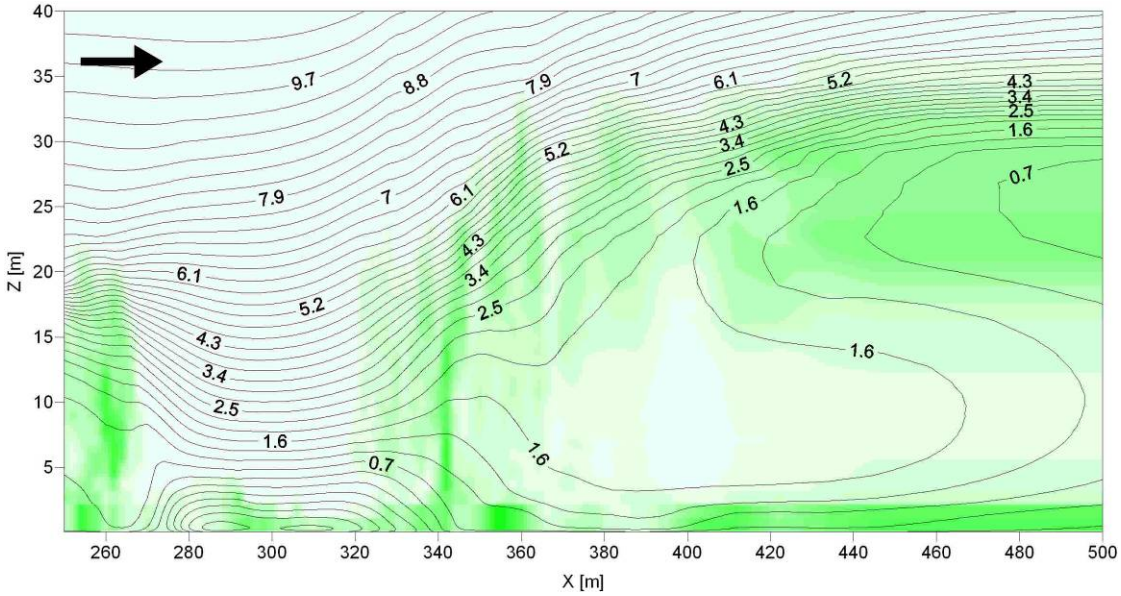

Fig. 5: Simulated horizontal wind speeds in m/s (black lines) with PAD distribution derived from LVS (green areas); black arrow depicts the flow direction

Acknowledgement

This study was supported by the Deutsche Forschungsgemeinschaft (DFG SPP 1276 MetStröm). Many thanks to Christian Feigenwinter and Roland Vogt (Uni Basel) for supplying some sonics and mental help; thanks also to the technical staff of IHM TUD, and to the students of Hydrology and Geography of the TU Dresden for the manpower. The authors would like to thank also Faro Europe GmbH for providing the laser scanner.

References

Aschoff, T., Holderied, M.W., Spiecker, H., 2006: Terrestrische Laserscanner zur Untersuchung von Wäldern als Jagdlebensräume für Fledermäuse. Photogrammetrie - Laserscanning - Optische 3D-Messtechnik (Beiträge Oldenburger 3D-Tage 2006, Hrsg. Th. Luhmann), Verlag Herbert Wichmann, 280-287.

Bienert, A., Scheller, S., Keane, E., Mohan, F., Nugent, C., 2007: Tree detection and diameter estimations by analysis of forest terrestrial laserscanner point clouds. ISPRS Workshop on Laser Scanning 2007 and SilviLaser 2007, Espoo, September 12-14, 2007, Finland, 50-55.

Feigenwinter, C., Bernhofer, C., Vogt, R., 2004: The influence of advection on the short term CO2-budget in and above a forest canopy. Bound.-Layer Meteorol. 113, 219-224.

Grünwald, T., Bernhofer, Ch., 2007: A decade of carbon, water and energy flux measurements of an old spruce forest at the Anchor Station Tharandt. Tellus 59B, 387–396.

Authors' addresses:

Dr. Ronald Queck (queck@forst.tu-dresden.de)
Institute of Hydrology and Meteorology, Dresden University of Technology
Pienner Straße 23, D-01737 Tharandt, Germany

Dipl.-Ing. Anne Bienert (anne.bienert@tu-dresden.de)
Institute of Photogrammetry and Remote Sensing, Dresden University of Technology
Helmholtzstraße 10, D-01069 Dresden, Germany

Dipl.-Hydrol. Stefan Harmansa (stefan.harmansa@tu-dresden.de)
Institute of Hydrology and Meteorology, Dresden University of Technology
Pienner Straße 23, D-01737 Tharandt, Germany

The SLF boundary layer wind tunnel - an experimental facility for aerodynamical investigations of living plants

Benjamin Walter, Christof Gromke, Michael Lehning

WSL Institute for Snow and Avalanche Research SLF, Davos, Switzerland

Abstract

The SLF boundary-layer wind tunnel is utilized to investigate the impact of living plants on air flow and soil erosion (Burri, 2009). Velocity measurements have been performed to identify the flow characteristics for different wind tunnel setups, e.g. over smooth floor, vegetation covered surfaces with spires and additional roughness elements in the fetch. Analyses of the results and comparison with literature show that a boundary layer flow suitable for further investigations of living plants is generated in the wind tunnel.

1. Introduction

Plants affect processes like erosion, transport and deposition of soil and snow that may occur when the atmospheric wind interacts with the ground. A lack of knowledge of the details of these processes exists due to their complexity. So far, artificial plant imitations instead of real living plants have been used in most wind tunnel studies. However, real plants display a highly irregular structure that can be extremely flexible and porous in contrast to the often rigid and non-porous artificial plant imitations. Due to their flexibility, real plants align with the flow at higher wind speeds (streamlining) and considerable changes in drag and flow regimes occur. Accordingly, significant differences in air flow and soil erosion can be expected in contrast to investigations using plant imitations. The novelty of our approach lies in the use of real living plants instead of artificial non-flexible imitations.

The SLF wind tunnel (Fig. 1) is situated at 1640 m a.s.l. in Davos, Switzerland. The wind tunnel has thus far been used to investigate threshold wind speeds for snow transport (Clifton et al., 2006), to investigate snow ventilation (Clifton et al., 2008) and saltation of fresh snow (Guala et al., 2008) and to improve saltation models (Clifton and Lehning, 2008). For this contribution, velocity measurements have been performed using two-dimensional hot-wire anemometry (HWA) to identify the flow conditions produced in the wind tunnel for different setups. Basic flow characteristics over a smooth floor setup without plants and the boundary layer development over a vegetation covered surface have been investigated. The first has already been analyzed in detail in a previous work (Ambühl, 2004). The latter has been done with and without spires and additional rigid roughness elements in the fetch. Influences of streamwise pressure gradients and the implications on the flow field have been studied. Integral length scales have been calculated for different positions within the vegetation canopy and compared to literature. Power spectral densities have been determined and compared to the von Karman spectrum. The results provide basic information and are a first step of investigating shear stress partitioning within living plants using Irwin sensors.

2. Basic theory

The mean horizontal wind velocity $u(z)$ in the constant stress layer of a boundary layer flow can be described by means of the logarithmic law $u(z) = u_*/\kappa \ln((z-d)/z_0)$. u_* is the friction velocity, $\kappa = 0.41$ the von Karman constant, z the height above the ground, d the zero plane displacement height and z_0 the aerodynamic roughness length. Turbulent fluctuations u', v' and w' are superimposed to the mean flow in the x, y and z direction, respectively. Important turbulence characteristics are described by the shear stress velocity $(- \overline{u'w'})^{1/2} = (\tau_t(z)/\rho)^{1/2}$, the integral length scale $L_u(z)$ and the power spectral density $S_{uu}(f)$ (e.g. Gromke et al., 2005; e.g. Gromke, 2009). The shear stress velocity increases from zero at the surface to a constant value in the logarithmic layer (friction velocity u_*) and decreases to zero in the free stream. Using Taylor's hypothesis of frozen turbulence (Stull, 1988), the integral length scale $L_u(z)$ is defined by

$$L_u(z) = \frac{u(z)}{\sigma_u^2(z)} \int_0^\infty \overline{u'(z,t)u'(z,t+\tau)}\, d\tau \ , \tag{1}$$

where the integrand is the autocorrelation function of $u'(z,t)$. $L_u(z)$ is a measure for streamwise spatial dimensions of the largest gusts. The power spectral density

$$S_{uu}(z,f) = \int_{-\infty}^{\infty} \overline{u'(z,t)u'(z,t+\tau)}\ e^{-i2\pi f\tau} d\tau \tag{2}$$

is the Fourier transform of the autocorrelation function and gives the distribution of turbulent kinetic energy in the frequency domain.

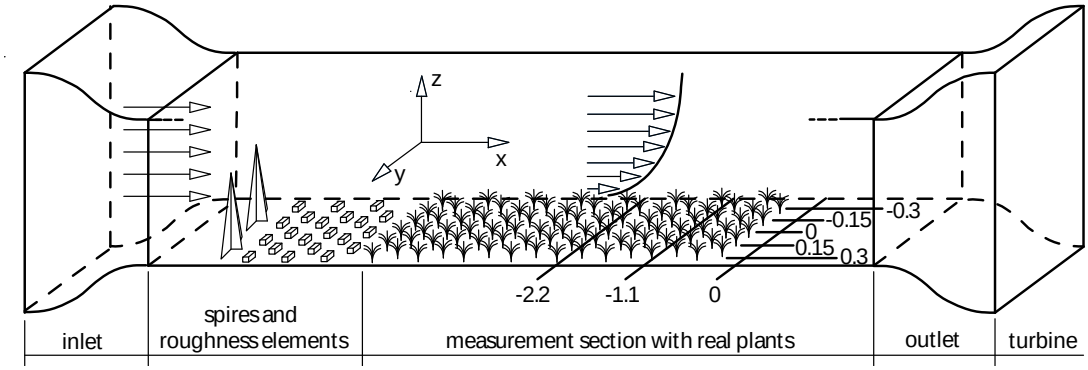

Fig. 1: Sketch of the SLF boundary layer wind tunnel (length x width x height = 14 m x 1 m x 1 m); the wind tunnel operates in suction mode; measurement positions are denoted; all values are given in meters

3. Basic flow characteristics - smooth floor experiments

Velocity measurements have been performed over a smooth wooden floor in the empty wind tunnel without spires and roughness elements to characterize the basic flow conditions. Vertical profiles of the horizontal velocity $u(z)$ have been measured at $x = y = 0$ m (Fig. 1) for different free stream velocities U_δ. Normalizing the profiles by U_δ resulted in a collapse of the velocity profiles (not shown here). Hence, a Reynolds number independent flow is produced.

The lateral homogeneity and the influences of the side walls on the air flow have been investigated by means of velocity profiles at five lateral positions. The three profiles around the centre of the tunnel at y = -0.15, 0, 0.15 m and x = 0 m are reasonably homogeneous with mean wind speed $u(z)$ deviations less than 6% (not shown here). Decelerated wind speeds in the outer velocity profiles next to the side walls are within acceptable limits.

4. Air flow above living plants

Velocity measurements at various positions between and above real plants (Fig. 2) have been performed. Streamwise pressure gradients, the development of the boundary layer as well as integral length scales and power spectral densities have been investigated and compared to literature data for rough wall turbulent boundary layers.

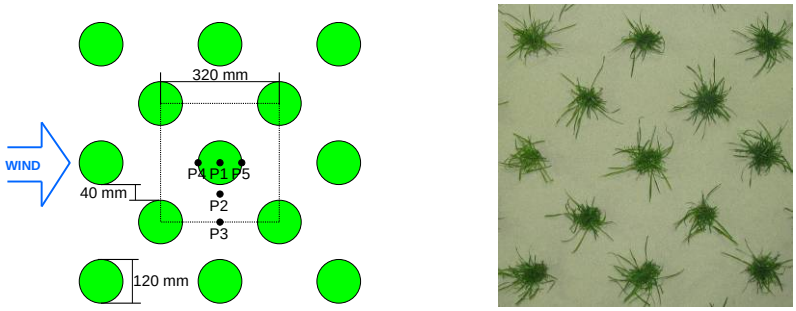

Fig. 2: Sketch and photograph of vegetation canopy with measurement positions

4.1 Streamwise pressure gradients

Pressure gradients along the flow direction of natural atmospheric boundary layer flows are negligible on typical wind tunnel dimensions. Hence, prevailing streamwise pressure gradients have to be eliminated in a wind tunnel in order to simulate a natural boundary layer flow. In a wind tunnel with constant cross section, the free stream velocity U_δ has to increase in x-direction due to the growth of the boundary layer thickness δ. This results in streamwise negative pressure gradients. The pressure gradients can be avoided by adjusting the ceiling of the wind tunnel in order to keep the free stream velocity constant. As can be seen from Fig. 3, in case of a non-adjusted ceiling, the free stream velocity layer is not present since we find $du/dx \neq 0$ and $du/dz \neq 0$ also above the boundary layer and thus $(- \overline{u'w'})^{1/2} \neq 0$ as well (profile 5). Contrary, in case of an adjusted ceiling with vanishing pressure gradient, the shear stress velocities $(-\overline{u'w'})^{1/2}$ are zero indicating the existence of a free stream velocity layer.

4.2 The boundary layer development

The boundary layer above the plants has to be sufficiently developed in the measurement section to perform reliable measurements. Vertical shear stress velocity profiles at various positions are used to investigate the streamwise increase of the boundary layer thickness δ (Fig. 3). The boundary layer thickness δ is defined as the height above the ground where $u(z) = 0.99U_\delta$ and $- \overline{u'w'} = 0$. An increase of δ from 370 mm at x =

-2.2 m to 500 mm at $x = 0$ m is found (profiles 1-3). Spires and artificial roughness elements in the fetch result in an increased boundary layer thickness in the measurement section (profile 4). That both - $u'w'$; $\overline{}$ profiles with and without spires and roughness elements collapse quite well at $x = 0$ up to a height of $z \approx 250$ mm (profile 1 and 4) is an indication of a sufficiently developed boundary layer in the interesting range close to the vegetation canopy.

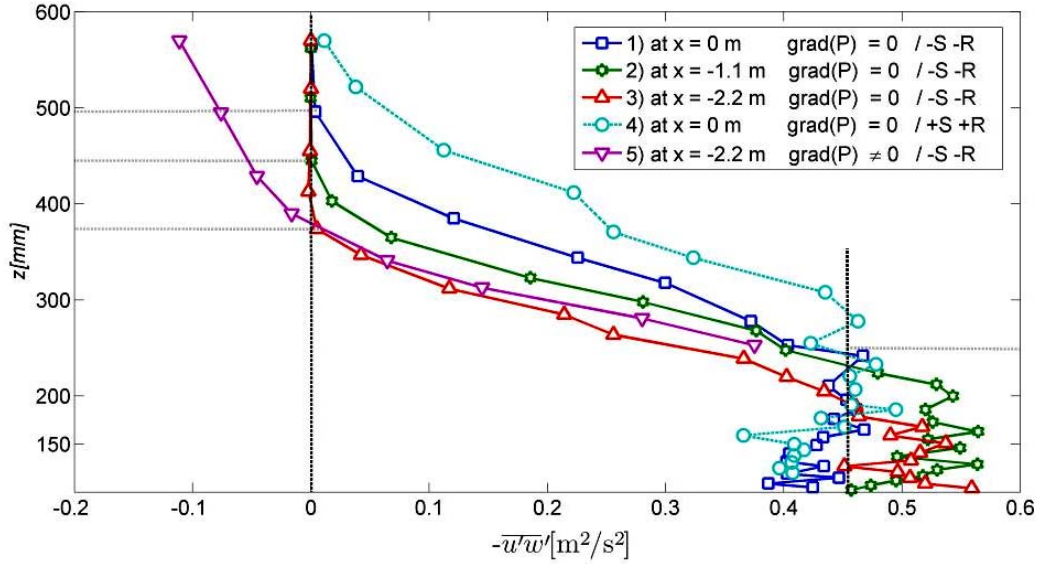

Fig. 3: Vertical shear stress velocity profiles - $u'w'$; $\overline{}$ with and without pressure gradients and with (+S +R) and without (-S -R) spires and roughness elements

4.3 Integral length scales

The integral length scales $L_u(z)$ and $L_w(z)$ shown in Fig. 4 have been calculated at five measurement positions (Fig. 2) using equation (1).

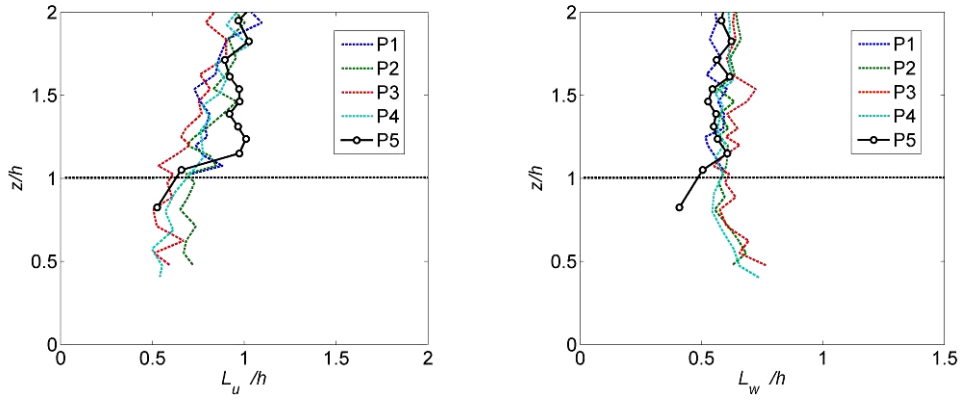

Fig. 4: Normalized integral length scale profiles $L_u(z)/h$ and $L_w(z)/h$ (h: canopy height) at positions P1-P5

A criteria for Taylor's hypothesis is that the turbulence intensity $I_u(z) = \sigma_u(z)/u(z) < 0.5$. This is fulfilled for all measurement positions P1-P5. A comparison of the measurements with literature (Raupach, 1991) shows good agreement, with $L_u/h \approx 1$ and $L_w/h \approx 0.5$ at the canopy height. A strong decrease of both $L_u(z)$ and $L_w(z)$ at z/h ≈ 1 is found at the measurement position P5 directly leeward of a plant. The plant accelerates the decay of gusts into smaller scales, which is reflected by smaller integral length scales.

4.4 The power spectral density (PSD)

The distribution of turbulent kinetic energy in the frequency domain is given by the power spectral density $S_{uu}(f)$ (Eq. (2)) which can be described by the von Karman spectrum (e.g. Gromke, 2009)

$$\frac{f\,S_{uu}(f)}{\sigma_u^2} = \frac{4\,f_n}{(1+70.78\,f_n^2)^{5/6}} \tag{3}$$

with $f_n = f\,L_u(z)/u(z)$. The normalized values of $S_{uu}(f)$ calculated from a 60 seconds HWA measurement time series (f = 20 kHz, z = 450 mm, U_δ = 15 m/s) are shown in Fig. 5. The measurement data fit the von Karman spectrum well and show the increase of the spectrum in the energy production range up to $f_n \approx 0.1$. This range contains the bulk of turbulent kinetic energy, where turbulent kinetic energy is produced by shear. In the inertial subrange, turbulent kinetic energy is neither produced nor dissipated but handed down to smaller scales and the spectrum decreases with a slope of m = -2/3 (Kaimal and Finnigan, 1994). At the high frequency end of the spectrum, turbulent kinetic energy is dissipated and converted into internal energy. This dissipation range is not described by the von Karman spectrum. The smallest structures of a turbulent flow in the dissipation range are called the Kolmogorov micro-scales. They are governed by the dissipation rate ε and the kinematic viscosity ν. The Kolmogorov time scale is defined as $\tau_k = (\nu/\varepsilon)^{1/2}$ (Wissink, 2006). In our case, τ_k can be estimated using $\nu = \nu_{air} = 1.5e^{-5}$ m^2/s and $\varepsilon \sim U^3/L$ where U and L are characteristic macroscopic velocity and length scales. The corresponding frequency $f_n^{Kolmogorov}$ is calculated by

$$f_n^{Kolmogorov} = \frac{1}{\tau_k}\frac{L_u(z)}{u(z)} \tag{4}$$

and is also shown in (Fig. 5). With U = $u(z)$ = 13.7 m/s and L ≈ δ ≈ 0.5 m, $f_n^{Kolmogorov} \approx 300$ and is within one order of magnitude with the smallest scales as seen from the measured spectrum.

5. Conclusions

The investigations show that the SLF boundary layer wind tunnel is well suited for future experiments on shear stress partitioning with living plants using Irwin sensors. The adjusted ceiling allows to produce boundary layer flows with vanishing pressure gradients resulting in sufficiently developed boundary layers in the measurement section. Spires and additional roughness elements in the fetch lead to an increased boundary layer thickness over the plant canopy. The comparison of integral length scales and power spectral densities show good agreement with established literature data.

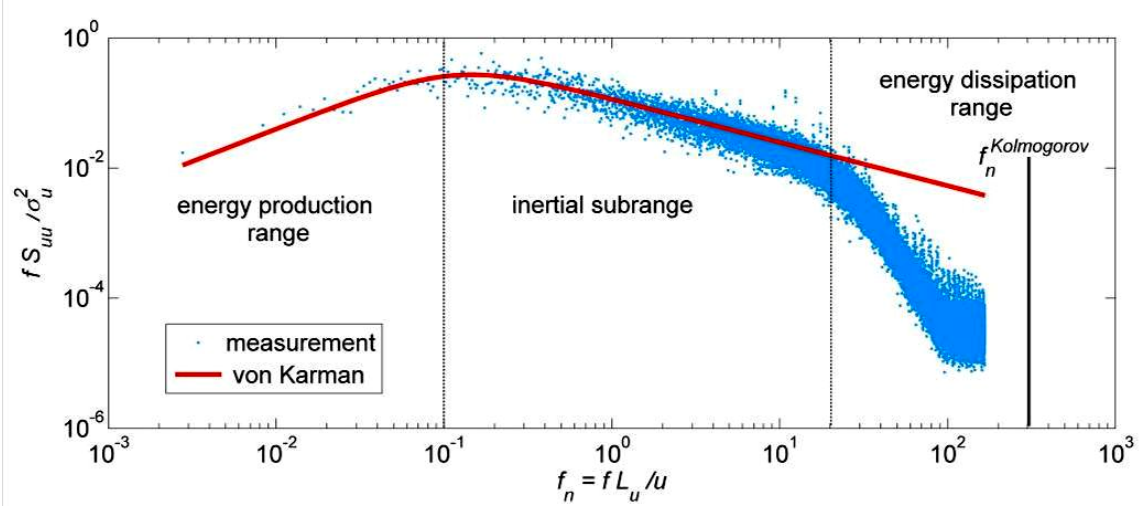

Fig. 5: Measured normalized power spectral density $S_{uu}(f)$ and von Karman spectrum given by Eq. (3)

Acknowledgement

The authors are indebted to the Vontobel Foundation and the Swiss National Science Foundation, Switzerland, for funding this research project.

References

Ambühl, D., 2004: Simulation of an atmospheric boundary layer in a wind tunnel. Term Paper, Institute of Fluid Dynamics, ETH Zürich, pp. 56.

Burri, K., Gromke, C., Graf, F., 2009: A wind tunnel study of Aeolian sediment transport and PM_{10} emission in grass canopies of different plant densities. Ber. Meteor. Inst. Univ. Freiburg No. 19, 39-44.

Clifton, A., Rüedi, J.-D., Lehning, M., 2006: Snow saltation threshold measurements in a drifting-snow wind tunnel. J. Glaciol. 52, 585-596.

Clifton, A., Manes, C., Rüedi, J.-D., Guala, M., Lehning, M., 2008: On shear driven ventilation of snow. Bound. Layer Meteorol. 126, 249-261.

Clifton, A., Lehning, M., 2008: Simulations of wind tunnel snow drift using a semi-stochastic model. Earth. Surf. Process. Landforms 33/14, 2156-2173.

Gromke, C., Ruck, B., 2005: Die Simulation atmosphärischer Grenzschichten in Windkanälen, 13. GALA Fachtagung, Cottbus, Germany, 51-1 - 51-8.

Gromke, C., 2009: Einfluss von Bäumen auf die Durchlüftung von innerstädischen Strassenschluchten. Dissertation, Institut für Hydromechanik, Universität Karlsruhe, pp. 142.

Guala, M., Manes, C., Clifton, A., Lehning, M., 2008: On the saltation of fresh snow in a wind tunnel: profile characterization and single particle statistics. J. Geophys. Res., F03024 pp.113.

Kaimal, J.C., Finnigan, J.J., 1994: Atmospheric boundary layer flows - their structure and measurements. Oxford University Press, pp. 289.

Raupach, M. R., 1991: Rough-wall turbulent boundary layers. Appl. Mech. Rev. 44, pp. 25.

Stull, R. B., 1988: An introduction to boundary layer meteorology. Kluwer Academic Publishers, Boston, pp. 666.

Wissink, J. G., 2006: Large eddy simulation in fluid mechanics. Lectural notes, Institute for Hydromechanics, University of Karlsruhe (KIT), Germany, pp. 49.

Authors' address:

Benjamin Walter (walter@slf.ch)
Christof Gromke (gromke@slf.ch)
Michael Lehning (lehning@slf.ch)
WSL Institute for Snow and Avalanche Research SLF
Flüelastrasse 11, CH-7260 Davos, Switzerland

A wind tunnel study of aeolian sediment transport and PM_{10} emission in grass canopies of different planting densities

Katrin Burri[1,2], Christof Gromke[1], Frank Graf[1]

[1]WSL Institute for Snow and Avalanche Research SLF, CH-7260 Davos Dorf, Switzerland
[2]ETH Zurich, Institute for Integrative Biology IBZ, CH-8092 Zurich, Switzerland

Abstract

In this study, wind tunnel experiments were performed with the grass species *Lolium perenne* planted in quartz sand. Sediment transport and PM_{10} emission were studied in four levels of canopy density with nominal plant coverages C_v = 55%, 15%, 3% and 0% and corresponding frontal area indices λ = 0.42, 0.11, 0.02 and 0, respectively. Both total sediment mass flux and PM_{10} emission decreased approximately exponentially with increasing plant cover. It was also found that vegetation profoundly changed the characteristics of vertical sediment flux profiles, with decreasing flux fractions near the ground in denser plant canopies. Spatial and temporal information on typical erosion and deposition patterns within the plant canopies were gained by using coloured quartz sand. The normalised friction velocities (u_*/U_δ) showed a maximum for medium values of λ, indicating a change from the wake interference to the skimming flow regime.

1. Introduction

World wide, wind erosion and desertification are most alarming processes of environmental degradation. Not only do they cause tremendous losses of fertile soil, but they also seriously affect human health. Pulmonary tuberculosis (silicosis) is one of the major diseases that have been linked to mineral fine dust (PM_{10}) in the atmosphere (Griffin *et al.* 2001). It is widely accepted that the re-establishment of an intact vegetation cover is the most effective measure against wind erosion. However, despite numerous investigations, the mechanisms responsible for the protective effect of vegetation are still not completely understood. Since the phenomenon involves multiple interactions between soil, plants and atmosphere, it is particularly difficult to quantify the efficiency of vegetation in reducing wind erosion. As an alternative to field investigations, wind tunnel experiments offer the advantage to control specific parameters within this complex system.

The innovative part of the present wind tunnel experiments is the use of living plants instead of artificial imitations or dead plant parts. Although imitations of vegetation have become more and more sophisticated, they do not behave like real plants. Up to now, most investigations addressing vegetation aspects have been performed with cylindrical obstacles or other artificial substitutes to mimic plants (e.g. Raupach *et al.* 1980, Musick *et al.* 1996, Poggi *et al.* 2004, Zhu *et al.* 2007). In this study, wind tunnel experiments were performed with living grass tussocks of *Lolium perenne*, including measurements of sediment transport and PM_{10} emission in four levels of canopy density.

2. Experimental setup and measurement techniques

The experiments were performed in the suction-type wind tunnel of the WSL Institute for Snow and Avalanche Research SLF in Switzerland (Clifton *et al.* 2006, Walter *et al.* 2009). For providing a vegetated surface in the wind tunnel, eight trays (1 x 1 m^2) were planted with *Lolium perenne* and aligned in the 8 m test section of the wind tunnel (Fig. 1). To create a readily erodible surface, a 1 cm thick layer of quartz sand (grain sizes 0.4 – 0.8 mm) was placed on top of the planted soil. The third and fifth tray downstream was filled with red and blue quartz sand, respectively, for gaining information on typical erosion and deposition patterns within the plant canopies.

Four levels of vegetation cover were tested, including 0, 5, 24 and 91 tussocks of *Lolium perenne* per square meter (Table 1). The distribution of the plants followed the same pattern of staggered rows in all the experiments to exclude effects of different arrangements. The mean height of the grass tussocks was approximately 10 cm.

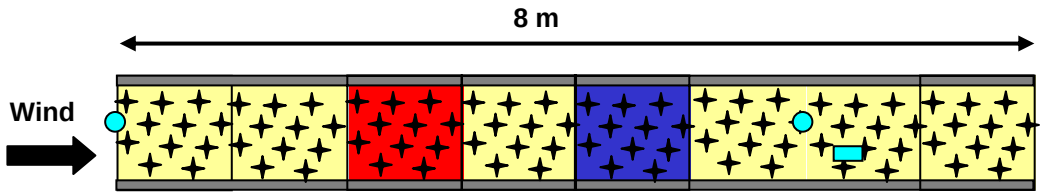

Fig. 1: Schematic of the wind tunnel test section, ○ = inlet nozzles of PM_{10} aerosol monitors. ▭ = sediment sampler

Table 1: Experimental conditions of the wind tunnel experiments with differently dense planted and bare sand

Frontal area index λ	**0.00**			**0.02**		**0.11**	**0.42**
Horizontal vegetation cover C_v [%]	0	0	0	3	3	15	55
Planting density [plants / m^2]	0	0	0	5	5	24	91
Mean friction velocity u_* [m/s]	0.6	0.6	0.6	0.7	0.7	1.0	0.8
Duration of erosive event [s]	120	124	124	256	174	610	7224
Air temperature [°C]	-6.6	-6.4	-2.5	12.2	7.3	7.4	9.9
Relative air humidity [%]	81.7	84.4	77.6	58.1	81.3	68.3	54.5
Specific air humidity [g/kg]	2.3	2.4	3.0	6.2	6.2	5.2	4.9
Relative humidity of sand pore air [%]	89.8	70.2	80.2	81.1	92.0	84.9	82.5
Matric potential of the sand [MPa]	-34.0	-45.0	-27.7	-27.8	-10.8	-21.4	-25.1

For measuring aeolian sediment flux, a modified WITSEG sampler was used (Dong *et al.* 2004). With 60 collecting boxes, each of 1 cm height, the sampler allowed measuring the vertical profile of aeolian sediment transport. PM_{10} concentrations were measured with two aerosol monitors (TSI DustTrak^{TM} 8520) at the beginning and the end of the test section, respectively. Thus, the difference between the two measurements could be attributed to the PM_{10} emitted from the test section. Capacitive relative humidity sensors (SHT11, Sensirion AG) were used for controlling the humidity of the sand layer and the air. During experiments, image sequences were taken through the perspex roof of the wind tunnel for getting information on the temporal development of erosion and deposition processes.

2-D hot-wire anemometry was applied to measure turbulent and mean flow properties above and within the grass canopies. These measurements were done once for each level of vegetation density at a wind speed below the sediment transport threshold.

3. Results and discussion

3.1 Wind speed profiles

The vertical profile of the horizontal mean wind velocity U(z) over the unplanted sand surface indicated a boundary layer thickness of approximately 28 cm (Fig. 2, left). With increasing vegetation cover, the boundary layer increased up to 40 cm. The vertical profiles of shear stress velocity $\left(\overline{-u'w'}\right)^{1/2} = (\tau_t(z)/\rho)^{1/2}$ showed that the inertial sublayer, identified by constant shear stress velocities (herein referred to as friction velocity u_*), was progressively higher with increasing vegetation cover, indicating an increase of the roughness sublayer thickness (Fig. 2, right).

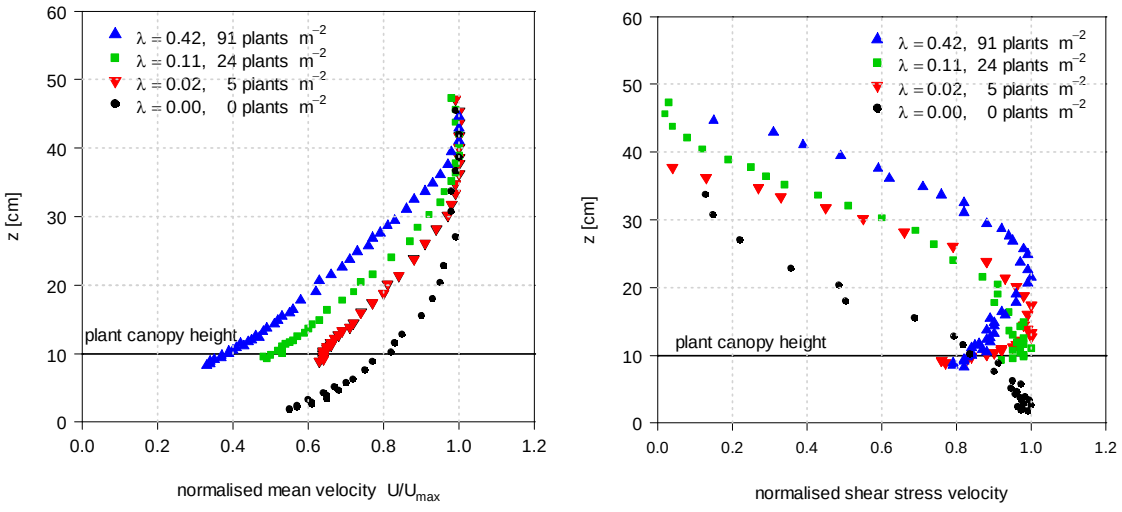

Fig. 2: Vertical profiles of normalised mean wind velocity U (left) and shear stress velocity $\left(\overline{-u'w'}\right)^{1/2} = (\tau_t(z)/\rho)^{1/2}$ (right), each profile corresponds to a single measurement series at a wind speed below the sediment transport threshold

A linear relationship was found between the shear stress velocities just above the plant canopies and the free stream velocity U_δ (Fig. 3, left). The normalised friction velocities (u_*/U_δ) showed a maximum λ (0.06) for medium values of the frontal area index (0.11), indicating a change from the wake interference flow to the skimming flow regime (Fig. 3, right).

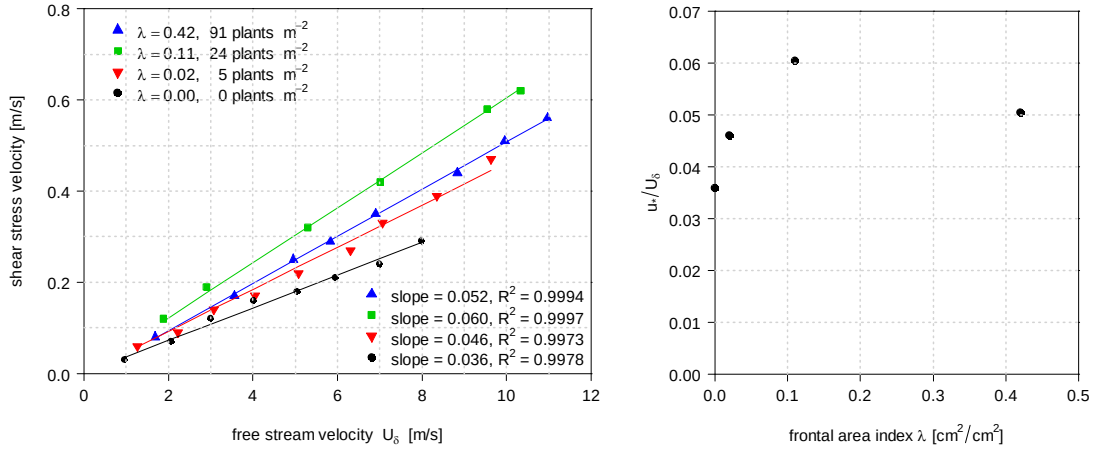

Fig. 3: Shear stress velocities vs. free stream velocity U_δ (left); for each level of canopy density, shear stress velocities were measured just above the plant canopies at various free stream velocities; normalised friction velocities (u_*/U_δ) vs. frontal area index λ (right)

3.2 Sediment transport and PM_{10} emission

Both total sediment flux and PM_{10} emission decreased approximately exponentially with increasing plant cover (Fig. 4, left), which is in accordance with wind erosion field studies (Lancaster & Baas 1998, Allgaier 2008).

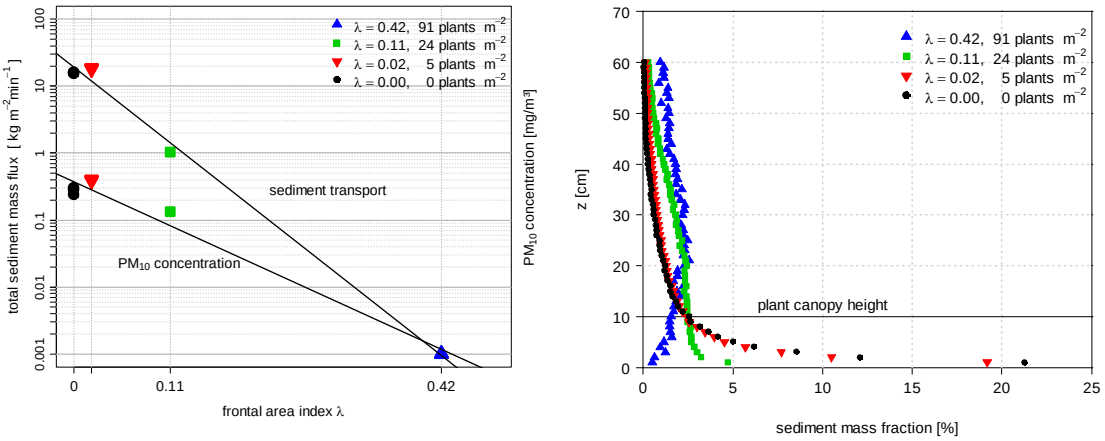

Fig. 4: Total sediment mass flux and PM_{10} emission (left); vertical profiles of sediment mass fraction (right)

Compared to the unplanted control, a vegetation coverage C_v of only 15% reduced the total sediment mass flux and PM_{10} by a factor of 15 and 2, respectively. Both processes were reduced to virtually zero with a vegetation coverage C_v = 55 %. However, in the very sparse grass canopy with C_v = 3%, sediment transport and PM_{10} emission tended to be slightly higher than in the unplanted control. This is attributed to the development of vortical structures in the lee of the tussocks (Logie 1982, Sutton & McKenna Neuman 2008) and to the triggering of erosion by oscillating movements of grass halms on the sand surface. It was also found that vegetation profoundly changed the characteristics of vertical sediment flux profiles, with decreasing flux fractions near the ground in denser plant canopies (Fig. 4, right).

3.3 Erosion and deposition patterns

The approach of using coloured quartz sand proofed useful for visualizing characteristic erosion and deposition patterns around plants as well as ripple formation (Fig. 5). Detailed image analysis is planned for gaining spatial and temporal information on the observed erosion and deposition processes.

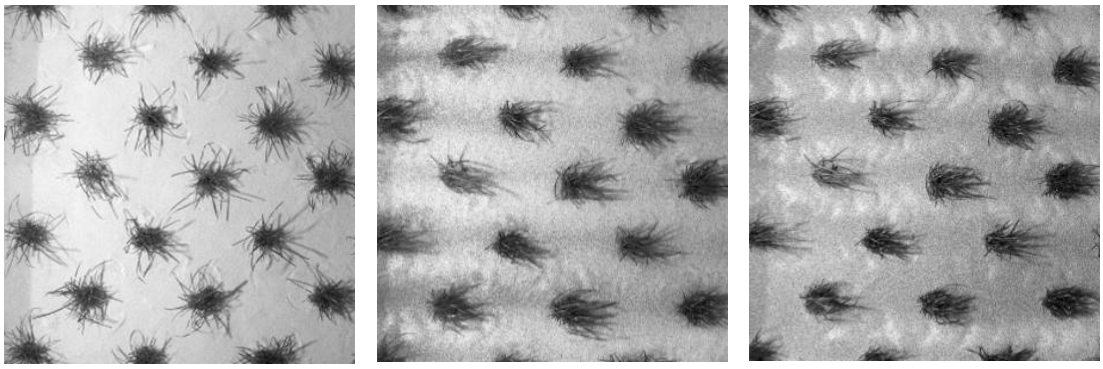

Fig. 5: Three frames from an image sequence captured through the perspex roof of the wind tunnel; dark (red) sand is invading from upstream (left)

4. Conclusions

The novelty of the present wind tunnel study was the use of living plants instead of artificial imitations. Results showed that even relatively sparse plant canopies provided substantial protection against wind erosion. For plant coverage C_V = 15% (λ = 0.11), the total sediment mass flux and PM_{10} emission rate were reduced to 7% and 50%, respectively, in comparison to the unplanted control. Increasing the plant coverage to C_V = 55% (λ = 0.42) resulted in negligible sediment mass transport and PM_{10} emission rates.

Living plants in wind tunnel experiments allow to studying aspects of biological wind erosion control which are not observable when using artificial roughness elements. They therefore provide additional information with regard to modelling and controlling wind erosion processes.

References

Allgaier, A., 2008: Aeolian Sand Transport and Vegetation Cover. In: Breckle SW et al. (eds.) Arid Dune Ecosystems. Ecological Studies 200, Springer-Verlag Berlin, Heidelberg.

Clifton, A., Rüedi, J.D., Lehning, M., 2006: Snow saltation threshold measurements in a drifting-snow wind tunnel. Journal of Glaciology 179, 585-596.

Dong, Z., Sun, H., Zhao, A., 2004: WITSEG sampler: a segmented sand sampler for wind tunnel test. Geomorphology 59, 119-129.

Griffin, D.W., Kellog, C.A., Shinn, E.A., 2001: Dust in the wind: Long range transport of dust in the atmosphere and its implications for global public and ecosystems health. Global Change Human Health 2, 20-33.

Lancaster, N., Baas, A., 1998: Influence of vegetation cover on sand transport by wind: Field studies at Owens Lake, California. Earth Surface Processes and Landforms 23, 69-82.

Logie, M., 1982: Influence of roughness elements and soil moisture of sand to wind erosion. Catena Supplement, 1, 161-173.

Musick, H.B., Trujillo, S.M., Truman, C.R., 1996: Wind-tunnel modelling of the influence of vegetation structure on saltation threshold. Earth Surface Processes and Landforms 21, 589-605.

Poggi, D., Porporato, A., Ridolfi, L., Albertson, J.D., Katul, G.G., 2004: The effect of vegetation density on canopy sub-layer turbulence. Boundary-Layer Meteorology 111, 565-587.

Raupach, M.R., Thom, A.S., Edwards, I., 1980: A wind-tunnel study of turbulent flow close to regularly arrayed rough surfaces. Boundary-Layer Meteorology 18, 373-397.

Sutton, S.L.F., McKenna Neuman, C., 2008: Sediment entrainment to the lee of roughness elements: Effects of vertical structures. Journal of Geophysical Research 113, F02S09, doi:10.1029/2007JF000783.

Walter, B., Gromke, C., Lehning, M., 2009: The SLF boundary-layer wind tunnel - an experimental facility for aerodynamical investigations on living plants. Ber. Meteor. Inst. Univ. Freiburg No. 19, 31-37.

Zhu, W., van Hout, R., Katz, J., 2007: On the flow structure and turbulence during sweep and ejection events in a wind-tunnel model canopy. Boundary-Layer Meteorology 124, 205-233.

Authors' address:

Katrin Burri (burri@slf.ch)
Dr. Frank Graf (graf@slf.ch)
Dr. Christof Gromke (gromke@slf.ch)
WSL Institute for Snow and Avalanche Research SLF
Flüelastrasse 11, CH-7260 Davos Dorf (Switzerland)

Implications of tree planting on pollutant dispersion in street canyons

Christof Gromke[1,2], Bodo Ruck[2]

[1]WSL Institute for Snow and Avalanche Research SLF, Davos, Switzerland
[2]Institute for Hydromechanics IfH, University of Karlsruhe, Germany

Abstract

Traffic pollutant dispersion processes inside urban street canyons with avenue-like tree planting have been studied in wind tunnel experiments. Tree planting of different crown porosities and their effects on the pollutant concentrations at the canyon walls have been investigated for wind approaching perpendicular to the street axis. The results show that avenue-like tree planting in street canyons lead to overall increases in traffic originated pollutant concentrations in comparison to the tree-free reference case. Maximum increases in concentrations of 80 % have been measured at the building walls in the street canyon central part where the dispersion processes are affected strongest by tree planting.

1. Introduction

Traffic emissions generally dominate air quality issues in urban areas. Critical situations arise in dense built-up inner city areas which are formed by urban street canyons suffering from limited ambient air exchange and high pollutant concentrations. Vegetation inside urban street canyons even complicates the situation, since it affects the prevailing flow field and, therefore, pollutant dispersion and exchange processes. In particular, in the case of avenue-like tree planting where the lower and the upper street level parts are separated by a tree crown layer, the air exchange with the above roof wind is hindered.

In the present study, wind tunnel measurements of traffic-originated pollutant concentrations and dispersion processes in urban street canyons with trees are presented. Implications of two-rowed avenue-like tree planting with different crown porosities on pollutant concentrations inside an urban street canyon are discussed, complementing the investigations with single-rowed planting documented in Gromke and Ruck (2007), Gromke et al. (2008), Gromke (2009), Gromke and Ruck (2009a), Gromke and Ruck (2009b) and Balczó et al. (2009). Moreover, a new and promising method has been established for the small scale modeling of trees for the purpose of wind tunnel studies. Special emphasis is laid on the description of this method and its justification/verification by fluid dynamical similarity considerations.

2. Street canyon setup, measurement techniques and boundary layer simulation

The wind tunnel experiments have been performed in a model street canyon of scale M=1:300. A canyon of length L to building height H ratio L/H=10 and street width W to building height H ratio W/H=2 with typical two-rowed avenue-like tree planting has been investigated (Fig. 1). The release of traffic exhausts was realized by four tracer gas (sulphur hexafluoride SF_6) emitting line sources embedded in the street ground.

Electron Capture Detection (ECD) has been used to analyze the air/tracer gas mixtures which have been sampled inside the street canyon at positions y/H=0.04 in front of the canyon walls. The resulting concentrations have been normalized according to

$$c^{+} = \frac{c\, u_H\, H}{Q_T/l} \tag{1}$$

with c the measured concentration, u_H the velocity of the undisturbed flow at building height H and Q_T/l the tracer gas source strength per unit length.

A typical urban atmospheric boundary layer flow with power law exponents of α=0.30 for the mean velocity profile and α_I=-0.36 for the turbulence intensity profile, approaching perpendicular to the canyon length axis, has been generated in the wind tunnel (Gromke and Ruck, 2005). Experimental studies with parallel and inclined approaching flow directions can be found in CODASC (2008) and in Gromke (2009). The Reynolds number Re, based on the building height H and the velocity u_H, is equal to 37.000 and ensures a Reynolds number independent flow field.

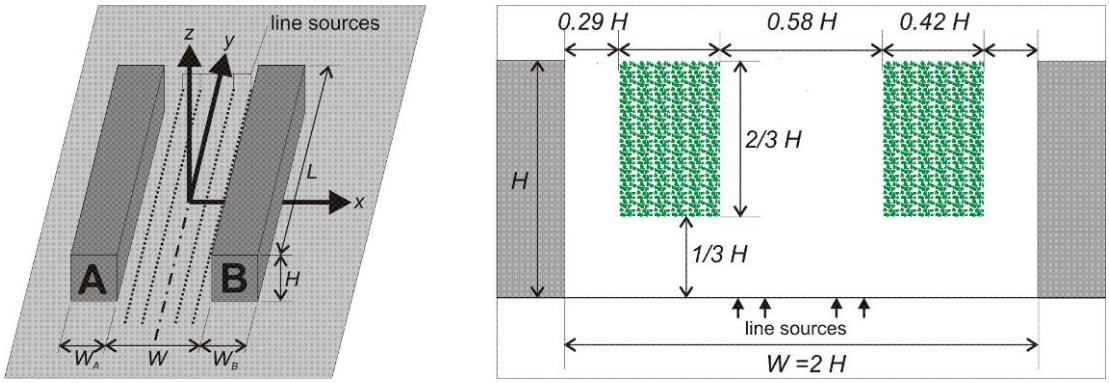

Fig. 1: Street canyon geometry and tree planting arrangement (W_A=W_B=H)

3. Small scale modeling of trees and similarity criterion

Trees, more precisely tree crowns, are porous objects and permeable to air flow. Flows past porous objects differ crucially from flows past non-porous counterpart objects. Characteristic differences can be found in the drag and in the wakes. Due to large volume specific surfaces of porous objects, skin friction becomes important. It can no longer be neglected as with non-porous objects, where the pressure difference on the windward and leeward side dominates the drag. Furthermore, wakes of porous objects extend further downstream and the leeward recirculation zone is often detached (Gromke and Ruck, 2008). In summary: due to their porosity, tree crowns show unique aerodynamic properties in comparison to non-porous bodies which have to be accounted for in wind tunnel.

As stated above, a new method has been developed for the small scale modeling of trees. The modeling of porous tree crowns has been realized using custom-made lattice cages constituting cubes with cross-sections of 0.42 H width and 0.67 H height (Fig. 2). These lattice cages have been aligned symmetrically along the street axis with the top facing the roof level. Spanning the street canyon of length L, the cages have been divided into 31 cells of 0.32 H depth each. A filament/fiber-like synthetic wadding material has been used to fill the cells, whose purpose was simply to facilitate a uniform distribution of the wadding material throughout the entire length of the lattice cage, see

also Gromke and Ruck (2009b). Different crown porosities/permeabilities have been realized by filling all the cells homogeneously with defined masses of wadding material. Pore volume fractions of P_{Vol}=97.5 % (herein referred to as high crown porosity) and P_{Vol}=96 % (herein referred to as low crown porosity), typical for crown porosities of deciduous trees have been modeled (Ruck and Schmidt, 1986; Gross, 1987). By filling each cell with the wadding material, avenue-like tree planting of high stand densities with interfering neighboring tree crowns have been modeled (ρ=1). In the same way, tree planting of lower stand densities with free space in-between can be realized by filling only every second, every third, and so forth, cage cell (corresponding to ρ=0.5, ρ=0.33, etc.) However, in the present paper, tree planting of high stand density (ρ=1) with interfering crowns are treated exclusively. Measurement results obtained with tree planting of lower stand density can be found in CODASC (2008) and in Gromke (2009).

The aerodynamic characteristics of the model trees are not sufficiently and definitely determined by their crown porosities. In fact, the internal crown structure, i.e. the pore size distribution, the arrangement and form of the crown constituting material and its surface properties are also important. In order to account for all these factors, the pressure loss coefficient λ [m^{-1}] has been determined for wadding material samples with pore volume fractions of P_{Vol}=97.5 % (high crown porosity) and P_{Vol}=96 % (low crown porosity) in forced convection conditions, according to

$$\lambda = \frac{\Delta p_{stat}}{p_{dyn}\, d} = \frac{p_{windward} - p_{leeward}}{(1/2)\, \rho u^2 d} \tag{2}$$

with Δp_{stat} the difference in static pressure windward and leeward of the porous sample in forced convection conditions, p_{dyn} the dynamic pressure, u the mean stream velocity and d the porous sample thickness in streamwise direction. Measurements resulted in pressure loss coefficients of λ=80 m^{-1} and λ=200 m^{-1} for the model tree crowns of high (P_{Vol}=97.5 %) and low (P_{Vol}=96 %) porosity, respectively.

In order to justify the chosen modeling approach and to base it on a scientific sound foundation, a fluid dynamical similarity consideration is needed. Pressure loss coefficients λ of artificially arranged natural vegetation elements simulating wind shelter belts have been determined by Grunert et al. (1984). Their measurements resulted in pressure loss coefficients $\lambda_{full\ scale}$ ranging from 0.4 m^{-1} to 13.4 m^{-1} with the majority lying in the range of 1.0 $m^{-1} < \lambda_{full\ scale} < 3.0\ m^{-1}$.

The derivation of similarity criterion is based on energy considerations and expressed by the postulation that the normalized pressure losses (normalized by the dynamic pressure p_{dyn}) have to be equal in full scale (nature) and small scale, i.e.

$$[\Delta p / p_{dyn}]_{full\ scale} = [\Delta p / p_{dyn}]_{small\ scale} \tag{3}$$

which, with Eq. (2), yields to

$$\frac{\lambda_{full\ scale}}{\lambda_{small\ scale}} = \frac{d_{small\ scale}}{d_{full\ scale}} = M\,. \tag{4}$$

In words: The ratio of the pressure loss coefficients has to be equal to the model scaling factor M (here M=1:300). Calculating the required small scale pressure loss coefficients $\lambda_{small\ scale}$ is now straightforward and using the values found by Grunert et al. (1984), one

obtains 120 $m^{-1} < \lambda_{small\ scale} < 4000\ m^{-1}$ whereas the great majority lies in the range of 300 $m^{-1} < \lambda_{small\ scale} < 900\ m^{-1}$.

Thus, the realized pressure loss coefficients of the high (λ=80 m^{-1}, P_{Vol}=97.5 %) and low (λ=200 m^{-1}, P_{Vol}=96 %) porosity model tree crowns match the lower limit of Grunert's down-scaled values. However, it has to be noted that the vegetation structures investigated by Grunert et al. (1984) appear, from visual impression, to be quite dense compared to usual tree crowns. Based on preceding wind tunnel experiments and on the concentration measurements (Gromke and Ruck, 2009b), it was concluded that the model trees realistically simulate the aerodynamic characteristics of full scale trees and their implications on the flow field.

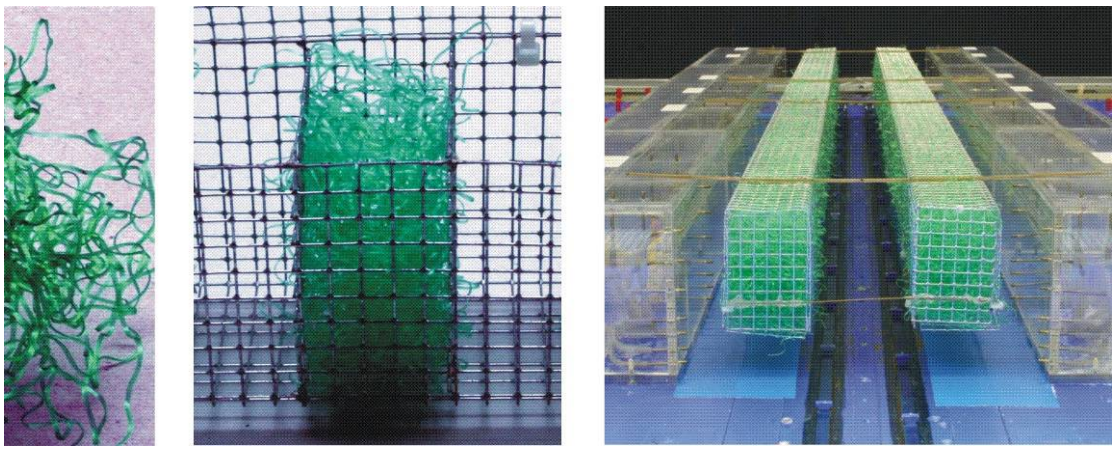

Fig. 2: Filament/fiber-like wadding material; wadding material incorporated in single cage cell; street canyon with two-rowed avenue-like tree planting (W/H=2)

4. Results and discussion

4.1 Street canyon W/H=2 without tree planting

As a reference, traffic pollutant dispersion in a tree-free street canyon is discussed initially. Fig. 3 shows that the pollutant charge close at the leeward wall A is considerable higher than at the windward wall B. This phenomenon is due to the prevailing canyon vortex which transports the near street level released traffic pollutants to wall A before they are diluted by vertical air exchange at the roof level. Towards the street canyon ends, the influence of the corner eddies becomes visible. These large scale vortex structures serve for additional lateral air exchange and thus to the steady concentration decrease when approaching the street canyon ends.

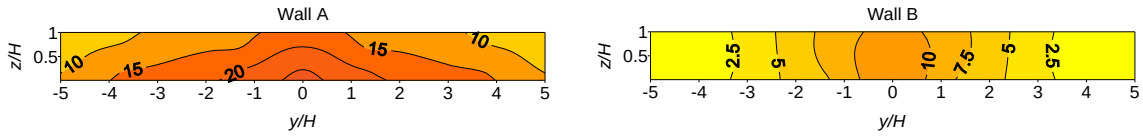

Fig. 3: Normalized pollutant concentrations [-] close to the walls A and B of the tree-free street canyon (reference case)

4.2 Street canyon W/H=2 with tree planting of high crown porosity (P_{Vol}=97.5 %)

For the street canyon with tree planting of high crown porosity, increases in concentrations at the leeward wall A and decreases at the windward wall B (Fig. 4) are found in comparison to the tree-free reference case (Fig. 3). The relative increases in the canyon central part of wall A are about 60 %, whereas the relative decreases in the central part of wall B are about 30 %. Calculating the wall average concentration changes yields a relative increase of 40 % at wall A and a decrease of 25 % at wall B. In summary, it remains an average relative increase in concentrations at the canyon walls of 23 % for the street canyon with tree planting. This is attributed to the blocking of the laterally entering corner eddies by the tree crowns at the canyon outer parts and to reduced ventilation of the gap between the upstream oriented planting and the leeward wall A.

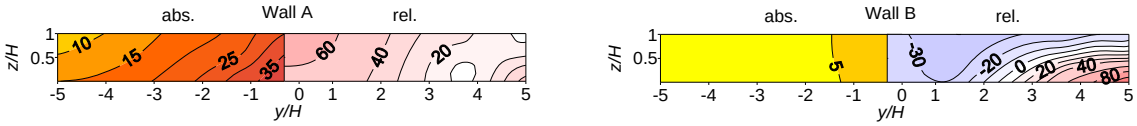

Fig. 4: Normalized pollutant concentrations [-] in the street canyon with tree planting of high crown porosity (P_{Vol}=97.5%) and relative deviations in concentrations [%] related to the reference case of the tree-free street canyon (Fig. 3)

4.3 Street canyon W/H=2 with tree planting of low crown porosity (P_{Vol}=96 %)

In the case of lower crown porosity (P_{Vol}=96 %), the overall pollutant concentration pattern (Fig. 5) is similar to that found for the high crown porosity tree planting shown in Fig. 4. The major difference is that the changes relative to the tree-free reference case are slightly stronger pronounced with increased maximum pollutant concentrations at the pedestrian level near the central part of wall A. Concentration increases at wall A of maximum 80 % in the canyon central part and in average of 41 % and decreases at wall B of maximum 40 % and in average of 32 % are found, resulting in an overall increase in wall near pollutant concentrations of 22 %.

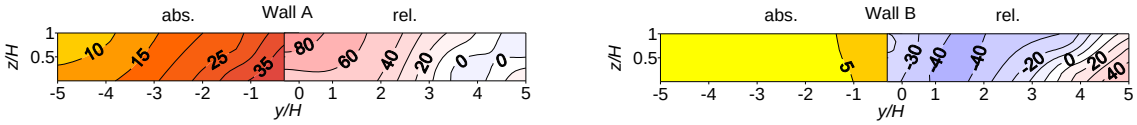

Fig. 5: Normalized pollutant concentrations [-] in the street canyon with tree planting of low crown porosity (P_{Vol}=96%) and relative deviations in concentrations [%] related to the reference case of the tree-free street canyon (Fig. 3)

5. Conclusions

Avenue-like tree planting in street canyons leads to overall higher traffic-originated pollutant concentrations in comparison to the tree-free reference case. In particular, higher pollutant concentrations at the leeward wall A and lower concentrations at the windward wall B were found for flow approaching perpendicular to the street canyon axis. These effects are stronger pronounced the lower the tree crown porosity is. Maxi-

mum relative increases in pollutant concentration of 41 % for the wall average and of 80 % for localized spots in the canyon central part have been found in the presence of the tree planting with low crown porosity (P_{Vol}=96 %). These results clearly show that the impact of avenue-like tree planting on pollutant dispersion and concentration inside urban street canyons have to be considered carefully. The reduced street canyon ventilation performance may result in critical exceedances of pollutant concentration limits and cause hazardous conditions for the residents. It is recommended to design avenue-like tree planting of low planting density and to employ tree species of high crown porosity (correlating with high permeability), in order to avoid high traffic-originated pollutant concentrations and hazardous conditions.

Acknowledgments

The authors are indebted to the Deutsche Forschungsgemeinschaft DFG for financial support (grant Ru 345/28).

References

Balczó, M., Gromke, C., Ruck, B., 2009: Numerical modeling of flow and pollutant dispersion in street canyons with tree planting. Meteorologische Zeitschrift 18, 197-206.

CODASC, 2008: Concentration data of street canyons. Internet data base, www.codasc.de.

Gromke, C., Ruck, B., 2005: Die Simulation atmosphärischer Grenzschichten in Windkanälen. Proc. 13. GALA Fachtagung "Lasermethoden in der Strömungsmesstechnik", 51/1-51/8.

Gromke, C., Ruck, B., 2007: Influence of trees on the dispersion of pollutants in an urban street canyon - Experimental investigation of the flow and concentration field. Atmospheric Environment 41, 3287-3302.

Gromke, C., Ruck, B., 2008: Aerodynamic modeling of trees for small scale wind tunnel studies. Forestry 81, 243-258.

Gromke, C., Buccolieri, R., Di Sabatino, S., Ruck, B., 2008: Dispersion modeling study in a street canyon with tree planting by means of wind tunnel and numerical investigations - Evaluation of CFD data with experimental data. Atmospheric Environment 42, 8640-8650.

Gromke, C., Ruck, B., 2009a: Effects of trees on the dilution of vehicle exhaust emissions in urban street canyons. International Journal of Environment and Waste Management 4, 225-242.

Gromke, C., Ruck, B., 2009b: On the impact of trees on dispersion processes of traffic emissions in street canyons. Boundary-Layer Meteorology 131, 19-34.

Gromke, C., 2009: Einfluss von Bäumen auf die Durchlüftung von innerstädtischen Straßenschluchten. Dissertationsreihe am Institut für Hydromechanik IfH der Universität Karlsruhe (TH), Heft 2008/2, Karlsruhe 2009.

Gross, G., 1987: A numerical study of the air flow within and around a single tree. Boundary Layer Meteorology, 40, 311-327.

Grunert, F., Benndorf, D., Klingbeil, K., 1984: Neuere Ergebnisse zum Aufbau von Schutzpflanzungen. Beiträge für die Forstwissenschaft 18, 108-115.

Ruck, B., Schmidt, F., 1986: Das Strömungsfeld der Einzelbaumumströmung. Forstwissenschaftliches Centralblatt 105, 178-196.

Authors' addresses:

Dr. Christof Gromke (gromke@slf.ch)
WSL Institute for Snow and Avalanche Research SLF
Flueelastr. 11, CH-7260 Davos-Dorf, Switzerland

Prof. Dr. Bodo Ruck (ruck@uka.de)
Institute for Hydromechanics, University of Karlsruhe
Kaiserstr. 12, D-76128 Karlsruhe, Germany

Turbulent structure behind tree

Motoki Kakizaki[1], Mikio Takahashi[1], Hitoshi Ishikawa[2], Shunsuke Yamada[2]

[1]Division of Mechanical Engineering, Tokyo University of Science, Japan
[2]Department of Mechanical Engineering, Tokyo University of Science, Japan

Abstract

The purpose of this study is to investigate the turbulent flow structure behind a tree as basic research of windbreak forests. An actual living tree was used as the test specimen in a wind tunnel experiment. The turbulent wake structure behind the tree was experimentally measured by an X-type hot wire probe that allows the meaurement of two velocity components. We used a young "*Cupressus Macrocarpa*" tree which is an evergreen with needle-shaped leaves. The main flow velocity U_∞ was 10 m/s, which is approximately the velocity of a natural calm wind. The Reynolds number, based on U_∞ and the maximum crown width d of the living tree, was 5.6×10^4. It was found that the flow structure in the wake of the tree has strong downwash flow from the crown part of the tree. In the downstream region, the flow moves toward the center of the wake.

1. Introduction

Wind damages, such as fallen trees and wind-blown sand, has been a serious problem for a long time in many countries. For example, in Japan, typhoon Man-yi in 2007 caused an estimated at 600 million dollars of damage in farming, forestry and the fishery industry. In addition, the fallen trees lead to collapsed buildings and heavily congested traffic.

One solution to prevent wind damage is planting windbreak forests. However, the mechanism of wind protection of trees is not well known. At present, the distance of each tree in a tree planting is decided not by fluid dynamics but by empirical rules, which is based on the growth rate and branch spread of the trees. The study of windbreak forests has typically been done using wind-tunnel experiments. Torita (1997) found that, 50-70% of density was more effective for protecting a broad area from the strong wind. In his research of windbreak hedges is 30, 50 and 100% density. Other report is that 50% density provided the best storm protection.

Although shelter density, distance of neighboring trees, has been discussed, the turbulent structure behind a tree has not been thoroughly studied for its effect on the windbreak forests. The purpose of this study is to investigate the turbulent flow structure behind a tree as basic research to prevent wind damage in windbreak forests. An actual living tree was used as the test specimen in a wind tunnel experiment. The turbulent structure behind the tree was experimentally measured with an X-type hot wire probe that allows the measurement of two velocity components.

2. Experimental setup

Experimental setup is shown in Fig.1. The experiment was carried out in a blow-up type wind tunnel with a working section 250 mm high and 250 mm wide. One primary advantage of our study is the use of actual living trees as test specimens. Actual living

trees have features that are impossible to recreate with an artificial tree model. These features include the flow permeability of branches and leaves, the flexibility of the trunk and branches and the ability to sway in the downstream direction. As our specimen, we used a young "*Cupressus Macrocarpa*" tree, which is an evergreen with needle-shaped leaves (Fig. 2). The reason for using the cupressus is that its leaf shape is similar to this type of tree is planted in windbreak forests in Japan. The height of the tree specimen is about 170 mm. The section of the tree with branches and leaves is called the "crown" of the tree. In our experiment, the maximum crown width d is about 80 mm.

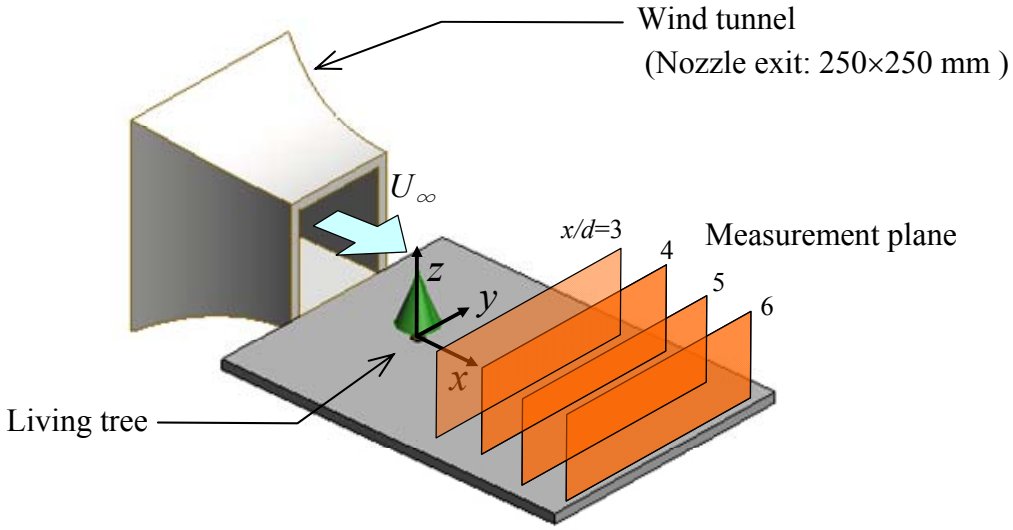

Fig. 1: Experimental setup

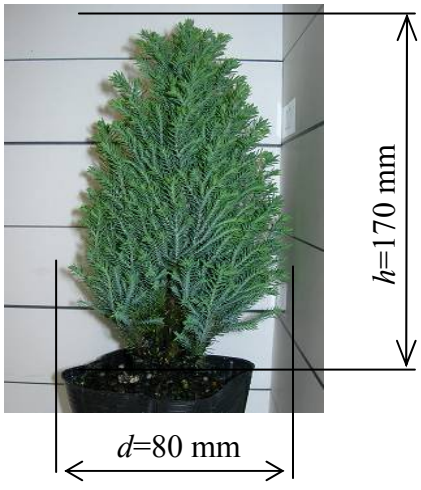

Fig. 2: Test specimen: a living tree (*Cupressus Macrocarpa*) with needle-shaped leaves

The coordinate origin is set at the soil line of the living tree. The x axis is in the direction of the main flow, the y axis is at a right angle to the x axis and the z axis is the height direction of the tree. Flow velocity components u, v and w for each x, y and z direction in the wake of the tree were measured by an X-type hot wire probe in the measurement plane x/d = 3,4,5 and 6. Main flow velocity U_∞ was 10 m/s, which is approximately the velocity of a natural calm wind. The Reynolds number, based on U_∞ and the maximum crown width d of the living tree, was 5.6×10^4.

3. Results

First, we focus on velocity profiles v and w behind the tree (Fig. 3). The velocity profile just behind the tree shows complex and nonaxisymmetric distributions, because the growth conditions of the tree, such as the length of branches and density of leaves, are also complex. As the flow goes downstream, the v component, which the flow goes towards the center of the wake increases; hence, a reverse flow region is closed at x/d=4. This occurs because of the turbulent structure, Karman vortex street shedding from the tree, is influenced by flow permeability. In the wake of a porous body such as a tree, the Karman vortex street is confirmed farther in the downstream region than in the wake of a normal bluff body. A similar tendency was shown by Miyata (2001), who conducted an experiment on a permeable hollow cylinder. The permeable hollow cylinder was a wire net rolled in the form of a normal cylinder.

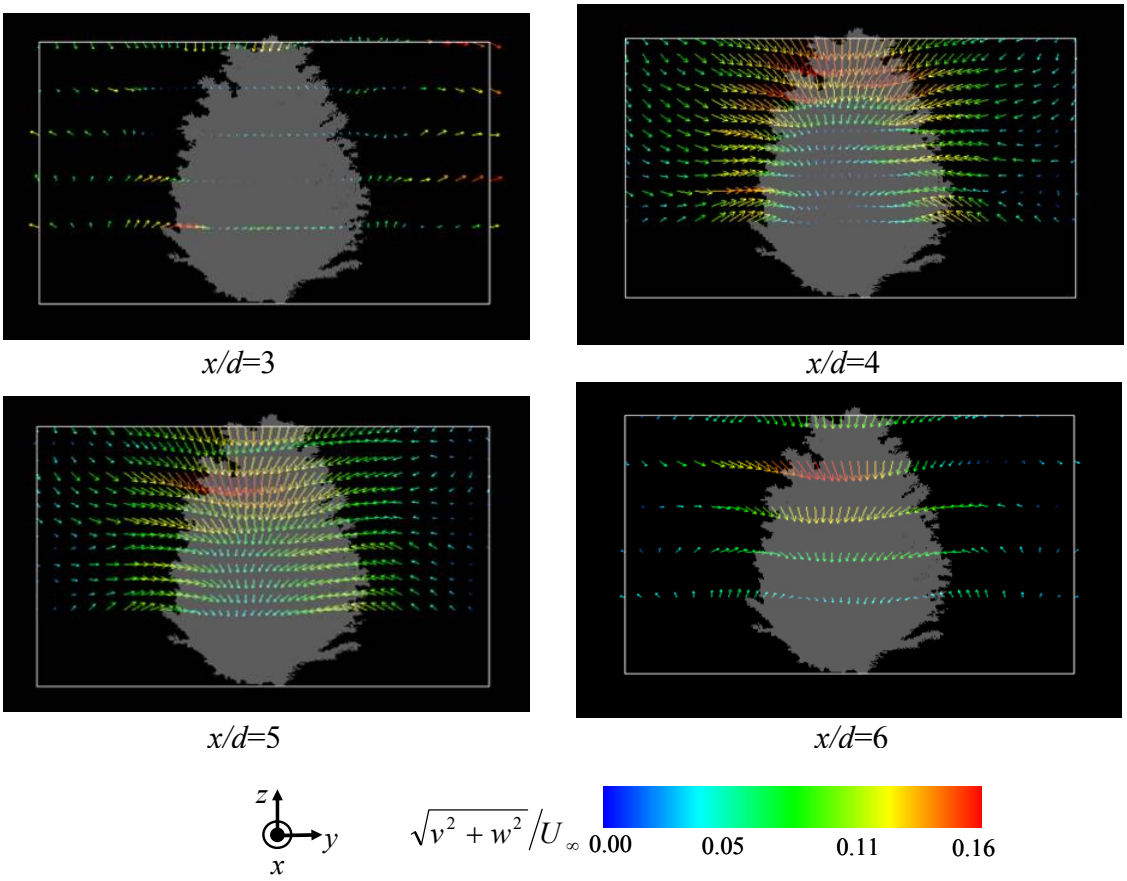

Fig. 3: Velocity profiles v and w behind the tree

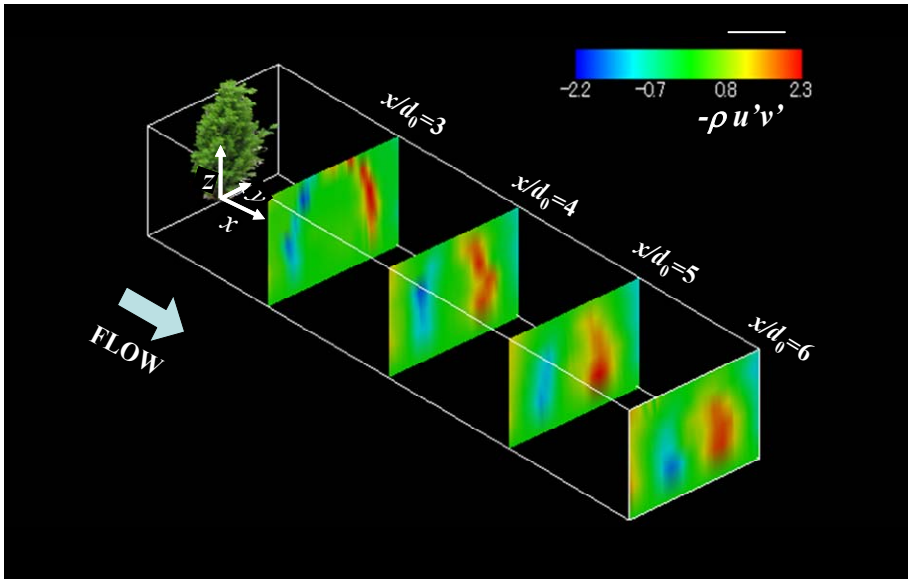

Fig. 4: Reynolds stress profile $-\rho\overline{u'v'}$ behind the tree

It is thought that the role of the wire net is similar to the leaves of a tree. For x/d=5, strong downwash flow from the top of the tree is observed.

Next, we observed that the Reynolds stress shows the momentum transport generated by the turbulence (Fig. 4). The Reynolds stress behind the conifer in the near wake region is smaller than that of the normal cylinder. We think that the flow passes through the crown of the tree, which has the permeability of branches and leaves, because the velocity gradient just behind the tree is smaller than that of the normal cylinder. Therefore, the momentum transportation in the tree's near wake is less than that in the normal cylinder's wake. This is probably due to the permeability of branches and leaves, through which the flow passes.

4. Conclusions

In this study, the turbulent structure behind a conifer was measured in a wind tunnel experiment. It was found that the wake of the tree has a downwash flow, which strengthened as the flow moved downstream and also when the flow moved toward the center of the wake. The momentum transportation in the near wake is less than that in the normal cylinder's wake.

References

Torita, H., Fukuchi, M., 1997: Studies on thinning in shelterbelt considering the effect of reducing wind speed - By the result of wind tunnel experiment. Bulletin of the Hokkaido Forestry Research Institute No. 34.

Miyata, M., Komeda, Y., 2001: Flow past 2D permeable hollow cylinder in uniform stream. Conference Proc. of Fluid Mech. Division, JSME, CD-ROM.

Authors' address:

Prof. Dr. Hitoshi Ishikawa (ishi@rs.kagu.tus.ac.jp)
Dr. Shunsuke Yamada (yamadas@rs.kagu.tus.ac.jp)
Department of Mechanical Engineering, Tokyo University of Science
Kudan-kita 1-14-6, Chiyoda-ku, Tokyo 102-0073, Japan

Large-eddy simulation of the aerodynamic interactions between canopy roughness sublayer turbulence and tree-sway motions

Hong-Bing Su[1], Mark Rudnicki[2], April Hiscox[3], Vincent Webb[2], David Miller[2]

[1]Department of Geography, East Carolina University, USA
[2]Department of Natural Resources and the Environment, University of Connecticut, USA
[3]Department of Environmental Sciences, Louisiana State University, USA

Abstract

The overall goals of this study are to incorporate tree-sway physics into Large-Eddy Simulation (LES) of canopy roughness sublayer (CRSL) turbulence in and above forest canopies, and to use the coupled LES-tree-sway-model to study the aerodynamic interactions between CRSL coherent gusts and tree-sway motions over a range of atmospheric conditions and canopy morphology. The focus of this presentation is to quantify the influences of tree-sway motions on the characteristics of CRSL turbulence in and above a horizontally homogeneous forest by comparing two LES runs with and without coupling with a tree-sway model.

1. Introduction

Turbulence winds in the CRSL drive forest-atmosphere exchange of heat, water and carbon, and transport and diffusion of pollen, seeds and spores. However, the complex architecture of forest ecosystems and the oscillations of trees have significant influences on turbulence structures in the atmospheric boundary layers (ABL) by imposing both mechanical (drag) and thermal (via energy balance of vegetation elements) forces.

Since the pioneering work of Shaw and Schumann (1992), the LES is proving to be a valuable tool that is aiding our understanding of CRSL turbulence structures in and above horizontally homogeneous plant canopies on flat ground (Kanda and Hino 1994, Dwyer et al. 1997, Shen and Leclerc 1997, Su et al. 1998, 2000, Patton et al. 2001, 2003, Shaw and Patton 2003, Fitzmaurice et al. 2004, Watanabe 2004, Yue et al. 2007, Dupont and Brunet 2008). An important element in modeling CRSL turbulence is the parameterization of drag force imposed by canopy elements. This is because work done against the form drag by airflow transfers both mean kinetic energy (MKE) and turbulent kinetic energy (TKE) at scales greater than canopy elements to wake scale kinetic energy (WKE), short-circuits the inertial cascade of TKE and enhances the overall dissipation (Shaw and Seginer 1985, Wilson 1988). Finnigan and Mulhearn (1978) stated: "It is relatively simple to show that in the expression for the mean aerodynamic drag in a waving cereal canopy, terms containing the motions of the plants explicitly are of the same order as those involving only the mean and fluctuating velocities of the airflow". Thus, considering plant motions could lead to a significant difference in modeled drag force. Furthermore, Shaw and Patton (2003) argued that the canopy drag has a large impact on both the resolved and unresolved components of an LES flow field.

We are aware of two LES studies involving flexible canopies, one is a 2-D LES of a reed field (Ikeda et al. 2001), and the other is a 3-D LES of a short crop (Dupont et al. 2008). However, previous LES of CRSL in and above forest canopies did not explicitly simulate the motions of individual trees. Therefore, the effects of tree-sway motions on CRSL turbulence characteristics produced by the earlier LES are unknown.

2. The large-eddy simulation (LES) of ABL

For a neutrally stratified ABL, the LES explicitly resolves the temporal evolutions of spatially filtered velocity $\tilde{u}_i$, kinematic pressure $\tilde{p}/\rho$ (defined as a deviation from the horizontal average P/ρ which is prescribed as an external larger-scale horizontal mean pressure-gradient-force, and ρ is the density of air) in a 3-D array of grids by solving the following set of equations:

$$\frac{\partial \tilde{u}_i}{\partial t} = -\frac{\partial \tilde{u}_i \tilde{u}_j}{\partial x_j} - \frac{1}{\rho}\frac{\partial P}{\partial x_i} - \frac{\partial \tilde{p}^*}{\partial x_i} - \frac{\partial \tau_{ij}}{\partial x_j} + f_C \varepsilon_{ij3} \tilde{u}_j - F_i \tag{A-1}$$

$$\frac{\partial \tilde{u}_j}{\partial x_j} = 0 \tag{A-2}$$

$$\frac{\partial^2 \tilde{p}^*}{\partial x_i^2} = \frac{\partial}{\partial x_i}\left\{ -\frac{\partial \tilde{u}_i \tilde{u}_j}{\partial x_j} - \frac{\partial \tau_{ij}}{\partial x_j} + f_C \varepsilon_{ij3} \tilde{u}_j - F_i \right\} \tag{A-3}$$

where $\sim$ denotes a spatial filtering operation, δ_{i3} is the Kronecker delta, ε_{ij3} is the alternating unit tensor, f_C is the Coriolis parameter, i (= 1, 2, 3) is the directional index for the x-, y-, z-direction in a Cartesian coordinate, F_i is the drag force imposed by plant elements. In the isotropic quantity $\tilde{p}^* = \tilde{p}/\rho + 2e/3$, $e = \left(\widetilde{u_k u_k} - \tilde{u}_k \tilde{u}_k\right)/2$ is the subfilter-scale (SFS) kinetic energy.

The SFS fluxes τ_{ij} are parameterized (Moeng 1984, Moeng and Wyngaard 1988) as:

$$\tau_{ij} = \widetilde{u_i u_j} - \tilde{u}_i \tilde{u}_j - \frac{2}{3} e \delta_{ij} = -K_m \left(\frac{\partial \tilde{u}_i}{\partial x_j} + \frac{\partial \tilde{u}_j}{\partial x_i} \right) \tag{A-4}$$

where the SFS eddy-diffusivity for momentum is parameterized as $K_m = C_K l_\Delta e^{1/2}$, in which C_K is a model coefficient, $l_\Delta = \left[(1.5\Delta x)(1.5\Delta y)(\Delta z) \right]^{1/3}$ is a length scale, and Δx, Δy, Δz are grid dimensions.

A prognostic equation for e is also solved:

$$\frac{\partial e}{\partial t} = -\tilde{u}_i \frac{\partial e}{\partial x_i} - \tau_{ij} \frac{\partial \tilde{u}_i}{\partial x_j} + \frac{\partial}{\partial x_i}\left(2K_m \frac{\partial e}{\partial x_i} \right) - \varepsilon - \varepsilon_{fd} \tag{A-5}$$

where the free-air dissipation is parameterized as $\varepsilon = C_\varepsilon e^{3/2} / l_\Delta$ with C_ε as a model coefficient (Moeng, 1984). The enhanced dissipation in the canopy is parameterized as $\varepsilon_{fd} = 8 C_d a_p \sqrt{e/3}$ (Shaw et al., 2003), in which C_d is a drag coefficient and a_p is the plant area density.

The drag force is typically parameterized as:

$$F_i = C_d a_p \left|\tilde{V}\right| \tilde{u}_i \,. \qquad \text{(A-6)}$$

If tree-sway motions are not considered as in most previous LES of airflow in forest canopies, $\tilde{V} = \left[\tilde{u}_k \tilde{u}_k\right]^{1/2}$ is the magnitude of instantaneous resolved-scale wind vector. The procedures of modifying $\tilde{V}$, F_i and ε_{fd} to explicitly account for tree-sway motions are described below.

3. The mechanical model of tree-sway motion

In this initial effort, we adopt a simple mass-spring-damper model that treats each tree as a straight and rigid beam attached to the ground via a rotary spring with a rotary dashpot damper (Fig. 1a). The main forces applied to the tree are gravity and wind-induced drag (Fig. 1b), while the resistance forces are due to stem elasticity, root-soil-plate weight, soil shear strength and root strength (Fig. 1c).

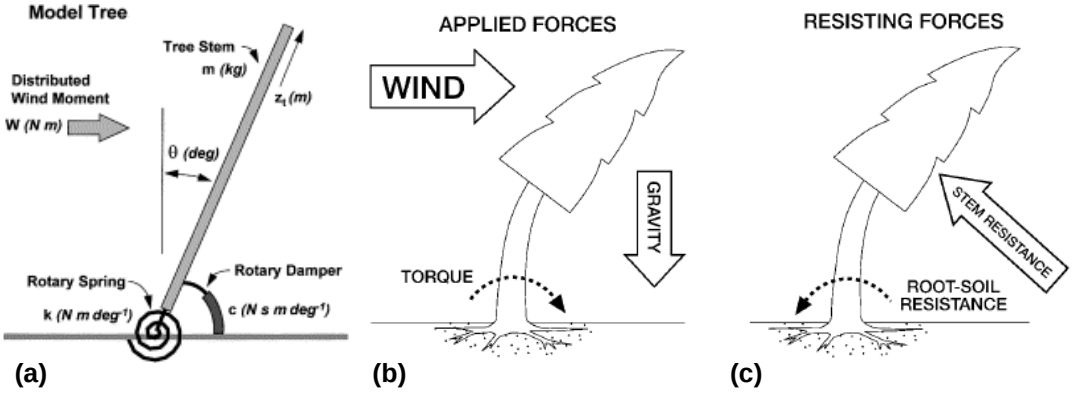

Fig. 1. (a) Mass-spring-damper model of a whole tree: the stem is treated as a rigid rod with mass m attached to the ground via a rotary spring and a rotary dashpot damper (Flesch and Wilson, 1999); (b) and (c) are from Peltola (2006).

Similar to Flesch and Wilson (1999), the equation of motion for a whole tree (with a height of h_t and a total mass of m) may be written as:

$$I\frac{\partial^2\theta_i}{\partial t^2} + D\frac{\partial\theta_i}{\partial t} + E\theta_i = \int_0^{h_t} F_i^p(z_t)\cos(\theta_i) z_t dz_t + \int_0^{h_t}\left[G(z_t) - F_3^p(z_t)\right]\sin(\theta_i) z_t dz_t \qquad \text{(B-1)}$$

where θ_i is the angular displacement in the i-direction (i = 1, 2 for the x- and y-direction in the Cartesian coordinate), z_t is the distance from the ground to a point along the main tree stem, $I = \int_0^{h_t} \rho_p(z_t) V_p(z_t) z_t^2 dz_t$ is the moment of inertial (ρ_p and V_p are the density and volume of tree elements), $D = 2D_r\omega_n I$ is the internal damping coefficient (ω_n is the natural frequency of the tree, and D_r is a non-dimensional reference damping

coefficient as a measure of how quickly the oscillations decay in terms of a time scale D/I), E is the spring constant, $F_i^p(z_t)$ is wind-induced drag force in the *i*-direction, and the drag force in the vertical direction $F_3^p(z_t)$ is combined with the gravitational force $G(z_t) = \rho_p(z_t)V_p(z_t)g$.

Several simplifications to (B-1) may be made as in Flesch and Wilson (1999). The first is to assume the tree is a cylindrical rod with its total mass uniformly distributed over its height so that $I = m \cdot h_t^2 / 3$. The second is to assume $F_3^p(z_t)$ is small so that it may be neglected. The third is to assume θ_i is small so that $\int_0^{h_t} G(z_t) z_t \sin(\theta_i) dz_t \cong mgh_t\theta_i / 2$, which is moved to the left-hand-side of (B-1) and combined with $E\theta_i$. An effective stiffness is then defined as $E_e = E - mgh_t / 2$ and $\omega_n^2 = E_e / I$.

4. Coupling tree motion model and LES

Interactions between turbulent wind fields in the CRSL and the tree motions are modeled by coupling the tree-sway equation and the LES equations via the drag forces $F_i^p(z_t)$ in (B-1) and F_i in (A-1) and (A-3), and the enhanced dissipation ε_{fd} in (A-5).

Similar to the 2-D LES of Ikeda et al. (2001), we adopt tandem grid systems (Fig. 2a, 2b), in which the "LES grids" (dashed boxes) are fixed in space whereas the "plant grids" (solid boxes) move with individual trees. The vertical LES grid size is 2 m or 1/10 of the model tree height (20 m), and the horizontal dimensions of the "LES grids" are set to 2m x 2m, as typically used in previous LES of CRSL. Here we set the "plant grids" also to $(2m)^3$. However, the "plant grids" do not have to have the same dimensions as the "LES grids". For example, the horizontal dimensions of the "plant grids" can be set to the maximum crown dimensions measured in the field (Fig. 2c).

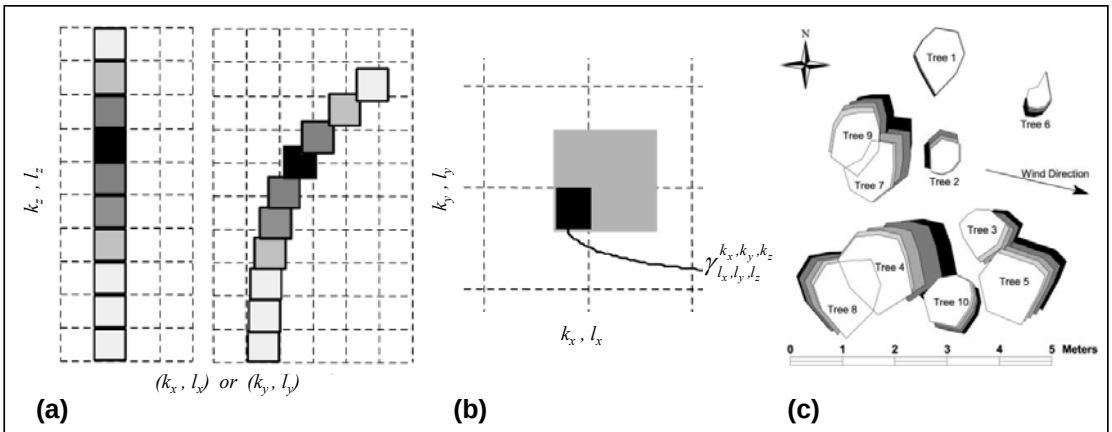

Fig. 2. (a) and (b) Tandem grid systems modified from Ikeda et al. (2001): dashed lines are LES grids, solid lines are plant grids; (c) Maximum crown dimensions of 10 trees and their movements measured at five consecutive time steps with an interval of 0.1 second. Black and white indicate the first and last time steps (Rudnicki et al., 2001).

Let l_x, l_y, l_z and k_x, k_y, k_z denote grid indices for the "LES grids" and the "plant grids" in the x-, y-, z-directions in the Cartesian coordinate, we have,

$$F_i(l_x,l_y,l_z) = \sum_{k_x,k_y,k_z} C_d \gamma_{l_x,l_y,l_z}^{k_x,k_y,k_z} a_p(k_x,k_y,k_z) \left|\tilde{V}\right| \left[\tilde{u}_i(l_x,l_y,l_z) - u_i^p(k_x,k_y,k_z)\right] \quad \text{(C-1)}$$

$$F_i^p(k_x,k_y,k_z) = \sum_{l_x,l_y,l_z} \rho C_d \gamma_{l_x,l_y,l_z}^{k_x,k_y,k_z} a_p(k_x,k_y,k_z) \left|\tilde{V}\right| \left[\tilde{u}_i(l_x,l_y,l_z) - u_i^p(k_x,k_y,k_z)\right] \quad \text{(C-2)}$$

$$\left|\tilde{V}\right| = \left\{\sum_{i=1}^{3}\left[\tilde{u}_i(l_x,l_y,l_z) - u_i^p(k_x,k_y,k_z)\right]^2\right\}^{1/2} \quad \text{(C-3)}$$

where $a_p(k_x,k_y,k_z)$ is the vegetation area density for a given "plant grid" (k_x, k_y, k_z) and $\gamma_{l_x,l_y,l_z}^{k_x,k_y,k_z}$ is the volume that this grid overlaps with the "LES grid" (l_x, l_y, l_z) even though only the overlapping area in the x-y plane is shown in Fig. 2b, $\tilde{u}_i$ and u_i^p are the velocities of corresponding LES and plant grids. For i = 1, 2 in the horizontal directions,

$$u_i^p(z_t) = z_t \frac{\partial \theta_i}{\partial t} cos(\theta_i) \quad \text{(C-4)}$$

and in the vertical direction (i = 3), we have,

$$u_3^p(z_t) = z_t \frac{\partial \theta_1}{\partial t} sin(\theta_1) + z_t \frac{\partial \theta_2}{\partial t} sin(\theta_2) \quad \text{(C-5)}$$

5. Results

At the time of submission of this extended abstract, the LES runs are being carried out. Results will be presented at the conference.

Acknowledgement

This work is funded by the US National Science Foundation through the Physical and Dynamic Meteorology Program in the Division of Atmospheric Sciences (ATM-0840191 for Su, ATM-0840147 for Rudnicki, ATM-0913018 for Hiscox). The first-author would like to acknowledge the computational support provided by the National Center for Atmospheric Research (NCAR), and a mixed MPI-OpenMP version of the LES code provided by Drs. Peter Sullivan and Ned Patton at NCAR.

References

Dupont, A., Brunet, Y., 2008: Influence of foliar density profile on canopy flow: A large-eddy simulation study. Agric. For. Meteorol. 148, 976-990.

Dupont, S., Py, C., de Langre, E., Hemon, P., Gosselin, F., Brunet, Y., 2008: Modelling waving crops using large-eddy simulation. 28th Conf. on Agric and For. Meteorol. American Meteorological Society, Orlando, FL.

Dwyer, M.J., Patton, E.G., Shaw, R.H., 1997: Turbulent kinetic energy budgets from a large-eddy simulation of airflow above and within a forest. Boundary-Layer Meteorol. 84, 23-43.

Finnigan, J.J., Mulhearn, P.J., 1978: Modeling waving crops in a wind tunnel. Boundary-Layer Meteorol. 14, 253-277.

Fitzmaurice, L., Shaw, R.H., Paw U, K.T., Patton, E.G., 2004: Three-dimensional scalar microfront systems in a large-eddy simulation of vegetation canopy flow. Boundary-Layer Meteorol. 112, 107-127.

Flesch, T.K., Wilson, J.D., 1999: Wind and remnant tree sway in forest cutblocks. II. Relating measured tree sway to wind statistics. Agric. For. Meteorol. 93, 243-258.

Ikeda, S., Yamada, T., Toda, Y., 2001: Numerical study on turbulent flow and honami in and above flexible plant canopy. Inter. J. Heat Fluid Flow 22, 252-258.

Kanda, M., Hino, M., 1994: Organized structures in developing turbulent flow within and above a plant canopy using a large eddy simulation. Boundary-Layer Meteorol. 68, 237-257.

Moeng, C.-H., 1984: A large-eddy-simulation model for the study of planetary boundary-layer turbulence. J. Atmos. Sci. 41, 2052-2062.

Moeng, C.-H., Wyngaard, J.C., 1988: Spectral analysis of large-eddy simulations of the convective boundary layer. J. Atmos. Sci. 45, 999-1022.

Patton, E.G., Davis, K.J., Barth, M.C., Sullivan, P.P., 2001: Decaying scalars emitted by a forest canopy: a numerical study. Boundary-Layer Meteorol. 100, 91-129.

Patton, E.G., Sullivan, P.P., Davis, K.J., 2003: The influence of a forest canopy on top-down and bottom-up diffusion in the planetary boundary layer. Quart. J. Roy. Meteorol. Soc. 129, 1415-1434.

Peltola, H.M., 2006: Mechanical stability of trees under static loads. American J. Botany 93, 1501-1511.

Rudnicki, M., Silins, U., Lieffers, V. J., Josi, G., 2001: Measure of simultaneous tree sways and estimation of crown interactions among a group of trees. Trees-Struc. Func. 15, 83-90.

Shaw, R. H., Seginer, I., 1985: The dissipation of turbulence in plant canopies. Preprint, 7th Symp. Turbulence Diffusion, American Meteorological Society, Boulder, CO, 200-203.

Shaw, R.H., Schumann, U., 1992: Large-eddy simulation of turbulent flow above and within a forest. Boundary-Layer Meteorol. 61, 47-64.

Shaw, R.H., Patton, E.G., 2003: Canopy element influences on resolved- and subgrid-scale energy within a large-eddy simulation. Agric. For. Meteorol. 115, 5-17.

Shen, S., Leclerc, M.Y., 1997: Modeling the turbulence structure in the canopy layer. Agric. For. Meteorol. 87, 3-25.

Su, H.-B., Shaw, R.H., Paw U, K.T., Moeng, C.-H., Sullivan, P.P., 1998: Turbulent statistics of neutrally stratified flow within and above a sparse forest from large-eddy simulation and field observations. Boundary-Layer Meteorol. 88, 363-397.

Su, H.-B., Shaw, R.H., Paw U, K.T., 2000: Two-point correlation analysis of flow within and above a forest from large-eddy simulation. Boundary-Layer Meteorol. 94, 423-460.

Watanabe, T., 2004: Large-eddy simulation of coherent turbulence structures associated with scalar ramps over plant canopies. Boundary-Layer Meteorol. 112, 307-341.

Wilson, J.D., 1988: A second-order closure model for flow through vegetation. Boundary-Layer Meteorol. 42, 371-392

Yue, W., Parlange, M.B., Meneveau, C., Zhu, W., van Hout, R., Katz, J., 2007: Large-eddy simulation of plant canopy flows using plant-scale representation. Boundary-Layer Meteorol., 124, 183-203.

Authors' addresses:

Prof. Dr. Hong-Bing Su (suh@ecu.edu)
Department of Geography, East Carolina University
Greenville, NC 27858, USA

Prof. Dr. Mark Rudnicki (mark.rudnicki@uconn.edu)
Mr. Vincent Webb (vincent.webb@uconn.edu)
Prof. Dr. David Miller (david.r.miller@uconn.edu)
Department of Natural Resources and the Environment, University of Connecticut
Storrs, CT 06269, USA

Prof. Dr. April Hiscox (ahiscox@lsu.edu)
Department of Environmental Sciences, Louisiana State University
Baton Rouge, LA 70803, USA

Modelling forest canopy motion using a porous elastic approach

David Pivato, Sylvain Dupont, Yves Brunet

INRA, UR1263 EPHYSE, Villenave d'Ornon, France

Abstract

In order to investigate the possibility of modelling plant motion at the landscape scale, an equation for canopy plant motion, forced by the instantaneous wind flow, is introduced in a large-eddy simulation (LES) airflow model, previously validated over homogeneous and heterogeneous canopies. The canopy is simply represented as a poroelastic continuous medium, which is similar in its discrete form to an infinite row of identical stems. In a first step only one linear mode of plant vibration is considered. The two-way coupling between plant motion and the wind flow occurs through the drag force term. This coupled model is validated against data recorded over an alfafa canopy, whose motions have been analysed elsewhere in great details from video recordings. It is shown that the model is able to reproduce the well-known phenomenon of *honami*. The model is then extended to a forest canopy using the first flexible vibration mode, and compared to the previous model and a finite-element model of a tree. The simplified models are shown to be as efficient as the finite-element model. Finally, the possibility of using such a porous elastic approach for studying forest canopy motion at landscape scale is discussed.

1. Introduction

Because of the complexity of the various processes responsible for windthrow in heterogeneous landscapes, modelling both plant and flow dynamics should provide tools allowing quantification of tree vulnerability to windload at any position in heterogeneous environments. Over the last decade it has been demonstrated that the Large-Eddy Simulation (LES) technique can be applied at the vegetation scale and can reproduce the main features of turbulent flow observed over homogeneous vegetation canopies as well as downwind from forest leading edges. While turbulent wind flow over plant canopies has been widely studied, coherent motions of plant canopies and their strong interactions with the wind flow have received little attention so far. Possibly the most detailed study on wind-plant interaction was performed by Py et al. (2005) and Py et al. (2006) from a video-recording experiment of alfalfa and wheat crop motions. It was found that for a specific range of flow velocities, flow and vegetation canopy may move in phase.

Developing and validating such a computational tool for better understanding wind-plant interaction is the subject of the present study. For this purpose, an equation of plant motion has been introduced into an atmospheric LES model where model, the canopy is represented as a poroelastic continuum. This representation is similar in its discrete form to an infinite row of identical mechanical oscillators where only one linear mode of plant vibration was first considered. The two-way coupling between plant motion and wind flow occurs through the drag force term. This modified LES model is validated against the video-recorded data of alfalfa crop motion performed by Py et al. (2005). The model is then extended to the first flexible vibration modes and compared with the previous model and a finite element model.

2. Material and methods

LES allows one to have access to instantaneous dynamical fields and is consequently able to simulate the wind gusts responsible for plant motions (Dupont et al., 2008a). The LES model used in this study (ARPS) was initially developed to simulate convective and cold-season storms as well as weather systems at larger scales. A detailed description of the standard version of the model and its validation cases are available in the ARPS User's Manual. We modified the model so as to simulate turbulent flows over plant canopies at very fine scales.

In LES models, the canopy is usually simply represented by a drag-force term in the momentum equation, with no account for plant motions. This drag-force approach is implemented by adding a pressure and viscous drag-force term in the momentum equation and by adding a sink term in the equations for subgrid-scale turbulent kinetic energy in order to represent the acceleration of the dissipation of turbulent eddies in the inertial subrange. Hence, the two-way coupling between plant motion and the wind flow occurs through the drag-force term.

In order to investigate the possibility of modelling plant motion at the landscape scale, we introduced an equation for plant motion (1), forced by the instantaneous wind flow, in a LES model previously validated over homogeneous (Dupont and Brunet, 2008a) and heterogeneous (Dupont and Brunet, 2008b) canopies:

$$M\frac{\partial^2 X(z,t)}{\partial t^2}+C\frac{\partial X(z,t)}{\partial t}+KX(z,t)=\rho\int_0^h C_d A_f^{tree}\left|u-\frac{\partial X(z,t)}{\partial t}\right|\left(u-\frac{\partial X(z,t)}{\partial t}\right)dz \quad (1)$$

where $X(z,t)$ is the plant displacement in the wind direction, M is the mass, C the damping coefficient, K the stiffness coefficient. The term on the right-hand side represents the drag force term and is proportional to the relative velocity between the wind u and the plant deflection velocity $\partial X(z,t)/\partial t$. In this term, C_d is the mean plant drag coefficient and A_f^{tree} is the frontal area density. Here, the canopy is simply represented as an infinite row of identical mechanical linear oscillators (Fig.1).

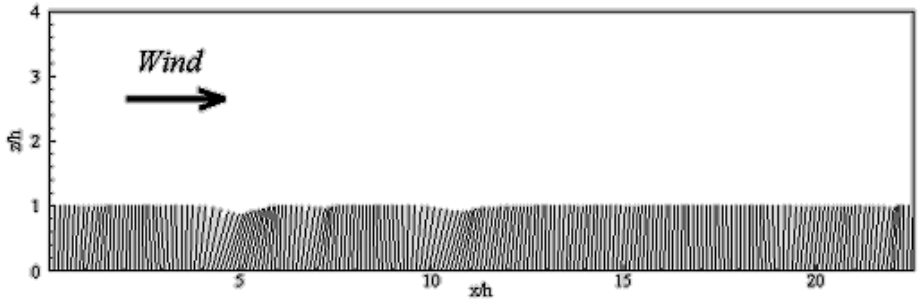

Fig. 1: Canopy represented as an infinite row of identical mechanical oscillators

The model is then extended to a forest canopy by considering a flexible vibration mode, instead of a linear one for the crop canopy. The tree displacement can be written as follow (de Langre, 2008):

$$X(z,t) = \sum_{i=1}^{n} q_i(t)\Phi_i(z) \quad (2)$$

where i is the mode number, q_i the modal displacement and Φ_i the mode shape.

Projecting the equation of plant motion (1) on each mode Φ_i, we obtain a system of equation for each modal displacement q_i:

$$m_i \frac{d^2 q_i(t)}{dt^2} + c_i \frac{dq_i(t)}{dt} + k_i q_i(t) = \rho \int_0^h C_d A_f^{tree} \left| u - \Phi_i \frac{dq_i(t)}{dt} \right| \left(u - \Phi_i \frac{dq_i(t)}{dt} \right) \Phi_i dz \quad (3)$$

where m_i is the ith modal mass, c_i is the ith modal damping, k_i the ith modal stiffness and the term on the right-hand side represents the ith modal drag force (De Langre, 2008). In this study, only the first mode shape is considered. In what follows one application of this model to a Maritime Pine forest is performed.

3. Application over an alfalfa crop canopy

In a first step the model has been validated for an alfalfa canopy with rigid stems whose motions have been analyzed in great details from video recordings (Dupont et al., 2009).

Fig. 2 shows instantaneous wind-plant interactions simulated by the LES model. Here is represented a time sequence of wind velocity and plant motion in a vertical streamwise slice over a 0.90 s period for the high wind speed case. The background color shows the intensity of the streamwise wind velocity component, the arrows the wind direction, and the white stems sketch canopy plants where plant displacements have been accentuated in order to provide a better view of the waving structures. At t = 0 s, a wind gust penetrates within the canopy around x = 8h, inducing a forward deflection of a group of plants. Then, after the gust passage, plants spring back (t = 0.30 s), and vibrate around their axis (t = 0.60 and 0.90 s), before they are damped and hit by another gust. The magnitude and velocity of plant motions were observed in agreement with measurements provided by Py et al. (2006).

Fig. 3 shows an instantaneous three-dimensional view of the simulated alfalfa crop motion. The dark patches appearing on the crop surface correspond to regions where plants are highly deflected downwind with the passage of strong wind gusts as observed in Fig. 2. We observed from crop motion animation that these patches move essentially in the wind direction. Wind gusts inducing plant swaying are characterized by large positive values of u and large negative values of w (figure not shown). This is the signature of sweep motions, *i.e.* downward turbulent structures, which constitutes part of the sweep-ejection cycle of coherent structures in canopy flows. They are induced by the development or impingement of turbulent coherent structures at canopy top. These wavelike crop motions are known as *honami* waves. We observed that the wavelength of these coherent waving patches is in agreement with that deduced from video recordings and exhibits the same dependence with mean wind velocity as the measurements. (Dupont et al., 2009).

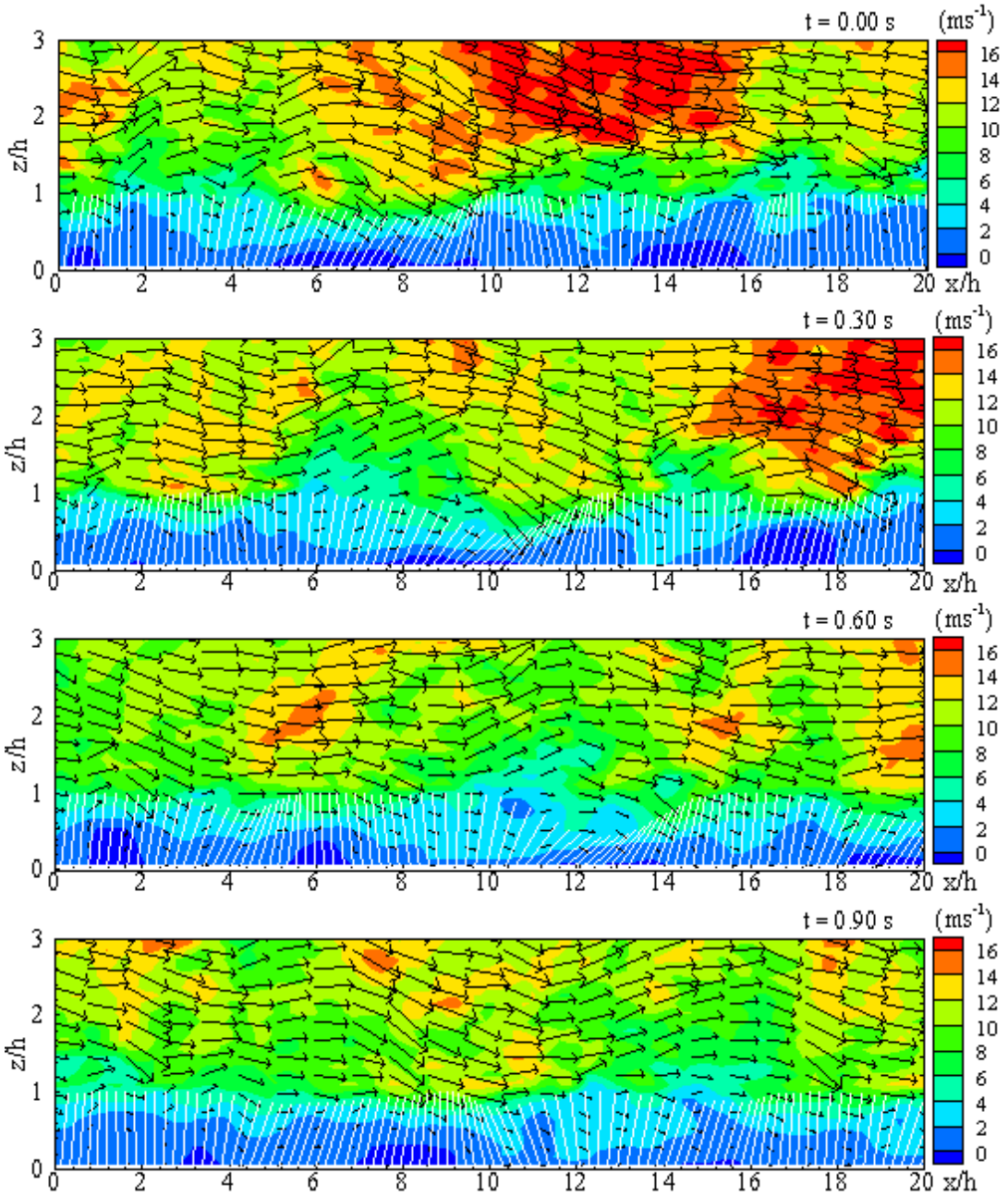

Fig. 2: Streamwise cross section of instantaneous wind-plant interaction at 0.30 s intervals during a period of 0.90 s; the background color represents the magnitude of the streamwise wind velocity, the arrows the wind vectors, and the white stems sketch plant displacement; for a better visualization, angular plant displacement was multiplied by a factor of 5 (Dupont et al., 2009)

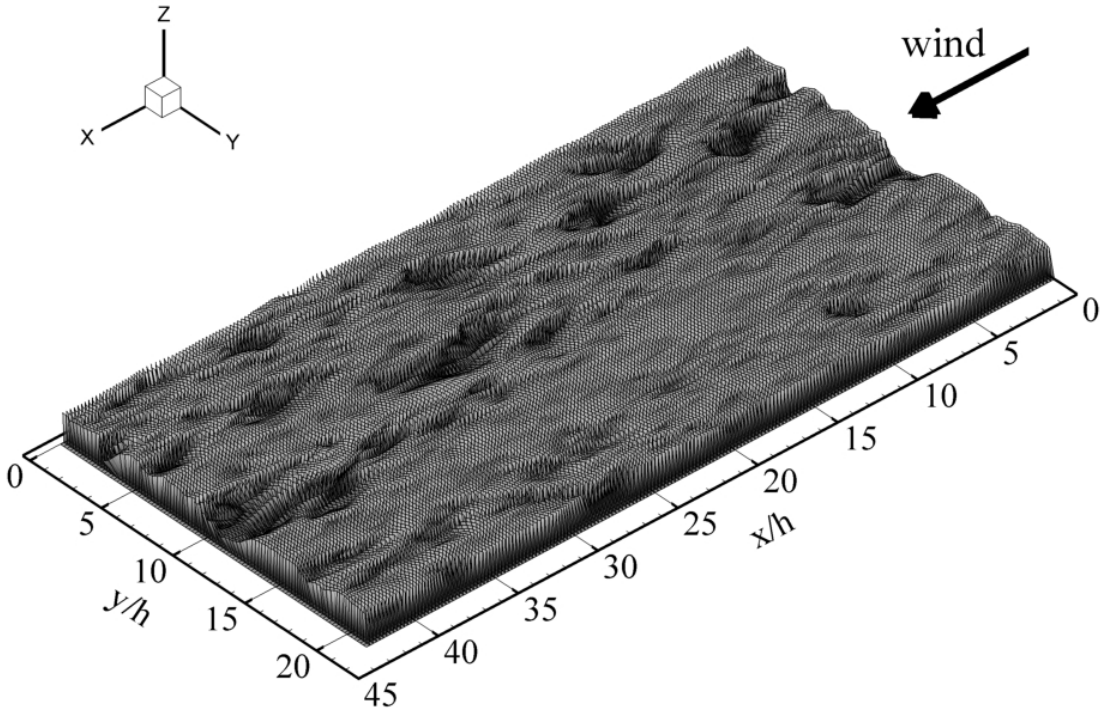

Fig. 3: Simulation of alfalfa crop motion (Dupont et al., 2009)

4. Extension of the model to a forest canopy

In a second step the model is extended to a forest canopy by considering the first flexible vibration mode (Fig. 4), instead of a linear one for the crop canopy.

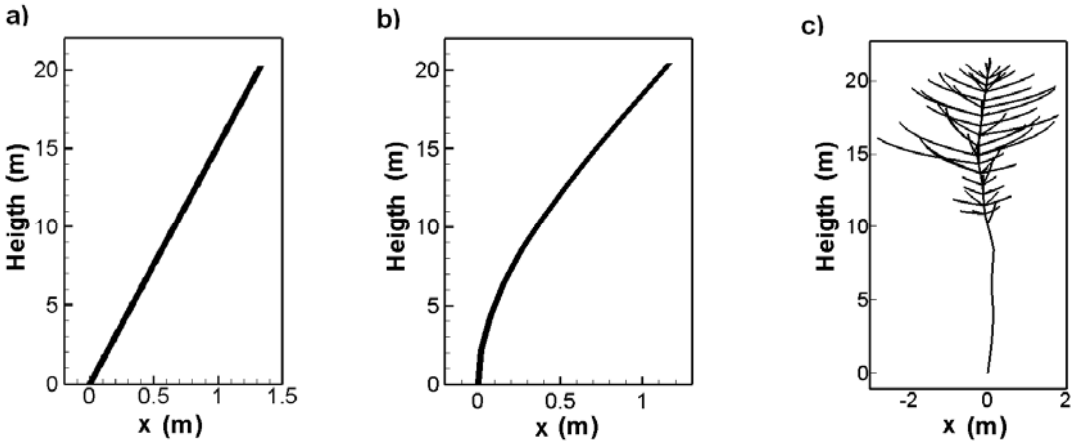

Fig. 4: Comparison between 3 models: (a) linear model, (b) flexible model, (c) finite element model

To compare the flexible model with the initial linear model and with a finite-element model of tree (Sellier et al. 2008), we compute the streamwise displacement of the tree for each model at the heights of 10 m and 20 m. The three models are submitted to the same wind forcing, extracted from the LES model.

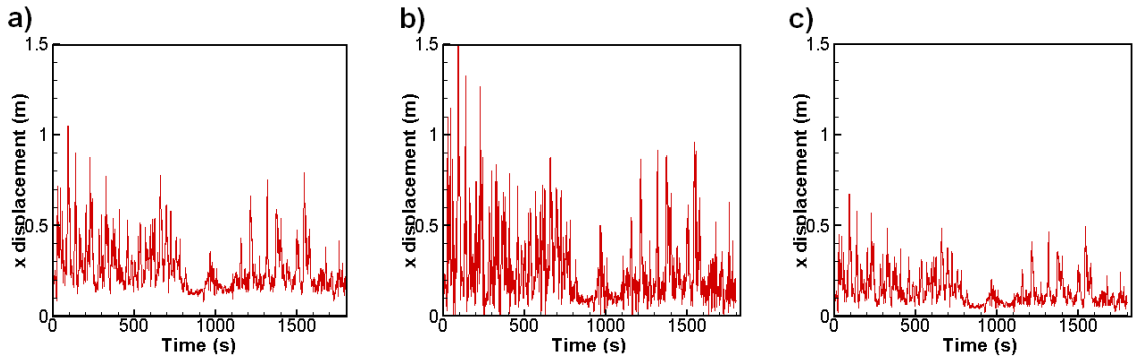

Fig. 5: Results for the streamwise displacement at 10 m: (a) linear model, (b) flexible model, (c) finite-element model

The streamwise displacement for the linear model, the flexible model and the finite-element model has the same shape but not exactly the same magnitude (Fig. 5). This is due to the mass, the damping and the stiffness being linearly distributed for the simplified models whereas for the finite-element model these characteristics are distributed over the whole tree architecture (*i.e.* trunk, foliage, etc.). This could be improved by distributing mass, damping and stiffness according to the foliar area A_f. Moreover, the same computation performed at 20 m (figure not shown) confirms this hypothesis: the flexible model provides the same streamwise displacement as the finite-element model.

4. Conclusion

A novel three-dimensional two-way coupled model between wind flow and canopy plant motion has been presented. This model consists of an atmospheric large-eddy simulation (LES) model coupled with a simple mechanical oscillator equation for crop plant motion. The canopy is represented as a poroelastic continuous medium, which is similar in its discrete form to an infinite row of identical stems. Only one linear mode of plant vibration was first considered. In a second step the model is extended to a flexible vibration mode. Applied over an alfalfa crop canopy we observed that the model is able to simulate *honami* motion usually observed over cereal crops in windy days. The extended model as well as the linear model can be good substitutes to more complex model (*e.g.*, finite-element models) and allow flow simulations over forests to be performed. In the future, we intend to model stem and tree breakage using non-linear mechanics and fracture mechanics in our model.

Acknowledgement

Financial support from the ANR programme “Chêne-Roseau”, involving Inra, Inria and Ecole Polytechnique, is gratefully acknowledged.

References

de Langre, E., 2008: Effects of wind on plants. Annu. Rev. Fluid Mech. 40, 141-68.

Dupont, S., Brunet, Y., 2008a: Influence of foliar density profile on canopy flow: a large-eddy simulation study. Agric. For. Meteorol. 148, 976-990.

Dupont, S., Brunet, Y., 2008b: Edge flow and canopy structure: a large-eddy simulation study. Boundary-Layer Meteorol. 126, 51-71.

Dupont, S., Brunet, Y. , 2009: Coherent structures in canopy edge flow: a large-eddy simulation study. J. Fluid Mech. 630, 93-128.

Dupont, S., Gosselin, F., Py, C., de Langre, E., Hemon, P., Brunet, Y., 2009: Modelling waving crops using Large-Eddy Simulation: comparison with experiments and a linear stability analysis. J.Fluid Mech., submitted.

Py, C., de Langre, E., Moulia, B., Hemon, P., 2005: Measurement of wind-induced motion of crop canopies from digital video images. Agric. For. Meteorol. 130, 223-236.

Py, C., de Langre, E., Moulia, B., 2006: A frequency lock-in mechanism in the interaction between wind and crop canopies. J. Fluid Mech. 568, 425-449.

Sellier, D., Brunet, Y., Fourcaud, T., 2008: A numerical model of tree aerodynamic response to a turbulent airflow. Forestry 81, 279-297.

Author's address:

David Pivato (david.pivato@bordeaux.inra.fr)
INRA, UR1263 EPHYSE
71 avenue Edouard Bourlaux, F-33883 Villenave d'Ornon, France

Tree motion in heterogeneous forests: a coupled flow-tree simulation study

Yves Brunet[1], Sylvain Dupont[1], Pascal Roux[1], Damien Sellier[2]

[1]INRA, UR1263 EPHYSE, Villenave d'Ornon, France
[2]SCION, Rotorua, New Zealand

Abstract

Landscape heterogeneities such as forest edges, clearings or gaps, as well as the presence of topography, induce spatial variations in turbulence properties that may have considerable impact on the aerodynamic sollications exerted on the trees. The heterogeneity in the damages caused by windstorms in forested landscapes can be partly attributed to such spatial variations in windload. We investigate here the impact of landscape heterogeneity on tree motion using a coupled flow-tree modelling approach. The simulation of flow fields is provided at fine spatial and temporal resolution by a large-eddy simulation (LES) model and the simulation of tree movements induced by instantaneous wind forces is provided by a mechanistic, dynamical model of tree behaviour. One-way coupling of the models is ensured by forcing the mechanical tree model with instantaneous velocity fields computed by the LES model, so that the tree response to a fluctuating wind field can be predicted at any location in a virtual landscape. Using this coupled model we illustrate the influence of canopy architecture on the streamwise variations in tree motion in two cases: a forest edge flow and a flow over a forested hill. The ultimate aim of the approach is to provide guidance for sustainable forest management practices.

1. Introduction

Landscape heterogeneities such as forest edges, clearings or gaps, as well as the presence of topography, substantially alter mean velocity and turbulence fields. They induce spatial variations in turbulence properties that may have considerable impact on the aerodynamic sollications exerted on the trees. The observed heterogeneity in the damages caused by windstorms in forested landscapes can be partly attributed to such spatial variations in windload. In the perspective of designing sustainable forest management practices, it is therefore of importance to better understand the coupling between wind flow and tree motion.

Because of the complexity of the processes responsible for windthrow in heterogeneous landscapes, modelling both plant and flow dynamics should provide adequate tools for allowing tree vulnerability to windload to be quantified at any position in heterogeneous environments. Over the past few years it has been shown that Large-Eddy Simulation (LES) of flow dynamics can reproduce the main features of canopy flow in horizontally homogeneous canopies (e.g., Dupont and Brunet, 2008a), across canopy edges (e.g., Dupont and Brunet, 2008b,c and 2009) and over forested hills (e.g., Dupont et al., 2008). In parallel, mechanistic models have been developed to simulate plant dynamics (e.g., Kerzenmacher and Gardiner, 1998; Moore and Maguire, 2005). More recently a new model has been developed to simulate the dynamics of a tree forced by a field of fluctuating velocities (Sellier et al., 2008). This model has been validated using field measurements of turbulent velocities and tree movements.

Here we couple a LES flow model with this latter model for tree dynamics, in order to simulate tree motion at any given position in a heterogeneous forested landscape. We

use the coupled model in two distinct situations: a forest edge flow and a flow over a forested hill. In both cases we illustrate the influence of stand density and canopy architecture on the streamwise variations in tree motion and mechanical stresses.

2. Turbulent flow and plant motion models

LES provides instantaneous dynamical fields and is consequently able to simulate the wind gusts responsible for plant motions. The LES model used in this study (ARPS) was initially developed to simulate convective and cold-season storms as well as weather systems at larger scales. It is a three-dimensional (3D), non-hydrostatic, compressible model where Navier-Stokes equations are written in terrain-following coordinates. The model solves the conservation equations for the three wind velocity components, pressure and potential temperature. At such high spatial resolution as is required here, these equations are filtered so that all turbulent structures larger than the filter scale are explicitly solved by the model (which is the case of most turbulent eddies generated by wind shear), while smaller turbulent structures (subgrid-scale turbulent motions) are modelled through a 1.5-order turbulence closure scheme. A detailed description of the standard version of the model and its validation cases is available in the ARPS User's Manual. The model was modified so as to simulate turbulent flows over plant canopies at very fine scales (Dupont et al., 2008a). The canopy is implemented in the model by adding a pressure and viscous drag-force term in the momentum equation and by adding a sink term in the equations for subgrid-scale turbulent kinetic energy and its dissipation. The latter term accounts for the acceleration of the dissipation of turbulent eddies in the inertial subrange. The grid is orthogonal in the horizontal direction and stretched in the vertical direction. This modified model has been validated in various cases: homogeneous canopy flow (Dupont and Brunet, 2008a), edge flow (Dupont and Brunet, 2008b) and flow over a forested hill (Dupont et al., 2008).

A dynamic model has also been developed to analyse the mechanical response of trees submitted to a turbulent airflow (Sellier et al., 2008). It is based on a standard motion equation written in matrix form:

$$M\,q'' + D\,q' + K\,q = F + G$$

where M, D and K are the inertia, damping and stiffness matrices of the structure, respectively; F is the column vector of the aerodynamic drag and G the column vector of gravitational forces; q'', q' and q are the column vectors of acceleration, velocity and displacement, respectively. The terms Mq'' and Dq' represent the inertia forces and dissipative forces, respectively. This equation is solved at all places on a given 3D tree structure, using the finite-element method, after the structure has been divided into a finite number of 3D beam elements with associated elastic properties. The term allowing coupling with the flow is the drag term F, that is a function of the drag coefficient, the plant area exposed to the wind (frontal area density), the wind velocity and the displacement velocity of the tree elements. Instantaneous values can be ascribed to the wind velocity, so that the dynamic model can be forced by wind values recorded at high frequency. The model was validated against experimental data collected during 30 min in a pine forest canopy (Sellier et al., 2008). In the original version of the model the equation system was solved using the Abaqus software. In the present study the open-access Cast3m software has been used. At the current stage only small displacements have been considered, so that non-linear processes cannot be properly accounted for.

Forcing the tree model by measured turbulent time series is adequate for validation purposes. However this approach becomes limiting for characterizing the tree behaviour in various environments or for performing sensitivity studies to tree architecture for example. Indeed, velocity fields strongly depend on canopy structure and landscape heterogeneities. In other words, the forcing functions have to be adapted to each case. LES provides a powerful solution to this problem: for a given tree architecture and plantation pattern, it can indeed generate time series of instantaneous 3D wind velocity that can be used to generate adequate forcing drag terms. The procedure is then as follows: (1) choose a particular tree architecture (tree 1 of Sellier et al., 2008, was used here); (2) assume a plantation density, that can be variable in space, throughout the LES domain; (3) run the LES model over a certain time period, after the leaf area density has been calculated at each grid point; (4) run the dynamic model at given locations of interest, using the velocity field calculated locally as a forcing function to the drag term on all tree elements. Two types of heterogeneities have been treated here using this procedure: a forest edge flow and a flow over a forested hill.

3. Forest edge flow

The density of the pine forest was chosen so as to correspond to the forest canopy described in Sellier et al. (2008), where the leaf area index (LAI) was 1.83. Two cases have been considered, i.e. with and without an understorey. The understorey was obtained by adding leaf area uniformly between the soil surface and the crown basis, so that the added frontal area density was equal to that of the crown.

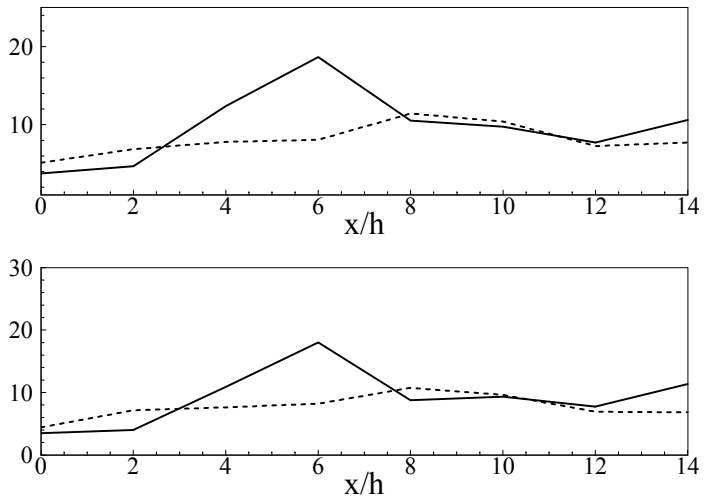

Fig: 1: Top: streamwise variation in the streamwise tree displacement ratio (maximum/mean), downstream from the forest edge. Bottom: streamwise variation in the Von Mises stress ratio (maximum/mean), downstream from the forest edge. Case of a pine forest canopy of LAI = 1.83, with (solid line) or without (broken line) an understorey. The edge is located at x/h = 0.

In each case 30-min time series were computed at various locations downstream of the edge, for variables such as tree deflection at various heights, axial stress, shearing stress,

torsional stress, flexural stress, Von Mises stress, etc. As trees may adapt their structure to local mean conditions, tree vulnerability may be estimated to a first approximation from the ratio between extreme and mean values of these variables (Dupont and Brunet, 2008c). As an example, Fig. 1 represents maximum tree displacement and Von Mises stress observed over the simulated period at height $z = 17$ m (middle of the crown layer), normalised by their mean value. Both variables exhibit similar patterns. With no understorey they show a slight increase down to about $x/h = 8$, and they tend to stabilize further downstream to an equilibrium value. In the presence of a thick understorey they both show a marked peak at $x/h = 6$ where they take about twice their value with no understorey. They then quickly decrease down to $x/h = 8$, where they take an equilibrium value. These results can be interpreted by looking at the spatial variations in the velocity statistics (not shown here): in the first case the absence of understorey allows the flow to adapt slowly and smoothly to the canopy, due to the presence of a sub-canopy wind jet starting at the edge, in the sparsest layers of the canopy, whereas in the second case the tree behaviour results from the combination of the strong intermittency observed in the upper canopy in the region $1 < x/h < 6$ and the development of a region of strong turbulence after $x/h \approx 4$. It is interesting to note that this peak at $x/h = 6$ cannot be seen on related variables such as the gust factor (Dupont and Brunet, 2008c), often used as a surrogate for tree vulnerability. This underlines the interest of our coupled flow-tree approach.

4. Flow over a forested hill

In the second case study we focus on the forested hill considered by Dupont et al. (2008) after the work of Finnigan and Brunet (1995). The simulated hill is 30 m in height H and 84 m in length L (half hill width at mid-hill height). The forest canopy has the same characteristics as those considered in the edge flow study. Two cases, with and without an understorey, were also considered.

Fig. 2 shows the same variables as Fig. 1, for this hill flow. In both understorey cases the tree deflection and Von Mises stress ratios tend to decrease slightly from positions upstream of the foot of the hill up to the top of it. The absolute magnitude of the displacement and stress slightly increases but, as the flow velocity increases within the canopy on its way up to the hill top, their mean values increase too, at a slightly larger rate. In the understorey case both variables exhibit a marked peak at about $x/L = 2.5$, i.e. near the downwind foot of the hill. This region is located somewhat upstream than the region identified by Dupont et al. (2008) as being particularly intermittent and strongly dominated by sweep motions. With no understorey a slight maximum is visible on the Von Mises stress ratio, but a little less downstream ($x/L \approx 2$) than in the previous case.

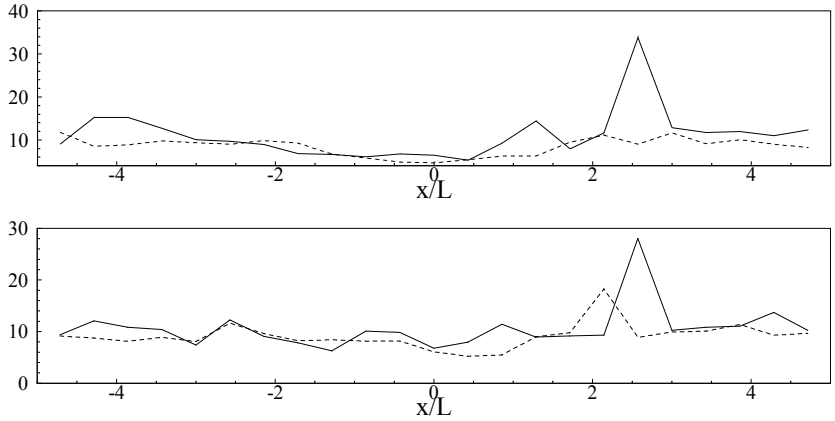

Fig: 2: Top: streamwise variation in the streamwise tree displacement ratio (maximum/mean), along the hill. Bottom: streamwise variation in the Von Mises strain ratio (maximum/mean), along the hill. Case of a pine forest canopy with (solid line) or without (broken line) an understorey. The hill top is located at x/L = 0.

5. Conclusion

A one-way coupled model between turbulent flow and plant motion has been presented. It consists in using a LES model in various landscape and canopy configurations to produce time series of instantaneous velocity components, and later use these velocities to force a dynamic tree model. Two cases have been explored, an edge flow and a flow over a forested hill. In the absence of any understorey (which is typically the case of a maritime pine forest) the streamwise variations in tree displacement and internal stress are fairly smooth. However, when the leaf area is distributed over the whole depth of the canopy, regions of larger tree vulnerability to windload were identified, at a few canopy heights downstream of the edge in the first case, and at 2-3 hill length scales in the second one. This preliminary study shows the potential of this approach since these particular regions could not be a priori identified on the sole basis of the mean wind and turbulence fields. A more systematic study will be carried out in the future, in order to cover a wider range of canopy and landscape configurations.

Acknowledgement

Financial support from the ANR programme “Chêne-Roseau”, involving Inra, Inria and Ecole Polytechnique, is gratefully acknowledged.

References

Dupont, S., Brunet, Y., 2008a: Influence of foliar density profile on canopy flow: a large-eddy simulation study. Agric. For. Meteorol. 148, 976-990.

Dupont, S., Brunet, Y., 2008b: Edge flow and canopy structure: a large-eddy simulation study. Boundary-Layer Meteorol. 126, 51-71.

Dupont, S., Brunet, Y., 2008c: Impact of forest edge shape on tree stability: a large-eddy simulation study. Forestry 81, 299-315.

Dupont, S., Brunet, Y., 2009: Coherent structures in canopy edge flow: a large-eddy simulation study. J. Fluid Mech. 630, 93-128.

Dupont, S., Brunet, Y., Finnigan, J.J., 2008: Large-eddy simulation of turbulent flow over a forested hill: validation and coherent structure identification. Q. J. Roy. Meteorol. Soc. 134, 1911-1929.

Finnigan, J.J., Brunet, Y., 1995: Turbulent airflow in forests on flat and hilly terrain. In : Wind and Trees. Coutts, M.P., Grace, J. (Eds.), Cambridge University Press, Cambridge, 3-40.

Kerzenmacher, T., Gardiner, B.A., 1998: A mathematical model to describe the dynamic response of a spruce tree to the wind. Trees 12, 385-394.

Moore, J.R., Maguire, D.A., 2005: Natural sway frequencies and damping ratios of trees: influence of crown structure. Trees 19, 363-373.

Sellier, D., Brunet, Y., Fourcaud, T., 2008: A numerical model of tree aerodynamic response to a turbulent airflow. Forestry 81, 279-297.

Author's address:

Dr. Yves Brunet (yves.brunet@bordeaux.inra.fr)
INRA, UR1263 EPHYSE
71 avenue Edouard Bourlaux, F-33883 Villenave d'Ornon, France

Forest scale cellular automata model of wind interacting with trees

Spencer Hall[1], Anthony Selino[1], Michael Jones[1], Mark Rudnicki[2]

[1]Department of Computer Science, Brigham Young University, USA
[2]Department of Natural Resources and the Environment, University of Connecticut, USA

Abstract

Computational models of tree sway at the forest scale may lead to improved understand of how forests withstand wind. Increasing frequency and severity of wind events will make this understanding more important. A cellular automata model of forest sway is constructed and used to count collisions and tree fall for a forest containing over 1,000 trees. As the accuracy of the model improves, it may yield valuable insights into sway behaviour at the forest scale.

1. Introduction

Wind and tree interaction at the forest scale create a complex dynamic system. Many questions can be asked about the ecology of this system, but it is difficult to design real-world experiments which might answer these questions. For example, investigations of crown-crown collisions during major wind events at the forest scale would require instrumenting hundreds or thousands of crowns.

Ecologists are struggling to predict the structure and function of ecosystems in a rapidly changing global environment which is altering ecosystems with unprecedented results. A mechanistic understanding of the dynamics of tree stability and failure (Baker 1995, James et al. 2006) is critical to predict how forest structure and function would respond to future global environmental changes (Dale et al. 2001), in particular more frequent and stronger windstorms (Emanuel 2005, Trapp et al. 2007). The purpose of this work is to create an experimental system for understanding the ecological implications of wind and tree interaction at the forest scale.

In this project, we aim to combine results from forestry ecology literature with appropriate computational methods to create predictive models of wind and tree interaction at the forest scale. Fig. 1 shows such a cellular automata model containing just over 1,000 trees and two wind fields approaching from the top left and right. The tree sway dynamics are patterned after empirical results and computational methods are used to reduce to cost of detecting collisions.

Computer scientists have generated models of tree motion which scale to forests and are visually plausible (Di Giacomo et al. 2001, Zhang et al. 2006, Diener et al. 2008). We plan to build on that work by replacing stochastic or simple periodic models of wind with more accurate models of wind gust structure. Cellular automata are a good model for this system as the behavior of the forest arises from the interactions of neighboring trees.

In the next section, we briefly outline key computational concepts on which our work is based. Section 3 contains a discussion of our methods and Section 4 contains selected data generated from the preliminary model. We close with conclusions about computational model of forest sway in Section 5.

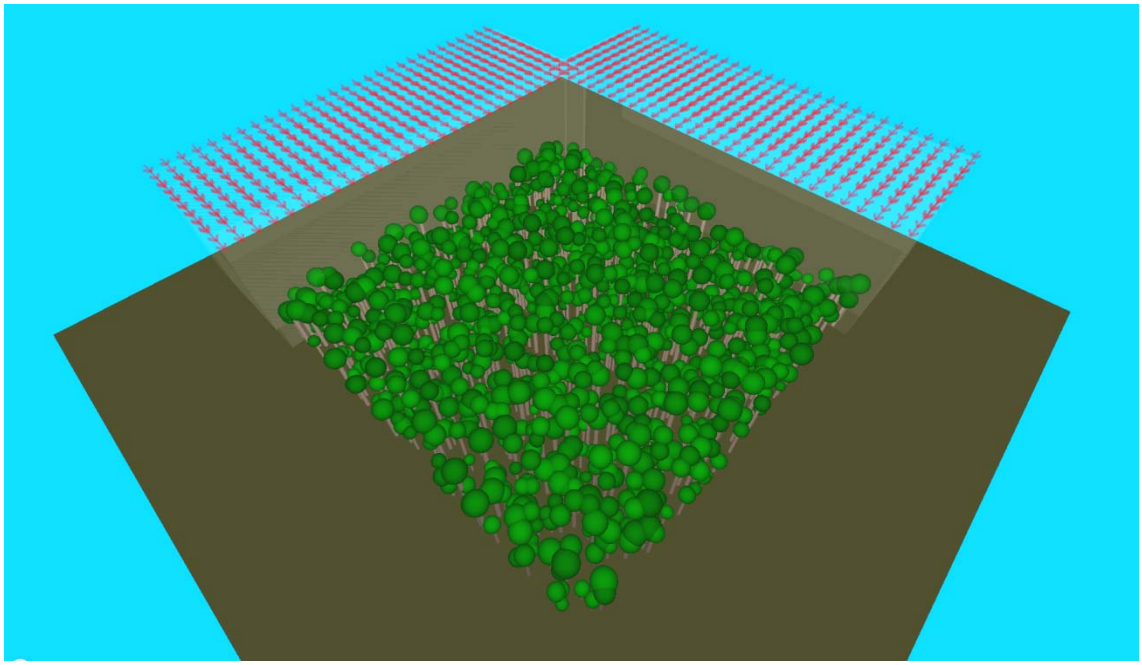

Fig. 1: Forest sway model with over 1,000 trees and two wind fields

2. Key computational concepts

Our model is based on cellular automata. In this context, automata are computational devices which transition between a finite set of discrete states based on input and the current state. Cellular automata are a kind of automata in which the transition relation depends not only on the local state and input but also on the states of neighboring automata in some fixed area.

Vizualization of the model is accomplished using the OpenGL 3D graphics library (see (OpenGL Architecture Review Board et al. 2007) for an introduction) together with the GLUT extensions (Kilgard 2009). OpenGL, and similar libraries such as DirectX, simplify the creation of interactive 3D applications. The disadvantage of graphics libraries is that they require certain degree of programming skill such as might be found in undergraduate computer science students in the 3rd or 4th year. The compelling advan-tage is the potentially for use of precompiled display lists which run directly on the graphics processing unit (GPU) and can significantly increase computational efficiency.

The model is a physical simulation based on Newtonian principles. The design of such simulations must be done carefully to balance numerical stability, accuracy and computational efficiency. Parent's textbook (Parent 2008) on algorithms in computer animation contains a good introductory discussion of issues in physical simulation.

3. Experimental design

Our computational experiments were conducted using a cellular automata model of forest sway implemented in C++. The model is instrumented to measure active colli-sions and trees fallen for each simulation cycle. The model consists of a forest which is com-

prised of trees, wind and the forces which act on the tree. Gravity is not included in the model. Each component is described in the following paragraphs.

Forest model. The cellular automata model of a forest consists of a grid, trees, a transition function and input. The grid is a rectangular partitioning of the forest floor. Trees populate some of the grid cells following a uniform random distribution which allows variation in height and diameter at breast height (dbh). The transition function describes tree/tree interaction, tree/wind interaction and single tree dynamics. The input to the transition function is neighboring trees' crown positions and wind speed. The wind speed is sampled at a single point in the wind field. Given these inputs, the transition function computes the next tree state which is the position of the crown center in the next simulation step.

Tree model. A single tree consists of a bole and crown parameterized by crown height (m), diameter at breast height (cm), crown radius (m), and tilt in x and y (radians) where x and y are horizontal dimensions of the spatial model. A torsion spring located at the base of the tree approximates the tree's response to wind loading as shown in Fig. 2.

In this model, the aboveground biomass (kg) of the tree is estimated using the biomass equation

$$bm = e^{\beta_0 + \beta_1 \ln dbh(cm)} \tag{1}$$

from (Jenkins et al. 2004) for trees with dbh larger than 2.5cm and treating each tree as a spruce. The moment of inertia at the bole base (kg m^2) is computed by estimating the bole's mass as 80 percent of the total aboveground biomass and treating the bole as an infinitely thin rod and the tree's crown as a sphere.

The natural sway frequency of the tree together with the moment of inertia give the spring constant κ for the for the radial spring at the base of the bole. We use the natural sway frequency

$$f = .0766 + 3.1219 \frac{dbh(cm)}{totalHeight^2} \tag{2}$$

from Moore (2004) where $totalHeight$ is the sum of the crown height and crown radius.

Wind model. Wind fields are modelled as 2 dimensional arrays of 3 dimensional vectors. A wind field has a speed, which is independent of the magnitude of the wind vectors, heading and frequency. Wind fields travel through the forest at a specified speed, heading and frequency. Wind interacts with trees in a 2 dimensional plane in which the wind vector at the centre of the crown acts uniformly on the entire tree. Trees do not influence the wind field.

Forces acting on a tree. Three forces act on trees: elasticity in the bole, wind and collisions with other tree. Each force creates a torque at the base of the bole. Elasticity in the bole is modelled by the torsion spring centred at the base of the bole.

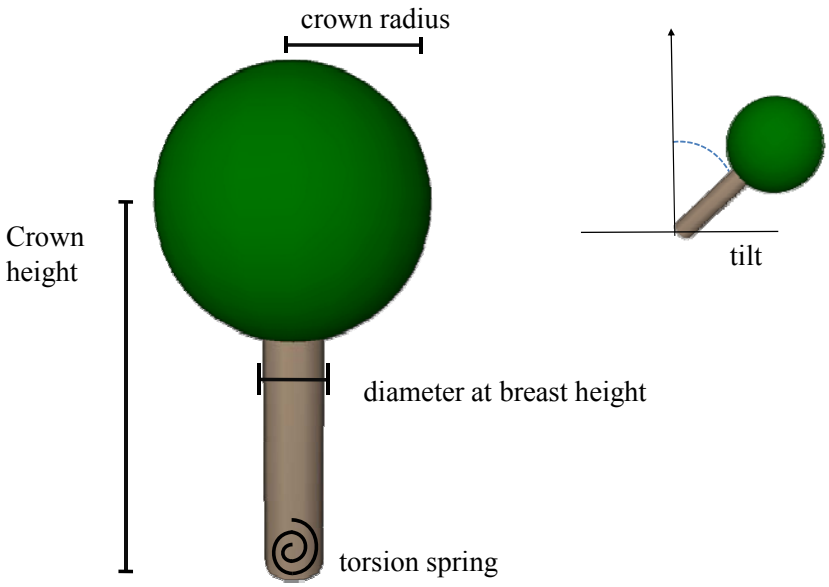

Fig. 2: Model of a single tree using in a cellular automata model of forest sway

Wind velocity, measured at the crown centre, is converted to a force, F_w (Newtons), at the centre of the crown using an aerodynamic drag equation in which the force is proportional to the square of the wind velocity

$$F_w \propto \frac{v^2 \rho C_d A}{2} \tag{3}$$

where $\rho = 1.204$ (kg/m^2) is the atmospheric density and $C_d = 0.69$ is the averaged estimated coefficient of drag for western hemlock in wind speeds ranging from 4 to 20 m/s (Rudnicki et al. 2004) and A (m^2) is the frontal area of the crown and bole. The force is then converted to a torque at the base of the bole. The value of F_w was scaled by a tuneable parameter to match simulation results against expected behaviour using the Beaufort scale.

Collision forces are computed when two crowns collide. The collision force is computed by transferring velocity from one tree to the other. The transferred forces are located at the crown centre and then converted to a torque at the base of the bole. Collisions are not energy preserving. A more accurate model would locate collision forces at the actual point of collision rather than the crown centre.

4. Preliminary results

Active collisions and felled trees were recorded during each simulation cycle for 9 different wind gust intensities. Active collisions are collisions in which two crowns overlap and one crown has velocity greater than or equal to 1 meter per second. Felled trees measures the number of trees fallen due to windthrow. Figs. 3 and 4 contain the results. In each graph, "B*n*" refers to Beaufort scale value *n*. Actual wind speed is the low end of the range specified at Beaufort scale value *n*.

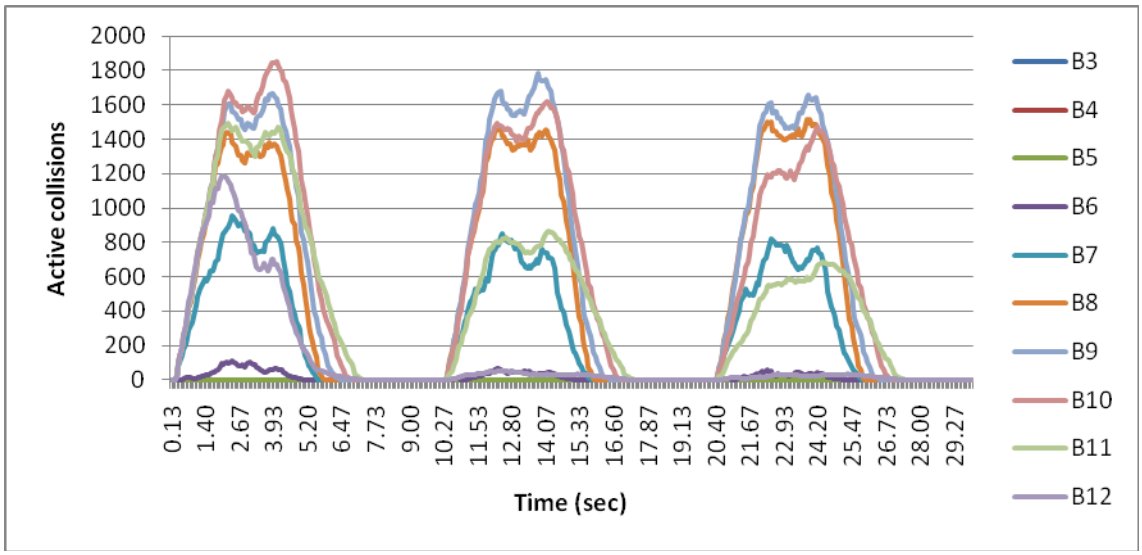

Fig: 3: Number of active collisions for a randomly generated forest in 9 different wind gust conditions

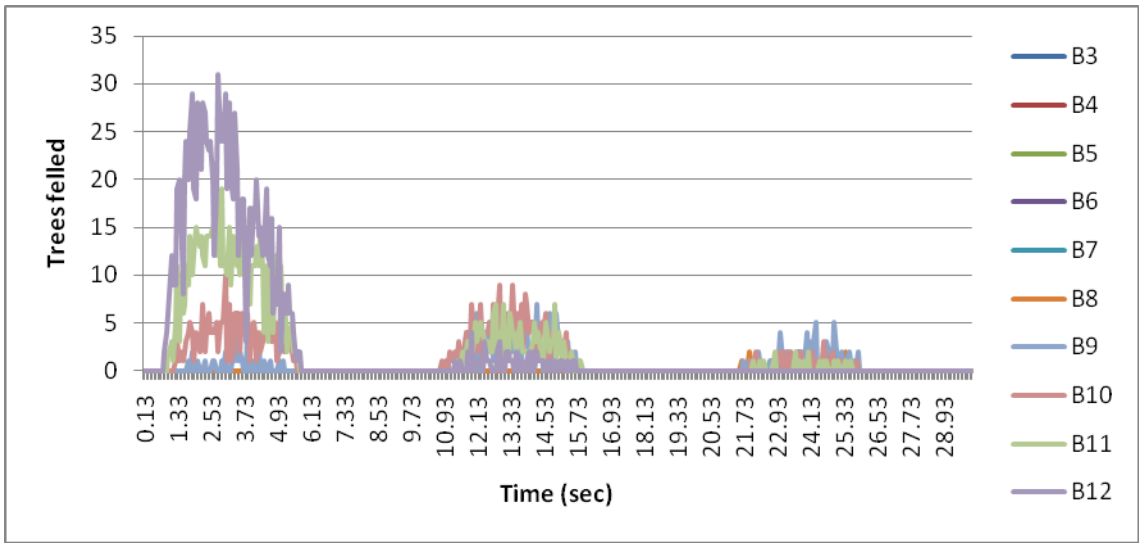

Fig: 4: Number of trees felled in a randomly generated forest in 9 different wind gust conditions

The time resolution of the simulation was 15 Hertz, wind gusts travelled at 20 meters per second and arrive every 10 seconds. The random forest contains a total of 1,280 trees distributed over 22,500 m^2. The average tree height is 8 m and the average dbh is 11.2 cm.

5. Conclusions

Cellular automata models of tree sway at the forest scale are a feasible model for investigating the interaction of wind and trees at the forest scale. The key computational insights which make the model tractable are simplifying collision detection and represent-

ing motion by changing what is stored in a cell location, rather than moving crowns into different cells. The results generated by the model are reasonable, but the validity of the model is based on tuning the wind force to match expected results rather than building bottom-up from empirical data, as advocated in (Camazine et al. 2001).

References

Baker, C. J., 1995: The development of a theoretical model for the windthrow of plants. Journal of Theoretical Biology 175, 355.

Camazine, S., Deneubourg, J.-L., Franks, N.R., Sneyd, J., Theraluz, G., Bonabeau, E., 2001: Investigation of Self-Organization. Self-Organization in Biological Systems. Princeton University Press, 69-87.

Dale, V.H., Joyce, L.A., McNulty, S., Neilson, R.P., Ayres, M.P., Flannigan, M.G., Hanson, P.J., Irland, L.C., Lugo, A.E., Peterson, C.J., Simberloff, D., Swanson, F.J., Stocks, B.J., Wotton, B.M., 2001: Climate change and forest disturbances. Bioscience 51, 723-734.

Di Giacomo, T., Capo, S., Faure, F., 2001: An interactive forest. Proceedings of the Eurographics workshop on Computer Animation and Simulation. Springer-Verlag New York, Inc., Manchester, UK.

Diener, J., Rodriguez, M., Baboud, L., Reveret, L., 2008: Wind projection basis for real-time animation of trees. Computer Graphics Forum 28, 533-540.

Emanuel, K., 2005: Increasing destructiveness of tropical cyclones over the past 30 years. Nature 436, 686-688.

James, K.R., Haritos, N., Ades, P.K., 2006: Mechanical stability of trees under dynamic loads. American Journal of Botany 93, 1522-1530.

Jenkins, J.C., Chojnacky, D.C., Heath, L.S., Birdsay, R.A., 2004: Comprehensive database of diameter-based biomass regressions for North American tree species. United States Dept. of Agriculture.

Kilgard, M., 2009: The OpenGL Utility Toolkit (GLUT) Programming Interface API Version 3.

OpenGL Architecture Review Board, Shreiner, D., Woo, M., Neider, J., Davis, T., 2007: OpenGL Programming Guide: The Official Guide to Learning OpenGL, Version 2.1. 6th edition. Addison-Wesley Professional.

Parent, R., 2008: Computer animation: Algorithms and Techniques. 2nd edition.

Rudnicki, M., Mitchell, S.J., Novak, M.D., 2004: Wind tunnel measurements of crown streamlining and drag relationships for three conifer species. Canadian Journal of Forestry Research 34, 666-676.

Trapp, R.J., Diffenbaugh, N.S., Brooks, H.E., Baldwin, M.E., Robinson, E.D., Pal, J.S., 2007: Changes in severe thunderstorm environment frequency during the 21st century caused by anthropogenically enhanced global radiative forcing. Proceedings of the National Academy of Sciences 104, 19719-19723.

Zhang, L., Song, C., Tan, Q., Chen, W., Peng, Q., 2006: Quasi-physical simulation of large-scale dynamic forest scenes. Advances in Computer Graphics. Springer, Hangzhou, China, 735-742.

Authors' addresses:

Spencer Hall (spencerhall@roberthall.net)
Anthony Selino (aselino@byu.edu)
Prof. Dr. Michael Jones (mike.jones@byu.edu)
Department of Computer Science, Brigham Young University
3328 TMCB, Provo, UT 84602 USA

Prof. Dr. Mark Rudnicki (mark.rudnicki@uconn.edu)
Department of Natural Resources and the Environment, The University of Connecticut
U-4087, 1376 Storrs Road, Storrs, CT 06269 USA

Responses of Scots pine trees to near-surface airflow

Dirk Schindler, Hannes Fugmann, Jochen Schönborn, Helmut Mayer

Meteorological Institute, Albert-Ludwigs-University of Freiburg, Germany

Abstract

The wind-induced vibration behaviour of adjacent, plantation-grown Scots pine trees was analysed by spectral methods and by the biorthogonal decomposition. Results from wavelet analyses demonstrate that covariation between wind loading in the range of the arrival frequency of coherent structures and wind-induced displacement of the sample trees was strong. Although several characteristic frequencies of tree vibration in response to wind excitation could be determined from Fourier energy spectra, covariation between wind loading and tree response in the range of these frequencies was weak. However, characteristic vibration mode shapes were associated with each of the peaks in the Fourier spectra. Most of the energy of the wind, which was transferred into tree movement, was dissipated by the deformation of the stem.

1. Introduction

Trees start to vibrate in response to turbulent wind loading. The amplitude of these vibrations is thought to be a function of the acting wind load. In many previous studies (e.g. Mayer, 1987; Gardiner, 1992; Peltola, 1996; Flesch and Wilson, 1999) it was demonstrated that the dominant, characteristic response of conifers to turbulent wind loading is sway at frequencies in the range of the fundamental sway frequency of their stem. However, these studies focused on the response of the stem because wind loads that surpass its wind load resistance normally cause fatal wind damage and have diverse implications on forest ecology and forestry (Quine and Gardiner, 2007).

There are only a few authors (e.g. Sellier et al., 2006; Moore and Maguire, 2008; Rodriguez et al., 2008) that analysed higher order vibration of coniferous trees. In general, higher order mode vibration may be induced by temporal and spatial variations of the wind load as well as by mass and stiffness and their distributions within the structure under investigation. Associated with the characteristic response frequencies are characteristic forms (modes) of stem deformation amplitude.

The purpose of this study is to raise some crucial issues related to the wind-induced displacement of plantation-grown Scots pine trees. The dynamic sway behaviour of the Scots pine trees' stems in response to wind excitation was analysed and the resultant vibration modes are presented. Their relevance for stem displacement damping is discussed.

2. Data and methods

Near-surface airflow properties and responses of neighbouring trees to wind excitation were monitored in a planted Scots pine (*Pinus sylvestris* L.) forest. The forest is located in Southwest Germany in the southern upper Rhine valley (Mayer et al., 2008). Several measurement campaigns were carried out over the period 2005 to 2008 in order to determine characteristic, dynamic tree responses to turbulent wind loading.

Different configurations of biaxial clinometers (model 902-45, Applied Geomechanics, USA) were used to sample (10 Hz) the angular position of the sample trees. Sonic anemometers (USA-1, Metek, Germany; Young, 81000 V, USA) were used to measure (20 Hz) near-surface airflow properties. They were mounted to scaffold towers, which were set up close to the Scots pine trees. For example, Fig. 1 is a top view of a group of 29 adjacent Scots pine trees that is surrounded by four measurement towers to which sonic anemometers were mounted.

Spectral methods (Fourier and wavelet analyses) as well as the biorthogonal decomposition (Aubry et al., 1991; Hémon and Santi, 2003) were applied in order to analyse the absorption of energy from turbulent airflow and the corresponding dynamic responses of the sample trees.

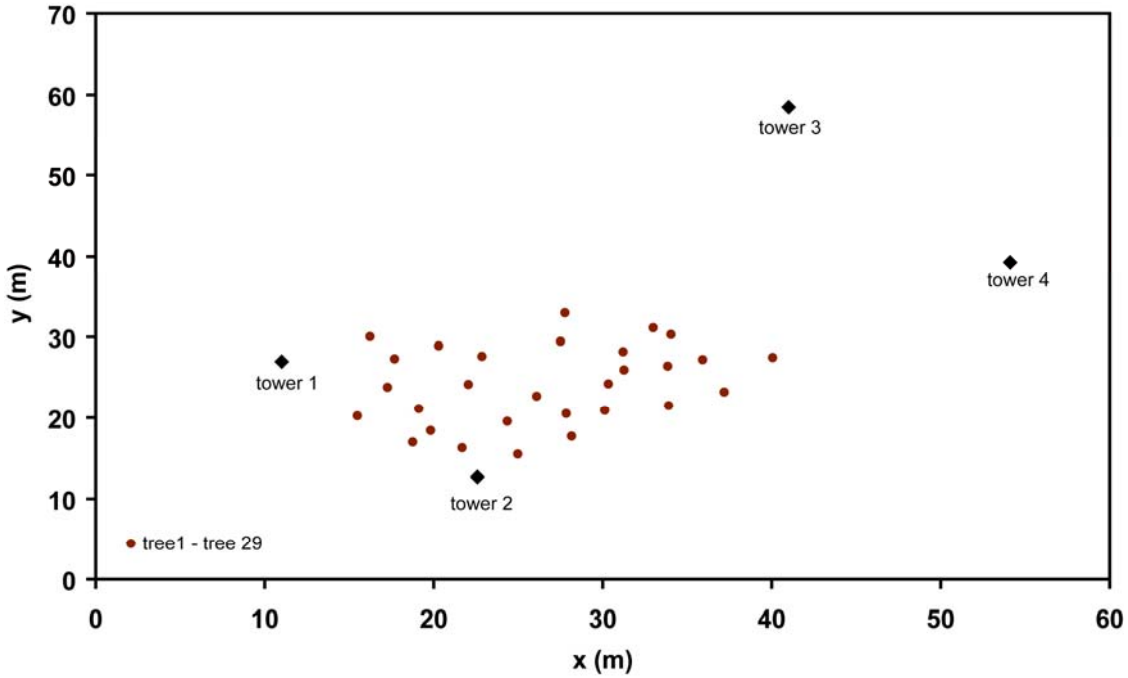

Fig. 1: Top view of a group of 29 adjacent Scots pine trees surrounded by four measurement towers to which sonic anemometers were mounted; the sonic anemometers were used to monitor near-surface airflow properties

3. Results and discussion

Results from Fourier analyses carried out in preceding studies (e.g. Mayer, 1987; Gardiner, 1992; Peltola, 1996; Flesch and Wilson, 1999) indicate that wind energy transfer into movement of conifers is very efficient in the range of the damped natural sway frequency. In contrast to these findings, results from this study demonstrate that absorption of energy of turbulent wind by the sample trees was rather weak in this frequency range. By means of wavelet coherence calculations it can be shown that covariation between airflow properties and along wind response of individual trees was strong in the range of frequencies at which organised, turbulent structures arrive at the trees. Large tree displacements arise as a result from impulsive wind loading exerted by coherent struc-

tures (Gardiner, 1995; Schindler, 2008) rather than from wind loading by turbulence elements in the range of the fundamental sway frequency of the sample trees. For example, in Fig. 2 the global wavelet coherence spectrum GWCS (Torrence and Webster, 1999), which was calculated from fluctuations of the longitudinal wind vector component u´ and from along wind tree displacement y over the hourly interval between 13:00 and 14:00 CET on 21st march 2008, is presented. GWCS is very low in the range of the natural sway period (≈ 3.5 s) of the sample tree under investigation. The most pronounced GWCS-peak can be identified in the range of 40 to 50 s. Schindler (2008) has shown that the arrival frequency of coherent structures is about 46 s over this hourly interval. This finding indicates that regardless of the dominant tree response in the range of the natural sway period of the stem to turbulent wind loading, the wind energy transfer into tree movement is strong especially in the range of the arrival frequency of coherent structures. However, the wind speed range observed during this study was too narrow and covered no potentially destructive high wind speeds that are suited to analyse the effects of a potential convergence of the arrival frequency of coherent structures and the damped natural sway frequency of the sample trees.

The wavelet calculations in this study were realized with wavelet software provided by C. Torrence and G. Compo. The software is available at URL:
http://atoc.colorado.edu/research/wavelets/.

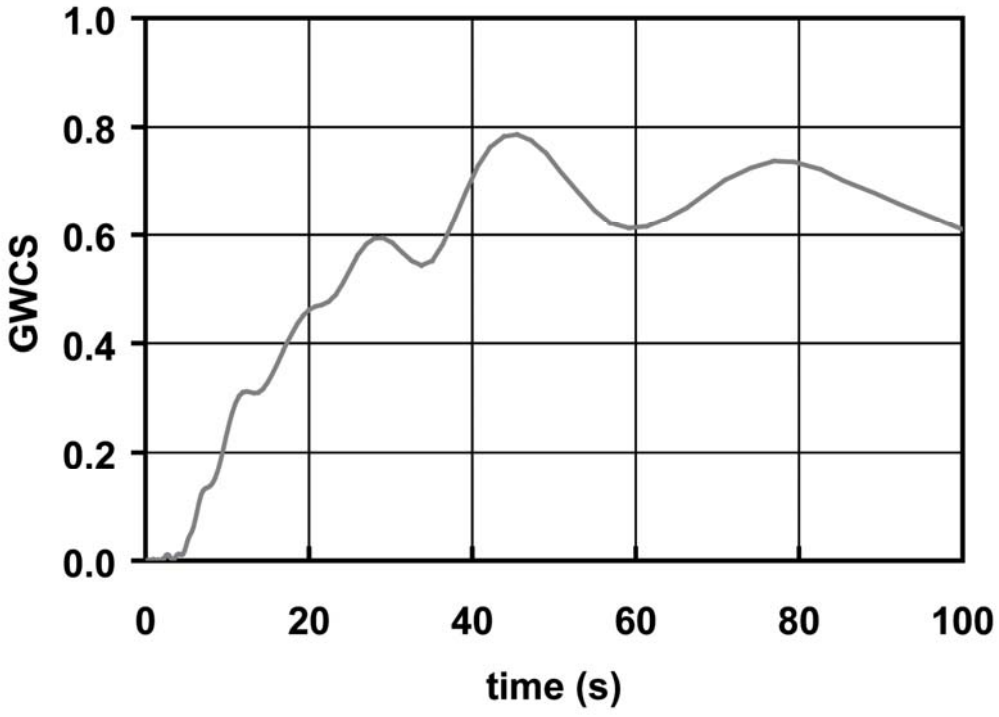

Fig. 2: Global wavelet coherence spectrum (GWCS) calculated from fluctuations of the longitudinal wind vector component u´ and from along wind tree displacement y over the hourly interval between 13:00 and 14:00 CET on 21st March 2008

Classical Fourier energy spectra were calculated from tree displacement records in order to determine characteristic frequencies at which the sample trees show most pronounced responses to turbulent wind loading. For a group of sample trees it was possible to determine a maximum of four characteristic vibration frequencies for both horizontal stem displacement directions. The mean mode shapes associated with these frequencies were computed by means of the biorthogonal decomposition. Furthermore, the results from BOD-calculations demonstrate that the first two vibrational modes contained at least 97 % of total tree displacement signal energy in the observed wind speed range. In Fig. 3 the mean mode shapes related to the first four vibration modes in along wind direction for a wind speed range at canopy height between 3 and 4 m s^{-1} are illustrated. The mode shapes are very similar to the mode shapes known for a clamped-free beam (e.g. Thomson and Dahleh, 1998; Hodges and Pierce, 2006).

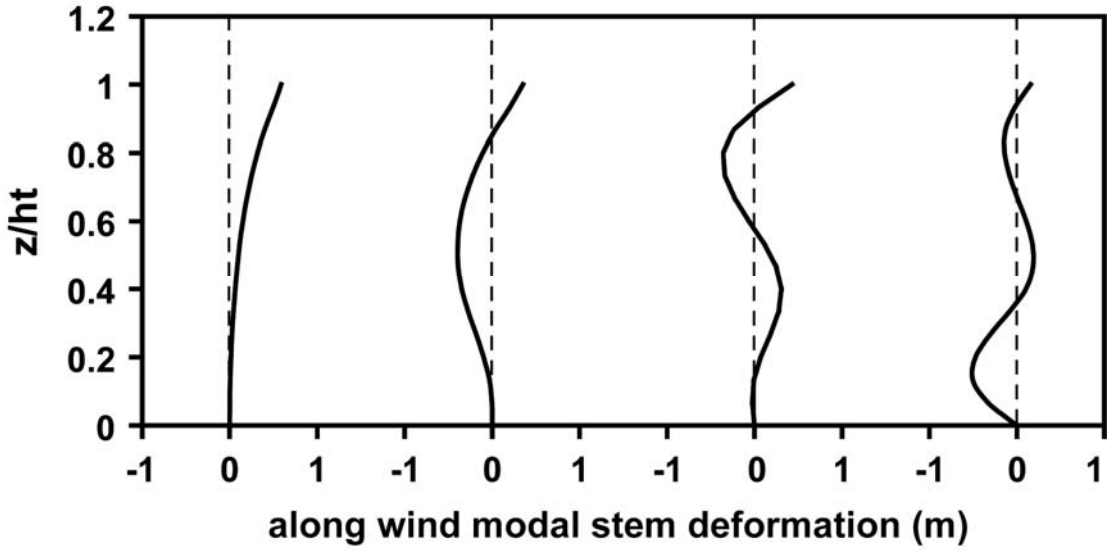

Fig. 3: Shapes of the first four deformation modes of the stem of a Scots pine tree; ht is the sample tree height, z is the height above ground level

Since the presented mode shapes are very similar to the mode shapes of a clamped-free beam it was assumed that only little energy of the swaying tree was dissipated in the rhizome. Otherwise, the modal stem deformations would have been more similar to those of a spring-restrained, hinged-free beam (Hodges and Pierce, 2006).

Due to the fact that the first vibration mode contained the greater part of the tree displacement signal energy even at the lowest recorded wind speeds at canopy height, and because the crowns of the sample trees are rather small, it was also assumed that

- multiple mass damping (James et al., 2006; Spatz et al., 2007) induced by the crowns,
- effects of the foliage (Sellier and Fourcaud, 2005)

were of minor importance for stem displacement damping.

In the observed wind speed range by far most of the energy absorbed by the trees from the wind seemed to be dissipated by the first vibration mode of the stem.

4. Conclusions

Although classical Fourier analyses allowed for the detection of characteristic frequencies at which the sample trees responded well to turbulent wind loading, these frequencies are of limited use as indicators of the covariation between turbulent wind loading and dynamic tree responses in the observed wind speed range. Wavelet analyses revealed that the covariation between wind-induced tree displacement and wind loading is strong in the range of the arrival frequency of coherent structures. It is rather weak in the range of the damped natural sway frequency of the sample trees.

In contrast to findings from other studies most of the energy of the wind, which was absorbed by individual Scots pine trees, was dissipated by the first mode of stem deformation. Crowns and foliage of the Scots pine trees contributed only little to stem displacement damping. The wind load resistance of individual sample trees seems to primarily rely on the deformation of the stem. The contribution of friction between neighbouring trees to stem displacement damping is still to be clarified.

Acknowledgements

The grant of the German Research Foundation (DFG SCHI 868/1) for this work is appreciated. In addition, this investigation was partly performed within the project ‘Development of a risk map for storm damages in forests and forest-significant models for storm damages as bases for methods to reduce storm damages in forests in Baden-Württemberg’, which is part of the RESTER-network (‘Strategies for the reduction of the storm damage risk for forests’) within the research program ‘Challenge climate change’. The authors would like to thank the Ministry for the Environment of the German federal state Baden-Württemberg for the financial support of this project.

References

Aubry, N., Guyonnet, R., Lima, R., 1991: Spatiotemporal analysis of complex signals: theory and applications. J. Stat. Phys. 64, 683-739.

Flesch, T.K., Wilson, J.D., 1999: Wind and remnant tree sway in forest cutblocks. II. Relating measured tree sway to wind statistics. Agric. For. Meteorol. 93, 243-258.

Gardiner, B.A., 1992: Mathematical modelling of the static and dynamic characteristics of plantation trees. In: J. Franke, A. Roeder (eds.), Mathematical modelling of Forest Ecosystems. Sauerländer’s Verlag, Frankfurt am Main, 40-61.

Gardiner, B.A., 1995: The interactions of wind and tree movement in forest canopies. In: M.P. Coutts, J. Grace (eds.), Wind and Trees. Cambridge University Press, Cambridge, 41-59.

Hémon, P., Santi, F., 2003: Applications of biorthogonal decompositions in fluid-structure interactions. J. Fluids Struct. 17, 1123-1143.

Hodges, D.H., Pierce, G.A., 2006: Introduction to Structural Dynamics and Aeroelasticity. Cambridge Aerospace Series, Cambridge University Press, Cambridge.

James, K.R., Haritos, N., Ades, P.K., 2006: Mechanical stability of trees under dynamic loads. Am. J. Bot. 93, 1522-1530.

Mayer, H., 1987: Wind-induced tree sways. Trees 1, 195-206.

Mayer, H., Schindler, D., Holst, J., Redepenning, D., Fernbach, G., 2008: The forest meteorological experimental site Hartheim of the Meteorological Institute, Albert-Ludwigs-University of Freiburg. Ber. Meteor. Inst. Univ. Freiburg, No. 16, 17-38.

Moore, J.R., Maguire, D.A., 2008: Simulating the dynamic behavior of Douglas-fir trees under applied loads by the finite element method. Tree Physiol. 28, 75-83.

Peltola, H., 1996: Swaying of trees in response to wind and thinning in a stand of Scots pine. Bound.-Layer Meteor. 77, 285-304.

Quine, C.P., Gardiner, B.A., 2007: Understanding how the interaction of wind and trees results in windthrow, stem breakage, and canopy gap formation. In: E.A. Johnson, K. Miyanishi (eds.), Plant Disturbance ecology – The process and the response. Elsevier, Amsterdam, 103-155.

Rodriguez, M., de Langre, E., Mulia, B., 2008: A scaling law for the effect of architecture and allometry on tree vibration modes suggests a biological tuning to modal compartmentalization. Am. J. Bot. 95, 1523-1537.

Schindler, D., 2008: Responses of Scots pine trees to dynamic wind loading. Agric. For. Meteorol. 148, 1733-1742.

Sellier, D., Fourcaud, T., 2005: A mechanical analysis of the relationship between free oscillations of Pinus pinaster Ait. saplings and their aerial architecture. J. Exp. Bot. 56, 1563-1573.

Sellier, D., Fourcaud, T., Lac, P., 2006: A finite element model for investigating effects of aerial architecture on tree oscillations. Tree Physiol. 26, 799-806.

Spatz, H.-C., Brüchert, F., Pfisterer, J., 2007: Multiple resonance damping or how do trees escape dangerously large oscillations? Am. J. Bot. 94, 1603-1611.

Thomson, W.T., Dahleh, M.D., 1998: Theory of vibration with applications. Prentice-Hall, London.

Torrence, C., Webster, P.J., 1999: Interdecadal changes in the ENSO-monsoon system. J. Clim. 12, 2679-2690.

Authors' address:

Dr. Dirk Schindler (dirk.schindler@meteo.uni-freiburg.de)
Hannes Fugmann (hannfug@web.de)
Dipl.-Forstw. Jochen Schönborn (jochen.schoenborn@meteo.uni-freiburg.de)
Prof. Dr. Helmut Mayer (helmut.mayer@meteo.uni-freiburg.de)
Meteorological Institute, Albert-Ludwigs-University of Freiburg
Werthmannstr. 10, D-79085 Freiburg, Germany

Experimental investigations of a walnut tree multimodal dynamics

Mathieu Rodriguez[1,2], Bruno Moulia[1], Emmanuel de Langre[2]

[1]INRA & Université Blaise Pascal, Clermont-Ferrand, France
[2]Ecole Polytechnique, Palaiseau, France

Abstract

Experimental data on the frequencies of a walnut tree are presented. These are derived from several kinds of tests using protocols that are commonly used in vibration analysis: pull and release test, hammer impact tests and wind excitation test. The results from these experiments are then used to validate an analytical approach based on the allometry of the tree. This is made possible by a detailed digitization of the tree geometry.

1. Introduction

Over the last decades, time-dependent dynamic effects have been found to play a major part in wind deformations of trees and windbreaks. However, the dynamic interactions between wind and trees are complex issues (Niklas, 1992). Wind velocity has a large spectrum of eddy size and frequency, as well as mean vertical profiles (de Langre, 2008). Most trees also have a branched architecture with different modes of branching (monopodial vs. sympodial) depending on species, up to 11 orders of axes, and reiterated patterns of various sizes and positions (Barthelemy and Caraglio, 2007). A first approach is to tackle this complexity is to focus first on the oscillatory elastic behaviour of the structure (for examples in trees, see Sellier et al., 2006; Moore and Maguire, 2008). A few authors have used modal analysis on trees (e.g., Fournier et al., 1993; Sellier et al., 2006; Moore and Maguire, 2008). All have concluded that modes involving significant branch deformation could rank in-between modes deforming mainly the trunk (Fournier et al., 1993; Sellier et al., 2006). Experiments from Moore and Maguire (2005) and Sellier and Fourcaud (2005) confirmed the excitation of several modes in a conifer trees under wind load, with again some of the modes having their deformation mainly located on branches. Although not using modal analysis, James et al. (2006) also showed that the measured frequency spectra of the responses under wind excitation of four trees with different architectures, including conifers, two eucalyptus and a palm tree, were also significantly dependent on the branching system. Moreover, James et al. (2006) and Spatz et al. (2007) argued that such multimodal dynamics including branch deformation could be beneficial to the tree by enhancing aerodynamic dissipation through a mechanism called multiple resonance damping or multiple mass damping.

In a recent paper, Rodriguez et al. (2008) showed that there exist a relation between the architecture of a tree and its modal organization. More specifically, the ratio between frequencies of flexural modes was directly related to the length/diameter allometry and to the ratio between diameters below and above branching. In their paper, this was validated on frequencies computed from the digitized geometry. Here, we aim at comparing with measured frequencies.

2. Experiments

An experimental investigation of a walnut tree (Juglans regia L.) dynamics has been conducted. The investigated walnut tree is an isolated tree. It is 4.2m high and has a 7.7cm diameter at 1.3m high (Fig. 1). It also has up to eight orders of branching. Preliminarily to the experiment on the tree dynamics, the geometry of the tree (positions, orientations, diameters of the stem segments, and the topology of branching points) was recorded in great details through 3D magnetic digitizing. During the experiment, an electromagnetic system (3Space Fastrak; Polhemus Inc., Colchester,VT, USA) has been used to record the tree dynamics. It consists in creating a magnetic field, around the tree, in which the 3D positions of magnetic sensors can be tracked. Four sensors were positioned on four successive segments of branches of the tree, starting from the trunk. During experiments, sensors were tracked at 30Hz with 1mm spatial resolution. A sonic anemometer was also installed a few meters from the tree to record the wind velocity. For wind excitation, the spectra from both wind velocity and sensors' signals were computed.

Fig. 1: Walnut tree, left: general features, right: digitized geometry; the dots show the position of displacement sensors

Two types of excitation protocols were applied to experimentally investigate the dynamical characteristics of the walnut tree: i) localized controlled excitations and ii) distributed and wide spectrum excitation through natural wind. Localized excitations were obtained through impacts with pull-release tests with a rope and hammer impact. They were applied to four positions corresponding to each segment bearing a sensor, in two orthogonal directions. Spectral analysis was applied to analyze the response of the walnut to these excitations. Figs. 2, 3 and 4 show typical responses that were measured. The spectra show that frequencies of modes could be well defined.

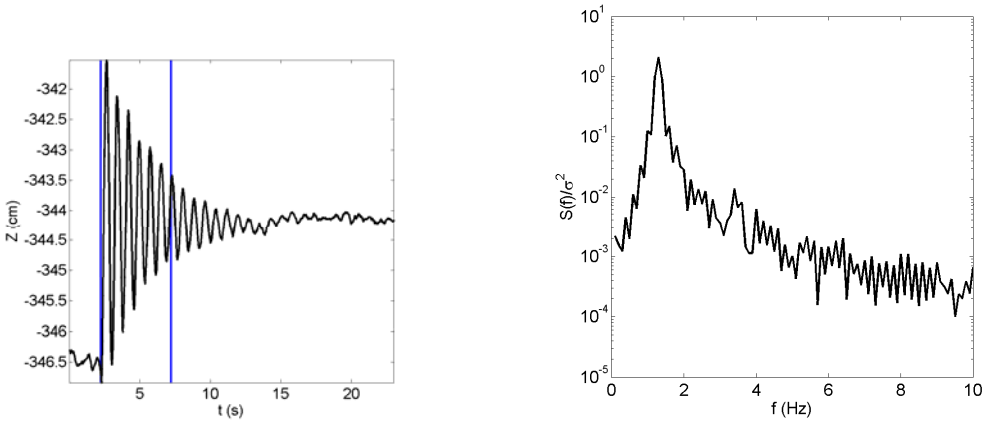

Fig. 2: Pull and release test: typical results, left: displacement as a function of time, right: corresponding spectrum

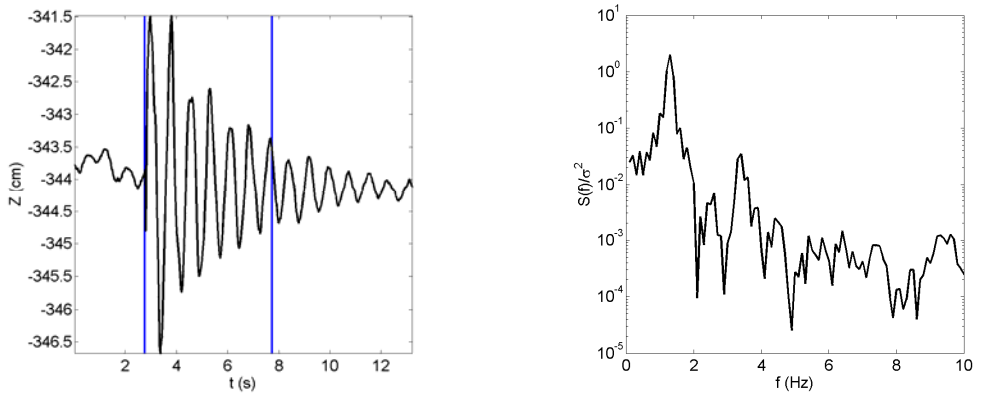

Fig. 3: Hammer impact test: typical results, left: displacement as a function of time, right: corresponding spectrum

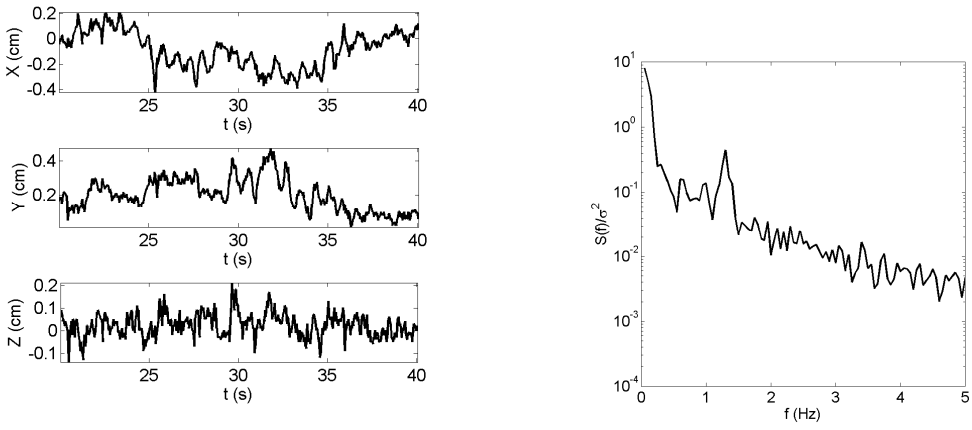

Fig. 4: Response under wind excitation, left: displacements as a function of time, right: corresponding spectrum

3. Comparison with scaling laws

Using data from digitization the relation between length and diameters of segments could be analyzed. Fig. 5 shows that a relation $D \approx L^{\beta}$ with $\beta \approx 0.8$ could be inferred. Similarly the parameter that relates diameters before and after branching is deduced from digitized data, giving $\lambda \approx 0.3$. These two parameters allow deriving the ratio between frequencies, following the results given in Rodriguez et al. (2008). This is also shown in Fig. 5, in comparison with measured frequencies.

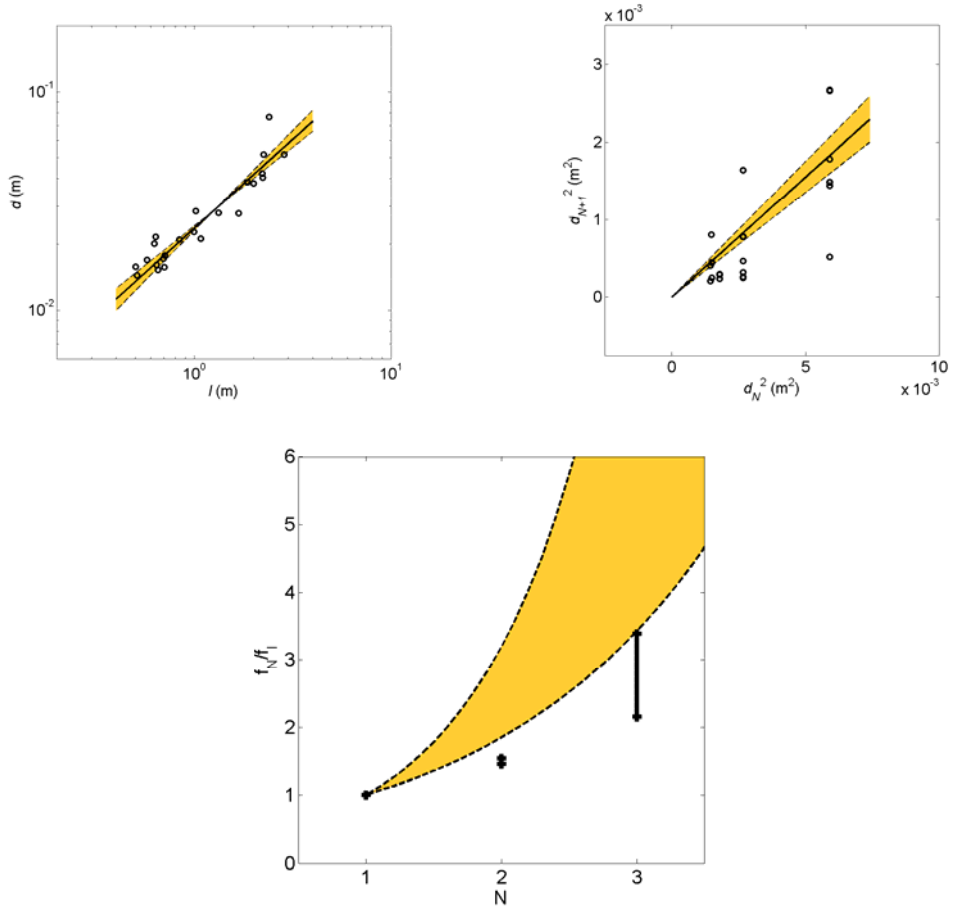

Fig. 5: Comparison between measured frequencies and prediction derived from the allometry of the tree; top left: length/diameter allometry; top right: relation between diameters of successive segments; bottom: measured frequencies and the range predicted from the data above, the shaded zone shows the 90% confidence intervals

5. Conclusions

All these results show that it is possible to infer the organization of modes in a given tree from data derived statistically from its geometry. Other results (not presented here for the sake of brevity) show that frequencies computed by finite elements, lead to very similar values. Moreover, detailed results show that the simultaneous use of pull and release tests, hammer impact tests and wind motion test give consistent results.

Acknowledgement

The authors acknowledge the financial support of the French ANR program "Chene-Roseau" number Blanc062-134798, and the joint CNRS-INRA PhD scholarship for the first author. The help of Boris Adam, Nicolas Donès, Pascal Hémon, Stéphane Ploquin in the experiments is acknowledged.

References

Barthelemy, D., Caraglio, Y., 2007: Plant architecture: A dynamic, multilevel and comprehensive approach to plant form, structure and ontogeny. Annals of Botany 99, 375-407.

Coutand, C., Moulia, B., 2000: A biomechanical study of the effect of a controlled bending on tomato stem elongation. II. local mechanical analysis and spatial integration of the mechanosensing. Journal of Experimental Botany 51, 1825-1842.

de Langre, E., 2008: Effects of wind on plants. Annual Review of Fluid Mechanics 40, 141-168.

Fournier, M., Rogier, P., Costes, E., Jaeger, M., 1993: Modélisation mécanique des vibrations propres d'un arbre soumis aux vents, en fonction de sa morphologie. Annales des Sciences Forestieres 50, 401-412.

Fournier, M., Stokes, A., Coutand, C., Fourcaud, T., Moulia, B., 2005: Tree biomechanics and growth strategies in the context of forest functional ecology. In A. Herrel, T. Speck, and N. Rowe [eds.], Ecology and biomechanics: A biomechanical approach of the ecology of animals and plants, 1-33. CRC Taylor & Francis, Boca Raton, Florida, USA.

Gardiner, B.A., Quine, C.P., 2000: Management of forests to reduce the risk of abiotic damage - A review with particular reference to the effects of strong winds. Forest Ecology and Management 135, 261-277.

Gardiner, B.A., 1992: Mathematical modelling of the static and dynamic characteristics of plantation trees. In J. Franke and A. Roeder [eds.], Mathematical modelling of forest ecosystems, 40-61. Sauerländer, Frankfurt/Main, Germany.

Gerardin, M., Rixen, D., 1994: Mechanical vibrations: Theory and application to structural dynamics. Wiley, Chichester, UK.

James, K.R., Haritos, N., Ades, P.K., 2006: Mechanical stability of trees under dynamic loads. American Journal of Botany 93, 1522-1530.

Mayer, H., 1987: Wind-induced tree sways. Trees - Structure and Function 1, 195-206.

McMahon, T.A., Kronauer, R.E., 1976: Tree structures: Deducing the principle of mechanical design. Journal of Theoretical Biology 59, 443-466.

Moore, J.R., Maguire, D.A., 2005: Natural sway frequencies and damping ratios of trees: influence of crown structure. Trees - Structure and Function 19, 363-373.

Moore, J.R., Maguire, D.A., 2008: Simulating the dynamic behaviour of Douglas-fir trees under applied loads by the finite element method. Tree Physiology 28, 75-83.

Moulia, B., Coutand, C., Lenne, C., 2006: Posture control and skeletal mechanical acclimation in terrestrial plants: implications for mechanical modeling of plant architecture. American Journal of Botany 93, 1477-1489.

Niklas, K.J., 1992: Plant biomechanics: An engineering approach to plant form and function. University of Chicago Press, Chicago, Illinois, USA.

Niklas, K.J., 1994: Plant allometry: The scaling of form and process. University of Chicago Press, Chicago, Illinois, USA.

Rodriguez, M., de Langre, E., Moulia, B., 2008: A scaling law for the effects of architecture and allometry on tree vibration modes suggests a biological tuning to modal compartmentalization. American Journal of Botany 95, 1523-1537.

Sellier, D., Fourcaud, T., 2005: A mechanical analysis of the relationship between free oscillations of *Pinus pinaster* Ait. saplings and their aerial architecture. Journal of Experimental Botany 56, 1563-1573.

Sellier, D., Fourcaud, T., Lac, P., 2006: A finite element model for investigating effects of aerial architecture on tree oscillations. Tree Physiology 26, 799-806.

Sinoquet, H., Rivet, P., Godin, C., 1997: Assessment of the three dimensional architecture of walnut trees using digitising. Silva Fennica 31, 265-273.

Spatz, H.-C., Brüchert, F., Pfisterer, J., 2007: Multiple resonance damping or how do trees escape dangerously large oscillations? American Journal of Botany 94, 1603-1611.

Telewski, F.W. 2006. An unified hypothesis of mechanoperception in plants. American Journal of Botany 93, 1466-1476.

Authors' addresses:

Mathieu Rodriguez (Mathieu.rodriguez@ladhyx.polytechnique.fr)
Dr. Emmanuel de Langre (delangre@ladhyx.polytechnique.fr)
Department of Mechanics, LadHyX, Ecole Polytechnique-CNRS, 91128 Palaiseau,

Dr. Bruno Moulia (Moulia@clermont.inra.fr)
UMR547 PIAF, INRA, Univ Blaise Pascal,
234, avenue du Brézet 63100 Clermont-Ferrand - France F-63100 Clermont Ferrand

Empirical modeling of long-term storm damage data in forests of Southwestern Germany: Judging the impact of silviculture

Axel Albrecht[1], Ulrich Kohnle[1], Marc Hanewinkel[1], Juergen Bauhus[2]

[1]Forest Research Institute Baden-Wuerttemberg, Germany
[2]University of Freiburg, Institute of Silviculture, Germany

Abstract

We analyzed a vast data source of storm damaged trees comprising of single tree and forest stand characteristics in Southwestern Germany. During the reference period of the data set (1950-2007) the majority of storm damage occurred as a result of winter storms in the years 1999, 1990 and 1967. We applied classification and regression tree (CART) methods as well as statistical modeling techniques (generalized linear mixed models, hurdle modeling) in order to consider distributional characteristics and spatial correlations in the data set appropriately. The results enable ordering the explanatory parameters into groups according to their significance for the explanation of storm damage. Forest, soil, wind and site parameters are thus evaluated, and illustrate the impact of silvicultural interventions on storm damage.

1. Introduction

Storm damage in forests is of crucial importance for forest management since it alters the ecosystem abruptly by turning over trees or breaking their stems (Mayer 1987). As a consequence, salvaging the damaged timber is necessary in order to avoid timber depreciation and – especially in coniferous forests – bark beetle infestations. Another effect of storm damage on forest management may be the necessity of replanting or regenerating the damaged forest stands. These effects may lead to important economic losses (Rottmann 1986, Quine 1995). Since storm damage is a constant natural risk and hard to prevent, it may best be considered in the mid- and long-term forest planning processes. Therefore, the main risk factors of storm damage have to be evaluated.

Selective **thinnings** are a common silvicultural practice in Germany with one to three thinning operations per decade in each stand. Besides other risk factors for storm damage such as tree species, stand height, topography and soil properties, these interventions alter the forest stands and thus their storm hazard. In large-scale empirical studies, detailed data on thinnings prior to a storm event are often not available. The few studies with quantitative information on thinnings indicate, however, that the storm resistance of stands is temporarily reduced after these interventions (König 1995, Müller 2002). 3 to 8 years after a thinning, a stand's canopy grows together again and the branches of neighboring trees touch each other again and form collective stability by reinforcing each other (Nielsen 1995). Besides this effect of temporary destabilization, a long-term effect of stabilization is reported by some authors, presumably driven by giving the individual trees more growing space and thus allowing firmer and deeper root anchorage (Kuhr 1999, Redde 2002). Up to today it is not clear how important these thinning effects are when compared to other risk factors. Most variables characterizing thinnings take into consideration information about the amount of removed timber, the time interval and intensity of thinnings and the average diameters of removed trees. A good overview of thinning variables is given in Karlsson and Lennart (2005).

The two main objectives of the study are the consideration of damage data explicitly from several storm events simultaneously and the quantitative analysis of the impact of silvicultural treatment on storm damage.

2. Data and methods

We examined a special source of empirical storm damage data not yet analyzed. The data from the long-term growth and yield experimental plots were available at the Forest Research Institute of Baden-Wuerttemberg (Southwestern Germany). These precise time series data comprise single tree information as well as stand level attributes such as stand density, prior and current silvicultural treatment, soil and site conditions, and orographic exposure. In a first step, the analytical method "classification and regression trees" (CARTs) was applied to both the stand-level and the single-tree-level data sets. CARTs are based on variance partitioning and yield decision tree graphs as a visual output (Venables and Ripley 2002, p. 255, Maindonald and Braun 2007). Key elements are choosing the split variables and their threshold values in order to separate the damaged from the undamaged trees or stands.

In a second step, statistical modeling was applied to both the stand-level and the single tree-level damage data A four-step modeling approach was applied in order to extract the main risk factors for general stand-level occurrence of storm damage (1), for the occurrence of total stand damage (2) and for partial storm damage in the stands (3). The estimated stand-level probability of step 3 was then refined in order to describe the damage potential for single trees within each partially damaged stand (4). The modeling concept and the sequence of the modeling steps are visualized in Fig. 1 and follow the logic of hurdle modeling.

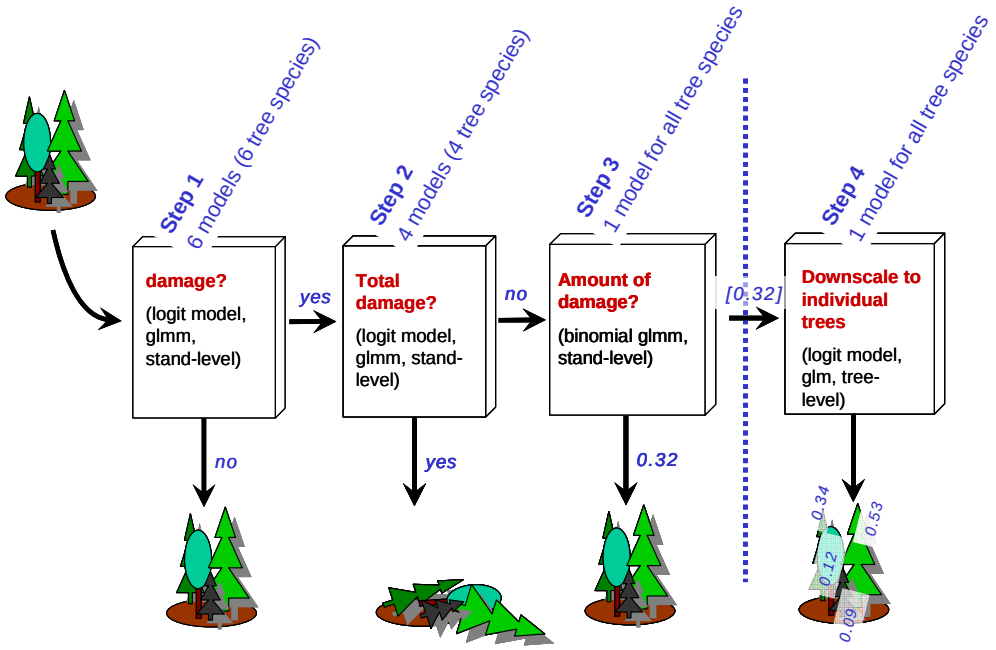

Fig. 1: Flowchart scheme of the modeling steps for the statistical modeling of empirical storm damage data (hurdle model)

In these four steps of statistical modeling, a total of 12 models were fit. In order to summarize the great number of models of our study we present only the impact of variable groups. For each of the selected predictor variables in the 12 statistical models, and also for each split criterion of the CARTs, we calculated a weighting factor that accounted for the weight of the respective model or decision tree. Since the different tree species were represented with different frequencies in the data set, this calculation was necessary for the correct presentation of the summarized results (for calculation formulae see Albrecht 2009, p. 104). However, for the presentation of the silvicultural impact we list the respective variables individually.

3. Results and discussion

With the CART methods it was not possible to summarize the impact of tree species. As shown in Table 1, these methods indicate tree and stand dimensions as the most important variable group for analyzing storm damage (56%). Especially the dominant stand height played the most important role in this group, but also the mean diameter of the trees within a stand had explanatory value. The second most important variable group was the silvicultural interventions (18%), which were dominated by the years since the last thinning and the amount of timber removed by the thinning. Third and fourth most important were the stand density variable group and the historic stand density group (10 and 15% respectively). h/d-ratio, site and soil properties as well as orographic information had little explanatory value.

Table 1: Summarized impact of the predictor variable groups for the analysis of storm damage, separately for the two analysis methods "Classification and Regression Trees" (CART) and statistical modeling; for regrouping the single variables' impact into variable groups, a weighting calculation was applied

variable group	***impact***	
	CART	*statistical modeling*
species		29%
tree/stand dimension	56%	27%
h/d-ratio	0%	15%
stand density	15%	2%
silvicultural intervention	18%	21%
site/soil	0%	3%
historic density	10%	0%
orography/wind data	1%	2%

The tree species is the most important information for the analysis of storm damage if analyzed with the statistical models (29%). Also very important are the tree and stand dimensions (27%). These two variable groups and the group 'silvicultural intervention' (21%) explain the largest part of storm damage risk. The impact of orography and wind data is rather small (2%). This ranking of variable groups is in good accordance with the other research method, the CARTs. However, different rankings are given for the h/d-

ratio, the stand density and the historic stand density. The impact of these variable groups was characterized differently by the two methods.

These results indicate that forest characteristics are most important for analyzing long-term storm damage data consisting of several storm events. Knowing the tree species and the tree or stand dimensions accounts for over half of the explained impact. But as quantified by the two different analytical methods independently, also the silvicultural interventions play an important role for the explanation of storm damage. These findings are remarkable, since additionally to the forest characteristics data on the meteorological and geographic conditions were also available. However, it appeared that soil properties, modeled wind data and the topographic situation (TOPEX to distance index, Wilson 1984, Ruel et al. 1997, Scott and Mitchell 2005) had comparatively little impact.

Table 2: Impact of the silvicultural predictor variables for the analysis of storm damage, separately for the two analysis methods "Classification and Regression Trees" (CART) and statistical modeling; the column on the far right summarizes the impact of both methods by variable groups

		damage impact by direction of impact				*damage impact within silvicultural variables*
	variable	*CARTs*		*statistical modeling*		
#		-	+	-	+	
1	thinning quotient				3.1%	
2	thinning quotient previous intervention		3.5%			38%
3	thinning quotient of past 10 years				8.3%	
4	relative removed volume				0.2%	
5	relative removed volume previous intervention	0.1%			3.7%	
6	relative removed volume of past 10 years				1.0%	21%
7	absolute removed volume		2.6%			
8	absolute removed volume previous intervention	0.7%				
9	years since intervention		11.0%		2.4%	35%
10	cumulated removals			2.2%		6%
		18%		**21%**		**100%**

In order to describe more precisely the impact of **silvicultural treatment** on storm damage the following Table 2 displays the impact of the single predictor variables. The first column contains the variable names sorted by groups. These groups contain information on the thinning quotient (variables 1-3), the amount of timber removed by a thinning (variables 4-8), the years since the last intervention prior to the storm event (variable 9) and the cumulated removed timber. Variables 1-3 were calculated as the average diameter of removed trees divided by the average diameter of all trees before the removal. Variables describing the relative removed volume (4-6) were calculated as the amount of timber removed divided by the amount of timber before the removal. The suffix 'previous intervention' characterizes the variable's value at the time of the previous intervention, as opposed to the current one. The suffix 'of past 10 years' stands for the average value of the respective variable during the past 10 years. The sum of the column 'CARTs' is equivalent to the impact value of the variable group 'silvicultural intervention' in Table 1 (and analogously for 'statistical modeling'). For a further summary we calculated the impacts by silvicultural variable groups (column on the far

right). The results give the proportion of explanatory power for each silvicultural variable group within the total explanatory power by all silvicultural variables. This summary was calculated for both analytical methods together.

Storm damage increases with higher values of the thinning quotient as becomes apparent by the positive direction of impact of the three variables in this group. Thus, silvicultural interventions destabilize stands the more they remove dominant trees. This finding appears plausible since dominant trees usually have a better structural rooting system (Kuhr 1999). Comparable results of other studies are not known to the authors. The second group of variables also showed an increasing impact on storm damage. Thus, the majority of the variables coding the amount of removed timber (variables 4-8) indicate that the stability of stands is decreased with increasing thinning amounts. The two occurrences with contradictory direction of impact (variables 5 and 8) appear in the CARTs methods but carry little overall explanatory power (0.1 and 0.7%) and are therefore negligible. The findings concerning augmented storm risk with higher thinning volumes are in good accordance with the results of other studies (Cremer et al. 1982, Schmid-Haas and Bachofen 1991, Müller 2002) and are probably due to a temporary disruption of the coherent canopy structure. Other studies were able to quantify that thinnings in general have a damage increasing effect, but could not state weather this impact was continuous with increasing amounts of timber removed (König 1995, Nielsen 1995, Aldinger et al. 1996, Jalkanen and Mattila 2000, Dobbertin 2002, Mason 2002, Achim et al. 2005). However, all these findings indicate that the collective stability is reduced through thinning operations.

4. Conclusion

Silvicultural interventions appeared to be the third most important group of variables in order to characterize storm risk while knowledge on tree species and on tree or stand dimensions are first and second most important. Although a wide range of potential predictor variables describing soil conditions, orographic exposure and modeled wind speeds was available, storm damage appeared more dependent on forest information and silvicultural treatment. Thus, especially silvicultural regimes removing the dominant trees from stands may need reconsideration under the aspect of risk avoidance, since the thinning quotient proved to be an important variable for storm damage analysis. Our findings indicate that storm damage analyses should always comprise detailed information on the forests and, if possible, also on the silvicultural past.

References

Achim, A., Ruel, J.-C., Gardiner, B.A., Laflamme, G., Meunier, S., 2005: Modelling the vulnerability of balsam fir forests to wind damage. Forest Ecol. Manage. 204, 35-50.

Albrecht, A., 2009: Sturmschadensanalysen langfristiger waldwachstumskundlicher Versuchsflächendaten in Baden-Württemberg. Freiburger Forstliche Forschung Band 42.

Aldinger, E., Seemann, D., Konnert, V., 1996: Wurzeluntersuchungen auf Sturm-wurfflächen 1990 in Baden-Württemberg. Mitt. Ver. Forstl. Standortskunde u. Forstpflanzenzüchtung 38, 11-24 (in German).

Cremer, K.W., Borough, C.J., McKinnel, F.H., Carter, P.R., 1982: Effects of sto-cking and thinning on wind damage in plantations. New Zealand Journal of Forestry Science 12, 244-268.

Dobbertin, M., 2002: Influence of stand structure and site factors on wind damage com-paring the storms Vivian and Lothar. Forest Snow and Landscape Research 77, 187-205.

Gardiner, B.A., Byrne, K.E., Hale, S., Kamimura, K., Mitchell, S.J., Peltola, H., Ruel, J.-C., 2008: A review of mechanistic modelling of wind damage risk to forests. Forestry 81, 447-463.

Hanewinkel, M., Hummel, S., Albrecht, A., 2009: Assessing natural hazards in forestry for risk management: a review. in review.

Jalkanen, A., Mattila, U., 2000: Logistic regression models for wind and snow dam-age in northern Finland based on the National Forest Inventory data. Forest Ecol. Manage. 135, 315-330.

Karlsson, K., Lennart, N., 2005: Modelling survival probability of individual trees in Norway spruce stand under different thinning regimes. Canadian Journal of Forest Research 35, 113-121.

König, A., 1995: Sturmgefährdung von Beständen im Altersklassenwald. Dissertation, Technische Universität München (in German).

Kuhr, M., 1999: Grobwurzelarchitektur in Abhängigkeit von Baumart, Alter, Standort und sozialer Stellung. Dissertation, University Göttingen (in German).

Maindonald, J., Braun, J., 2007: Data analysis and graphics using R - An example-based approach. Cambridge University Press, Cambridge.

Mason, W. L., 2002: Are irregular stands more windfirm? Forestry 75, 347-355.

Mayer, H., 1987: Wind-induced tree sways. Trees 1, 195-206.

Müller, F., 2002: Modellierung von Sturm-, Schnee- und Rotfäulerisiko in Fichtenbe-ständen auf Einzelbaumebene. Dissertation, Technische Universität München (in German with English abstract).

Nielsen, C.C.N., 1995: Recommendations for stabilisation of Norway spruce stands based on ecological surveys. In: Coutts, M. P. and Grace, J. (eds.), Wind and Trees. Cambridge University Press, Cambridge, 424-435.

Quine, C., 1995: Assessing the risk of wind damage to forests: practice and pitfalls. In: Coutts, M. P. and Grace, J. (eds.), Wind and Trees. Cambridge University Press, Cambridge, 379-403.

Redde, N., 2002: Risiko von Sturm und Folgeschäden in Abhängigkeit vom Standort und von waldbaulichen Eingriffen bei der Umwandlung von Fichtenreinbeständen. Berichte des Forschungszentrums Waldökosysteme, Reihe A, Band 179 (in German).

Rottmann, M., 1986: Wind- und Sturmschäden im Wald. J. D. Sauerländer's, Frankfurt a. M. (in German).

Ruel, J.-C., Pin, D., Spacek, L., Cooper, K., Benoit, R., 1997: The estimation of wind exposure for windthrow hazard rating: comparison between Strongblow, MC2, Topex and a wind tunnel study. Forestry 70, 253-266.

Schindler, D., Grebhan, K., Albrecht, A., Schönborn, J., 2009: Modelling the wind damage probability in forests in Southwestern Germany for the 1999 winter storm 'Lothar'. Int. J. Biometeorol. DOI 10.1007/s00484-009-0242-3.

Schmid-Haas, P., Bachofen, H., 1991: Die Sturmgefährdung von Einzelbäumen und Beständen. Schweizerische Zeitschrift für das Forstwesen 142, 477-504 (in German).

Scott, R.E., Mitchell, S.J., 2005: Empirical modelling of windthrow risk in partially harvested stands using tree, neighbourhood, and stand attributes. Forest Ecol. Manage. 218, 193-209.

Venables, W.N., Ripley, B.D., 2002: Modern applied statistics with S. Springer, New York.

Wilson, J.D., 1984. Determining a topex score. Scottish Forestry 38, 251-256.

Authors' addresses:

Dr. Axel Albrecht (axel.albrecht@forst.bwl.de)
PD Dr. Ulrich Kohnle (Ulrick.Kohnle@forst.bwl.de)
Prof. Dr. Marc Hanewinkel (Marc.Hanewinkel@forst.bwl.de)
Forest Research Institute Baden-Wuerttemberg
Wonnhaldestr. 4, D-79100 Freiburg,, Germany

Prof. Dr. Juergen Bauhus (juergen.bauhus@waldbau.uni-freiburg.de)
Institute of Silviculture, University of Freiburg
Tennenbacher Str. 4, D-79106 Freiburg, Germany

The WINDA-GALES wind damage risk planning tool

Kristina Blennow[1], Barry Gardiner[2]

[1]Southern Swedish Forest Research Centre, Swedish University of Agricultural Sciences, Sweden
[2]Forest Research, Roslin, UK

A wind damage risk forest management planning tool, WINDA-GALES, has been developed. The tool has added functionality compared to the WINDA system of models on which it is based (Blennow & Sallnäs 2004; Blennow & Olofsson 2008). WINDA-GALES can be used to evaluate silviculture strategies and forest planning options with respect to the probability of wind damage. Using climate scenario data and a description of the state of the forest under climate change, the potential probability of wind damage under a changed climate can be estimated (cf. Blennow et al. 2009).

WINDA-GALES provides a geographically explicit environment for stand-wise calculation of the probability of exceeding critical wind speeds for wind damage in a landscape (Fig. 1). The calculations are sensitive to the stability of the forest as well as to the local wind climate.

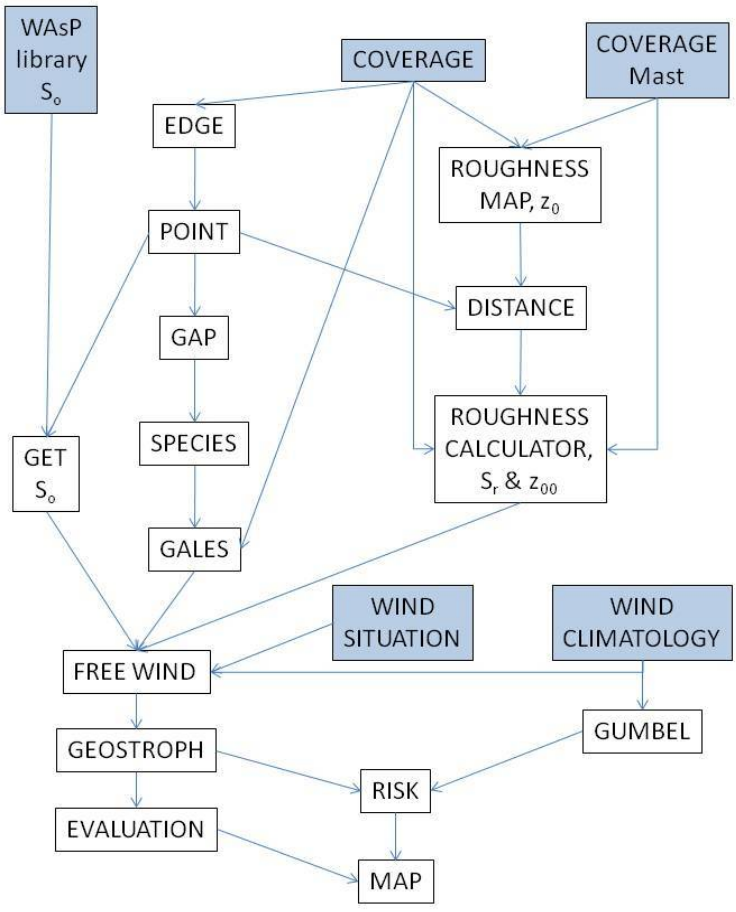

Fig. 1: Flow chart of routines in the WINDA-GALES planning tool, input in blue boxes

The GALES model is used to estimate the stability of the forest stand in terms of critical wind speeds for uprooting and stem breakage at the stand edge or inside the stand (Gardiner et al. 2000). Spatial variables used as input to GALES are estimated using a geographical information system. Calculated critical wind speeds are linked to the geostrophic wind by taking into account effects of the terrain surrounding the stand using a rationale developed for the WAsP airflow model (Mortensen et al. 1993). Input data on speed-up coefficients due to the local topography, S_o, are calculated using the WAsP airflow model and are kept separately in a library. The effect of up-stream roughness changes, S_r, on the wind is estimated according to Kaimal and Finnigan (1994) and the average up-stream roughness length, z_{00}, is estimated using a procedure by Troen & Petersen (1989). The critical wind, U_0, of direction D_0 and at height z above the zero plane displacement height, is cleaned of the effects of topography and surface roughness using

$$U(z) = \frac{U_0(z)}{(1 + S_o(D_0))(1 + S_r(D_0))}$$

where $U(z)$ is the free stream wind speed. Assuming the logarithmic wind–profile for neutral stratification (Thom, 1971), the friction velocity, u_{*0}, is calculated using

$$u_{*0}(D_0) = \frac{\kappa U(z)}{\ln\left(z / z_{00}(D_0)\right)}$$

where κ is the von Kármán constant, here assumed equal to 0.4. $U(z)$ is linked to the geostrophic wind, G, aloft. This is done using Tennekes' derivation of the geostrophic drag law

$$G = \frac{u_{*0}}{\kappa}\sqrt{\left\{\ln\left(\frac{u_{*0}}{f z_{00}}\right) - A\right\}^2 + B^2}$$

where f=2*(the earth's rate of rotation in rad/s)*sin(latitude), and where A and B are dimensionless constants (Kristensen et al. 2000). The numerical values A=1.8 and B=4.5 were used, as recommended by Mortensen et al. (1993) and Troen & Petersen (1989).

The annual probability of exceeding the critical geostrophic wind speed is calculated from a time series of geostrophic wind data using extreme value statistics by Gumbel (1958). The geostrophic wind data can be obtained by linking observed surface wind to the geostrophic wind in a similar way as above, or using output from a regional climate model. The latter option also provides opportunities to calculate the probability of wind damage based on climate change scenario data.

Acknowledgement

This study was carried out as part of the EC FP7 funded MOTIVE project entitled 'Models for Adaptive Forest Management' (ENV-2008-1:226544). Many thanks are due to Magnus Mossberg for programming assistance.

References

Blennow, K., Sallnäs, O., 2004: WINDA - A system of models for assessing the probability of wind damage to forest stands within a landscape. Ecological Modelling 175, 87-99.

Blennow, K., Olofsson, E., 2008: The probability of wind damage under a changed wind climate. Climatic Change 87, 347-360.

Blennow, K., Andersson, M., Bergh, J., Sallnäs, O., Olofsson, E., 2009: Potential climate change impacts on the probability of wind damage in a south Swedish forest. Climatic Change, in press.

Gardiner, B., Peltola, H., Kellomäki, S., 2000: Comparison of two models for predicting the critical wind speeds required to damage coniferous trees. Ecological Modelling 129, 1-23.

Gumbel, E.J., 1958: Statistics of Extremes. Columbia University Press, New York, 375 pp.

Kaimal, J.C., Finnigan, J.J., 1994: Atmospheric Boundary Layer Flows. Oxford University Press, 289 pp.

Kristensen, L. Rathmann, O., Hansen, S.O., 2000: Extreme winds in Denmark. Journal of Wind Engineering and Industrial Aerodynamics 87, 147–166.

Mortensen, N.G., Landberg, L., Troen, I., Petersen, E.L., 1993: Wind atlas analysis and application program (WAsP). Technical Report I-666(EN), Risø National Laboratory, Roskilde, Denmark.

Thom, A.S., 1971: Momentum absorption by vegetation. Quarterly Journal of the Royal Meteorological Society 97, 414–428.

Troen, I., Petersen, E.L., 1989: European Wind Atlas, Risø National Laboratory for Commission of the European Communities Directorate-General for Science and Development.

Authors' addresses:

Assoc. Prof. Kristina Blennow (Kristina.Blennow@ess.slu.se)
Southern Swedish Forest Research Centre, Swedish University of Agricultural Sciences
P.O. Box 49, SE-230 53 Alnarp, Sweden

Prof. Barry Gardiner (Barry.Gardiner@forestry.gsi.gov.uk)
Forest Research, Northern Research Station, Roslin, Midlothian EH25 9SY, Scotland

Modelling wind damage for managed and old-growth stands in Québec

Axel Wellpott[1,2], Barry Gardiner[2], Jean-Claude Ruel[1]

[1]Université Laval, Département des sciences du bois et de la forêt, Sainte-Foy, Québec, Canada
[2]Forest Research, Northern Research Station, Roslin, Midlothian EH25 9SY, Scotland, UK

Abstract

Clear cutting has been the traditional silvicultural practice for most of eastern Canadian forests for many decades. However, more recently there has been a shift towards partial cutting regimes, in which individual trees are left standing mainly to improve the ecological value of the site and speed up the process of natural regeneration. Due to decreased stand density and the creation of gaps those stands are probably more vulnerable to wind damage than those managed with a traditional approach, which might counterbalance any beneficial aspects.

A quantification of the wind risk of an area is desirable to support decision processes in designing cutting plans. Here we present the results from a spatial modelling approach. The model design as well as the sensitivity of its modules are discussed. A major factor for uncertainty is the coarse resolution of the stand data information. A better model performance could be achieved using more data sources like remote sensing.

1. Introduction

The shift in silvicultural practise towards partial cutting regimes raises concerns about the wind stability of the remaining thinned stands. In general a higher thinning intensity is associated with a higher likelihood of wind damage and it is therefore desirable to quantify the wind risk for a large area.

Wind risk models are a suitable tool to estimate the impact of different thinning intensities on the wind stability of all stands in an area. Such results can deliver valuable information that can be used in for forest management decisions.

2. Study area

The study area is in the North Shore region located in the province of Québec, Canada (50°12‘N, 68º14‘W), about 450 km north-east of Québec city. The area is part of the spruce-moss ecological domain and its stands are old growth, unmanaged, and dominated by balsam fir (*Abies balsamea*) and black spruce (*Picea mariana*). The growing process in these stands is rather slow and the stand density is high.

3. pyFGE model

The model used in this study is a clone of the mechanistic British wind risk model ForestGALES (Gardiner et al., 2000), which has been used in many other studies to calculate the wind risk of forest stands. Due to its mechanistic approach it is easily adaptable for different tree species. The necessary information for the species parameterisation for the commercially most important eastern Canadian species has been derived from the

literature: (i) black spruce: Élie and Ruel, 2005; Bergeron et al., 2009 (ii) balsam fir: Achim et al., 2005a (iii) jack pine: Élie and Ruel, 2005; (iv) white spruce: Achim et al., 2005b.

4. Model runs and validation

The model input (Fig. 1) was derived from (i) forest maps, (ii) digital terrain models, and (iii) wind speed maps. The forest maps contain stand information, which are based on aerial photograph interpretation. The model input parameters that were extracted from the forest maps are stand density (stocking), stand height, species composition, and soil drainage. All parameters are encoded and classified which means that the numerical parameters can only be defined within a defined interval. For some of the parameters the classes span a rather wide region, which in turn can have a significant impact on the wind risk calculations for the stand.

The impact of partial cutting management was simulated by applying harvesting scenarios in which a certain percentage of trees (range: 10 to 40 %, step size: 10 %) was removed from the stands.

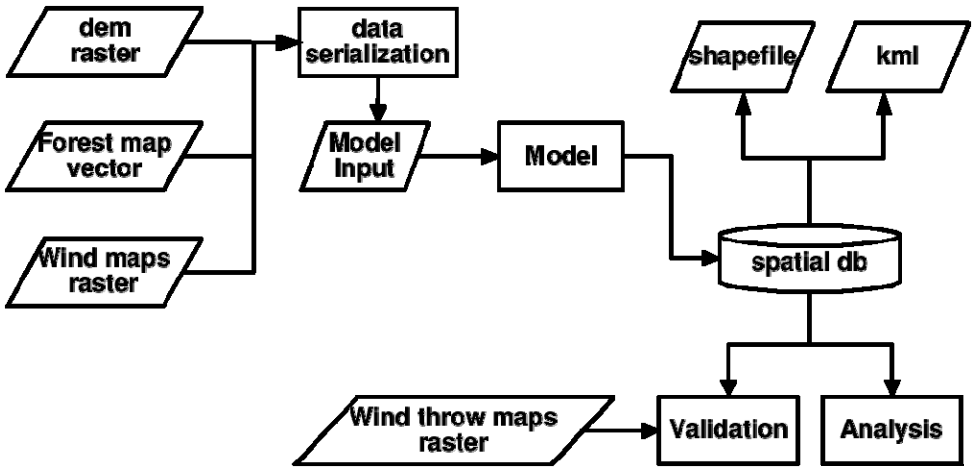

Fig. 1: Flow diagram of the model

5. Results

The study area comprises more than 35000 stands. Almost 45 % of those stands were identified as pure black spruce stands, where the individual stand area covers a size range from less than 100 m^{-2} up to 1.3 km^{-2}. All model input data are only available as classes at the stand level, so that it is not possible to account for internal stand variation, even if the stand is large. The fact that the model input is only available as classes has an impact on the uncertainty of the model calculations. Fig. 2 gives an example of the differences in critical wind speed estimates caused by the stocking and stand top height. Stocking classes cover a range of several 100 trees ha^{-1} and top height classes span several meters. The plot illustrates the differences in critical wind speed calculations, be-

tween model runs, for which the stocking and top height were set to the lower and upper limits of their classes. The figure shows that the uncertainty introduced by the top height parameter is significantly higher (median 4.71 ms^{-1}) than the one introduced by the stocking parameter (median: 0.95 ms^{-1}).

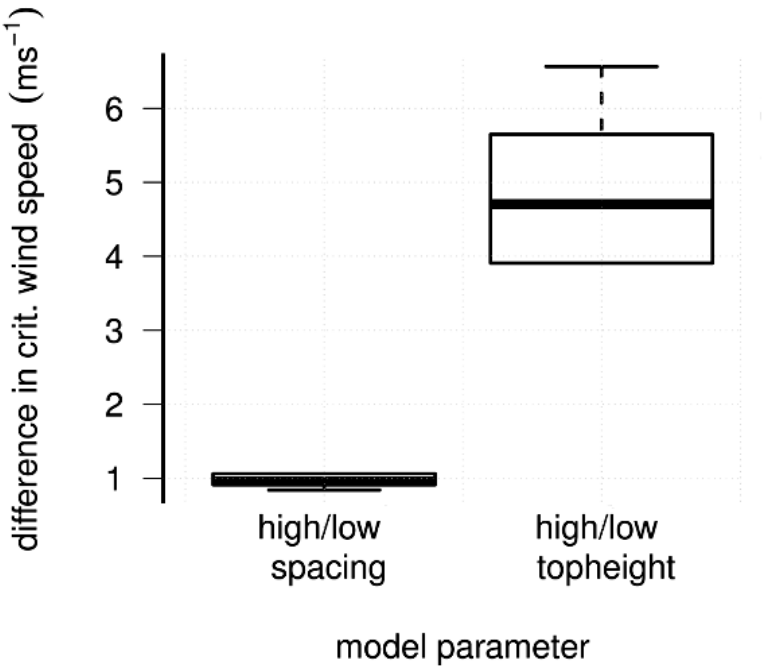

Fig. 2: Boxplot representation of the differences in model calculations for all black spruce stands (n=15303); left plot: differences between high/low stocking density; right plot: differences between high/low top height values

The impact of different thinning intensities on the critical wind speed for the study area can be seen in Fig. 3, where the calculated critical wind speed for all black spruce stands is plotted against the percentage of total area (2126 km^{-2}). The original (unthinned) stand is represented by the solid line, which is as expected the most stable scenario, with only ~15 % of the area experiencing damage at wind speeds up to 20 ms^{-1}.

The risk of wind damage increases with intensity of thinning. At 40 % thinning, a wind speed of 20 ms^{-1} would cause damage across ~85 % of the area.

A comparison of the critical wind speed values for the different thinning scenarios shows that the removal of 10 % of the trees lowers the critical wind speed by about 1 ms^{-1} (median) as it can be seen in Fig. 4. However in some circumstances a removal of 10 % can lower the critical wind speed by more than 2 ms^{-1}. Although these changes do not appear to be big, they can have a significant impact on the likelihood of wind damage for an individual stand, depending on the wind speed distribution at the site. In general the wind speed distribution is approximated by a 2-parameter Weibull distribution. Depending on its shape, differences as they were observed in the thinning scenario study, can shift the estimated return period from a value as high as several decades towards one of only a few years or even less.

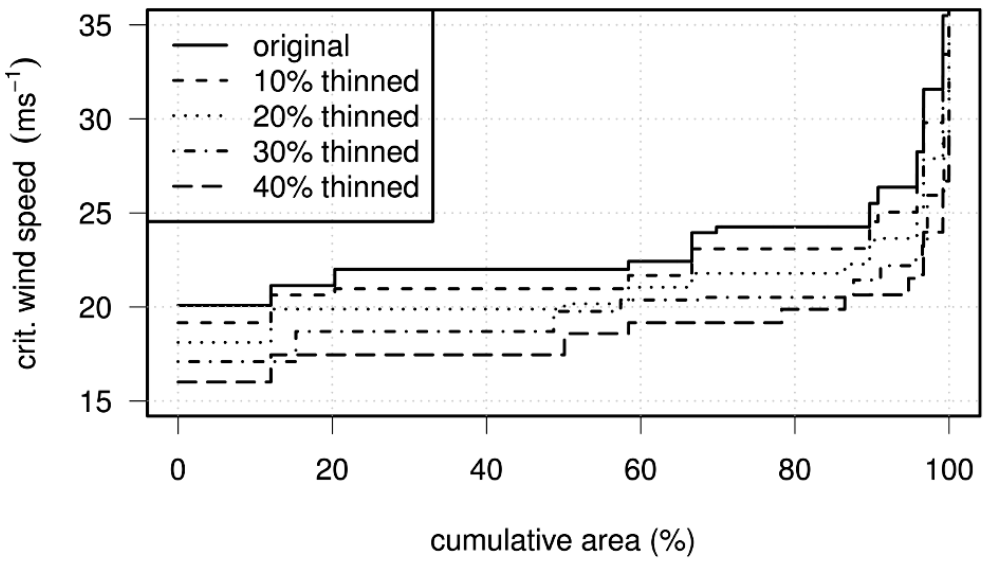

Fig. 3: Critical wind speed for all black spruce stands (n=15303) in the study area plotted against their cumulative area; lines represent different thinnig scenarios

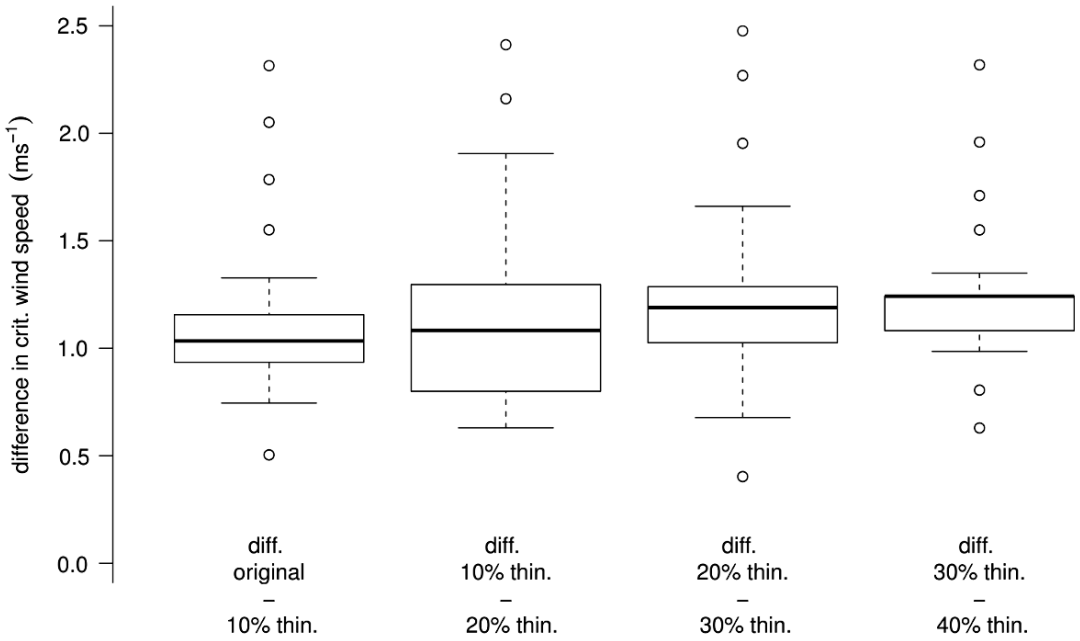

Fig. 4: Differences in critical wind speed between the thinning scenarios

6. Discussion

The model is very sensitive to the stand characteristics, which were derived from the forest map and are only available as rather coarse classes. As a consequence the model results need to be interpreted carefully at the stand level. However, these uncertainties should even out if the model's output is interpreted at the landscape scale rather than at

the stand level scale, so that the results are useful for strategic decision making and can support in the planing of thinning strategies in the area.

Further refinement of the model input and therefore more reliable results could be achieved if more data sources were used to determine the model input.

References

Achim, A., Ruel, J.-C., Gardiner, B.A., 2005a: Evaluating the effect of precommercial thinning on the resistance of balsam fir to windthrow through experimentation, modelling, and development of simple indices. Canadian Journal of Forest Research 35, 1844-1853.

Achim, A., Ruel, J.-C., Gardiner, B.A., Laflamme, G., Meunier, S., 2005b: Modelling the vulnerability of balsam fir forests to wind damage. Forest Ecology and Management 204, 37-52.

Bergeron, C., Ruel, J.-C., Èlie, J.-G., Mitchell, S.J., 2009: Root anchorage and stem strength of black spruce (*Picea mariana*) trees in regular and irregular stands. Forestry 82, 29-41.

Èlie, J.-G., Ruel, J.-C., 2005: Windthrow hazard modelling in boreal forests of black spruce and jack pine. Canadian Journal of Forest Research 35, 2655-2663.

Environment Canada, 2009: Atlas canadian d'énergie éolienne. [http://www.atlaseolien.ca/fr/index.php]

Gardiner, B.A., Peltola, H., Kellomäki, S., 2000: Comparison of two models for predicting the critical wind speeds required to damage coniferous trees. Ecological Modelling 129, 1-23.

Gardiner, B., Byrne, K., Hale, S., Kamimura, K., Mitchell, S.J., Peltola H., Ruel, J.-C., 2008: A review of mechanistic modelling of wind damage risk to forests. Forestry 81, 447-463.

Authors' addresses:

Dr. Axel Wellpott (axel.wellpott@gmail.com)
Forest Research, Northern Research Station
Roslin, Midlothian EH25 9SY, UK

Dr. Barry Gardiner (barry.gardiner@forestry.gsi.gov.uk)
Forest Research, Northern Research Station
Roslin, Midlothian EH25 9SY, UK

Dr. Jean-Claude Ruel (jean-claude.ruel@sbf.ulaval.ca)
Département des sciences du bois et de la forêt
Faculté de Foresterie et de Géomatique
Université Laval, Sainte-Foy, Québec, Canada G1K 7P4

Dynamics of windthrow risk in different forest ecosystems for 21st century (SRES A1B, B1)

Oleg Panferov[1], Andrey Sogachev[2], Claus Doering[1], Bernd Ahrends[1]

[1]Büsgen-Institute, Georg-August University of Göttingen, Germany
[2]Wind Energy Division, Risø National Lab. Sust. Energy, Tech. University of Denmark

Abstract

The probability and extent of wind damage in forest, depend not only on strength of a driving force itself (e.g. wind speed) but also on combinations of effecting agents and on a structure of forest stands. The damage-induced changes in forest structure strengthen or weaken the importance of different windthrow relevant climatic factors at local or even regional scales and thus increase or decrease the probability of the next damage event, creating positive or negative feedbacks. The present study investigates the projected developments of windthrow risks in different forests in 21st Century under conditions of SRES scenarios A1B and B1 (downscaled by CLM) taking into account windthrow-induced changes of forest structure. Risk assessment is carried out for the example region of Solling, Germany calculating water and energy balance of forest ecosystems with BROOK 90 (Federer et al. 2003) and wind loading on trees with Forest-GALES approach under assumption of horizontal homogeneity of forest stands. 85 years old spruce and pine forests are chosen as typical stands and cambisols, podzolic cambisols as typical soil types. The risks of windthrow/breaks for a certain forest stand result from daily combinations of soil water characteristics, wind load on trees with dynamical structure and of soil texture. Model output is aggregated over 30-years periods and compared to "present conditions" of 1981-2010. The results show considerable increment of windthrow risks towards 2100 relatively to "present state" caused by weak changes in precipitation and wind patterns and strong increase of mean air temperature, whereas the increment is higher for pine under A1B and for spruce under B1 scenario. It is shown that for Solling the wind damage induced changes of structure and microclimate provide a positive feedback i.e. - increase the probability of the next damage event.

1. Introduction

Wind damage is a major natural disturbance that can occur in European forests. It was pointed out that the management using decision support systems (DSS) can considerably reduce the risk of windthrow (Gardiner et al 2000). The DSS "Forest and Climate Change" which is currently being developed at the University of Goettingen will provide such a tool for the quantitative assessment of risks including the windthrow and drought for forest ecosystems under the conditions of changing climate (Jansen et al., 2008). The review of scientific literature by Albrecht et al. (2008) demonstrates that the uncertainties of the modelling projections for future storms strengths and frequencies are too large to develop a reliable adaptation strategy upon. On the other hand Peltola et al (1999) indicated that the projected future warmer weather is expected to increase the windthrow risk even without frequent storms, since the tree anchorage during the period between autumn and early spring will be reduced due to a decrease in soil freezing. Thus, the risk of windthrow whenever possible should be estimated as a result of the combined effect of several climatic factors. It is also very important to consider a feedback of each damage event on climatic forcing. The positive feedback of windthrow events on wind forcing in a forest gap was demonstrated by Panferov and Sogachev

(2008). This study investigates the wind damage in stands of three stocking degrees (SD), for two typical tree species: Norway spruce and Scots pine and for two soils under projected climatic conditions of SRES A1B and B1.

2. Materials and methods

a) Site description, tree species, soil conditions: The Solling highlands within the limits of 51.6°N to 52°N and 9.4°E to 9.8°E, i.e. about 1600 km^2 were chosen for investigation. Two tree species: Norway spruce and Scots pine are selected. Each species is represented by three stands with different SDs (stand densities). The correspondent characteristics of all stands are given in Table 1. To consider effects of different soil types and soil textures on root-soil resistance, rooting depth and soil moisture two different soils – cambisol and cambic podzol - are selected, which are typical for the investigation area. The soils are free draining soils, but with very contrasting physical soil characteristics and consequently with different rooting depth (Ahrends et al. in present Issue).

Table 1: Structural characteristics and model parameters for SD classes of two tree species: spruce and pine. a: (Schober, 1995); b: (Hammel & Kennel 2001)

Parameter	**Unit**	**Norway spruce**			**Scots pine**			**source**
age	years	85	85	85	85	85	85	a
stocking degree	[-]	1.0	0.8	0.6	1.0	0.8	0.6	a
stand density	tree ha^{-1}	706	564	423	561	447	335	a
tree height	m	26.6	26.6	26.6	22.3	22.3	22.3	a
DBH	cm	27.9	27.9	27.9	27.2	27.2	27.2	a
Max LAI	$m^2\ m^{-2}$	7.45	5.96	4.47	3.29	2.62	1.96	eq. (2)
Relative winter LAI	[-]	0.8	0.8	0.8	0.6	0.6	0.6	b
SAI	$m^2\ m^{-2}$	1.41	1.12	0.84	1.06	0.85	0.63	eq. (2)

b) Climate projections: The daily mean values of climate variables for A1B, B1 and for C20 with two runs per scenario are obtained from CERA data base (Lautenschlager et al., 2009). For all variables the time series of runs 1 and 2 of A1B and B1 are merged with correspondent runs of C20 so that continuous time series from 1960 to 2100 are built for both runs of A1B and B1. The calculations of abiotic risks with CLM data have been carried out according to the recommendations of Keuler et al (2007). Spatial averaging over the 9 CLM grid points to represent the study area is carried out for all climate characteristics. The calculations of abiotic risks have been done with daily resolution, separately with runs 1 and 2 for both merged C20-A1B and C20-B1. The results for each run are aggregated to annual means. To describe the tendencies of climate development the spatial mean values are then averaged over the 30-years periods: 1981-2010 (P0) – assumed as "actual state" or "reference period", 2011-2040 (P1), 2041-2070 (P2) and 2071-2100 (P3) and relative differences are calculated: $\Delta\varphi i = (\varphi i - \varphi 0) / \varphi 0 * 100\%$, where φi is the 30-years mean value of the spatially averaged climate variable listed above for the climatic period i = 0, 1, 2, 3. The analysis of climate scenarios

data (Fig. 1) shows that in both scenarios the daily mean (V_{av}) and maximal wind velocity (V_{max}) do not change strongly during 21st century. In A1B both V_{av} and V_{max} increase continuously towards P3 with $\Delta V_{av},3$ going up to 2.3% and $\Delta V_{max,3}$ up to 1.6%. In B1 the strongest increases – 1.6% for ΔV_{max} and 2.2% for ΔV_{av} occur from P0 to P1 exceeding the correspondent ΔV_{max} and ΔV_{av} values for A1B. Then decreases to P2 and increases slightly again in P3. The amount of precipitation also does not change much. Both scenarios project a weak increase of precipitation to $\Delta P1 \approx 6\%$ and then slightly monotonically decrease towards 2100 to $\Delta P3 \approx 5\%$. However, the air and soil temperatures increase monotonically (not shown) and rather strongly towards P3 with $\Delta T > 37\%$ in A1B and $\Delta T > 24\%$ in B1.

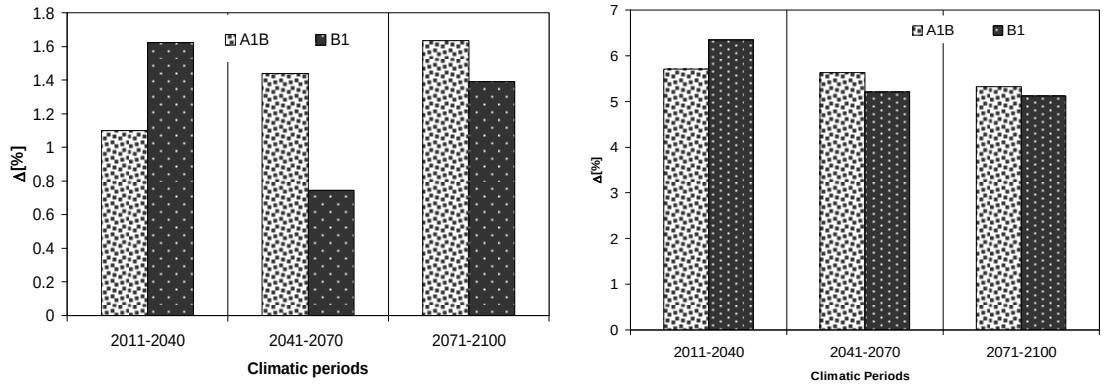

Fig. 1: The changes of annual mean values of daily averaged maximal wind velocity V_{max} (left panel) and precipitation sum (right panel) averaged over 30-years climatic periods relatively to the reference P0 (1981-2011) for two SRES scenarios: A1B and B1

c) Critical wind speed (CWS): The CWS for windbreak, CWS_{break}, and for overturning, CWS_{ot}, defined as the speed at the tree tops are calculated as in ForestGALES. The detailed description and discussions of approach are given in e.g. Gardiner et al. (2000). Additionally the factor accounting for physical support of neighbouring trees (Sup) as in Shelhaas (2007) is used. Influence of rooting depth is taken into account as the linear factor describing positive or negative deviation of tree anchorage and CWS relatively to "average" value (Peltola 1999). Similarly, the effect of soil moisture on windthrow is expressed as linear function of positive and negative deviations of water-holding capacity (WHC) relatively to its reference value: $WHC_{ref} = 0.6\ WHC_{t,s}$, for the certain combination of tree species (subscript "t") and soil type (subscript "s").

d) Risk assessment and feedbacks: In the numeric experiments following assumptions are made: 1) all forest stands are unmanaged; 2) no large gaps result from windthrow event - the windthrow damage is distributed evenly within the forest stand; 3) the survived vegetation is quantified as a share of total stand ($0 \le D \le 1$) which is a function of wind load. The minimal speed leading to windthrow is V_{min}= 8 m s^{-1} (correspondent load is denoted as F_{Vmin}) and the wind speed of $V_{abs.max}$= 40 m s^{-1} is set as the load of full damage, i.e. all trees in stand are damaged (Schelhaas et al., 2007) (correspondent load is denoted as $F_{Vabs,max}$). The relative load provided by actual wind is then:

$$F_{act} = 1 - \frac{F_{V\,abs,\max} - F_{V\,act}}{F_{V\,abs,\max} - F_{V\,\min}} \text{ and } D = 1 - F_{act}^{b} \ ,$$

where b = 3.73 is the best approximation of damage curves for unmanaged stand presented by Schelhaas et al. (2007). To assess the effects of forest structure changes resulting from windthrow events on the probability of next damage event the calculations are carried out in two ways. First – the damage is summed up during the 30-years period but the forest structure does not change. Second – the damage is summed up and the damaged trees are "removed" from the stand – accordingly the stand density and LAI decrease. The calculations with BROOK90 continue from the time point of damage with the new values of structural characteristics. The stand's microclimate changes which in turn enhances or inhibits the following windthrow events thus creating positive or negative feedbacks.

3. Results and discussion

Fig. 2 shows that generally the risk of windthrow damage increase towards 2100 for both spruce and pine stands of all SDs and densities, under the conditions of both scenarios and on both soils. The minimal increase of 10% could not be directly explained by the increase of a wind load alone which is rather weak (Fig. 1). It is obvious that for all climate and soil conditions the risks for the spruce stands are much higher than for pine stands of the same age – even the lowest risk spruce stand with SD=0.6 is higher than the highest risk pine stand with SD=1. The differences in damage values between climate scenarios are not really high for both species and soil types and vary around 2%. However, the patterns of risk's increase differ significantly between scenarios according to climatic signal: for the periods P0 and P1 the risks remain almost the same for both spruce and pine. For spruce on cambic podzol the risks are even slightly higher under B1 reflecting the higher increase of windspeed and precipitation (Fig. 1).

For P2 and P3 the stronger monotonical increase of wind speed under A1B leads to monotonical increase of windthrow risks which is higher than under B1. The latter is characterized by significant decrease of wind during P2 which, however, is not sufficient to decrease the risks. The increase of temperature and higher precipitation compensate the reduction of wind so that the risks remain at the same level as in P1 or even slightly increase. The influence of soil characteristics for two particular soil types is significant for spruce stands and almost negligible for pine ones (Fig. 2). The risks in spruce are higher for all stands on cambisol because of smaller rooting depth. The rates of risks increase are higher on cambic podzol during P0-P1, but during P2-P3 under A1B the rates decrease. Under B1 the risks increase during P2-P3 according to increase of windspeed. For both tree species the risks increase with decreasing of SD and of correspondent stand density which is one of the main factors in estimation of CWS. The analysis of effects of structure changes resulting from windthrow damage shows that the latter perform positive feedbacks increasing the risks of damage up to 4%. The magnitudes of additional feedback contributions to projected windthrow damage are similar for both scenarios and vary slightly for different soils in spruce stands. In pine stands that contribution is slightly lower and almost independent from soil type and SD.

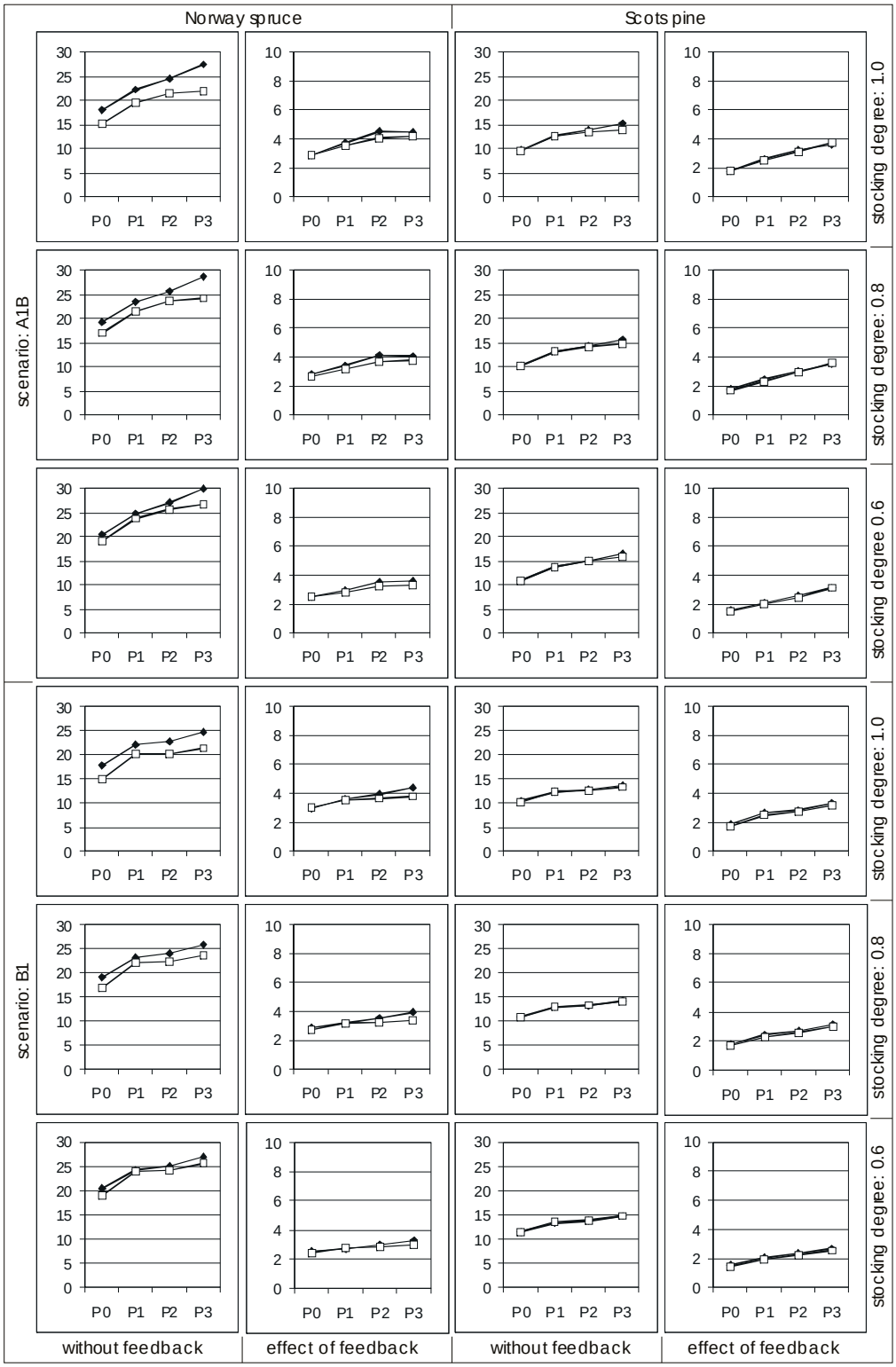

Fig. 2: Scenarios of absolute windthrow damage (%) for different tree species, stand densities and soil types: ─▲─: cambisol, ─□─: cambic podzol

5. Conclusions

The results of present study show that according to climate scenarios A1B and B1 the risks of windthrow damage in mature spruce and pine stands in Solling, Germany will increase up to 30% in 21st century. The magnitude of increment could not be explained by the increase of windspeed and is a result of joint influence of wind, increased temperature and soil water content causing the destabilisation of stands. The pine stands show lower probability of damage than spruce, where damage vary strongly depending on soil type. Within the same species stands with lower SD - with lower density - have higher damage risk. The changes of structure of damaged stands causing changes of microclimate, of wind load on remaining trees and stand stability should be taken into account when assessing projected risks.

Acknowledgements

This study was supported by the German Ministry for Education and Research (BMBF) within the frames of research initiative *klimazwei* (Project DSS-WuK) and by Ministry of Science and Culture of Lower Saxony (Program KLIFF). We gratefully acknowledge this support.

References

Ahrends, B., Jansen, M., Panferov, O., 2008: Effects of windthrow on drought in different forest ecosystems under climate change conditions. Ber. Meteor. Inst. Univ. Freiburg No. 19, 303-309.

Albrecht, A., Schindler, D., Grebhan, K., Kohnle, U., Mayer H., 2008: Klimawandel und Stürme über Europa - eine Literaturübersicht. FVA einblick 01/08, 20-23.

Federer, C.A., Vörösmarty, C., Feketa, B., 2003: Sensitivity of annual evaporation to soil and root properties in two models of contrasting complexity. J. Hydro. 4, 1276-1290.

Gardiner, B., Peltola, H., Kellomäki, S., 2000: Comparison of two models for predicting the critical wind speeds required to damage coniferous trees. Ecol. Model. 129, 1–23.

Granier, A., et al., 2007: Evidence for soil water control on carbon and water dynamics in European forests during the extremely dry year: 2003. Agric. For. Meteor. 143, 123-145.

Hammel, K., Kennel, M. 2001: Charakterisierung und Analyse der Wasserverfügbarkeit und des Wasserhaushalts von Waldstandorten in Bayern mit dem Simulationsmodell BROOK90. Forstliche Forschungsberichte München Nr. 185, 148 S.

Lautenschlager, M., Keuler, K., Wunram, C., Keup-Thiel, E., Schubert, M., Will, A., Rockel, B., Boehm, U., 2009: Climate simulations with CLM, Data Stream 3: European region MPI-M/MaD. World Data Center for Climate. DOIs: 110.1594/WDCC/CLM_C20_1_D3;2 10.1594/WDCC/CLM_C20_2_D3;310.1594/WDCC/CLM_A1B_1_D3;410.1594/WDCC/CLM_A1B_2_D3;510.1594/WDCC/CLM_B1_1_D3;610.1594/WDCC/CLM_B1_2_D3.

Leckebusch, G.C., Renggli, D., Ulbrich, U., 2008: Development and application of an objective storm severity measure for the Northeast Atlantic region. Meteorol. Z., 17, 575-587.

Panferov, O., Sogachev, A., 2008: Influence of gap size on wind damage variables in a forest Agric. For. Meteor. 148, 1869-1881.

Peltola, H., Kellomäki, S., Väisänen, H., Ikonen, V.-P., 1999: A mechanistic model for assessing the risk of wind and snow damage to single trees and stands of Scots pine, Norway spruce, and birch. Can. J. For. Res., 29, 647-661.

Roeckner, E., Brasseur, G.P., Giorette, M., Jacob, D., Jungclaus, J., Reick, C., Sillmann, J., 2006: Klimaprojektionen für das 21. Jahrhundert. Max-Planck-Institut f. Meteor., Hamburg. 28 S.

Schelhaas, M.-J., Kramera, K., Peltola, H., van der Werf, D.C., Wijdeven, S.M.J., 2007: Introducing tree interactions in wind damage simulation. Ecol. Model. 207, 197–209.

Authors' addresses:

Dr. Oleg Panferov (opanfyo@uni-goettingen.de)
Büsgen-Institute, Chair Bioclimatolgy, University of Göttingen
Büsgenweg 2, D-37077 Göttingen, Germany

Dr. Andrey Sogachev (anso@risoe.dtu.dk)
Wind Energy Department, Risø – DTV
P.O. Box 49, DK-4000 Roskilde, Denmark

Dr. Bernd Ahrends (bahrend@uni-goettingen.de)
Claus Doering (cdoerin@gwdg.de)
Büsgen-Institute, Chair Soil Sciences, University of Göttingen
Büsgenweg 2, D-37077 Göttingen, Germany

The development of a wind risk model for irregular stands

Barry Gardiner[1], Sophie Hale[1], Axel Wellpott[1,2], Bruce Nicoll[1]

[1]Forest Research, Northern Research Station, Roslin, Midlothian EH25 9SY, Scotland
[2]Université Laval, Département des sciences du bois et de la forêt, Sainte-Foy, Québec, Canada

Abstract

Modelling wind risk to forests has concentrated to date on damage within uniform stands. However, as continuous cover forestry becomes more widely practised, models will be required that can predict the risk of damage to individual trees within any stand structure. The key to building such models is developing an understanding of the response to wind loading of individual trees of different sizes. In earlier work on nine trees in a mature Sitka spruce stand (Wellpott, 2008) a turning moment coefficient (T_C) was derived as a measure of the maximum turning moment experienced by a tree in response to a given wind speed. It was found that simple competition indices (*CI*), derived from the proximity and relative size of neighbouring trees, could be used to estimate T_C for individual trees.

We have now analysed additional data collected within five different treatments in a Sitka spruce spacing experiment (Gardiner et al., 1997) and from a 2-storey larch stand (Wellpott, 2008). The wind loading, wind speeds and tree locations relative to their neighbours were available from both sites and provided T_C and *CI* for individual trees. Altogether 29 trees were compared across the three experiments and due to the large differences in tree height (h) (8.7-31.9 m) the data were normalised by h^3 (h = tree height) as suggested from earlier wind tunnel experiments (Stacey et al., 1994). We found that the data collapsed onto a single curve giving a strong relationship between T_C/h^3 and *CI*. Further field measurements are underway in order to obtain a more comprehensive data set to fully validate the relationship.

The relationship between competition index and turning moment coefficient provides a method for calculating the response to individual trees to wind loading. This allows the calculation of differences in risk of damage across a stand and to build risk models for complex stand structures.

1. Introduction

Modelling wind risk to forests has concentrated to date on damage within uniform stands. For example, ForestGALES, which is a PC-based wind risk model parameterised for British conditions, calculates the probability of damage to the average tree within a uniform forest stand. However, as continuous cover forestry becomes more widely practised, models will be required that can predict the risk of damage to individual trees within any stand structure.

Key to building such models is developing an understanding of the response to wind loading of individual trees of different sizes. Wellpott (2008) measured turning moment on nine trees in a mature Sitka spruce stand, and derived a turning moment coefficient (T_C) as a measure of the maximum turning moment experienced by a tree in response to a given wind speed:

$$T_C = M_{max}/u^2$$

where M_{max} (Nm) is maximum turning moment experienced in a 10 minute period, and u (ms^{-1}) is the average wind speed at the canopy top for over that period.

Wellpott (2008) found that simple competition indices (CI), derived from the proximity and relative size of neighbouring trees, could be used to estimate T_C for individual trees (Fig. 1). See Appendix for details of the different competition indices.

This paper describes analysis of data from two additional forest stands, to test the wider applicability of the relationship found by Wellpott (2008).

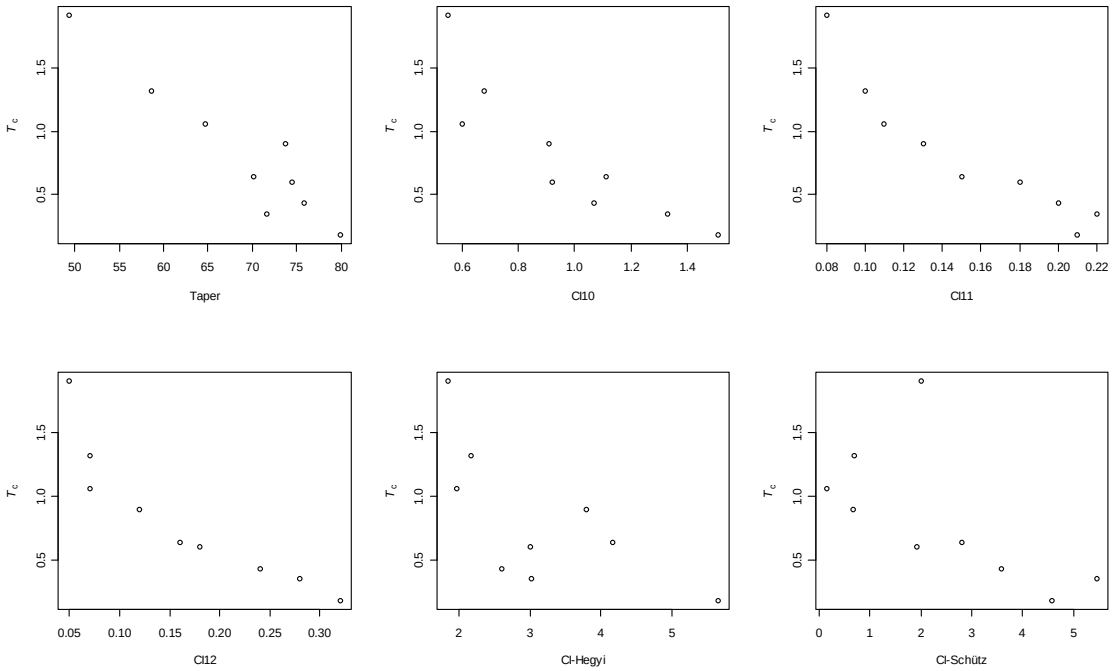

Fig. 1: Turning moment coefficients (T_C) plotted against taper (h/d) and five competition indices for the nine trees at Clocaenog, redrawn from Wellpott (2008)

2. Methods

Data were available from two additional forests, of varying species and structure, as described below. In all stands, turning moments were measured using orthogonal strain transducers, and each tree was calibrated by applying a known load. Wind speed was measured at the canopy top. Diameter at 1.3 m (d) of all trees in each plot was measured. For details of experimental setup, refer to Gardiner et al. (1997) and Wellpott (2008). Measurements of wind loading and wind speeds were analysed to calculate T_C. Mapped tree positions within all plots were processed using Voronoi polygons to objectively identify the neighbours for each sample tree, enabling calculation of competition indices. Of those indices presented by Wellpott (2008), the three based on proximity and d (CI10, CI11 and CI12; see Appendix) were calculated for all sample trees. CI-Hegyi and CI-Schütz were not used as they also require crown dimensions and, based on the Clocaenog data, offered no improvement over the simpler indices.

Kershope

In 1989, Gardiner et al. (1997) measured the wind loading on 11 trees in a Sitka spruce spacing experiment at Kershope Forest, Cumbria (55º 7' N, 2º 42' W). The stand was planted in 1967 at 1.8 x 1.7 m spacing (3200 stems ha^{-1}), and respaced in 1975 to various spacing patterns and densities. Summary characteristics of the five plots used in this study are given in Tables 1 and 2. The number of data runs obtained for each sample tree is shown in Table 2. Where more than one run was obtained for a particular tree, values of T_C presented represent an average of individual runs.

Table 1: Stand characteristics for the three sites

	Clocaenog	Kershope	Kyloe	Kyloe
Species	Sitka spruce	Sitka spruce	European larch	Sitka spruce
Age (yrs)	54	22	59	Not known
Mean height (m)	27	12	25	11
Spacing (m)	5.9	1.8 - 4.9[†]	9.2	Not recorded
[*]Height range (m)	22.8 - 31.9	10.4 - 12.7	21.0 - 27.6	8.7 - 11.3
[*]Diameter range (m)	28.5 - 59.8	14.2 - 22.6	33.7 - 40.6	12.1 - 21.4
[*]*h*/*d* range	0.49 - 0.80	0.47 - 0.88	0.54 - 0.68	0.53 - 0.77

[*] sample trees only
[†] see Table 2

Table 2: Plot characteristics and sample trees at Kershope

Plot number	Treatment[*]	Spacing (m)	Spacing:height	Tree ID (No. of data runs)		
1715	1	1.8	0.14	25 (1)	71 (13)	121 (1)
1709	2	2.4	0.21	34 (1)	70 (4)	
1710	3	2.8	0.24	56 (4)	64 (3)	
1713	4	3.4	0.32	26 (3)	45 (4)	
1707	6	4.9	0.45	21 (4)	43 (1)	

[*] see Gardiner et al. (1997) for treatment descriptions

Kyloe

Measurements were made in 2006 in Kyloe Wood in Northumberland (55º 38' N, 1º 55' E). This was a European larch stand (age 59 years), with a naturally-regenerated Sitka spruce understorey in part of the stand. Wind loading was measured on nine trees: two from the single storey larch, four from the overstorey larch, and three from the understorey Sitka spruce. Stand characteristics are included in Table 1. Understorey trees were excluded from the calculation of Voronoi polygons, in order that the presence of an understorey tree would not cause an overstorey tree to be excluded as a neighbour.

3. Results

Fig. 2 shows T_C plotted against CI10, CI11 and CI12 for Kershope and Kyloe. It can be seen that for all graphs, there is a general decrease in T_C as CI increases, although there is substantially more scatter than shown by the Clocaenog trees (Fig. 1). T_C values from Kershope are an order of magnitude smaller than those at Clocaenog. T_C values from Kyloe span a wide range and overlap with the other two sites. Values of competition indices for the three sites are of the same order of magnitude.

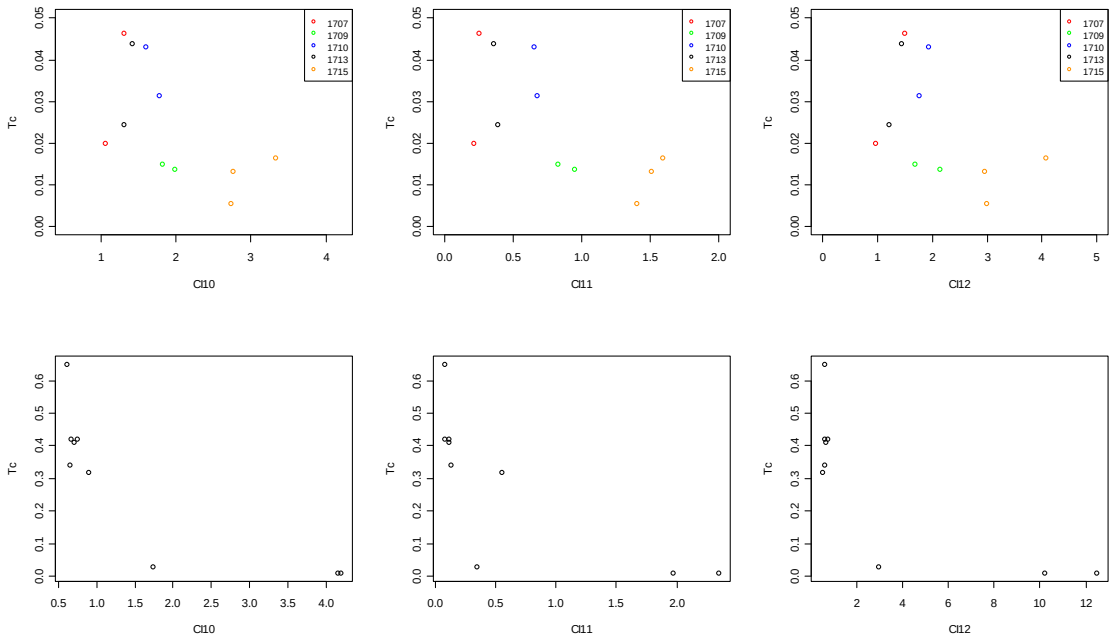

Fig. 2: Turning moment coefficients (T_C) plotted against three competition indices for the experimental trees at Kershope (top three panels) and Kyloe (lower three panels); note the difference in scale for the y-axis; the y-axis in Fig. 2 has been multiplied by 10^6 for clarity of presentation

To accommodate the large difference in tree height across the three sites (8.7 to 31.9 m), the turning moment coefficient data from all sites were normalised by h^3 (h = tree height) as suggested from earlier wind tunnel experiments (Stacey et al., 1994). These

are presented in Fig. 3, and it can be seen that the values of T_C/h^3 for all sites fall within the same range.

The relationship between T_C/h^3 and both CI11 and CI12 showed some separation between the three sites. For CI10, however, the data collapsed onto a single curve, giving a strong relationship between T_C/h^3 and CI. The solid line shown on Fig. 3 represents a preliminary best-fit to the data, and can be used to estimate T_C from CI for an individual tree where the diameter and proximity of neighbours are known. The turning moment experienced by that tree for a given wind speed can then be calculated.

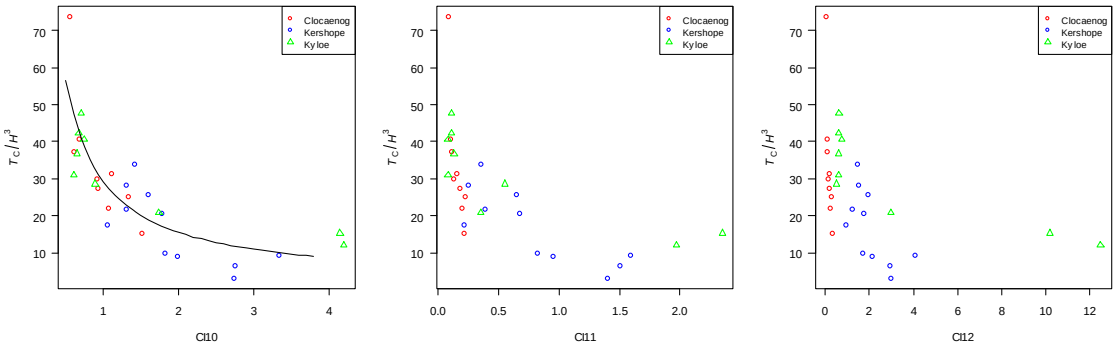

Fig. 3: Normalised turning moment coefficients (T_C/h^3) plotted against three competition indices for the experimental trees at Clocaenog, Kershope and Kyloe; note that the y-axis has been multiplied by 10^6 for clarity of presentation; a preliminary fit has been made to the data in the first panel (black line), which has the relationship $T_C/h^3 = 1.79 + 27.4/\text{CI10}$

4. Discussion

The scatter at Kershope is unsurprising as the data are essentially from five different plots, rather than from a single plot as at the other two sites. Spacing/height varies from 0.14 to 0.45, and differences between individual sample trees within a plot at Kershope are largest in the more widely spaced plots.

The wide range of T_C values recorded at Kyloe is consistent with the difference in tree size between the overstorey and understorey. The low values of T_C measured for the understorey Sitka spruce trees (0.01 to 0.03) were very similar to those recorded for the trees at Kershope (0.01 to 0.05), which were of a similar size (Table 1).

5. Conclusions

The collapse of the data sets from Clocaenog, Kershope and Kyloe onto a single line is very encouraging, particularly given the differences in both species and structure of the forest stands. Competition indices, which are used widely within forest growth modelling, offer a potentially useful tool for apportioning wind energy across individual trees of different sizes within a forest stand. This allows us to calculate the differences in risk

of damage across a stand and to build a risk model for complex stand structures. Further field measurements are underway in order to obtain a wider data set to fully validate the relationship.

References

Gardiner, B.A., Stacey, G.R., Belcher, R.E., Wood, C.J., 1997: Field and wind tunnel assessments of the implications of respacing and thinning for tree stability. Forestry 70, 233-252.

Hegyi, F., 1974: A simulation model for managing jack-pine stands. In: J. Fries (Ed.) Growth models for tree and stand simulation. Royal College of Forestry, Stockholm, pp. 74-90.

Rouvinen, S., Kuuluvainen, T., 1997: Structure and asymmetry of tree crowns in relation to local competition in a natural mature Scots pine forest. Can. J. For. Res. 27, 890-902.

Schütz, J.P., 1989: Zum Problem der Konkurrenz in Mischbeständen. Schweiz. Z. Forstwes. 140, 1069-1083.

Stacey, G.R., Belcher, R.E., Wood, C.J., Gardiner, B.A., 1994: Wind flows and forces in a model forest. Boundary-Layer Meteorol. 69, 311-334.

Wellpott, A. 2008. The stability of continuous cover forests. PhD thesis. University of Edinburgh. pp. 160.

Appendix

Formulae for calculation of the competition indices presented in the report.

From Rouvinen and Kuuluvainen (1997):

$$CI_{10} = \sum_{i=1}^{n} \frac{d_j / d_i}{D_{ij}} \qquad CI_{11} = \sum_{i=1}^{n} \frac{d_j / d_i}{D_{ij}^2} \qquad CI_{12} = \sum_{i=1}^{n} \frac{\left(d_j / d_i\right)^2}{D_{ij}}$$

From Hegyi (1974):
$$CI_{Hegyi} = \sum_{i=1}^{n} \frac{\left(R_j / R_i\right)^{1.3}}{D_{ij}^{0.4}}$$

From Schütz (1989):
$$CI_{Schütz} = \sum_{i=1}^{n} 0.5 - \frac{D_{ij} - \left(R_j + R_i\right)}{\left(R_j + R_i\right)} + 0.65 \cdot \frac{h_i - h_j}{D_{ij}}$$

where:

d is tree diameter at 1.3 m (cm)

i, j represent subject and neighbour tree, respectively

D_{ij} is distance between subject and neighbour tree (m)

h is tree height (m)

R is mean crown radius (m)

n is number of neighbours

For $CI_{Schütz}$, a neighbouring tree is only counted as a competitor if the calculated value is larger than zero.

Author's address:

Dr. Barry Gardiner (barry.gardiner@forestry.gsi.gov.uk)
Forest Research, Northern Research Station
Roslin, Midlothian EH25 9SY, UK

Measuring vibrations of a single, solitary broadleaf tree

Jochen Schönborn, Dirk Schindler, Helmut Mayer

Meteorological Institute, Albert-Ludwigs-University of Freiburg, Germany

Abstract

The vibration behaviour of aerial parts of a fully leafed Norway maple (*Acer platanoides*) tree as well as near-surface airflow properties around the tree are monitored since July 2009. After a short description of the experimental set-up, preliminary results from branch displacement measurements are presented. The first analyses of wind-tree interaction revealed that the sway pattern of aerial parts of the sample tree is very complex and anisotropic.

1. Introduction

Damping of wind-induced tree sways is caused by aerodynamic drag (e. g. Mayhead, 1973; Amiro, 1990; Rudnicki et al., 2004; Sellier and Fourcaud, 2005), structural damping/multiple resonance damping (e. g. Sellier and Fourcaud, 2005; James et al., 2006; Spatz et al., 2007; Moore and Maguire, 2008; Rodriguez et al., 2008), and viscous damping of the wood (Milne, 1991; Wood, 1995). Within forests stands friction between neighbouring trees may also be an important mechanism for the reduction of wind-induced tree movement (Milne, 1991).

Since the vibration behaviour of the aerial parts of forest trees contributes to whole tree movement damping, their responses to turbulent wind loading were analysed in detail in the past (e. g. Mayer, 1987; Peltola et al., 1993; Gardiner, 1992, 1994, 1995; Peltola, 1996, Kerzenmacher and Gardiner, 1998; Flesch and Wilson, 1999; Schindler, 2008). However, most of these studies focused on the dynamic responses of the stem of individual coniferous forest trees. Results from these studies mainly covered characteristics of the first mode of stem deformation.

During the last few years, multimodal vibration behaviour of all aerial parts in response to wind loading became an important research topic (e. g. James, 2003; Sellier and Fourcaud, 2005; James et al., 2006; Spatz et al., 2007; Moore and Maguire, 2008; Rodriguez et al., 2008) in wind-tree interaction research due to its relevance for whole tree movement damping. Anyhow, so far only a few field studies (e. g. James, 2003; James et al., 2006) were carried out in order to study the multimodal vibration behaviour of broadleaf trees under real wind situations. The objective of this field study is therefore to measure and analyse the dynamic responses of the aerial parts of a broadleaf tree, which seasonally loses its foliage, on turbulent wind loading.

2. Experimental set-up

Dynamic responses of a single, fully leafed Norway maple (*Acer platanoides*) tree on wind loading are measured since July 2009. The maple tree is located in the Zartener Becken (Freiburg-Ebnet, 380 m a.s.l.) approx. 5 km (47°58´52.04´´N, 7°55´10.46´´E) to the east of Freiburg. Its height equals to 12.5 m and its diameter at breast height is 37 cm. The length, diameter, inclination, and orientation of all branches with a diameter greater than 2 cm at branch point were measured.

Wind-induced vibration behaviour of the trunk and selected branches (up to the 7th order) with different orientation is monitored (10 Hz) by 29 biaxial clinometers (SCA121T-D05, VTI Technologies Oy, Finland). On the branches (diameter > 2 cm at branch point), the inclinometers were mounted at 2/3 of the distance between two branch points of different order.

Characteristics of the near-surface airflow are monitored (10 Hz) with 17 ultrasonic anemometers, which are mounted on four scaffold towers (Fig. 1). The towers were set up in the four cardinal directions close around the tree. At each tower four ultrasonic anemometers were mounted at 12 m ($z_1/h = 1.0$), 9 m ($z_2/h = 0.75$), 6 m ($z_3/h = 0.5$) and 3 m height ($z_4/h = 0.25$). In addition, one sonic anemometer is used to monitor airflow properties above the sample tree at 16 m. Since airflow from west and east dominates at the measurement site, the sonic anemometers were oriented to the north and south in order to minimize the influence of the measurement towers to on the turbulence measurements.

A commercial PC is used to store all sampled data. The inclinometers are scanned via Data Acquisition System Laboratory Software (DASYLab, National Instruments, Germany). Andreas Christen (Department of Geography, UBC) provided the software used to retrieve sonic anemometer data.

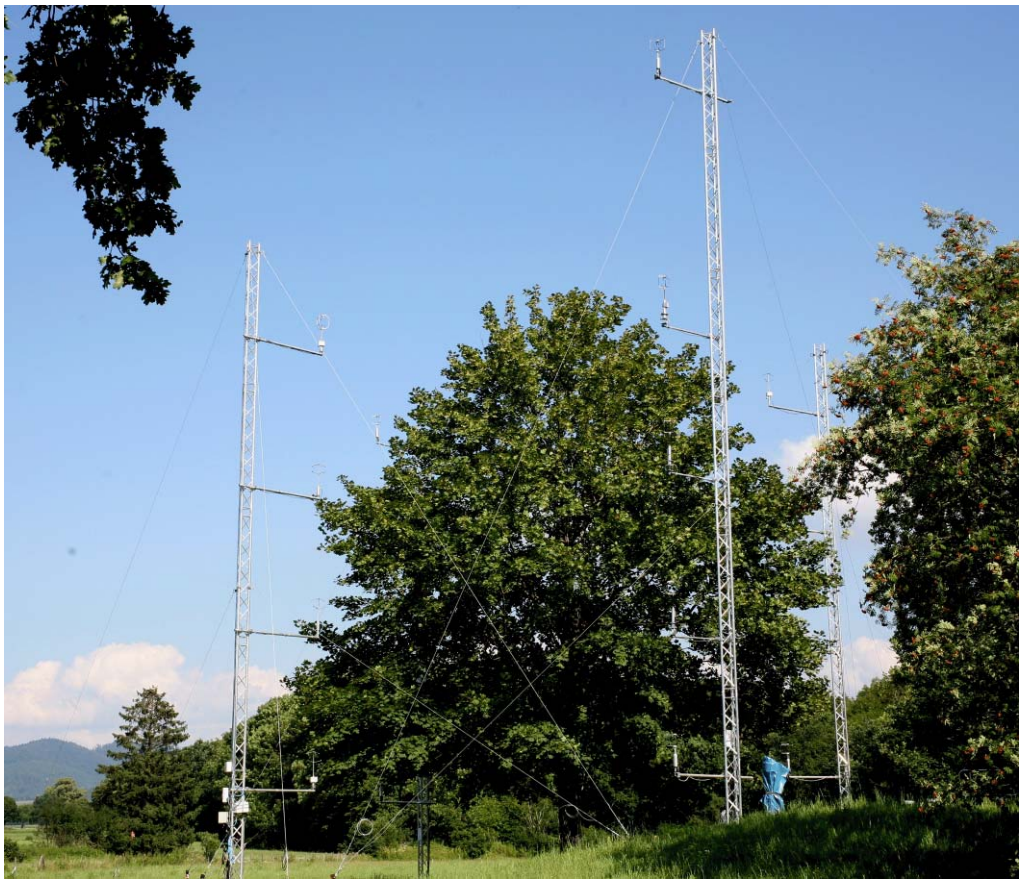

Fig. 1: Fully leafed Norway maple (*Acer platanoides*) tree and measurement towers that carry sonic anemometers at the field site in Freiburg-Ebnet

3. Preliminary results

In Fig. 2, the vertical displacement component y (deg) which is measured at three different distances (0.5 m, 1.0 m, 1.8 m) from the tree's stem of one, slightly upward angled branch (branch no. 15) is shown. With increasing distance from the stem, the values of y increase. It is noticeable that the branch is mainly displaced into one direction. It does not sway back and forth in response to wind loading. After a decrease in wind loading it returns in a position close to its normal position, a displacement pattern similar to the displacement pattern reported by James (2003).

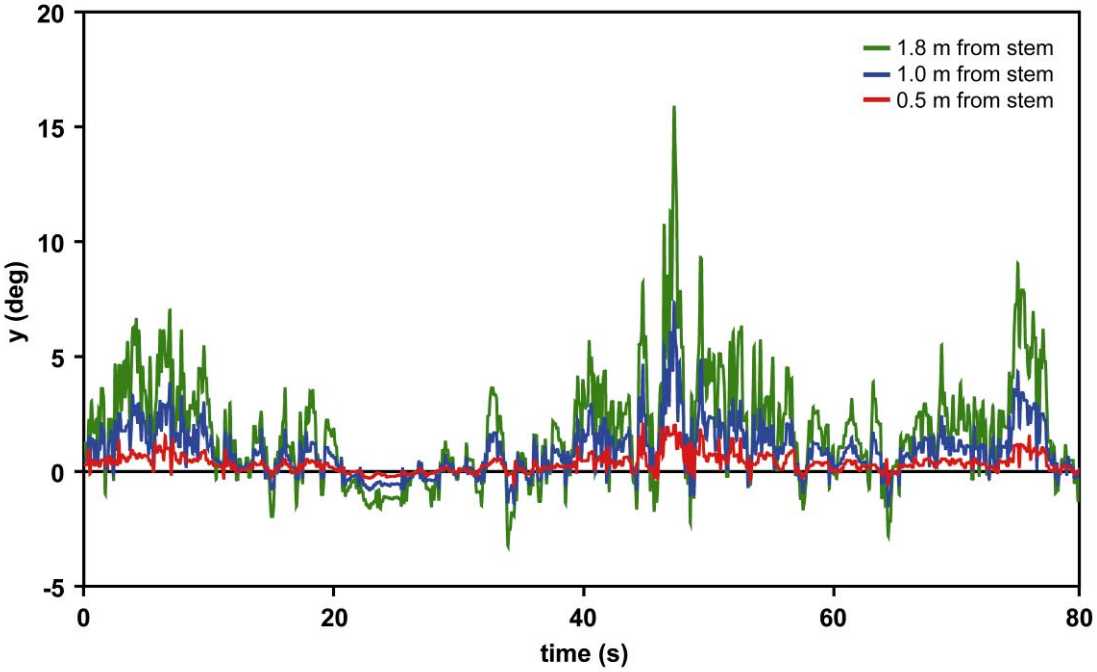

Fig. 2: Vertical displacement y (deg) of a first order branch (branch no. 15) of the Norway maple tree, measured over a period of 80 s at 0.5 m, 1.0 m and 1.8 m distance from the tree's stem

In order to analyse periodicities in the vibration behaviour of the sample tree's branches, a Fourier analysis was carried out. Fig. 3 is a representation of three Fourier energy spectra ($fS_y(f)/\sigma_y^2$), which were computed over an hourly interval from the vertical displacement component y of branch no. 15 which was measured at three different distances (0.5 m, 1.0 m, 1.8 m) from the tree's stem.

The energy spectra show several distinct peaks. These peaks indicate different modes of branch deformation with frequencies in the range of 0.45 Hz (only displacement series measured at 1.8 m distance from stem), 1.3 Hz, 1.8 Hz, and 3.8 Hz.

A further notable feature of the tree's vibration behaviour is the highly anisotropic excitation of its branches by turbulent wind loads. The direction of wind loads determines the response characteristics of the sampled branches. For example, branches oriented

into the direction of an arriving wind load are strongly excited while branches on the reverse side of the tree show no response.

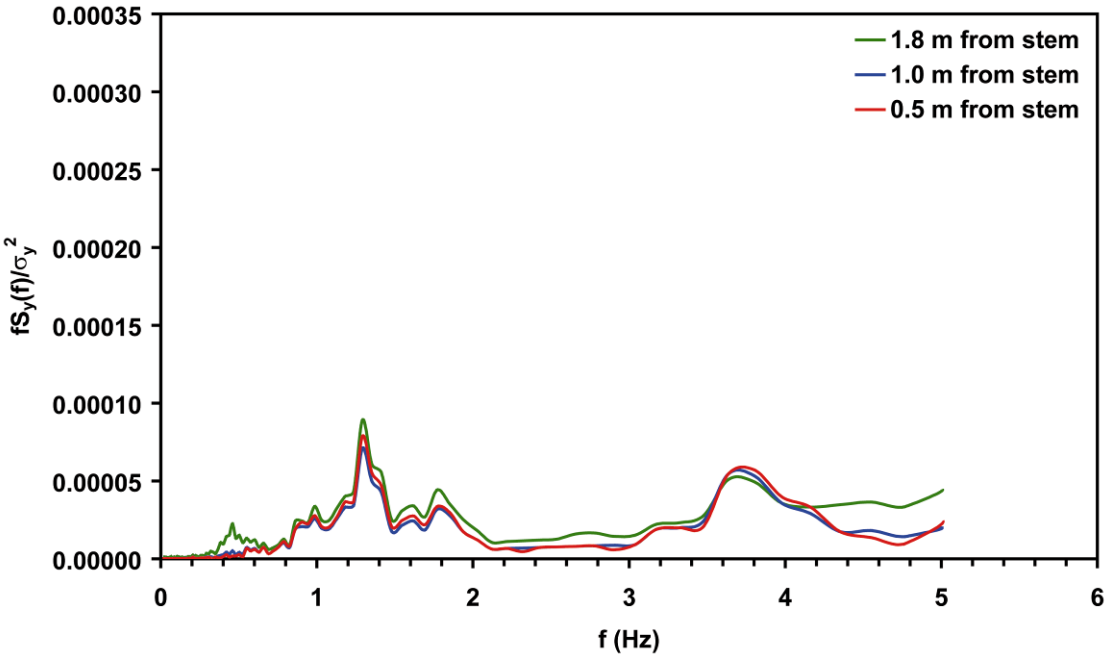

Fig. 3: Spectral energy ($fS_y(f)/\sigma_y^2$) calculated from an hourly series of vertical branch displacement y, which was measured at three different distances (0.5 m, 1.0 m, 1.8 m) from the sample tree's stem

Since the maple tree seasonally loses its foliage, the displacement measurements will continue over the leafless period in winter in order to investigate the effect of foliage on the vibration behaviour of the aerial tree parts.

References

Amiro, B.D., 1990: Drag coefficients and turbulence spectra within three boreal forest canopies. Bound.-Layer Meteor. 52, 227-246.

Flesch, T.K., Wilson, J.D., 1999: Wind and remnant tree sway in forest cutblocks. I. Measured winds in experimental cutblocks. Agric. For. Meteorol. 93, 229-242.

Gardiner, B.A., 1992: Mathematical modelling of the static and dynamic characteristics of plantation trees. In: J. Franke, A. Roeder (eds.), Mathematical modelling of Forest Ecosystems. Sauerländer's Verlag, Frankfurt am Main, 40-61.

Gardiner, B.A., 1994: Wind and wind forces in a plantation spruce forest. Bound.-Layer Meteor. 67, 161-186.

Gardiner, B.A., 1995: The interactions of wind and tree movement in forest canopies. In: M.P. Coutts, J. Grace (eds.), Wind and Trees. Cambridge Univ. Press, Cambridge, 41-59.

James, K., 2003: Dynamic loading of trees. J. Arboriculture 29, 165-171.

James, K.R., Haritos, N., Ades, P.K., 2006: Mechanical stability of trees under dynamic loads. Am. J. Bot. 93, 1522-1530.

Kerzenmacher, T., Gardiner, B., 1998: A mathematical model to describe the dynamic response of a spruce tree to the wind. Trees 12, 385-394.

Mayer, H., 1987: Wind-induced tree sways. Trees 1, 195-206.

Mayhead, G.J., 1973: Some drag coefficients for British forest trees derived from wind tunnel studies. Agric. Meteorol. 12, 123-130.

Milne, R., 1991: Dynamics of swaying of Picea sitchensis. Tree Physiol. 9, 383-399.

Moore, J.R., Maguire, D.A., 2008: Simulating the dynamic behavior of Douglas-fir trees under applied loads by the finite element method. Tree Physiol. 28, 75-83.

Peltola, H., 1996: Swaying of trees in response to wind and thinning in a stand of Scots pine. Bound.-Layer Meteor. 77, 285-304.

Peltola, H., Kellomäki, S., Hassinen, A., Lemettinen, M., Aho, J., 1993: Swaying of trees as caused by wind: analysis of field measurements. Silva Fennica 27, 113-126.

Rodriguez, M., de Langre, E., Moulia, B., 2008: A scaling law for the effects of architecture and allometry on tree vibration modes suggests a biological tuning to modal compartmentalization. Am. J. Bot. 95, 1523-1537.

Rudnicki, M., Mitchell, S.J., Novak, M.D., 2004: Wind tunnel measurements of crown streamlining and drag relationships for three conifer species. Can. J. For. Res. 34, 666-676.

Schindler, D., 2008: Responses of Scots pine trees to dynamic wind loading. Agric. For. Meteorol. 148, 1733-1742.

Sellier, D., Fourcaud, T., 2005: A mechanical analysis of the relationship between free oscillations of Pinus pinaster Ait. saplings and their aerial architecture. J. Exp. Bot. 56, 1563-1573.

Spatz, H.-C., Brüchert, F., Pfisterer, J., 2007: Multiple resonance damping or how do trees escape dangerously large oscillations? Am. J. Bot. 94, 1603-1611.

Wood, C.J., 1995. Understanding wind forces on trees. In: M.P. Coutts, J. Grace (eds.), Wind and Trees. Cambridge University Press, Cambridge, 133-164.

Authors' address:

Dipl.-Forstw. Jochen Schönborn (jochen.schönborn@meteo.uni-freiburg.de)
Dr. Dirk Schindler (dirk.schindler@meteo.uni-freiburg.de)
Prof. Dr. Helmut Mayer (helmut.mayer@meteo.uni-freiburg.de)
Meteorological Institute, Albert-Ludwigs-University of Freiburg
Werthmannstrasse 10, D-79085 Freiburg, Germany

Application of yield surfaces in three-dimensional VHM load space to the stability of trees under wind loading

Tim Newson[1], Padmavathi Sagi[1], Craig Miller[1], Stephen Mitchell[2]

[1]Dept. of Civil Engineering, Faculty of Engineering, University of Western Ontario, Canada
[2]Dept. of Forest Sciences, Faculty of Forestry, University of British Columbia, Canada

Abstract

This paper describes a numerical parametric study using finite element analysis designed to apply the VHM load space method to tree stability under wind loading. Combined vertical, horizontal and moment loads have been applied to a rigid, monolithic root-plate system and conditions required for instability and rotational failure investigated. Comparison has been made with data from a windthrow event associated with a tornado in Ontario, and the findings are discussed in light of wind loading of trees and the complex loading states that lead to wind-throw of trees.

1. Introduction

Resistance to windthrow is a complex interaction between topography, climate, soil type and state, location of the water table and the biomechanics of the tree and its roots. Mechanistic approaches to modelling windthrow are currently limited to semi-empirical relationships linking wind speeds to basal bending moments. Rigorous examination of the biomechanics of the *soil-root-tree* system is still developing. The loading resistance of shallowly buried structural foundations undergoing combined vertical, horizontal and moment loadings is a fundamental geotechnical engineering problem (e.g. Meyerhof, 1953). More recently, the performance of offshore foundations, subjected to cyclical wind and wave loads, has been investigated using three-dimensional VHM load space methods that bound combinations of vertical, horizontal and moment load that cause failure (e.g. Gourvenec & Randolph, 2003). The aim of this investigation is to assess the feasibility of applying these methods to predict the resistance of trees to windthrow. It is assumed that the tree is subjected to combination of vertical (V), horizontal (H) and moment (M) loadings due to self weight and wind loading as shown in Fig. 1. The wind velocity field [u(z)] applies a spatially variable horizontal load to the tree [H(z)], which is typically estimated using drag equations of the form (e.g. Peltola and Kellomaki, 1993):

$$H(z) = \frac{\rho_{air}}{2} C_d A_f(z) u(z)^2 \qquad (1)$$

where: ρ_{air} = fluid density, C_d = drag coefficient, $A_f(z)$ = frontal area and u(z) = wind velocity.

For the purpose of adopting the load space method, a resultant force (H) is assumed to be applied to the tree through the centroid of the vertical wind pressure diagram. The self weight of the tree and root-plate system constitutes the vertical load (V). Thus the 'tree' is assumed to be bounded by the interface of the soil and the root-plate beneath the tree. Since the tree stem acts as a cantilever under the action of these forces, the flexural rigidity of the stem contributes to an additional 'out of balance' component for

the moment (M) that is applied to the base of the tree stem. Thus the tree is required to resist the combination of these three forces, V, H and M to prevent windthrow.

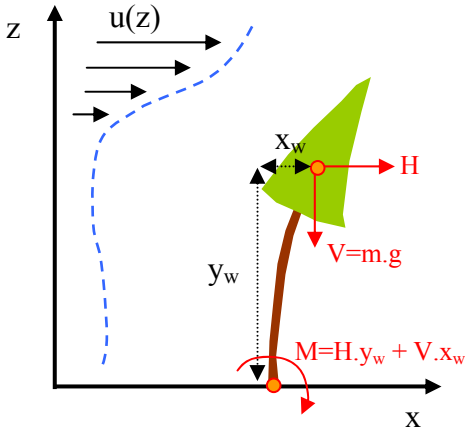

Fig. 1: Applied loading due to self weight and wind loading

2. Numerical methodology

The approach for modelling the root-soil system is based on a number of simplifications and this paper should be treated as a first approximation of this system. The windthrow behaviour of the soil and roots have been investigated using two dimensional plane-strain finite element analysis (with the software PLAXIS®). The soil has been modelled assuming *undrained* soil conditions and a Mohr-Coulomb elastic-perfectly plastic material behaviour. The soil material parameters are the friction angle, (ϕ_u), undrained shear strength (c_u), Young's modulus (E), Poisson's ratio (ν) and unit weight (γ).

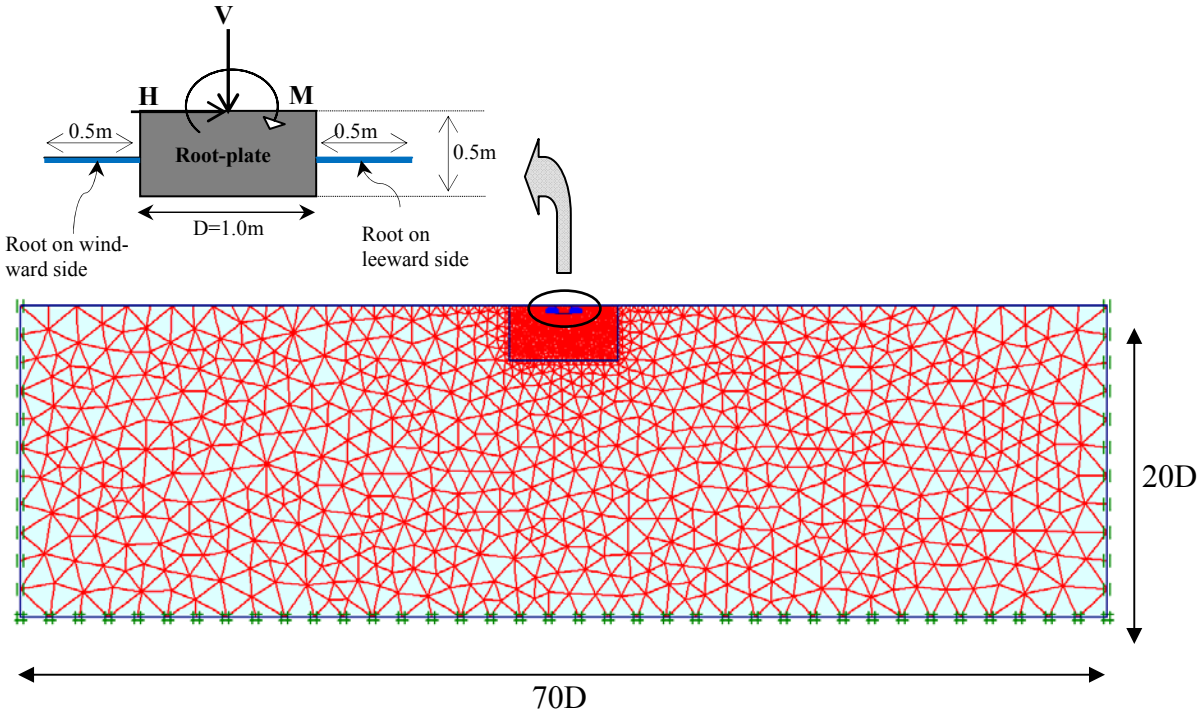

Fig. 2: Generated mesh and boundary conditions

The soil and root system within the 'root plate' has been modeled as a rigid, rectangular monolithic body with unit weight equivalent to that of the soil. Since much of the root system and adjacent soil appears to remain intact during windthrow events, this is thought to be reasonable. The mechanical effect of roots on the leeward and windward side of the tree that extend beyond the root plate has been accounted for by modelling thin, rigid inclusions in the soil attached to the sides of the root plate. Rather than explicitly modelling each of the exposed roots, the stabilising effect of the exposed root 'mass' has been approximately modelled using this approach. Both the root plate and exposed 'roots' have been modelled as non-porous linear elastic materials with Young's modulus (E), Poisson's ratio (ν) and unit weight (γ). A typical finite element mesh and the model geometry used in this study are shown in Fig. 2. The soil and root-plate were modelled using 15-noded triangular elements, which provide fourth order interpolation for displacements; typically about 3000 elements were used for the whole domain. Smooth, rigid boundaries were located sufficiently far from the root system to not interfere with failure mechanisms or stresses in the deforming zone.

Two forms of analysis were performed: (a) where the soil was assumed to remain in intimate contact with the root plate throughout the loading and (b) where detachment of the root plate was allowed. To model this 'breakaway' case, the root plate was surrounded by slip elements, allowing detachment to occur between the root plate and the soil, simulating tensile failure of the soil. A weak interface between the root plate and soil on the plate base and sides was created with a strength parameter reduction factor (R_{int}). This provides a reduced interface friction and interface cohesion (adhesion) compared to the friction angle and the cohesion in the adjacent soil, and allows detachment/separation to occur. Combinations of horizontal, vertical and moment loads have been imposed on the root-plate system (as described below) and the resistive forces were calculated by summating the stresses at the integration points in the soil immediately adjacent to the edges of the root plate (on the sides and bottom).

One of the major aims of the numerical analyses was to investigate the yield envelopes for the root-soil systems in VHM load space. Of particular interest was the shape of the yield envelopes and the soil deformation mechanisms occurring around the root-plate at yield. Stress controlled probes applying prescribed combinations of vertical (V), horizontal (H) and moment (M) loads were increased in magnitude until large displacements occurred. From this approach, failure envelope points (combinations of V, H and M causing windthrow) were calculated. A limited parametric study was performed to assess the changes in the stability of the root-soil system, with varying root plate depth, soil strength, detachment and with/without exposed roots on the sides of the model. All of the root-plate models have assumed a rectangular root-plate with a width (D) =1.0m and a unit length in the orthogonal horizontal direction (due to the 2D constraint). The soil had an undrained shear strength of c_u=25kN/m^2, Young's modulus E = 2500 kN/m^2, Poisson's ratio ν=0.49 and it was assumed that there was no spatial variation in soil strength across the model. All of the failure envelopes have been plotted in a non-dimensional form (using $V'=V/A.c_u$; $H'=H/A.c_u$; $M'=M/A.D.c_u$).

3. Numerical analyses and results

The aspects investigated in the parametric study are (i) depth of the root-plate (d = 0.2 and 0.5 m, representing shallow and deep cases), (ii) 0.5 m long exposed roots modelled

on the windward and leeward sides of the root-plate and (iii) detachment effects between the root-plate and the surrounding soil (full attachment and an interface with only 10% strength & detachment capabilities). The first set of analyses are shown in Fig. 3, which compares shallow and deep root plates (D/d = 5 and 2) with no exposed roots and with full soil attachment only. The shallow system is shown in Fig. 3 (a) and shows the variation in states of H′ and M′ for different vertical loadings from V=0 to 90% of the vertical failure load (V_{ult}). A loading of H′=1 represents a pure sliding case (with no rotational force) and a loading of H′=0 represents a pure rotational case (with no horizontal force). Examples of windthrow found in nature will obviously fall between these two extreme cases. Increasing V is seen to reduce both the moment and horizontal capacity of the tree-root system. For the assumptions of no soil detachment and a shallow root-plate the 'peak' moment capacity occurs towards H′=0 for high V and towards H′=1 for low V. This is due to differences in the volume of soil mobilised beneath the root-plate when subjected to different combinations of V, H and M.

In comparison, the deep root-plate response shown in Fig. 3(b) indicates much higher horizontal and moment capacities. This is due to a greater mass of soil being mobilised at failure and additional resistive (active and passive) soil forces on the sides of the root-plate. Less differences are apparent between the different V loads and no moment peak is found near H′=1 for any of the cases. Both of the sets of envelopes shown in Fig. 3 represent theoretical variations in V that span a wider range than will be found in nature; trees will need to take advantage of their self weight for stability, but this should not be so high as to cause vertical failure of the soil beneath the root system! A preliminary investigation of tree mass and root-plate dimensions (e.g. Duncan & Nicoll, 1998; Cucchi et al., 2004) suggest that for typical soil undrained shear strengths, the mass of the tree will lie between the 0.03 < V/Vult < 0.2. Thus it is likely that trees rely partly on their mass to prevent windthrow, but seem to have self-optimised to avoid the penalties associated with very high masses compared to the soil strength below.

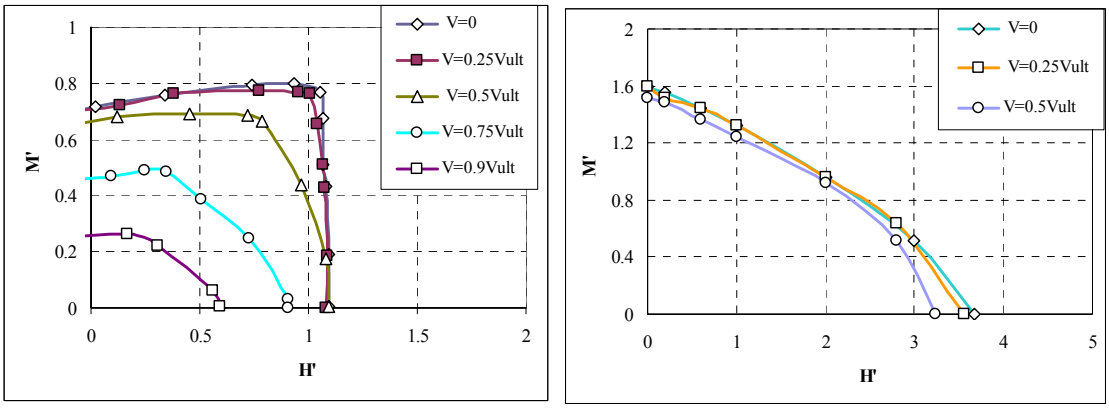

(a) Shallow root-plate (D/d=5) (b) Deep root-plate (D/d = 2)

Fig. 3: VHM failure envelopes for root-plate depth variations (no detachment)

The second set of analyses are shown in Fig. 4, for the deep root-plate systems only and show the effects of detachment of the root-plate from the soil beneath and the effect of

adding lateral and rotational restraint from the addition of exposed roots. Fig. 4(a) shows that detachment of the soil on the base and sides of the root-plate cause a 30-40 % reduction in capacity. Fig. 4(b) shows the envelopes for a deep, detachment case with additional support from exposed roots on the windward and leeward sides. The increase in capacity is seen to be similar to the attached cases shown in Figure 4(b). The roots have been modelled as extremely rigid inclusions (allowing detachment along their length), thus no bending is occurring and this increase in capacity is due to mobilisation of larger volumes of soil at failure. In nature, it would be expected that the bending, shear strength and tensile properties of the roots would dominate and create some rotational resistance, although at the expense of mobilising less soil volume.

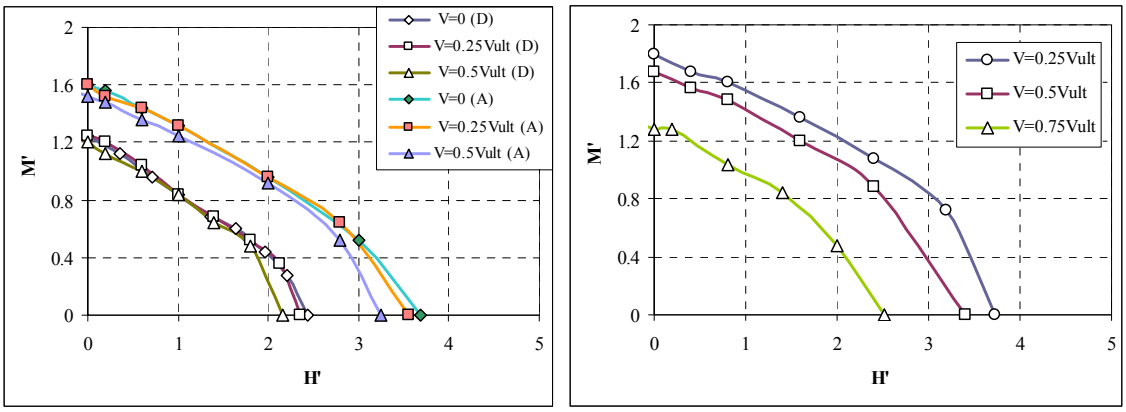

(a) Deep root-plate, with/without attachment (b) Deep root-plate, with roots/detachment

Fig. 4: VHM yield envelopes for variation in horizontal fixity and detachment

4. Windthrow case study

A tornado event caused a damage track 22 km long and 40 to 50 m wide across Southern Ontario in May 2007. Structural damage and storm signatures at more than one location indicated tornado damage in the lower end of the Fujita scale (F1 category, at approximately 36-42 m/s). Numerous trees were damaged along this track and two windthrown Poplar trees were studied by the authors. The height of the trees were (L) 25.9m and the diameter at breast-height (DBH) were 0.42m. The crown frontal area (A_f) was estimated to be 95 m^2 and the dimensions of the root-plate 2.5 x 2.5 m in plan, by approximately 1 m deep. Estimates of the critical windspeed for these trees have been made using the developed VHM envelopes. Since the soil shear strength at the site is unknown, estimates based on c_u = 15, 30 and 60 kPa have been made. Other assumptions were made: (a) the tree is a uniform, circular section cantilever and was loaded by a point load (H) at 3L/4 from the base, (b) the centre of mass of the tree is at 9.3m from the base, (c) the drag coefficient was C_d=0.2 and (d) the proportion of the horizontal capacity (H') mobilised was unknown and estimates based on 0.5, 1 and 2 were used.

For comparative purposes the deep, detached envelopes, with and without exposed roots were used to model the windthrow event. Figure 5 shows variations in the predicted wind speeds with changes in undrained shear strength and flexural rigidity of the tree (EI). These show reductions in the moment capacity and therefore lower critical wind-

speeds with reducing soil strength, no exposed roots and more flexible trees. As the trees become very rigid (as shown in Figure 5b) the critical windspeed appears to reach a threshold value for the given soil undrained shear strength (30 kN/m^2). The data also shows the importance of the proportion of the horizontal capacity mobilised by the forces, with reducing critical windspeeds. The estimated flexural rigidity of the trees lay between 7500 and 10000 kNm^2 and with an assumed c_u = 30 kN/m^2 and H′ = 2, the estimated windspeeds are between 34 and 56 m/s (respectively without and with exposed roots), which given the approximate nature of the analyses is reasonable.

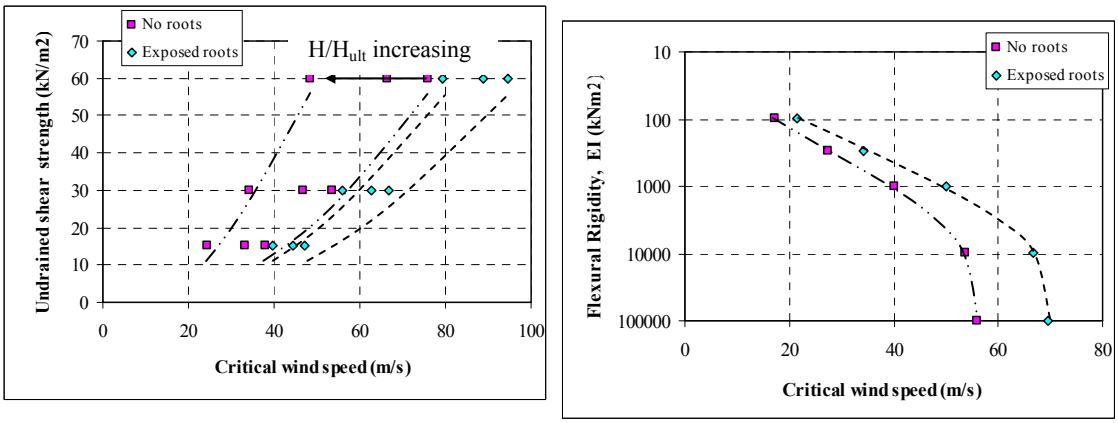

(a) Deep root-plate, with/without attachment (b) Deep root-plate, with root/detachment

Fig. 5: Predictions of critical windspeed for windthrow

5. Conclusions

This paper has described a numerical parametric study using finite element analysis designed to apply the VHM load space method to tree stability under wind loading. Combined vertical, horizontal and moment loads have been applied to a rigid, monolithic root-plate system and the conditions required for instability and rotational failure investigated. Comparison has been made with data from a windthrow event associated with a tornado in Ontario. The results show the importance of lateral and rotational stability from exposed roots and the low vertical stresses imposed by the self-weight of the trees. Despite the simplifications made, the method has provided reasonable estimates of the critical wind speeds for the windthrow event observed.

References

Gourvenec, S., Randolph, M., 2003: Effect of strength non-homogeneity on the shape of failure envelopes for combined loading of strip circular foundations on clay. Geotechnique 53, 575-586.

Meyerhof, G.G., 1953: The bearing capacity of foundations under eccentric and inclined loads. In Proceedings of the 3rd International Conference on Soil Mechanics and Foundation Engineering (ICSMFE), Zurich. Vol. I., 440-445.

Peltola, H., Kellomaki, S., 1993: A mechanistic model for calculating windthrow and stem breakage at stand edge. Silva Fennica 27, 99-111.

Author's address:

Associate Professor Tim Newson (tnewson@eng.uwo.ca)
Geotechnical Research Centre, Dept. Civil Engineering, University of Western Ontario
Spencer Engineering Building, London, Ontario, N6A 5B9, Canada

Root anchorage under the combined condition of wind pressure and intensive rainfall: tree-pulling experiments with controlled soil water content

Kana Kamimura[1], Kenji Kitagawa[2], Satoshi Saito[1], Hayahito Yazawa[3], Taichi Kajikawa[3], Hiromi Mizunaga[2]

[1]Forestry and Forest Products Research Institute, Japan
[2]Department of Forest Resources Science, Shizuoka University, Japan
[3]Centre for Education and Research of Field Sciences, Shizuoka University, Japan

Abstract

Root anchorage was examined under the condition of strong wind and intensive rainfall by conducting tree-pulling experiments with controlled water content in the soil. Wind damage in forests mainly results from typhoons, one of the tropical cyclones, in Japan. Typhoons frequently cause both strong wind and heavy rainfall. Current wind damage studies have focused on wind pressure, while the consideration of intensive water supply to the soil has been absent. Our aim is to analyse the effects of root anchorage when exposed to intensive water supply in the soil. Tree-pulling experiments were conducted for 30-year old hinoki trees (*Chamaecyparis obtusa* Sieb. et Zucc.), one of the most important commercial coniferous species in Japan, in experimental forests of Shizuoka University, Shizuoka Prefecture, Japan. Before the experiments, water was supplied on the soil surface area of 2 x 2 m^2 around a target tree up to 12.5, 25, 50, 100, 200, 400 mm of precipitation. We also examined soil resistance to vertical penetration, water content in the soil and root plate, and soil and root plate movement were additionally measured. Water content inside root plate significantly results in terms of the maximum turning moment at stem base (TMmax). Supplying water reduced soil resistance; however, no relationship was found between vertical resistance of soil and TM_{max}. Although further studies are required, additional impacts on root anchorage such as water content in the soil need to be considered for regions where both strong wind and heavy rainfall are expected.

1. Introduction

This study addressed root anchorage with the combined effects of strong wind and intensive soil water content by conducting tree-pulling experiments on the soil with a controlled water supply. Wind damage in forests has mainly resulted from typhoons, one of the tropical cyclones, in Japan (Chiba, 2000; Kamimura and Shiraishi, 2007). Generally, two types of meteorological characteristics are observed during a typhoon event; catastrophic wind alone or a combination of catastrophic wind and heavy rain. For instance, enormous numbers of trees were failed in Hokkaido Island in 2004 due to strong wind, while damage to forests in Toyama Prefecture during a typhoon event in 2004 was due to heavy rainfall (approximately 100 mm of precipitation for 10 hours recorded at the Fushiki meteorological station) and strong wind. Currently, there are research efforts associated with wind disturbance in forests. However, there is limited information regarding the influence of tree stability caused by a combination of wind pressure and intensive rainfall on soil.

Our aim was to analyse how root anchorage is affected by intensive water supply to the soil. To demonstrate tree uprooting we conducted tree-pulling experiments for 30-year old hinoki trees (*Chamaecyparis obtusa* Sieb. et Zucc.), one of the most important commercial coniferous species in Japan, in experimental forests of Shizuoka University,

Shizuoka Prefecture, Japan. In our study, the maximum turning moment at the stem base (TM_{max}) was considered as the factor to index root anchorage against wind pressure. We primarily supplied water to the soil at the certain level around the target tree, and then plastic flags were set on the surface soil to observe soil and root plate movement. The tree was then artificially pulled down using wire cable until recording the maximum force. Statistical analysis was conducted based on TM_{max} compared to tree characteristics and behaviour such as stem weight and soil movement. This study would be helpful to understand a part of tree stability under intricate conditions caused by typhoon (cyclone) and to improve procedures and analysis on tree-pulling experiments.

2. Methods

Ten 30-year old hinoki trees were selected, which were planted on the brown earth soil. Averages of tree height and diameter at breast height (dbh) were 16.6 m and 18 cm. The trees were located at latitude 34°54'26.6''N and longitude 137°44' 40.6''E in the Kamiatago Experimental Forest of Shizuoka University, Shizuoka Prefecture, Japan. Approximately, elevation is 340 m, slope is 20 degree, and slope aspect is ESE. Tree-pulling experiments were carried out from 1 to 4 June 2009. Mean temperature from 22 May to 4 June was approximately 17° centigrade. Little daily precipitation was recorded before and during the experiment except on 28 May and 3 June.

A 2 m x 2 m wood frame covered with a plastic sheet was previously set around a target tree in order to prevent water from running off. A 1-ton water tank was set near the study area and water was supplied by using a hosepipe from the tank to the stem base of the target trees. Water supply was controlled up to 12.5, 25, 50, 100, 200, 400 mm of precipitation in total. Before providing water we measured surface soil moisture using a hydro sensor (HydroSense TM, Campbell Scientific Australia Pty. Ltd.) at 4 points inside the frame at 20 cm depth from the soil surface. Additionally, before and after water supply soil resistance to vertical penetration was measured using a soil penetromenter (DIK-5521, Daiki Rika Kogyo Co. Ltd.) at 2 points inside the frame from the soil surface to 50 m depth. Soil moisture was further measured below (20 cm depth from the bottom of the root plate) and inside (20 cm inside from the bottom of the root plate) the root-soil plate after pulling down the tree. Before the experiments, tree height and dbh were measured. After supplying water, we set plastic flags with number tape, which were approximately 20 cm height and located at 20 cm apart between flags. Two video cameras and a digital camera were set at the upper and lower side of the target tree to record root-soil plate movement.

Procedure of tree-pulling experiments was mostly based on the previous studies (e.g., Nicoll *et al*., 2005; 2006). A tree was pulled down on a parallel with contour lines. Because there are different root anchorage confirmed by artificially pulling down or up a tree on slope conditions (Nicoll *et al*., 2005), it is important to select pulling direction to minimize experimental effects on anchorage. A tree was pulled down until the maximum force was identified and recorded. After pulling down a tree, we measured tree characteristics such as tree height and stem weight.

After the experiments, grid image files were created based on the video and camera images using IDRISI Andes (Clark Lab.) in order to calculate area and distance of soil movement and root plate. The area was ultimately classified depending on distance with a 0.1 m interval. Subsequently, TM_{max} was calculated for conducting statistical analysis

with tree and soil characteristics such as stem weight, tree height, dbh, water content, and root plate size by using SPSS (SPSS Inc.).

3. Results

All trees were uprooted during the experiments. Nine trees were used for this analysis because one of the target trees failed to record the maximum force. Average stem weight was 207.1 kg and TM_{max} was 30825.6 Nm. Root plate depth was from 0.52 to 0.91 m. Due to the measurement using the grid images, mean area of soil movement at the maximum force was approximately 1.4 m^2 and that of root plate was 1.0 m^2. The plate area of pull side, which is between the stem base and hinge position, was from 0 to 0.32 m^2.

Soil condition including water content showed various phenomena before and after supplying water. Response of soil from water supply varied even though these trees were located on the same site (similar soil type, slope and slope aspect). Water content below the plate was slightly correlated to mean root plate depth (*Sig.* = -0.670 at 0.05 level). In addition, total soil resistance was significantly reduced by supplying water (*Sig.* = -0.721 at 0.01 level). Soil resistance also increased from 10 to 30 cm depth from soil surface both before and after supplying water, while it did not considerably change from 30 to 50 cm depth except the resistance at 40 cm depth recorded before supplying water (Fig. 1). Although there was an exception, the soil layer deeper than 30 cm would become more stable than the shallower soil layer in terms of stiffness and response to water supply.

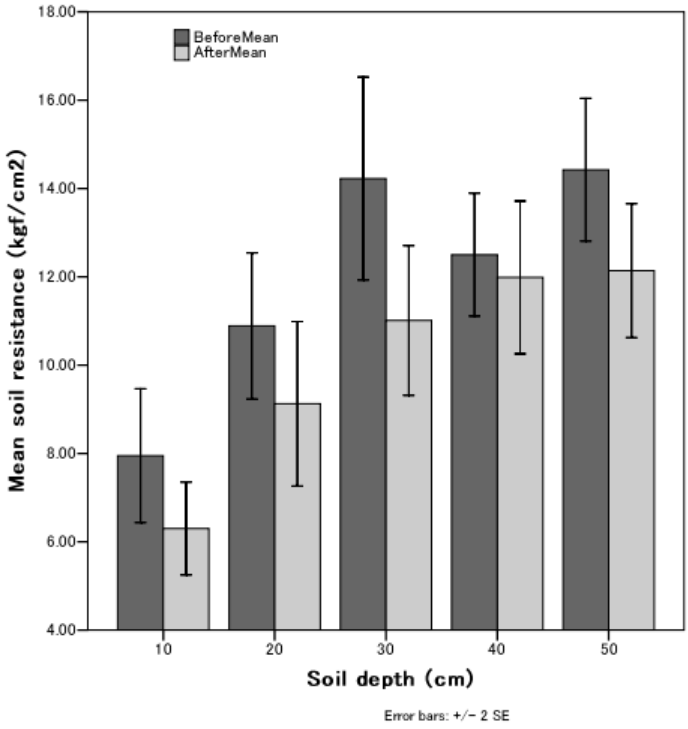

Fig: 1: Mean soil resistance (kgf/cm^2) measured at 10, 20, 30, 40, and 50 cm depth from the soil surface before and after supplying water

To examine tree stability, the relationship between TM_{max} and tree characteristics was statistically analysed using Pearson correlation (2-tailed). Stem weight, dbh, squared dbh multiplied by tree height (dbh^2h), mean root plate depth, root plate volume, water content below plate and inside plate were significantly correlated to TM_{max} at 0.05 level (Table 1). Soil resistance (stiffness) tended to decrease with supplying water. However, we did not find any relationship between TM_{max} and total soil resistance and TM_{max} and soil resistance at any depth from the soil surface.

Table 1: Pearson correlation ($p > 0.05$) of tree and soil characteristics significantly associated with TM_{max}. These physical characteristics of the pulled down trees and the soil condition were statistically correlated to TM_{max}.

Factors	n	Pearson correlation
Stem weight	9	0.683
dbh	9	0.727
dbh^2h	9	0.691
Root plate width	9	0.747
Root plate volume	9	0.676
Water content below root plate	9	-0.728
Water content inside root plate	8	0.827

Lateral surface area of the root plate located at certain distance from the stem position was more likely to be associated with root anchorage. For instance, the lateral root plate area at 0.6 - 0.7 m apart from the stem position indicated the significant effects to TM_{max} (*Sig.* = 0.836 at 0.01 level, n=8). This finding suggests that the more lateral root plate area at this position, a stronger root anchorage would be expected. No relationship was found between TM_{max} and hinge position, between TM_{max} and pull side area, and between TM_{max} and area of soil movement.

Several tree characteristics showed significant relationship to TM_{max} (Table 1). The correlation of stem weight and dbh^2h with TM_{max} tended to be lower than that in previous studies such as Achim *et al*. (2005) and Peltola *et al*. (2000). This would be due to limited tree size used for these experiments. Water contents below and inside the plate also indicated significant relationship with TM_{max}. This suggested that root anchorage would be reduced when water penetrates through root plate into deep layers of soil. On the other hand, root anchorage with high water content in the plate was better than that with less water content.

4. Discussion

Intensive water supply, in other words heavy rainfall, changed soil condition and root anchorage in this study site. The amount of penetrated water through the root plate and of the remaining water in the root plate was more likely to affect root anchorage. Additionally, water in the root plate would contribute to strength root anchorage by adding extra weight. This is because root plate is one of the keys to enhancing root anchorage (Coutts, 1986). On the other hand, water below the root plate would reduce root anchorage. When a tree is pulled or pressed strongly, a space is created between the soil and root plate. In wet soil, the space is more likely to be filled with water and to liquefy soil around the space (Ray and Nicoll, 1998). In addition, positive correlation was found

between the stem angle at the maximum force and water content below the root plate (*Sig.* = 0.639 at the 0.05 level), which means that a large stem displacement occurred with high water below the root plate. This indicates that the root plate will tend to slip caused by a liquid layer between root the plate and soil.

Soil resistance was not directly related to TM_{max}, while the resistance was mostly reduced due to water supply. Coutts (1986) indicated that soil resistance would be the most significant factor before applying the maximum force, and subsequently become less important on root anchorage compared with windward roots and weight. In addition, the tree used for the experiments tended to have deep root system. Our results showed that soil resistance deeper than 30 cm would become slightly stable compared with shallower soil layer. This might enhance anchorage of a deeper part of root plate. Consequently, vertical resistance of soil was less sensitive to root anchorage than other factors such as water content, which was directly associated with liquid soil under the root plate.

Although the tree sizes for the experiments were limited, we found additional factors associated with root anchorage, i.e. water contents below and inside the root plate. This would be because mechanical balance of tree components against pressure might be changed due to unusual water in the soil. Stem weight and dbh^2h are often beneficial when considering tree stability especially for mechanistic wind damage risk assessment model such as GALES (Gardiner *et al*., 2000), extra parameters would be required when the target regions for estimation is expected to receive both strong wind and heavy rainfall.

5. Conclusion

Root anchorage against wind pressure was examined under the condition of high water content in the soil. Our results revealed that intensive water supply certainly affected to the root anchorage in the study field. The amount of penetrated water through the root plate and of the remaining water in the root plate was more likely to be important for root anchorage. Soil resistance decreased with supplying water, but no significant relationship was found between soil resistance and TM_{max}. This indicated that vertical resistance of soil was not significant for root anchorage compared with the other factors such as water content, which was directly associated with change of soil condition under the root plate. Further study is required for tree stability under strong wind and heavy rainfall by considering oscillation of a stem caused by tree swaying, which also contributes to create space between the root plate and soil and to make soil more liquid.

Acknowledgement

We are grateful to Mr. Kawai and Mr. Adachi, undergraduate students of Shizuoka University, who greatly supported us for tree-pulling experiments. This study was funded by Japan Society for the Promotion of Science as a Grant-in-Aid for Scientific Research for “Canopy disturbance and recovery associated with wind damage risk (Research Project Number: 20380088)”.

References

Achim, A., Ruel, J.-C., Gardiner, B.A., Laflamme, G., Meunier, S., 2005: Modelling the vulnerability of balsam fir forests to wind damage. For. Ecol. Manage. 204, 35-50.

Chiba, Y., 2000: Modelling stem breakage caused by typhoons in plantation Criptomeria japonica forests. For. Ecol. Manage. 135, 123-131.

Coutts, M.P., 1986: Components of tree stability in Sitka spruce on peaty gley soil. Forestry 59(2), 173-197.

Kamimura, K., Shiraishi, N., 2007: A review of strategies for wind damage assessment in Japanese forests. J. For. Res. 12, 162-176.

Nicoll, B.C., Achim, A., Mochan, S., Gardiner, B.A., 2005: Does steep terrain influence tree stability? A field investigation. Can. J. For. Res. 35, 2360-2367.

Nicoll, B.C., Gardiner, B.A., Rayner, B., Peace, A.J., 2006: Anchorage of coniferous trees in relation to species, soil type, and rooting depth. Can. J. For. Res. 36, 1871-1883.

Peltola, H., Kellomäki, S., Hassinen, A., Granander, M., 2000: Mechanical stability of Scots pine, Norway spruce and birch: and analysis of tree-pulling experiments in Finland. For. Ecol. Manage. 135, 143-153.

Ray, D., Nicoll, B.C., 1998: The effect of soil water-table depth on root-plate development and stability of Sitka spruce. Forestry 71, 169-182.

Authors' addresses:

Dr. Kana Kamimura (kanak@affrc.go.jp)
Department of Forest Policy and Economics, Forestry and Forest Products Research Institute
1 Matsunosato, Tsukuba-shi, Ibaraki 305-8687, Japan

Mr. Kenji Kitagawa (duck-goose-fly@shizudai-yuho.com)
Department of Forest Resources Science, Shizuoka University
836 Ohya, Suruga-ku, Shizuoka-shi, Shizuoka 422-8529, Japan

Dr. Satoshi Saito (stetsu@affrc.go.jp)
Department of Plant Ecology, Forestry and Forest Products Research Institute
1 Matsunosato, Tsukuba-shi, Ibaraki 305-8687, Japan

Mr. Hayahito Yazawa (kamiatago-yazawa@r7.dion.ne.jp)
University Forest (Kamiatago region), Shizuoka University
1623-1 Nishifujidaira, Tenryu-ku, Hamamatsu-shi, Shizuoka 431-3531, Japan

Mr. Taichi Kajikawa (nakakawane-kajikawa@s3.dion.ne.jp)
University Forest (Nakakawane region), Shizuoka University
298-7 Motofujikawa, Kawanehonnmachi, Haibara-gun, Shizuoka 428-0311, Japan

Prof. Dr. Hiromi Mizunaga (mizunaga@agr.shizuoka.ac.jp)
Department of Forest Resources Science, Shizuoka University
836 Ohya, Suruga-ku, Shizuoka-shi, Shizuoka 422-8529, Japan

Genetic variability in 3D coarse root architecture in *Pinus pinaster*

Frédéric Danjon[1], Emmanuelle Eveno[1], Frédéric Bernier[2], Jean-Paul Chambon[2], Pablo Lozano[1], Christophe Plomion[1], Pauline Garnier-Géré[1]

[1]INRA, UMR 1212 BioGeCo, Bordeaux-Cestas, France
[2]INRA, Unité Expérimentale, Bordeaux-Cestas, France

Abstract

The *Pinus Pinaster* Landes forest experienced recently very large damage through windthrow. 3D coarse root architecture was measured in a 5-6-years-old provenance x progeny test. Both by a high throughput phenotyping procedure on 1150 trees and by precise 3D digitizing of 71 root systems. French atlantic coast provenances showed a strong unique and deep taproot, and a large root biomass. The provenances of dry areas showed more shallow roots, but no differences in root length could be found. No genetic variation for circular distribution of shallow root and no family variance for root architecture could be found in this planted trees. This variability in root architecture of *P. pinaster* may be due to natural selection for anchorage and for drought.

1. Introduction

The south-western France Landes forest covers one million hectares of mono-specific intensively managed *Pinus Pinaster* stands on very poor sandy spodosols. It provides however nearly 1/5 of the wood volume produced in France. *P. pinaster* shows a poor stem straightness (Danjon 1994) and stands are regularly damaged by windthrow including two big storms (Martin & Klaus) who reduced the stocking from 159 M° m3 mid-1999 to 90 M° m3 mid-2009. From an intensive study of coarse root architecture (Danjon et al 2005), it is now known that a good stability of both sapling and mature trees is achieved in sandy soils when ca. 10-years-old-trees possess both a strong, vertical, deep and unique taproot and shallow roots all around the stump (Danjon et al. 2005, Danjon et al. 2009, Fourcaud et al. 2008).

Coarse root 3D architecture and its relationship with stability were intensively studied in samples of about 12 trees per treatment in a chrono-sequence and in various factorial experiments (e.g. Danjon et al. 1999a & 2005, Khuder et al. 2007). It was shown that young trees are anchoraged by a strong taproot like a pole, guyed by an array of symmetric surface roots. Older root systems are sinker roots systems, with a large diameter growth of the Zone of Rapid Taper (ZRT) of laterals roots on stump and of secondary sinkers forming a sort of cage holding the soil and guyed by shallow roots (Danjon et al. 2005). This cage defines the root-soil plate which forms during uprooting. As the secondary sinkers grow from the shallow roots and *P. pinaster* trees do not regenerate new surface roots from the stump, a homogeneous array of surface roots in saplings is needed to provide a large root soil plate to large trees (Atger & Edelin 1995). Soil preparation and planting techniques could influence largely the growth of the tap root and of shallow laterals. Nowadays, planting of genetically improved material makes 80% of newly established stands. The current improved populations were selected from the local populations, but with global change, the base of this population may be enlarged by crosses with provenances from the Mediterranean area, which is dryer. Therefore a better knowledge of genetic variability of coarse root architecture is needed.

And an improvement of trees stability may be achieved by a selection for rooting characteristics in the breeding program using high-throughput phenotyping.

2. Material and methods

A provenance x progeny test was established in the nursery of the research station of Pierroton 30 km south-west of Bordeaux (France). The soil is a sandy spodosol with a water-table raising to about 50 cm depth in winter and going down to 2 m depth late summer. Yearly rainfall is about 900 mm, dominant wind is from the north-west. The populations where sampled in 5 large geographic units including populations from West of France (8 populations), Corsica (4), Spain (9), Morocco (1) and Tunisia (1) covering a large part of the natural range of the species. The populations originated from areas where altitude and rainfall range between 10/1600 m and 350/1400 mm respectively (Table 1 - Fig. 1). Each population is represented by 20 to 30 open pollinated half sib families randomly chosen in the forest. Seeds were sown in turf plugs in May 2003 and planted 6 months later in the field in 9000 single-tree plots with 75 x 75 cm spacing. Tree height and diameter were measured periodically.

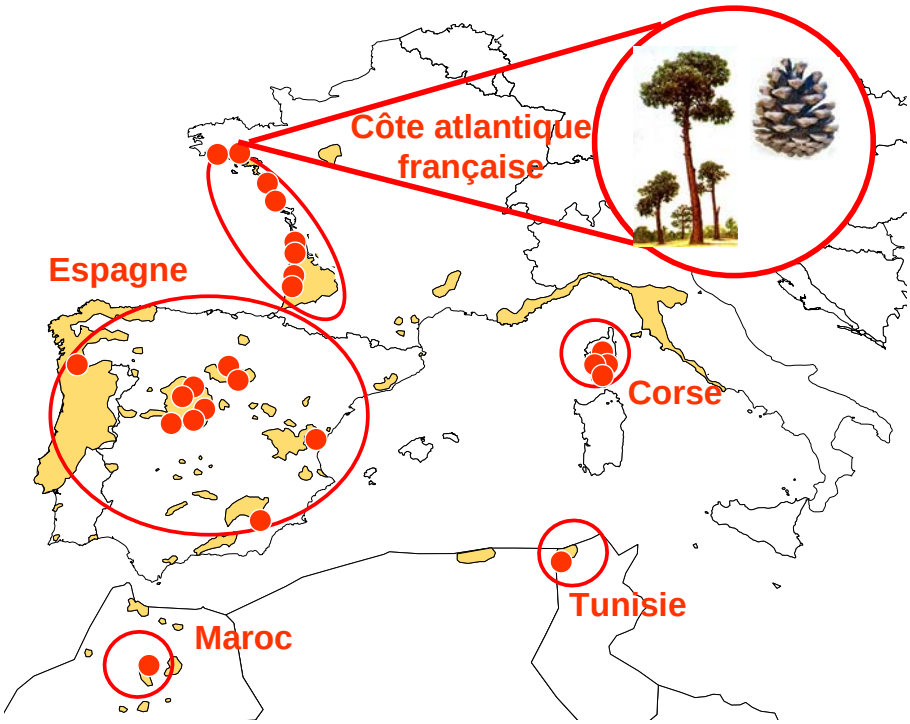

Fig. 1: Sampling of the provenances in Europe and North-Africa

In December 2007, stem height and diameter at 80 cm were measured on 1140 trees with 5 cm mean DBH, the stem was tagged south with XY coordinates and the trees pulled vertically with a logging crane for root measurement, the roots were cleaned with a high pressure lance before measurement. A manual high throughput phenotyping

technique was set-up to assess the genetic variability in root architecture. Entire trees were disposed 6 by 6 on a horizontal plank screwed on two threstles.

Table 1: List of populations sampled and their geographic coordinates

Country	Origin of stand	Sampling location	n°	Depart-ment	Lati-tude	Longi-tude	Alti-tude	Rain-fall	Number of
							(m)	(mm)	Progenies
France	Corsica	Restonica	2	2B	42.27	9.12	700	850	30
France	Corsica	Pineta	11	2A	41.97	9.03	750	1300	30
France	Corsica	Pinia	15	2A	42.02	9.5	10	699	30
France	Corsica	Aullène	10	2A	41.67	9.05	1105	UD	30
France	W Atlantic Coast	Petrock	40	40	44.05	-1.32	35	950	30
France	W Atlantic Coast	Mimizan	41	40	44.13	-1.3	37	950	30
France	W Atlantic Coast	Le Verdon	43	33	45.57	-1.22	12	950	30
France	W Atlantic Coast	Hourtin	42	33	45.17	-1.13	30	950	30
France	W Atlantic Coast	Olonne/mer	44	85	46.57	-1.83	20	650	30
France	W Atlantic Coast	St Jean de Monts	45	85	46.77	-2.02	20	650	30
France	W Atlantic Coast	Pleucadec	46	56	47.78	-2.33	80	855	30
France	W Atlantic Coast	Erdeven	47	56	47.65	-3.13	17	800	30
Spain	Noroeste	San Cipriano	27	Po	42.08	-8.42	310	1575	21
Spain	Montaña Soria-Burgos	San Leonardo de Yagüe	25	So	41.82	-3.07	1100	686	30
Spain	Meseta Castellana	Bayubas de Abajo	26	So	41.53	-2.9	904	470	30
Spain	Meseta Castellana	Coca	22	Sg	41.22	-4.5	788	440	30
Spain	Meseta Castellana	Cuellar	23	Sg	41.4	-4.32	887	440	30
Spain	Sierra de Gredos	Arenas de San Pedro	21	Av	40.2	-5.08	1359	1398	30
Spain	Sierra de Gredos	Cenicientos	20	M	40.27	-4.48	935	1398	20
Spain	Sierra de Guadar-rama	Valdemaqueda	24	M	40.5	-4.3	820	771	20
Spain	Sierra de Espadán	Ahín	28	Cs	39.9	-0.33	700	637	30
Spain	Sierra de Oria	Oria	29	Al	37.52	-2.37	1232	351	30
Morocco		Tamrabta	30		33.71	-4.74	1600	950	25
Tunisia		Tabarka	50		36.65	8.54			30

We measured:

- the stem base straightness (deviation of the stem base from the main line of the upper part of the stem + orientation of leaning) and collar diameter;
- total depth of root system, length, inclination, diameter at base, middle and end of two main taproots;
- the diameter at the base of the sinkers, separating primary and secondary taproots;

- the diameter at 5 cm from the base of all shallow second order roots larger than 2 mm diameter, recorded in 8 circular sectors, starting with the NE sector, in two categories, horizontal and oblique (> 45° < 66°) roots; cross sectional area of roots provide generally a good estimation of root volume downstream the root (Coutts 1983);
- the size in degrees and azimut of the two largest circular sectors without any root;
- a subjectif rate of circular distribution of shallow laterals ranging from zero (all roots in the same azimut) to 1 (homogeneous circular distribution in root number and size);
- several miscellianous characteristics like the number of cones or the degree of branching of the taproot were also recorded.

Less than 10 mn by one people per tree was spent for the whole procedure including uprooting. All root measurements were made by the first author.

In January 2009, after the Klaus storm, in a remaining - undamaged part of the test, 4 trees in each of 18 families (one well growing and one bad growing per provenance) from 7 provenances of Corsica, Spain, Morocco, France were sampled for 3D digitizing of root architecture. The north and soil level was tagged with a screw and the trees were uprooted with a logging crane after removing ca. 15 cm of soil in 2 m radius with a shovel and an air lance to get the shallow roots. The main objective was to test if measuring only the distal CSA of shallow roots gives good information on the biomass and length of these roots, independently from the provenance.

For the measurements, the base of the stem was attached with straps to a large 2m longboard buried with an angle of 55° from the soil surface. A sort of 4 x 4 m ring with four levels of ropes attached to four trees was set-up around the board. Each horizontal root which often reached more than 2 m were attached to the ring with a small paper clip and a strap cut from a bicycle tube. 20 000 segments and 5000 axes were measured using this new technique for rapid positioning of the root system (for a description of the measurement technique see Danjon et al. 1999b and Danjon & Reubens 2008). Analysis was made according to Danjon et al. 2005 and Danjon & Reubens 2008, using an architectural analysis procedure.

3. Results

In the 1140 trees, high country, provenance and family effects were found for stem volume and collar diameter (Table 2). The Moroccan population had a significantly smaller stem compared to the others and France and Corsica was larger than Spain, there was a large provenance and family variability for stem characters. The French provenances, and to a lesser extent the Corsican had certainly a larger root biomass because they showed a larger relative root base cross sectional area (CSA/collar diameter).

The French provenances had a larger relative sinker roots volume (7.9% on the stem instead of 4 to 6%). The French populations showed a larger rooting depth than the other provenances except the Tunisian one, and the Moroccan had a very low rooting depth. The Moroccan provenance had a larger proportion of shallow root CSA (53%) and the French and Corsican a lower proportion in this character. The Corsican trees showed significantly more oblique roots (7% vs 3 to 4.5) In French and Tunisia provenances, 88% of sinkers volume was allocated to the taproot, conversely it was only 75% for Corsican and Moroccan provenances.

Table 2: High throughput phenotyping on 1150 trees, anova, effect of country, provenance, family and bloc; mean for each country, CSA = cross sectional area of roots at 5 cm from base

		Country	Provenance	Bloc	Family	Corsica	Spain	Morocco	France	Tunisia
Collar diameter		2.9e-18	6.0e-32	0.115	0.001	4.6	4.36	3.14	4.69	4.69
$(\text{Stem volume})^{0.33}$	cm	1.3e-33	3.2e-53	0.614	0.001	11.1	10.1	7.39	11.3	11.1
$(\text{CSA root})^{0.5}$/collar diameter		5.5e-27	5.1e-29	0.004	0.047	0.769	0.747	0.733	0.796	0.72
horizontal root CSA	%	1.8e-11	1.4e-19	0.00513	0.151	36.4	45	52.9	41.3	38.6
oblique root CSA	%	0.0005	0.039	0.104	0.655	7.07	4.6	2.93	3.39	4.64
volume(sinkers/stem)		9.0e-12	9.1e-14	0.0151	0.161	6.09	6.3	4.43	7.85	5.54
Maximal depth		7.1e-27	1.3e-22	0.0038	0.514	52.7	51.7	36.5	56.8	53.1
Number of tap roots		1.2e-09	1.4e-09	0.098	0.502	3.4	2.96	3.52	2.46	3.78
taproot vol. in sinkers	%	1.2e-14	4.3e-13	0.106	0.168	75.9	82.1	74	87.6	84.6
Stem leaning	cm	3.57e-21	1.31e-30	0.327	0.387	1.87	3.67	3.47	2.55	6.28
%deformed roots	%	1.19e-12	3.92e-09	0.00129	0.435	26	34.8	33	35	47.1
Sector without roots	deg.	0.0174	0.0013	0.0195	0.605	147	130	120	132	101
circular symmetry		0.0019	0.000145	0.0155	0.628	11.6	10.8	10.2	10.9	9
%CSA leeward	%	0.0727	0.0673	0.119	0.0861	0.119	0.156	0.157	0.151	0.126
%CSA windward	%	0.487	0.972	0.0764	0.596	0.137	0.148	0.125	0.133	0.146

And French provenances grew a significantly lower number of sinkers (2.5). The root systems showed about 35% of deformed root, deformation was higher for the Tunisian trees and lower for the Corsican which is surprising. The circular symmetry of shallow second order laterals was low (average score 10/20) and showed low genetic variability, only the Tunisian provenance showed significantly worse symmetry and high stem leaning. Genetic effects for windward/leeward reinforcement were not significant. Family effects for root architecture traits were generally not significant, except the relative root base cross sectional area.

In the 71 trees for which 3D digitizing of root was performed (Table 3), we did not find significant differences in tree size at population level but large differences between families, which is due to the sampling. Genetic variability in maximum radial distance and total root length where poorly significant. French provenance 45 had larger rooting depth, the Moroccan one smaller rooting depth. Larger variability was found concerning the relative number of roots per root system and the inter-lateral length on second order roots. Provenances from the drier areas (29 & 30) were more branched, have a distinctly lower proportion of taproot in root volume, a larger ZRT, more relative shallow root volume beyond ZRT and longer shallow order 2 axes. The Spanish provenance 27 and the French one's have generally more deep root volume, length and number.

Proximal and distal sinkers volume did not exhibit significant differences between provenances. The Corsicans and the Moroccan provenances had more sinkers beyond ZRT. The stump is a major component of coarse root reaching 40% of extracted root volume. Root volume excluding stump, was in average allocated at 25% to taproot, 20% to ZRT, 40% to shallow roots beyond ZRT, 5% to sinkers below ZRT, 0.5 % to sinkers beyond ZRT, 6% to oblique roots, 2.5% to roots at intermediate depth and 0.2% to deep roots.

Table 3: Character obtained from 3D digitizing of root architecture on 71 trees, anova, effect of provenance, family and bloc; mean for each provenance, % by root type, volume is stump excluded, except for the stump

		Factors effects			Corsica		Spain		Mo-rocco	France	
		Pop	Bloc	Fam	11	15	27	29	30	41	45
Collar diameter	cm	0.108	0.678	0.001	4.24	4.6	4.87	3.66	3.61	4.78	4.93
Max radial distance	cm	0.04	0.012	0.058	142	135	176	160	120	161	172
Maximal depth	cm	0.0002	0.051	0.042	-43.1	-49.7	-53.3	-42.3	-39.7	-53	-57.5
Root length	cm	0.401	0.028	0.025	2290	2810	2300	3090	2460	2630	2800
number axes/collar diam		0.0002	0.131	0.013	16.8	15.5	12.9	20.6	21.2	17.1	14.7
inter-lateral length order 2	cm	0.0004	0.126	0.476	8.77	11.5	14	13.5	9.16	16.7	16.5
		% by root type									
Stump volume	%	0.205	0.002	0.907	42.1	42.4	42.3	37.5	41.1	39.9	38.4
Tap root volume	%	0.001	0.041	0.295	27.5	28.8	32.7	14.1	16.7	30	32.5
Proximal sinkers volume	%	0.152	0.479	0.716	9.86	7.33	4.97	2.3	7.94	1.21	3.54
Distal sinkers volume	%	0.416	0.22	0.372	0.14	0.33	0.86	0.92	1.03	0.32	0.14
Oblique roots volume	%	0.343	0.323	0.195	8.53	7.18	4.69	6.95	5.13	1.64	9.44
ZRT volume	%	0.005	0.336	0.793	14.4	13.8	18.8	23.8	22.2	20.6	17.3
Horizontal far volume	%	0.005	0.236	0.015	37.8	38.4	36.5	49.9	46.1	42.9	33.5
Intermediate depth vol.	%	0.0269	0.969	0.797	1.74	4.07	0.92	1.99	0.92	3.09	3.17
deep roots volume	%	0.289	0.82	0.742	0.05	0.1	0.57	0.009	0.001	0.2	0.35
Sinker length	%	0.036	0.691	0.808	3.58	1.9	1.84	0.93	2.95	0.84	1.22
Deep root length	%	0.002	0.46	0.97	0.19	0.35	0.55	0.094	0.01	0.36	1.14
Nb sinkers under ZRT	%	0.024	0.803	0.532	5.04	3.19	2.41	1.9	4.25	1.1	1.7
Nb deep roots	%	6.67e-05	0.36	0.926	0.9	2.22	3.2	0.85	0.11	2.45	7.33

4. Discussion and conclusion

P. pinaster sapling from all provenances grew a taproot system, with a low amount of oblique roots or intermediate depth roots, therefore, *P. pinaster* can really be considered as a taproot species in young age. *P. pinaster* from windy areas, south west France, and to a lower extent from Corsica developed a stable root system with a big and deep tap-root and a large root biomass. P. pinaster apparently show natural selection for stability. However, none of the populations could compensate by secondary growth a uneven circular distribution of shallow roots and reinforcements in the wind direction could not be found.

Provenances from dry areas developed more shallow and more branched roots. In this experiment, the regeneration of a taproot after planting was not too bad. However, a large root deformation was observed: that's certainly why the circular distribution of shallow root was generally not homogeneous. These will result in unstable adult trees. Appropriate planting techniques have to be employed for all populations.

Acknowledgements

The planting and maintenance of the experiment was founded by the TreeSnip european project.

References

Atger, C., Edelin, C., 1995: A case of sympodial branching based on endogenous determinism in root system: Platanus hybrida Brot. Acta. Bot. Gallica 142, 23-30.

Coutts, M.P., 1983: Root architecture and tree stability. Plant Soil 71, 171-188.

Danjon. F., 1994: Heritabilities and genetic correlations for estimated growth curves parameters in maritime pine. Theor. Appl. Genet. 89, 911-921.

Danjon, F., Bert, D., Godin, C., Trichet, P., 1999: Structural root architecture of 5-year-old Pinus pinaster measured by 3D digitising and analysed with AMAPmod. Plant Soil 217:49-63.

Danjon, F., Sinoquet, H., Godin, C., Colin, F., Drexhage, M., 1999b: Characterisation of structural tree root architecture using 3D digitising and AMAPmod software. Plant Soil 211, 241-258.

Danjon, F., Fourcaud, T., Bert, D., 2005: Root architecture and windfirmness of mature Pinus pinaster (Ait.). New Phytologist 168, 387-400.

Danjon, F., Reubens, B., 2008: Assessing and analyzing 3D architecture of woody root systems, a review of methods and applications in tree and soil stability, resource acquisition and allocation. Plant and Soil 303, 1-34.

Danjon, F., Drénou, C., Dupuy, L., Lebourgeois, F., 2009: Racines, sol mécanique de l'ancrage de l'arbre et stabilité in : La forêt face aux tempêtes. Y. Birot, G. Landmann, I. Bonhême, coord. Coll. Synthèses, Quae Ed. Paris. 155, 176.

Fourcaud, T., Ji, J.N., Zhang, Z.Q., Stokes, A., 2008. Understanding the impact of root morphology on overturning mechanisms: a modelling approach. Annals of Botany 101, 1267-1280.

Khuder, H., Stokes, A., Danjon, F., Gouskou, K., Lagane, F., 2007: Is it possible to manipulate root anchorage in young trees? Plant & Soil 294, 87-102 + erratum Plant Soil (2007) 295, 293-295.

Authors' address:

Dr. Frédéric Danjon (fred@pierroton.inra.fr)
INRA, UMR 1212 BioGeCo, Domaine de l'Hermitage
Pierroton, F-33610 Gazinet, France

Extreme wind speeds as a natural disturbance agent in spruce forests in Latvia

Janis Donis, Maris Rokpelnis, Guntars Snepsts, Juris Zarins

Latvian State Forest Research Institute "Silava", Latvia

Abstract

Wind is one of the most important natural disturbance agents in boreal forests. Goal of our research was to clarify impact of extreme winds on spruce forests in Latvia. Therefore we made estimates of dose - response relationships and probabilities of extreme wind speeds.

1. Introduction

Several authors (Mönkkönen, 1999, Kuuluvainen, 2002) have opinion that sustainable forest management could be provided by emulating natural or historical disturbance regime and forest structures created by disturbances. It is assumed that in Latvia on mesic and wet mesotrophic mineral soils spruce stands have succession disturbance regime, while on eutrophic mineral, wet mineral and wet peat soils – gap dynamics (Angelstam et al. 2005). Fire is assumed to be most important natural disturbance agent in boreal regions (Angelstam 1998) nevertheless wind could be of the same importance. Role of wind as agent of natural disturbance is not evaluated so far in Latvia.

Goal of our research was to clarify impact of extreme winds on spruce forests in Latvia. Therefore we made estimates of dose - response relationships and probabilities of extreme wind speeds.

2. Material and methods

Information about wind speed in the gusts during windstorm of January 2005 in Latvia obtained from Latvian Environmental, Geological and Meteorological Agency (LEGMI) and the Swedish Meteorological and Hydrological Institute (SMHI). Wind speed during windstorm of January 8, 9, 2005 reached 15 -18 ms^{-1} and 30 - 35 ms^{-1} in the gusts in the Eastern and Western part of Latvia respectively according to SMHI data and 24-27 ms^{-1} and 30-40 ms^{-1} according to LEGMI data.

LEGMI provided statistical data about long-term (1977-2005) wind speeds from 13 meteorological stations which were used to calculate probabilities of extreme wind speeds based on Gumbel distribution. Damage caused by wind during windstorm January 2005 surveyed in all stands which were in 170 one km^2 squares distributed evenly over territory of Latvia. For 75 squares DTM (20*20m grid) was generated. Average aspect and slope for each stand and exposure was calculated based on DTM and information about height of neighbouring stands. Information about sanitary clear-cuttings in 2005 is obtained from State Forest Service. In total we used information about 1541 surveyed spruce stands and 6423 sanitary clear-cutting areas. Data processing and analysis is done using MS Excel, SPSS 14 (ANOVA, binary logistic regression) and ArcGIS 9.2. In binary logistic analysis as variables were wind speed, mean tree height, as dummy variables were used: time since last thinning (none or more than 10 years, 1-2 years, 3-5 years, 6-10 years), aspect (plane, windward, leeward, 45 degrees windward,

135 degrees windward), dominant landcover type in windward position (forest, agriculture land, bog, clearcut, roads or other infrastructure objects, young stand up to 6m high).

3. Results

Wind speed in different parts of Latvia during storm was not equal (see Fig. 1a) therefore damage rate (expressed as product of damaged stands in sample plots and percent of damaged volume) as well was different (Fig. 1b)

Out of 1358 surveyed spruce stands some form of damage was found in 595 (44%) of stands with average damage rate 4% of total volume. In the regions with higher wind speeds in the stands older than 60 years in average 12% of volume is damaged, while in regions with lower wind speeds only 3%.

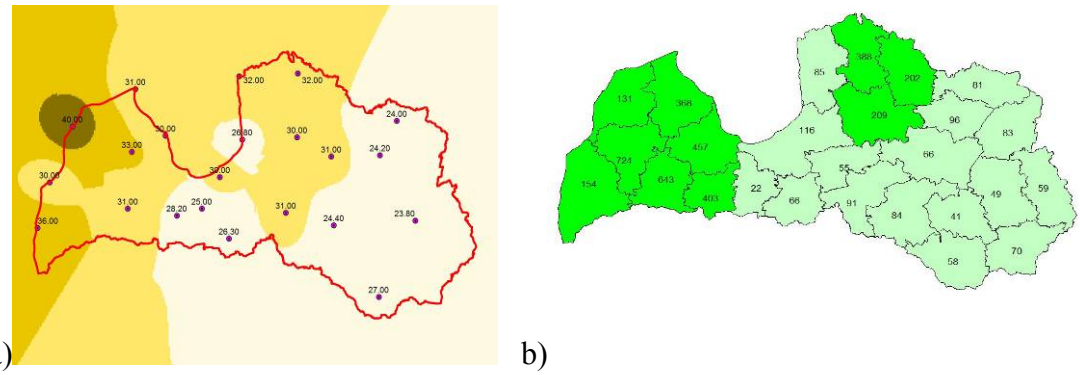

a) b)

Fig. 1: a) Gust wind speed during Storm January 8/9 2005 based on LEGMI data
b) Damage rate as % of damaged stands multiplied by % of damaged volume

ANOVA revealed that average damaged area (S) (sanitation cuttings) in mature spruce stands (older than 80 years) significantly differs between regions of high wind speeds (more than 20 ms^{-1}) and low wind speeds (less than 20 ms^{-1}) N=2614, (S_{aver} =0.87 ha and S_{aver}=0.72 ha respectively) (F=11.03; p=0.01). Also we found out that between eutrophic wet peat and eutrophic mineral soils there is significant difference (S_{aver} =0.46 ha and S_{aver} =1.48 ha) (F=4,378; p<0,001). We concluded that in managed spruce forests wind disturbance is different from that assumed to be natural (gap disturbance).

Binary logistic regression explained 31% of data variation (Nagelkerke R Square 0,314); correctly detected 55-59% of damaged stands (Table 1). Analysis revealed that most important factors influencing damage are wind speed, height of the trees, time after thinning and neighbouring clear cutting areas (Table 2).

Table 1: Logistic regression classification table

Observed			Predicted					
			Selected Cases(a)			Unselected Cases(b,c)		
			Damage Code		Percentage Correct	Damage Code		Percentage Correct
			0	1		0	1	
Step 1	Damage Code	0	376	89	80.9	402	89	81.9
		1	116	169	59.3	131	169	56.3
	Overall Percentage				72.7			72.2

a selected cases code NE 1
b unselected cases code EQ 1
c some of the unselected cases are not classified due to either missing values in the independent variables or cate gorical variables with values out of the range of the selected cases.

Table 2: Variables in the equation of Logistic regression

		B	S.E.	Wald	df	Sig.	Exp(B)	95,0% C.I.for EXP(B)	
								Lower	Upper
Step 1(a)	Wind speed	.141	.038	13.511	1	.000	1.151	1.068	1.241
	Hdom	.118	.011	111.011	1	.000	1.125	1.101	1.150
	Thinning_Dummy_1	3.088	.773	15.958	1	.000	21.937	4.821	99.814
	Thinning_Dummy_1	1.105	.333	10.983	1	.001	3.019	1.571	5.802
	Thinning_Dummy_3	.497	.391	1.621	1	.203	1.644	.765	3.535
	W clearcut	.506	.561	.814	1	.367	1.659	.553	4.976
	Constant	-5.461	.823	43.993	1	.000	.004		

a variable(s) entered on step 1: W clear cut.

Long term wind data analysis revealed (Table 3) that probability that wind speed will exceed 20 ms^{-1} in the Western part of Latvia is 2 to 10 times in 100 years, while in the Central Eastern part only 1 to 2 times in 100 years.

Table 3: Probability of 10 minutes average wind speed over specified value in different parts of Latvia (example)

Meteorological station	Location	10 minutes average wind speed m/s						
		10	12	14	16	18	20	22
Liepāja	Western	100	100	94.9	63.2	29	11.2	4.1
Stende	Western	99.4	73.3	30.4	9.8	2.9	0.9	0.3
Ainaži	Central	100	95	48.2	15	4.2	1.2	0.3
Bauska	Central	89.4	39.9	11.3	2.9	0.7	0.2	0.0
Alūksne	Eastern	71.3	23.8	6.4	1.7	0.5	0.1	0.0
Daugavpils	Eastern	97.9	57.4	18.3	4.9	1.3	0.4	0.1

4. Discussion

Available data gives us only rough estimate of wind speeds during storm January 8/9, 2005. But both LEGMI and SMHI data shows clear West-East gradient. Wind speed in the gusts in western part of Latvia was almost 2 times higher than in Eastern part. Damage as rate in regions with higher wind speeds was 4 times higher than in rest of the country. More vulnerable are spruce stands on eutrophic mineral soils than on eutrophic wet peat, which could be explained by fact that on mineral soils spruces are higher and usually commercial thinnings are more often carried out on mineral soils rather than on peat soils. Binary logistic regression revealed that time since last thinning is significant factor, increasing probability of wind damage. Aspect and slope in this analysis did not appeared as significant factors, which could be explained with fact that sample stands were relatively even terrain, and in the single stand represented by average slope and aspect values of 20*20m grid was not representative indicator.

Despite of relatively small area of Latvia (6.4 mill ha), probability of extreme wind speeds is different in different parts of Latvia and probability of wind speed with more than 20 ms^{-1} in Eastern and central part of Latvia is 5-10 times lower than in Western part, therefore, precautionary management activities, should not be the same even assuming that managers have the same attitude to risk.

5. Conclusions

Probability of extreme wind speeds (more than 20 ms^{-1}) in western parts of Latvia 5-10 times higher than in central and eastern part of Latvia. In managed spruce forests wind disturbance is different from that assumed to be natural (gap disturbance). Between eutrophic wet peat and eutrophic mineral soils there is significant difference in average salvage cutting areas (S_{aver} =0.46 ha and S_{aver} =1.48 ha)

Acknowledgement

Research was financed by Forest Development Funding of Ministry of Agriculture of the Republic of Latvia.

References

Angelstam, P.K., 1998: Towards a logic for assessing biodiversity in boreal forests. In: Assessment of biodiversity for improved forest planning. Forest Sciences 51, 301-314.

Angelstam, P.K., Kuuluvainen, T., 2004: Boreal forest disturbance regimes, successional dynamics and landscape structures - a European perspective. Ecological Bulletins 51, 117- 136.

Angelstam, P.K., Bērmanis, R., Ek, T., Šica, L., 2005: Bioloģiskās daudzveidības saglabāšana Latvijas mežos. Noslēguma ziņojums. (Conservation of Biological Diversity in Forests of Latvia) (in Latvian) VMD, LVM. 95p.

Kuuluvainen, T., 2002: Disturbance dynamics in boreal forests: defining the ecological basis of restoration and management of biodiversity. Silva Fennica 36, 5-10.

Mönkkönen, M., 1999: Managing Nordic boreal forest landscapes for biodiversity: ecological and economical perspectives. Biodiversity and Conservation 8, 85-99.

Sousa, W.P., 1984: The role of disturbance in natural communities. Ann. Rev. Ecol. Syst. 15, 353-391.

Author's address:

Janis Donis (janis.donis@silava.lv)
Latvian State Forest Research institute "Silava"
Rigas street 111, Salaspils, LV-2169, Latvia

Windthrow effects on soil properties, earthworm biomass and species diversity in Hyrcanian forests of Iran

Yahya Kooch, Seyed Mohsen Hosseini

Department of Forestry, Faculty of Natural Resources, Tarbiat Modares University, Iran

Abstract

This paper focuses the effects of tree uprooting on some of soil properties, earthworm biomass and species diversity in Sardabrood forests of Chalous that is located in Hyrcanian forest, northern Iran. For this purpose, twenty seven single - tree gap sites in mixed beech forests were found, seventeen sites dominated by beech (Fagus orientalis Lipsky) and ten by hornbeam (Carpinus betulus L.) at 700 - 1300 m altitude range. Four microsites were distinguished including mound top (mound), the pit bottom (pit), the gap in the canopy (gap) and closed canopy (canopy) at each site. Soil samples were taken at 10cm depth from all microsites. The earthworms were collected simultaneously with the soil sampling by hand sorting. Soil acidity, water content, total carbon, total nitrogen and carbon to nitrogen ratio measured in the laboratory. The impact of uprooting disturbance on soil properties were found, significantly. Total earthworm number and biomass differed significantly among mentioned sites and microsites. Number and biomass of earthworms showed decreasing trend from undisturbed (closed canopy) to disturbed sites (gap, pit and mound). This trend is mainly caused by number and biomass of endogeic ecological group of earthworms. The windthrow generally reduced the activity and abundance of the earthworms.

1. Introduction

The most important type of disturbsnces in the temperate forests is blowdowns connected with the direct disturbance of soils (Ulanova, 2000). Tree uprooting (Fig. 1) has important influences on forest ecology and implications for forest management. Ice storms, firing and other factors may cause uprooting, but wind is the most common cause. Windthrow events have significant impacts on forest structure, species composition, gap succession and microtopography (Phillips, et al. 2008).

Earthworms are perhaps the most important soil organisms in terms of their influence on organic matter breakdown, soil structural development, and nutrient cycling, especially in productive ecosystems. Despite of the vast increase in scientific literature on earthworms in recent years, much remains to be known in their basic biology and ecology (Kooch, et al. 2008). However, the determination of a relationship among biomass and diversity of earthworms with pit and mound disturbances and soil properties are essential for management of forest ecosystems.

The golal of this study was to investigate of windthrow effects on soil properties, earthworm biomass and species diversity in hyrcanian forests of Iran that is the first survey in these forests.

2. Materials and methods

This research performed in Sardabrood forests that are located in the lowland and midland of Mazandaran province in north of Iran with the area of 2347 ha (between 36˚ 37´

30″, 36° 40′ 52″ northern latitude, and between 51° 7′ 50″, 51° 12′ 51″ eastern longitude).

Fig. 1: Uprooted single - tree by windthrow event

Mean annual precipitation of the study area were from 237.6 to 47.5 mm at the Noushahr city metrological station, which is 10Km far from the study area. Presence of logged and bare roots of trees is indicating rooting restrictions and soil heavy texture. Twenty seven single - tree gap sites in mixed beech forests were found, seventeen sites dominated by beech (Fagus orientalis Lipsky) and ten by hornbeam (Carpinus betulus L.) at 700 - 1300 m altitude range. Four microsites were distinguished including mound top (mound), the pit bottom (pit), the gap in the canopy (gap) and closed canopy (canopy) at each site. Soil samples were taken at 10cm depth from all microsites. Large live plant material (root and shoots) and pebbles in each sample were separated by hand and discarded. The soil samples were air - dried and sieved. Soil acidity (with an electrode), water content (by drying soil samples at 105° C for 24 hours), total carbon (Walkey and Black method), total nitrogen (Kjeldahl method) and carbon to nitrogen ratio measured in the laboratory. The earthworms (Fig. 2) were collected simultaneously with the soil sampling by hand sorting, washed in water and weighed with mili gram precision. Species of earthworms were identified by external characteristics using the key of BOUCH. Biomass was defined as the weight of the worms after drying for 48 hours on filter paper at room temperature (60°C) (Edwards and Bohlen, 1996).

Kolomogorov - Smirnov test used as normality test and Levene test for data homogeneity test. Analysis of variance (one - way ANOVA) and Duncan comparison were used to find differences in soil characteristics of the microsites. Nonparametric Kruskal - Wallis analysis of variance and Mann - Whitney comparison were used to find differences in earthworm's number and biomass of sites and microsites, because in some cases there was no homogeneity of variance. The relationships between microsites and earthworms species were analysed by Principle Component Analysis (Mc Cune and Mefford, 1999).

Fig. 2: Earthworm's representative of different ecological groups: (a) Epigeic species, such as Dendrodrilus rubidus, inhabit organic rich surface layers and feed mainly on surface organic matter. (b) Endogeic species, such as Octolasion tyrtaeum, consume more mineral soil than epigeic species, and mix mineral and organic soil layers together. (c) Aneceic species, such as Lumbericus terrestries, live in deep vertical burrows, feed mainly on surface litter, and incorporate litter into the soil as well as transporting mineral soil to the surface from deeper soil layers (Kooch et al., 2007)

3. Results

Analysis of variance is indicating (Table 1) soil characteristics have significant differences in investigated microsites of beech and hornbeam sites. The maximum and minimum of acidity were observed in mound and canopy microsites, respectively for both of sites.

Table 1: Mean of soil characteristics in different microsites of sites

Site	Microsite	pH	Water content	Carbon	Nitrogen	Carbon to nitrogen ratio
Beech	Mound	6.82 (0.03)a	15.98 (0.84)d	2.59 (0.13)b	0.12 (0.006)c	21.05 (1.39)ab
	Pit	6.11 (0.09)b	55.72 (1.97)a	2.68 (0.18)b	0.12 (0.003)c	22.00 (1.69)a
	Gap	6.68 (0.04)a	29.38 (1.26)c	3.00 (0.16)ab	0.17 (0.008)b	17.67 (1.37)bc
	Canopy	6.03 (0.07)b	43.80(1.75)b	3.34 (0.15)a	0.24 (0.006)a	14.04 (0.68)c
Hornbeam	Mound	7.66 (0.05)a	14.84 (0.84)c	2.35 (0.04)b	0.11 (0.005)b	20.37 (0.90)a
	Pit	7.43 (0.01)b	53.74 (4.32)a	2.37 (0.29)b	0.13 (0.007)b	18.67 (2.75)a
	Gap	7.65 (0.04)a	37.61 (2.39)b	3.04 (0.17)a	0.25 (0.006)a	12.05 (0.74)b
	Canopy	7.34 (0.08)b	37.49 (2.34)b	2.84 (0.03)ab	0.26 (0.007)a	10.95 (0.38)b

Values are the means ±St. error of the mean (in parenthesis); within the same column the means followed by different letters are statistically different ($P < 0.05$)

The most water content (moisture) devoted in pit microsite and the lesat was observed on mound. In beech site, maximum of carbon related to canopy and the lesat devoted on mound microsite, but in hornbeam site, the highest observed in gap microsite. Nitrogen had higher amounts in canopy and lesat value related to mound. Carbon to nitrogen ratio was less in canopy and the highest amounts observed in pit for beech site and on mound in hornbeam site. Analysis of data showed that number and biomass of earthworm's ecological groups had significant differences among microsites and sites. Earthworm's number and biomass had more amounts in canopy and the lesat were observed on mound microsites. Hornbeam site involved more abundance of earthworms in compare to beech site.

4. Discussion

Soil acidity had significant differences in microsites as the most and least amounts devoted in mound and canopy microsites, respectively. Thus, it is conceivable that gap creation increased soil acidity and low pH observed in canopy microsite. Faguetum litters have low pH, but within gaps because of disturbance creation and extensive changes, the decomposition velocity is higher and organic matter cycles are better in compare to canopy. Therefore, the soil pH includs higher amounts in gap microsite that is according to the reults of Muscolo et al. (2007) research. The mean of soil characteristics indicating pit had the most water content and least value found in mound microsite that is similar to Barton et al. (2000) research. Pay attention to obtained results, gap creation decreased soil water content and central areas of gaps (mound microsite) had less moisture in comarison to border areas (gap microsite). Water content changes are very variable in different forest ecosystems (Gagnon et al. 2003). Chen et al. (1999) mentioned that gap creation in forest ecosystems are due to moisture decreasing and temperature increasing in superficial soils.

Thick humus layers creats appropriate positions for moisture preservation in forest lands. Spong character under closed canopy will increase water and moisture preservation capacities in comparison with positions without closed canopy. Disturbance and gap creation are due to decomposition of these layers and transmission to beneath horizons. Humour reduction within gaps can be related to solar radiation and incraesing of microclimate temperature (Page and Cameron, 2006). In beech site, the maximum of carbon found in canopy and least value devoted on mound microsite whereas in hornbeam site, the most amount of carbon observed in gap microsite. Clinton and Baker (2000) reported the following distribution pattern for organic carbon at Coweeta Basin in North Carolina one year after a windthrow event: 2.15% mound, 2.11% pit wall, 1.42% pit bottom, and 4.73% in the undisturbed area. Thus, the change of carbon amounts is different in diverse forest ecosystems. Nitrogen had higher value in canopy and the least related to mound. It is considerable that soil characteristics had different reactions to various microsites. It is possible that changing bacterias of organic nitrogen to mineral form are activiting in special temperature range. Therefore, soil temperature has multiple effects and this reason the correlation values of positive and negative in nitrogen content are mentioned in different studies (Schmidt, et al. 2002). The presence of microbial agents and oozing of created acids by activity of these organisms have important role in carbon storage (Frazer, et al. 1990).

Carbon to nitrogen ratio found less in canopy and the most value observed in pit for beech site and mound in hornbeam site. Barton et al. (2000) investigated the amounts of carbon, nitrogen and carbon to nitrogen ratio in various microsites of pit and mound feature. He found that the most amount of these characters were devoted to undisturbed areas and significant differences showed with the other microsites. Totally, the most earthworms are sensitive to soil acidity as theirs number and biomass reduce in soils with low pH. In beech site, epigeic ecological groups found in pit and canopy microsites that were in relation to moisture high amounts within these microsites. Almost, 80 to 90 % of earthworms fresh weight constitued of water, thus soil moisture are essential for theirs live and will kill by reason of soil drying (Saleh Rastin, 1978). With considering moisture of 55.72 % in pit microsite, this moisture amount is due to more gathering of epigeics. In hornbeam site, earthworm's different groups were found in studied microsites except of mound microsite. Mounds create hilly surfaces on superficial soil and include more soil volume and temperature in compare to other surfaces (Londo, 2001).

On the other hand, soil temperature is effcetive on number and biomass of earthworms and distribution. Therefore, low moisture and high temperature created fatal conditions for earthworms on mound microsite (Nachtergale et al. 2002). Due to theses reasons no earthworms were found in mound microsite in both of sites. Nachtergale et al. (2002) mentioned that the increase of epigeics biomass in pits is a response to more gathering of trees litters within this microsite. Pits creation in forest floor produce an especial condition as is due to increase of litter thickness and water content, thus the epigeics biomass will increase. Carbon to nitrogen ratio in closed canopy microsite is due to assemblage of earthworms diverse groups in this microsite of hornbeam site. Totally, it is mentionable that suitable temperature and moisture, lack of inappropriate chemical compostions such as tanan, ploy fenol and low carbon to nitrogen ratio (especially in closed canopy microsite) created appropriate conditions for increasing of biologic activities of earthworms in hornbeam site in compare to beech site. Therefore, presence and aboundance of earthworm's diverse groups are more visible in hornbaem site. Results of this resaerch are indicating that the most impact on endogeic ecological group of earthworms. These earthworms group werent visible in disturbed areas (gap, pit and mound). It is imagined that this earthworms group are more sensitive to severe light condition and created temperature within gap in compare to other earthworm groups. With considering this group have more excavation ability opposit to other groups (Kooch, et al. 2008), thus they migrated to deeper layers of soil and no endogeic found in 0 - 10 cm depth. Whereas, in closed canopy regarding to less light and temperature conditions of soil surface, endogeics migrated to soil surface.

5. Conclusion

Results of this study showed that earthworms can be as bioindicator for evaluation of forest stands changes after disturbance events. The windthrow generally reduced the activity and abundance of the earthworms. Our results suggest that windthrow should be considered as an effective factor on pedodiversity that are tied to forest ecology. This is significant for evaluating forest management policies and practices with respect to impacts on soil and also for the use of soils as indicators of forest ecosystems.

References

Barton, D., Corey, C., Baker, R., 2000: Catastrophic windthrow in the southern Appalachians: characteristics of pits and mounds and initial vegetation responses. Forest Ecology and Managemen. 126, 51-60.

Chen, J., Saunders, S.C., Crow, T.R., Naiman, R.J., Brosofski, K.D., Mroz, G.D., Brook Shire, B.L., Franklin, J.F., 1999: Microclimate in forest ecosystem and landscape ecology. Bioscience 49, 288-297.

Clinton, B.D., Baker, C.R., 2000: Catastrophic windthrow in the Southern Appalachians: characteristics of pit and mounds and initial vegetation responses. Forest Ecology and Management 126, 51-60.

Edwards, C.A., Bohlen, P.J., 1996: Biology and Ecology of Earthworms. Chapman and Hall, London, 426 pp.

Gagnon, J.L., Jokele, E.J., Moser, W.K., Huber, D.A., 2003: Dynamics of artificial regeneration gaps within alongleaf pine flatwoods ecosystem. Forest Ecology and Management 172, 133-144.

Kooch, Y., Jalilvand, H., Bahmanyar, M.A., Pormajidian, M.R., 2008: Abundance, biomass and vertical distribution of earthworms in ecosystem units of Hornbeam forest. Journal of Biological Sciences 8, 1033-1038.

Kooch, Y., Jalilvand, H., Bahmanyar, M.A., Pormajidian, M.R., Shahbeiki Gilkalayee, M., 2007: The effective soil factors on distribution of earthworms in forest ecosystem units. 10th congress of soil sciences in Iran, 221-223 (in Persian).

Londo, A.J., 2001: Bucket mounding as a mechanical site preparation technique in wetlands. NIAF 18, 7-13.

Mc Cune, B. and M. Mefford. 1999. Multivariate Analysis of Ecological data Version 4.17. MJM Software. Gleneden Beach, Oregon, USA, 233 pp.

Muscolo, A., Sidari, M., Mercurio, R., 2007: Influence of gap size on organic matter decomposition, microbial biomass and nutrient cycle in Calabrian pine (Pinus laricio, Poiret) stands. Forest Ecology and Management 242, 412-418.

Nachtergale, L., Ghekiere, K., Schrijver, A.D., Muys, B., Lussaert, S., Lust, N., 2002: Earthworm biomass and species diversity in windthrow sites of a temperate lowland forest. Pedobiologia 46, 440-451.

Page L.M., Cameron, A.D., 2006: Regeneration dynamics of Sitka spruce in artificially created forest gaps. Forest Ecology and Management 221, 260-266.

Phillips, J., Marion, D.A., Tukington, A.V., 2008: Pedologic and geomorphic impacts of a tornado blowdown event in a mixed pine - hardwood forest. Catena 75, 278-287.

Saleh Rastin, N., 1978: Soil biology. Publishing of Tehran University, 325 pp (in Persian).

Schmidt, I.K., Jonasson, S., Shaver, G.R., Michelsen, A., Nordin, A., 2002: Mineralization and distribution of nutrients in plants and microbes in four arctic ecosystems: responses to warming. Plant and Soil 242, 93-106.

Ulanova, N.G., 2000: The effects of windthrow on forests at differential spatial scales: a review. Forest Ecology and Management 135, 155-167.

Authors' address:

Yahya Kooch, PhD candidate of Forestry (yahya_kooch@yahoo.com)
Assoc. Prof. Seyed Mohsen Hosseini (hosseini@modares.ac.ir)
Faculty of Natural Resources, Tarbiat Modares University
Noor, Mazandaran, Iran

Acclimation and growth response of Norway spruce advance regeneration after release

Marek Metslaid, Kajar Köster, Floortje Vodde, Kalev Jõgiste

Institute of Forestry and Rural Engineering, Estonian University of Life Sciences, Estonia

Abstract

The present study is focused on the growth response and acclimation of advance regeneration of Norway spruce after release (clear-cut). The sampling of advance regeneration trees was carried out in four permanent sample plots in the Järvselja Experimental Forest of the Estonian University of Life Sciences. We found that when advance regeneration is released from overstorey competition by a windstorm or a regeneration cut, it is able to occupy the available growing space and to form a new young stand. Shoot and needle morphology can reflect the relative growth and acclimation to new environmental conditions. Shoot length and needle mass increase in subsequent years tend to stabilise 4-5 years after release. The acclimation in terms of accelerated height and diameter growth seems to start in 2-3 years after release.

1. Introduction

Stand-levelling windstorms and clear-cut logging often leave advance regeneration of varying size and age distribution in place (Frelich, 2002). An understanding of acclimatised growth response of trees is fundamental to predict forest successional dynamics and forest regeneration in managed stands after partial or complete release of advance regeneration (Wright et al., 2000). Norway spruce (*Picea abies* (L.) Karst.) is one of the shade-tolerant tree species, which can produce a viable population of advance regeneration that can exist long periods beneath the canopy of a mature forest stand (Jeansson et al., 1989; Lundqvist and Fridman, 1996). This advance growth can be utilized for forest regeneration (Greene et al., 2002; Kuuluvainen, 2002). However, little is known about how such released trees acclimate to the new environmental conditions and about their subsequent growth performance.

Earlier research suggested that needle characteristics provide the best indication of performance: new needles are greater by size compared to older needles. The particular questions of interest in this study are how Norway spruce advance regeneration acclimatised to understorey conditions reacts to subsequent release that exposes the trees to full sunlight, and how these features could be used to predict sapling performance after release.

2. Material and methods

2.1 Plot characteristics

The growth response and acclimation of advance regeneration of Norway spruce trees was studied in four permanent sample plots in the Järvselja Experimental Forest of the Estonian University of Life Sciences.

The first plot (1) was established on a 2.5-ha clear-felled area harvested during the winter of 1995/1996. The site type is *Oxalis-Myrtillus* and the site index is bonitet 1. Before felling, the stand consisted of 70% Norway spruce, 20% silver birch (*Betula pendula*

Roth) and 10% trembling aspen (*Populus tremula* L.). The volume of the stand before clear-cutting was 338 m^3 ha^{-1}. Trees were sampled in two patches.

The second plot (2) was established on a 1.1 ha clear-felled area harvested during the winter of 1999/2000. The site type is *Oxalis-Myrtillus* and the site index is bonitet 1. The main canopy consisted of 90% Norway spruce, Scots pine (*Pinus sylvestris* L.) making up the balance. The volume of the stand before clear-cutting was 288 m^3 ha^{-1}. Most of the advance regeneration trees were located in one large group, but 15 trees were distributed separately in a second group.

The third plot (3) is a 0.6 ha stand situated next to the first, but beneath a dense canopy cover. The site index is bonitet 1 and the site type is *Oxalis-Myrtillus*. The old canopy comprised 60% of Norway spruce, 30% of trembling aspen and 10% of silver birch. The volume of the stand is 329 m^3 ha^{-1}. The advance regeneration trees were unevenly distributed in several patches. The overstorey of the stand has not been removed yet.

The fourth plot (4) was established on a clear-felled area cut in winter 2001/2002. The size of the clear-cut was 2.1 ha. The site type is *Myrtillus* and the site index is bonitet 3. The old canopy comprised 65% Norway spruce, 30% silver birch, and 5% Scots pine. The volume of the stand before clear-cutting was 287 m^3 ha^{-1}. Most of the advance regeneration trees were located in one large group.

Plot size and configuration varied; the plot size was adjusted to accommodate 100 trees of various sizes and competition status. Because the density and tree size varied, plot size and shape were not fixed. All trees within the plot perimeter were measured to include competition effects, but if a group exceeded 100 trees, only a sub-area was sampled. In this case, the trees neighbouring sample trees were also measured, even though they fell outside the sample plot, but were within a 2-m radius of the sampled trees. These trees were taken into account in calculating the competition index. If the group was too small to include 100 trees, additional trees were selected. The trees were tagged with numbered metal labels and the stem locations mapped. The number of trees on plots included in the final analysis varied, depending on how many trees survived until the end of the observation period.

2.2 Field and laboratory measurements

Measurements on advance regeneration trees were made at the end of each growing season and included tree height, diameter at the root collar. In addition, the length of the top shoot (leader) was recorded.

At each measurement, a lateral shoot was sampled randomly from the upper third of each tree crown. Visual criteria were applied to ensure that no damaged shoots or any with extreme growth were included in the sampling. This shoot from the upper third of the crown was always compared with a similarly selected shoot from the same tree from the previous year. The shoots and needles collected were assumed to reflect the growth capacity of the tree during the previous year. Excised shoots were taken to the laboratory where shoot length was measured and the number of needles counted. Needles were dried at 70 °C for 72 h and weighed.

Trees on plot 1 were sampled destructively after five years' growth in full light conditions. Basal discs were removed and tree rings were measured using WINDENDRO

(Regent Instruments) (the width of each growth ring was measured and averaged from two radii).

2.3 Data analysis

We have described essential characteristics of advance growth.

The index of competition was calculated for each tree:

$$K = \sum_{K=1}^{N} \left(\frac{H_k}{H_0} * \frac{1}{S_k} \right) \qquad (1)$$

where K is index of competition, H_k is the height of the competitor tree, H_0 is height of the tree and S_k is the distance from the competing tree (Hegyi, 1974).

MS Excel (Microsoft, Redmond, WA), STATGRAPH (Version 5.0; STSC) and SAS software (version 8.0; SAS Institute, Cary, NC) were used for all correlation and regression analyses. Correlation analysis was used to describe relationships between needle and shoot variables and the diameter increment. Growth dependencies over the years were subjected to simple regression analysis. Regression equations were fitted for different combinations of variables to obtain the best growth predictions. Tree increment was related to the previous increment and needle mass. The general linear model procedure of SAS software was applied to study the relationships between variables.

3. Results

Growth trends of diameter and height of the sample advance regeneration trees are shown in Figs. 1 and 2. The mean height and diameter values were also calculated for the year 2008. The variations in tree dimension were quite high. Plot 2 variables had higher values, because the trees were higher and the measurements on this plot started at second year at full light. The acceleration in height growth starts on third year after release, whereas the acceleration in diameter growth starts on second year after release.

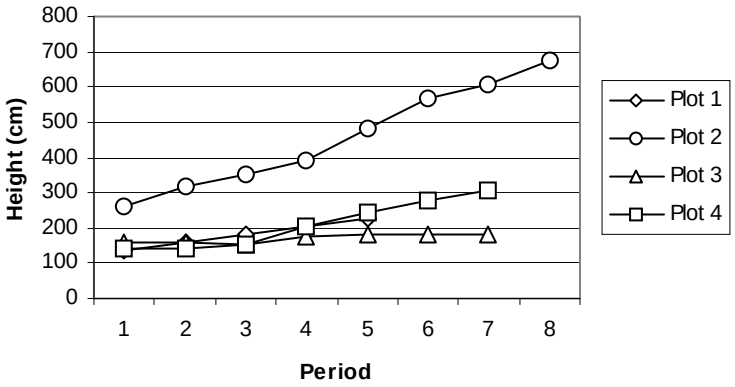

Fig. 1: Mean height of the trees by period (measurement year) on permanent sample plots

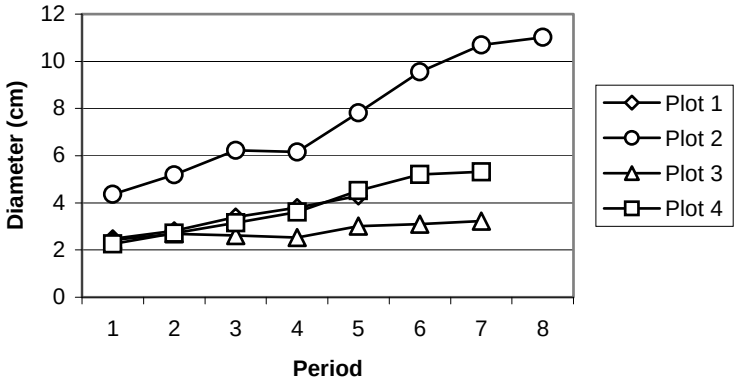

Fig. 2: Mean diameter of the trees by period (measurement year) on permanent sample plots

The basic shoot characteristics (shoot length and needle mass) were provided (Table 1). The variation in shoot dimensions was rather high. Mean values of the shoot characteristics show a generally increasing trend, except plot 3 beneath a dense canopy cover. On plot 1, the dry year of 1999 (Period 4) stands out as an exception.

Table 1: Sample shoot characteristics of Norway spruce advance regeneration trees

Plot	Year	Needle mass (g)			Shoot length (cm)		
		Mean	Min	Max	Mean	Min	Max
Plot 1	1996	0.40	0.02	1.29	9.4	2.0	20.7
	1997	0.39	0.05	1.26	9.2	1.9	29.0
	1998	0.49	0.05	1.83	12.4	2.5	33.8
	1999	0.37	0.06	1.11	11.6	3.4	29.0
	2000	0.57	0.07	1.73	13.4	2.0	37.8
Plot 2	2001	0.41	0.14	1.03	10.9	3.5	18.3
	2002	0.77	0.08	1.80	18.3	1.5	33.4
	2003	0.81	0.10	1.81	20.5	2.7	36.5
	2004	0.94	0.09	1.88	23.9	2.3	37.7
	2005	1.18	0.07	2.40	29.2	6.5	47.0
	2006	1.83	0.20	4.21	25.8	6.2	40.0
	2007	1.37	0.16	3.75	25.5	5.5	48.5
Plot 3	2002	0.19	0.05	0.41	8.4	3.7	14.2
	2003	0.13	0.03	0.40	5.9	2.6	13.2
	2004	0.19	0.03	0.58	8.6	2.2	16.7
	2005	0.19	0.02	0.47	8.6	2.7	14.5
	2006	0.30	0.05	0.69	8.3	3.3	14.4
	2007	0.21	0.03	0.53	7.8	2.6	14.3
Plot 4	2002	0.20	0.03	0.59	5.2	1.5	10.5
	2003	0.30	0.05	0.78	8.4	3.1	14.8
	2004	0.40	0.05	1.02	11.8	3.1	25.0
	2005	0.55	0.02	1.42	15.0	3.2	28.2
	2006	1.03	0.04	2.75	17.2	2.2	33.5
	2007	0.78	0.03	2.77	16.8	2.6	38.0

Correlation analysis between different shoot and needle variables of advance regeneration showed high correlations between shoot needle mass and other shoot characteristics of current and consecutive years (Metslaid et al., 2005b). Shoot length and needle mass in consecutive years can be used to describe the response dynamics of advance regeneration.

The best regression equation combining different tree variables for growth was following ($n = 457$, $R^2 = 0.81$, RMSE = 0.70) (Metslaid, 2008):

$$\ln I_{g_{(t+1)}} = a_0 + a_1 \ln I_{g(t)} + a_2 K_t + a_3 \ln G_t + a_4 \ln M_t \qquad (2)$$

where I_g is basal area increment, K_t is competition index, G is basal area at ground level and M_t is needle mass of shoots from the upper third of the tree crown at time t.

4. Discussion

Shoot and needle morphology can reflect relative growth, acclimation to different light conditions and indicate the performance of advance regeneration after release. Shoot length and needle mass in consecutive years help to describe the growth dynamics of the advance regeneration trees.

The acclimation of the new shoots of Norway spruce to the release takes place within 4-5 years after release. Valkonen et al. (1998) reported that the time for estimating tree growth should be at least 5 years.

Following release, the understorey trees are subjected to a major environmental change that influences shoot structure. Shoot growth depends on tree growth, especially in Norway spruce, which has a plastic crown structure that is dependent on light conditions (Sellin, 2001). Kneeshaw et al. (2002) found that understorey release causes an immediate growth response in roots but a more gradual response in aerial tree parts, which is in accordance with the findings in present study. The degree of shoot vigour could indicate the degree of acclimation of the tree to the new growing conditions. Tree size before the release influences the rate of acclimation (Kneeshaw et al., 2002). Metslaid et al. (2005a) found that after release the basal area increment increased in all trees, but the timing of growth resumption depended on previous growth.

5. Conclusions

Shoot length and needle mass increase in subsequent years tend to stabilise 4-5 years after release. The acclimation in terms of accelerated height and diameter growth seems to start in 2-3 years after release.

Advance regeneration trees can be used for forest regeneration, but spruce-dominated forests would need dense groups of advance regeneration to be tended and the proportion of hardwood species to be reduced in order to prevent severe competition. For mixed-species stands where birch (and other deciduous species) and spruce are establishing at different times it is possible to regulate tree species composition by saving and promoting the growth of the desired tree species during forest management.

Acknowledgements

The study was financially supported by Estonian Science Foundation Grants 4127 and 4980 and by Estonian Research Council, Target Financing Projects SF0432486s03 and SF0170014s08. This research was supported by European Social Fund's Doctoral Studies and Internationalisation Programme DoRa.

References

Frelich, L., 2002: Forest dynamics and disturbance regimes. Studies from temperate evergreen-deciduous forests. Cambridge University Press, Cambridge. 266 pp.

Hegyi, F., 1974: A simulation model for managing Jack-pine stands. IUFRO Working Party. S4.01-4. Rapp. Uppsats. Instn. Skogsprod. Skogshögsk. 30, 74–90.

Jeansson, E., Bergman, F., Elfing, B., Falck, J., Lundqvist, L., 1989: Natural regeneration of pine and spruce. Proposal for a research program. Swedish University of Agricultural Sciences. Department of Silviculture. Report NO. 25, 67 pp.

Kneeshaw, D.D., Williams, H., Nikinmaa, E., Messier, C., 2002: Patterns of above- and below-ground response of understory conifer release 6 years after partial cutting. Can. J. For. Res. 32, 255-265.

Kuuluvainen, T., 2002: Disturbance dynamics in boreal forests: Defining the ecological basis of restoration and management of biodiversity. Silva Fenn. 36, 5-11.

Lundqvist, L., Fridman, E., 1996: Influence of local stand basal area on density and growth of regeneration in uneven-aged *Picea abies* stands. Scand. J. For. Res. 11, 364-369.

Metslaid, M., Ilisson, T., Vicente, M., Nikinmaa, E., Jõgiste, K., 2005a: Growth of advance regeneration of Norway spruce after clear-cutting. Tree Physiol. 25, 793-801.

Metslaid, M., Ilisson, T., Nikinmaa, E., Kusmin, J., Jõgiste, K., 2005b: The recovery of advance regeneration after disturbances: acclimation of needle characteristics in *Picea abies*. Scand. J.For. Res. 20 (Suppl. 6), 112-121.

Metslaid, M., 2008. Growth of advance regeneration of Norway spruce after clearcut. PhD Thesis, Estonian University of Life Sciences, Tartu.

Sellin, A., 2001: Morphological and stomatal responses of Norway spruce foliage to irradiance within a canopy depending on shoot age. Environ. Exp. Bot. 45, 115-131.

Valkonen, S., Saksa, T., Saarinen, M., Moilainen, M., 1998: Alikasvos vapauttamisen jälkeen (Advance growth after release). In: Moilainen, M., Saksa, T. (Eds.), Alikasvokset metsänuudistamisessa. Varjosta valoon (Advance Growth in Forest Regeneration. From Shade to Light). Metsälehti Kustannus, 33–53 (in Finnish).

Wright, E.F., Canham, C.D., Coates, K.D., 2000: Effects of suppression and release on sapling growth for 11 tree species of northern, interior British Columbia. Can. J. For. Res. 30, 1571-1580.

Authors' address:

Dr. Marek Metslaid (marek.metslaid@emu.ee)
Dr. Kajar Köster (kajar.koster@emu.ee)
MSc. Floortje Vodde (floorvodde@hotmail.com)
Prof. Kalev Jõgiste (kalev.jogiste@emu.ee)
Institute of Forestry and Rural Engineering, Estonian University of Life Sciences
Kreutzwaldi 5, 51014 Tartu, Estonia

Windthrow impacts in riparian leave-strips

Stephen J. Mitchell, Devesh Bahuguna, Yosune Miquelajauregui, Tim Shannon

Department of Forest Sciences, University of British Columbia, Canada

Abstract

The riparian buffers experiment at the University of British Columbia research forest was commenced in 1998. In this experiment 0m buffer (fully harvested), 10 m, 30 m and unharvested (control) treatments were replicated three times within 70 year old uniform structured stands dominated by western hemlock (*Tsuga heterophylla*). Approximately 15 % of the retained trees were windthrown in the 10 m buffer treatment, and 10 % in the 30 m wide treatment, primarily in the first 2 years following harvest of adjacent timber. Windthrown trees were smaller than the average tree. Stand self-thinning is an additional source of mortality, particularly in the control and 30 m buffers. Eight years after harvest, 90% of the windthrown trees were still suspended above the stream channel. The area of exposed soil is related to the diameter and number of uprooted trees, but only 14 % of uprooted trees were in a position to deliver sediment to the stream channels. Results of this study have been integrated into ForestGALES_BC to model windthrow impacts on streams.

1. Introduction

Changes in forest practices regulations in British Columbia and the northwest United States in the past two decades have lead to greater protection of small streams during timber harvesting. Forest policies require retention of treed buffer strips along larger stream channels with fish populations (Wang et al., 2002). These unharvested strips are intended to minimize impacts of forest management activities on water quality, aquatic ecosystems and riparian community diversity (BCMOF, 1995). The transfer of large woody debris (LWD) from streamside forests to stream channels is an important long term role of these buffers. Windthrow is a major source of tree-falls in newly exposed buffers, and to design effective riparian prescriptions we need to understand the potential impacts of windthrow in both the short and longer term.

2. Windthrow component of small streams study

This study was a component of a larger integrated study of forest management impacts on small streams. The small streams riparian buffers experiment is located in the foothills of the Coast Mountains, approximately 60km east of Vancouver, British Columbia. The climate is maritime and characterized by dry, warm summers and wet, cool winters. Total precipitation ranges between 2200 mm and 3000 mm per year and falls primarily as rain. The stands in the study area are dense, uniform second growth forests that naturally regenerated following logging and wildfire in the 1930s. The tree species include western hemlock (*Tsuga heterophylla* (Raf.) Sarg.), western redcedar (*Thuja plicata* Donn ex D.Don), Douglas-fir (*Pseudotsuga menziesii* (Mirb.) Franco), paper birch (*Betula papyrifera* Marsh.), and red alder (*Alnus rubra* Bong.).

Two buffer width treatments (10 m and 30 m on each side of the stream), and unharvested controls were each replicated three times within the riparian buffers experiment. Harvesting commenced in the fall of 1998. Understory and overstory vegetation plots

were measured annually. These vegetation plots are 15 m long and 4 m wide, run lengthwise parallel to the stream, and are repeated at 2 m and 15 m from the stream bank on each side of the stream. These 4 strip-plot clusters are replicated at two locations along the stream within each treatment unit and represented vegetation for the buffer experiment (Miquelajauregui, 2008) and provide tree mortality data for the LWD study. Within each strip plot the species, dbh, height and status (standing live, standing dead, uprooted) were recorded for each tree in each year since 1998. LWD transects were established up the centre of each stream within each treatment unit in the summer of 2006 using the protocol of Moore et al. (2002) as a basis for sampling and measurements. Since each treatment unit is at least 150m long, we chose a LWD transect length of 150m. For downed trees to be tagged and measured they needed to be: fallen or windthrown since 1998, having at least a portion of the log length within (or above) the active channel and greater than 7.5 cm in diameter at the mid creek.

3. Key results

After harvest in 1998, 12 % and 6 % of initially live standing trees were blown down in the first and second years in the 10 m and 30 m buffer treatments respectively. There was minimal new windthrow in subsequent years until 2006 when winter storms brought these numbers up to 15 % and 10 % in the buffers, and to 9 % of trees in the control treatments (Fig. 1). In these dense second growth stands, there is still a significant amount of annual mortality in standing trees, amounting to 30 % of initially live trees in the controls and 15 % each in the 10 m and 30 m buffers after 8 years. The average diameter of live, dead and windthrown trees were 35, 13 and 26 cm respectively for all treatments pooled. A total of 291 logs (spanning and in-creek) were recorded in the stream transects and 75% of these were oriented diagonally or perpendicularly to the stream. Even 8 years after harvesting and the post-harvest pulse of windthrow, 90% of logs in the 10m and 30m buffer treatments were still elevated above the creek.

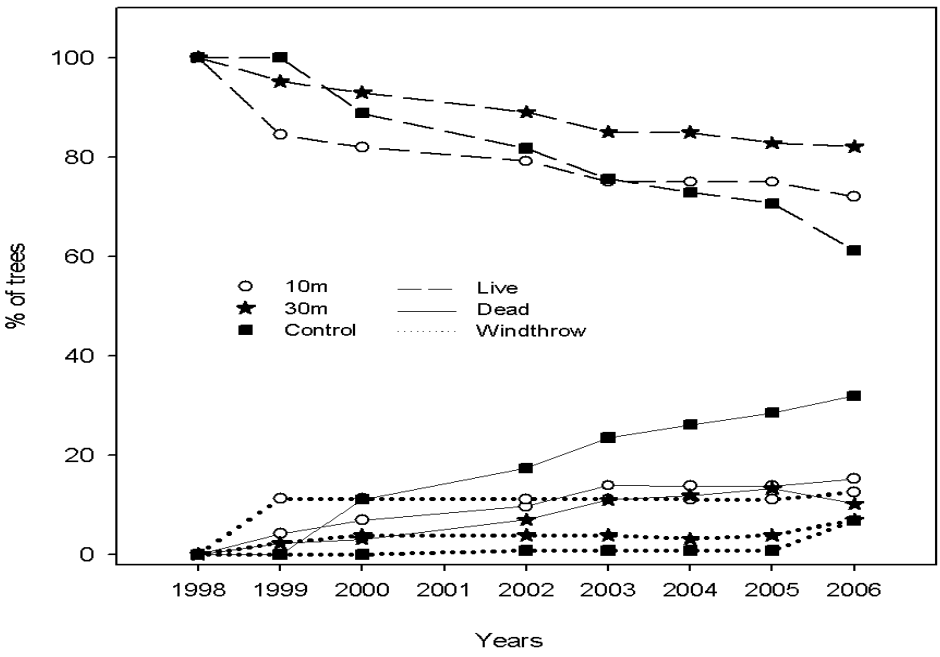

Fig. 1: Percentage of trees by status and treatment from 1998 to 2006

There were no significant differences in the average number of decayed logs in decay classes 1 (Bartels *et al* 1985; fresh LWD) and 2 (fine branches decayed) between buffer widths, however there were three times as many logs in decay class 3 (bark sloughing and sapwood decayed) in the 30 m buffer than in the 10 m and control treatments. The proportion of logs in advanced stages of decay was higher for in-creek logs than for spanning logs (Fig. 2). Height above stream was positively correlated with log diameter. These streams were constrained by a combination of hillslopes and fluvial terraces. Log height above stream was negatively correlated with the width of stream terraces. Logs decay most rapidly at the upper end where they contact the ground and in consequence, the more decayed logs were also shorter (Fig. 3).

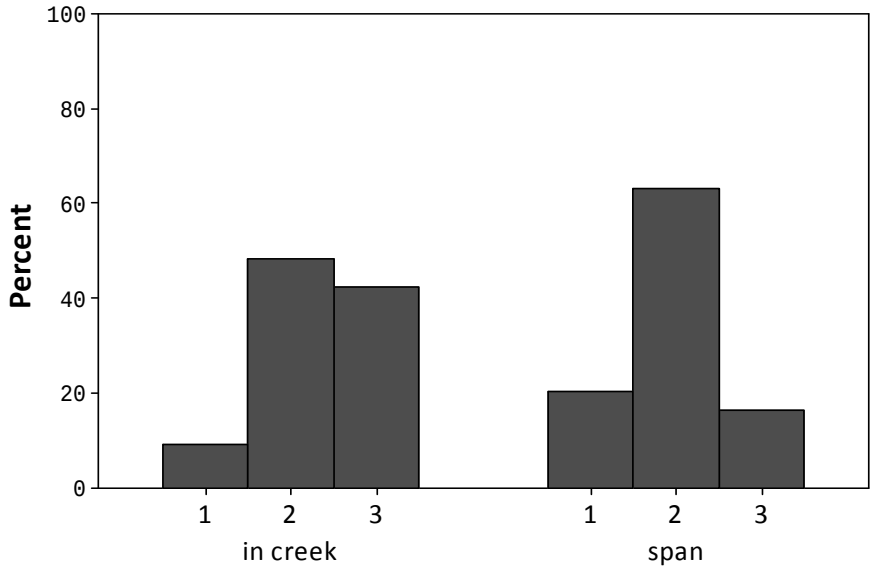

Fig: 2: Percent of in-creek and spanning logs by decay classes (Bartels et al. 1985), all size classes and treatments pooled

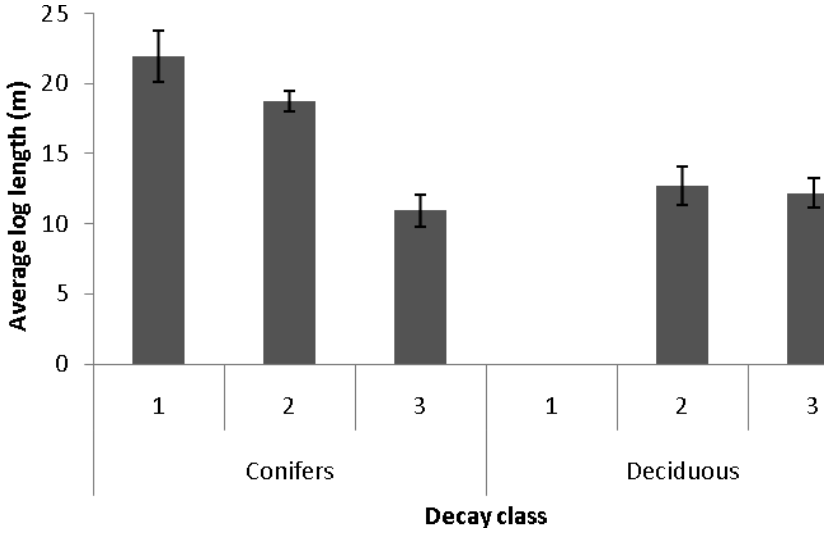

Fig: 3: Average log length (m) by decay classes and species group

Fourteen percent of the post-harvest windthrown trees delivered some sediment to the stream. Most of this was associated with trees within 5 m of the stream bank. The soil area exposed by uprooted trees was greatest in the 10 m buffer treatment. Area exposed per uprooted tree is positively related to tree diameter (r=0.60). These observations have implications for assessing windthrow impacts on streams and for riparian LWD modeling. None of the LWD recruitment models reported in the literature explicitly model the geometry and decay process of windthrown trees. By introducing a digital elevation model of stream valley geometry into our spatially explicity windthrow prediction model ForestGALES_BC, we are able to characterize the initial position and dimensions of individual windthrown trees (Fig. 4). We have also added a log decay function that reduces effective log diameter in annual time steps until the log is no longer able to support its own weight and drops to new ground support points. Further documentation of the decay rates of various species in riparian buffers will be necessary to refine species and site-specific decay coefficients.

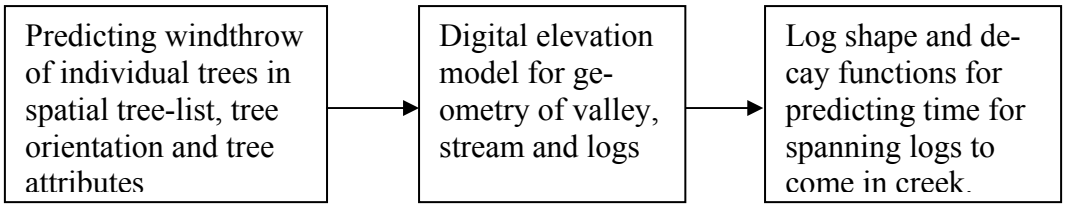

Fig: 4: Architecture of LWDSPAN windthrow recruitment model

4. Conclusions

In riparian buffers, recruitment of logs into stream channels where they can play a role in stream morphology lags the post-harvest pulse of windthrow by many years. This lag time depends on the size, species and initial condition of the logs, and their direction of fall relative to the geometry of the stream valley. These components can be characterized in submodels for LWD recruitment models. Logs that initially span the stream are in a state of advanced decay before they enter the stream channel and this has implications for their in-stream role and residence time and needs further investigation. Both windthrown trees and trees that died as a result of intertree competition were smaller than the average tree within the stand. Few windthrown trees were located in a fashion that would lead to the introduction of sediment into the stream channel.

Acknowledgement

The research was financially supported by BC Forest Science Program. We would like to thank Malcolm Knapp Research Forest's staff for their help during field work. We would also like to thank UBC Windthrow Research Group for their help in field data collection.

References

Bartels, R., Dell, J.D., Knight, R.L., Schaefer, G., 1985: Dead and down woody material. In: Brown, E.R., (Ed.).Management of wildlife and fish habitats in forests in western Oregon and Washington. USDA For. Serv. Pub. No. R6-FoWL-192. Portland, Oregon. 171-186.

B.C. Ministry of Forests (BCMOF), 1995: Riparian Management Area Guidebook. Ministry of Forests, Victoria, BC.

Miquelajauregui, Y., 2008: Vegetation community development in small stream buffers eight years after harvesting at Malcolm Knapp Research Forest. MSc Thesis, The University of British Columbia, Vancouver BC.

Moore, K., Jones, K., Dambacher, J., 2002: Methods for stream habitat surveys. Oregon Department of Fish and Wildlife. Aquatic Inventories Project. Natural Production Program. Version 12.1, Corvallis, OR.

Wang, X.L., Klinka, K., Chen, H.Y.H., de Montigny, L., 2002: Root structure of western hemlock and western redcedar in single- and mixed-species stands. Can. J. For. Res. 32, 997-1004.

Author's address:

Dr. Stephen Mitchell (stephen.mitchell@ubc.ca)
Department of Forest Sciences, University of British Columbia
3041-2424 Main Mall, Vancouver, BC, Canada V6T1Z4

Integrated use of two dimensional airflow model Aquilon and mechanistic model HWIND for risk assessment of tree stands to wind damage

Heli Peltola[1], Sylvain Dupont[2], Veli-Pekka Ikonen[1], Hannu Väisänen[1], Ari Venäläinen[3], Seppo Kellomäki[1]

[1]University of Joensuu, Faculty of Forest Sciences, Finland
[2]INRA, France
[3]Finnish Meteorological Institute, Finland

Abstract

In this work, we will apply a two dimensional airflow model Aquilon together with a mechanistic model HWIND for risk assessment of wind damage in Scots pine (*Pinus sylvestris*) and Norway spruce (*Picea abies*) stands under a range of forest configurations in Finnish conditions. In the above context, Aquilon will provide for HWIND vertical wind profiles for different forest configurations, including either a clear-cut area or another shorter stand upwind the stand edge considered to have a risk. HWIND will then predict the critical wind speeds needed for wind damage. Based on these simulations, we will demonstrate how the critical wind speeds are affected by different tree and stand characteristics at the downwind stand edges of clear-cut areas and by shelter provided by another shorter stand upwind the stand edge considered to have a risk for Scots pine and Norway spruce stands.

1. Introduction

Forest damage caused by high wind speeds and storms has during the past decades caused significant economic losses in forestry both in central and northern Europe. For example, in January 1990 and December 1999 about 100 and 175 million m^3 of timber was damaged in these regions by storms. Again, in January 2005 a storm damaged about 70 million m^3 of timber in southern Sweden, but spared Finland. So far, the most destructive storm damages observed in Finland have occurred in December 2001, when two separate storms (named as Pyry and Janika) blew down about 7 million m^3 of timber in southern Finland. The economic impacts of damage are particularly severe in managed forests because of the reduction in the yield of recoverable timber, increased costs of harvesting in damaged forests, and timber price reductions due to the quality decrease of damaged timber and additional unscheduled cutting operations.

In Finland, even relatively low wind speeds have caused significant damage (e.g. Janika: 10-min mean wind of 15-19 m/s; Pyry: 8-13 m/s, coupled with wet and heavy snow load of 30 kg/m^2 crown area). In addition to the properties of wind, also individual tree and stand characteristics and site conditions affect the susceptibility of tree stands to damage. Determining appropriate management practices for reducing the risk of damage is a complicated task because the probability of damage changes as a consequence of tree growth, interactions between neighbouring stands, and management actions (see e.g. Zeng et al. 2006). When risk assessment is concerned in Finnish conditions, the most crucial question is how the new clear-cuts will affect the local wind speeds and the wind loading on trees adjacent to the clear-cut areas.

For the assessment of risk of wind-induced damage, we should understand the mechanisms of tree stability and the resistance of trees against strong winds (Gardiner et al., 2000; 2008). Mechanistic models such as HWIND (Peltola et al., 1999), GALES/ ForestGales (Gardiner et al., 2000; 2008) and FOREOLE (Ancelin et al., 2004) were developed for this purpose, i.e. predicting the critical wind speeds needed for uprooting or breaking trees at stand edges or within stands (evenaged stands) under a range of silvicultural conditions, based on the properties of the trees and stands.

In this work, we will apply a two dimensional airflow model Aquilon together with a mechanistic model HWIND for risk assessment of wind damage in Scots pine (*Pinus sylvestris*) and Norway spruce (*Picea abies*) stands under a range of forest configurations in Finnish conditions. Based on these simulations, we will demonstrate how the critical wind speeds are affected by different tree and stand characteristics at the downwind stand edges of clear-cut areas and by shelter provided by another shorter stand upwind the stand edge considered to have a risk for Scots pine and Norway spruce. As a comparison, we will use corresponding predictions done by HWIND, applying a logarithmic wind profile at the upwind stand edge (see Zeng et al. 2009).

2. Outlines for the component models and simulations

2.1 Outlines for the Aquilon model simulations

The Aquilon model is a CFD type model that has been adapted to canopy flow (Foudhil et al., 2005). Turbulence is modelled statistically with a k-ε closure scheme. The flow equations in the canopy are modified to account for the drag forces and the production of turbulent kinetic energy by the vegetation. The dynamic part of the model has been previously validated in 2D cases (continuous and discontinuous vegetation canopies), against wind-tunnel and in-situ measurements (Foudhil et al., 2005), and in a 3D heterogeneous urban park (Dupont and Brunet, 2006).

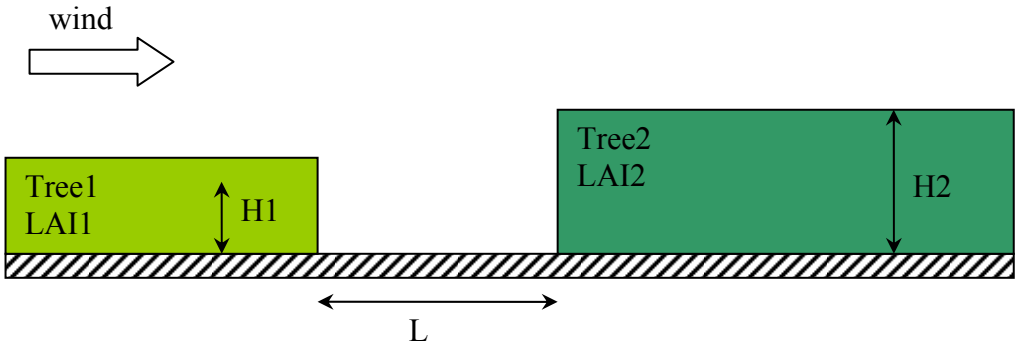

Fig. 1: Layout for the Aquilon simulations and examples of simulated wind profiles for Scots pine and Norway spruce at -0.5 tree heights before the downwind edge considered to have a risk; figure legends: L = clear-cut area, H1 = height of upwind tree stand (Tree1) with leaf area index (LAI) of 1 and H2 = height of downwind stand at risk (Tree2) with LAI of 2

In this work, Aquilon will provide vertical wind profiles for HWIND at upwind stand edge with different forest configurations, including either a clear-cut area (L) or another shorter stand (H1) upwind the stand edge (H2) considered to have a risk (see Fig. 1, Table 1). The simulated relative wind profiles at -0.5 tree heights before the edge are then used as input for further HWIND computations on critical wind speeds.

Table 1: Simulated cases by Aquilon for Norway spruce (NS) and Scots pine (SP)

Cases	L (m)	H1 (m)	H2 (m)	LAI1	LAI2	Tree1	Tree2
1, 4	Infinity	-	20.0	-	1	-	NS, SP
2, 5	Infinity	-	20.0	-	2	-	NS, SP
3, 6	Infinity	-	20.0	-	3	-	NS, SP
7, 8	200.0 (10 h)	20.0	20.0	2	2	NS, SP	NS, SP
9, 10	100.0 (5 h)	20.0	20.0	2	2	NS, SP	NS, SP
11,15	0.0	5.0	20.0	2	2	constant	NS, SP
12, 16	0.0	10.0	20.0	2	2	constant	NS, SP
13, 17	0.0	5.0	20.0	2	1	constant	NS, SP
14, 18	0.0	10.0	20.0	2	1	constant	NS, SP
19, 21	0.0	15.0	20.0	2	2	constant	NS, SP
20, 22	0.0	15.0	20.0	2	1	constant	NS, SP
23	400 (20 h)	20.0	20.0	2	2	NS	NS
24	800 (40 h)	20.0	20.0	2	2	NS	NS

We simulated by Aquilon the two dimensional airflow: i) over forest clearing (gap perimeter corresponding 5 and 10 tree heights of downwind stand height) and consequently for downwind stand edge of clearing, but also ii) in the conditions when there existed upwind stand instead of open area, with relative height of 25, 50 and 75 % of that of downwind stand height for Scots pine and Norway spruce (with average tree height of 20 m and diameter at breast height of 20 cm, and crown ratios of 40 and 70% for Scots pine and Norway spruce, with leaf area index (LAI) of 2, corresponding 700 stems/ha). We also used LAI of 1 and 3 in some cases to study the sensitivity of results on upwind edge stand density. Similarly, we simulated cases with large perimeters (from 20 h to infinity) as a comparison to above described cases.

2.2 Outlines for the HWIND model simulations

The HWIND model was originally developed to calculate the mean critical wind speeds of one hour average needed to uproot or break Scots pine, Norway spruce and birch (*Betula* spp.) trees at different distances from the downwind edge of a newly created clear-cut area (see Peltola et al., 1999). In the model, a tree is assumed to be uprooted if the maximum bending moment exceeds the resistance of the root-soil plate. Respectively, the stem is assumed to be broken if the breaking stress exceeds the critical value of modulus of rupture.

A good agreement has been demonstrated between HWIND, GALES and FOREOLE models at newly created stand edge conditions (see Ancelin et al., 2004), despite of the

fact that HWIND was originally designed to calculate the critical wind speeds at upwind stand edges in Finnish conditions, whereas GALES and FOREOLE were designed to calculate them within forest stands for British and French conditions. HWIND has also predicted critical wind speeds in line with those speeds actually caused damage in Finnish and Swedish conditions (see e.g. Talkkari et al., 2000; Blennow and Sallnas, 2004). The properties of the HWIND model, its parameters, inputs and the validity of its outputs have been discussed previously by Peltola et al. (1999), Gardiner et al. (2000, 2008), Blennow and Sallnäs (2004) and Zeng et al. (2006, 2009).

Zeng et al. (2009) recently modified slightly the parametrization of logaritmic wind profile in HWIND in order to consider also a shelter effect by another shorter stand upwind the stand edge considered to have a risk (i.e. resulting lower wind loading). However, this theoretical approch has not yet been validated based on experimental data or airflow simulations. In this sense, Aquilon simulations offer now possibility to validate HWIND model's assumption for logarithmic profile at upwind stand edge considered to have a risk. Therefore, we will make corresponding simulations by HWIND for upwind stand edges, by applying a logarithmic wind profile (see in details, Peltola et al. 1999, Zeng et al. 2009).

Based on HWIND simulations, we will analyze how the critical wind speeds are affected by: i) tree and stand characteristics (e.g. tree height, diameter and breast height, stand density) at the downwind stand edges of clear-cut areas (with different sizes) and ii) shelter provided by another shorter stand (i.e. height varies from 0, 25, 50 and 75 % of that of downwind stand edge at risk) upwind the stand edge considered to have a risk in Scots pine and Norway spruce. We consider here only uprooting as wind damage type regardless of tree species because it is in Finnish conditions the most typical type of wind damage under unfrozen soil conditions. The range used for different tree and stand characteristics in simulations correspond well the range observed in sample trees of forest inventory data representing permanent inventory plots in southern Finland.

3. Example results of simulations

The model simulations showed in general, that increase in tree height of the downwind stand or perimeter of the upwind stand decreased the critical wind speeds needed to uproot trees regardless of tree species. Increasing dbh/height-ratio of the downwind stand or shelter (relative tree height) offered by the upwind stand increased the critical wind speeds (Figs. 2 and 3). In Norway spruce with longer crown (crown ratio of 70% in simulations), the shelter effect of upwind stand height was stronger than in Scots pine (crown ratio of 40%). Norway spruce needed also on average lower wind speeds for damage than Scots pine. The simulated results by the Aquilon and HWIND differed also in some cases significantly from those by HWIND (see Fig. 2). For Fig. 3, the critical wind speeds at canopy top were transformed by the logarithmic wind profile into corresponding wind speeds at 10 m above ground at the stand edge of clear cut area (following original HWIND approach).

In general, the probability for strong wind speeds and, thus, risk of damage, differ also spatially much in Finland. Thus, the risk considerations are especially important on areas having high probabilities of damage (e.g. in Helsinki (south coast) probabilities for winds < 17 m/s are highest), when decisions for management of forests are made.

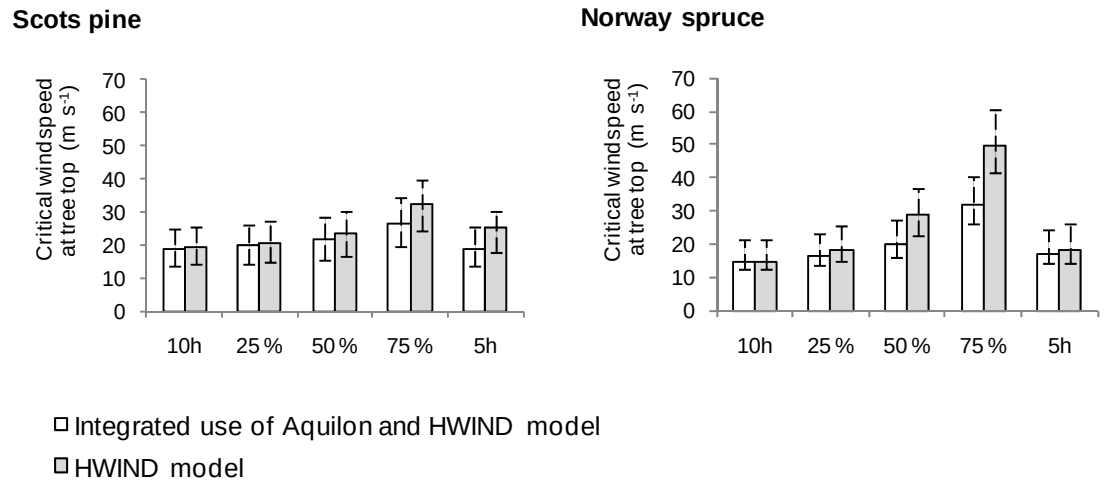

Fig. 2: Examples of predicted critical wind speeds: i) a clear-cut area (with perimeters of 5 and 10 tree heights (h) of downwind stand edge), and ii) another shorter stand (with relative height of 25, 50 and 75% of downwind stand edge) upwind the stand edge, considered to have a risk; the tree height = 20 m, stem taper = 1:100 for bars and 1:75 and 1:125 for error bars

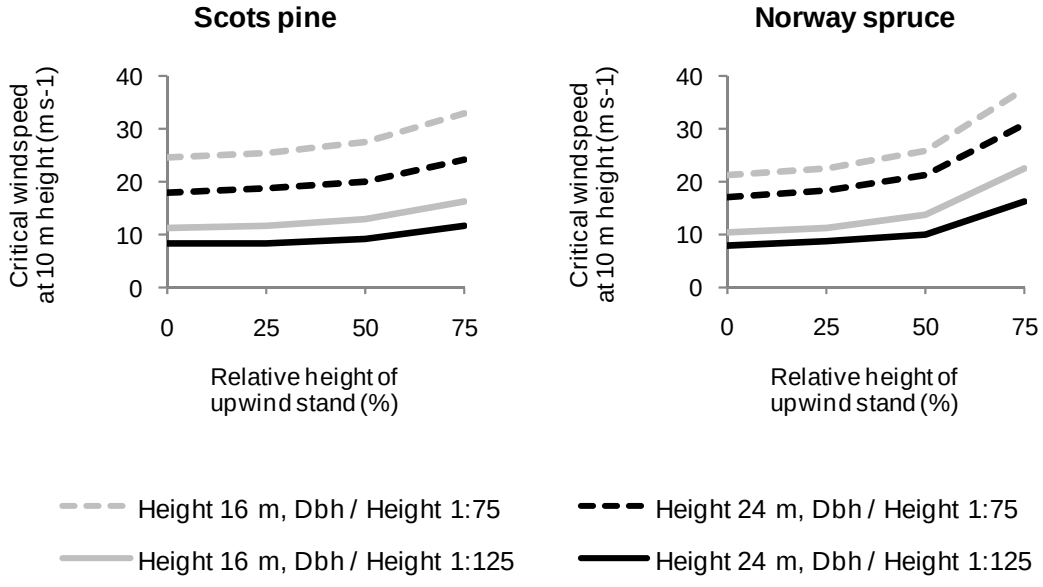

Fig. 3: Predictions for critical wind speeds (by Aquilon and HWIND) for trees of varying sizes with different forest configurations (see legends in Fig. 2); perimeter of clear-cut area is 10x downwind stand edge height

4. Conclusions

Compared to the integrated use of Aquilon and HWIND models, HWIND predicted alone larger critical wind speeds for Scots pine especially when the relative height of upwind stand, providing shelter for downwind stand edge at risk, increased significantly

or when perimeter of clear-cut area decreased. In Norway spruce, corresponding shelter effect differences were even more evident. This results from the fact that the modified logaritmic profile parametrization used in HWIND (see Zeng et al. 2009) seemed to output too low wind speeds in lower tree canopy compared to the Aquilon, resulting underestimation of the wind loading on trees and thus, overestimation of the shelter effect. Anyway, modelling tools like demonstrated in this work could support the decision making of forest managers when considering the silvicultural risks by wind.

References

Ancelin, P., Courbaud, B., Fourcaud, T., 2004: Development of an individual tree-based mechanical model to predict wind damage within forest stands. Forest Ecology and Management 203, 101-121.

Blennow, K., Sallnäs, O., 2004: WINDA - a system of models for assessing the probability of wind damage to forest stands within a landscape. Ecological Modelling 175, 87-99.

Dupont S., Brunet Y., 2006: Simulation of turbulent flow in an urban forested park damaged by a windstorm. Boundary-Layer Meteorol. 120, 133-161.

Foudhil, H., Brunet, Y., Caltagirone, J. P., 2005: A k-ε model for atmospheric flow over heterogeneous landscapes. Env. Fluid Mech. 5, 245-267.

Gardiner, B.A., Peltola, H., Kellomäki, S., 2000: Comparison of two models for predicting the critical wind speeds required to damage coniferous trees. Ecological Modelling 129, 1-23.

Gardiner, B., Byrne, K., Hale, S., Kamimura, K, Mitchell, S.J, Peltola, H., Ruel, J.C., 2008: A review of mechanistic modelling of wind damage risk to forests. Forestry 81, 447-463.

Peltola, H., Kellomäki, S., Väisänen, H., Ikonen, V-P., 1999: A mechanistic model for assessing the risk of wind and snow damage to single trees and stands of Scots pine, Norway spruce and birch. Canadian Journal of Forest Research 29, 647-661.

Zeng, H., Peltola, H., Talkkari, A., Strandman, H., Venäläinen, A., Wang, K., Kellomäki, S., 2006: Simulations of the influence of clear-cuttings on the risk of wind damage on a regional scale over a 20-year period. Canadian Journal for Forest Research 36, 2247-2258.

Zeng, H., Peltola, H., Väisänen, H., Kellomäki, S., 2009: The effects of fragmentation on the susceptibility of a boreal forest ecosystem to wind damage. Forest Ecology and Management, in print.

Authors' addresses:

Dr. Heli Peltola (Heli.Peltola@joensuu.fi),
Dr. Veli-Pekka Ikonen (Veli-pekka.Ikonen@joensuu.fi),
Mr. Hannu Väisänen (Hannu.Vaisanen@joensuu.fi)
Prof. Dr. Seppo Kellomäki (Seppo.Kellomaki@joensuu.fi)
Faculty of Forest Sciences, University of Joensuu
Yliopistokatu 7, FI-80101 Joensuu, Finland

Dr. Sylvain Dupont (sdupont@bordeaux.inra.fr)
INRA, UR1263 Ephyse
71 Avenue Edouard Bourlaux, F-33140 Villenave d'Ornon, Cedex, France

Dr. Ari Venäläinen (Ari.venalainen@fmi.fi)
Finnish Meteorological Institute
Erik Palmen place 1, FI-00101 Helsinki, Finland

Tree damages in Lisbon during southern windstorms

António Lopes, Marcelo Fragoso

Centre for Geographical Studies / CLiMA Research Group
(Climate and Environmental Changes)
Universidade de Lisboa, Portugal

Abstract

Street trees can cause damages when they fall during windstorms. In the last years it was observed an increasing number of falling trees and branches during extreme windy events. In the city of Lisbon the most of the falls occurs from October to December. Strong wind is generally a trigger to put poorly adapted or weakened/sick trees down. Local authorities must consider the costs of damages versus urban forest maintenance. From the period of 1990-2008 more than 32% of windstorms caused one or two falls and 16 % damaged vehicles parked in the streets. It was estimated that the partial cost of damages in vehicles is about 100 000€ per year in Lisbon. During southern windstorms, 56 % of the falls occurred in N/S oriented streets and only 23.4 % in W/E streets, revealing a good agreement between storm and street directions.

1. Introduction

Urban trees can cause injures in persons and damages to the cars when they fall during windstorms. In the last years falling trees were monitored in the city of Lisbon and a database (from 1990 to 2008), with the location of fallings trees and branches was constructed from the records of the Lisbon fire brigade (Lopes et al, 2008), which contains the damages in the cars parked in the streets. It was added the wind speed in the last 3, 6 and 12 hours before the call to the fireman, and street morphologic characteristics (H/W, street dominant direction, etc.).

The most representative species in Lisbon's streets are the European nettle tree (Celtis australis L.), the plane tree (Platanus hybrida Brot.), lime trees (Tilia spp.), blue jacaranda (Jacaranda mimosifolia D. Don), box elder maple (Acer negundo L.) and different species of poplars (Populus alba L., Populus nigra L. and Populus canescens). Poplars are the principal trees that fall probably due to their age in the city of Lisbon and poor adaptation to the urban soils (Soares and Castel-Branco, 2007).

The majority of the falls (Fig. 1) occurs from October to December (Lopes et al, 2008). From an inventory of 128 windstorm days in Lisbon from 1990 to 2006, large-scale atmospheric circulation patterns were investigated (Fragoso and Lopes, 2008 and 2009). It was found that frontal cyclones over Western Europe with W or SW winds over Portugal (30.5 %) and low system with SW or S winds (38.3 %) are the main circulation systems that cause the tree falls. The analysis of CAPE index from 59 soundings (for the same period) shows that instability increases in Autumn, when the occurrence of convective storms is dominant (CAPE Index in Autumn 661 J/kg; 301 J/kg in Winter; 263 J/kg in Spring and 543 J/kg in Summer) (Fragoso and Lopes, 2008).

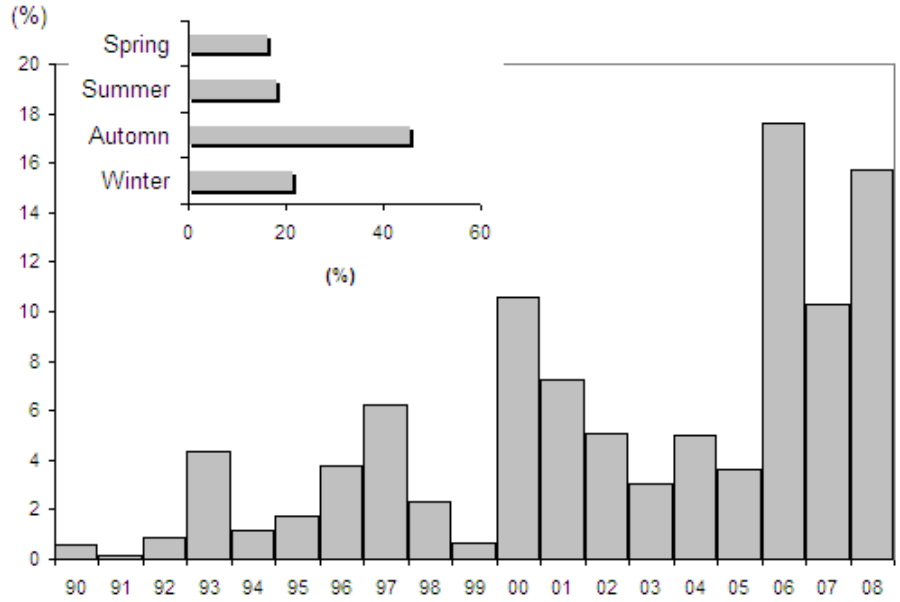

Fig. 1: Percentage of trees and branches that fell during windstorms in the period of 1990–2008

2. Objectives and methodology

The main goals of this research are: *i*) to verify if there is any correlation between wind direction and the orientation of the streets; *ii*) to assess the damages in vehicles parked in the streets during southern windstorms; *iii*) to identify wind risk areas in a central neighbourhood of Lisbon (along Av. EUA), with a micrometeorological model (ENVI-met®, by Michael Bruse & Team), (Bruse and Fleer, 1998).

The initial database was obtained from the information compiled by the Lisbon Fire Brigade and Rescue Services (*Regimento de Sapadores Bombeiros de Lisboa - RSBL*), which handles emergency calls. The database has certain limitations: a) the difference of time registered by the fire brigade (that corresponds to the time of the emergency call and not to the tree fall) and the occurrence which remains unknown; b) the occurrences recorded refer only to the incidents that caused disturbances or damages to people. This initial database (that includes, for the recent years, the vehicles affected by the falls) was completed with the geographical coordinates of each occurrence, some morphometric characteristics of the streets (H/W, main orientation, special features, etc.), and the wind speed and direction in *Gago Coutinho* Meteorological station (near the Airport), registered at the hour of the call and in the 3, 6 and 12 hours before the call. Due to the ongoing update of the database some results are only presented for the period of 1990 to 2006 (especially the relation between windstorm and street orientations).

3. Results

There is a good correlation between the number of street trees in each neighbourhood and the falls (Lopes et al, 2008) which indicates that they depend on the environment that is generally unfavourable for most arboreous species. Strong wind is generally a trigger to put poorly adapted or weakened/sick trees down. The distribution of tree falls

in Lisbon between 1990 and 2006 (the last two years are not yet implemented in the GIS system) is shown in Fig 2. The major part of them occurs in the streets with greats number of trees, in the axis of Campo Grande/Baixa (downtown) (Fig. 2b A), Campolide, Campo de Ourique e Alcântara (B), in the northeast part of the city (Encarnação and Chelas - C), and in the Benfica neighbourhood (D). Near the Tagus bank the falls are much less although riverside is well planted of trees. Further investigation should attend other factors like the influence of turbulence and fyto-sanitary problems. In the Expo 98 area there has been fewer occurrences because it is a new neighbourhood, build-up after the 1998 Lisbon World Exposition and consequently with very young and healthy trees.

Although it is recognized that trees brings many benefits to the urban environment the maintenance of the urban forest of a metropolitan area, like Lisbon region, by a single organization (usually the City Hall, or by small groups of locals in closed commonholds with the agreement of the local authorities) it is very difficult, expensive and requires a great number of experts (from landscape planners to gardeners).

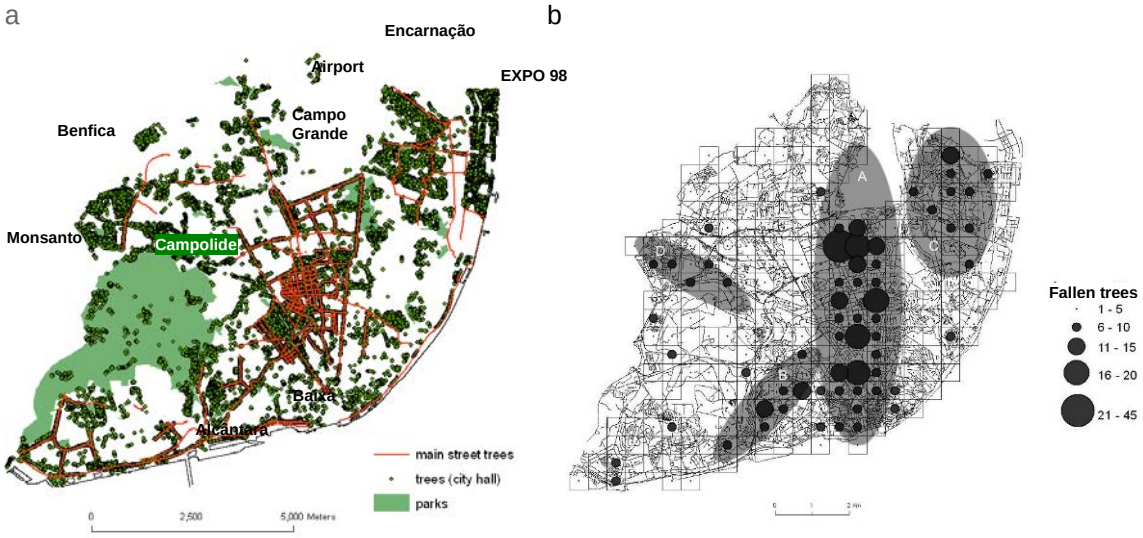

Fig. 2: Urban forest system (a) and fallen trees and branches (b) in Lisbon (1990-2006)

But the practice of letting "nature" take care about pruning (through the wind action), and the temptation of nothing do to control plagues and other problems, must be avoid. Evidence of damages caused by falling trees during windstorms let us conclude that the authorities must consider the costs of damages versus the costs of urban forest maintenance. And if it is difficult to carry on with the forest maintenance in a great urban area, it is possible to surgically intervene in the areas with a great risk of tree falls during windstorms. As far as we know, in Lisbon, any study has been done to account the damages of tree falls. A first attempt was carried out to assess damages in the vehicles parked in the streets. From the period of 1990- 2008 more than 32 % of occurrences registered by the fireman brigade caused one or two trees or branches falls and more

than 10 % caused four falls (Fig. 3). Should these numbers be neglected? From a total of 1680 falls, 16 % damaged vehicles parked in the streets. Taking into account the average value to repair a vehicle during 3 days and the car rental service during that period, it was estimated that every year the partial cost of damages is about 100 000€ in Lisbon (some effort have been done to add the fire brigade rescue services into account as well as other indirect costs).

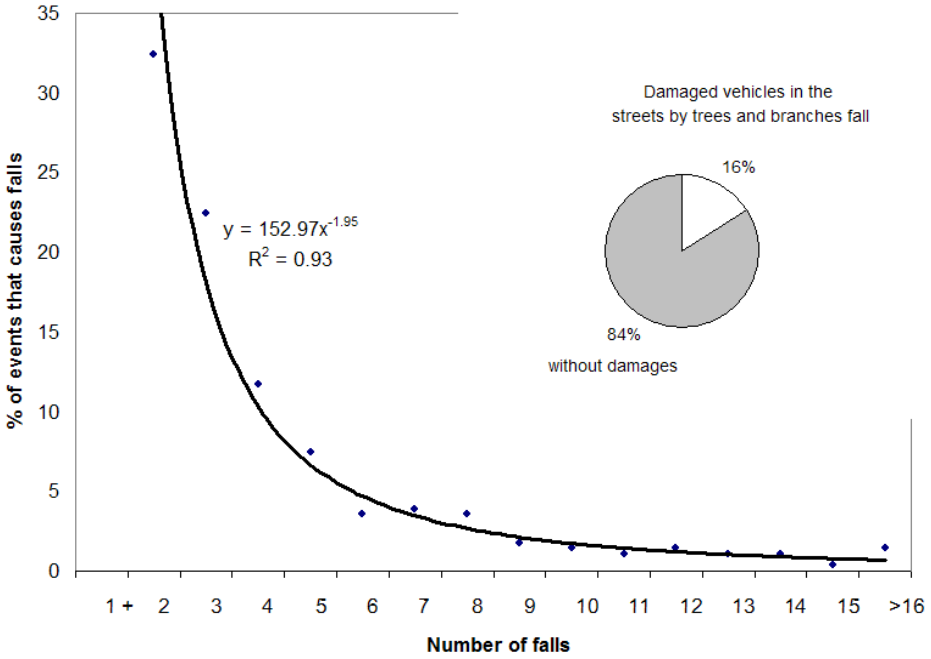

Fig. 3: Relations between windstorms and tree falls; the white part inside the circle represents the percentage of trees that damages vehicles parked in the streets

An attempt was made to correlate the trees that falls during southern windstorms (from October to December, 1990-2006 period) with urban morphology. A total of 410 tree falls and 125 branches falls were included in this part of the study (Table 1).

Table 1: Relation between street orientation and tree/branch falls during southern windstorms

General street orientation	Trees	*(%)*	Branches	*(%)*	Total trees and branches falls	*(%)*
N/S	238	*44.5*	64	*12.0*	302	*56.4*
E/W	90	*16.8*	35	*6.5*	125	*23.4*
Squares	50	*9.3*	20	*3.7*	70	*13.1*
Not well defined	32	*6.0*	6	*1.1*	38	*7.1*
Total	410	*76.6*	125	*23.4*	535	*100*

These storms have an average wind speed of about 9.5 m/s in the previous 12 hours before the call to the fireman brigade and the most frequent (modal) value was 11 m/s. The relation between wind direction and the street direction where the falls occurs is quite evident: more than 56 % of the falls occurred in N/S oriented streets, 23.4 % in W/E streets. The rest (20.2 %) occurred in squares or in streets with no predominant orientation.

A three-dimensional microclimate model containing the buildings and trees in a neighbourhood of central Lisbon (Fig. 4) was constructed. The initial conditions were set to the characteristics of southern windstorms (9 m/s; SW wind). The areas of strong wind acceleration were identified and compared with the pattern of the tree falls in that area. This can be a valuable tool to define the areas of mechanic wind risk and can be easily applied in urban planning.

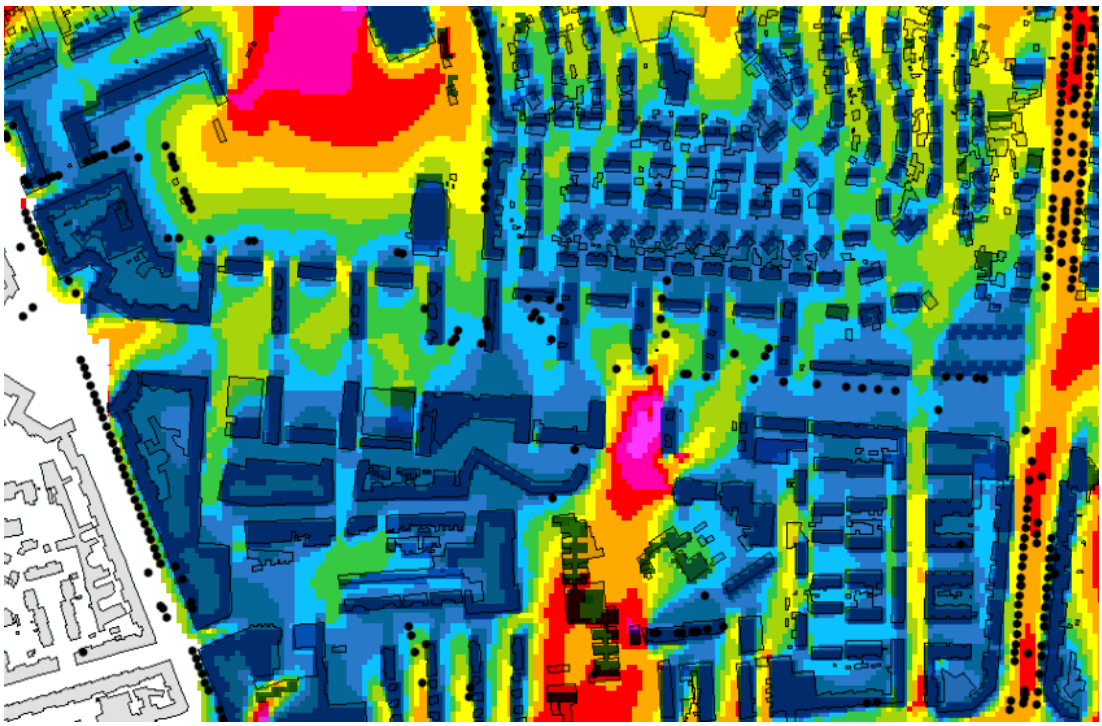

Fig. 4: Windstorm simulation with Envi-met software (Bruse and Fleer, 1998) in a central neighbourhood of Lisbon (Av. EUA); "Cut off" wind speed at 5 m high; yellow, red and pink colours represents wind estimation superior to 7 m/s.

4. Conclusions

The majority of tree and branch falls due to windstorms in the city of Lisbon occurs from October to December when wind speed exceeds 7 m/s. It is evident that the falls has increased in the last years probably due to environmental degradation. The wind can be only a factor that triggers more exposed specimen. Trees located in N/S oriented streets in the city centre are more exposed to these extreme events. Damages in the vehicles parked in the streets should not be neglected and more profound studies on costs/benefits regarding the maintenance of the urban forest should be implemented.

Microclimate models can be used to identify the areas of strong wind accelerations and mechanic wind risk. This can provide valuable information to urban designers and planners in order to ameliorate the practises of plantation of new street trees.

Acknowledgement

This research was undertaken within the scope of the project 'Climate and urban sustainability. Perception of comfort and climatic risks (URBKLIM)', funded by FCT (POCI/GEO/61148/2004).

References

Bruse, M., Fleer, H., 1998: Simulating surface-plant-air interactions inside urban environments with a three dimensional numerical model. Environ. Modell. Softw. 13, 373-384.

Fragoso, M.; Lopes, A., 2008: Windstorms in Lisbon: atmospheric circulation patterns and sounding derived stability indices. Abstracts of the 8th Annual Meeting of the European Meteorological Society/7th European Conference on Applied Climatology, Vol. 5, ISSN 1812-7053.

Lopes, A., Oliveira, S., Fragoso, M., Andrade, J., Pedro, P., 2008: Wind risk assessment in urban environments: the case of falling trees during windstorm events in Lisbon. In: K. Střelcová et al (Eds.), Bioclimatology and Natural Hazards, Springer, 55-74.

Soares, A.L, Castel-Branco, C., 2007: As Árvores da cidade de Lisboa. Floresta e Sociedade. Uma história em comum. Ed. Público/FLAD, 289-333.

Author's address:

António Lopes (antonio.lopes@campus.ul.pt)
Centre for Geographical Studies / Institute of Geography and Spatial Planning
Universidade de Lisboa
Al. da Universidade, Edifício FLUL, 1600-214 Lisboa, Portugal

Assessing risk and adaptation options to storms in European forestry

Mart-Jan Schelhaas[1], Geerten Hengeveld[1], Zbigniew W. Kundzewicz[2,3]

[1]Alterra, Wageningen UR, the Netherlands
[2]Research Centre for Agricultural and Forest Environment,
Polish Academy of Sciences, Poznań, Poland
[3]Potsdam Institute for Climate Impact Research, Potsdam, Germany

Abstract

Risks can theoretically be described as the combination of hazard, exposure and vulnerability. Using this framework, we evaluated the historical and future development of risk of wind damage in European forestry at the national level. Risk for wind damage in forests is expected to increase mainly as a consequence of increase in exposure (total growing stock) and vulnerability (defined by age class and tree species distribution). Projections of future wind climate are very uncertain, but an increase in hazard (storminess) cannot be ruled out. Adaptation options should aim to limit the increase in exposure and vulnerability. Only an increase in harvest level can stop the current build-up of growing stock, while at the same time it will lower vulnerability through the reduction of the share of old and vulnerable stands. Changing species from conifers to broadleaves helps to reduce vulnerability as well. Lowering vulnerability by decreasing the rotation length is only effective in combination with a higher demand for wood. Due to data limitations, no forecast of future damaged timber amount by storms was possible.

1. Introduction

European forests are among the most intensively managed forests in the world. Despite the intensive use, the forest area and growing stock are increasing, and this development is projected to continue for at least several decades to come (Schelhaas et al. 2006). At the same time, damage due to natural disturbances seems to increase (Schelhaas et al., 2003). Possible causes are such changes in the forest, but climate change could play a role as well. Given projected increases in forest resources and changes in storm climate, risk for wind damage to forests might increase considerably. One way to react to this development is to adapt forest management. This paper aims to evaluate the historic evolution of possible drivers and indicators of risk of wind damage in forests and to asses how adaptation measures in forestry could contribute to reduction of adverse consequences of future climate change. Countries assessed are Finland, the United Kingdom, Denmark and the Czech Republic.

2. Theoretical framework

Risks, such as the risk for natural disturbances, can theoretically be described by the combination of hazard, exposure and vulnerability (Kron, 2002). Any change to one of these components will lead to a corresponding change in risk level. Hazard is defined as the probability of occurrence and the magnitude of a particular disturbance agent. Exposure is the amount or value of the goods (or services) that can be damaged, including for example the number of people present in the area. Vulnerability expresses the resistance of the subject under study to the damaging agent, i.e. how easily damage will occur.

The hazard of wind is entirely related to the wind climate. European countries with Atlantic coastlines generally experience higher wind speeds, with Ireland and the United Kingdom in particular having a rather severe wind climate. Also, mountainous regions generally experience a more severe wind climate due to topographical influences. Wind speeds are usually presented as hourly average (ECMWF, 2009). Since wind damage to forests generally occurs during events with high wind speeds, we take the maximum observed average hourly wind speed in a year as indicator for the wind climate.

Storms can influence all forest functions and services, like timber production, water and soil protection, biodiversity and landscape amenity. Exposure is defined as the value of all these functions. However, many of these are difficult to quantify. Wind damage is usually reported in terms of wood volume damaged, so we take total growing stock volume as a proxy for exposure to wind damage.

Age (as a proxy for tree height) and tree species composition are found to be important indicators of vulnerability of forests. These two can usually be extracted from historic inventory data for a range of European countries, and from model simulations for the future. We developed the following vulnerability indicator:

$$V = \frac{\sum_{j} (a_{j,young} \times b_{j,young} + a_{j,mature} \times b_{j,mature})}{a} \quad (1)$$

where V is the vulnerability, $a_{j,young}$ and $a_{j,mature}$ the area of tree species group j below and above a certain threshold, $b_{j,young}$ is the relative vulnerability of young stands of tree species group j, $b_{j,mature}$ is the relative vulnerability of mature stands of tree species group j and a the total forest area Table 1 gives an overview of the groupings of tree species, relative vulnerability scores and threshold ages used, based on literature review. The relative vulnerability ranges from 1 (low vulnerability) to 6 (high vulnerability), and thus also the calculated total vulnerability score can range between 1 and 6.

Table 1: Vulnerability scoring of tree species

Tree species group (j)	$b_{j,young}$	$b_{j,mature}$	Threshold age
Broadleaves except poplar	1	3	80
Poplar	1	4	10
Conifers other than Norway and Sitka spruce	1	4	40
Norway and Sitka spruce	1	6	40

3. Data and methods

Historical growing stock for 1950 and 2000 was taken from Kuusela (1994) and MCPFE (2007) respectively. Vulnerabilities were calculated from relevant national inventory reports as close as possible to these dates. Historical data on damaged volume by wind were taken from the Database on Forest Disturbances in Europe (Schelhaas et al. 2001), for the period since 1948 whenever available. Historical wind hazard was calculated from the Re-Analysis data at ECMWF (2009), including data for the period 1948-2007. For each grid cell (250 by 250 km), the maximum observed wind speed

(hourly average) per year was extracted. From this series, also the average maximum annual wind speed was calculated, giving an indication of the severity of the wind climate. A GIS was used to calculate national averages.

For the development of future exposure and vulnerability under various adaptation measures, the European Forest Information Scenario model (EFISCEN V3.1.3) was applied. EFISCEN is a model that simulates the development of forest resources at scales from provincial to European level (Schelhaas et al., 2007). The core of the EFISCEN model was developed by Sallnäs (1990). EFISCEN is mostly used as a tool to evaluate and compare different scenarios. For the baseline scenario, wood demand was assumed to increase slightly. We assumed that climate change would have no influence on the forest growth level. In addition to the baseline, the following four adaptation scenarios were considered: (1) Increased harvest level (max): By increasing the harvest level, exposure to wind damage could be decreased; (2) Rotation length decrease (rotdec): A 10-year decrease in rotation length could decrease the forest area at risk for wind damage; (3) Tree species change (sp_change): Regeneration of coniferous area was for 50% done by broadleaved species, to reduce vulnerability; (4) A combination of the other three, aimed at minimising wind risk (max_rotdec_sp_change). We were not able to obtain reliable wind speed projections for the prediction of future wind hazard. Therefore we chose to assume no change in future wind climate and to discuss possible future changes in a qualitative way.

4. Results

The maximum annual wind speed that can be expected above land is clearly linked to distance to the Atlantic Ocean and other seas. The United Kingdom is fully exposed to depressions coming from the Atlantic and on average experiences an annual maximum wind speed of 19.4 m/s (Table 2). Denmark is a bit more sheltered with values of 18.1 m/s. In Finland the average annual maximum is 10.4, while in the Czech Republic it is 12.2 m/s. The Czech Republic reported the highest amount of damaged timber in the period 1948-2007 with 107.7 million m^3 (Table 2). Damage in the other three ranged from 16.0 in Poland to 19.7 million m^3 in Finland.

Due to its skewed age class distribution, the United Kingdom shows the lowest vulnerability of the countries under study. It increased from 1.6 in 1980 to 1.7 in 2000, but was projected to increase to 3.6 by 2100 under the baseline scenario. Denmark showed a similar development, with little change between 1951 (2.0) and 2000 (2.2), but a drastic increase to 3.6 in 2100 under the baseline scenario. Due to the harvest of older stands in Finland, vulnerability decreased from 3.9 in 1952 to 3.0 in 2000. Under the baseline scenario, it is expected to increase to 3.2. Vulnerability in Czech Republic was stable over the last half a century at 3.5 and is hardly expected to change over the coming century. Decreasing rotation lengths had in all countries only a very minor effect on the vulnerability. Increasing the harvest level had not much effect in the Czech Republic (-0.1 point), but a high effect in Denmark (-1.5) and the United Kingdom (-1.9). Changing the species distribution towards broadleaves resulted in a decrease of the vulnerability in the range of 0.5 (Untied Kingdom) to 0.8 (Czech Republic). The combination of these three scenarios gave the highest reductions of vulnerability, with a reduction just below 1 point for the Czech Republic to a reduction of 2.4 in the United Kingdom.

Table 2: Indicator values for wind risk

		Finland		Denmark	
Wind speed	historic	1948-2007	10.4	1948-2007	18.1
Vulnerability	historic	1952	3.9	1951	2.0
	historic	2000	3.0	2000	2.2
	baseline	2100	3.2	2100	3.6
	maximum harvest	2100	2.8	2100	2.1
	rotation decrease	2100	3.1	2100	3.5
	species change	2100	2.5	2100	2.8
	max_rotdec_sp_change	2100	1.8	2100	1.6
Exposure (Mm^3)	historic	1952	1538	1950	39
	historic	2000	2091	2000	74
	Baseline	2100	3237	2100	272
	maximum harvest	2100	1998	2100	146
	rotation decrease	2100	3033	2100	265
	species change	2100	2779	2100	242
	max_rotdec_sp_change	2100	1247	2100	150
Damage	historic (Mm^3, total in period)	1948-2007	19.7	1948-2007	16.0
	historic (total compared to 2000)		0.9		21.5

		United Kingdom		Czech Republic	
Wind speed	historic	1948-2007	19.4	1948-2007	12.2
Vulnerability	historic	1980	1.6	1950	3.5
	historic	2000	1.7	1994	3.5
	baseline	2100	3.6	2100	3.6
	maximum harvest	2100	1.7	2100	3.5
	rotation decrease	2100	3.5	2100	3.5
	species change	2100	3.1	2100	2.8
	max_rotdec_sp_change	2100	1.2	2100	2.8
Exposure (Mm^3)	historic	1950	110	1950	322
	historic	2000	267	2000	631
	Baseline	2100	1168	2100	1103
	maximum harvest	2100	355	2100	899
	rotation decrease	2100	1134	2100	1021
	species change	2100	1073	2100	925
	max_rotdec_sp_change	2100	334	2100	870
Damage	historic (Mm^3, total in period)	1948-2007	17.9	1948-2007	107.7
	historic (total compared to 2000)		6.7		17.1

Exposure, expressed as the total timber volume in a country, is strongly related to the forest area in a country. Denmark only has little timber volume (74 million m^3 in 2000) in comparison with Finland (over 2 billion m^3 in 2000). All countries showed a huge

increase in timber volume over the period 1950-2000, and this increase is projected to continue towards 2100. Decreasing the rotation age or changing the tree species composition only had a minor effect on the exposure. Increasing the harvest level had a strong effect, but could in many cases not avoid an increase in exposure in 2100 as compared to 2000. The combination of the three scenarios yielded an exposure in 2100 comparable to the increasing harvest scenario, only in Finland was the reduction of exposure more pronounced.

5. Discussion and conclusions

Over the last 50 years, the European forests have changed considerably. In most parts of Europe the forest area expanded, the growing stock increased and the forest has become older. Under the baseline scenario, these trends are expected to continue until 2100. It is still uncertain how climate change will affect future risk to wind damage in forests, but the projected increase in exposure and vulnerability will increase the risk considerably. Only an increase in harvest level can stop the current build-up of growing stock, while at the same time it will lower vulnerability through the reduction of the share of old and vulnerable stands. Changing species from conifers to broadleaves helps to reduce vulnerability as well. Lowering vulnerability by decreasing the rotation length is only effective in combination with a high demand of wood.

Projections of future wind climate are difficult with the current generation of climate models, especially concerning extreme events. The majority of the current generation of models show, for a future warmer climate, a poleward shift of storm tracks, with greater storm activity at higher latitudes (cf. Kundzewicz et al., 2004). Even if the wind climate would not change, we can expect an increasing risk for wind damage in forests due to the expected large increase in exposure and vulnerability under the baseline scenario. If we assume an increase in storminess, the risk would increase even further.

Unfortunately we were not able to fit a regression model on the data, so we cannot make predictions on future risks under the difference scenarios. One cause is doubts about the quality of the wind speed dataset (Smits et al., 2005), but also the quality and completeness of the damage dataset must be looked at with care. For example, Holmsgaard (1986) estimated that although a good overview exists for Denmark for the major storm damage to forest in the 20th century, only half of the total damage was included in his overview, the rest consisting of smaller windthrows. If a year when no damage is reported is considered as a year with no damage, the regression results are heavily influenced by these data points, since they are many. This would lead to an underestimation of the risk in severe events. If these years are excluded, only little data remains.

Vulnerability to wind damage of a particular forest stand can be modified by many factors, like thinning regime, regeneration method, species mixture and occurrence of openings in the forest at the windward side (Quine et al., 1995). These were not included in our study, but must be taken into account in studies at the landscape and stand level scale.

Acknowledgement

This study was financed by the European Commission through the ADAM project (Adaptation and Mitigation: Supporting European climate policy, FP7-018476). The research is part of the strategic research programmes “Sustainable spatial development of ecosystems, landscapes, seas and regions" and “Climate change”, funded by the Dutch Ministry of Agriculture, Nature Conservation and Food Quality, and carried out by Wageningen University Research centre. Furthermore we would like to thank Emil Cienciala and Zuzanna Exnerová from IFER for their help in obtaining historical forest inventory data for the Czech Republic.

References

ECMWF, 2009: European Centre for Medium-Range Weather Forecasts, www.ecmwf.int. Cited 2 February 2009.

Holmsgaard, E., 1986: Historical development of wind damage in conifers in Denmark. In: Minimizing Wind Damage to Coniferous Stands (ed. Communities, CotE), pp. 2–4. Lövenholm Castle, Denmark.

Kron, W., 2002: Flood risk = hazard x exposure x vulnerability. In: Wu M. et al. (ed.) Flood Defence, Science Press, New York.

Kundzewicz, Z.W., Bärring, L., Giannakopoulos, Ch., Graczyk, G., Leckebusch, G., Palutikof, J., Pińskwar, I., Radziejewski, M., Schwarb, M., Szwed, M., Ulbrich, U., 2004: Changes in extremes occurrence. Part II. Impact on selected sectors. Papers on Global Change 11, 143-150.

Kuusela, K., 1994: Forest Resources in Europe 1950-1990. Research Report 1, European Forest Institute. Cambridge University Press.

MCPFE, 2007: State of Europe’s forests 2007. The MCPFE Report on Sustainable Forest Management in Europe. Ministerial Conference on the Protection of Forests in Europe, Liaison Unit Warsaw, Poland.

Quine, C., Coutts, M., Gardiner, B., Pyatt, G., 1995: Forests and wind: Management to minimize damage, Forestry Commission Bulletin 114. HMSO, London.

Sallnäs, O., 1990: A matrix growth model of the Swedish forest. Studia Forestalia Suecica 183, Swedish University of Agricultural Sciences, Faculty of Forestry. Uppsala, Sweden.

Schelhaas, M.J., Eggers, J., Lindner, M., Nabuurs, G.J., Pussinen, A., Päivinen, R., Schuck, A., Verkerk, P.J., van der Werf, D.C., Zudin, S., 2007: Model documentation for the European Forest Information Scenario model (EFISCEN 3.1). Wageningen, Alterra, Alterra report 1559, EFI Technical Report 26, Joensuu, Finland.

Schelhaas, M.J., Nabuurs, G.J., Schuck, A., 2003: Natural disturbances in the European forests in the 19th and 20th centuries. Global Change Biology 9, 1620-1633.

Schelhaas, M.J., van Brusselen, J., Pussinen, A., Pesonen, E., Schuck, A., Nabuurs, G.J., Sasse, V., 2006: Outlook for the development of European forest resources. A study prepared for the European Forest Sector Outlook Study (EFSOS). Geneva Timber and Forest Discussion Paper, ECE/TIM/DP/41. UN-ECE, Geneva.

Schelhaas, M.J., Varis, S., Schuck, A., 2001: Database on forest disturbances in Europe (DFDE). European Forest Institute, Joensuu, Finland. http://www.efi.fi/projects/dfde/. Cited 2 February 2009.

Smits, A., Klein Tank, A.M.G., Können, G.P., 2005: Trends in storminess over the Netherlands, 1962–2002. International Journal of Climatology 25, 1331-1344.

Authors' addresses:

Dr. Mart-Jan Schelhaas (martjan.schelhaas@wur.nl)
Dr. Geerten Hengeveld
Alterra, Wageningen University Research,
PO Box 47, 6700 AA Wageningen, The Netherlands

Prof. Dr. Zbigniew W. Kundzewicz
Potsdam Institute for Climate Impact Research
Telegrafenberg A51, PO Box 60 12 03, D-14412 Potsdam, Germany

Salvage decision scheme in The Netherlands

Anne Oosterbaan

Alterra, Wageningen UR, The Netherlands

Abstract

After the storm of January 2007 a research project has been carried out with the aim of developing a decision support tool for forest managers to decide which part of windfallen wood should be left in the forest and which part should be salvaged, based on economic, social and nature conservation criteria.

3 years of research around plots with different degrees of storm damage in Scots pine-stands gave better insight in:

- economic aspects: financial costs/benefits and influencing factors when damaged wood is left in the forest,
- insects: to discover which insect species develop in the dying stems, stem parts have been investigated under conditioned cirumstances,
- pathogens: inventories of pathogens developing on the dead wood have been carried out each year,
- development of natural regeneration,
- development of herb and moss vegetation.

Based upon the results of these investigations a decision scheme will be developed and presented.

1. Introduction

In The Netherlands heavy storms occur every 10-20 years, and an increase in storm frequency seems likely. Often forests are not spared in such events. In all cases storm damaged trees posing imminent risk to people or properties will be removed first. Then the question should be answered what storm timber should be salvaged and how much will be left in the forest. This question is not so easy to answer. At one hand, storm wood in the forest will give more dead wood and this will enhance biodiversity (Bijlsma en Ten Hoedt 2006, Grasveld en Imming 1987, Koop et al 1990), but on the other hand it represents a loss in revenue, especially when larger quantities are damaged. Also further activities in the stand like thinning or control of unwanted species can cost more. Also a relevant question is how the average forest visitor views greater quantities of storm wood. For an informed answer to the question of how much storm wood in the forest should be left, a complex balancing of the various aspects is required. Commissioned by the Ministry of LNV in 2007, a project was launched to investigate the importance of different aspects on hand of developments in a series of stands with different amounts of storm wood. The ultimate goal of this project is to develop a support tool which gives forest managers information to take an informed decision about the quantities of storm wood to be left in the forest. This tool will be compiled in the course of 2009. This article gives an overview of the current research with a number of hitherto obtained results.

2. Research project

In cooperation with the Dutch State Forest Service a series of stands of Scots pine with different quantities of storm wood was selected in 2007 (e.g. Fig. 1). These stands were monitored for:

- growth and vitality,
- development of tree, shrub, herb and mosslaye,
- presence of insects that depend on dead wood,
- presence of fungi that depend on dead wood.

In the second year forest visitors were asked for their opinion about different quantities of storm wood in the forest. A desk-study was carried out for economic aspects of storm wood.

The results of these studies have to deliver the basic information for a decision support tool for forest managers to take well informed decisions about the quantities of storm wood to leave in the forest behind.

Fig. 1: Scots Pine stand with much storm wood (Veluwe, The Netherlands)

3. Methods

During the period 2007-2009 in 2 series of stands of Scots pine (*Pinus sylvestris)* with different quantities of storm wood (much > 100 m3, moderate 10-50 m3 and storm

wood removed), the stand growth and vitality and the development of tree, shrub, herb and mosslayer were recorded (in 3 plots per storm wood level).

During the first, second and third year, the presence of insects that depend on dead wood was recorded in the same stand series. In the first year only a field recording was carried out (to be expected bark beetles) and a number of trees were partly peeled with the aim to obtain an indication of the activity of bark beetles. In the second and third year stemparts of the trees were brought under conditioned circumstances and investigated for insects.

In all 3 years a recording of fungi that depend on dead wood has been carried out by macroscopic evaluation of fruiting bodies in the field. In the summer of the second year 150 forest visitors, who passed a stand with a high level of storm damage, were asked for their opinion about the phenomenon and background of storm wood in the forest. The desk-study for economic aspects of storm wood focused on the costs and benefits of different amount of storm wood and at what point salvage should be emphasized.

4. Preliminary results of investigations

Insects

Behind the bark of the pine developed a series of bark beetles, predators, parasitic wasps, fungi and fungus eaters. It is noteworthy that in this study a number of new species for our country are found. The investigation further showed that in areas with many storm damaged trees larger numbers of *Tomicus piniperda L.* , *Phaenops cyanea* and wasps beauty seemed to be compared with plots with little storm wood. This phenomenon can be caused by a kind of magnetic force by the large number of stems. In addition, the sunny plots are attractive for warm-liking species like blue pine beetle. *Phaenops cyanea* can be a danger for unhealthy trees (Moraal 2008, Wermelinger et al. 2008).

Opinion of forest visitors

The survey of 157 passers of a heavily damaged storm plot showed that almost all respondents found the appearance of the forest important. Approximately three quarters of the respondents considered the storm plot natural and varied. On the degree of attractiveness, the opinions differed: more than one third judged attractive but 20 % pronounced unattractive.

Economics

When answering whether storm wood from a financial point of view should be harvested or not, different factors play a role:

- total amount of timber to be harvested and sold,
- number of trees per hectare (density) that is blown and damaged,
- diameter of the storm wood and the species,
- type of storm damage,
- safety,
- timber prices.

Calculations for different diameters and price levels indicates that it is always financially attractive to harvest storm wood thicker than 30 cm DBH, while harvesting stems < 15 cm DBH is not worthwhile. Furthermore, the additional operating costs (due to the lying trees) in the next 20 years are not very high.

5. Conclusions

The following interim conclusions can be drawn:

- within a relatively short time a considerable diversity of insects develops in the dying pine stems,
- most of the forest visitors can agree with leaving a rather high amount of wind blown trees in the forest,
- additional operating costs, by leaving storm damaged trees in the stand, are not too high.

References

Bijlsma, R.J., ten Hoedt, A., 2006: Spectaculaire bryologische ontwikkelingen op en rond dood naaldhout in "Neerlands Thüringen" (Zuidoost-Veluwe). De Levende Natuur 5, 208-212.

Grasveld, P.C.M., Imming, J.W.T.M., 1987: Natuurlijke ontwikkeling op stormvlakten in Drente. Intern Rapport 87/31. Rijksinstituut voor Natuurbeheer. Leersum. 64 p.

Koop, H., Berris, L., Wolf, R., 1990: Stormschade, wind in de zeilen voor natuurontwikkeling in bossen. Nederlands Bosbouw Tijdschrift 10, 318-324.

Moraal, L., 2008: Blauwe dennenprachtkever in stormhout- nieuw fenomeen. Vakblad Natuur, Bos, Landschap 2, 20-21.

Wermelinger, B., Rigling, A., Schneider Mathis, D., Dobbertin, M., 2008: Assessing the role of bark- and wood-boring insects in the decline of Scots pine (*Pinus sylvestris*) in the Swiss Rhone valley. Ecological Entomology 33, 239-249.

Author's address:

Ing. Anne Oosterbaan (anne.oosterbaan@wur.nl)
Wageningen University Research
Droevendaalsesteeg 3, NL-7608 PB Wageningen, The Netherlands

Parametric modelling of trees and using integrated CAD/CFD tools: application to create a planting pattern for new forests

Amir Mosavi

University of Debrecen, Hungary

Abstract

This project presents a simulation based design method in order to approach the safer built forest planting patterns against the wind. Planting the trees based on the suggested patterns which are modelled and simulated according to the topological map of the site, trees' shading, number of trees/planting space, kind of trees and finally wind behaviour is expected to make the future forests much safer against the wind´s attack. For the reason of modelling and simulation the forest environment the recent technological advances in CAD and CAE are applied. The result of this research shows that how the planting pattern could be effective in order to reduce the speed of wind at the position of each tree. For this reason the process of simulation and optimisation continues till finding the optimal pattern.

1. Introduction

For the reason of planting new forest there are many standard planting patterns available, which are just for the planting the smooth landscapes. These patterns have been developed according to the basic and static design factors including kind of trees, soil material, usual climatic condition and sun. In fact these patterns might deliver high risk of being affected by wind. In order to reach the optimal pattern, the dynamic objectives such as wind must be also included to the process. Behaviour of wind in the different landscapes, according to topographic characteristics differs. Wind is an undefined force which in the different topographic scenarios reacts unexpectedly. Wind is deviated with obstacles, rocks, hills, buildings, utility locations, detention ponds and etc. The objects have effects on wind speed, direction and flow. One of the few tools for limiting the speed of wind in order to minimize the effect of wind is option of positioning the trees at the time of planting.

According to the knowledge of Computational Fluid Dynamics, which simulates and analyzes the fluid movements, right positioning of the trees in the site could reduce the speed of the wind at identified points. Based on this fact the target is to reduce the speed of wind by at least five percent at the trees´ positions with just design and optimizing the planting patterns.

Usually trees are planted in rectangular spacing which makes working with planting equipments much easier and the process of planting is done faster. Created corridors make the access to any part of forest possible. There are also dozen geometrical planting patterns available with identified advantages and disadvantages which are widely utilized. Geometrical planting patterns are the methods of planting in the smooth fields. Such these planting patterns have not application in the planting the hilly lands and non-smooth sites.

2. Review

Researchers have tried to simulate the condition of forest with advanced tools of Computer Aided engineering (CAE), which are usually utilized for the industrial applications rather than environmental. For instance, the wind is simulated by Computational Fluid Dynamics (CFD) tools. Also there are projects, which the tree is modelled applying the Computer Aided Design (CAD) tools. Reviewing these projects declare that it is tried to bring the advanced computer design and simulation technologies and make them involved in this regard.

The related researches could be studied in two subjects. First subject deals with the researches regarding built forest planting patterns and second one is related to wind simulations. Many research activities have been recently done related to traditional planting patterns in order to improve their functioning and performance according to the identified static objectives.

Note that in this paper the phrase of objective refers to the forest environmental factors, which have effects on forest sustainable, growing and survival which are subjected to be optimized.

Based on these researches now there is useful knowledge available, which could be trusted for further research. For instance it is possible to find out the maximum number of trees in the limited area of site [5]. There are also many researches, which went a bit further to simulate and optimize the new objectives such as trees' shading for the reason of creating effective planting patterns which deliver more sun and balance it for all trees.

Harja et al. (2004) introduced a computer tool, which simulates the trees' shading according to the kind of tree [1]. As sometimes two or more types of trees are planted in the site, the introduced computer tool has ability to deal with that. In this research the plantings patterns are designed just according to the one objective and one design variable. Identified objective is amount of sun and design variable is the kind of tree.

Meanwhile there is other kind of researches, which have done in the area of wind simulation and its effect on trees. The outcomes of these researches deliver more information and understandings about wind behavior and characteristics and also present the possibility of analyzing and calculation the speed of wind at the identified points.

In most of the researches, the planting patterns are tried to be introduced via a mono-objective optimization, which means the one single objective is the aim of design and optimization the planting pattern and besides the methods of the optimization are mostly based on trial and error approaches.

Because the lack of technologies in the proper modelling and simulation of the objectives and also absence of a tool in order to couple simulations, an effective method for design the planting pattern based on the all involved objectives of the site has not yet been introduced.

In order to find the optimal design of the planting pattern, forest condition must be simulated and the arrangement of the pattern must be optimized in order to make all objectives satisfied.

The weakness of the reviewed projects could be concluded as follow. The following list shows the factors which have not being yet utilized because the lack of the technologies:

(i) effective optimisation tool,

(ii) involving all objectives,

(iii) involving all design values and factors,

(iv) coupling the simulation tools together,

(v) parallel running the simulations,

(vi) integrating the Computer Aided Design with Computer Aided Design tools,

(vii) modelling the non-smooth landscapes.

Note, almost all simulations have focused on the smooth landscapes. Although the simulation process is effective but the applied optimisations method is not able to satisfy the objectives. Most of the time the work flows have based on mono-objective optimisation which result non-accurate outputs.

3. Methodology

Reviewed papers showed that an effective method for designing the planting patterns based on the topographic characteristic of site has not yet been introduced. But the recent advances in computer technology deliver more possibilities to generate a method based on them.

Recent computer technologies which have utilized here are listed as follow:

(i) advances in Computational Fluid Dynamics (CFD) tools for wind simulation,

(ii) Computer aided Design (CAD) tools and surface lofting techniques for topology modelling,

(iii) Computer aided Design (CAD) parametric modelling tools which are going to applied for tree modelling,

(iv) multi-objective optimization based design for controlling the process.

With introduced technologies design factors are simulated and according the design objective planting pattern is going to be optimized. Design factors and variables are listed as follow:

(i) kind of trees,

(ii) tree's shading,

(iii) topography map of the site,

(iv) planting space and number of trees in the site.

Objectives are identified and listed as follow:

(i) the speed of wind at the position of each tree, in order to minimize the effect wind on trees is supposed to be minimized;

(ii) number of tree in the site, in order to fully utilized the site is supposed to be maximized;

(iii) amount of sun for each tree, for the reason to have maximum growing is supposed to be maximized.

However, sometimes objectives don't need simulation. Just its effect on design appears as a value which limits the action of other simulation.

(A) Planting space and number of trees in the site

Besides planting pattern, spacing is other important factor of planting. Distance between trees is dependent on the kind of trees and also the reason of planting. With the right spacing, it is possible to plant enough number of trees to fully utilize the field meanwhile providing sufficient space for growing. Planting space could be easily defined as a constant value by according to the species and available experiences regarding the growing of that special species. Planting space doesn't need simulation. Its effect appears as a constant value. Value of distance applies a limitation onto process which means during simulation of further objectives the distance between trees must be in an identified span.

(B) Kind of trees

Based on the climate condition of the site and maybe other factors, kind of tree is identified. So according the shape of the tree, parametric model of tree is created is in Computer Aided Design tools. Parametric modelling as mentioned before is the state of the art technology of computer modelling. This technology gives the ability of modelling the tree and with changing the parameters of design the other models of tree in different size automatically could be presented. Applying this technology deliver the ability of having the tree's models in different ages and different seasons. Afterwards based on the kind of tree, number of trees and minimum distance between trees a parametric model of all available trees is created. Fig. 1 shows the parametric model of an example tree.

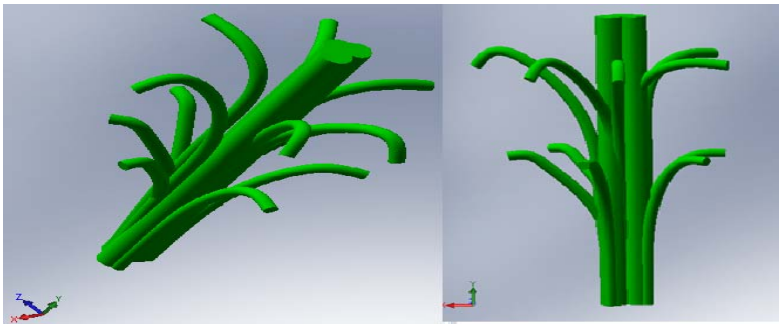

Fig. 1: Shows two different views of the parametric model of a tree

(C) Trees' shading

Three are a few number of simulation packages which are effective in order to position the trees according to deliver equal amount of sun during the day for all trees. Theses computer packages hold information about the shapes and sizes of about all kind of trees. According these information trees' shading are simulated in forest.

(D) Topology map of the site

Traditionally topology maps are indicated the shape of the landscapes by using contours lines. Besides satellite photos have became more accurate in order to present the shape of the landscape. These photos utilized the variety of colures instead of counter lines to present the topology characteristics. Figs. 2 and 3 show topology map and satellite photo, respectively.

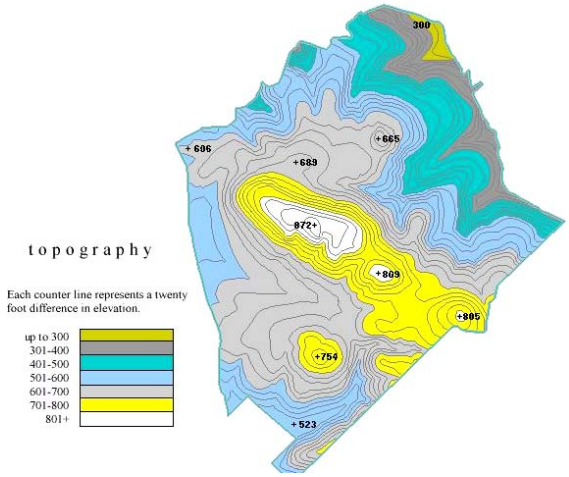

Fig. 2: Shows a topographical map of an example landscape [8]

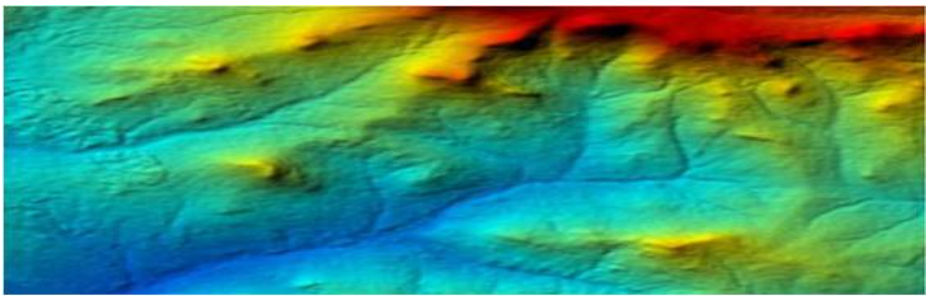

Fig. 3: Shows a satellite topographic map [8]

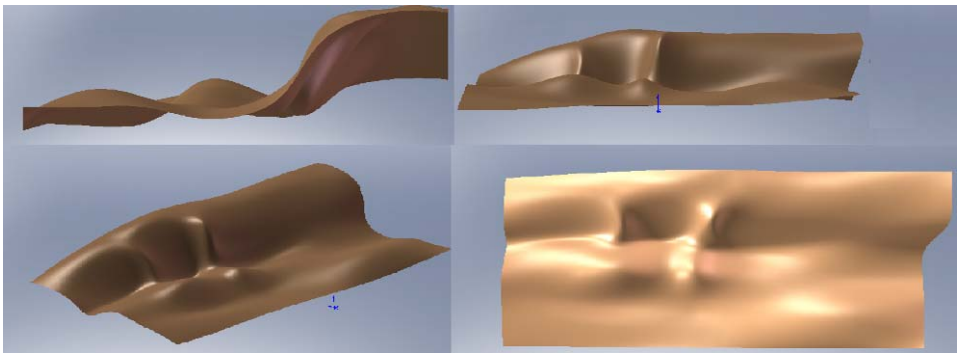

Fig. 4: Shows four different views of the result of the converted topographic map, which is available in Fig. 3, into CAD package applying loft techniques

(E) Wind behaviour

Computer Aided Engineering packages (CAE) according to the speeds and directions of wind could simulate the wind behaviour. The information of wind's speed could be collected from annual wind distribution map of the area of the site. Fig. 5 shows an example of annual wind distribution map.

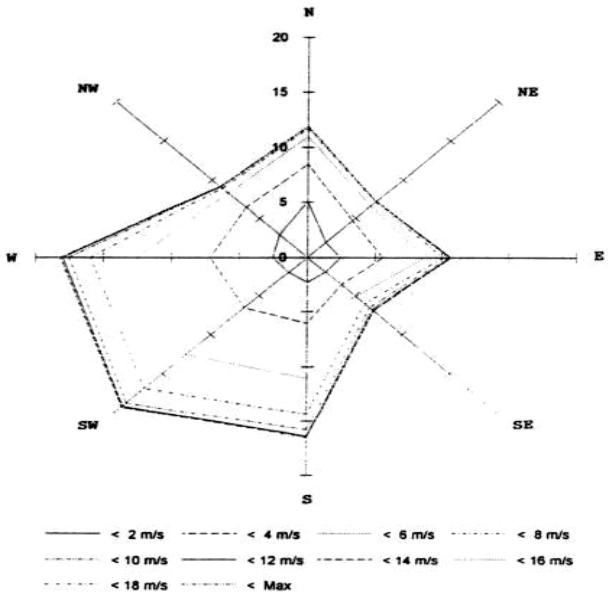

Fig. 5: Shows the annual wind distribution

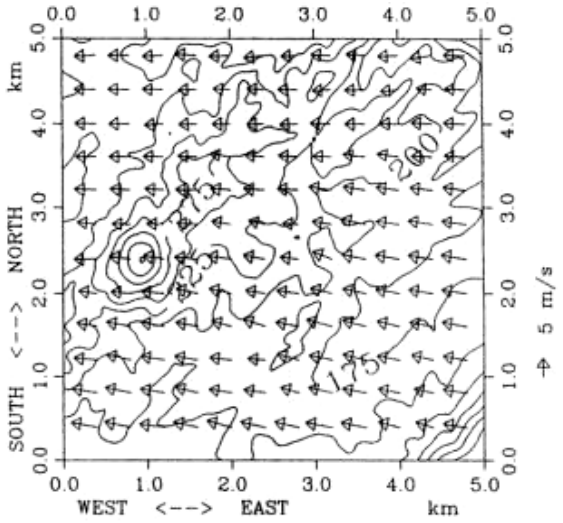

Fig. 6: Shows the annual wind determination

The information regarding directions of wind is collectable from annual wind determination map. Fig. 6 shows an example of annual wind determination map. Based on this information which identifies the wind characteristics, CAE which have the Computational Fluid Dynamics (CFD) simulation tools could simulate the process. CAD model

of the site and also the parametric CAD model of trees are imported into CFD package. After a series of initializing the speeds and directions of wind, simulation process is started.

In order to run all involved simulations at the same time in parallel mode and also for the reason of applying constant value, spans, and limitations in the simulation process, a new computer package is utilized. This computer package is able to couple simulation packages together. This state of the art computer tool which is called multi-objective optimization controls the objectives' simulations and based on the asked results continues till achieving the expected results.

The parametric model of the group of trees in CAD is combined with CAD topology model of landscape. Fig. 7 shows the initial parametric modelling of forest holding a random planting patter.

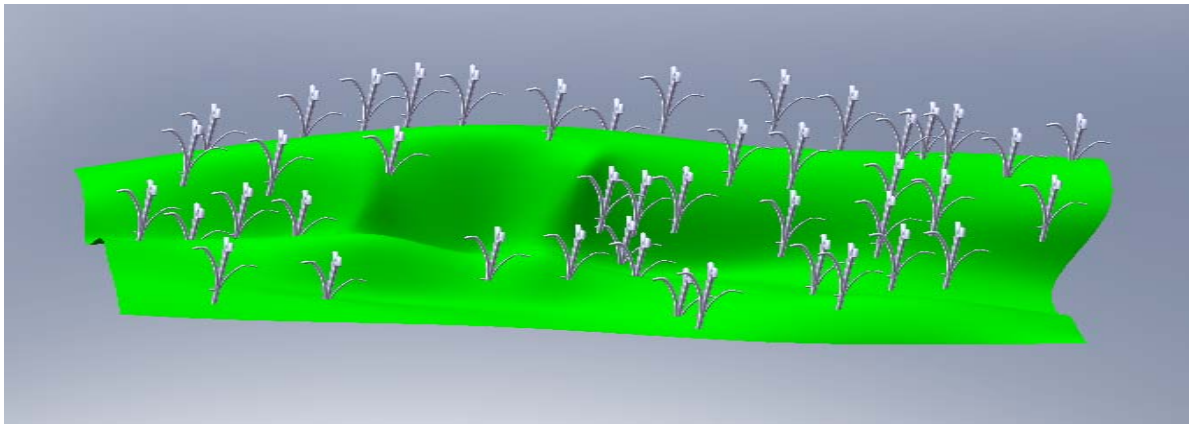

Fig. 7: Shows the initial parametric modelling of forest holding a random planting pattern

Based on the area of the site and planting space the maximum number of trees in site is calculated. According to the number of trees in the site also initial pattern - which is randomly selected - a complete parametric model of trees is created. Parametric model of forest is completely under control of optimization package. After modelling the forest is done the simulation could be started. There are two simulations available for operate, firstly SExI for shading simulation secondly ANSYS CFX for wind simulation. SExI is initialized based on species of tree and ANSYS CFX based on wind distribution/determination annual diagrams. Automatic Multi-objective optimization package of the modeFRONTIER is utilized for the reason of optimization and arranging the process. modeFRONTIER runs the simulations in parallel mode. Optimizer package couples CAD package with CFD and SExI. Results of optimization as the speed of wind at the position of trees are listed for twenty different patterns' arrangement. Finally the result of process is presented as an optimal planting pattern as it is available in Fig. 8.

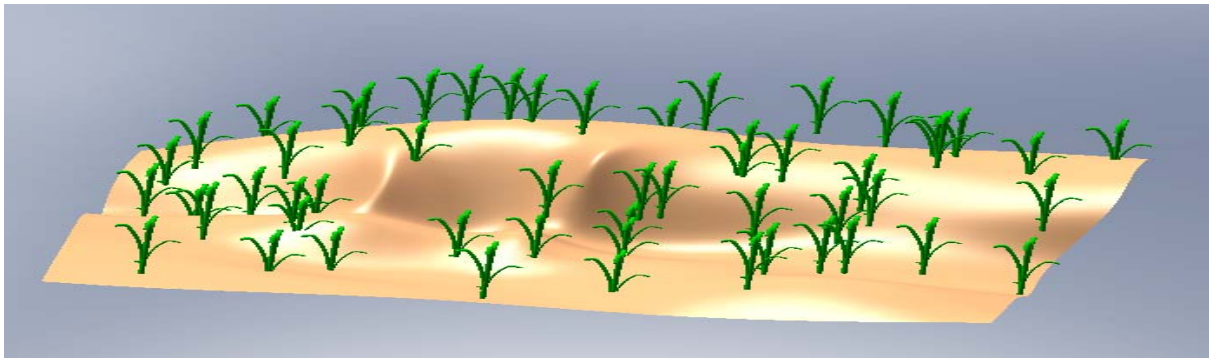

Fig. 8: Shows the optimal planting pattern of forest after optimisation which delivers seven percent lower wind speed at the positions of trees

4. Conclusions

Optimization package automatically simulated and optimized the objectives. Results of simulations have been also automatically appeared as a CAD model. The presented workflow of simulation and design process was an example of environmental simulation and design which could be useful in simulation of further environmental subjects. Approaching the optimal planting pattern is the result of successful coupling CAD and CFD.

This method of design which is based on optimization could deliver the result faster and more accurate. The results show that the planting pattern has effect on reducing the speed of the wind at the positions of trees by seven percent. Because of some reasons such as non-accurate model of trees, mistakes of converting topographic map into CAD, direction of the wind and etc the result is not accurate but it could be trustable.

The presented optimal planting pattern has much to learn and study. Taking a look at optimal model and focusing on the area without trees shows that leaving some place empty on the site might reduce the speed of wind. Other points regarding optimal model of forest are listed below. These gathered points as the results of optimizations because of the few number of simulated patterns are not certainly true. In order to have more trustable results, the number of the simulated patterns must be increased:

(i) minimizing the distance between trees reduce the speed of the wind in some places,

(ii) high risk places which have high speed wind are leaved free,

(iii) area with high slope are not good place for planting, maybe it causes increasing the speed of wind on the places of other trees or maybe in this area the speed of wind is naturally high.

References

[1] Harja, D., Vincent, G., Purnomosidhi, P., Rahayu, S., Joshi, L., 2004: World Agroforestry Centre (ICRAF). Bogor, 2IRD, Montpellier.
[2] Coutts, M.P., Grace, J., 1995: Wind and trees. Cambridge University Press.
[3] McCreary, D.D., 2001: Regenerating rangeland oaks in California. ANR Publications.
[4] Lantagne, D., 2009: Tree planting in Michigan. http://www.for.msu.edu/extension/ExtDocs/treeplnt.htm reviewed by June 2009.

[5] www.Wordagroforestry.org/sea/products/afmodels/SExI, reviewed by June 2009.

[6] Mosavi, A., 2009: Automatic multi-objective surface design optimisation using CAD/CAE. ANSYSItalian Conference, Bergamo, Italy.

[7] Anderson, S., 2009: Introduction to growing christmas trees. http://www.osuextra.com reviewed by June 2009.

[8] www.brownlemur.com, satellite topographic map, reviewed by June 2009.

Author's address:

Amir Mosavi (A.Mosavi@math.unideb.hu)
Faculty of Informatics, University of Debrecen
Egyetem ter 1, H-4200 Debrecen, Hungary

Wood degradation after windthrow in a northern environment

Jean-Claude Ruel, Alexis Achim, Raul Espinoza Herrera, Alain Cloutier

Wood and forest sciences department, Laval University, Quebec, Canada

Abstract

Severe windthrows often require special salvage operations that lead to increased costs and reduced product value. In northern environments, the cold climate could contribute to slower rates of wood degradation and provide a wider window for salvage logging. The study was conducted in northeastern Quebec (Canada), in a severe windthrow which occurred in 2006 in a region already touched by partial windthrow in 2003. Logs from the damaged area were collected for two species: *Abies balsamea* and *Picea mariana*. Logs were obtained from three classes of degradation based on visual estimates and from living trees. Each log was sawn and one piece of lumber was selected from each to determine MOR, MOE and visual grade. The exact time of mortality was determined through dendrochronology. Results show that the visual grade of *Picea* lumber from trees that died one or two years before sampling was comparable to that from living trees. Some degradation was seen for trees that died 3-4 years before sampling and increased thereafter. Degradation of *Abies* wood properties was faster. MOE was not reduced until 6 years after windthrow. MOR decreased after 3-4 years in *Picea* but no effect could be detected in *Abies*, due to a huge variation.

1. Introduction

Windthrow is an important disturbance in many forests of the world (Bergonzini and Laroussinie 2000). Direct loss in value can occur when the bole breaks or splits, especially if this occurs in the bottom log. The rate of infestation by decay fungi will be a function of tree species, water content and temperature (Pischedda 2004). Most insects that attack wood prefer dying or recently cut trees. However, some of them require more than one year to complete their life cycle (Graham and Knight 1965).

Severe and extensive windthrows often require special responses that include salvage plans and log storing strategies. Volumes salvaged after windthrow have reached record values in 2006-07 in Quebec (Vaillancourt 2008). Salvage operations lead to increased costs related to operational harvesting difficulties and can require additional road access in some regions. In the northern parts of the Canadian boreal forests, logging still takes place in virgin areas where no prior road access is available, meaning that new access roads need to be built when a salvage operation is conducted. However, given the cold climate, wood degradation could be slower than in other parts of the world which could extend the period under which wood can be salvaged. In these conditions, a good knowledge of the rate of wood degradation becomes crucial. In this study, we document the effect of time since death on visual grade, mechanical wood properties and timber value for two major species typical of the eastern boreal forest of Canada.

2. Methods

The study was conducted in eastern Quebec, Canada (50°12 ᴵN, 68º14ᴵ W). The climate is cold and humid (Annual mean temperature: -2.5 to 0^{o}C; Annual precipitations: 1300 mm; (Robitaille et Saucier 1998)). The area is dominated by black spruce (*Picea*

mariana (Mill.) B.S.P.) and balsam fir (*Abies balsamea* (L.) Mill.) growing in pure or mixed stands. Stands in the study area were generally old (84% of the area >90 years), which is typical of virgin stands of the region.

From 2003 to 2006, the study area was strongly affected by windthrow. A first partial windthrow occurred in 2003, followed by a major event in 2006. Over this period, a total of 88 000 ha was impacted by different levels of windthrow. The last major event affected more than 20 000 ha and led to an important salvage plan.

Field sampling was conducted in 2007. It took advantage of the fact that trees that had died at different times could be sampled on the same site. Since a proportion of stems had not been windthrown, living trees could also be sampled on the site. Additional balsam fir trees, presumably dead in 2003, were sampled on a second site close by, since balsam fir was not abundant enough on the first site. An additional older windthrow was also sampled for black spruce. This was not attempted for balsam fir since this species is known to be more prone to decay.

A total of 167 trees were sampled with an objective of around 20-30 trees per species and windthrow age. An approximate time since death was associated with each tree in the field, based on external appearance. The bottom 8-foot log of each stem was collected and marked with paint, according to its estimated time of death and species. Log diameter ranged from 9 to 28 cm for black spruce and from 11 to 30 cm for balsam fir. The exact time of death was determined from dendrochronological analyses made on a disk collected at the end of the log using a master chronology established from living trees. This exact dating forms the basis for comparisons of lumber properties.

Each log was processed with a portable sawmill. A lumber piece next to the slab was selected to determine lumber grade and mechanical properties. Three samples were taken from each slab to determine water content. Lumber of each species was dried separately following a species adapted schedule. Each piece of dried lumber was visually graded according to the NLGA Standard Grading Rules (NLGA, 2000) for “Structural Light Framing” (NLGA article 124). For each piece of lumber, the modulus of elasticity (MOE) and modulus of rupture (MOR) in static bending were determined. The lumber was tested edgewise according to ASTM standards.

3. Results

Measured time of death was closely linked to field estimates. For black spruce trees presumably dead prior to 2003, 4 had died in 2003 (Table 1). None of these had died in 2001 or 2002. Time of death was thus reclassified. Trees that died in 2005 or 2006 form the 2006 group whereas trees that died in 2004 and 2003 are grouped in the 2003 class. Time of death ranged from 1976 to 2000 for old black spruce windthrows.

Most of the lumber from living balsam fir trees was classified as grade 2 or better (Fig. 1). In trees that had been dead for one year, grade 3 becomes more abundant than grade 2. In trees that died in 2003, grade 3 becomes the most frequent. For black spruce, the vast majority of living and recently dead trees qualified for grades 1 and Select. Inferior grades became more frequent for trees that died in 2003. No lumber from the oldest windthrows qualified for grade 2 or better.

Table 1: Number of trees by estimated and measured year of mortality

Species	Estimated year of mortality	Measured year of mortality				
		2006	2005	2004	2003	Before 2003
Black spruce	2006	25	1			
	2003	1			21	4
	Before 2003				4	17
Balsam fir	2006	10	1	1	2	
	2003			2	15	1

The standard NLGA select grade allows for some insect holes. Six out of the 22 pieces of lumber from recently dead (2006) black spruces contained insect holes. Since specific markets do not accept insect holes, a premium class is added where no insect hole is allowed. About half of the living or recently dead black spruces qualified for this class. Almost no trees that died in 2003 (3%) met these standards.

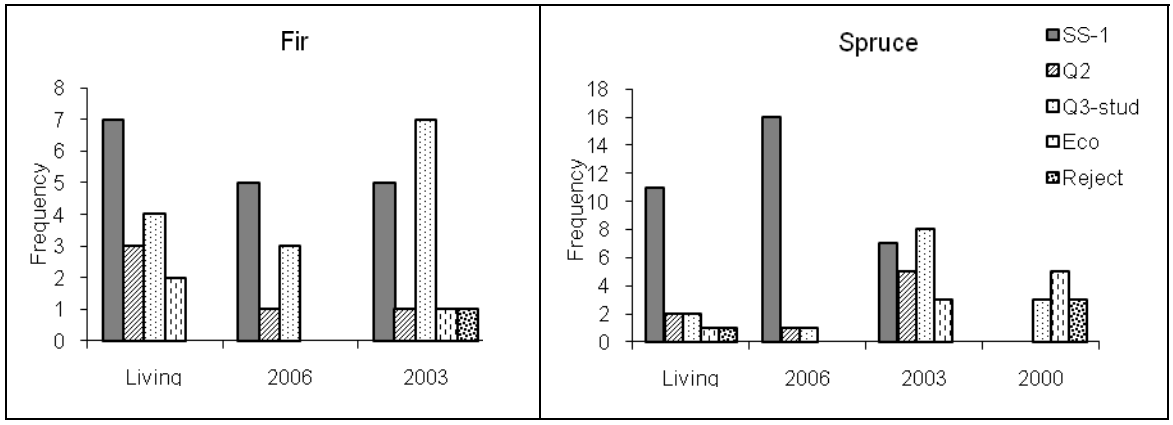

Fig. 1: Lumber visual grades by year of mortality

For both species, the water content of slabs decreased from living trees to trees that died in 2003 (Fig. 2). An increase in water content was observed for old black spruce windthrows (2000). Although water content remains above the fibre saturation point, black spruce trees that died in 2003 come close to it.

Mechanical properties of balsam fir lumber did not vary with year of mortality (Fig. 3). However, variability becomes high in trees that died in 2003. For black spruce lumber, a reduction in MOE was observed in old windthrows only (Fig. 4). A reduction of MOR occurred earlier since trees that died in 2003 had lower values in comparison with living trees.

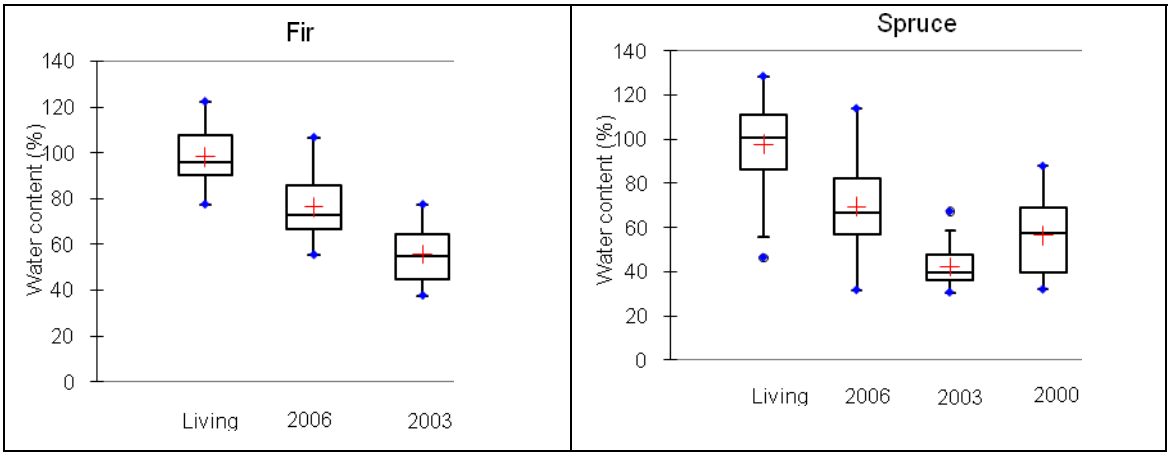

Fig. 2: Water content of slabs by year of mortality

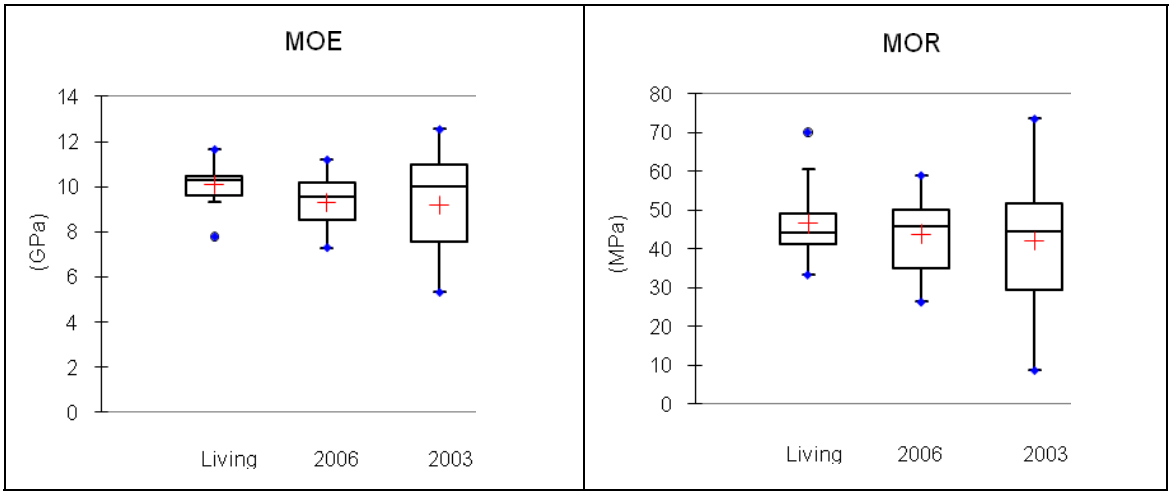

Fig. 3: Mechanical properties of balsam fir lumber according to year of mortality

4. Discussion

The first impact of windthrow on wood characteristics was a reduction of water content in slabs. According to Pischedda (2004), the high water content of freshly dead wood makes it a poor substrate for fungus development. Soon after death however, the water content starts to drop so that significant decreases were noted after one year. The fact that the crown is still attached to the uprooted tree hastens the decrease in water content.

Lumber of trees that had been dead for one year showed few signs of degradation. After one year, the visual grade after drying was not seriously affected for either species, considering that the Select, no 1 and no 2 grades are generally sold at the same price. Hence the product value after one year should not be affected, as long as the recovery rates are not reduced. Mechanical properties (MOE and MOR) of both species were also not affected after one year. According to Wilcox (1978), toughness, or the ability to withstand shock loading, is generally the property most sensitive to decay. The strength properties would be the next most sensitive, but the relative sensitivity of MOE and MOR seems to differ between studies.

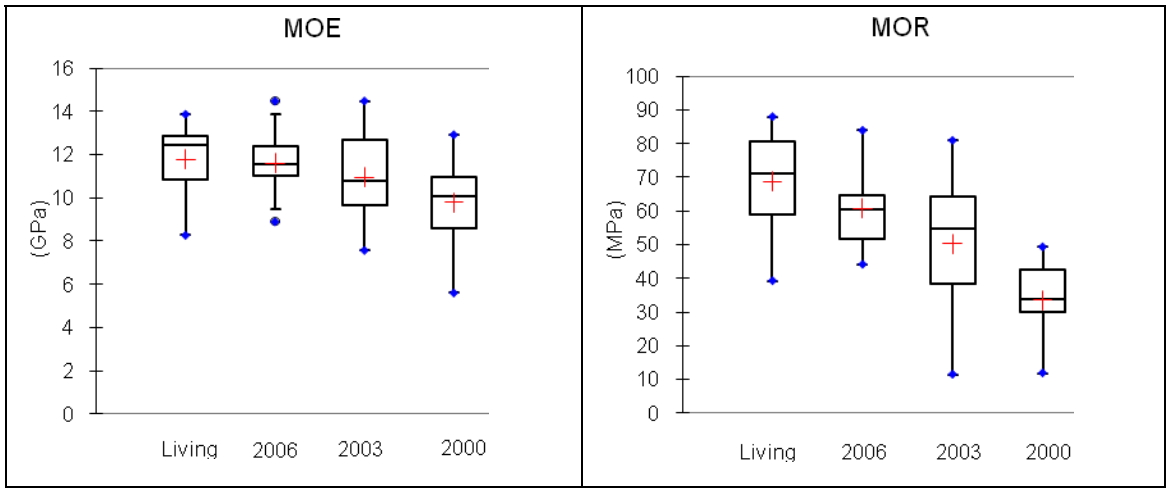

Fig. 4: Mechanical properties of black spruce lumber according to time of death

Insect holes in black spruce did not cause additional reduction in premium lumber yield after one year. According to Graham and Knight (1965), freshly dead trees would be the most attractive for wood boring insects, suggesting that most of the infestation would occur during the first year after windthrow. However, some species, like the common *Monochamus scutellatus*, can require more than one year to complete their life cycle, depending on conditions of temperature and humidity (Graham et Knight 1965). This could explain that decreases in premium lumber yield were not observed after one year but became important thereafter.

For trees that had been dead for 4 years, important signs of degradation were seen for both species. For balsam fir lumber, no 3 grade became dominant whereas, for black spruce, it increased strongly at the expense of no 1 grade. Mechanical properties of balsam fir were not significantly reduced but became quite variable. For black spruce, MOE was not affected but MOR was reduced. Strong reductions in water content in slabs were also observed for both species. Low water content could become a problem when processing slabs for pulp and paper. In a market based on visual grading and given the current price structure, wood degradation would appear to have a negligible impact on product value as long as lumber recovery rates are not affected. However, this level of degradation could have an impact for specific markets, especially when insect holes are not accepted.

For black spruce that had been dead for 7 years or more, wood degradation became evident. This category includes a wide range of time since death, from 7 to 31 years. The best grade was not obtained and rejects were found. MOE values were slightly reduced whereas MOR showed important reductions in comparison with living trees.

5. Conclusion

The rate of wood degradation after windthrow varies between species, with degradation occurring more rapidly for balsam fir. For balsam fir, small decreases are noticed after one year for visual grade and water content. MOE and MOR became quite variable for trees that had been dead for 4 years. For black spruce, visual grading was not affected until the trees have been dead for 4 years. Even at that stage, the product value would

probably not be seriously affected as long as the market can tolerate some insect damage. Black spruce MOR was reduced 4 years after windthrow whereas MOE was only reduced for the oldest windthrows. Hence, salvage operations should consider both the species and the market.

Acknowledgements

The authors are indebted to Fonds Québécois de la Recherche sur la Nature et les technologies for financial support and Abitibi-Bowater inc. for sample collection. We also wish to thank Benoit Brossier for conducting the dendrochonological work.

References

Bergonzini, J.-C., Laroussinie, O., 2000: Les écosystèmes forestiers dans les tempêtes. Institut pour le développement forestier, Paris.

Bouchard, M., Pothier, D., Ruel, J.-C., 2009: Severe windthrow in the boreal forests of eastern Quebec. . Can. J. For. Res. 39, 481-487.

Graham, S.A., Knight, F.B., 1965: Principles of forest entomology. 4th ed. Mc Graw-Hill Book Company, New York.

Grayson, A.J., 1987: The 1987 storm impacts and responses. Forestry commission bulletin. 87.

NLGA, 2000: Règles de classification pour le bois d'oeuvre canadien. Commission nationale de classification des sciages, Vancouver. C.B., pp. 276.

Pischedda, D., 2004: Guide technique sur la récolte et la conservation des chablis.

Robitaille, A., Saucier, J.-P., 1998: Paysages régionaux du Québec méridional. Publications du Québec.

Swift, M.J., Heal, O.W., Anderson, J.M., 1979: Decomposition in terrestrial ecosystems. University of California Press., Berkeley and Los Angeles.

Vaillancourt, M.A., 2008: Effets des régimes de perturbation par le chablis sur la biodiversité et les implications pour la récupération. Min. Ress. Nat. et Faune du Québec.

Wilcox, W.W., 1978: Review of literature on the effects of early stages of decay on wood strength. wood and fiber 9, 252-257.

Authors' address:

Dr. Jean-Claude Ruel (jean-claude.ruel@sbf.ulaval.ca)
Alexis Achim (alexis.achim@sbf.ulaval.ca)
Raul Espinoza Herrera (raul.espinoza-herrera.1@ulaval.ca)
Alain Cloutier (alain.cloutier@sbf.ulaval.ca)
Université Laval, Département des sciences du bois et de la forêt
2405, rue de la Terrasse, Québec (Québec) Canada G1V 0A6

A decision making tool to manage storm damage in Wallonia

Simon Riguelle[1], Jacques Hébert[2], Benoit Jourez[1]

[1]Laboratory of Wood Technology, Public Service of Wallonia, Belgium
[2]Unit of Forest and Nature Management, Gembloux Agricultural University, Belgium

Abstract

In order to efficiently manage post-storm damages, a software was developed to be used as a decision support system by the public authorities in order to take the best decisions as soon as possible after a storm event. This tool provides an overview of the present situation and compares the efficiency of several prospective simulations. The model was built on the basis of previous storm events in Europe and its parameters were defined after a comprehensive literature review. The System Dynamics theory was used to simulate the complex scheme of post-storm management operations (inventory, sale, harvesting, transport, storage and transformation). The operator can modify thirty parameters to simulate the crisis situation.

1. Introduction

Recently, several dramatic storms struck Europe. These events not only had a huge impact on forest resources: they also destabilized the wood market and the whole sector of wood transformation. Indeed in many cases, whereas a fast and suitable reaction should minimize the storm impacts, the extent of the damage, the lack of preparation and the major distress of the actors compromise such a strategy. In order to manage efficiently post-storm damage, we developed a software that would be used as a decision support system by the public authorities (politics and administration).

This research was a regional priority and has been funded for four years by the Forest and Nature Department (DNF). The scope of this software is the Walloon forest (southern Belgium), which represents 80 % of the national forest area. Thus, the simulations results must only be considered at the regional scale. The aim of this work was to develop a tool that should help a crisis unit to take the best decisions as soon as possible after the storm, by (i) showing an overview of the present situation, (ii) comparing efficiency of several prospective simulations. The model was built on the basis of previous windthrow events in Europe and its parameters were defined after a comprehensive literature review.

2. Modeling the post-storm damage system

We used the System Dynamic theory to simulate the post-storm damage management. This approach has a very wide scope and is particularly adapted to environmental or sustainable development models. The system representation in terms of stocks and flows, its extreme flexibility and the feedbacks analysis are the main advantages of this method. On the other hand, this kind of model generally needs plenty of data to run correctly. Thus, their identification and estimate are very important, since the model is extremely sensitive to initialization values. The second step is to draw a schematic view of the system that represents the various stocks and flows and to establish the main relationships (Fig. 1).

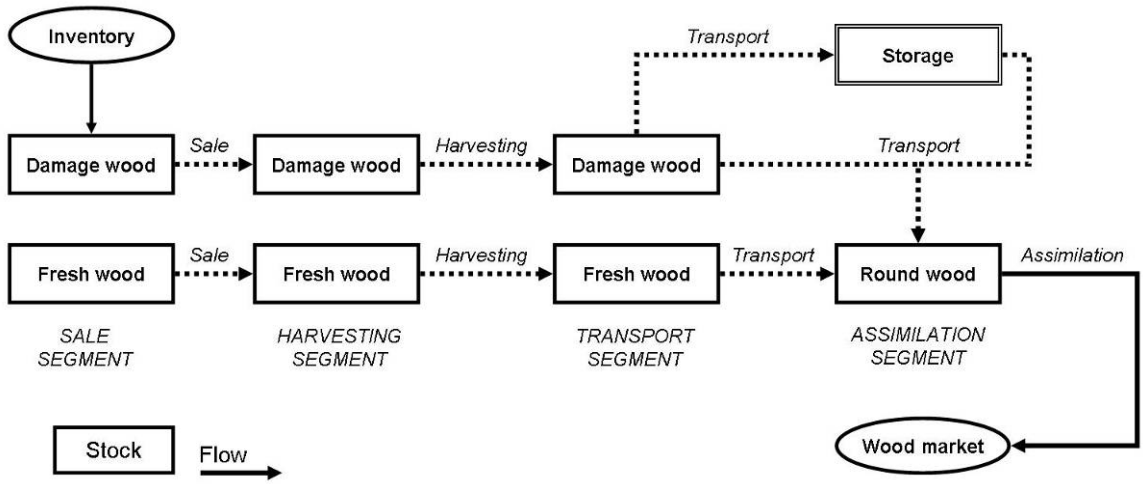

Fig. 1: Schematic representation of post-storm management system; stocks are linked by flows; inventory box is the main entry; wood market box is the main exit

3. Main entries, parameters and options of the system

The main entry system is the volume of damage, which can be estimated in a very short time (3 days) by using the plot network of the Walloon Permanent Forest Inventory. About thirty parameters can be modified by the operator to simulate the crisis situation (Table 1). They relates to the four segments sale, harvesting, transport and storage, transformation.

As part of the transport capacity is dedicated to the timber storage operations, the transport and storage operations are interdependent and are thus considered together. The assimilation segment includes all the outlets of the first transformation market: sawing, pulp/paper, panels, wood energy. The total capacity of transformation is the sum of the specific capacities of these four operations. Exported volume is an exit of the system preliminary to this segment, whereas imported volumes act oppositely.

4. Use of the software

The software is coded in VBA and thus is very didactic and simple to use. The results corresponding to the various scenarios are automatically recorded in a report for each treated case. These reports will be used by the crisis managers and the public authorities to discuss about the best strategies. Before using the software, the user has to set up the parameters – for instance wood prices, harvesting capacity or number of trucks – to get a first view of the situation (basic situation). Afterwards these parameters can be modified to check the impacts of those choices on the crisis management.

Eventually, the graphic file displays the results of these prospective studies and, for each step of post-storm management, the wood stocks and the speed to which they are emptied can globally be evaluated at different times. However, the conclusions which come out from the analysis cannot be repeated for all the crisis situations because they are valid only for the specific scenario. The tool will not solve the problems in place of

the authorities but can help them to take the best decision as soon as possible after the storm.

Table 1: Crisis system parameters for each segments and short description of them

N°	Parameters	Description
	Sale	
1	Annual sale of fresh wood (m³/an)	Sale's capacity of local market before the storm
2	Amount to sell (%)	Part of damaged timber and fresh wood brought to the market
3	Resiliency time (month)	Delay before the return at the initial level
4	Sale differential (± %)	Increasing or decreasing of sale capacity after the storm
5	Exchange rate (%)	Part of fresh wood that to exchange for damaged wood
6	Sales repartition (% / month)	Sale's rhythm for damaged and fresh timber after the storm
7	Repartition of sale capacity (%)	Choice between damaged wood and fresh wood
8	Payment delays (month)	Activated for a limited period or deactivated
9	Wood devaluation (€/m³)	For each type of damage (broken, uprooted and standing trees)
10	Wood prices (€/m³)	Before and after the storm, for the four group of species
	Harvest	
11	Inaccessibility of cutting areas	Accessibility or weather restrictions periods
12	Harvesting rate (%)	Part of the wood sold before the storm but no yet cut after
13	Harvesting delays (month)	Activated for a limited period or deactivated
14	Harvesting units	Number of harvesters, skidders and lumberjack available
15	Harvesting system	Choice between three systems (mechanized, mixed, manual)
16	Repartition of harvest rate (%)	Choice between damaged timber and fresh wood
	Transport and Storage	
17	Forest inaccessibility (day)	Weather restrictions
18	Transport characteristic values	Number of trucks, mean distance (km), gross tonnage (T)
19	Type of transport	Direct (industries) or indirect (industries and/or storage places)
20	Repartition of transport rate (%)	Between damaged timber and fresh wood
21	Repartition of transport rate (%)	Between damaged timber species
22	Storage	Activate / Deactivate
23	Amount of storage (m³)	Wood quantity stored for each species
24	Storage method	Type of conservation (wet, dry or oxygen exclusion storage)
25	Storage duration (month)	Minimal and / or maximal time period
	Transformation	
26	Reduce work periods (day)	E.g. annual closing periods
27	Export level (m³/year)	Wood annual exports for each species after the storm
28	Import rate (%)	Increasing or decreasing import level after the storm
29	Transformation output (%)	Potential increase

5. Example: a case analysis

The basic situation is modelled starting from a volume of damage of 8 million cubic meters (two annual harvests in Wallonia). The default values of the system are as follows: (i) higher sale capacity of 50%, timber exchange of 5%, (ii) 100 harvest units (a unit includes one harvester, one skidder and one logger) and average reduction in the output of 20%, (iii) 100 trucks available, average way of 50 km between forests and transformation units, authorized travelling total weight (PTRA) of 44 T. Fig. 2 shows the system evolution for these parameters.

Regarding the basic scenario, the harvest and transport capacities clearly seem insufficient if the main objective is to harvest and transport the damaged wood within the first two years. The operator can modify the options of the decision-making tool to try to reach this goal. As the crisis system is dynamic, when the user modifies parameters relating to harvest segment, the basic situation for the segments "Transport" and "Assimilation" will be consequently modified. Thus the research of most adapted strategy must be done step by step and the backing consequences for the other segments must always be considered. The best post-storm strategy will optimizes the mobilization of damaged wood with the lower costs and without disadvantaging a particular branch of industry. Fig. 3 shows the evolution of harvest segment for the different case studies. The increase of the harvest units allows reducing the crisis duration for one or two years. Furthermore, the deferment of the remaining harvesting operations by 24 month relieves the forest sector and reduces the crisis impacts.

A similar analysis can be made for transport segment (Fig. 4): the maximum value culminates at 4 million m^3 two years after the storm - when the harvesting operations are finished - and the total duration of transport reaches almost four years. The positive impacts of timber storage and authorized truck weight increase from 44 to 55 T are obvious, as show on Fig. 4. The analysis of assimilation segment (Fig. 5) demonstrates a progressive accumulation of wood that cannot be transformed after four years. Measures can be taken to control the provisioning: slowing down the importations, increasing the exports, or storing wood at medium and long term.

6. Software validations and monitoring

The decision-making tool underwent a series of validations with several experts (public and private owners, merchants, conveyers, sawyers, scientific and forest experts). The Regional Crisis Unit and the universities were also consulted. Furthermore, the software has to be regularly updated to be fully effective in a crisis context. This monitoring consist in several tasks: (i) the update of data, default values and parameters of the model (ii) the realization of prospective simulations before the storm's high risk periods (autumn, winter), (iii) the improvement of the software's functionalities following the experience feedbacks after a real crisis. The concept of prospective analysis illustrates one of the main goals of the tool: the anticipation of the crisis' impacts and the research of operational solutions before the next catastrophe.

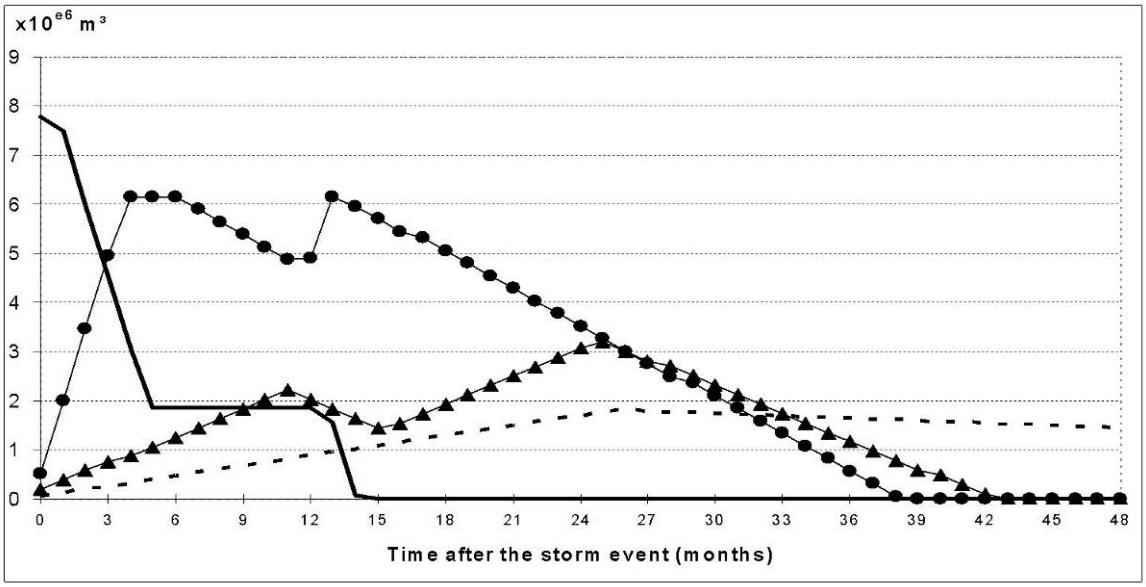

Fig. 2: Evolution of the successive segments for a basic scenario: sale (—); harvesting (—•—); transport (—▲—); transformation (- - - -)

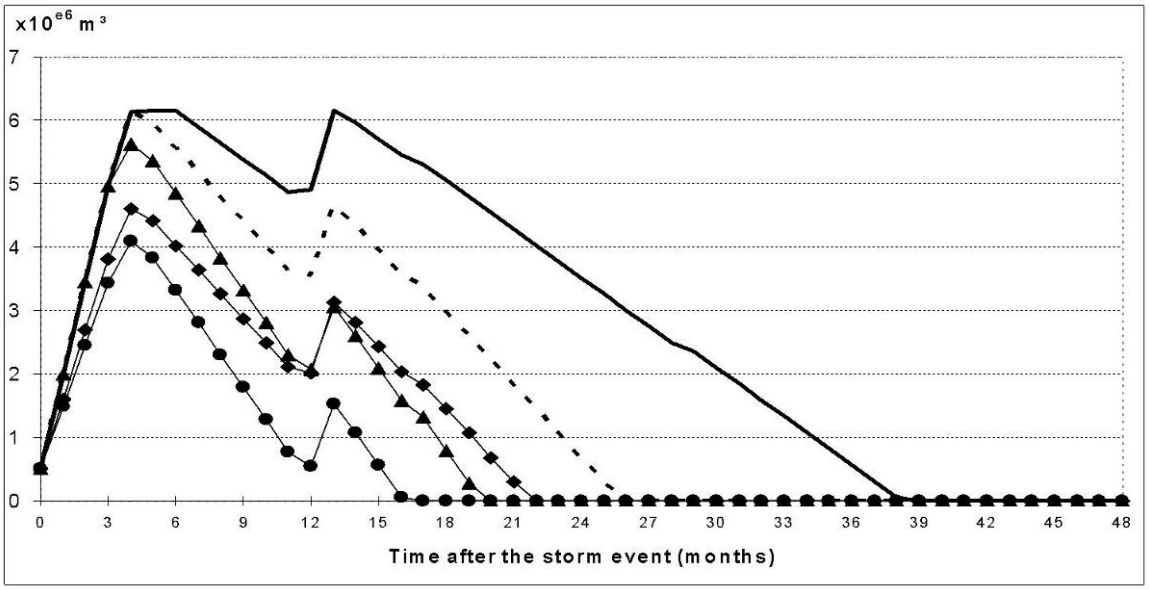

Fig. 3: Evolution of harvesting segment: basic scenario (—); 150 harvesting units (- - - -), 200 harvesting units (—▲—); 150 harvesting units and delay of 24 months (—◆—); 200 harvesting units and delay of 24 months (—•—)

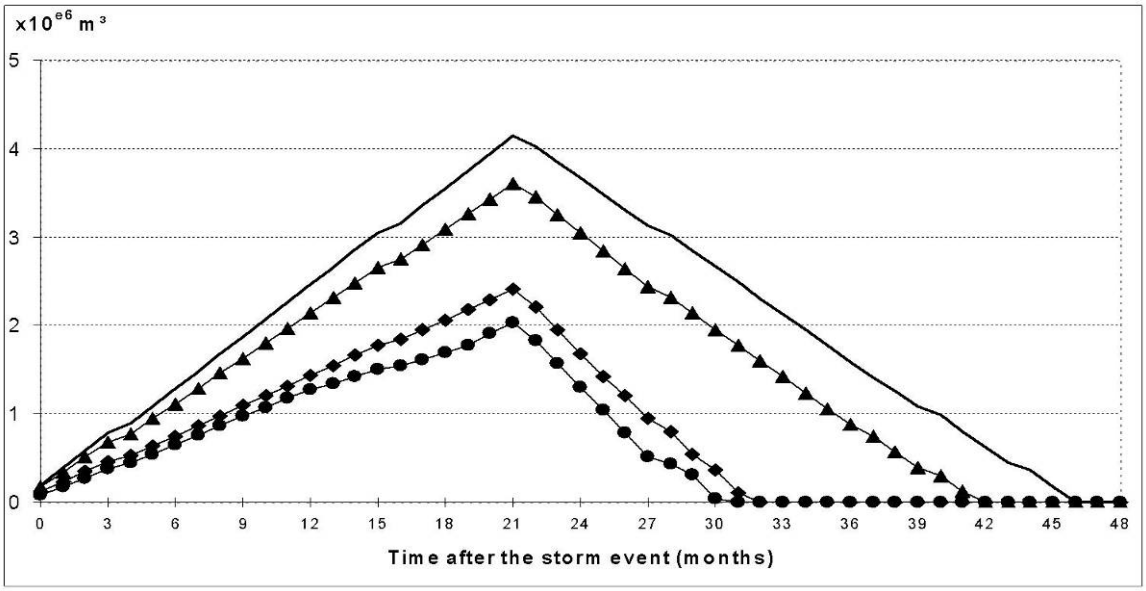

Fig. 4: Evolution of transport segment: basic scenario (—); truck PTRA of 55T (—▲—); timber storage (—◆—); timber storage and truck PTRA of 55T (—•—)

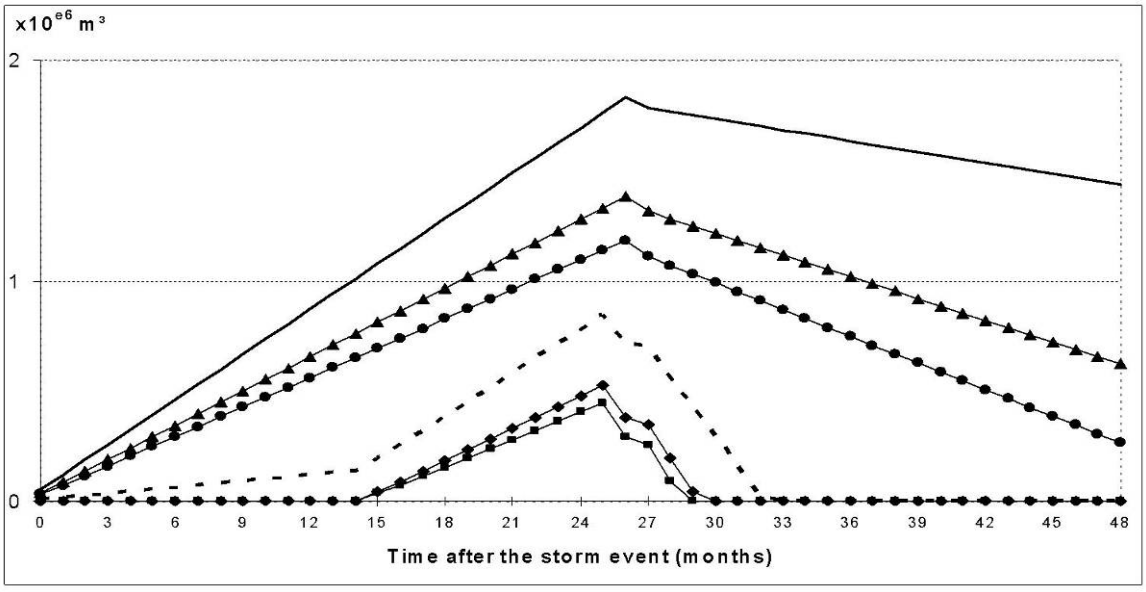

Fig. 5: Evolution of assimilation segment: basic scenario (—); drop of importations by 25% (—▲—); timber export of 10% (—•—); timber storage (▪ ▪ ▪ ▪); drop of importations by 25% and timber storage (—◆—); timber export of 10% and timber storage (—■—)

7. Conclusion

The recent storm events - Lothar and Martin in 1999, Kyrill in 2007 and Klaus in 2009 - were very wrenching for European forests. Thus decision-making supports are more and more important to face these dramatic events in the ongoing crisis context. Now, the crisis managers will be able to compare their strategies with the scenarios analysis and even to reject some of them or consolidate others. The first simulation results show a great potential to predict the post-storm damage evolution and the bottlenecks which have to be solved to improve the post-storm management. Obviously, a validation in real conditions should confirm the tool's efficiency and the possibility to extend its scale. Moreover, a technological watching must be done by regional forest services to ensure that the software will stay up-to-date and functional at any time.

Nevertheless, the software in its first version does not integrate yet the economic aspects related to the potential scenarios, which should not prevent the managers to keep in mind this strategic aspect. Expert testimony and professional experience of the whole sector will indeed remain paramount to achieve an optimal strategy. In addition the operator cannot read the simulated values of stocks like foreseeable results because it is only the relative comparison of scenarios that could be interpreted. Finally, it is obvious that all the partners of the forest sector will have to work in close collaboration to reduce storm impacts, in particular to get the required data in the shortest reasonable time after the calamity.

Authors' addresses:

Ir. Simon Riguelle (simon.riguelle@spw.wallonie.be)
Laboratory of Wood Technology, Public Service of Wallonia
Avenue Maréchal Juin 23, B-5030 Gembloux, Belgium

Prof. Dr. Jacques Hebert (hebert.j@fsagx.ac.be)
Unit of Forest and Nature Management. Gembloux Agricultural University.
Passage des Déportés 2, B-5030 Gembloux, Belgium

Dr. Benoit Jourez (benoit.jourez@spw.wallonie.be)
Laboratory of Wood Technology, Public Service of Wallonia
Avenue Maréchal Juin 23, B-5030 Gembloux, Belgium

Comprehensive evaluation of the effects of wet and dry deposition of various ionic species, atmospheric ozone, and mineral weathering on plant growth by using Plant Growth Stress Model: estimated growth of pine tree for hypothetical 100 years in Ijira lake area, Central Japan

Toshihiro Kitada, Yohei Suzuki, Tomoyuki Katagiri

Department of Ecological Engineering, Toyohashi University of Technology, Japan

Abstract

A plant growth-stress model was developed and coded with C compiler; the model's basic concept is the same as PGSM by EPRI (1993). By using this model with various inputs such as hourly meteorological parameters, ozone, SO_2, and CO_2 concentrations, and wet deposition of ionic species, plant growth (a type of Japanese pine tree) was simulated for hypothetical 100 years; Among the factors, effects of wet deposition, O_3 concentration, and CO_2 concentration on the plant growth were focused.

1. Introduction

Ijira Lake is located in the northern part of Noubi Plain, Japan (see star symbol in Fig. 1). Near the lake a monitoring site for acidic deposition etc. is operated by Ministry of Environment, Japan and Gifu Pref. for about 20 years. As can be inferred from Fig. 1, the area is routinely affected by the huge emission sources in Nohbi Plain, where the cities of Nagoya, Toyota, etc. are located, under prevailing local flows of land/sea breeze and mountain/valley wind (Kitada et al., 1998, 2000a). Thus to know a sustainable emission level in the plain in terms of preservation of mountainous environment nearby is an important task. As a step to the goal, we have performed hypothetical plant

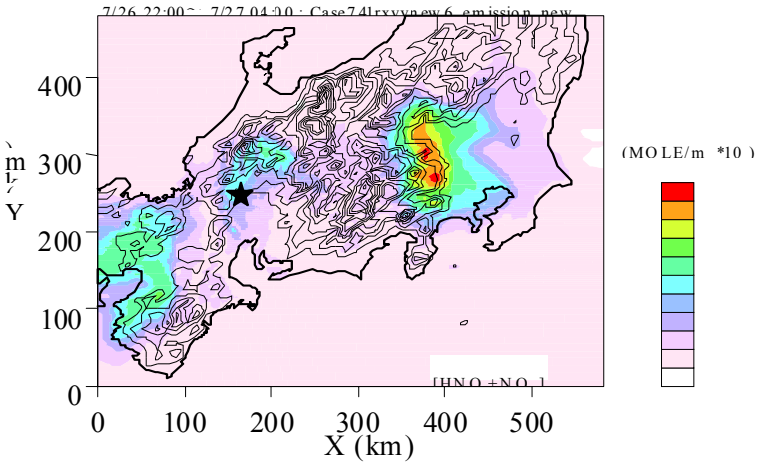

Fig. 1: Calculated distribution of HNO3+NO3- dry deposition for one night on land/sea breeze day (Kitada et al., 2000b); the star symbol shows the location of Ijira Lake in Gifu Pref., Central Japan

growth simulation for 100 years in Ijira Lake area by using the Plant Growth Stress Model (PGSM) by EPRI with various scenarios.

The PGSM (EPRI, 1993) simulates tree physiology, soil hydrology, and soil biogeochemistry. We applied the PGSM to 100 years hypothetical growth of pine tree in Ijira Lake area (see "star" symbol in Fig. 1), and studied effects of ozone concentration, wet and dry deposition of various ionic species, and mineral weathering on hypothetical plant growth (pine tree) for 100 years. In the base case, observed values of ozone, aerosols (SO4= etc.), and chemical constituents of precipitation for two years (1997 and 1998) as well as meteorological data were repeatedly used to prepare the data for the hypothetical 100 years. Various scenarios: (1) no mineral weathering, (2) no ionic deposition through precipitation (but only hydrogen ion concentration was kept as it was), (3) increased ozone concentration, (4) increased acid deposition, and (5) increased both

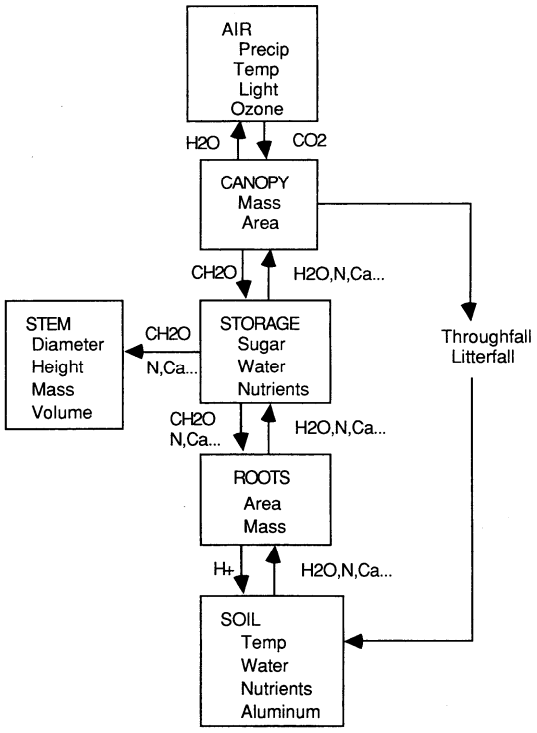

Fig. 2: Schematic representation of the modeled system in PGSM, the model tree is encircled with a dashed line

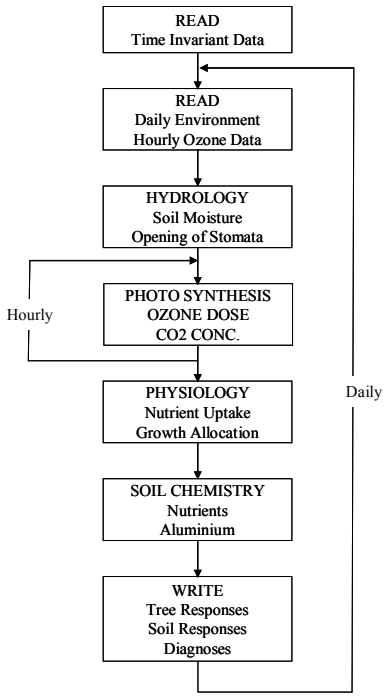

Fig. 4: Overall computational sequence of the PGSM

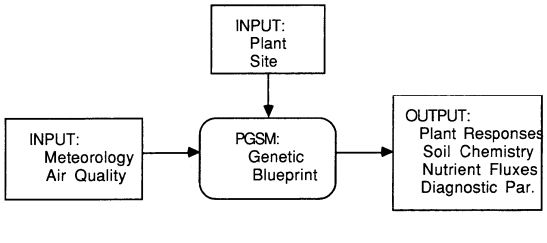

Fig. 3: Overview of PGSM (Plant Growth Stress Model)

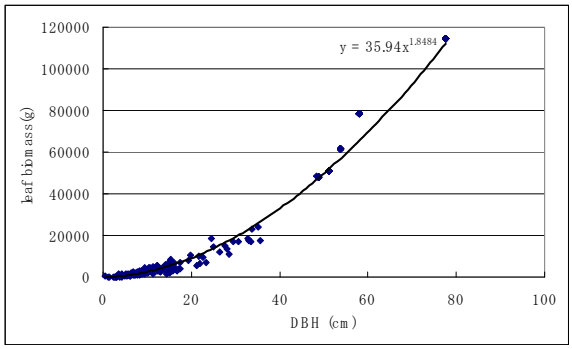

Fig. 5: Japanese red pine in the Ijira Lake area: leaf biomass (g) vs. DBH (cm)

ozone concentration and acid deposition.

2. PGSM (Plant Stress Growth Model)

PGSM (EPRI, 1993) calculates a tree growing by simulating tree physiology, soil hydrology, and soil biogeochemistry. PGSM models a tree as in Fig. 2. The tree is assumed to consist of four parts of "canopy", "storage", "stem", and "roots". The storage stores the organic matter (sugar) produced by photosynthesis as well as water and nutrients extracted from the soil. The sugar, water, and nutrients are then used to grow biomass of the tree such as stem, canopy, and roots. The tree growing is subject to the environmental influence of atmospheric conditions such as temperature, light, precipitation, relative humidity, ozone, acid deposition, etc.

Fig. 3 shows an overview of the PGSM (EPRI, 1993). The time series of meteorology and air quality data are provided in the input files. In addtion, tree and site characteristic data have to be given so that the model can simulate how the tree grow and react to environmental conditions of air and soil. Fig. 4 represents overall computational sequence of the PGSM (EPRI, 1993). Photosystheis influenced by light condition, water availability, and ozone concentration is hourly calculated. Calculated tree responses are recorded daily.

3. Input data for tree growing simulation in Ijira Lake area, Central Japan

3.1 Tree characteristics

A tree in the PGSM is characterized by leaf biomass, root biomass, stem biomass, and tree height, and these quantities are related to DBH (Diameter at Breast Height) of the tree. In this study, Japanese red pine and Japanese ceder were chosen as typical tree species in the area. By using tables of existing tree biomass sorted with the tree age for Japanese red pine (Gifu Pref. Office, 1984) and Japanese Ceder (Dept. Forestry, Gifu Pref. Office, 1992) in the Ijira Lake area, relations between DBH and leaf area, root biomass, stem biomass, and tree height were determined as in Table 1. Fig. 5 illustrates the relation of DBH and leaf biomass for Japanese red pine in the area.

Table 1: Relations between DBH (cm) and leaf biomass (g), root biomass (g), stem biomass (g), and tree height (m) for Japanese red pine and Japanese cedar in the Ijira Lake area, Gifu Prefecture

Red Pine	$Leaf=35.9DBH^{1.85}$	$Root=29.3DBH^{2.32}$	$Stem=29.4DBH^{2.63}$	$Height=1.04DBH^{0.88}$
Cedar	$Leaf=99.5DBH^{1.65}$	$Root=20.21DBH^{2.39}$	$Stem=44.94DBH^{2.47}$	$Height=1.78DBH^{0.69}$

3.2 Meteorological data

Meteorological data in the year 1997 and 1998 were used for the simulation. The data at Gifu-Hokubu site by AMeDAS (Automatic Meteorological Data Acquisition System, Japan Meteorological Agency) include daily values of wind speed, maximum and

minimum temperatures, precipitation, humidity, and atmospheric pressure. Light intensity is calculated directly from latitude of the site, time, cloudiness, and the site location information such as slope angle, and direction of the slope.

3.3 Atmospheric environmental data

Wet deposition data of various chemical species were available every two weeks in 1994. Dry deposition was calculated from measured SPM concentration with an assumption on its chemical composition. Fig. 6 shows yearly-averaged chemical composition of the precipitation in 1994, and Fig. 7 illustrates monthly precipitation and average pH values.

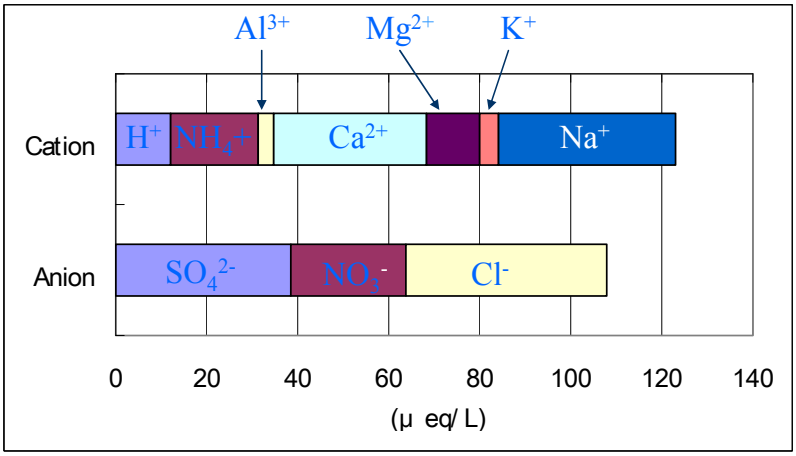

Fig. 6: One year-averaged chemical composition of the precipitation in the Ijira Lake area; ion balance of the precipitation was maintained by reducing concentrations of the cations, except for hydrogen ion, proportionally to their ratios in the total cation concentrations less hydrogen ion concentration

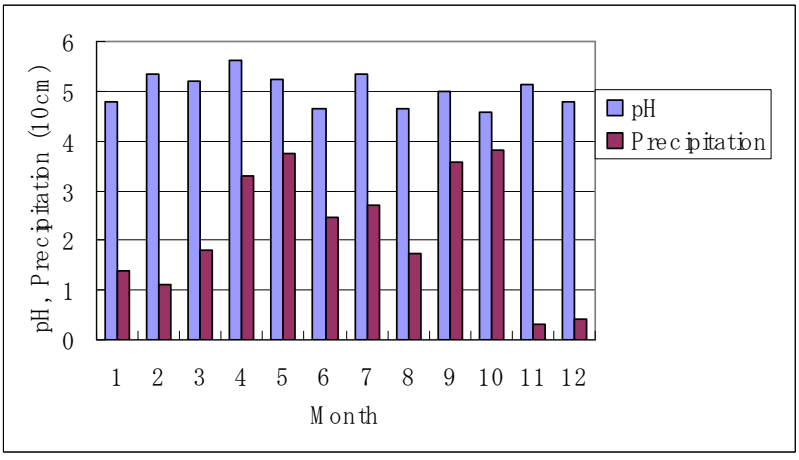

Fig. 7: Sample of monthly variation of precipitation data in 1998

Hourly ozone concentration data in 1997 and 1998, obtained at Gifu-Hokubu site by Gifu Prefectural Office, were used for simulation. Fig. 8 shows yearly frequency of hourly ozone concentration data in 1997 as an example.

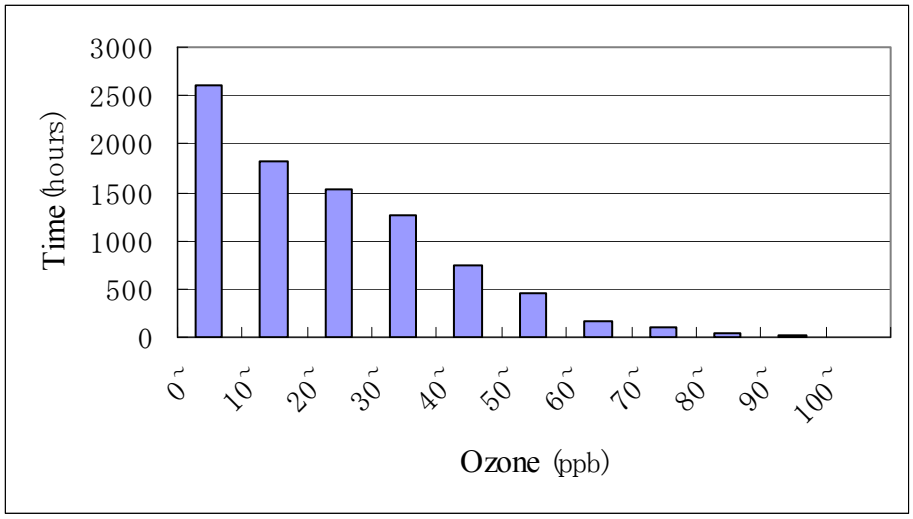

Fig. 8: Accumulated hours of ozone concentration in 1997

3.4 Site data

Site data include physical characteristics such as watershed area and width, and latitude and longitude, hydrological data such as evapotranspiration related parameters, soil hydrological data, soil chemistry, soil rates, and minerals. They were all provided in a report by Ministry of Environment, Japan (1998). Among them, composition of minerals and its weathering rate are listed in Table 2.

Table 2: Weathering rate and mineral composition at the Ijira Lake area, Gifu Prefecture

	Ca	Mg	K	Na
Weathering Rate (yr^{-1})	10^{-5}	10^{-5}	10^{-8}	10^{-5}
Composition (meq/100g)	3.6	59.2	55.9	22.0

4. Hypothetical 100 year growth simulation of Japanese red pine: simulation cases

To see effects of various factors on the growth of Japanese red pine in the Ijira Lake area, hypothetical 100 year simulation was performed. The factors considered are mineral weathering, wet deposition, and ozone concentration. The meteorological and atmospheric data described in the section 3 were repeated to do the 100 year simulations.

Table 3 lists the simulation cases. Case 8~10 use CO_2 concentration and temperature for IPCC SERES-A1F1, A1B and A1T.

Table 3: Simulation cases

	Mineral weathering	Wet deposition	O_3 concentration	CO_2 & Temperature
Case 1	0	0	0	normal
Case 2	normal	0	0	normal
Case 3	0	normal	0	normal
Case 4	normal	normal	0	normal
Case 5	normal	normal	normal	normal
Case 6	normal	normal	#	normal
Case 7	normal	normal	&	normal
Case 8	normal	normal	normal	A1FI (IPCC_SERES)
Case 9	normal	normal	normal	A1B (IPCC_SERES)
Case 10	normal	normal	normal	A1T (IPCC_SERES)

Ozone concentration below 30 ppb was raised to 30 ppb.

& Ozone concentration was doubled, and then the concentration below 30 ppb was raised to 30 ppb.

5. Results and discussion

Fig. 9a shows 100 year growth of the tree for case 1-4, and Fig. 9b for case 5-7. In Figs. 9a,b, leaf area is used as an indicator of the growth. From Figs. 9a,b, the followings can be observed:

(1) Importance of mineral weathering: Case 1 and 3 do not include mineral weathering process, and show death of the tree after 20 years, indicating the mineral weathering should be the most important process for the tree growth.

(2) Possible importance of wet deposition as sources of some ionic species: Case 2 does include mineral weathering but not wet deposition through precipitation. The leaf area in case 2 (Fig. 9a) shows oscillation with very large amplitude after 80 years, indicating possible death of the tree. In this case, only hydrogen ion concentration (pH) in precipitation was maintained by assuming hypothetical anion concentration which does not have physiological effect. This suggests that precipitation provides ions useful for the tree growth; Ca^{2+} and K^{+} provided by the precipitation (see Fig. 6) were identified by the model as possible important species for the tree's growth.

(3) Toxic effect of ozone: ss shown in Fig. 9b, case 6 in which ozone concentration is set always above 30 ppb starts to show an oscillation of leaf area. Moreover, the doubled ozone concentration with minimum ozone forced above 30 ppb (case 7) suggests further oscillation with larger amplitude and even prohibits the tree growing as indicated in decrease of average leaf area (Fig. 9b).

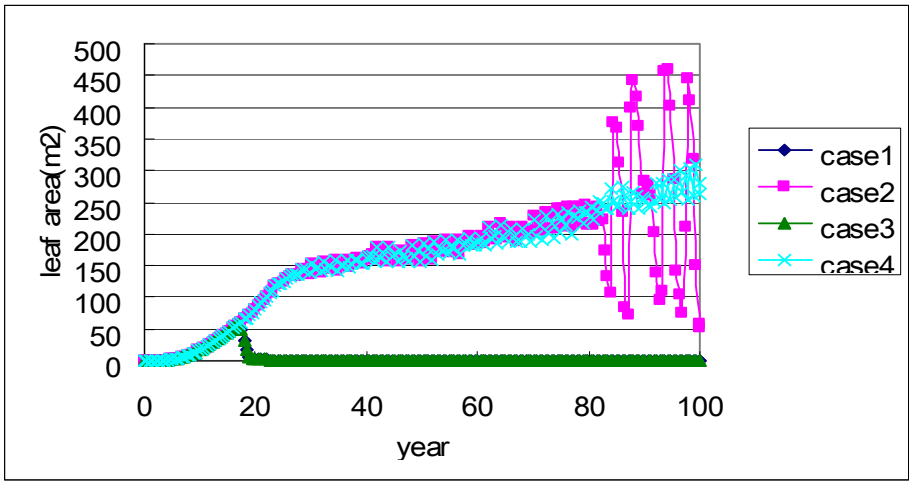

Fig. 9a: 100 year growth simulation of Japanese red pine in the Ijira Lake area: effects of mineral weathering, ions supply through precipitation, and ozone concentration; see Table 3 for case 1-7

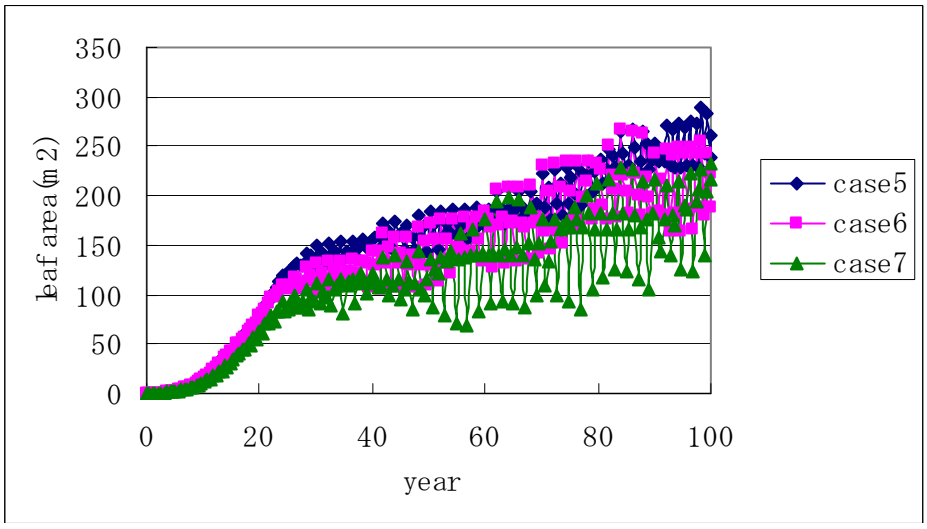

Fig. 9b: Same as in Fig. 9a but for case 5-7

(4) Effect of IPCC SERES_A1 scenarios: Fig. 10 illustrate 100 years' variation of DBH in Case 5 (normal) and Case 8~10 (IPCC SERES_A1 scenarios). Figs. 11a and 11b show changes of CO_2 and temperature based on the scenarios (IPCC SERES_A1) which were used for calculation in Case 8~10. Fig. 10 predicts A1

scenarios could lead to 12~16 % excess growth of the pine tree compared with the normal case (Case 5; CO2 is assumed constant at about 380 ppm) after 100 years.

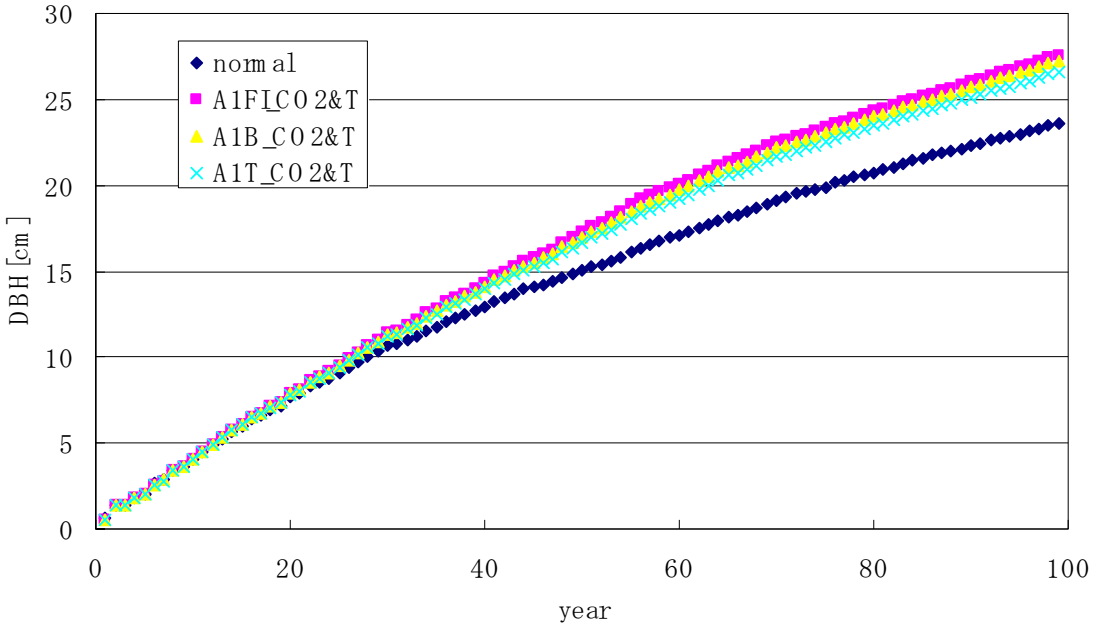

Fig. 10: Temporal change of DBH (Diameter at Breast Height) of Japanese red pine tree for Case 5 (normal), and IPCC SERES: Case 8 (A1FI), 9 (A1B), and 10 (A1T)

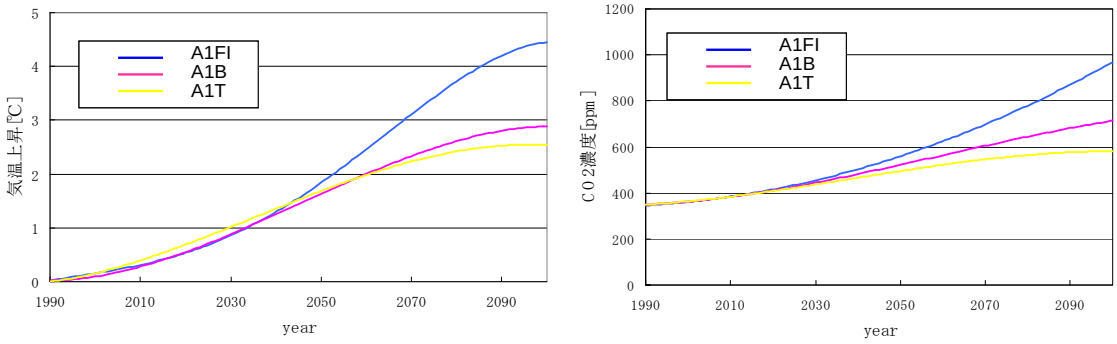

(a) Increase of average temperature from 1990 (b) Average CO2 concentration

Fig. 11: 100 years' changes of CO_2 and temperature according to IPCC scenarios of (a) increase of average temperature in K, and (b) average CO_2 concentration (ppm); these were used for simulations Case 8-10 (see Table 3).

Acknowledgement

This work was supported in part by Ministry of Education, Culture, Sports, Science and Technology, Japan through the research grant for Toyohashi University of Technology on "Strategic Planning for Regional Sustainability in Prefectural Cross-border Areas" in 2006~2010.

References:

Gifu Prefectural Office, Dept. of Forestry, 1984: Report on the Japanese Red Pine Biomass in Gifu Prefecture, 87 pp.

Gifu Prefectural Office, Dept. of Forestry, 1992: Report on the Japanese Cedar Biomass in Gifu Prefecture, 21 pp.

EPRI, 1993: The Response of Plants to Interacting Stresses: PGSM Ver. 1.3 Model Documentation, EPRI TR-101880.

Kitada, T., Okamura, K., Tanaka, S., 1998: Effects of topography and urbanization on local winds and thermal environment in the Nohbi Plain, Coastal region of central Japan: a numerical analysis by meso-scale meteorological model with a k- ε turbulence model. J. Appl. Meteorology 37, 1026-1046**.**

Kitada, T., Okamura, K., Nakanishi, H., Mori, H., 2000a: Production and transport of ozone in local flows over central Japan: a comparison of numerical calculation with airborne observation. Air Poll. Modeling and Its Application XIII, Plenum Press, 95-106**.**

Kitada, T., Ishizaka, Y., Okamura, K., 2000b: Proc. Int. Symp. On Oxidants/Acidic Species and Forest Decline in East Asia, JST/CREST, 67-74.

Ministry of Environment, Japan, 1998: Research Report on Acid Rain: Influence on Soil, 151 pp.

Authors' address:

Prof. Dr. Toshihiro Kitada (kitada@earth.eco.tut.ac.jp)
Mr. Yohei Suzuki
Mr. Tomoyuki Katagiri
Department of Ecological Engineering, Toyohashi University of Technology
Tempaku-cho, Toyohashi, 441-8580 Japan

Analyses of the annual, winter time and extreme geostrophic wind speeds in northern Europe based on GCMs

Hilppa Gregow, Kimmo Ruosteenoja, Ari Venäläinen

Finnish Meteorological Institute, Finland

Abstract

In this work we analyse the geostrophic wind speed in Europe with five global climate scale models: ECHAM5, MIROC3, BCCR, CSIRO and CNRM. The focus is on annual, winter time (September-April) and extreme geostrophic wind speeds (V_g) of the lowest model level. The detailed description will be given of changes in Finland. The maximum geostrophic wind speed return levels are calculated only for Helsinki (60°N, 25°E). The main finding is that in most of the models even if the mean annual winds increase by 0-5 % in Finland the extreme winds decrease by 1-6%.

1. Introduction

Wind and also snow are known to cause annual damage to forests in northern Europe (e.g., Quine 1995, Nilsson et al. 2005, Nykänen et al. 1997). In Finland we know that during the last 40-50 years the greatest risk to wind exposure has been close to the sea and the lakes that dominate in the eastern Finland and the higher elevated areas such as exist especially in northern part of Finland (Gregow et al. 2008).

The worst storm damages is northern Europe have happened in southern Sweden where in January 2005 about 75 million cubic metres of timber was lost (e.g. Alexandersson 2005). In Finland the latest major storm wind damages have taken place in southern and central parts of Finland in 2001 (e.g. Pellikka and Järvenpää 2003) and in eastern and central parts of Finland in 2002. Then altogether nearly 10 million cubic meters of timber was lost. The former damages took place in November with unfrozen soil conditions and the latter in July due a suddenly developed smaller scale storm. Mostly the storm wind damages have taken place in autumn – the very well remembered storms in Finland in 1978, 1982 and 1985 and 2001 have happened during the months of September-November. According to Solantie (1983) in the storm of September 1982 the maximum geostrophic wind speeds were 43-44 ms^{-1} and the gusts causing destruction were about 65 % (30 ms^{-1}) of the geostrophic wind speeds.

The influence of climate change on storminess has been studied eg. by Leckebush et al. 2008. According to them the total hemispheric number of extreme cyclones will decrease but in the Northeast-Atlantic the number of extreme cyclones will increase. Therefore this work concentrates on analysing the lowest model level geostrophic wind speed V_g. The intension is to find out how the V_g varies annually, during the colder season and in the extremes in the GCM's. The winds will be analysed in grids that are between 100-200 km depending on the model's resolution.

2. Data and methods

We used five global scale climate models: ECHAM5, MIROC3, BCCR, CNRM and CSIRO (CMIP3) also used in the IPCC report. In simplicity we compared the lowest model level V_g of the climate of today to the equivalents of the future climate. In ECHAM5, MIROC3 and CNRM the control climate covers years 1971-2000 and in BCCR years 1971-1998 and in CSIRO 1960-1980 and 1990-2000 (Table 1). The future climate estimates are available for 2046-2065 and 2081-2100, in case of BCCR the latest period covers 2081-2098. Scenarios compared were A1B, B1 and A2.

Table 1: Information on the global climate models used

Country	GCM	Control climate	Future climate	Scenarios
Germany	ECHAM 5	1971-2000	2046-65 and 2081-2100	A1B,B1, A2
Japan	MIROC3	1971-2000	2046-65 and 2081-2100	A1B,B1
Norway	BCCR	1971-1998	2046-65 and 2081-2100	A1B,A2
France	CNRM	1971-2000	2046-65 and 2081-2100	A1B,B1, A2
Australia	CSIRO	1961-1980 and 1991-2000	2046-65 and 2081-2100	A1B,B1, A2

The geostrophic wind speeds were analysed in an area from 10°W, 35°N to 50°E 85°N. The absolute values of the mean annual and the mean winter time (meaning September-April) geostrophic wind speeds were analysed as in changes of the absolute values and as in changes in percentages. The maximum geostrophic wind speeds were analysed in four locations. These were Rovaniemi, Joensuu and Helsinki from Finland and Goteborg from southern Sweden (Table 2). The return levels of the extreme geostrophic wind speeds were calculated for Helsinki by means of the "peak over threshold" (POT) method (Coles 2001), utilizing the extRemes toolkit software package developed in NCAR (e.g. Katz et al. 2005).

Table 2: The cities used for closer analysis of maximum Vg

City and location	Lat (°N)	Lon (°E)
Helsinki	60	25
Joensuu	62.5	30
Rovaniemi	67.5	25
Göteborg	57	12

3. Results

3.1 Control climate averages in Finland

According to the GCM simulations the mean annual V_g has been between 6 ms^{-1} and 9 ms^{-1}. The highest annual V_g is seen in the control climate of CSIRO which is very distinct from the other models. It gives local maximums with V_g above 12 ms^{-1} on the Gulf of Bothnia (Fig. 1). On land the greater the distance is from the sea the weaker the winds are being 8 ms^{-1} in the eastern and northern Finland. ECHAM5 gives the next highest V_g and then MIROC3 the third highest values. The lowest V_g are seen in BCCR (Fig. 1) and CNRM control climate.

The winter time (September-April) V_g is somewhat higher than the annual equivalent: in ECHAM5 8-10 ms^{-1}, in MIROC3 between 8-9 ms^{-1} and in BCCR between 6-8 ms^{-1} (Fig. 2).

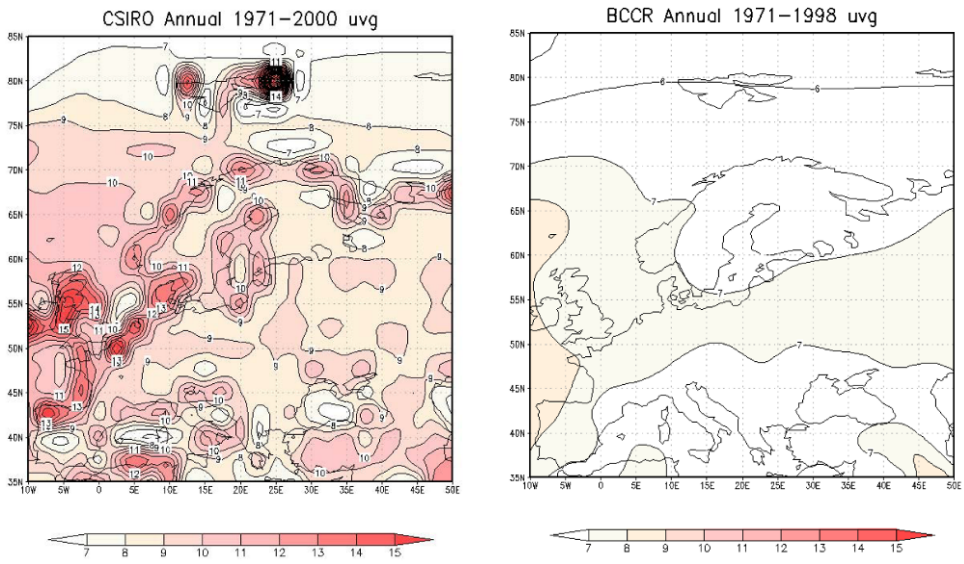

Fig. 1: Control climate analysis of the mean annual geostrophic wind speeds in CSIRO and BCCR at the lowest model level in Europe

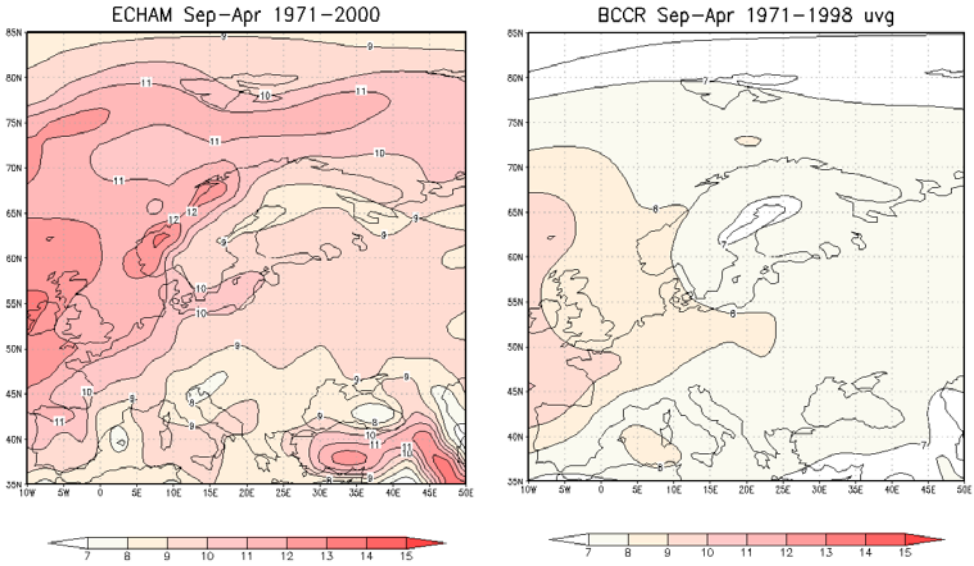

Fig. 2: Control climate analysis of the mean winter time geostrophic wind speeds in ECHAM5 and BCCR at the lowest model level in Europe

3.2 Future climate 2046-65 and 2081-2100 averages in Finland

The models estimate the meal annual geostrophic wind speed to be between 6-10 ms^{-1}. The highest annual wind speeds appear in the CSIRO A2-scenario which gives local

maximums with wind speeds above 13 ms^{-1} on the Gulf of Bothnia. On land the greater the distance is from the sea the weaker the winds are being 8 ms^{-1} in the eastern and northern Finland.

According to ECHAM5 the winter time geostrophic wind speeds will change slightly in Finland. Based on the scenario A1B excluding the southwestern Finland the geostrophic wind will decrease (by 0-2.5 %) in 2046-2065 and increase again (by 0-2.5 %) in 2081-2100 (Fig. 3). The scenario A2 gives 0-2.5 % increase for 2046-2065 and also 0-2.5 % increase for 2081-2100. The scenario B1 strengthens the geostrofic wind speed in 2046-2100 in southern most Finland by 2.5 % but in the north the geostrophic winds will not change or rather decrease by 0-2.5 %.

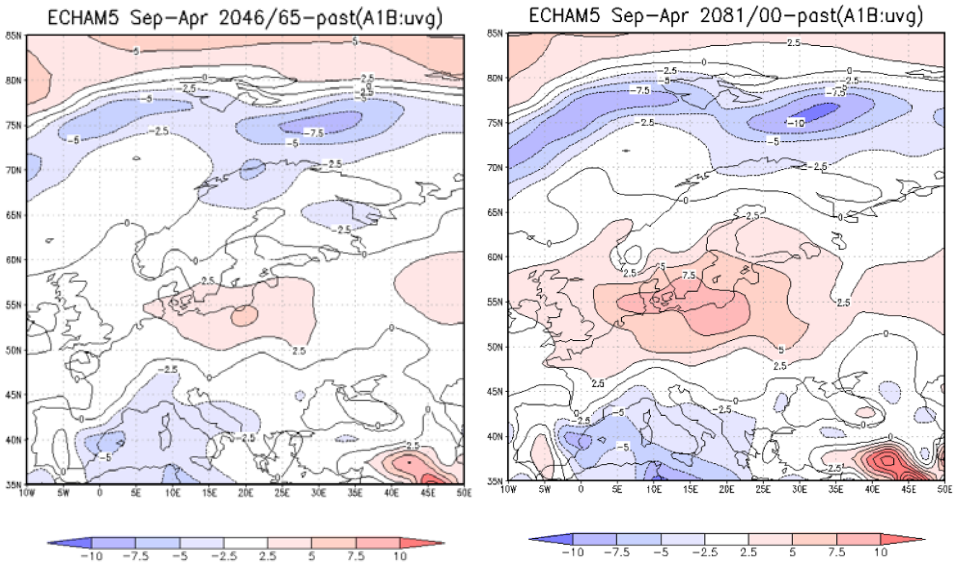

Fig. 3: The change in geostrophic wind speeds in percentages according to ECHAM5 and scenario A1B when comparing the future climate estimates to the control climate; in northern most Europe the winds will decrease especially over the sea; in southern parts of northern Europe the winds will increase

According to MIROC3 and scenario A1B the V_g would increase by 2.5 % first in the southern areas and in 2081-2100 throughout the country. Very similar trend is seen in the B1-scenario. According to BCCR the future climate would become windier than it is today. The increase would take place gradually from south to north being 2.5-5 % depending on the scenario used in 2081-2098.

According to CNRM the winter time geostrophic winds would increase by some 2.5 % in Finland until 2065 and 5-10 % until 2100 using the scenario A1B. On the contrary CSIRO and the scenario A1B gives a signal of weakening of the winds: in 2046-65 in western and central parts of Finland by 0-5 %. In 2081-2100 CSIRO increases the winds closer to the control climate level.

3.3 Changes in return levels of winter time maximum geostrophic wind speeds

In the cities chosen for this work (Table 2) the maximum geostrophic wind speeds vary mainly between 15 and 35 ms^{-1} (Fig. 4). However again the model CSIRO makes an exception: according to CSIRO control climate the geostrophic wind speeds have been twice above 45 ms^{-1} in Helsinki (Fig. 4).

According to the extreme value analysis and the 10, 50 and 100 year return levels in the control climate and then the future climate only BCCR will have increasing extremes (in Helsinki) in the area where it also suggested that the annual and winter time averages would increase (Table 3). The other models get weaker extremes for the 10, 50 and 100 year return levels in the future than in the control climate and in case of CNRM only very small changes. Based on the return level estimates the model CSIRO is not in balance in northern Europe.

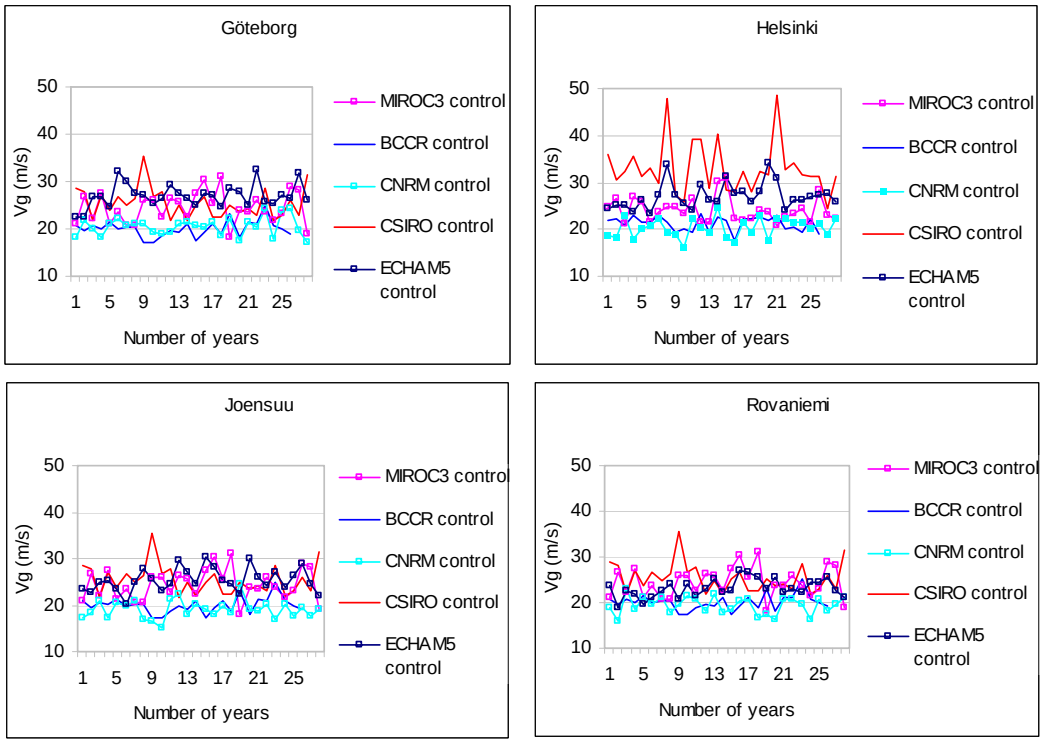

Fig. 4: The maximum geostrophic wind speed in Goteborg (Sweden), Helsinki, Joensuu and Rovaniemi (Finland) in the control runs of ECHAM5, MIROC3, BCCR, CNRM and CSIRO; the max winds are mainly between 15-35 ms^{-1}

Table 3: The 10, 50 and 100 years return levels of V_g based on the control climate and the future climate using scenario A1B; the estimates are shown for Helsinki

Control climate return levels and averages of all models (average 1) and all but CSIRO (average 2) Helsinki

Return level (years)	ECHAM5	BCCR	MIROC3	CNRM	CSIRO	Average1	Average2
10	30,5	23,0	27,6	23,0	40,0	28,8	28,4
50	34,8	23,3	33,3	24,3	48,0	32,7	29,6
100	36,8	23,3	36,4	24,7	51,7	34,6	30,3

Climate A1B 2046-65 return levels and averages of all models (average 1) and all but CSIRO (average 2) Helsinki

Return level (years)	ECHAM5	BCCR	MIROC3	CNRM	CSIRO	Average1	Average2
10	30,3	23,6	26,2	22,8	46,9	30,0	26,9
50	31,7	25,5	27,2	24,6	79,8	37,7	27,5
100	32,1	26,1	27,5	25,2	105,0	43,2	27,7

Climate A1B 2081-100 return levels and averages of all models (average 1) and all but CSIRO (average 2) Helsinki

Return level (years)	ECHAM5	BCCR	MIROC3	CNRM	CSIRO	Average1	Average2
10	28,7	25,1	28,6	22,9	38,3	28,7	27,8
50	30,6	26,6	31,1	24,6	46,1	31,8	28,5
100	31,3	27,0	31,9	25,3	49,9	33,1	28,9

Changes in percentages 2046-65 A1B climate - control climate Helsinki

Return level (years)	ECHAM5	BCCR	MIROC3	CNRM	CSIRO	Average1	Average2
10	-1 %	3 %	-5 %	-1 %	17 %	3 %	-4 %
50	-9 %	10 %	-18 %	1 %	66 %	10 %	-5 %
100	-13 %	12 %	-24 %	2 %	103 %	16 %	-6 %

Changes in percentages 2081-100 A1B climate - control climate Helsinki

Return level (years)	ECHAM5	BCCR	MIROC3	CNRM	CSIRO	Average1	Average2
10	-6 %	9 %	4 %	-1 %	-4 %	0 %	-1 %
50	-12 %	14 %	-7 %	1 %	-4 %	-1 %	-2 %
100	-15 %	16 %	-12 %	3 %	-4 %	-3 %	-2 %

4. Conclusions

According to the global scale climate models ECHAM5, MIROC3, BCCR, CSIRO and CNRM the geostrophic wind speeds in Finland have been and will be between 6-10 ms^{-1} during winter time – annually somewhat weaker and the maximum geostrophic wind speeds between 15-35 ms^{-1}. An increase of 2.5-5% in the annual and winter time V_g could take place and most probably so in southern Finland; larger increase is seen in southern Baltic Sea and its surroundings. In Finland elsewhere the climate models indicate that there will be natural variability in the wind climate – some decades weaker some decades stronger. Based the analyses the mean annual geostrophic wind speeds will increase 0-5 % in Finland but the extremes will decrease 1-6 %. The model CSIRO seems unstable at least from the extreme analysis point of view.

References

Alexandersson, H., 2005: Den stora januaristormen 2005. Väder och Vatten 1/2005. 11 p. (In Swedish)

Coles, S., 2001: An introduction to statistical modeling of extreme values. Springer-Verlag, London.

Gregow, H., Venäläinen, A., Peltola, H., Kellomäki, S., Schultz, D., 2008: Temporal and spatial occurrence of strong winds and large snow load amounts in Finland during 1961-2000. Silva Fennica 42, 515–534.

Katz R. W., Bruch, G.S., Parlange, M.B., 2005: Statistics of extremes: Modelling ecological disturbances. Ecology 86, 1124-1134.

Leckebush, G.C., Donat, M., Ulbrich, U., Pinto, J.G., 2008: Mid-latitude Cyclones and Storms in an Ensemble of European AOGCMs under ACC. Clivar Exchanges, Vol. 13(3).

Nilsson, C., Stjernquist, I., Bärring, L., Schlyter, P., Jönsson, A.M., Samuelsson, H., 2004: Recorded storm damage in Swedish forests 1901-2000. Forest Ecology and Management, 199, 165-173.

Nykänen, M-L., Peltola, H., Quine, C., Kellomäki, S., Broadgate, M., 1997: Factors affecting snow damage of trees with particular reference to European conditions. Silva Fennica 31, 193-213.

Pellikka, P., Järvenpää, E., 2003: Forest stand characteristics and wind and snow induced forest damage in boreal forest. Proc. Int. Conference on Wind Effects on Trees, University of Karlsruhe, Germany, 269-276.

Solantie, R., 1983: Metsän myrskytuhojen ja tuulennopeuden vastaavuus alueittain Suomessa. Metsä ja Puu 2: 9-11. (In Finnish)

Authors' address:

Hilppa Gregow (hilppa.gregow@fmi.fi)
Kimmo Ruosteenoja (kimmo.ruosteenoja@fmi.fi)
Ari Venäläinen (ari.venalainen@fmi.fi)
Finnish Meteorological Institute
Erik Palmen place 1, PO.Box 503, FI-00101 Helsinki, Finland

Wind speed variation over the leeward region according to vegetation under the strong wind

Woo-Sik Jung[1], Jong-Kil Park[2], Hwa Woon Lee[3], Eun-Byul Kim[1], Hyo-Jin Choi[1]

[1]Dept. of Atmospheric Environment Information Engineering/Atmospheric Environment Information Research Center, Inje University, Gimhae, Korea
[2]School of Environmental Science Engineering/ Atmospheric Environment Information Research Center, Inje University, Gimhae, Korea
[3]Dept. of Atmospheric Science, Pusan National University, Busan, Korea

Abstract

We have investigated the wind speed variations over the leeward region when the strong wind by typhoon blows. For this, we have employed "Envi-met" micro-scale atmospheric numerical model to simulate the effect of surface boundary conditions, This model is applied for two cases which are characterized by land use. Under the same wind speed and direction, the first, base case having natural geographical condition shows the weakest wind speed around lee side of Chunsudae, Gadeok island in Busan, Korea. The others which remove the vegetation represent the stronger wind speed than base case. The main factor of this result is the surface friction by vegetation. The distinct variation of wind is found at offshore area between Chunsudae and the southern part of village, but the northern part, which is apart from Chunsudae, shows a small variation of wind pattern. The weakening of wind speed around residential area is a maximum of 4~8m/s when the wind blows in the village as strong as 55m/s. The gust wind speed is weakened about 7~17m/s in this case if the coefficient of gust wind adapted as 1.75.

1. Introduction

The weather elements such as wind and air temperature are influenced greatly by topographical condition nearby. Especially, wind is not only influenced by geographical and topographical conditions of the area but also by the buildings, etc in the narrow area. When strong wind such as typhoon blows, topographical effects by vegetation become bigger.

Therefore, we tried to examine the micro-scale wind speed variations of the leeward area by vegetation change of Chunsudae, Gaduk island in Busan, Korea as shown in the Fig. 1. For this, we used 'Envi-met' micro-scale atmospheric numerical model to examine the change of the wind fields according to topographical conditions with vegetation and without vegetation when a typhoon approaches.

2. Model description

2.1 Envi-met model

Envi-met model used in this study is developed by the Michael Bruse (1998), the professor of the Bochum University in Germany and it is a model updated in 2004. The Envi-met model is a microscale model about the surface, building, vegetation, and reciprocal action of the atmosphere in the urban area and the merit of this model is that it can make a clear pattern of microscale atmosphere and it not only simulate the surface of a hard wall of a building but also simulate the soft canopy such as a forest. Envi-met

model is composed with atmospheric model, vegetation model, soil model, and the numerical formula about the surface and building.

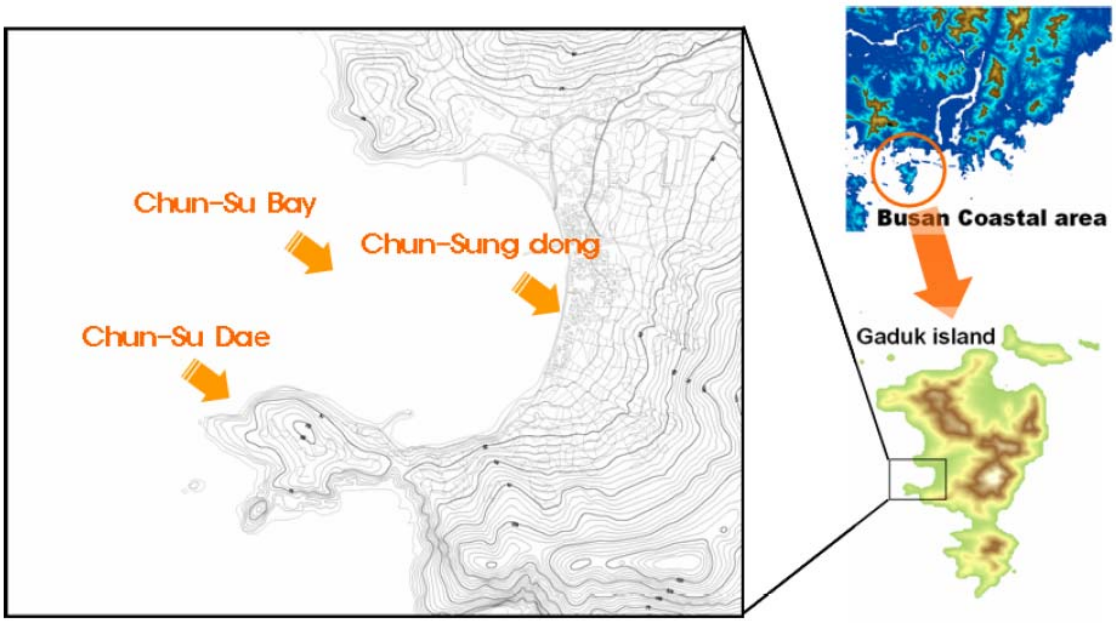

Fig. 1: Geographical condition around Chunsudae, Gaduk island in Busan, Korea

2.2 Model domain

In this study, we have set the domain as following condition to predict the variation of the wind velocity and wind direction in the village according to the change of the vegetation in Chunsu-dae. The computational area is horizontally 2,000 m for the east-west scope and 1,600 m for the north-south scope which horizontal grid size is 40m, number of grid point is 50 for the east-west direction and 40 for the north-south direction. And vertically 950m is divided into 25 layers and for the detail computation of surface boundary layer, the vertical grid layer interval becomes larger as it goes to upper layer (telescoping method, 20%). The topographic and vegetation input data which is to predict the wind flow field is composed as the Fig. 2.

2.3 Verification of modelling result

To verify the validity of the modeling result, we used the metrological data observed from the Automatic Weather station (AWS) established on the rooftop of the building in the village. Also, used one hour observed data at the 3 site in the same area by using a portable weather station during November 16 and 17, 2005. As a result (Table 1), we found that the observed wind data was very similar with the value obtained by the Envi-met model. From these results, we could decide that the value obtained from the model is credible enough to predict and check the wind fields in the offing and village including Chunsudae.

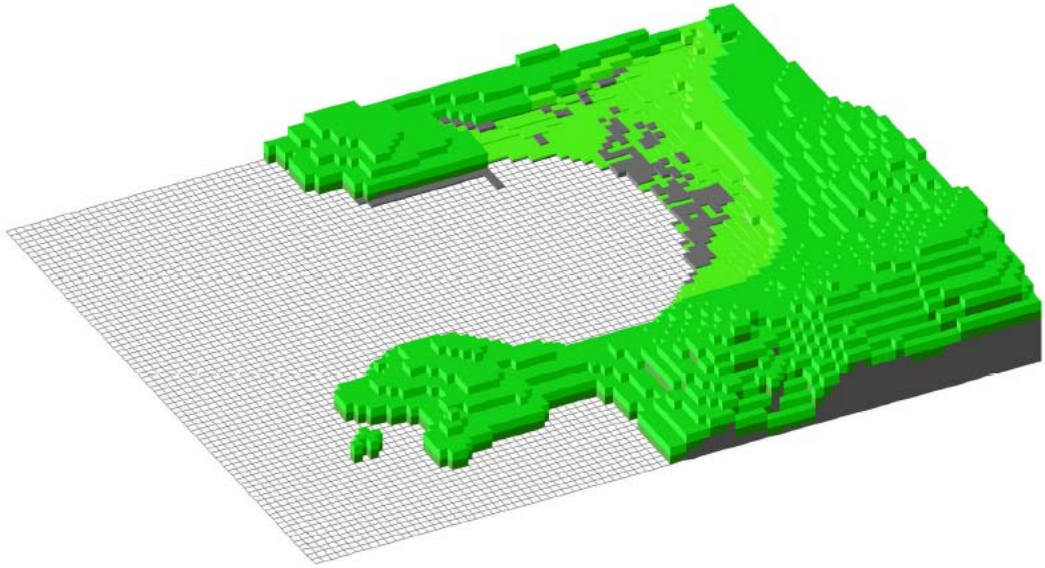

Fig. 2: Surface boundary outlines of Envi-met model

Table 1: Comparision of the observed with calculated wind speed (WS) and wind direction (WD)

		16 November, 2005				17 November, 2005		
		1400 LST				0000LST	0900LST	1800LST
		P1	P2	P3	AWS	AWS	AWS	AWS
WS (m/s)	OBS	3.1	3.6	3.6	4.6	1.9	1.1	2.1
	CAL	3.8	3.7	3.7	4.4	1.9	1.2	2.2
WD (degree)	OBS	290	280	280	285	55	93	23
	CAL	284	281	283	286	57	94	23

3. Results and Discussions

3.1 Designing the numerical experiment

We analyzed the quality and degree of the change of the wind field with layers in base case considering vegetation and natural state topography in Chunsudae and in bare case eliminating the vegetation without the change of the topography (Fig. 3). And also, to find out the wind velocity's effect on Chunsudae, we saw the change of the wind field when the potential maximum wind velocity by typhoon is 55 ms^{-1} on the surface condition (Jung et al., 2006). Lastly, we have considered specific wind direction, 260 degree, which is able to give a wind potential damage by typhoon in the village.

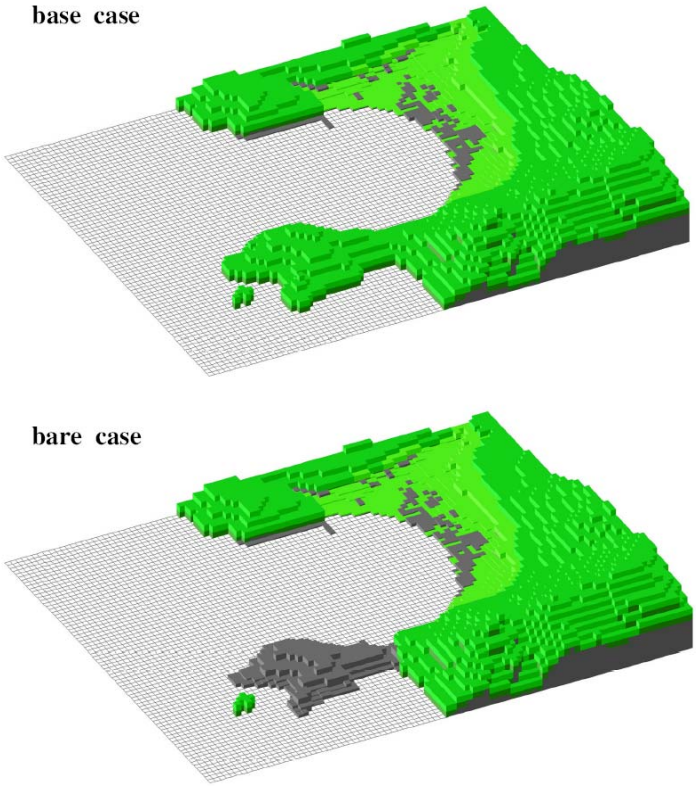

Fig. 3: Surface boundary condition over the Chunsudae: base case (up) is considering vegetation and natural state topography in Chunsudae and bare case (down) indicates surface boundary condition eliminated the vegetation without the change of the topography

3.2 Variation of wind vector

3.2.1 Modelling result of base case

Topography of Chunsudae is like a hilly area which the center is high with a 52 m height and getting low as it goes to the edge. Also, it has a vegetation condition which is covered with pine trees generally about 15~20 m tall. When 260° wind blows in 55 ms^{-1} toward the Chunsudae with this vegetation condition, the result is as follows. The Fig. 4(a) shows the wind vector of 3 m height above sea level. An inflow which is the west wind toward the Chunsudae and the village shows the clear change of the wind direction and the weakening of wind velocity in the leeward, back of the Chunsudae (east part of Chunsudae). Especially, in the leeward of north part of Chunsudae, we found that the wind pattern was very different because of the vortex which flew around the Chunsudae and by this, wind direction of the south area of the village was the north-west wind.

But in the center of the village and the north area shows the west wind which is similar with the inflow wind pattern. Besides, there is a big change of the wind direction and velocity along the north-west coast line of Chunsudae and at the edge of the Chunsudae's opposite side shows similar change of wind direction and velocity. Similar wind field distribution shows in the altitude of 20 m (Fig. 4(b)), too.

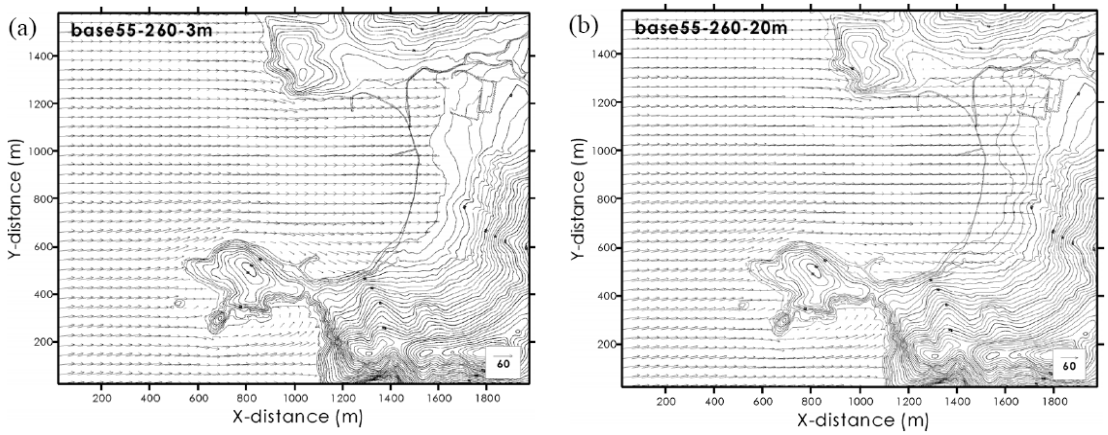

Fig. 4: Wind vector distributions of (a) 3 m height above sea level and (b) 20 m height above sea level in base case of 55 ms^{-1} inflow

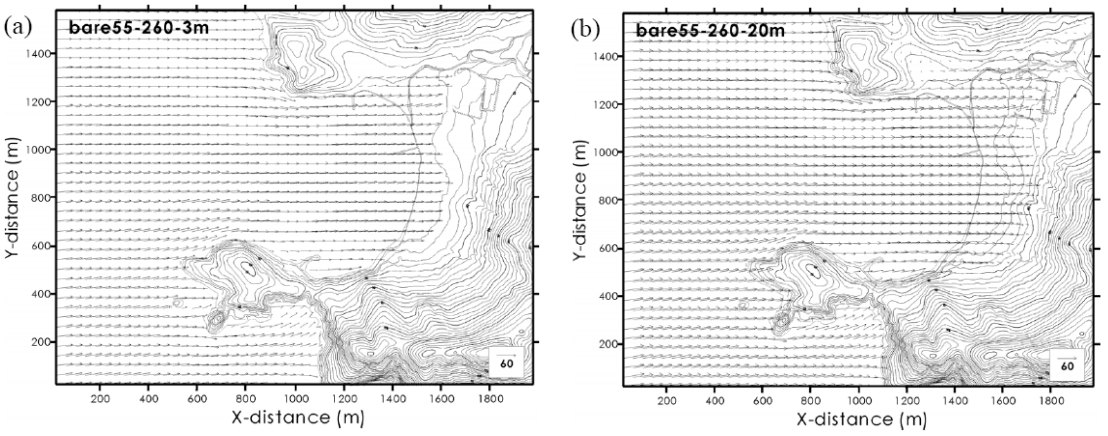

Fig. 5: Same as Fig. 4 except for bare cases

3.2.2 Modelling result of bare case

Under the surface boundary condition felling all the pine trees with 15-20 m tall without the change of the topography, the results of the numerical simulation was as follows (Fig. 5). Fig. 5(a) shows the wind vector distribution of 3 m height above sea level. Generally there is no big difference with the base case but in the north-west area of Chunsudae shows clear difference. This difference is well shown in Fig. 6. This figure represents the wind field of 3 m height above sea level in both the base case and the bare case. The red color vector is the result of the base case and the black color vector is the result of the bare case. We can see the clear difference of the wind direction and the velocity in the backside of the Chunsudae which is the leeward region about the inflow wind of 260° direction. Especially, it shows clear difference in the north-west and the south-west coastal region of Chunsudae. It seems like there is no big difference in the size of the vector which shows the wind velocity's intensity but if we see the size of the unit vector (60 ms^{-1}) at the foot of the figure in the right side, the little difference of the size of an arrow is about 10~15 ms^{-1} difference of the wind velocity. This distinct difference of the wind direction and the wind velocity is because of the vegetation effect,

we think. Also in this study, when there is no vegetation in Chunsudae the friction is relatively small. So the change of the wind direction and velocity is small but when there is lots of vegetation in the area the friction becomes bigger as it comes closer to the coastline and the change of the wind direction and velocity becomes bigger. But when it goes to the ocean floor far from the land, the displacement of wind direction and velocity becomes gradually small in the leeward, backside of the Chunsudae. This is same as the general definition of a windbreak that a windbreak effects the range of 5~6 times distance of a vegetation tall and the range of 30~35 times distance of the leeward direction (www.sanrimji.com). In case of a forest on the slope, the effect of windbreak is higher in the leeward than in the windward. But the weakening the wind velocity by the windbreak make a difference according to the vegetation density, topography, wind direction and wind velocity, etc.

In this study we find out the similar result with the general case. Fig. 5(b) is the result of the wind field of 20 m height above sea level. When we see the result of this, it is not that different with the wind field of the 3 m height that we have seen before. But even in this altitude the wind direction and velocity shows clear difference in the leeward, backside of the Chunsudae about inflow direction

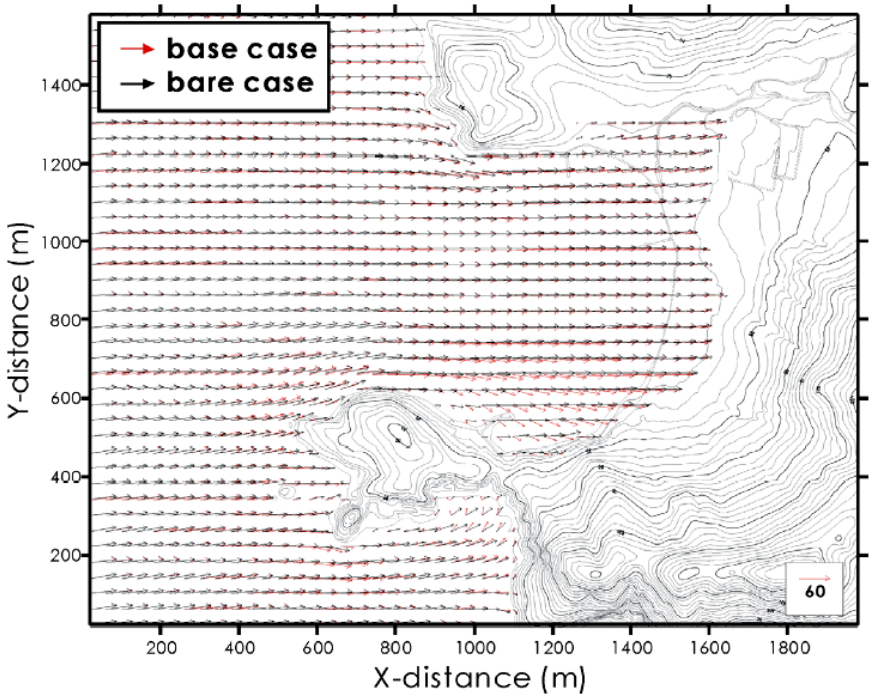

Fig. 6: Comparison of wind vectors of base with 20m cases at 3m above sea level

4. Summary and conclusions

In this study, under the strong wind such as typhoon we analyzed the variation extent of wind direction and wind velocity in the leeward of Chunsudae with topographical condition using the Envi-met model. For this, we compared the base case which is in the natural topographic condition and the bare case which is in the condition with no vegetation without the change of the topography. When we made the strong wind with same

direction of 260°, the wind velocity was weak in the base case compared to the bare case. The difference of wind velocity is about 10~15 ms^{-1}, especially the weakening of wind speed around residential area is a maximum of 4~8 ms^{-1} when the wind blows in the village as strong as 55 ms^{-1}. This explains that when the vegetation is eliminated, the wind become stronger in the leeward of topography.

Acknowledgement

This work was funded by the Korea Meteorological Administration Research and Development Program under Grant CATER 2006-3303.

References

Bruse, M., 1988: Development of a micro-scale model for the calculation of surface temperatures in structured terrain. MSc Thesis, Inst. Geo. Univ. Bochum.

Jung, W.S., Park, J.K., Lee, H.W., 2006: An analysis on influence of geographical variation induced by development affecting to the local scale wind environment - numerical simulation using the Envi-met model. J. Korean Society for Atmospheric Environment 22, 888-903 (in Korean).

http://www.sanrimji.com(2009.06.21)

Authors' addresses:

Assistant Prof. Dr. Woo-Sik Jung (wsjung1@inje.ac.kr)
Department of Atmospheric Environment Information Engineering/Atmospheric Environment Information Research Center, Inje University
Gimhae, Korea

Prof. Dr. Jong-Kil Park (envpjk@inje.ac.kr)
School of Environmental Science Engineering/Atmospheric Environment Information Research Center, Inje University
Gimhae, Korea

Prof. Dr. Hwa Woon Lee (hwlee@pusan.ac.kr)
Dept. of Atmospheric Science, Pusan National University
Busan, Korea

Ph. D. Candidate, Eun-Byul Kim (star2713@nate.com)
Department of Atmospheric Environment Information Engineering, Graduate School, Inje University
Gimhae, Korea

Ph. D. Candidate, Hyo-Jin Choi (space-chj@hanmail.net)
Department of Atmospheric Environment Information Engineering, Graduate School, Inje University
Gimhae, Korea

GIS-based modeling for evaluation of wind damage probability in forests in Southwest Germany

Karin Grebhan, Dirk Schindler, Helmut Mayer

Meteorological Institute, Albert-Ludwigs-University of Freiburg, Germany

Abstract

The weights of evidence (WofE) methodology and logistic regression models (LRM) were used for GIS-based estimation of the wind damage probability (P_{DAM}) in the forests across the federal state of Baden-Wuerttemberg (Southwest Germany). P_{DAM}-calculations were based on the storm damages caused by the severe winter storms 'Vivian'/'Wiebke' and 'Lothar'. For each storm event six out of 20 tested evidential themes were favorably associated with wind damage in the forests. Out of these six evidential themes soil type, geology, and soil moisture were important predictor variables for P_{DAM} after both storm events. Further important evidential themes related with 'Vivian'/'Wiebke' were slope, altitude, and soil drainage. Maximum gust speed, forest type, and soil acidification were further predictor variables that were favourably associated with P_{DAM} after 'Lothar'. On the basis of the combined evidential themes, for each storm event GIS-based wind damage probability maps were produced. These maps were then classified into zones of high, moderate and low wind damage probability. The WofE-methodology predicted wind damage with an overall success rate of 76 % after 'Vivian'/ 'Wiebke' and 78 % after 'Lothar'. The area under the ROC curve calculated from the LRM results for P_{DAM} after 'Vivian'/ 'Wiebke' equalled to 78 %. After 'Lothar' the area under the ROC curve amounted to 79 %. The most wind damage-prone regions within the study area are the northern Black Forest, the northern Upper Rhine Valley, and the Swabian Alb.

1. Introduction

The federal state of Baden-Wuerttemberg (Southwest Germany), which was the study area (35,752 km^2), represents one of the most densely wooded (38 %) federal states in Germany. Its topography is rather complex. Striking elements are the Black Forest, the Swabian Alb, and the upper Rhine valley. In the past, severe winter storms like 'Vivian'/'Wieb-ke' in February 1990 (Schüepp et al., 1994; Goyette et al., 2001) and 'Lothar' in December 1999 (Clarke, 2001; Ulbrich et al., 2001) caused large amounts of wind damaged timber (LFV, 1994; Kronauer, 2000). For example, 'Lothar' blew down about 30 million m^3 of timber in Baden-Wuerttemberg, which is about three times the annual cut. The monetary loss in the forests of Baden-Wuerttemberg resulting from 'Lothar' was estimated at € 770 million (Hartebrodt, 2004).

Owing to both the large study area and the lack of comprehensive long-term tree and stand damage data across the study area, two statistical, data-driven approaches were chosen to assess the wind damage probability (P_{DAM}) in the forests of Baden-Wuerttemberg. For P_{DAM}-assessment, the weights of evidence methodology (WofE) and common logistic regression models (LRM) (Hosmer and Lemeshow, 2000) were applied. The Spatial Data Modeller (Sawatzky et al., 2008), which is a free ArcGIS® software (ESRI, Redlands, CA) extension, was used to carry out the WofE-methodology. The statistical software SAS® 9.2 (SAS Institute, Cary, NC) was used to accomplish the logistic regression analyses. The P_{DAM}-results are based on wind damage data, which

- recently became available within the framework of the CORINE Land Cover 2000 (CLC2000) project (Keil et al., 2005),
- orginate from forest inventories (ZN_{Sturm}).

The main objectives of the study were to identify the most important evidential themes for study area-wide P_{DAM}-assessment and to prepare a GIS-based P_{DAM}-quantification for forest managers. The final P_{DAM}-maps are thought of as tools useful for supporting decision making in silviculture.

2. Methods

The GIS-based mapping of P_{DAM} followed seven steps (Schindler et al., 2009):

- WofE-based division of all continuous evidential themes into classes,
- calculation of WofE-weights for each class of the evidential themes,
- generalization of the evidential themes,
- application of conditional independence test,
- combination of the most relevant and conditionally independent evidential themes by applying WofE and logistic regression analyses in order to calculate P_{DAM}-values,
- double Application of the Youden index (Baker et al., 2007) to divide P_{DAM}-values into classes,
- evaluation of WofE- and logistic regression models.

The starting database for model building and subsequent area-wide estimation of P_{DAM} encompassed the following evidential themes:

- topographical themes: elevation, slope, aspect, slope form, topographic exposure, minimum distance to next ridge;
- soil conditions and geological themes: soil type, soil substrate, soil depth, soil moisture, soil acidification, groundwater affected soils, backwater affected soils, geology;
- forest themes: forest type, minimum distance to forest edge, minimum distance to western forest edge (the main wind direction during winter storms over the last 30 years (Heneka et al. 2006);
- meteorological and hydrological themes: maximum gust speed field of ‘Lothar’ (spatial resolution: 1 × 1 km), minimum distance to next river.

All evidential themes in vector format were converted into raster format with a cell resolution of 50 × 50 m. Due to the resolution of the satellite images and the mapping procedures applied in CLC2000 (Keil et al. 2005), the minimum size of identifiable storm damaged areas after ‘Lothar’ was 5 ha.

3. Results

The strongest relationship between

- wind damaged areas due to 'Vivian'/'Wiebke' and predictor variables was found for soil type, soil moisture, soil drainage, geology, slope, and altitude;
- wind damaged areas resulting from 'Lothar' and predictor variables was found for forest type, soil type, geology, soil moisture, soil acidification, and maximum gust speed.

The evidential themes were used to produce area-wide P_{DAM}-maps with a resolution of 50 × 50 m. After

- 'Vivian'/'Wiebke', the highest P_{DAM}-values were predicted for coniferous forest growing on strongly acidic, fresh to moist soils on loess loam at slopes of less than 5 degrees;
- 'Lothar', the highest P_{DAM}-values were predicted for coniferous forests growing on fresh to moist soils on bunter sandstone formations – provided that 'Lothar' maximum gust speed exceeded 35 m s^{-1}.

Based on the Youden index the probability maps were classified into three P_{DAM}-classes representing low, moderate, and high wind damage probability. In Fig. 1 map extracts of WofE-based P_{DAM}-estimates after 'Vivian'/'Wiebke' (Fig. 1a) and 'Lothar' (Fig. 1b) are shown for the area to the south of the city of Pforzheim.

The degree of discrimination between non-storm damage and storm-damage of

- WofE (area under the success rate curve) was 76 % for 'Vivian'/'Wiebke' and 78 % for 'Lothar',
- LRM (area under to the ROC curve) between non-storm damage and storm-damage was 78 % for 'Vivian'/'Wiebke' and 79 % for 'Lothar'.

The degree of discrimination realized can be compared to results presented for other studies (e.g. Mitchell et al. 2001; Scott and Mitchell, 2005).

4. Conclusions

The most important outcome of this study is that, for the first time, there is a GIS-based area-wide quantification of P_{DAM} in the forest of Baden-Wuerttemberg. An area-wide quantification of P_{DAM} did not exist until now. The produced P_{DAM}-maps are intended to be useful tools for supporting decision making in silviculture towards a reduction of wind damage in forests.

For further refinement of the presented results the next step in the area-wide P_{DAM}-estimation will be the conflation of all available data into one dataset and carrying out multinomial P_{DAM}-assessment across both storm events.

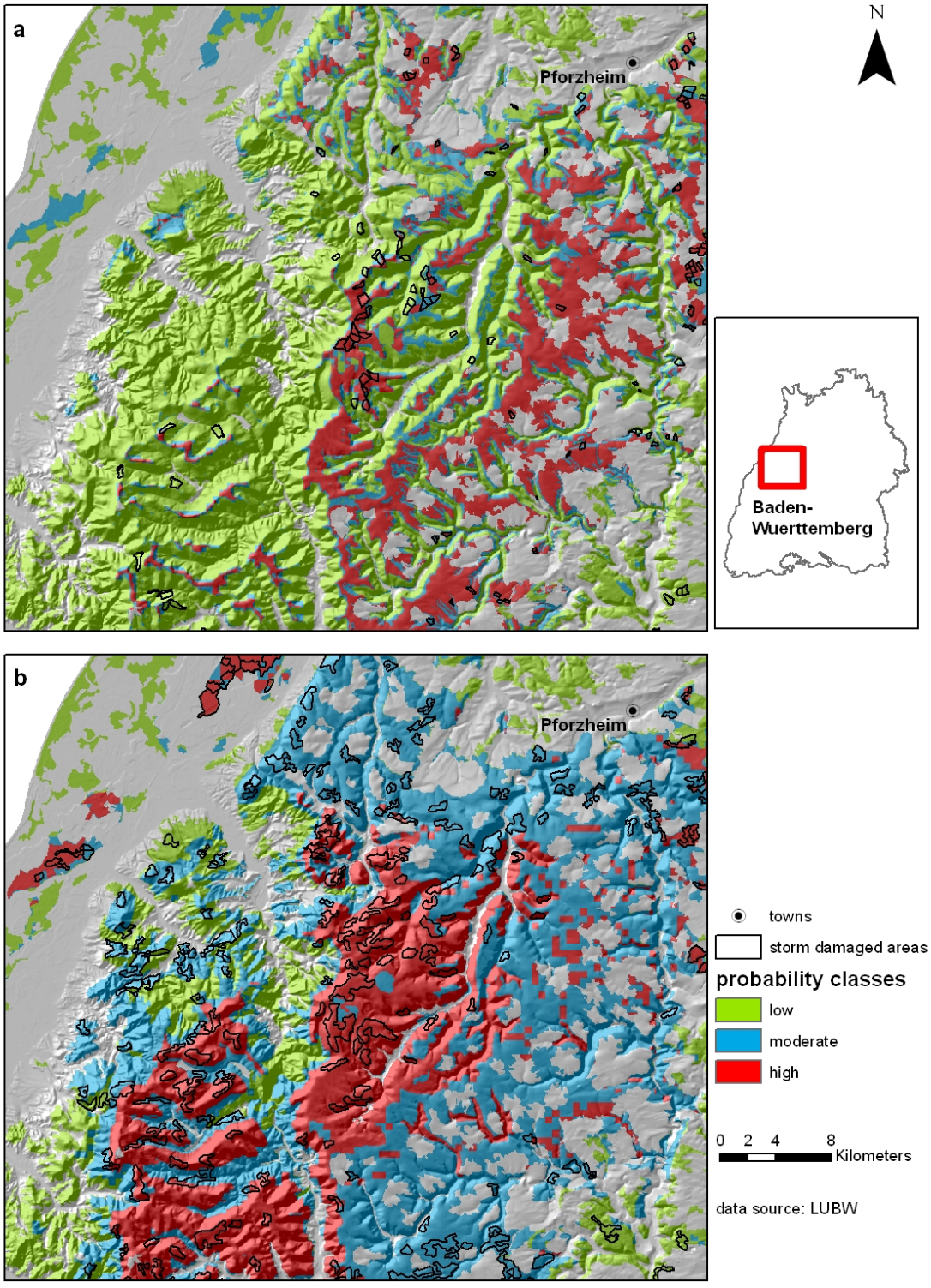

Fig. 1: Map extracts showing the WofE-classified wind damage probability (P_{DAM}) after (a) the winter storm 'Vivian'/'Wiebke', and (b) after the winter storm 'Lothar' (LUBW: State Agency for Environmental Protection Baden-Wuettemberg)

Acknowledgement

This investigation was performed within the project 'Development of a risk map for storm damages in forests and forest-significant models for storm damages as bases for methods to reduce storm damages in forests in Baden-Württemberg', which is part of the RESTER-network ('Strategies for the reduction of the storm damage risk for forests') within the research program 'Challenge climate change'. The authors would like to thank the Ministry for the Environment of the German federal state Baden-Württemberg for the financial support of this project.

References

Baker, S.G., Kramer, B.S., 2007: Peirce, Youden, and Receiver Operating Characteristic Curves. Am. Stat. 61, 343-346.

Clarke, R., 2001: Lothar and Martin. WMO Bulletin 50, 54-59.

Goyette, S., Beniston, M., Caya, D., Laprise, R., Jungo, P., 2001: Numerical investigation of an extreme storm with the Canadian Regional Climate Model: the case study of windstorm VIVIAN, Switzerland, February 27, 1990. Clim. Dyn. 18, 145-168.

Hartebrodt, C., 2004: The impact of storm damage on small-scale forest enterprises in the southwest of Germany. Small-scale Forest Economics, Management and Policy 3, 203-222.

Heneka, P., Hofherr, T., Ruck, B., Kottmeier, C., 2006: Winter storm risk of residential structures - model development and application to the German state of Baden-Württemberg. Nat. Haz. Earth Sys. Sci. 6, 721-733.

Hosmer, D.W., Lemeshow, S., 2000: Applied Logistic Regression. John Wiley & Sons, New York, 375 pp.

Keil, M., Kiefl, R., Strunz, G., 2005: CORINE Land Cover 2000 – Germany. Final Report – Wessling, 80 pp.

Kronauer, H., 2000: Tagung des Forstvereins Baden-Württemberg. Nach Lothar: Neue Wälder - neue Wege? AFZ 17, 919.

LFV, 1994: Dokumentation der Sturmschäden 1990. Schriftenreihe LFV Baden-Württemberg 75, 9-61.

Mitchell, S.J., Hailemariam, T., Kulis, Y., 2001: Empirical modeling of cutblock edge windthrow risk on Vancouver Island, Canada, using stand level information. For. Ecol. Manage. 154, 117-130.

Sawatzky, D.L., Raines, G.L., Bonham-Carter, G.F., Looney, C.G., 2008: Spatial Data Modeller (SDM): ArcMAP 9.2 geoprocessing tools for spatial data modelling using weights of evidence, logistic regression, fuzzy logic and neural networks. http://arcscripts.esri.com/ details.asp?dbid=15341.

Schindler, D., Grebhan, K., Albrecht, A., Schönborn, J., 2009: Modelling the wind damage probability in forests in Southwestern Germany for the 1999 winter storm 'Lothar'. Int. J. Biometeorol. DOI 10.1007/s00484-009-0242-3.

Schüepp, M., Schiesser, H.H., Huntrieser, H., Scherrer, H.U., Schmidtke, H., 1994: The Winterstorm "Vivian" of 27 February 1990: About the Meteorological Development, Wind Forces and Damage Situation in the Forests of Switzerland. Theor. Appl. Climatol. 49, 183-200.

Scott, R.E., Mitchell, S.J., 2005: Empirical modelling of windthrow risk in partially harvested stands using tree, neighbourhood, and stand attributes. For. Ecol. Manage. 218, 193-209.

Ulbrich, U., Fink, A.H., Klawa, M., Pinto, J.G., 2001: Three extreme storms over Europe in December 1999. Weather 56, 70-80.

Authors' address:

Dipl.-Geogr. Karin Grebhan (karin.grebhan@meteo.uni-freiburg.de)
Dr. Dirk Schindler (dirk.schindler@meteo.uni-freiburg.de)
Prof. Dr. Helmut Mayer (helmut.mayer@meteo.uni-freiburg.de)
Meteorological Institute, Albert-Ludwigs-University of Freiburg
Werthmannstrasse 10, D-79085 Freiburg, Germany

A dynamic tree sway model

Hannes Fugmann, Dirk Schindler, Helmut Mayer

Meteorological Institute, Albert-Ludwigs-University of Freiburg, Germany

Abstract

The proposed anisotropic, mathematical model can be used to simulate the sway of a Scots pine tree resulting from a tree-pulling test in the direction of the pulling force to a reasonable degree. However, under real wind conditions the model's ability to simulate the dynamics of wind-induced tree vibrations is limited. Possible sources of the model's simulative inability arise from sporadic decoupling of the tree response from near-surface airflow, effects of cross-coupling of the two horizontal displacement components, changes in instantaneous wind load frequency and tree response frequency, and the insufficient description of the acting wind load.

1. Introduction

In a planted Scots pine (*Pinus sylvestris* L.) forest (mean stand height: 14.5 m) located in the southern upper Rhine valley (Southwest Germany, 47°56´04´´N, 7°36´02´´E, 201 m a.s.l.) adjacent to the forest meteorological experimental site Hartheim (Mayer et al., 2008), both wind-induced stem displacement of a Scots pine tree and near-surface airflow properties were monitored over the period October 2005 to April 2006. Properties of near-surface airflow were measured (sampling rate: 20 Hz) by eight ultrasonic anemometers (USA-1, METEK, Germany), which were mounted on a 28 m high traingular lattice tower. The measurement tower was set up in a small canopy gap a few meters away from the sample tree.

Angular position of the sample tree (tree height: 14.6 m) was measured (sampling rate: 10 Hz) by three biaxial clinometers (model 902-45, Applied Geomechanics, USA), which were mounted on its stem at the three heights hc_1 = 1/7ht, hc_2 = 3/7ht, and hc_3 = 5/7ht, ht being the sample tree height. These heights were assumed to be approximately the heights of the antinodal points of vibration of the 4th normal mode of a clamped-free beam. Angular position (degree) measurements were converted into wind-induced stem displacement (m) in x- and y-direction along the stem of the tree. Its displacement between z = 0 m to the top height was estimated for 0.2 m intervals using cubic spline interpolation (Schindler, 2008). In addition, tree-pulling tests were carried out in order to determine the sample tree's stiffness matrix **K**.

2. Model description

The mathematical, dynamic tree sway model, which was built in order to simulate the dynamic behaviour of a Scots pine (*Pinus sylvestris* L.) tree in response to turbulent wind loading, is based on a model used to simulate deflections of a cantilever (Kerzenmacher and Gardiner, 1998; Nash, 1998; Petersen, 2000). In the model the Scots pine tree is reproduced as a one-sided fixed beam (Fig. 1), which is divided into 1 m beam segments. To each of the hinged segment points, values of mass m_j (j = 1, …, 15) are assigned. The coordinates y_j (m) of the upper endpoints of the segments corresponds with the values of stem displacement in the streamwise direction. Based on lateral wind loading, the movement of the joints between the segments can be

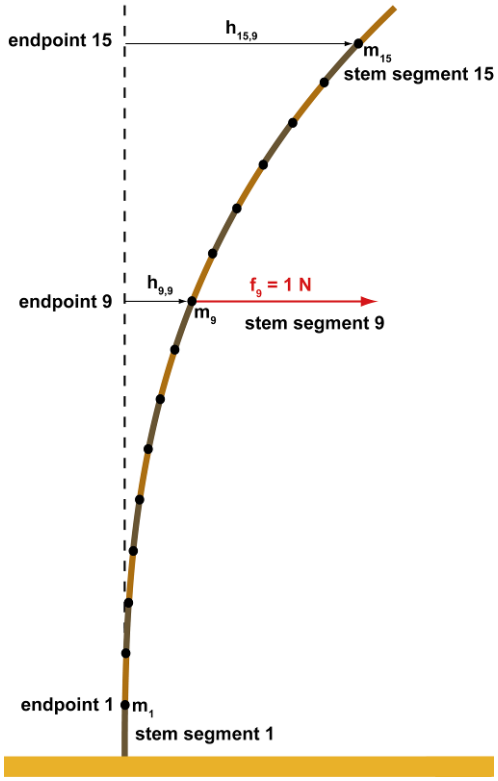

Fig. 1: Model of a one-sided fixed beam used to simulate tree sway resulting from tree-pulling tests and induced by turbulent wind loading

described by a set of n coupled differential equations, which are solved by application of the normal mode solution.

If the wind load, which was approximated from the vertical wind velocity profile for 0.2 m intervals by cubic spline interpolation, acts on the endpoints of the hinged segments then the displacement of each endpoint can be simulated by the differential equation

$$\mathbf{M}\ddot{\mathbf{y}} + \mathbf{D}\dot{\mathbf{y}} + \mathbf{K}\mathbf{y} = \mathbf{F} \tag{1}$$

where $\mathbf{M}$ is the n × n mass matrix whose elements are m_{ij} (i, j = 1, …, 15), $\mathbf{D}$ is the n × n viscous damping matrix whose elements are d_{ij}, $\mathbf{K}$ is the n × n stiffness matrix whose elements are k_{ij}, $\mathbf{F}$ is the n × 1 load vector whose elements are f_j, and $\mathbf{y}$ is the n × 1 stem displacement vector whose elements are y_j.

The mass matrix $\mathbf{M}$ is the diagonal matrix

$$\mathbf{M} = \begin{bmatrix} m_1 & 0 & \dots & \dots & 0 \\ 0 & m_2 & \dots & \dots & \dots \\ \dots & \dots & \dots & \dots & \dots \\ \dots & \dots & \dots & m_{n-1} & 0 \\ 0 & \dots & \dots & \dots & m_n \end{bmatrix} \tag{2}$$

where

$$m_j = \rho_w \cdot \pi \cdot r_j^2 + bm_j \quad (3)$$

with r_j as the mean radius of segment j, ρ_w as the wood density of the stem, and bm_j as the branchmass associated with segment j.

The calculation of **K** is based on the flexibility matrix **H**. **H** is the inverse of **K**. The j^{th} column of **H** is the vector that describes the displacement of each endpoint when exposed to a unit load (N) at the j^{th} endpoint.

Since the rope used to pull the sample tree was attached at only one height (9.0 m), stem displacement is known only at the pulling height. In order to determine displacement of other endpoints of stem segments, Maxwell's reciprocity relation (Kelly, 1996) was applied which implies that $h_{ij} = h_{ji}$. Stem displacement above the tree-pulling height was linearly extrapolated up to the top of the tree.

Under the assumption of proportional damping, **D** is then calculated from **M** and **K** as

$$\mathbf{D} = \alpha\mathbf{M} + \beta\mathbf{K} \quad (4)$$

where α und β are constants that were determined from free vibration conditions while conducting tree-pulling tests.

The wind load vector was calculated as

$$f_j = F(j) = \rho_a \, c_d \, A_{seg}(j) |u(j)| u(j) \quad (5)$$

where ρ_a is the air density, c_d is the drag coefficient, $A_{seg}(j)$ is the canopy area per stem segment, and u(j) is the streamwise wind speed at the heights of the endpoint of segment j.

Since Eq. (1) cannot be solved by numerical methods at this point, it was decoupled by means of the normal mode solution. The j^{th} mode shape vector for natural frequencies is given by

$$\left(\mathbf{K} - \omega_j^2 \mathbf{M}\right) a_j = 0 \quad (6)$$

where

$$a_j = \begin{Bmatrix} a_{1,j} \\ \dots \\ a_{n,j} \end{Bmatrix} \quad (7)$$

is the mode shape vector of eigenfrequency ω_j. This leads to the eigenvalue-eigenvector problem

$$\mathbf{M}^{-1} \mathbf{K} \, a_j = \omega_j^2 \, a_j \quad (8)$$

a_j and a_i (for i, j = 1, …, 15 and $i \neq j$) are mode shape vectors for the 15-degree-of-freedom system that are related to ω_i and ω_j. These mode shapes satisfy the following orthogonality conditions:

$$a_j^T \mathbf{M} a_i = 0 \tag{9}$$

$$a_i^T \mathbf{M} a_j = 0 \tag{10}$$

When the mode shape vectors are conflated to the modal matrix **A**

$$\mathbf{A} = \begin{bmatrix} a_{1,1} & a_{1,2} & \cdots & a_{1,15} \\ a_{2,1} & a_{2,2} & & \\ \vdots & & \ddots & \vdots \\ a_{15,1} & & \cdots & a_{15,15} \end{bmatrix} \tag{11}$$

then the matrix products

$$\mathbf{A}^T \mathbf{M} \mathbf{A} \tag{12}$$

$$\mathbf{A}^T \mathbf{K} \mathbf{A} \tag{13}$$

are diagonal matrices.

By introducing the new displacement coordinates z = z(t), which are defined by

$$y = \mathbf{A} z \tag{14}$$

Eq. (1) can be transformed to

$$\mathbf{M A} \ddot{\mathbf{z}} + \mathbf{D A} \dot{\mathbf{z}} + \mathbf{K A z} = \mathbf{F} \tag{15}$$

Multiplying Eq. (15) by $\mathbf{A}^T$ leads to

$$\mathbf{A}^T \mathbf{M A} \ddot{\mathbf{z}} + \mathbf{A}^T \mathbf{D A} \dot{\mathbf{z}} + \mathbf{A}^T \mathbf{K A z} = \mathbf{A}^T \mathbf{F} \tag{16}$$

where $\widetilde{\mathbf{M}} = \mathbf{A}^T \mathbf{M A}$ is the modal mass matrix, $\widetilde{\mathbf{D}} = \mathbf{A}^T \mathbf{D A}$ is the modal damping matrix, $\widetilde{\mathbf{K}} = \mathbf{A}^T \mathbf{M A}$ is the modal stiffness matrix, and $\widetilde{\mathbf{F}} = \mathbf{A}^T \mathbf{F}$ is the modal force vector. Equation (16) represents a set of decoupled differential equations, which can be solved numerically. The retransformation of the z- to y-coordinates gives the stem displacement at the endpoints of the 1 m stem segments as a function of time.

3. Results and Discussion

The performance of the model was assessed by comparing simulated tree sway against (1) tree sway from a tree-pulling test and (2) tree sway under real wind conditions. The estimate of the tree sway frequency used in the model was obtained from the sway period of the tree after it was released from the pulling rope during a tree-pulling test. This frequency estimate corresponds to the tree's damped free vibration frequency.

The model reproduced tree sway resulting from the tree-pulling tests quite well (Fig. 2). Nonetheless, over time the tree's instantaneous sway frequency (Feldman, 2008) in-

creased from 0.240 to 0.256 Hz and the simulated tree displacement started to lag behind the measured tree displacement. Under real wind conditions the model's simulative ability was distinctly reduced compared to the simulations of tree displacement resulting from tree-pulling tests. For example, over the period of 200 s presented in Fig. 3 there are only short sections when measured and simulated tree displacement agree well.

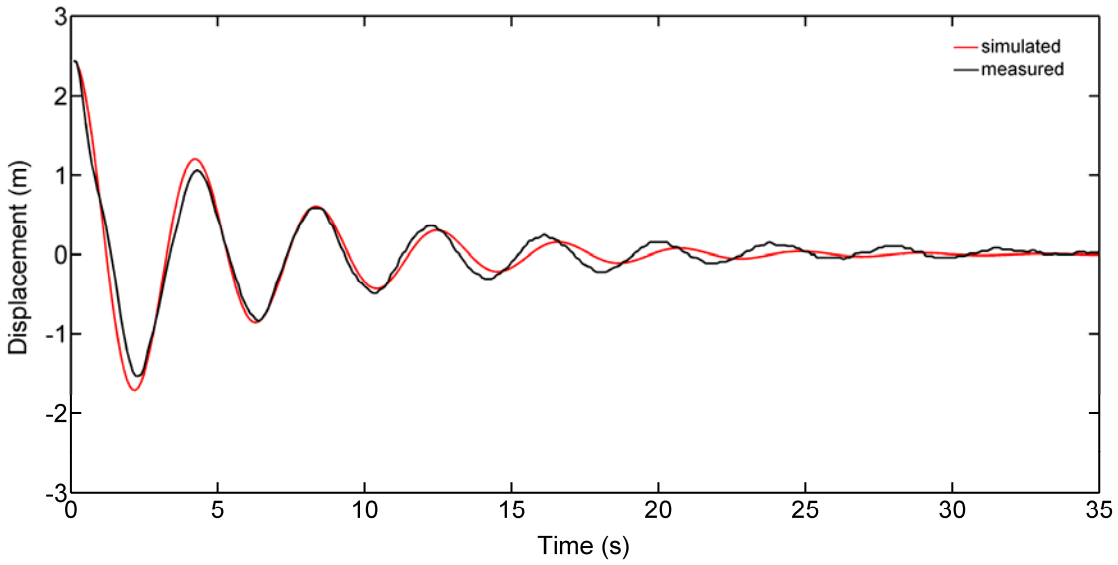

Fig. 2: Measured and simulated sway of a Scots pine tree at 11 m height over a period of 35 s after release from the pulling rope

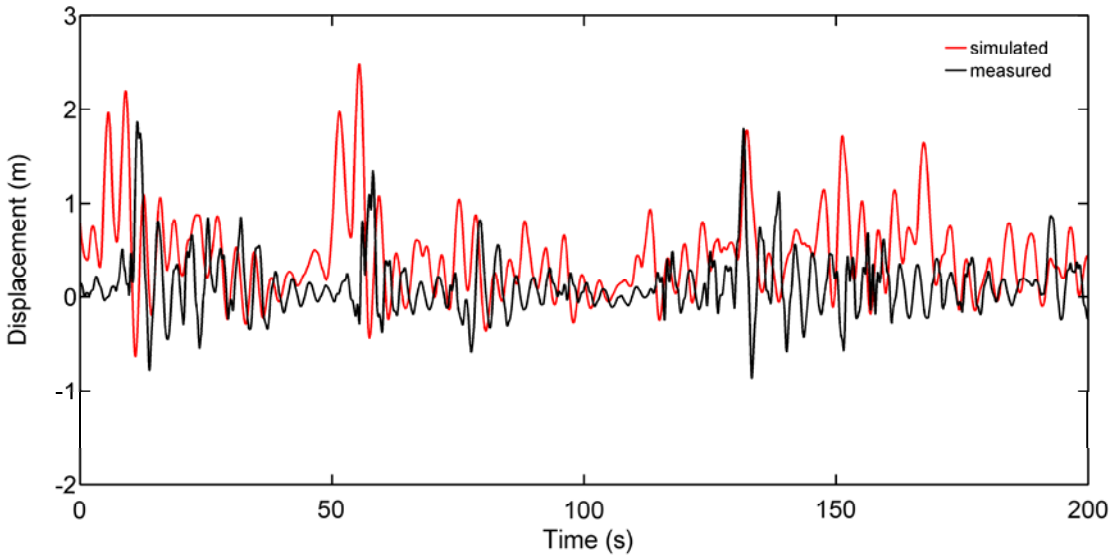

Fig. 3: Measured and simulated sway of a Scots pine tree at 11 m height over a period of 200 s under real wind conditions

Most of the time simulated tree displacement did not agree with measured tree displacement. Frequency as well as amplitude of measured tree displacement is weakly reproduced by the model. Reasons that cause the reduction in the model's simulative ability are sporadic decoupling of tree response from near-surface airflow, effects of cross-coupling of the two horizontal displacement components, changes in instantaneous wind load frequency and tree response frequency, and the insufficient description of the acting wind load.

4. Conclusions

The proposed model in its present state might be of use when simulating tree sways that result from tree-pulling tests. It cannot be applied to adequately simulate wind-induced tree sway because it is not capable to reproduce frequency and amplitude of measured tree displacement over prolonged periods of time.

Improved performance of the model might be achieved with an adequate inclusion of a better approximation of the acting wind load, of periods during which the tree is decoupled from wind loading, and of cross-coupling of the horizontal tree displacement components.

Acknowledgement

This investigation was performed within the project 'Development of a risk map for storm damages in forests and forest-significant models for storm damages as bases for methods to reduce storm damages in forests in Baden-Württemberg', which is part of the RESTER-network ('Strategies for the reduction of the storm damage risk for forests') within the research program 'Challenge climate change'. The authors would like to thank the Ministry for the Environment of the German federal state Baden-Württemberg for the financial support of this project.

References

Feldman, M., 2008: Theoretical analysis and comparison of the Hilbert transform decomposition methods. Mech. Syst. Signal Pr. 22, 509-519.

Kelly, S.G., 1996: Schaum's outline of theory and problems of mechanical vibrations. McGraw-Hill, New York.

Kerzenmacher, T., Gardiner, B., 1998: A mathematical model to describe the dynamic response of a spruce tree to the wind. Trees 12, 385-394.

Mayer, H., Schindler, D., Holst, J., Redepenning, D., Fernbach, G., 2008: The forest meteorologyical experimental site Hartheim of the Meteorological Institute, Albert-Ludwigs-University of Freiburg. Ber. Meteor. Inst. Univ. Freiburg Nr. 17, 17-38.

Nash, W.A., 1998: Schaum's outline of strength of materials. McGraw-Hill, New York.

Petersen, C., 2000: Dynamik der Baukonstruktionen. Vieweg, Braunschweig.

Schindler, D., 2008: Responses of Scots pine trees to dynamic wind loading. Agric. For. Meteorol. 148, 1733-1742.

Authors' address:

Hannes Fugmann (hannfug@web.de)
Dr. Dirk Schindler (dirk.schindler@meteo.uni-freiburg.de)
Prof. Dr. Helmut Mayer (helmut.mayer@meteo.uni-freiburg.de)
Meteorological Institute, Albert-Ludwigs-University of Freiburg
Werthmannstrasse 10, D-79085 Freiburg, Germany

Expansion of heavily damaged windthrow areas through tree mortality in surrounding areas

Kajar Köster, Kalev Jõgiste, Floor Vodde, Marek Metslaid

Institute of Forestry and Rural Engineering, Estonian University of Life Sciences, Estonia

Abstract

When a forest with certain stand characteristics gets hit by a storm, part of the stands is entirely windthrown, some of them partly and some remain undamaged. The division between these categories depends on storm and stand characteristics. The remaining trees either 1) continue as living healthy trees, 2) are damaged but recover, 3) die and fall down later on either because they were initially damaged at the storm event or because they suffer from post-storm effects. We used sequential surface photography, aerial photos and photo-derived data to evaluate tree mortality in a windthrow area in eastern Estonia, where a storm occurred in 2001. The study is based on aerial photos from different years and on photographs taken annually of the edge of three completely destroyed areas with total canopy destruction in which no salvage-logging took place and wind-felled trees were left after disturbance as they were. In total, 137 spruce trees (*Picea abies* (L.) Karst.) along the forest edge were observed over a seven-year period. A transition matrix model was used to examine tree mortality dynamics and patterns. At the end of the seven-year period, only 10% of the spruce trees survived in areas surrounding the windthrow. The mortality was highest in the second year after disturbance and the probability of a tree falling (both dead trees and living trees) was high over the entire study period. According to local observations, *Ips typographus* caused most of the tree deaths, but as the insect outbreak alone cannot explain the large proportion of falling trees in the area, co-influences of other factors were also important.

1. Introduction

Disturbances exert strong control over the species composition and structure of forests. Among different natural disturbance factors wind damage is playing an active role in the successional cycle of forests (Bouget and Duelli, 2004). Wind disturbances can have short- and long term effects, on the secondary succession of vegetation, canopy closure, and dead wood decay (Bouget and Duelli, 2004). Extreme wind can damage trees by uprooting them, snapping their trunks, or causing bending to occur, resulting in blowdown of canopy trees (Brassard and Chen, 2006). Wind-felled Norway spruce (*Picea abies*, L.) offers breeding ground for a wide range of insects and pests (Eriksson *et al.*, 2005), which in case of more severe windstorms may lead to a population outbreak and subsequent attacks on living spruce trees (Schroeder, 2001). It is well known that large-scale outbreaks of the spruce bark beetle (*Ips typographus* L.) will develop when large numbers of fallen spruce trees are left in the forest after storm or other disturbances (Peltonen, 1999; Göthlin et al., 2000; Nageleisen, 2001; Hedgren et al., 2003; Meier et al., 2003; Okland and Berryman, 2004). Generally *I. typographus* prefers to reproduce in wind-felled or otherwise damaged trees, but in some situations it is also able to damage and kill living trees in large numbers (Schroeder, 2001). Retention of wind-felled trees may increase the risk of consequential tree mortality (Duelli and Obrist 1999, Wichmann and Ravn 2001, Eriksson *et al*. 2007). The fear for insect outbreaks and fire makes the majority of forest managers choose for salvage logging.

Therefore, little is known about what will happen with damaged areas if they are left untouched. One observation has been that the damaged areas start to expand (Rizzo et al. 2000, Worrall and Harrington 2005). This study intends to investigate the dynamics and turnover of spruce trees along the edge of recently wind-damaged areas.

2. Material and methods

The areas for the assessment of tree mortality were located in the former Tudu Forest District (59º11′ N 26º52′ E) in Eastern Estonia, which experienced severe windthrow on 16 July 2001. Norway spruce is the dominant species, with lesser amounts of European aspen (*Populus tremula* L.), silver birch (*Betula pendula* Roth.) and downy birch (*Betula pubescens* Ehrh.). The study areas include stands on Eutric Gleysols and Calcaric Cambisols (FAO *et al.*, 1998; Reintam *et al.*, 2001), *Filipendula* and *Myrtillus* forest site types (Lõhmus, 1984) being most commonly represented. Formerly the forests were under protection (landscape preserve), meaning that they have been unmanaged for decades. The stand ages ranged from 110 to 160 years.

For studying the tree mortality after windthrow**,** photographs were taken from three completely damaged areas with total canopy destruction. A Nikon D50 digital single-lens reflex camera with 6.1 million pixel elements was used to capture the images. The camera location and photo point remained the same, as we used permanent markers for that purpose. The first picture was taken at the end of January in the winter of 2002, six months after disturbance. This photo image is regarded as the initial stage of measurements. Local observations were carried out to visually determine the causes of mortality. In the first picture, we numbered every spruce that we could distinguish on the image and later verified what changes took place in subsequent years. Multiple observers worked with the first picture until all of them got the same tree count. We placed each tree into one of four classes in every year: living tree - tree shape and crown not damaged; standing dead tree - with no needles detected; damaged tree - at least 25% decrease in crown density; fallen tree - disappeared from picture. In total 137 spruce trees were observed during the seven-year period. We used a transition matrix to determine the probabilities with which trees in different classes moved to another class. This matrix was then of the form:

$$A=\begin{pmatrix} p_{11} & p_{12} & p_{13} & \cdots & p_{1n} \\ p_{21} & p_{22} & p_{23} & \cdots & p_{2n} \\ p_{31} & p_{32} & p_{33} & \cdots & p_{3n} \\ \cdots & \cdots & \cdots & \cdots & \cdots \\ pn_1 & pn_2 & pn_3 & \cdots & pnn \end{pmatrix}$$

where p_{1n} was the probability of transition to class 1 from n time intervals.

Multiplication of this matrix, A, by a column vector $x_{(t)}$ that describes the tree state class at time t, gives the tree state class at time $t + 1$.

3. Results and discussion

During a seven year period, approximately 10% of the spruces survived in areas surrounding the windthrow. The largest number of damaged/suffering trees (more than 22% on average) was found in the second year after disturbance (Table 1). The transition probability matrix (Table 1) demonstrated that most of the damaged trees died during the second year after disturbance, but some recovered.

Table 1: Transition probability matrices: the columns represent transitions from each class initially at time *t*, while the rows represent transitions to each class one time interval later (*t*+1); class group codes are: 1 - living tree; 2 - damaged tree; 3 - fallen tree; 4 - standing dead tree

		1	2	3	4
Number of trees in 2002		105	5	0	27
2002-2003	*p<0.0001*				
	1	0,277	0,000	0,000	0,000
	2	0,204	0,015	0,000	0,000
	3	0,044	0,000	0,000	0,036
	4	0,241	0,022	0,000	0,161
2003-2004	*p<0.0001*				
	1	0,248	0,036	0,000	0,000
	2	0,015	0,058	0,000	0,000
	3	0,000	0,007	0,073	0,007
	4	0,015	0,117	0,000	0,372
2004-2005	*p<0.0001*				
	1	0,219	0,036	0,000	0,000
	2	0,036	0,022	0,000	0,000
	3	0,015	0,007	0,131	0,124
	4	0,015	0,007	0,000	0,387
2005-2006	*p<0.0001*				
	1	0,219	0,036	0,000	0,000
	2	0,007	0,015	0,000	0,000
	3	0,007	0,000	0,277	0,073
	4	0,022	0,007	0,000	0,336
2007-2008	p<0.001				
	1	0,109	0,000	0,000	0,000
	2	0,000	0,000	0,000	0,000
	3	0,109	0,022	0,467	0,088
	4	0,036	0,007	0,000	0,161

Note: Differences between matrices were tested by chi-square (χ^2) test

The most rapid change in the number of living trees took place during the second year after disturbance, but a remarkably high recovery of damaged trees was observed every year. The number of standing dead trees increased till the third year after disturbance, later the number decreased as these trees started to fall down. Table 1 shows that the probability of a standing dead tree falling down was greatest at the end of the fourth year, but in general a considerable number of standing dead trees fell each year. The early falling of standing dead trees implies to the co-influence of various disturbance

types. It usually takes some decades for standing dead trees to fall because of decomposition (Storaunet and Rolstad, 2002; Storaunet, 2004; Storaunet and Rolstad, 2004), mainly because of drying out after death (Krankina and Harmon, 1995). The root systems of living spruces were probably damaged by storms or fungi, thus weakening the trees. In that case bark beetles killed the trees and these standing dead spruces fell so early because of their damaged root system.

4. Conclusions

At the end of the seven-year period, only 10% of the spruce trees survived in areas surrounding the windthrow. The mortality was highest in the second year after disturbance and the probability of a tree falling (both dead trees and living trees) was high over the entire study period. According to local observations, *Ips typographus* caused most of the tree deaths, but as the insect outbreak alone cannot explain the large proportion of falling trees in the area, co-influences of other factors were also important. Probably root rot in combination with bark beetle may be responsible for the early collapse of standing dead wood).

Acknowledgements

This study was supported by a grant from the Estonian Environmental Investment Fund, the Estonian Ministry of Education and Science grant SF0170014s08 and by the Estonian Science Foundation grant 6087.

References

Bouget, C., Duelli, P., 2004: The effects of windthrow on forest insect communities: a literature review. Biological Conservation 118, 281-299.

Brassard, B.W., Chen, H.Y.H., 2006: Stand Structural Dynamics of North American Boreal Forests. Critical Reviews in Plant Sciences 25, 115-137.

Eriksson, M., Pouttu, A., Roininen, H., 2005: The influence of windthrow area and timber characteristics on colonization of wind-felled spruces by *Ips typographus* (L.). Forest Ecology and Management 216, 105-116.

FAO, ISSS, ISRIC, 1998: World reference base for soil resources. World Soil Resources Rep. 84.

Göthlin, E., Schroeder, L.M., Lindelöw, A., 2000: Attacks by *Ips typographus* and *Pityogenes chalcographus* on windthrown spruces (*Picea abies*) during the two years following a storm felling. Scand. J. For. Res. 15(5), 542-549.

Hedgren, P.O., Schroeder, L.M., Weslien, J., 2003: Tree killing by *Ips typographus* (Cleoptera: Scolytidae) at stand edges with and without colonized felled spruce trees. Agricultural and Forest Entomology 5(1), 67-74.

Krankina, O.N., Harmon, M.E., 1995: Dynamics of the dead wood carbon pool in northwestern Russian boreal forests. Water, Air and Soil Pollution 82, 227-238.

Lõhmus, E., 1984: Eesti metsakasvukohatüübid (Estonian forest site types) ENSV ATK IJV, Tallinn (in Estonian).

Meier, F., Gall, R., Forster, B., 2003: Ursachen und Verlauf der Buchdrucker-Epidemien (*Ips typographus* L.) in der Schweiz von 1984 bis 1999. Schweizerische Zeitschrift für Forstwesen 154, 437-441.

Nageleisen, L.-M., 2001: Monitoring of bark and wood-boring beetles in France after the December 1999 storms. Integrated Pest Management Reviews 6, 159-162.

Okland, B., Berryman, A., 2004: Resource dynamic plays a key role in regional fluctuations of the spruce bark beetles *Ips typographus*. Agricultural and Forest Entomology 6, 141-146.

Peltonen, M., 1999: Windthrows and dead-standing trees as bark beetle breeding material at forest-clearcut edge. Scand. J. For. Res. 14, 505-511.

Reintam, L., Rooma, I., Kull, A., 2001: Map of soil vulnerability and degradation in Estonia. In: Stott, D.E., Mohtar, R.H., Steinhard, G.C. (Ed.), Sustaining the Global Farm. 10th International Soil Conservation Organization Meeting, USDA-ARS NSERL, May 24-29, 1999, Purdue University, 1068-1074.

Rizzo, D.M., Slaughter, G.W., Parmeter, J.R. Jr., 2000: Enlargement of canopy gaps associated with a fungal pathogen in Yosemite Valley, California. Canadian Journal of Forest Research 30, 1501-1510.

Schroeder, L.M., 2001: Tree mortality by the bark beetle *Ips typographus* (L.) in storm-disturbed stands. Integrated Pest Management Reviews 6, 169-175.

Storaunet, K.O., 2004: Models to Predict Time Since Death of *Picea abies* Snags. Scand. J. For. Res. 19, 250-260.

Storaunet, K.O., Rolstad, J., 2002: Time since death and fall of Norway spruce lgs in old-growth and selectively cut boreal forest. Can. J. For. Res. 32, 1801-1812.

Storaunet, K.O., Rolstad, J., 2004: How long do Norway spruce snags stand? Evaluating four estimation methods. Can. J. For. Res. 34, 376-383.

Worrall, J.J., Lee, T.D., T.C. Harrington, T.C., 2005: Forest dynamics and agents that initiate and expand canopy gaps in Picea-Abies forests of Crawford Notch, New Hampshire, USA. Journal of Ecology 93, 178-190.

Authors' address:

Dr. Kajar Köster (kajar.koster@emu.ee)
Prof. Dr. Kalev Jõgiste (kalev.jogiste@emu.ee)
MSc. Floor Vodde (floorvodde@hotmail.com)
Dr. Marek Metslaid (marek.metslaid@emu.ee)
Institute of Forestry and Rural Engineering, Estonian University of Life Sciences
Kreutzwaldi 5, Tartu 51014, Estonia

Windstorm damage in coniferous forests in Galicia (NW Spain) under different thinning treatments

Eva P. Roca Posada, Juan G. Álvarez González, Alberto Rojo Alboreca

Unidade de Xestión Forestal Sostible (UXFS), Universidade de Santiago de Compostela, Lugo, Spain

Abstract

Extra tropical cyclone Klaus hit southern France and northern Spain on January 23th and 24th 2009, causing severe damage to forests in its path. The extreme gust wind speeds reached up to 198 km/h in Galicia (NW Spain), the most productive forestry region of Spain. In this area, the wind destroyed about 1.2 million cubic meters of wood, approximately 25% of the region annual harvest. The storm also affected the thinning trials established by the Sustainable Forest Management Unit (UXFS) for the four major commercial conifers in Galicia (*Pinus radiata* D. Don, *Pinus pinaster* Ait., *Pinus sylvestris* L. and *Pseudotsuga menziesii* Mirb. Franco).

To assess the susceptibility of forests to wind damage, as affected by the stand and tree characteristics and management, becomes extremely important to face the predicted increase on the frequency of extreme weather events under climate change. This study evaluates the damage produced on each of those trials and the causes of the differences among them and compares the effect of the different treatments carried out in the plots (heavy thinning from below, light thinning from below, mixed thinning with crop tree designation and control without thinning) on the occurrence of wind damage during storms. The data collected is analyzed to determine the tree characteristics (diameter at breast height, crown size, total height, slenderness ratio and Hart-Becking index) more relevant to windthrow susceptibility.

1. Introduction

Wind damage to trees is considered as a major problem in managed forests, where it can result in huge economic losses because of the reduction in the yield of recoverable timber, the increased costs of unscheduled operations and the resulting problems in forestry planning. In addition, broken and uprooted trees left in forests can lead to detrimental insect attacks on the remaining plants (Schroeder and Eidmann, 1993). In Europe, the estimated average storm damage over the period 1950-200 is 18.7 million m^3 of wood (Schelhass *et al.*, 2003) and several projections suggest an increase in frequency and severity of extreme events under climate change (IPCC, 2007).

On January 2009 23th and 24th southern France and northern Spain were affected by a severe windstorm associated with extra-tropical depression Klaus. During passage, strong gust wind speeds of up to 198 km/h were measured in the Autonomous Community of Galicia, NW Spain (Meteogalicia, 2009). In this region, where forests occupy 68% of the surface and annual harvest accounts for almost 50% of the Spanish harvest, the estimated total area affected was 32502 ha. Approximately 1.2 million m^3 of timber was damaged, equivalent to about 25% of its total annual harvest. The most affected species were *Pinus radiata* D. Don, *Pinus sylvestris* L. and *Pinus pinaster* Ait.

The windstorm also affected some of the thinning trials belonging to the network established by the research group Sustainable Forest Management Unit (UXFS, its acronym in Galician) from the University of Santiago de Compostela. We used this event to study the relative influence of site, stand and tree factors on wind damage.

The scope of this study is to obtain an evaluation of the susceptibility to windthrow, in relation to site attributes, stand conditions and tree characteristics, that leads to a more profound understanding of the processes and patterns of damage, in order to aid to the development of silvicultural strategies to minimize the risk of wind damage (Gardiner and Quine, 2000; Peltola *et al*., 2000a).

2. Material and methods

Data used

In 2003 the UXFS began the installation of thinning trials sites for the main commercial conifers in Galicia. Nowadays, there are six trial sites installed throughout the region: two in a *Pinus radiata* plantations (both situated on the same stand but originated from two different seed sources: New Zealand and Galicia), two in naturally regenerated stands of *Pinus pinaster* (one for the coastal ecoregion of the species and another one for the interior ecoregion), one in a *Pinus sylvestris* plantation, and the latest in a *Pseudotsuga menziesii* (Mirb.) Franco plantation. Each test site consists on a variable number of plots (depending on the availability of land with homogeneous characteristics) of different size depending on the initial stand density, where three or four thinning treatments (differing in type and intensity of thinning) have been tested:

- No thinning (N): control plot, there is no extraction of trees except the extraction of the dry and dying individuals, recorded as natural mortality.
- Light thinning from below (L): 75-90% of the control plot basal area remaining. It focuses on extracting the lower diameter classes but, occasionally, it can affect thicker trees if attacked by insects or diseases or if they are dying, forked or twisted.
- Heavy thinning from below (H): 60-80% of the control plot basal area remaining. It affects the thinner trees, some codominant trees and, sometimes, dominant trees if they have any of the characteristics aforementioned.
- Mixed thinning with crop tree designation (C): 70-80% of the control plot basal area remaining. Trees belonging to all the sociological classes are extracted to benefit the selected crop trees, leaving those individuals that do not compete directly with them.

The data used in this study was obtained from the periodical inventories of the five thinning trials located in the Lugo province (see Table 1). Data from the coastal *Pinus pinaster* trial (province of Ourense) was not used because its climatic conditions vary greatly from the rest of the stands, due to its distant geographical position. In each plot, all trees are labelled with a number and the following variables are measured in each inventory: two measurements of diameter at breast height (*DBH*) to the nearest 0.1 cm, with callipers; total height (*H*) and crown base height (*CBH*) to the nearest 0.1 m with a digital hypsometer, in a representative sample of trees distributed in proportion to number of trees per diameter class (in the latest plots established all heights are measured); two cross measurements of the crown diameter (D_c), on the same sample in which the heights were measured; and the height of the thicker 100 trees per hectare within each plot in order to calculate the dominant diameter (D_0) and height (H_0). Descriptive variables were also recorded for each tree (i.e. if they were dying, forked, leaning, etc.). For the trees whose *H*, *CBH* and D_c were not measured, equations were adjusted for each site using the data available from all the previous inventories. Further tree variables cal-

culated from the inventory data for each tree tallied were: length of living crown (L_c), crown ratio (R_c, defined as the *CBH:H* ratio) and crown volume (V_c, assuming a conical shape of the crown). Individual tree data from 7072 trees were used in this study.

The stand variables calculated for each inventory were: stand age (T), stand basal area (BA), number of trees per hectare (N), mean height (H_m), mean and dominant slenderness coefficient (SC_m and SC_0 respectively, defined as the *H:DBH* ratio) and the Hart-Becking spacing Index (HI, the ratio between the average distance between trees and H_0). Only alive trees were included in the calculations. In addition, data on the number of trees per hectare and stand basal area removed in thinning operations were available (N_{int} and BA_{int} respectively), as well as the elapsed time since the treatment (t_t). The mean values of these variables are shown in Table 1.

After the storm an additional inventory to monitor the damage caused by wind was carried out in all plots. The number of trees damaged and the type of damage (snapped or uprooted) were recorded (see Table 1).

No climate data could be introduced into the model because there was no available information of the precise meteorological conditions within the plots during the storm. However, all the stands are located in a reduced area in which it is very likely that the general wind conditions were quite homogeneous.

Table 1: Summary of the main characteristics of the thinning trials established by UXFS in Lugo province (Galicia, NW Spain)

Site	**BegonteG**[1]				**BegonteNZ**[1]				**Bacurín**[1]			**Corgo**				**Becerreá**			
species	*Pinus radiata* (Galicia)				*Pinus radiata* (NZ)				*Pseudotsuga menziesii*			*Pinus pinaster* (interior)				*Pinus sylvestris*			
no. plots	12				12				8			4				4			
plots size (m)	30x30				30x30				30x30			50x50				46x46[2]			
thinning date	April 2004				April 2004				February 2007			March 2008				March 2008			
inventory date	December 2007				November 2007				November 2006			December 2007				January 2008			
age (yr)	17				17				19			24				36			
altitude (m)	455				457				482			560				1090			
aspect (º)	214				175				191			157.5				118			
slope (%)	3.1				6.7				5.0			8.0				18.0			
treatments	N	L	H	C	N	L	H	C	N	L	C	N	L	H	C	N	L	H	C
N_{int} **(%)**	0.79	24.1	20.3	23.8	1.05	29.5	47.2	34.7	1.01	29.4	15.8	3.87	48.2	57.8	47.7	0	15.5	33.6	14.0
BA_{int} **(%)**	0.72	11.1	41.8	20.0	0.5	11.7	26.3	27.6	0.81	21.9	19.8	0.26	21.3	47.5	22.7	0	14.2	28.7	13.6
N	1524	1174	974	1085	1471	1084	871	1024	1089	169	926	1726	1118	824	1203	770	938	604	911
BA	32.9	29.9	19.5	27.7	34.7	35.2	32.5	30.0	36.0	28.5	26.9	60.9	38.7	32.0	46.7	39.6	43.7	32.3	41.0
D_g	16.6	18.1	19.5	18.1	17.3	20.4	21.8	19.3	20.5	21.7	19.2	21.2	21.0	22.2	22.3	25.6	24.4	26.1	23.9
D_0	28.5	27.6	28.5	27.3	28.4	31.3	30.3	31.0	26.7	26.1	26.7	30.8	29.0	27.5	31.5	32.9	32.1	32.2	32.3
H_m	15.4	16.6	16.5	17.5	16.1	18.0	19.1	17.9	13.6	14.0	13.0	14.7	17.1	15.1	16.1	13.3	14.1	14.3	13.8
H_0	19.2	19.7	18.7	18.2	19.8	20.9	21.3	21.4	14.9	15.0	14.9	16.7	18.8	15.8	17.7	14.0	15.1	15.6	14.7
SC_m	0.9	0.91	0.82	0.85	0.91	0.86	0.88	0.91	0.68	0.65	0.70	0.74	0.83	0.69	0.76	0.53	0.59	0.56	0.59
SC_{100}	0.67	0.72	0.66	0.70	0.70	0.67	0.70	0.69	0.59	0.56	0.56	0.54	0.65	0.58	0.56	0.43	0.48	0.47	0.47
HI	13.4	14.9	17.2	16.7	13.2	14.6	15.9	14.6	20.3	24.1	22.0	14.4	15.9	22.1	16.3	25.7	21.6	26.1	22.5
$N_{damaged}$ **(%)**	0.24	0.64	0.38	3.44	0.76	1.03	0.43	0.72	0	0	0	11.1	18.4	10.6	15.4	11.1	4.28	8.99	6.02
$N_{uprooted}$ (%)	*30.7*	*0*	*30.5*	*21.2*	*35.6*	*34.5*	*33.2*	*17.6*	*0*	*0*	*0*	*4.5*	*0*	*12.5*	*2.4*	*0*	*0*	*0*	*23.1*
$N_{snapped}$ (%)	*0*	*37.3*	*0*	*47.9*	*33.3*	*36.6*	*0*	*17.6*	*0*	*0*	*0*	*95.5*	*100*	*87.5*	*97.6*	*100*	*100*	*100*	*76.9*
$BA_{damaged}$ **(%)**	0.08	0.5	0.3	5.6	0.57	1.7	0.47	0.9	0	0	0	12.2	18.3	9.79	13.3	8.61	2.57	6.25	5.72
$N_{uprooted}$ (%)	*30.7*	*0*	*30.5*	*16.2*	*35.6*	*34.5*	*33.2*	*4.8*	*0*	*0*	*0*	*5.4*	*0*	*11.5*	*3.2*	*0*	*0*	*0*	*14.7*
$N_{snapped}$ (%)	*0*	*37.3*	*0*	*52.9*	*33.3*	*36.6*	*0*	*30.3*	*0*	*0*	*0*	*94.6*	*100*	*88.5*	*96.8*	*100*	*100*	*100*	*85.3*

__N__: no thinning (control plots), __L__: light thinning from below, __H__: heavy thinning from below, __C__: mixed thinning with tree crop selection. (1) These trials include several repetitions of each treatment, data shown are the mean values (2) Plot size is uneven, size shown is the average plot size.

Statistical methods

Tree, stand and site characteristics were used as independent variables to model the probability that an arbitrary tree is undamaged by wind (p_0):

$$p_0 = \frac{\exp(\alpha_0 + \alpha_1 \cdot x_1 + \alpha_2 \cdot x_2 + ... + \alpha_n \cdot x_n)}{1 + \exp(\alpha_0 + \alpha_1 \cdot x_1 + \alpha_2 \cdot x_2 + ... + \alpha_n \cdot x_n)} \quad (1)$$

where $x_1, x_2, ..., x_n$ are the independent variables (see Table 2) and $\alpha_o, \alpha_{1,...,} \alpha_n$ are the parameters.The following model for the logit was fitted to the data using logistic regression:

$$\text{logit } (p_0) = \ln\left(\frac{p_0}{1 - p_0}\right) = \alpha_0 + \alpha_1 \cdot x_1 + \alpha_2 \cdot x_2 + ... + \alpha_n \cdot x_n \quad (2)$$

The same logistic analysis technique was used to asses the probability of an arbitrary tree being snapped or uprooted for the class of damaged plots (*dam*=1). Only tree characteristics were used to model the probability of these trees being uprooted (p_u):

$$p_u = \frac{\exp(\beta_0 + \beta_1 \cdot x_1 + \beta_2 \cdot x_2 + ... + \beta_n \cdot x_n)}{1 + \exp(\beta_0 + \beta_1 \cdot x_1 + \beta_2 \cdot x_2 + ... + \beta_n \cdot x_n)} \quad (3)$$

$$\text{logit } (p_u) = \ln\left(\frac{p_s}{1 - p_s}\right) = \beta_0 + \beta_1 \cdot x_1 + \beta_2 \cdot x_2 + ... + \beta_n \cdot x_n \quad (4)$$

where $\beta_0, \beta_1, ..., \beta_n$ are the estimated parameters.

For both models, the selection of site, stand and site variables was guided by the stepwise option within the logistic regression procedure in SAS (SAS Institute, 1990).

Table 2: Site, stand and tree variables used in the model

site variables	stand variables		tree variables	
altitude (m)	T (yr)	H_0 (m)	DBH (cm)	D_c (m)
mean slope (%)	t_t (months)	SC_m (m/cm)	H (m)	V_c (m^3)
aspect (º)	N (trees/ha)	SC_0 (m/cm)	SC (m/cm)	L_c (m)
	BA (m^2/ha)	HI (%)	CBH (m)	R_c
	D_g (cm)	BA_{int} (%)	bifurcation presence (0/1)	
	H_m (m)	N_{int} (%)	damage (0=undamaged/1=damaged)	
	D_0 (cm)		type of damage (0=uprooted/1=snapped)	

3. Results and discussion

3.1 Damage

The regression model for the probability of no damage (p_0) included three predictive variables: t_t, H_m and R_c. None of the site characteristics was included in the model, unlike the results obtained by several authors (e.g. Mayer *et al.*, 2005; Evans *et al.*, 2007). The probability assessment model given by the logistic analysis was:

$$p_0 = \frac{\exp(5.2157 + 0.0579 \cdot t_t - 0.3132 \cdot H_m + 3.3667 \cdot R_c)}{1 + \exp(5.2157 + 0.0579 \cdot t_{t)} - 0.3132 \cdot H_m + 3.3667 \cdot R_c)} \quad (5)$$

The model correctly classified 79.8% of the analyzed trees and the chi-square given by Hosmer and Lemeshow goodness-of fit-test was 78.70 (p=0.0005).

As expected in view of previous studies (Cremer *et al.*, 1982; Achim *et al.*, 2005), the risk of damage increases immediately after thinning, due to the drop of the collective stability as a consequence of a higher exposure to wind. But thinning also increases the availability of site resources and enables residual trees to rapidly increase in size and to adjust the allocation of stem, crown and roots growth to the parts where mechanical stresses are greater (Mitchell, 2000; Ruel *et al.*, 2003; Roberts *et al.*, 2007), thus greatly reducing the risk of damage over the time. The logical positive correlation between the mean height of the stand and the probability of damage has also been noted in many studies (e.g. Cremer *et al.*, 1982; Mayer *et al.*, 2005). Neither the present density nor the basal area of the stand were correlated with the probability of damage.

An unexpected finding is the lack of significance of the stand variables SC_m and SC_{100} that are typically used to asses the stability of stands (e.g. Cremer *et al.*, 1982; Becquey and Riou-Nivert, 1987).

According to the fitted model, the only tree characteristic that influences the risk of damage is R_c. This result contradicts several studies in which other tree variables are usually found to be significantly related to storm damage: *DBH* (Peltola *et al.*, 2000b; Nagel and Diaci, 2006), *H* (Gardiner *et al.*, 2000; Cucchi and Bert 2003; Ancelin *et al.*, 2004) and *SC* (Petty and Swain, 1995; Valinger and Fridman, 1997 and 1999; Achim *et al.*, 2005; Roberts *et al.*, 2007). In our model, mean stand height was more predictive than individual tree height, whereas diameter does not directly influence the probability of damage. However, crown length (and thus R_c) is related to *DBH*, so this variable may be including the effect of *DBH* on the risk of windthrow.

Probability of windthrow is lower for trees with a high proportion of living crown. Although trees with larger crowns will experience higher wind loads than small crowned trees, due to the higher surface area of the crown exposed to wind forces (Telewski, 1995), several studies have found that damaged trees had significantly smaller crowns than undamaged trees (Cucchi and Bert, 2003; Ancelin *et al.* 2004). A plausible explanation is that a large deep crown results in a lower centre of gravity of the tree, so that the turning moment produced by the crown weight for any given crown displacement will be smaller than it would be in a tree with a higher centre of gravity (Dunham and Cameron, 2000). Finally, large crowns may also be a reflection of adaptive growth to develop resistance to predominant winds and may be related with growth adaptation within the root system.

3.2 Type of damage

The predictor variables for the type of damage were *DBH*, *H* and L_c. The model obtained for the probability of uprooting (p_u) was:

$$p_u = \frac{\exp(0.825 \cdot DBH + 0.822 \cdot H + 2.234 \cdot L_c)}{1 + \exp(0.825 \cdot DBH + 0.822 \cdot H + 2.234 \cdot L_c)} \quad (6)$$

The model correctly classified 81.9% of the trees and the chi-square value of the Hosmer and Lemeshow test was 9.3778 (p=0.3118).

At the view of the results, thicker and taller trees are more prone to be overturned than to be snapped, and longer crowns also predispose trees to uprooting rather than snapping. This last finding agrees with the results obtained by Peltola *et al.* (1997) and Ancelin *et al.* (2004), whereas Dunham and Cameron (2000) did not found differences between crown sizes for the damage type. Uprooted trees have also been reported to be shorter than snapped trees by Putz *et al.* (1983). On the other hand, larger trees have been found to be more likely to snap than to uproot by Putz *et al.* (1983) and Nagel and Diaci (2006).

It is important to note that the strenth of the root anchorage and the wood propierties have a great infuence in the type of damage occurring in a wind storm (e.g. Coutts, 1983; Putz *et al.*, 1983; Peltola *et al.*, 2000a), so a more complete evaluation of the type of damage should include root system characteristics and mechanichal wood propierties that were not available for this study.

4. Conclusions

The model developed was able to predict affected versus unaffected stands with 80% accuracy and the type of damage with 82% accuracy. The most predictive variables to determine the storm impact were stand and tree variables. Particularly significant is the effect of the crown length (both absolute and relative) for the stability of trees. The results suggest that the usefulness of slender coefficients (H:DBH ratios) in determining trees vulnerability to wind damage may be in some cases overestimated, due to the lack of correlation between this parameter and the probability of windthrow found in this study. All these results must be considered as partial and must be taken cautiously, since currently only the first thinning intervention has been carried out in each site.

References

Achim, A., Ruel, J.-C., Gardiner, B.A., 2005: Evaluating the effect of precommerical thinning on the resistance of balsam fir to windthrow through experimentation, modelling and development of simple indices. Can. J. For. Res. 35, 1844-1853.

Ancelin, P., Courbaud, B, Fourcaud, T., 2004: Development of an individual tree-based mechanical model to predict wind damage within forest stands. For. Ecol. Manage. 203, 101-121.

SAS Institute, I., 2004: SAS/STAT™ User's Guide 9.1. Cary, NC.: SAS Institute Inc.

Becquey, J., Riou_nivert, P., 1987: L'existence de "zones d'estabilité" des peuplements, consequences sur la géstion. Rev. For. Fr. 39, 323-334. (in French).

Coutts, M.P., 1983: Root architecture and tree stability. Plant Soil 71, 171-188.

Cucchi, V., Bert, D., 2003: Wind-firmness in *Pinus pinaster* ait. Stands in Southwest France, influence of stand density, fertilisation and breeding in two experimental stand damaged during the 1999 storm. Ann. For. Sci. 60, 209-226.

Cremer, K.W., Borough, C.J., McKinnell, F,H., Carter, P.R., 1982: Effects of stocking and thinning on wind damage in plantations. NZ J. For. Sci. 12, 244-266.

Dunham, R.A., Cameron, A.D., 2000: Crown, stem and wood properties of wind-damaged and undamaged Sitka spruce. For. Ecol. Manage. 135, 73-81.

Evans, A.M., Camp, A.E., Tyrrell, M.L., Riely, C.C., 2007: Biotic and abiotic influences on wind disturbance in forests of NW Pennsylvania, USA. For. Ecol. Manage. 254, 44-53.

Gardiner, B.A., Peltola, H., Kellomaki, S., 2000: Comparison of two models for predicting the critical wind speeds required to damage coniferous trees. Ecol. Model. 129, 1-23.

Gardiner, B.A., Quine, C.P., 2000: Management of forests to reduce the risk of abiotic damage - a review with particular reference to the effects of strong winds. For. Ecol. Manage. 135, 261-277.

IPCC, 2007: Climate Change 2007: Synthesis Report. Contribution of Working Groups I, II and III to the Fourth Assessment.

Mayer, P., Brang, P., Dobbertin, M., Hallenbarter, D., Renaud, J.-P., Walther, L., Zimmermann, S., 2005: Forest storm damage is more frequent on acidic soils. Ann. For. Sci. 62, 303-311.

Meteogalicia, 2009: O fenómeno da cicloxénese explosiva, que afectou a Galicia o pasado venres, supero os rexitros históricos de refachos de vento na nosa comunidade. Informe de seguemento da cicloxénese explosiva 23/24 de xaneiro. Available at http://www.meteogalicia.es/pdfs/cicloxenese.pdf [retrieved 4th march 2009]. (in Galician).

Mitchell, S.J., 200: Stem growth responses in Douglas-fir and Stika spruce following thinning: implications for assessing wind-firmness. For. Ecol. Manage. 135, 105-114.

Nagel, T.A., Diaci, J., 2006: Intermediate wind disturbance in an old-growth beech-fir forest in southeastern Slovenia. Can. J. For. Res. 36, 629-638.

Peltola, H., Gardiner, B.A., Kellomäki, S., Kolström, T., Lässig, R, Moore, J., Quine, C, Ruel, J.-C., 2000a: wind and other abiotic risks to forests. For. Ecol. Manage. 135, 1-2.

Peltola, H., Kellomäki, S., Hassinen, A., Granander, M., 2000b: Mechanical stability of Scots pine, Norway spruce and birch: an analysis of tree-pulling experiments in Finland. For. Ecol. Manage. 135, 143-153.

Peltola, H., Nykänen, M.-L., Kellomäki, S., 1997: Model computations on the critical combination of snow loading and wind speed for snow damage of Scots pine, Norway spruce and Birch sp. at stand edge. For. Ecol. Manage. 95, 229-241.

Petty, J.A., Swain, C., 1985: Factors influencing stem breakage of conifers in high winds. Forestry 58, 75-84.

Putz, F. E., Phyllis, D. C., Lu, K, Montalvo, A., Aiello, A., 1983: Uprooting and snapping of trees: structural determinants and ecological consequences. Can. J. For. Res. 13, 1011-1020.

Roberts, S.D., Harrington, C.A., Buermeyer, K.R., 2007: Does variable-density thinning increase wind damage in conifer stands on the Olympic Peninsula? West. J. Appl. For. 22, 285-296.

Ruel, J.C., Larouche, C, Achim, A., 2003: Changes in root morphology after precommercial thinning in balsam fir stands. Can. J. For. Res. 33, 2452-2459.

Schelhaas, M.J., Nabuurs, G.J., Schuck, A., 2003: Natural disturbances in the European forests in the 19th and 20th centuries. Global Change Biol. 9, 1620-1633.

Schroeder, L.M., Eidmann, H.H. 1993: Attacks of bark and wood-boring Coleoptera on snow-broken conifers over a two-year period. Scandinavian Journal of Forest Research 8, 257-265.

Telewski, F.W., 1995: Wind-induced physiological and developmental responses in trees. In: Coutts, M.P. and Grace, J. (Eds.), Wind and Trees. Cambridge University Press, pp.237-263.

Valinger, E., Fridman, J., 1997: Modelling the probability o snow and wind damage in Scots Pine using tree characteristics. For. Ecol. Manage. 97, 215-222.

Valinger, E., Fridman, J., 1999: Models to assess the rislof snow and wind damage in Pine, Spruce, and Birch forests. Environmental Management 24, 209-217.

Authors' address:

Eva P. Roca Posado (eva.roca@usc.es)
Juan G. Álvarez González
Alberto Rojo Alboreca
Unidade de Xestión Forestal Sostible (UXFS), Departamento de Enxeñaría Agroforestal, Escola Politécnica Superior, Universidade de Santiago de Compostela
Campus Universitario s/n, 27002 Lugo, Spain

Inclusion of windthrow assessment in stand density management diagrams for even-aged stands

Marcos Barrio-Anta[1], Felipe Crecente-Campo[2], Pedro Álvarez-Alvarez[1], Fernando Castedo-Dorado[3]

[1]Department of Biology of Organisms and Systems, University of Oviedo, Spain
[2]Department of Agroforestry Engineering, University of Santiago de Compostela, Spain
[3]Department of Agricultural Engineering and Sciences, University of León, Spain

Abstract

A stand density management diagram (SDMD) for even-aged stands, which includes windthrow assessment as a specific management objective, is presented.

The average slenderness coefficient for the whole stand (defined as the ratio of average stand height to average stand diameter) was satisfactorily included in the SDMD for assessing the risk of windthrow. The slenderness coefficient isolines can be used to define general stability thresholds for species for which these values are quite well documented.

The methodology of superimposition on the diagram of the "zones of stability" primarily proposed by Becquey and Riou-Nivert (1987) for Norway spruce and silver fir stands in France is also shown. These zones of stability were applied to uniform conifer stands in temperate zones, and therefore complement the information given by the slenderness coefficient isolines.

The primary use of the diagram is to derive thinning schedules for even-aged stands by taking into account stand resistance to windthrow. However, it also allows rapid estimation of stand volume, stand biomass and carbon pools. This information can help silviculturists to make quick and easy comparisons among different thinning schedules in which both timber production and the risk of damage from wind are considered.

The model is of widespread potential use because the data required for the equations and diagrams are usually available from common timber inventories. In addition, it is relatively easy to develop alternative thinning schedules, and to compare these alternatives with economic and windthrow risk criteria, thereby facilitating management decisions.

1. Introduction

Wind damage to trees is considered as a major problem, particularly in managed forests, in which the damage can result in huge economic losses. Different types of modelling tools have been developed to help foresters estimate stand stability, i.e., the resistance of a stand to windthrow. Both mechanistic and empirical models have been used to evaluate the risk of damage. Mechanistic modelling applies the results of winching and wind tunnel studies to predict the critical wind speeds at which trees will fall. In empirical modelling, regression equations or indices are developed to relate windthrow incidence to site, stand, and/or tree attributes.

The simplest empirical stability indicator for single tree or stand dimensions is the slenderness coefficient (e.g., Oliveira, 1988; Wang et al., 1998; Wilson and Oliver, 2000; Hinze and Wessels, 2002), which is defined as the ratio of total height to diameter at breast height when both variables are measured in the same units. Several studies have shown that the value of the slenderness coefficient (SC) (considered as tree or stand index) is highly correlated to stem bending, windsnap and windthrow (Cremer et al.,

1982; Becquey and Riou-Nivert, 1987; Navratil, 1995; Wilson and Oliver, 2000; Wonn and O'Hara, 2001). Since the slenderness coefficient is primarily a function of spacing, it enables improvement of stand stability through density management (e.g., Wonn and O'Hara, 2001; Cameron, 2002).

Stand density management diagrams (SDMDs) are average stand-level models that graphically illustrate the relationships among yield, density and density-dependent mortality at all stages of stand development (Newton and Weetman, 1994). The use of SDMDs is one of the most effective methods for the design, display and evaluation of alternative density management regimes in even-aged stands. More specifically, SDMDs can be used to determine the initial spacing or thinning schedules required to achieve different management objectives.

The objective of the present study was to develop a methodology for construction of SDMDs, which enables consideration of the assessment of stand resistance to wind damage as a primary objective.

2. Construction of the basic SDMD

Structurally, SDMDs consist of a number of functional and empirical quantitative relationships that collectively represent the cumulative effect of various underlying competition processes on tree and stand yield variables. The SDMD proposed in the present study includes the relative spacing index (RS), the average stand slenderness coefficient and a system of two equations as basic components. In addition, dominant height is represented on the *x*-axis and the number of trees per hectare on the *y*-axis (the latter on a logarithmic scale), following the methods proposed by Barrio and Álvarez-González (2005).

The first step in the construction of the stand density diagram is to fit the non-linear system of the following two equations:

$$d_g = b_0 N^{b_1} H_0^{b_2} \tag{1}$$

$$V = b_3 d_g^{b_4} H_0^{b_5} N^{b_6} \tag{2}$$

where d_g = quadratic mean diameter, N = number of trees per hectare, H_0 = dominant height (defined as the mean height of the 100 thickest trees per hectare), and V = total stand volume.

The second step in the construction of the diagram involves representation of the isolines for the growing stock level (expressed by the RS) and for the stand variables included in the stand-level model (d_g and V). The isolines are obtained by solving for N in Eqs. (1)-(2) (see Barrio and Álvarez-González (2005) for more details).

3. Inclusion of the average stand slenderness coefficient in the SDMD

The most obvious way of calculating the stand slenderness coefficient is as the ratio between the average stand height and average stand diameter (e.g., Mitchell, 2000; Wonn and O'Hara, 2001; Hinze and Wessels, 2002), and this was therefore the definition used in this study for this coefficient.

The inclusion of the average stand SC in the SDMD is conditioned by the variables represented in the diagram (H_0, N, d_g, V). Therefore, the relationships between average stand height $(\overline{h})$ and average stand diameter $(\overline{d})$ and some of these stand variables must firstly be obtained. Accurate estimates of $\overline{h}$ and $\overline{d}$ can usually be obtained from H_0 and d_g, respectively, by simple linear relationships. For example, for radiata pine plantations in NW Spain, the following equations were obtained (Castedo-Dorado et al., 2009):

$$\overline{h} = -1.712 + 0.9574 H_0 \; ; \; R^2 = 0.968 \tag{3}$$

$$\overline{d} = -0.4155 + 0.9761 d_g \; ; \; R^2 = 0.998 \tag{4}$$

Therefore, in this example, we can express the stand slenderness coefficient as follows:

$$\mathrm{SC} = \frac{-1.712 + 0.9574 H_0}{-0.4155 + 0.9761 b_0 N^{b_1} H_0^{b_2}} \tag{5}$$

Representation of the isolines for slenderness coefficient involves solving Eq. (5) for N through a range of H_0 by setting SC constant:

$$N = \left(\frac{-1.712 + 0.9574 H_0 - (0.4155 \mathrm{SC})}{0.9761 b_0 H_0^{b_2} \mathrm{SC}} \right)^{1/b_1} \tag{6}$$

Fig. 1 shows the isolines corresponding to the 40-110 range of slenderness coefficient values superimposed on the SDMD for the case of radiata pine plantations. These isolines slope downwards from left to right, and are highly sensitive to stand density and dominant height. The expected size-density trajectories (i.e. the values of RS), the isolines for d_g and the isolines for V, were also included on the bivariate graph.

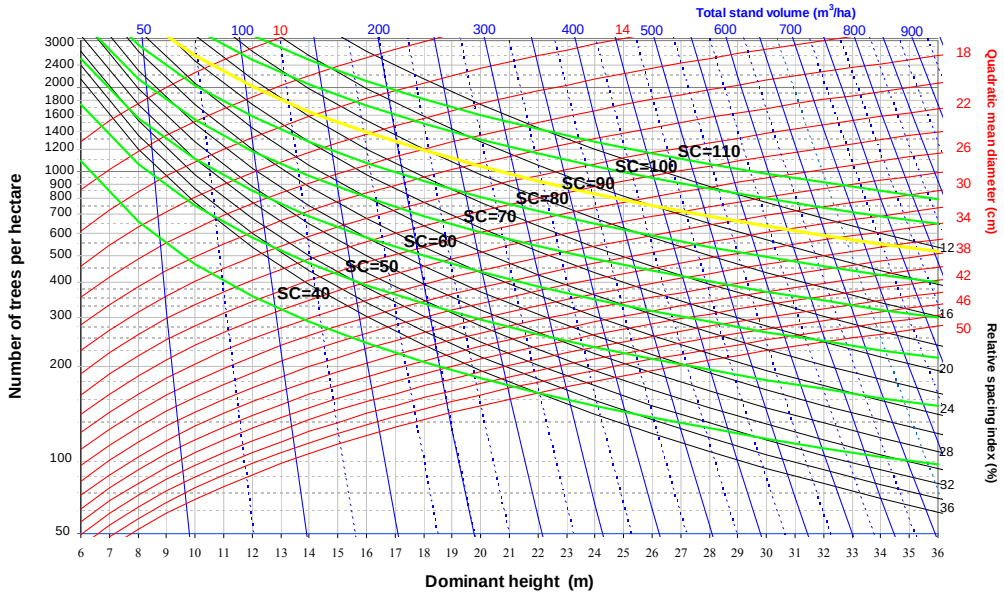

Fig. 1: SDMD for radiata pine stands including isolines for stand SC; the SC isoline of 90 considered as the stability thresholds for the species is highlighted in yellow

4. Inclusion of the "zones of stability" in the SDMD

The "zones of stability" primarily proposed by Becquey and Riou-Nivert (1987) for Norway spruce and silver fir stands in France can also be easily superimposed on the diagram. Becquey and Riou-Nivert (1987) used a plot of stand slenderness coefficient against stand dominant height to define three stability zones for stands (stable, not very stable and unstable) for observations made after a severe storm in 1982. The SC for inclusion in a stability zone decreased with greater tree heights: for stand heights between 20 and 30 m, unstable mean SC values were above 90; the mean SC value of stable stands was below 60 (Fig. 2).

Moreover, these stability zones are quite consistent with general stability thresholds for species for which these values are well documented (e.g. Cremer et al., 1982; Hinze and Wessels, 2002; Oliveira et al., 1988; Cucchi and Bert, 2003). In this way, the slenderness coefficient isolines of 90 and 75 considered as the stability thresholds for radiata pine and maritime pine, respectively, define quite adequately the limit between the stable and the intermediate zones of Becquey and Riou-Nivert (1987) (Fig. 2). The consistency of these results with findings of other authors suggests that general zones of stability exist for uniform conifer stands in temperate zones (Mitchell, 2000).

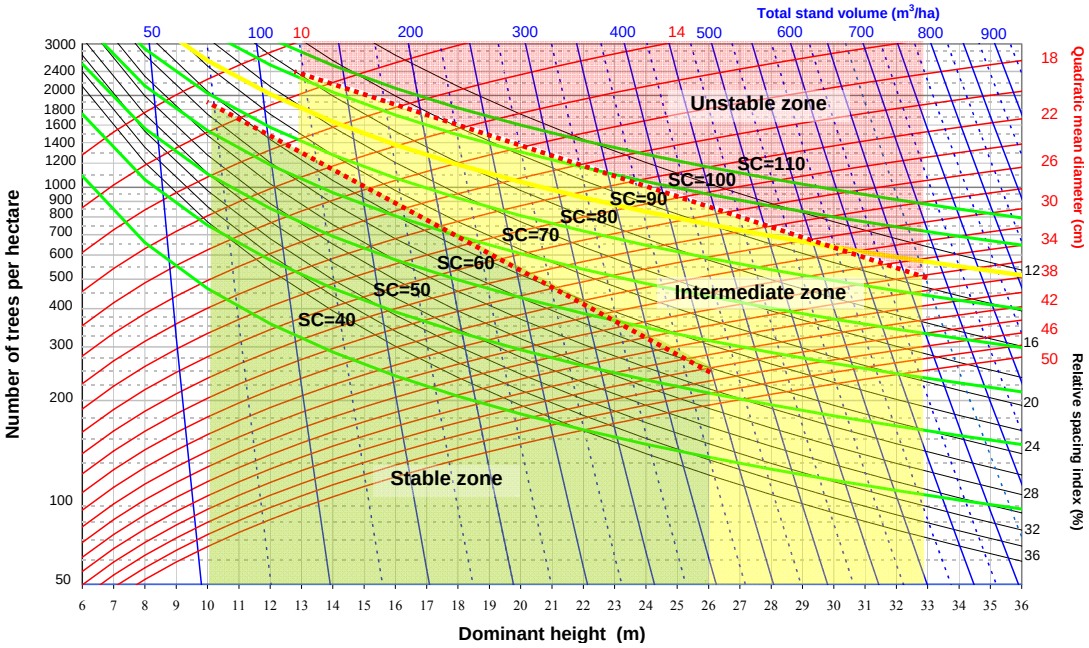

Fig. 2: Stand density management diagram for radiata pine stands including the zones of stability as defined by Becquey and Riou-Nivert (1987)

5. Applications of the SDMD in density management

The schedule of thinning operations within the framework of the SDMD proposed is determined by two factors: the target stand status at the rotation age and the windthrow risk. In other words, stand stability (explicitly defined by the stand SC isolines and "zones of stability") determines the "trajectories" of alternative density management regimes. In addition, locating current stands on the SDMD and projecting their future

growth can provide advance warning of future risk and indicate the potential benefits of thinning treatments.

For more details on developing thinning schedules using this type of SDMD, see Castedo-Dorado et al. (2009).

6. Conclusions and future research needs

The diagrams developed in this study were designed to derive thinning schedules for even-aged stands by taking into account stand resistance to windthrow. Two complementary tools were included in the SDMD for this purpose: the stand slenderness coefficient isolines and the "zones of stability" proposed by Becquey and Riou-Nivert (1987).

The value of the stand slenderness coefficient as a stability measure is supported by both mechanistic models of tree stability and empirical evidence. The stand SC isolines for the whole stand were demonstrated to be easily included in the stand density management diagram proposed. If assessment of the stability of the different crown classes within a stand is required, an estimation of the average SC for each crown class can also be included in the SDMD by relating it to the average stand SC.

Superimposition on the diagram of the "zones of stability" as proposed by Becquey and Riou-Nivert (1987) may also help in the assessment of wind damage vulnerability from stand dominant height and mean stand slenderness coefficient. Although these zones of stability have been applied to uniform conifer stands in temperate zones, tailored information for particular species and areas is desired.

It is well known that stand stability decreases immediately after thinning operations, and that this is much more evident with increasing tree height. This is due to the immediate effects of thinning on increasing the canopy roughness and wind load, and on decreasing the sheltering effects from surrounding trees. This, although very important in stand management, is not considered in the diagrams developed. Close examination of height increments and comparison with radial increments may be used in the future to identify the duration of this period of great disequilibrium shortly after thinning.

Finally, it must be emphasized that this study only focused on the use of SDMD to assess the stand hazard component of windthrow risk; other environmental factors should be considered in assessing the probability of damage at a given location.

Acknowledgement

The authors are indebted to the Spanish Ministry of Science and Innovation for funding research project No AGL-2008-02259/FOR.

References

Barrio, M., Álvarez-González, J.G., 2005: Development of a stand density management diagram for even-aged pedunculate oak stands and its use in designing thinning schedules. Forestry 78, 209-216.

Becquey, J., Riou-Nivert, P., 1987: L'existence de zones de stabilite des peuplements. Consequences sur la gestion. Revue Forstiere Francaise 39, 323-334.

Cameron, A.D., 2002: Importance of early selective thinning in the development of long-term stand stability and improved log quality: a review. Forestry 75, 25-35.

Castedo-Dorado, F., Crecente-Campo, F., Álvarez-Álvarez, P., Barrio-Anta, M., 2009: Development of a stand density management diagram for radiata pine stands including assessment of stand stability. Forestry 82, 1-16.

Cremer, K.W., Borough, C.J., McKinnel, F.H., Carter, P.R., 1982: Effect of stocking and thinning on wind damage in plantations. N. Z. J. For. Sci. 12, 244-268.

Cucchi, V., Bert, D., 2003: Wind-firmness in *Pinus pinaster* Ait. stands in Southwest France: influence of stand density, fertilisation and breeding in two experimental stands damaged during the 1999 storm. For. Ecol. Manage. 60, 209-226.

Hinze, W.H.F., Wessels, M.O., 2002: Stand stability in pines: an important silvicultural criterion for the evaluation of thinnings and the development of thinning regimes: management paper. South. A. For. J. 196, 37-40.

Mitchell, S., 2000: Forest health: preliminary interpretations for wind damage. For. Pra. Br., B.C. Min. For., Victoria, B.C. Stand Density Management Diagrams.

Navratil, S., 1995: Minimizing wind damage in alternative silvicultural systems in Boreal mixedwoods. Canada-Alberta Partnership Agreement in Forestry, Report 8033-124.

Newton, P.F., Weetman, G.F., 1994: Stand density management diagram for managed black spruce stands. For. Chron. 70, 65-74.

Oliveira, A.M., 1988: The H/D ratio in maritime pine (*Pinus pinaster*) stands. Proc. IUFRO Conference Forest Growth modelling and prediction. 1987, 881-888.

Wang, Y., Titus, S.J., LeMay, V.M., 1998: Relationships between tree slenderness coefficients and tree or stand characteristics for major species in boreal mixedwood forests. Can. J. For. Res. 28, 1171-1183.

Wilson, J.S., Oliver, C.D., 2000: Stability and density management in Douglas-fir plantations. Can. J. For. Res. 30, 910-920.

Wonn, H.T., O'Hara, K.L., 2001: Height:diameter ratios and stability relationships for four northern Rocky Mountain tree species. West. J. Appl. For. 16, 87-94.

Authors' addresses:

Dr. Marcos Barrio-Anta (barriomarcos@uniovi.es)
Department of Biology of Organisms and Systems, University of Oviedo
E.U. de Ingenierías Técnicas, C/ Gonzalo Gutiérrez Quirós, 33600 Mieres, Spain

Dr. Felipe Crecente-Campo (felipe.crecente@usc.es)
Department of Agroforestry Engineering, University of Santiago de Compostela
Escuela Politécnica Superior. Campus Universitario 27002 Lugo, Spain

Dr. Pedro Álvarez-Alvarez (alvarezpedro@uniovi.es)
Department of Biology of Organisms and Systems, University of Oviedo
E.U. de Ingenierías Técnicas, C/ Gonzalo Gutiérrez Quirós, 33600 Mieres, Spain

Dr. Fernando Castedo-Dorado (fcasd@unileon.es)
Department of Agricultural Engineering and Sciences, University of León
Campus de Ponferrada, Avenida de Astorga, 24400 Ponferrada, Spain

Digital video tracking imagery of tree movements in response to gusting airflow conditions

Pat Pickett

Artist, Los Angeles, California

Abstract

In order to trace the movements of trees over time and as they interact with gusting wind in a complex terrain, illustrations are produced using a 3-D tracking program. The animation of specific tree behavior will be based on digital information chosen from within field-gathered footage to show the paths of foliage, branch and tree movement. The biomechanical response of leaves, branches, limbs, canopy, and/or trunk displacement can be captured, and a story told of the effects of gusting wind conditions upon a single tree, and further, over the forest and/or across edge terrain. By choosing tracking points, as features, on trees from the entire framed landscape, the response of an individual tree in the foreground can be seen within the context of the surrounding canopy. The trailing imagery can illustrate specific wind loading strategies and show range of movement from crown to lower branches. Wind speed data are recorded in the field during filming and are provided for each digitally annotated, video-captured event. Gust excitation and sway response, as well as the characteristic movements of distinct elements, can be individually expressed in this process using the vocabulary of art.

1. Introduction

Art and science share the need to give visual expression to events, data, forces, ideas, etc - things that might not otherwise be seen. Working between the disciplines, I am interested in the physicality and expressiveness of measurable circumstances, and in the accumulation, over time, of this visual information.

My interest in the effects of wind on trees began in 1999 as part of a series of works designed to expand the definition of drawing to include marks made in response to the stimulation of an external phenomenon by an organism with distinct physical characteristics. I looked beyond traditional artistic responses to light and its' visual effects, to the environment for examples of forces that would only be made visible by their effects and corresponding response characteristics. I imagined visual residues accumulating around the branches of trees swaying in the wind.

I began with "Tree Drawings", in which I attached a pen to end of a branch and positioned a drawing surface (paper, panel, photo of the tree) below, in order to capture the track of the branch movement when excited by the wind. It was an experiment designed to begin to capture the movement of individual branches under a wide variety of wind conditions. Patterns emerged that were at once aesthetically pleasing and informative.

Building upon and proceeding from an analog representation of branch excitation, the digital video-tracking project is designed to more fully realize my original vision and to create a more dynamic picture event of tree behavior (Coutss and Grace, 1995; Elkins, 1999).

2. Measurable circumstances - the process

What follows is a snapshot of only the first steps taken in what will be a long-term motion-drawing project. Video footage is gathered while on drawing expeditions in the field, from a variety of wind conditions and terrain. This process does not require foreign tracking objects to be inserted into the tree. Relying solely on the video footage of the trees for tracking information will allow for the greatest flexibility in capturing the behavior of very tall trees, trees in difficult terrain, trees at a distance, and/or a larger view of the landscape.

Once in the studio, the footage is sorted and edited. Crucial to the process is finding digital tools that will provide dependable data for the array of compositing programs that will be utilized later on in the process to create the most expressive and animated pictures of tree movement. Using a 3-D tracking system, the footage of trees in gusting conditions is analyzed for the best examples of clearly identifiable tracking points (Figs. 1-5).

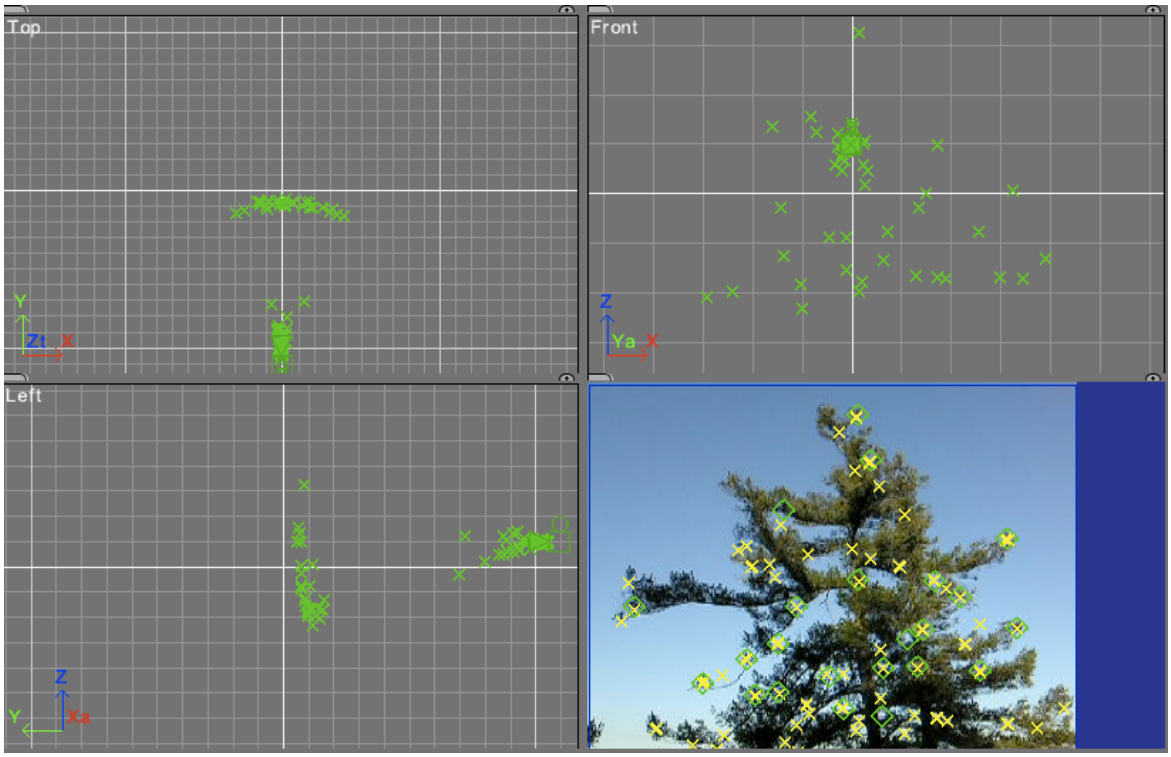

Fig. 1: Set to run automatically, the tracking program chooses 2-D points to solve for motion and, if they exist, to solve for 3-D coordinates; the top left, top right and bottom left graphs show the solved 3-D features from different perspectives; on bottom right - the completed tracking solutions within the video

Fig. 2: Tracking points (green squares), 3-D coordinates (yellow x's), and trails (blue and red looping lines)

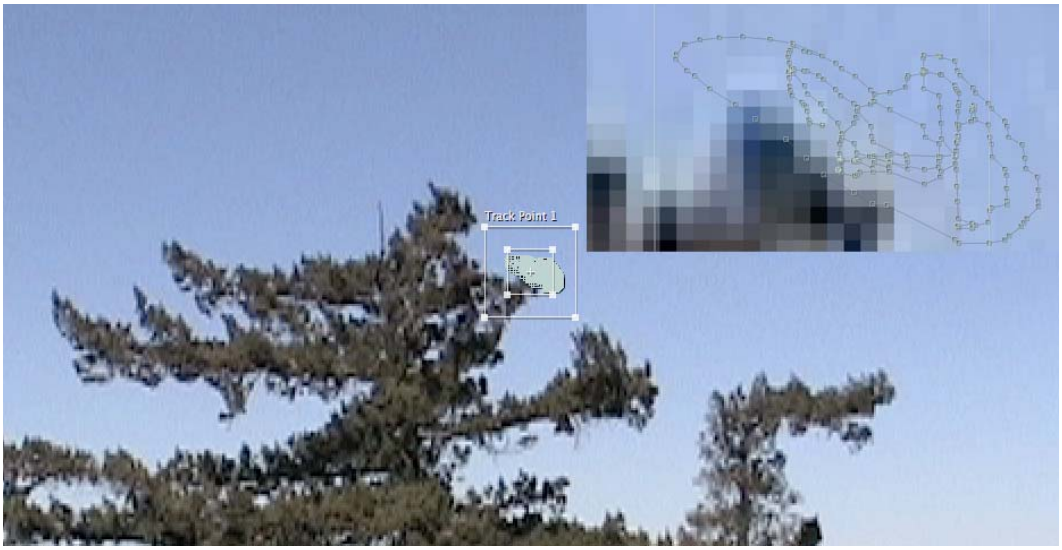

Fig. 3: Trails follow coordinates and serve as a tracer-picture of the path of the branch tip; these coordinates can be used in a compositing, animation package, or CAD program to render the trails as a 3-D model of the path; resulting ultimately in the ability to make pictures of the wind-effect-on-trees-event over time

Fig. 4: In supervised tracking, each feature is selected manually, monitored and corrected as needed in order to follow a selected set of pixels throughout the shot

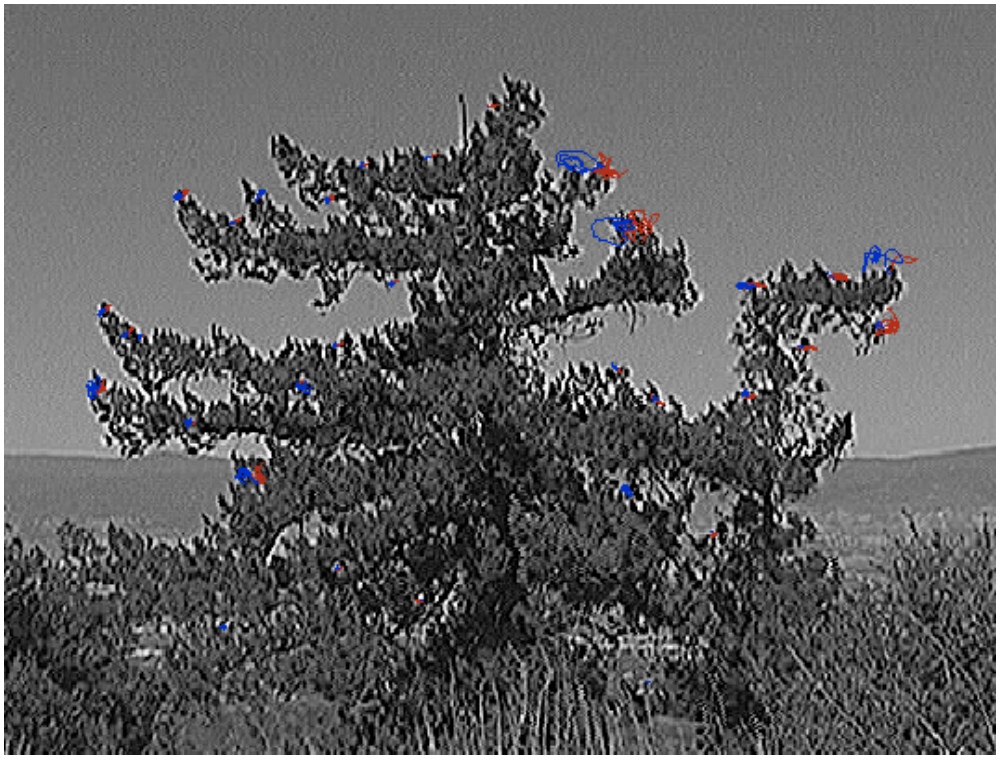

Fig. 5: Processed here for “edge” and “sharpen”, a black and white version allows for easier supervised tracking, especially at lower resolutions

3. Conclusion

Attempts to "picture" an event in nature, whether by drawings, paintings, graphs, diagrams, statistical modeling, measured experiments, or photographic processes, are but approximate responses and each tell only part of the story. The results so far in this project promise to provide an ongoing conversation between a phenomenon, its' direct record, and an artists' response. It will continue to evolve within the aesthetic language of art, and along the way hope to be of interest within the useful language of science.

Acknowledgements

I am indebted to Clint Hope, Chuck Harrison, Dimitri Negroponte and Eric Powers for their technical advice and assistance.

References

Coutts, M.P., Grace, J., 1955: Wind and Trees. Cambridge University Press, UK.

Elkins, J., 1999: The Domain of Images. Cornell University Press, Ithica.

Author's address:

Pat Pickett (ppickett@mindspring.com)
652 Sunnyhill Dr., Los Angeles, California 90065 USA

Effects of windthrow on drought risk in spruce and pine forest ecosystems under climate change conditions

Bernd Ahrends, Martin Jansen, Oleg Panferov

Büsgen-Institute, Georg-August University of Göttingen, Germany

Abstract

Forests are influenced by many disturbances, especially drought, windthrow, pest at-tacks, air pollution, and forest management. The climate change results in increasing frequency of weather extremes which will probably cause drought stresses in European forest ecosystems. By integrating several new features within two existing models, small-scale coupled process based modeling was carried out for the region of Solling, Germany. The results show considerable increment of drought risks towards 2100 compared to "present climate conditions", caused by changes in precipitation and increase of mean air temperature. It is shown that for Solling sites the wind damage induced changes of structure and microclimate provide a decrease on drought stress in the following years.

1. Introduction

The currently emerging global environmental changes expose forest ecosystems and woodlands to environmental factors which fundamentally differ in their combinations and dynamics from those experienced in the past. The climate change results in increasing frequency of weather extremes (Leckebusch et al. 2008), which may result in broad area damage events (e.g. drought, windthrow) in European forest ecosystems. The climatic changes forecast for Europe projects temperature rises, changed spatiotemporal distribution and intensity of precipitation, as well as the increased frequency of extreme anomalies. The climate projections of future annual precipitation for Central Europe show an increase of more intensive precipitation events in the winter and an increase in summer periods without precipitation (Roeckner et al. 2006). In combination with rising temperatures, an increase in the duration of hot periods in the summer is expected. These projections suggest that the risk of damage to trees will increase during the predicted climatic warming. Possible effects of the combination of warm and dry periods on forest ecosystems of Central Europe were observed for the summer 2003 (Granier et al. 2007). The intensity of these drought effects is strongly influenced by the local climate, site conditions and tree species. On the other hand Peltola et al. (1999) indicated that the projected future warmer weather is expected to increase the windthrow risk since the tree anchorage during the period between autumn and early spring will be reduced due to a decrease in soil freezing. Therefore, it is very important to take into account a feedback of each damage event on climatic conditions in the stands. There are direct and indirect feedbacks from windthrow on the soil water availability and the risk of drought stress, i.e. the changes of precipitation interception, transpiration, soil water regime, and radiation penetration. The present study focuses on the effect on the water regime for two typical tree species (spruce and pine) on different soil types (camisoles) under the projected climatic conditions of SRES A1B and B1.

2. Site description, tree species, soil conditions and climate projections

The Solling highlands within the limits of 51.6°N to 52°N and 9.4°E to 9.8°E, i.e. about 1600 km^2 were chosen for investigation. Two tree species: Norway spruce (Picea abies (L.) Karst) and Scots pine (Pinus Sylvestris, L.) were represented by three different stocking degrees each (Tab. 1). For most parameters we used the standard Brook90 parameter set (Federer et al. 2003, Hammel & Kennel 2002). To consider the effects of different soil types and soil textures on rooting depth, soil moisture and drought stress we select two different soils, which are typically for the investigation area (Tab. 2).

Table 1: Stand characteristics and model parameters for 3 stocking degree classes of Norway spruce and Scots pine, a: Schober (1995)

Parameter	**Unit**	**Norway spruce**			**Scots pine**			**source**
age	years	85	85	85	85	85	85	a
solid volume	$m^3_{(s)}$ ha^{-1}	561	449	337	333	266	200	a
stocking degree	[-]	1.0	0.8	0.6	1.0	0.8	0.6	a
stand density	tree ha^{-1}	706	564	423	561	447	335	a
tree height	m	26.6	26.6	26.6	22.3	22.3	22.3	a
DBH	cm	27.9	27.9	27.9	27.2	27.2	27.2	a
Max leaf are index	m^2 m^{-2}	7.45	5.96	4.47	3.29	2.62	1.96	see 3.2
Stem area index	m^2 m^{-2}	1.41	1.12	0.84	1.06	0.85	0.63	see 3.2

Table 2: Soil hydraulic parameters by texture class from Clapp & Hornberger (1978) at saturation (subscript "s") and at the upper limit of available water (subsc. "u")

Soil type	**depth**	**horizon**	**texture**	**stone**	Ψ_u	θ_u	θ_s	K_u
unit	[cm]	[-]	US-system	[%]	[kPa]	[-]	[-]	[mm/d]
cambisol	4-0	L/F	-	0	-34.4	0.650	0.863	3.70
	0-5	Ah	silt loam	9	-25.0	0.365	0.509	13.13
	5-90	Bw	loam	9	-8.5	0.324	0.472	6.27
	90-200	2R	loamy sand	72.5	-3.8	0.203	0.410	3.51
cambic podzol	8-0	L/F/H	-	0	-34.4	0.650	0.836	3.70
	0-5	AEh	silt loam	50	-25.0	0.365	0.485	13.13
	5-10	Bw(AEh)	silt loam	50	-25.0	0.365	0.485	13.13
	10-30	Bw	silt loam	50	-25.0	0.365	0.485	13.13
	30-60	Bw2	silt loam	72.5	-25.0	0.365	0.485	13.13
	60-200	R	silt loam	92.5	-25.0	0.365	0.485	13.13

where: ψ is matrix potential, K – hydraulic conductivity, θ – volumetric water fraction.

To represent the possible future climatic conditions, the calculations of two SRES climate scenarios A1B and B1 for a period of 2001-2100 as well as 20th century scenario

C20 for the period of 1960-2000 were done by coupled general circulation model -Max-Planck-Institute ocean model, ECHAM5-MPIOM, are used as defined in German framework program "klimazwei". The modelled data are downscaled using Climate Local Model, CLM, (Rockel et al. 2008) to a spatial resolution of 0.2°×0.2°. The daily mean values of climate variables for A1B, B1 and for C20 with two runs per scenario are obtained from CERA-database (Lautenschlager et al. 2009). For all variables the time series of runs 1 and 2 of A1B and B1 are merged with correspondent runs of C20 so that continuous time series from 1960 to 2100 are built for both runs of A1B and B1. Following notation is assumed in further analysis: A1B_1, A1B_2 and B1_1, B1_2 are correspondingly the merged runs 1 and 2 of C20-A1B and C20-B1. The simple A1B and B1 denote respective merged scenarios averaged over the two runs.

3. Model description

For small-scale coupled process based, we developed a modelling approach, by integrating several new features within two existing models, namely the BROOK90 model (Federer et al. 2003), for calculating the water balance of forest ecosystems and Forest-GALES approach for estimating a critical wind speed (CWS) Gardiner et al. (2000). The parameterisation and the modifications of Brook90 are described below. The detailed methodologies for critical wind speed (CWS) calculation were described for the windthrow risk assessment in Panferov et al. (in present Issue). Therefore, only the drought estimation will be outlined here. Granier et al. (2007) has identified for various forest eco-systems types 40% of relative extractable soil water (REW) as a critical limit, below which transpiration and gross primary production were sharply reduced by drought. So we calculate the drought stress duration (DSD) as follows:

$$DSD = \sum_{t=1}^{365} \begin{cases} 1 & if \quad REW < 0.4 \\ 0 & else \end{cases}$$

where REW is defined as a ratio between the actual (t) extractable soil water (EW_t) divided to the maximum (EW_m). EW is defined as difference between field capacity and wilting point in the rooting zone. To simulate the water balance of a given combination of tree species and age with certain soil type a 1D-SVAT model BROOK90 (Version 4.4e) is used. It is a detailed, process-oriented model that can be used as a reliable tool to investigate the potential effects of change in tree species, soil types and climate scenarios. For each soil horizon the parameters of the water retention curve and the hydraulic conductivity function are deduced from soil texture with the pedotransfer function of Clapp & Hornberger (1978). For the estimation of the effective rooting depth the rules from Czajkowski et al. (2009) are applied. The LAI is modeled by integration a litterfall model (Ahrends 2008) in the LAI model from Law et al. (2001). For the estimation of stem area index (SAI) we used the functions of Hammel & Kennel (2003). To assess the effects of forest structure changes resulting from windthrow events on the probability of next drought stress event the calculations are carried out in two ways. First - the drought stress indicators are summed up during the 30-years period but the forest structure does not change. Second - the drought stress is summed up and the damaged trees are "removed" from the stand - accordingly the stand density, LAI and SAI decrease. The calculations with BROOK90 continue from the time point of damage with the new values of stand characteristics. The BROOK90 calculations for all climate scenarios and runs are started 01.01.1960 and carried out with daily time step continuously for 140 years up to

2100. The evaluations of results are accomplished for the following four periods: P0: 1981-2010 – assumed as the "present conditions" or reference period, P1: 2011-2040, P2: 2041-2070, P3: 2071-2100.

4. Results and discussion

To characterize the projected climate conditions in 21st century in Solling area the CLM-data were post-processed. The data of A1B and B1 are aggregated to annual means (sums in case of precipitation). Spatial averaging over the 9 CLM grid points to represent the study area is carried out for all mentioned climate characteristics.

The spatial variations within the chosen area are very low so that the spatial means are assumed to be representative. To describe the tendencies of climate development the spatial mean values are averaged over the 30-years periods: P0 –P3 and relative differences are calculated: $\Delta\varphi_i = (\varphi_i - \varphi 0) / \varphi 0 * 100\%$, where φ_i is the 30-years mean value of the spatially averaged climate variable listed above for the climatic period i = 1, 2, 3. The analysis of climate scenarios shows for both scenarios an increase of precipitation to $\Delta P1 \approx 6\%$ and then slightly monotonically decreases towards 2100 to $\Delta P3 \approx 5\%$. However, the air and soil temperature increase monotonically and rather strongly towards P3 with $\Delta T > 37\%$ in A1B and $\Delta T > 24\ \%$ in B1. The differences in drought between tree species and soil types and the future projected development are plotted as mean yearly DSD for a given period. Fig. 1 clearly demonstrates that under the same conditions: climate scenarios, soil types and the same stocking degree the spruce stands have higher risk of drought stress, due to higher LAI values (Tab. 1) and a shallow root systems (Czajkowski et al. 2009). The results show that LAI is one of the crucial parameters determining model response of evapotranspiration, runoff and consequently duration of drought stress (Federer et al. 2003). Consequently when taking into account the effect of windthrow damage as feedback, the DSD decreases in all stands. The feedback contribution to drought reduction in pine stand generally remains very low.

As expected, the cambisol with the highest extractable soil water capacity (≈ 240 mm) shows the lowest duration values of drought stress in a plausible range. For example in 2003, Granier et al. (2007) found water stress durations of 28 to 172 days in various different forest ecosystems in Europe. When estimating the trends of DSD in 21st century comparing to present conditions, i.e. comparing the projected drought for periods 1, 2, 3 to the reference P0 (Fig. 1), it is obvious that the values generally decrease in the period 1 and sometimes also in the period 2 and then increase towards 2100. The decrease in drought in the first period could be explained by the increase of precipitation on the one hand and the slight increase of temperature in this period on the other hand. The changes are generally stronger under A1B condition than under B1. However, the contributions of feedback are of more complicated character depending on combination of scenarios, tree species and soil types. The pattern of drought calculated considering feedbacks is similar to the pattern of "standard" simulation itself (not show here) but shows lower values for all species and soils. The highest contribution of feedback can be observed in Period 3, when the windthrow risk is highest. It is caused by increase of air and soil temperature and by seasonal redistribution precipitation and critical windspeed during the 21th century.

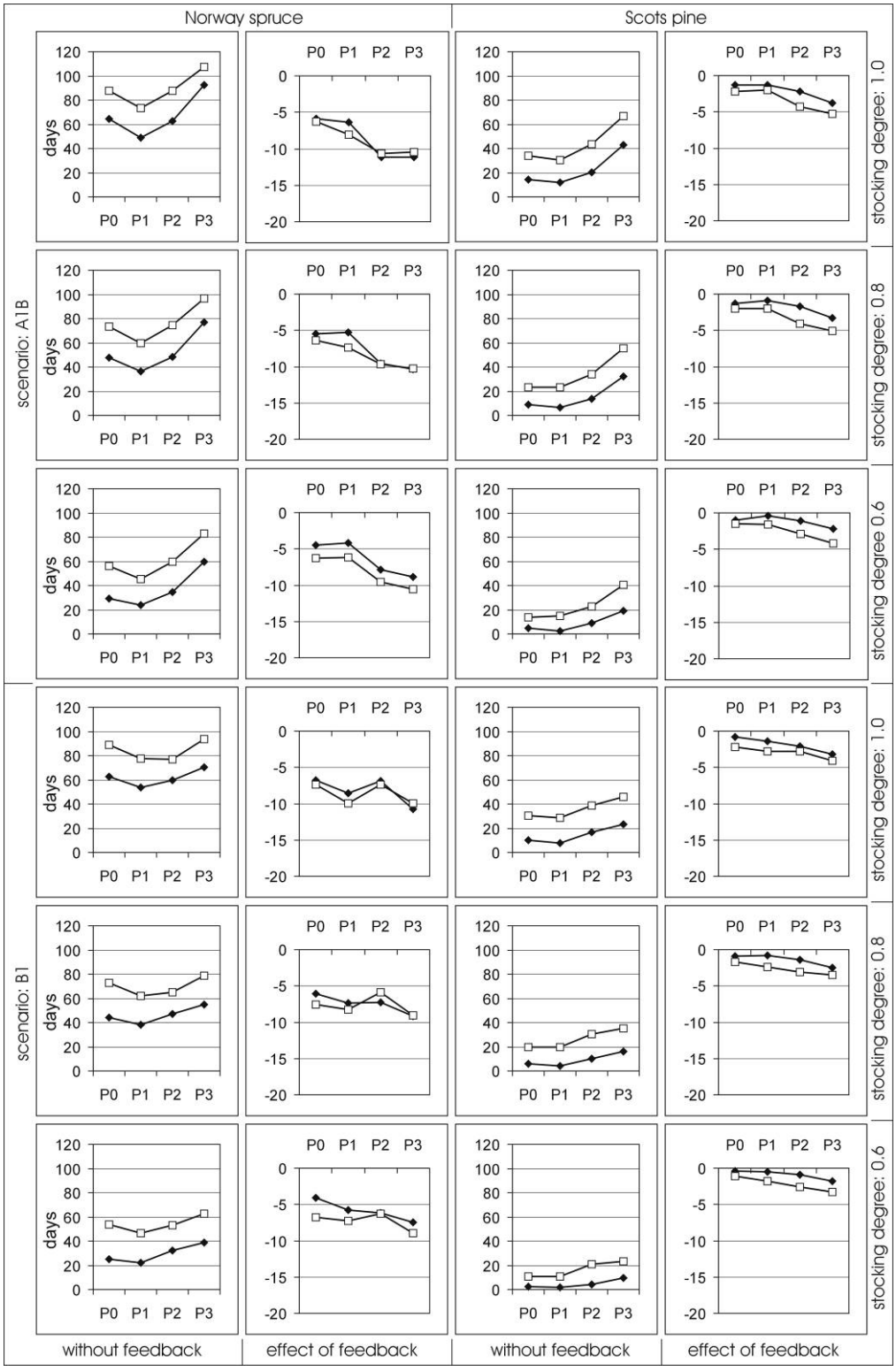

Fig. 1: Scenarios of drought stress duration (days per year) for different tree species, stocking degrees, and soil types. ─♦─: cambisol, ─□─: cambic podzol

5. Conclusions

The results of present study show: 1) considerable increment of drought risks towards 2100 compared to "present climate conditions", caused by changes in yearly precipitation distribution and increase of mean air temperature and (2) for Solling sites the wind damage induced changes of structure and microclimate provide a decrease on drought stress in the following years.

Acknowledgement

The study was financed by BMBF within the frames of joint project "Decision Support System - Forest and Climate Change" (DSS-WuK) and by Grant of Ministry for Science and Culture of Lower Saxony "KLIFF". We gratefully acknowledge this support.

References

Ahrends, B., 2008: Dynamische Modellierung der langfristigen Auswirkungen des Waldumbaus von Kiefernreinbeständen auf die Kohlenstoffspeicherung im Auflagehumus saurer Waldböden in Nordwestdeutschland. Horizonte, Bd. 21, 162 S.

Clapp, R.B., Hornberger, G.M., 1978: Empirical equations for some soil hydraulic properties. Water Resources Research 14, 601-603.

Czajkowski, T., Ahrends, B., Bolte, A., 2009: Critical limits of soil water availability (CLSWA) in forest trees - an approach based on plant water status. vTI agriculture and forest research 59, 87-93.

Federer, C.A., C. Vörösmarty, C., Feketa, B., 2003: Sensitivity of annual evaporation to soil and root properties in two models of contrasting complexity. J. Hydrol. 4, 1276-1290.

Gardiner, B., Peltola, H., Kellomäki, S., 2000: Comparison of two models for predicting the critical wind speeds required to damage coniferous trees. Ecol. Model. 129, 1-23.

Granier, A., et al., 2007: Evidence for soil water control on carbon and water dynamics in European forests during the extremely dry year: 2003. Agric. Forest Meteorol. 143, 123-145.

Hammel, K., Kennel, M., 2001: Charakterisierung und Analyse der Wasserverfügbarkeit und des Wasserhaushalts von Waldstandorten in Bayern mit dem Simulationsmodell BROOK90. Forstliche Forschungsberichte München No. 185.

Lautenschlager, M., Keuler, K., Wunram, C., Keup-Thiel, E., Schubert, M., Will, A., Rockel, B., Boehm, U., 2009: Climate simulations with CLM, data stream 3: European region MPI-M/MaD. World Data Center for Climate. DOIs: 1)10.1594/WDCC/CLM_C20_1_D3;2) 10.1594/WDCC/CLM_C20_2_D3;3)10.1594/WDCC/CLM_A1B_1_D3;4)10.1594/WDCC/ CLM_A1B_2_D3;5)10.1594/WDCC/CLM_B1_1_D3;6)10.1594/WDCC/CLM_B1_2_D3.

Law, B.E., van Tuyl, S., Cescatti, A., Baldocchi, D.D., 2001: Estimation of leaf area index in open-canopy ponderosa pine forests at different successional stage and management regimes in Oregon. Agric. Forest Meteorol. 108, 1-14.

Leckebusch, G.C., Renggli, D., Ulbrich, U. 2008: Development and application of an objective storm severity measure for the Northeast Atlantic region. Meteorol. Z. 17, 575-587.

Panferov, O., Sogachev, A., Döring, C., Ahrends, B., 2009: Dynamic of windthrow risk in different forest ecosystems for 21st century (SRES A1B, B1). Ber. Meteor. Inst. Univ. Freiburg No. 19, 119-125.

Peltola, H., Kellomäki, S., Väisänen, H., Ikonen, V.-P., 1999: A mechanistic model for assessing the risk of wind and snow damage to single trees and stands of Scots pine, Norway spruce, and birch. Can. J. For. Res. 29, 647-661.

Rockel, B., Will, A., Hense, A., 2008: The regional climate model COSMO-CLM (CCLM) Editorial. Meteorol. Z. 12, 347-348.

Roeckner, E., Brasseur, G.P., Giorette, M., Jacob, D., Jungclaus, J., Reick, C., Sillmann, J., 2006: Klimaprojektionen für das 21. Jahrhundert. Max-Planck-Institut für Meteorologie, Hamburg. 28 S.

Schober, R., 1995: Ertragstafeln wichtiger Baumarten bei verschiedener Durchforstung. 4. Aufl. Sauerländer. Frankfurt am Main. 166 S.

Authors' addresses:

Dr. Bernd Ahrends (bahrend@uni-goettingen.de)
Dr. Martin Jansen (mjansen@gwdg.de)
Büsgen-Institute, Chair Soil Science of Temperate and Boreal Ecosystems, University of Göttingen
Büsgenweg 2, D-37077 Göttingen, Germany

Dr. Oleg Panferov (opanfyo@uni-goettingen.de)
Büsgen-Institute, Chair Bioclimatolgy, University of Göttingen
Büsgenweg 2, D-37077 Göttingen, Germany

Effects of green tree retention on boreal forest understorey vegetation

Harri Hautala

Finnish Forest Research Institute, Vantaa Research Unit, Finland

Abstract

In green tree retention (GTR) felling, patches of initial forest are preserved in order to maintain some of the initial biological diversity over the long forest regeneration phase. However, the patches are often prone to tree uprooting and other edge-effects. This study from Southern Finland examines the effects of GTR felling to understorey vegetation in GTR patches, which were around 10 times larger than in the current practice. The patches were located on biologically rich swamped spruce forest on the basis of preceding biotope mapping. Understorey vegetation coverage and its' species numbers were measured from systematically located (according to distance from the patch edge and to cardinal point) permanent study plots during one pre-treatment year and two post-treatment years. One year after the felling, coverage of vascular plants increased in the GTR patches, while coverage of bryophytes decreased, respectively. In general, coverage of vascular plant species decreased slightly towards to the centre of the patch, while coverage of bryophytes increased, respectively. Two years after the felling, coverage of mosses in the southern side of the patches had declined on lower level if compared to the northern side. Species number of vascular plant species remained constant, but species number of bryophytes decreased significantly during the study period. In general, species number of bryophytes was slightly higher in the edges than in the centre of the patches, while number of vascular plants increased towards the interior and then steeply declined in the very centre of the patches. The results show that even in relatively large GTR patches, abundance of forest interior species (mainly bryophytes) reduces significantly after felling. This is probably due to the macroclimatic edge-effects from the felling area, which increased when high amount of uprootings was formed due to the strong wind events in the patches during the study period. Size and location of GTR patches should be considered carefully according to the local respective management objectives in order to better preserve the initial vegetation.

1. Introduction

Certain human activities, such as forestry, are nowadays rapidly changing our forests. This poses serious challenges for initial forest vegetation. Is it possible to maintain the initial structure and diversity of vegetation e.g. in the clear-felling areas over their regeneration period? Various new 'environmentally friendly' forest management methods have been introduced recently. One of these is green tree retention (GTR), where patches of initial forest are retained in the felling areas. GTR has gained popularity for example in Finland, as our ecological silviculture is focused on the managed tree stands (Mielikäinen & Hynynen 2003).

Although understorey vegetation is in a crucial role as the former of the biological matrix of forest on which majority of the species and ecosystem processes depend on, the scientific knowledge about the responses of understorey vegetation on GTR is exiguous. The development of boreal forest understorey vegetation is largely dependent on the existing tree layer (Hautala et al. 2005) and thus also forestry impacts on vegetation by way of changes on tree-layer structure (Økland et al. 2003). Simberloff (2001) has emphasized that if the main priority is to preserve the biodiversity of boreal forest, the monitoring should focus also on the effects of disturbances on species and not just the

disturbance processes. Previously, it has been shown that 0.01 ha sized retention tree groups (RTG's), even being larger than used in current Finnish practice, seem to be too small to maintain the initial diversity any better than clear-felling on stand-level (Jalonen and Vanha-Majamaa 2001).

The focus of this study is in the immediate responses of understorey vegetation in RTG's after clear-felling of the surrounding areas. It was hypothesized that: 1. Abundance (inc. coverage and species numbers) of field layer (vascular plants) will increase in the RTG's due to the changes in microclimate caused by the fellings, 2. abundance of ground layer (bryophytes) will decrease, and 3. abundance of vegetation will generally differ in the different parts of RTG's due to the edge-effects (e.g. increased light and ruderal species from clear-felling areas) so that vascular plants will favour edges and bryophytes will favour the interiors of the RTG's.

2. Material and methods

The study sites are located in southern-boreal vegetation zone in Heinävesi, eastern Finland (62°25' N; 28°37' E). The forests of this area have been managed intensively for the last 100 years. On the basis of biotope-mapping and measuring of different environmental variables from an area of 200 hectares in 1997, a group of forest patches were divided according to their type (see the details: Hautala et al. 2004). From this group, 11 homogenous paludified (biologically rich) spruce forest patches (with mean size of 0.2 ha) were chosen for the study sites. In the RTG's, understorey vegetation mean coverages (in percentages) and species numbers of all species were measured from the permanently marked sample plots with a circular 1 m^2 frame before (year 1998) and after felling of the surrounding areas (years 1999 and 2000). The systematical placement of the plots in the different parts in the RTG's is illustrated in Fig. 1. A paired-samples t-test was used to estimate the differences between the years. A linear regression analysis was used to detect whether the coverages and species numbers were dependent on the uprooting and distance from the edge of the RTG's. Arithmetic transformations were used for the variables, but original values are shown in the Figures. In statistics, SPSS 14.0.2 (17 Mar 2006) for Windows was used.

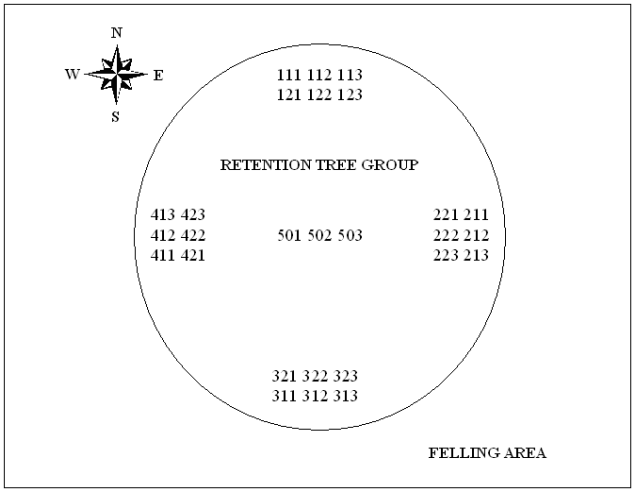

Fig. 1: The placement of the plots in the RG's

3. Results

Coverage of the field layer increased significantly ($P < 0.001$) between all years (excluding year-pair 1998-1999) during the study period (1998: 18.19 ± 0.76%; 1999: 17.09 ± 0.67%; 2000: 28.98 ± 1.16%), while coverage of the ground layer decreased significantly ($P < 0.001$) between all years (1998: 54.94 ± 1.57%; 1999: 42.45 ± 1.52%; 2000: 37.81 ± 1.32%). Coverage of the ground layer was slightly dependent on the uprooting percentage in the groups ($R^{2adj} = 0.339$, $P < 0.035$). Coverage of the field layer was higher in the S-side (vs. N-side) of the RTG's before the fellings, while coverage of the ground layer was higher in the N-side (vs. S-side) of the RTG's after the fellings (Fig. 2). In all years, coverage of the field layer decreased towards the centre of RTG (significantly in 1998: R = 0.152, $R^{2adj} = 0.021$, $P = 0.003$), while coverage of the ground layer increased significantly (1998: R = 0.215, $R^{2adj} = 0.044$, $P < 0.001$; 1999: R = 0.288, $R^{2adj} = 0.081$, $P < 0.001$; 2000: R = 0.193, $R^{2adj} = 0.035$, $P < 0.001$) (Fig. 3).

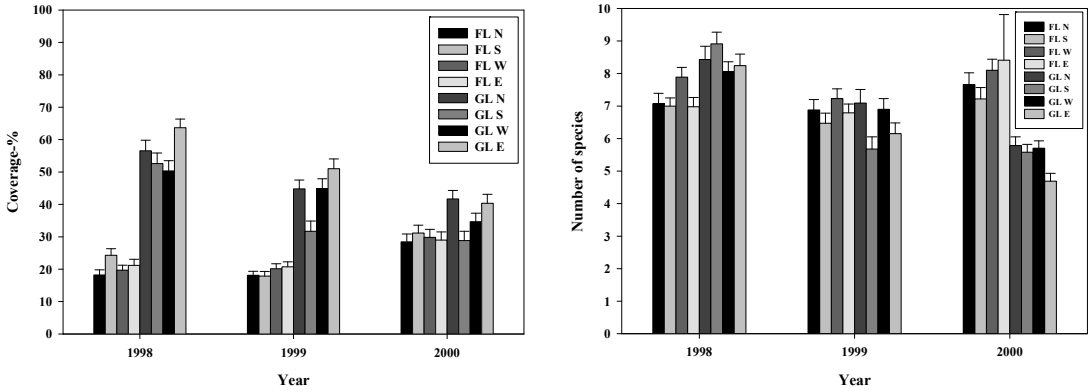

Fig. 2: Coverage percentage and number of species in the field (FL) and ground (GL) layers in north (N), south (S), west (W) and east (E) sides of the RG's during the study period (1998-2000)

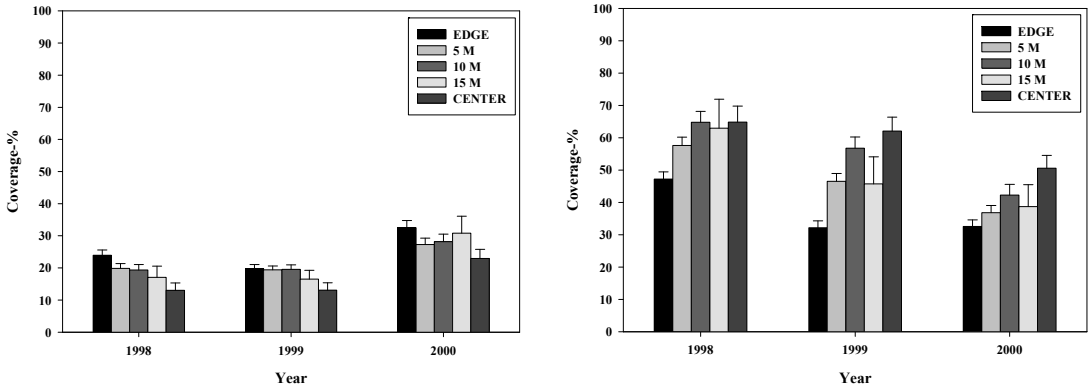

Fig. 3: Coverage percentage of the field (left) and ground (right) layers in the different distances from the edge of RG during the study period (1998-2000)

Number of the field layer species did not change significantly after the fellings (1998: 7.19 ± 0.15%; 1999: 6.83 ± 0.15%; 2000: 7.8 ± 0.37%), while number of the ground layer species decreased significantly decrease during the study period ($P < 0.001$) (1998: 8.34 ± 0.19%; 1999: 6.39 ± 0.19%; 2000: 5.37 ± 0.12%). Number of both the field and ground layer species did not differ significantly between N and S sides of the RTG's (Fig. 2.), while number of the ground layer species decreased significantly towards the centre of RTG in 1998 ($R = 0.176$, $R^{2adj} = 0.028$, $P = 0.001$) and in 2000 ($R = 0.181$, $R^{2adj} = 0.03$, $P < 0.001$) (Fig. 4).

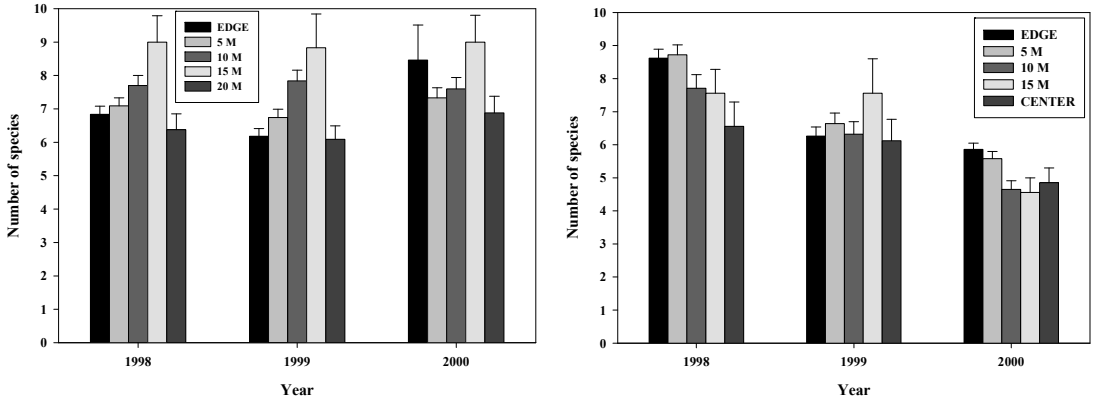

Fig. 4: Number of species in the field and ground layer in the different distances from the edge of RG during the study period (1998-2000)

4. Discussion

Generally, the hypotheses proved to be true. Field layer vegetation coverage increased clearly especially on the edges of the RTG's during the study period. It is known that dwarf shrubs *Vaccinium myrtillus* L. and *Vaccinium vitis-idaea* L., the dominant species on the plots, can regenerate totally in few years from macroclimatic changes caused by large-scale disturbance, such as clear-felling (Palviainen et al. 2005) and from small-scale disturbance targeted on plants themselves (Hautala et al. 2001). Macroclimatic conditions on the edges apparently released growth resources for these species.

Although the size of RTG's was over 10 times larger than in the current Finnish practice, the RTG's were subjected to local strong winds (possibly summer storms) which caused excessive tree uprooting in the groups especially during year 2000. The RTG's were located on paludified spruce forest patches, which were known to be susceptible to wind damage, especially as Norway spruce (*Picea abies*) was the domi-nating tree species on the biotope. It is possible that the high tree uprooting rates in the RTG's decreased the nutrient and water intake by trees and these resources became available for understorey vegetation. In the study of Halpern et al. (2005), slash accumulation and other disturbances connected to fellings were shown to decrease the understorey abundance in smaller retention tree groups. Similarly, species numbers in the ground layer decreased in this study. Also Haeussler et al. (2002), in their study from Canadian boreal forests, noticed that increasing forest practice disturbance severity decreased the diversity of non-vascular species.

The decline of abundance of forest interior species, including especially bryophytes, reflects the significant macroclimatic change in the RTG's after the felling and wind-caused tree uprooting. As the ecological purpose of GTR is to ensure the continuum of initial forest structures, the size and location of RTG's should be planned carefully in the individual forest management plans.

Acknowledgement

I wish to thank the following people who have participated in this study: Sanna Laaka-Lindberg, Marja-Leena Heinilehto, Ilkka Vanha-Majamaa, Jyrki Jalonen, Ahti Anttonen, Juhani Mäkinen, Jaakko Rokkonen, Ilkka Taponen, the organisations involved: FFRI, Metsäteho PLC, University of Helsinki, Finnish biodiversity program FIBRE (projects MONTA and RETREE): Jari Niemelä, Simo Kaila and Markus Strandström and Stora-Enso Ltd (Tornator PLC) providing the study areas. The study was financed by Academy of Finland, FFRI, Finnish Cultural Foundation, Maj and Tor Nessling Foundation, The Finnish Forest Foundation and especially The Finnish Society of Forest Science, who gave me a travel grant to the conference "Wind Effects on Trees" in Freiburg during October 2009.

References

Haeussler, S., Bedford, L., Leduc, A., Bergeron, Y., Kranabetter, J.M., 2002: Silvicultural disturbance severity and plant communities of the southern Canadian boreal forest. Silva Fennica 36, 307–327.

Halpern, C.B., McKenzie, D., Evans, S.A., Maguire, D.A., 2005: Initial responses of forest understories to varying levels and patterns of green-tree retention. Ecological Applications 15, 175-195.

Hautala, H. Tolvanen, A., Nuortila, C., 2001: Regeneration strategies of dominant boreal forest dwarf shrubs in response to selective removal of understorey layers. J. Veg. Sci. 12, 503-510.

Hautala, H., Jalonen, J., Laaka-Lindberg, S., Vanha-Majamaa, I., 2004: Impacts of retention felling on coarse woody debris (CWD) in mature boreal spruce forests in Finland. Biodiversity and Conservation 13, 1541-1554.

Hautala, H., Kuuluvainen, T., Hokkanen, E., Tolvanen, A., 2005: Spatial organization of understorey plant community at two sites of different fire history in a boreal forest. Community Ecology 6, 119-130.

Jalonen, J., Vanha-Majamaa, I., 2001: Immediate effects of four different felling methods on mature boreal spruce forest understorey vegetation in southern Finland. Forest Ecology and Management 146, 25-34.

Mielikäinen, K., Hynynen, J., 2003: Silvicultural management in maintaining biodiversity and resistance of forests in Europe-boreal zone: case Finland. Journal of Environmental Management 67, 47-54.

Palviainen, M., Finér, L., Mannerkoski, H., Piirainen, S., Starr, M., 2005: Responses of ground vegetation species to clear-cutting in a boreal forest: aboveground biomass and nutrient contents during the first 7 years. Ecol. Res. 20, 652-660.

Simberloff, D., 2001: Management of boreal forest biodiversity - a view from the outside. Scand. J. For. Res. Suppl. 3, 105-118.

Økland, T., Rydgren, K., Økland, R.H., Storaunet, K.O., Rolstad, J., 2003: Variation in environmental conditions, understorey species number, abundance and composition among natural and managed Picea abies forest stands. Forest Ecology and Management 177, 17-37.

Author's address:

Dr. Harri Hautala (harri.hautala@aka.fi)
Academy of Finland, Biosciences and Environment Research Unit,
P.O. Box 99 (Vilhonvuorenkatu 6), FI-00501 Helsinki, Finland

The effect of wind exposure on beech trees' canopy form and height in Caspian forests

Farshad Yazdian

Forestry Faculty, Cahools IAU University, Iran

Abstract

Beech tree occurs as a mountain tree in many forests in south of Caspian Sea except in eastern areas of low effective rainfall. It rarely grows under 250m and above 2500m altitude in south Caspian Sea areas and grows up to 50 m tall as a dominant in dense forests. The vertical structure of beech forest studied on three slope directions at three altitudes (500-1500-2300m). The results show there is a relationship between canopy form (height, bending) and wind speed and direction. Since the tallest trees were less than 20m, canopy form is different from trees above 20m height and it will depend on slope direction, altitude and wind speed and variation of them.

1. Introduction

Wind load is a function of wind speed and acceptable levels of risk must be associated with wind speeds and their probability of recurrence (Callen 2002). The trees become dwarfed if they are exposed to frequent dry wind. Sometimes, the effects of wind on tree morphology result from materials carried by wind rather than from the wind itself (Kimmins 1987, Zhu. et al. 2002).

In chronically windy locations, wind can also affect tree growth, resulting in permanent deformation. Robertson (1987) notes a number of investigators who have developed indices of deformation, which are related to wind speed. Cullen (2002) showed that wind speed about 20-30 km/h can move small branches and sometimes the small trees leaf being to sway and to make different of canopy form too.

2. Methods

Field work was carried out early in 2008 to collect data. About 9 sample plots (Table 1) were established at three altitudes (500, 1500 and 2300m) on three slopes (north, west and east). They were numbered 1, 2 and 3 (up to 500m); 4, 5 and 6 (up to 1500m); and 7, 8 and 9 m (up to 2300m). Field data were collected from a total plot with area about 400 square meters. Some characteristic data such as tree high, diameter at breast high, crown diameter (or radius), crown cover density and trunk slanting were measured. Diameter properties of trees over 50 years were measured. All of sample plots were dominated by beech (*Fagus orientalis* Lipsky) and hornbeam (*Carpinus betulus* L.) stands with crown covers created more than 50% by beech trees.

Weather information such as speed and direction of wind was obtained from meteorological station in the range zero, 1500 and 2200 m altitude.

Table 1: Numbers of sample plots at different altitudes and slop directions

Altitude (m)	Geographic directions		
	East	North	West
500	1	4	7
1500	2	5	8
2300	3	6	9

3. Results

The following results were derived from 9 sample plots. The average height and diameter of trees is more than 50 cm. Results are presented in Table 2.

Table 2: Study results related to beech trees in all sample plots on three altitudes and three slopes

Altitude(m)	500			1500			2300		
Slope	West	North	East	West	North	East	West	North	East
Plot NO.	1	2	3	4	5	6	7	8	9
d.b.h m	60	80	60	80	90	70	80	80	60
N*	4	4	4	6	5	6	2	4	4
E*	6	7	5	6	7	6	6	6	4
S*	6	6	5	7	7	6	4	4	4
W*	3	4	4	5	5	6	2	4	4
Canopy cover %	80	80	70	100	100	90	60	60	50
Trunk slant %	0	0	0	10	0	0	50	30	20
Wind speed direction %	50	50	0	60	40	0	70	30	0
Wind speed m/s	0	6	5	8	7	0	10	8	0

***** Four directions of canopy (north, west, south, east)

For example, the average height of largest trees in sample plot No, 5 (altitude 1500 m) is equal to 35 meters. Crown radiuses (Fig. 1) of beech trees for 4 geographical coordinates can show the rate of asymmetry of the crown due to wind effect. This study shows there is a relationship between wind and crown shape. The results show that on the altitude of 2300 m with western slope and a wind speed of 10 m/s trees is more asymmetry than sites with 1500 m of altitude or less.

Beech crowns on the eastern slope are more symmetrical than other slopes. Crown density of beech trees has its maximum on 1500 m altitude and appears to be minimum on 2300 altitude.

More than 50% of the trees on sites about 2300 m altitude and western slope are slanted. It is noteworthy that means of crown height, diameter and crown radius are presented.

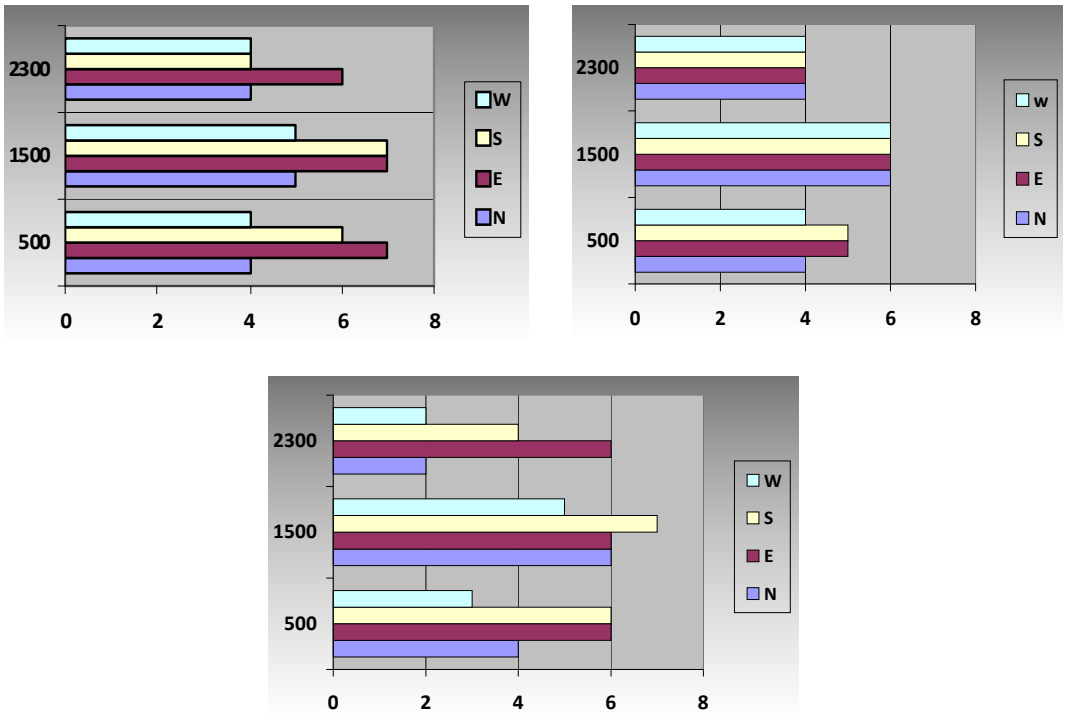

Fig. 1: Crown radius (m, horizontal axis) of beech trees on three altitudes (m a.s.l, vertical axis) and three slopes (upper left: North slope, upper right: East slope, bottom: West slope)

4. Discussion

- This study shows that wind speed and direction can affect canopy form.
- Only beech trees on 2000 m altitude are slanted.
- The study of wind speed on different altitude shows that wind speed more than 8 m/s will change the crown form and rate standing so that about 50% of beech trees on western slope and about 30% of them on northern slope are slanted
- Beech trees on the northern and western slopes have a crown asymmetry and for that reason the wind speed more influence than photo factor
- Previous mechanical damage to trees increases subsequent wind damage.
- Wind affects the morphology of stem and crown through influencing the distribution of growth.
- The foliage and buds of trees in the lee wind are less influenced.
- According to Zhu jiao-jun et al. (2004), wind not only causes extensive damages to trees in many parts of the world, also has more subtle effects on tree growth, tree morphology, and forest ecology as well.

Acknowledgement

The author is indebted to the Forest and Rangeland Organization and Chaloos IAU University for all of helping.

References

Kimmins, J.P., 1987: Forest Ecology. New York, Macmillan.

Cullen, S., 2002: Trees and wind: wind scals and speeds. Journal of Arboriculture 28(5).

Zhu, J.J., Matsuzaki, T., Li, F.Q., Gonda, Y., 2002: Theoretical derivation of risk - ratios for assessing wind damage in a costal forest. Journal of Forestry Research 13, 310-315.

Zhu, J.J., Matsuzaki, T., Matsuzaki, T., Jiang, F.Q., 2004: Wind on tree windbreaks. Beijing, China Forestry publishing house.

Author's address:

Dr. Farshad Yazdian (Farshad.yazdian@yahoo.com)
Islamic Azad University, Chaloos Branch, Chaloos
Mazandaran, Iran

Stem damage in radiata pine: observations with respect to site, silviculture and seedlot

Jennifer C. Grace, Carolyn Andersen, Rod Brownlie, Marika Fritzsche

Scion, Rotorua, New Zealand

Abstract

Radiata pine is the predominant plantation forestry species in New Zealand, planted across a wide range sites in terms of environmental conditions. Through the development and testing of a tree and branch growth model, TreeBLOSSIM, it became apparent that it was common for individual trees in experimental trials to have the occasional larger than expected branch, which appeared to result from incidences of stem breakage. As large branches impact on both stem wood properties and log use, it was important to gain a wider understanding of the incidence of stem breakage within New Zealand. An examination of qualitative stem description codes recorded in trials showed that the percentage of trees with stem breakage is highly variable and, depending on site conditions, silvicultural treatment and seedlot, can reach least 50%.

1. Introduction

New Zealand consists of two main islands, situated on the boundary of the Pacific and Indo-Australian tectonic plates and spanning from latitude 34°S to 48°S. As a result of the mountain ranges formed by tectonic activity and the latitudinal range, the country is very diverse in terms of environmental conditions. Recently it has been classified into 20 high-level environmental classes using a total of 15 different climate, landform and soil variables (Leathwick et al., 2003). Wind is not one of these 15 variables.

In 2003, plantation forestry occurred in 18 of the 20 high-level environments, but the percentage of the area covered by plantation forests exceeded 10% in only 4 environments (Leathwick et al., 2003). Since 2003, the area in plantation forestry has dropped by approximately 4% (Ministry of Agriculture and Forestry, 2003 and 2008), primarily due to conversion to dairy farms. As at 1 April 2008 the net stocked planted production forests covered an estimated 1.76 million hectares ± 5%. Seventy percent of the total forest area is located in the North Island, and 30 percent in the South Island. Radiata pine (*Pinus radiata* D.Don) accounts for 89% and Douglas fir (*Pseudotsuga menziesii*) for 6 % of the plantation forests (Ministry of Agriculture and Forestry, 2008).

Radiata pine silviculture has evolved through time with wide spacing and heavy thinning and pruning being favoured in the late 1980's and early 1990's (James, 1990). One large forest company recently developed a regime of planting 555 stems/ha and not thinning or pruning on most sites. Reasons given for this regime included a perceived lower premium for clearwood in 20 years due to increased availability of pruned trees, better techniques for manufacturing clearwood from unpruned logs, and improved plant quality with exceptional survival rates (Dyck and Thomson, 1999). The rotation age for radiata pine is currently is around 30 years (Ministry of Agriculture and Forestry, 2008).

There has been an active tree improvement programme for radiata pine since the 1950s and selections have been made to improve stem growth, stem straightness and resistance to the disease dothistroma. Selections have also been made to provide seedlots with dif-

ferent branching characteristics, wood density and reduced spiral grain (Radiata Pine Breeding Company Ltd, 2002).

Wind damage has been described as the most important risk factor to plantation forestry in New Zealand (Somerville, 1989). Several storms have caused widespread damage to forests in New Zealand. For example, Cyclone Bernie in 1982, and Cyclone Bola in 1988 caused major damage to forests in the North Island.

In terms of silviculture, the risk of wind damage is high in the first two years after thinning. Thinning after a mean crop height of 20 m also increases the risk (Ainsworth, 1989).

While the losses from large storms may be quantified, some losses due to wind have not been quantified (Somerville, 1989), for example:

- Toppling in recently planted trees and consequent butt sweep
- Stem malformation from leader loss
- Changes in wood properties including compression wood formation

Development and testing of a branch growth model highlighted the fact that stem malformations impacted on branching patterns, so this study was designed to provide an initial quantification of the extent of stem malformation in radiata pine using data from experimental trials planted between 1987 and 1991.

2. Crown architecture in radiata pine

A model of crown development in radiata pine (BLOSSIM) was developed that (1) predicted the underlying stem branching pattern (Grace et al., 1998) including the number of branch clusters in an annual shoot, (2) had the ability to utilise inventory measures of branching characteristics and (3) had the ability to link to sawing simulators (e.g. Pont et al., 1999). The mathematical equations in BLOSSIM were developed by destructively sampling a total of 49 near-rotation age radiata pine from 9 sites throughout New Zealand. The sample trees were selected to avoid stem malfor-mations, so BLOSSIM does not predict the effects of stem malformation. BLOSSIM was linked with an individual tree distance–independent growth model to create the model TreeBLOSSIM.

3. TreeD methodology

The performance of TreeBLOSSIM was tested using the TreeD methodology. TreeD is a photogrammetric image-based dendrometry system, which was developed for measuring stem and crown features on individual standing trees (Brownlie et al., 2007). There are two phases to the system. First, stereo digital images are taken of the sample tree and seven field parameters associated with that particular image/object environment are measured. Second, the field parameters are used to register the images in a computer, which allows the images to be viewed stereoscopically. The dimensions of any feature visible on the tree-stem can be measured and the position of the feature located in three-dimensional space. The system uses a full-frame digital SLR camera and a PC-based digital stereo viewing platform.

Comparison of branch diameters extracted from TreeD images with predictions from TreeBLOSSIM, highlighted that there were random occurrences of extremely large branches on trees that were supposedly free from stem defects, and that these were not well predicted by TreeBLOSSIM. Examining the TreeD images indicated that these large branches were either at a much steeper angle with respect to the stem than other branches (suggesting that the apical dominance of the stem had been impaired) and/or there was a kink in the stem at this point. It was therefore considered that such large branches had resulted from an incidence of stem breakage. Such large branches also impact on the within stem distribution of wood properties, with more compression wood likely to be present below clusters with large branches (Grace et al., 2006)., i.e. there is likely to be increased compression wood in the vicinity of any stem breakage.

4. Stem breakage in trials

Eighteen radiata pine trials, established in 1987, 1990 and 1991 (Tables 1 and 2) were then used to quantify the extent of stem breakage in radiata pine, and to determine whether this varied with the different silvicultural treatments applied and/or with the different seedlots planted. Each of the above trials consisted of at least 18 combinations of seedlot × silvicultural treatment, with 1 (1990, 1991) or 2 (1987) replicates. The combinations of seedlot × silvicultural treatment were common within, but not across, trial series.

The 1987 trial series contained six common silvicultural treatments (Table 1) and 4 common seedlots. These seedlots were rated as GF7, GF14, GF21 and GF13/LI28. The 1990 and 1991 trial series contained seven common silvicultural treatments (Table 2). The seedlots were GF6 (1991 trials), GF7 (1990 trials), GF14, GF16, GF25 and GF13/LI25. GF describes seedlots selected for improved growth and form, and LI describes seedlots selected for having less branch clusters. The higher the number the more improved the seedlot.

These trials have been measured on a regular basis for stem diameter and height. In addition a single “description code” may be recorded at each measurement describing any obvious features of the stem. Codes such as BW (basket whorl), DL (double leader), DT (dead, broken or defective top), FK (forked) MF (undefined malformation), ML (multileader), RC (ramicorn) and TO (top-out) are assumed to be related to stem breakage, probably caused by wind. The term stem breakage is used subsequently for all the above defects. Other codes relate to the shape of the stem. Only one code is recorded for each tree at each measurement, so the amount of stem breakage is probably underrepresented.

For each sample plot, the percentage of trees that had been ever been assigned one of the above stem breakage codes was calculated for each age of measurement. The data were plotted graphically to show trends with age. The percentages at age 13-years were analysed to determine the differences with respect to site, silvicultural treatment and seedlot, providing an initial quantification of stem breakage in radiata pine plantations.

Table 1: Silvicultural treatments applied in the 1987 series of trials

Treatment	Initial stems/ha	Final stems/ha	Mean crop height at time of thinning	Pruning
1	500	100	6.2 m	Yes
2	500	200	6.2 m	Yes
3	1000	400	6.2 m	Yes
4	1500	600	6.2 m	Yes
5	500	500	No thinning	No
6	500	200	20 m	Yes

Note: pruning treatment was either prune to leave 4 m of crown or prune to a stem diameter of 10 cm.

Table 2: Silvicultural treatments applied in the 1990 and 1991 series of trials

Treatment	Initial stems/ha	Final stems/ha	Mean crop height at time of thinning	Pruning
1	250	100	6.2 m	Yes
2	500	200	6.2 m	Yes
3	1000	400	6.2 m	Yes
4	500	200	6.2 m	No
5	1000	400	6.2 m	No
6	1000	600	6.2 m	No
7	1000	1000	No thinning	No

Note: pruning treatment was prune to leave 4 m of crown.

In all trials the percentage of trees that had been assigned one of the above stem breakage codes increased with increasing tree age. At age 13 years, the percentage of trees that had been assigned a stem breakage code varied from 10% to 39%. Trials on known exposed/windy sites had the higher incidence of stem breakage.

In the 1987 series of trials (Table 1), treatment 5 (plant 500 stems/ha with no thinning or pruning) consistently had the highest percentage of trees with stem breakage (between 21% and 51%). This treatment was very similar to that proposed by Dyck and Thompson (1999). The treatment with the lowest percentage of stem breakage (between 5% and 21%) was either treatment 3 or treatment 4. These had initial planting stockings of 1000 or 1500 stems/ha respectively and final stockings of 400 or 600 stems/ha respectively. The differences between the four seedlots were smaller than either the differences between sites or the differences between treatments. The seedlot with the highest GF rating had the least stem breakage on four of the six sites.

In the 1990 and 1991 trial series (Table 2) the treatment with the highest incidence of stem breakage (14% to 56% depending on site) was (apart from 1 site) either treatment 7 (initial stocking 1000 stems/ha with no thinning or pruning) or treatment 4 (initial stocking 500 stem/ha, thinned to 200 stems/ha with no pruning). The treatment with the least stem breakage varied between sites. Overall treatment 3 (initial stocking 1000 stems/ha, and thinned to 400 stem/ha) had the smallest incidence of stem breakage. There was generally a slight but non-significant reduction in stem breakage in the

pruned treatments compared to unpruned treatments with the same initial and final stocking. The difference in stem breakage between the different seedlots was only significant at two Central North Island sites. The seedlot with the highest GF rating generally, but not necessarily, showed the least amount of stem breakage.

5. Windthrow in trials

In 2008, one of the 1987 trials in the Central North Island suffered an endemic windthrow (Stathers et al. 1994). Prior to planting the land had been V-bladed to generate 0.5m to 1m tall mounds running parallel on an orientation of 288°, with pitches between 4 m and 6 m apart and each mound being 1 m to 2 m wide. Apart from the distinctive V-blading, the 48 plots had received a wide range of silvicultural treatments (Table 1) with final crop stockings varying between 100 and 600 stems/ha. It was observed that the low stocked plots at 100 or 200 stems/ha that had been thinned early and pruned lost no trees to windthrow, whereas highly stocked plots of 400 stems/ha or more, experienced extensive damage with many leaning and toppled trees. Damage seemed worst in plots where gusts blew across from a very low stocked area of 100 stems/ha before hitting a higher stocked plot above 300 stems/ha. Trees in the lower stocked areas had not been damaged by the wind, whereas the plots with 600 stems/ha were completely uprooted. Judging from the direction in which the trees fell, the wind had hit the stand at approximately 90° to the soil mounds, an angle at which the root systems were least able to withstand wind.

6. Conclusions/future research

By developing the integrated growth and branching model, TreeBLOSSIM, that predicted the underlying branching pattern of radiata pine, the importance of stem breakage to branch diameter was detected. To quantify the occurrence of stem breakage through out New Zealand, qualitative stem description codes were analysed. These analyses indicated that the percentage of trees with stem breakage can be over 50% depending on the site conditions, silvicultural treatment and seedlot planted. At age 13 years, the “plant and leave” treatments were particularly susceptible to stem breakage. It is recommended that the same analysis be repeated at the end of the rotation and that an inventory assessment be carried out to determine the value of the different treatments.

Modelling systems for radiata pine should be enhanced to incorporate the probability of and growth responses to stem breakage so that the value of different silviculture systems may be more accurately assessed.

Acknowledgement

The authors are pleased to acknowledge the New Zealand Government and the New Zealand forest industry for supporting these long-term trials and funding this analysis.

The trials were designed by Dr. M. Carson, Dr. S. Carson, Dr. P. Wilcox, and J. Hayes. Many people have contributed over the years to the collection of data from these trials.

References

Ainsworth, P., 1989: Wind damage in radiata pine: The Tasman experience. In: A. Somerville, S. Wakelin and L. Whitehouse (eds): Workshop on wind damage in New Zealand exotic forests. FRI Bulletin, No. 146. Forest Research Institute, Ministry of Forestry, pp. 6-9.

Brownlie, R.K., Carson, W.W., Firth, J.G., Goulding, C.J., 2007: An image-based dendrometry tool for standing trees. New Zealand Journal of Forestry Science 37, 153-168.

Dyck, B., Thomson, P., 1999: Carter Holt Harvey's Millenium Forestry. New Zealand Journal of Forestry 43, 2-4.

Grace, J.C., Blundell, W., Pont, D., 1998: Branch development in *Pinus radiata* - model outline and data collection. New Zealand Journal of Forestry Science 28, 182-194.

Grace, J.C., Pont, D., Sherman, L., Woo, G., Aitchison, D., 2006: Variability in stem wood properties due to branches. New Zealand Journal of Forestry Science 36, 313-324.

James, R.N., 1990: Evolution of silvicultural practice towards wide spacing and heavy thinnings in New Zealand. In: R.N. James and G.L. Tarlton (eds): New approaches to spacing and thinning in plantation forestry. FRI Bulletin No. 151. Forest Reseach Institute, N.Z. Ministry of Forestry, pp. 13-20.

Leathwick, J., Wilson, G., Rutledge, D., Wardle, P., Morgan, F., Johnston, K., McLeod, M., Kirkpatrick, R., 2003: Land Environments of New Zealand, Nga Taiao o Aotearoa. Pub. David Bateman Ltd.

Ministry of Agriculture and Forestry (MAF), 2003: A National Exotic Forest Description 2003. http://www.maf.govt.nz/mafnet/publications/nefd/national-exotic-forest-2003/, 64 pp.

Ministry of Agriculture and Forestry (MAF), 2008: A National Exotic Forest Description 2008. http://www.maf.govt.nz/mafnet/publications/nefd/national-exotic-forest-2008/index.htm, 68 pp.

Pont, D., Grace, J.C., Todoroki, C., 1999: Modelling the influence of radiata pine branching characteristics on visual timber grade. In: Nepveu, G. (ed.): Proceedings of third workshop "Connection between silviculture and wood quality through modelling approaches and simulation softwares". Publication Equippe de recherches sur la quality des bois. INRA- Nancy, France, pp. 63-71.

Radiata Pine Breeding Company Ltd., 2002. Rating the genetic quality of radiata pine. Information Bulletin No. 1. http://www.rpbc.co.nz.

Somerville, A., 1989: Tree wind stability and forest management practices. In A. Somerville, S. Wakelin and L. Whitehouse (eds): Workshop on wind damage in New Zealand exotic forests. FRI Buletin, No. 146. Forest Research Institute, Ministry of Forestry, pp. 38-58.

Stathers, R.J., Rollerston, T.P., Mitchell, S.J., 1994: Windthrow Handbook for British Columbia Forests. 32 pp.

Authors' address:

Dr. Jennifer C. Grace (jenny.grace@scionresearch.com)
Carolyn Andersen (carolyn.andersen@scionresearch.com)
Rod Brownlie (rod.brownlie@scionresearch.com)
Marika Fritzsche (marika.fritzsche@scionresearch.com)
Scion
Private Bag 3020, Rotorua, New Zealand

2nd International Conference

Wind Effects on Trees

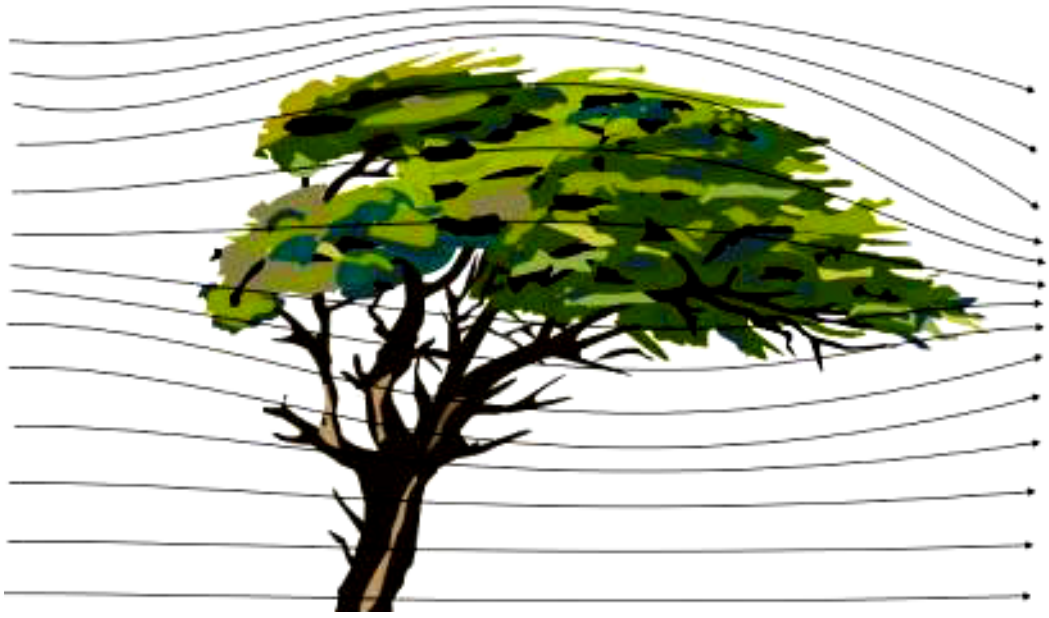

13-16 October 2009
Albert-Ludwigs-University of Freiburg, Germany

Program

2nd International Conference
Wind Effects on Trees

hosted by

Meteorological Institute, Albert-Ludwigs-University of Freiburg, Germany

in collaboration with:

Forest Research Institute Baden-Wuerttemberg, Freiburg, Germany

and

IUFRO Section 8.01.11

Conference website: www.wind2009.uni-freiburg.de

Meteorological Institute, Albert-Ludwigs-University of Freiburg
Werthmannstrasse 10, D-79085 Freiburg, Germany
Phone: +49/761/203-3590
Fax: +49/761/203-3586
e-mail: meteo@meteo.uni-freiburg.de
http://www.meteo.uni-freiburg.de

2nd International Conference "Wind Effects on Trees"

- Program outline -

Presentations in Freiburg (Auditorium (Aula), Albert-Ludwigs-University of Freiburg)

Tuesday, 13 October 2009:

08:00:	Registration
09:00 - 09:30:	Welcome addresses and organisation details
09:30 - 10:00:	Wind climatology: 1 oral presentation
10:00 - 10:30:	*Coffee break*
10:30 - 12:00:	Air flow at forest edges: 3 oral presentations
12:00 - 13:00:	*Lunch (buffet, foyer of the auditorium)*
13:00 - 15:30:	Air flow around trees: 5 oral presentations
15:30 - 16:00:	*Coffee break / Poster presentations*
16:00 - 18:00:	Aerodynamic interaction between wind and trees I: 4 oral presentations
18:00 - 20:00:	*Ice-breaker (foyer of the auditorium)*

Wednesday, 14 October 2009:

09:00 - 10:30:	Aerodynamic interaction between wind and trees II: 3 oral presentations
10:30 - 11:00:	*Coffee break / Poster presentations*
11:00 - 12:30:	Storm impacts and risk modelling I: 3 oral presentations
12:30 - 13:30:	*Lunch (buffet, foyer of the auditorium)*
13:30 - 14:30:	Storm impacts and risk modelling II: 2 oral presentations
14:30 - 15:30:	Mechanics of trees under wind loading: 2 oral presentations
15:30 - 16:00:	*Coffee break / Poster presentations*
16:00 - 17:30:	Failure criteria of trees: 3 oral presentations
19:00:	*Wine tasting at the State Viniculture Institute in Freiburg*

Thursday, 15 October 2009:

09:00 - 10:00:	Ecological dynamics and strong winds: 2 oral presentations
10:00 - 10:30:	*Coffee break / Poster presentations*
10:30 - 12:00:	Ecological dynamics following windthrow: 3 oral presentations
12:00 - 13:00:	*Lunch (buffet, foyer of the auditorium)*
13:00 - 14:30:	Silviculture, tree level management and harvest design to reduce wind damage I: 3 oral presentations
14:30 - 15:00:	*Coffee break*
15:00 - 16:00:	Silviculture, tree level management and harvest design to reduce wind damage II: 2 oral presentations
16:00 - 18:00:	Post storm damage responses: 4 oral presentations
18:00:	Closing session

Friday, 16 October 2009:

07:30:	Excursion to the Black Forest arranged by the Forest Research Institute Baden-Wuerttemberg

2nd International Conference "Wind Effects on Trees"

- Detailed program -

Oral presentations: 30 minutes, i.e. 20 minutes for presentation and 10 minutes for discussion

Tuesday, 13 October 2009:

08:00: Registration

09:00 - 09:20: Welcome addresses:

Prof. Dr. Helmut Mayer; Chair, Organising Committee, Freiburg, Germany

Prof. Dr. Heinz Rennenberg, Vice-Dean of the Faculty of Forest and Environmental Sciences, Albert-Ludwigs-University of Freiburg, Germany

09:20 - 09:30: Organisation details:

Prof. Dr. Helmut Mayer; Germany

Wind climatology (chair: Thomas Wohlgemuth, Switzerland)

09:30 - 10:00: Monika Rauthe (University of Karlsruhe / Forschungszentrum Karlsruhe, Germany), Michael Kunz:
A regional perspective on severe winter storms in a changing climate

10:00 - 10:30: **Coffee break**

Air flow at forest edges (chair: Mark Rudnicki, USA)

10:30 - 11:00: Cornelia Frank (University of Karlsruhe, Germany), Bodo Ruck, Michael Tischmacher:
About the influence of the windward edge structure on the flow characteristics at forest edges

11:00 - 11:30: Andrey Sogachev (Wind Energy Division, Risø-DTU, Roskilde, Denmark), Ebba Dellwik, Ferhat Bingöl, Jakob Mann
Airflow modelling near a forest edge

11:30 - 12:00: Cornelia Frank (University of Karlsruhe, Germany), Bodo Ruck:
About the influence of the stand density on the flow characteristics at forest edges

12:00 - 13:00: **Lunch (buffet, foyer of the auditorium)**

Air flow around trees (chair: Yves Brunet, France)

13:00 - 13:30: Ronald Queck (TU Dresden, Germany), Anne Bienert, Stefan Harmansa:
Modeling wind fields in tall canopies - towards better momentum distribution using 3D vegetation scans in high resolution

13:30 - 14:00: Benjamin Walter (WSL Institute for Snow and Avalanche Research SLF, Davos, Switzerland), Christof Gromke, Michael Lehning:
The SLF boundary layer wind tunnel - an experimental facility for aerodynamical investigations of living plants

14:00 - 14:30: Katrin Burri (WSL Institute for Snow and Avalanche Research SLF, Davos, Switzerland), Christof Gromke, Frank Graf:
A wind tunnel study of aeolian sediment transport and PM_{10} emission in grass canopies of different planting densities

14:30 - 15:00: Christof Gromke (WSL Institute for Snow and Avalanche Research SLF, Davos, Switzerland), Bodo Ruck:
Implications of tree planting on pollutant dispersion in street canyons

15:00 -15:30: Motoki Kakizaki (Tokyo University of Science, Japan), Mikio Takahashi, Hitoshi Ishikawa, Shunsuke Yamada:
Turbulent structure behind tree

15:30 - 16:00: **Coffee break / Poster presentations**

Aerodynamic interaction between wind and trees I (chair: Ulrich Kohnle, Germany)

16:00 - 16:30: Hong-Bing Su (East Carolina University, Greenville, NC, USA), Mark Rudnicki, April Hiscox, Vincent Webb, David Miller:
Large-eddy simulation of the aerodynamic interactions between canopy roughness sublayer turbulence and tree-sway motions

16:30 - 17:00: David Pivato (INRA, UR1263 EPHYSE, Villenave d'Ornon, France), Sylvain Dupont, Yves Brunet:
Modelling forest canopy motion using a porous elastic approach

17:00 - 17:30: Yves Brunet (INRA, UR1263 EPHYSE, Villenave d'Ornon, France), Sylvain Dupont, Pascal Roux, Damien Sellier:
Tree motion in heterogeneous forests: a coupled flow-tree simulation study

17:30 - 18:00: Spencer Hall (Brigham Young University, Provo, UT, USA), Anthony Selino, Michael Jones, Mark Rudnicki:
Forest scale cellular automata model of wind interacting with trees

18:00 - 20:00: **Ice-breaker** (drinks and finger-food in the foyer of the auditorium)

Wednesday, 14 October 2009:

Aerodynamic interaction between wind and trees II (chair: Bodo Ruck, Germany)

09:00 - 09:30: Dirk Schindler (Albert-Ludwigs-University of Freiburg, Germany), Jochen Schönborn, Hannes Fugmann, Helmut Mayer:
Responses of Scots pine trees to near-surface airflow

09:30 - 10:00: Mathieu Rodriguez (Ecole Polytechnique, Palaiseau, France), Bruno Moulia, Emmanuel de Langre:
Experimental investigations of a walnut tree multimodal dynamics

10:00 - 10:30: Andreas Detter (Brudi & Partner TreeConsult, Gauting, Germany), Erk Brudi, Frank Bischoff:
Engineering models for wind effects on solitary trees

10:30 - 11:00: **Coffee break / Poster presentations**

Storm impacts and risk modelling I (chair: Barry Gardiner, Scotland)

11:00 - 11:30: Axel Albrecht (Forest Research Institute Baden-Wuerttemberg, Freiburg, Germany), Ulrich Kohnle, Marc Hanewinkel, Juergen Bauhus:
Empirical modeling of long-term storm damage data in forests of South-western Germany: judging the impact of silviculture

11:30 - 12:00: Kristina Blennow (Southern Swedish Forest Research Centre, Swedish University of Agricultural Sciences, Alnarp, Sweden), Barry Gardiner:
The WINDA-GALES wind damage risk planning tool

12:00 - 12:30: Thomas Wohlgemuth (Swiss Federal Institute for Forest, Snow and Landscape Research, Birmensdorf, Switzerland), Tilo Usbeck, Matthias Dobbertin:
The relation of growing stock, wind speed and forest damage in the Zurich region from 1891 to 2007

12:30 - 13:30: **Lunch (buffet, foyer of the auditorium)**

Storm impacts and risk modelling II (chair: Dirk Schindler, Germany)

13:30 - 14:00: Oleg Panferov (Georg-August University of Göttingen, Germany), Andrey Sogachev, Claus Doering, Bernd Ahrends:
Dynamics of windthrow risk in different forest ecosystems for 21st century (SRES A1B, B1)

14:00 - 14:30: Barry Gardiner (Forest Research, Northern Research Station, Roslin, Midlothian, Scotland), Sophie Hale, Axel Wellpott, Bruce Nicoll:
The development of a wind risk model for irregular stands

Mechanics of trees under wind loading (chair: Emmanuel de Langre, France)

14:30 - 15:00: Jochen Schönborn (Albert-Ludwigs-University of Freiburg, Germany), Dirk Schindler, Helmut Mayer:
Measuring vibrations of a single, solitary broadleaf tree

15:00 - 15:30: Vincent A. Webb (University of Connecticut, Storrs, CT, USA), Mark Rudnicki:
Estimating wind forces and bending moments in a forest stand before and after thinning

15:30 - 16:00: **Coffee break / Poster presentations**

Failure criteria of trees (chair: Stephen J. Mitchell, Canada)

16:00 - 16:30: Tim Newson (University of Western Ontario, London, Canada), Padmavathi Sagi, Craig Miller, Stephen Mitchell:
Application of yield surfaces in three-dimensional VHM load space to the stability of trees under wind loading

16:30 - 17:00: Kana Kamimura (Forestry and Forest Products Research Institute, Tsukuba, Japan), Kenji Kitagawa, Satoshi Saito, Hayahito Yazawa, Taichi Kajikawa, Hiromi Mizunaga:
Root anchorage under the combined condition of wind pressure and intensive rainfall: tree-pulling experiments with controlled soil water content

17:00 - 17:30: Frédéric Danjon (INRA, UMR 1212 BioGeCo, Bordeaux-Cestas, France), Emmanuelle Eveno, Frédéric Bernier, Jean-Paul Chambon, Pablo Lozano, Christophe Plomion, Pauline Garnier-Géré:
Genetic variability in 3D coarse root architecture in Pinus pinaster

19:00: **Wine tasting at the State Viniculture Institute in Freiburg**

Thursday, 15 October 2009:

Ecological dynamics and strong winds (chair: Heli Peltola, Finland)

09:00 - 09:30: Scott Goodrick (US Forest Service, Athens, GA, USA), Brian Beckage:
Wind damage to a coastal forest during hurricane Wilma

09:30 - 10:00: Janis Donis (Latvian State Forest Research Institute "Silava", Salaspils, Latvia), Maris Rokpelnis, Gundars Snepsts, Juris Zarins:
Extreme wind speeds as a natural disturbance agent in spruce forests in Latvia

10:00 - 10:30: **Coffee break / Poster presentations**

Ecological dynamics following windthrow (chair: Jürgen Bauhus, Germany)

10:30 - 11:00: Scott Goodrick (US Forest Service, Athens, GA, USA), John Stanturf:
Hurricanes and fire: interacting disturbances in coastal forests of the southeastern United States

11:00 - 11:30: Marek Metslaid (Estonian University of Life Sciences, Tartu, Estonia), Kajar Köster, Floortje Vodde, Kalev Jõgiste:
Acclimation and growth response of Norway spruce advance regeneration after release

11:30 - 12:00: Stephen J. Mitchell (University of British Columbia, Vancouver, Canada), Devesh Bahuguna, Yosune Miquelajauregui, Tim Shannon:
Windthrow impacts in riparian leave-strips

12:00 - 13:00: **Lunch (buffet, foyer of the auditorium)**

Silviculture, tree level management and harvest design to reduce wind damage I (chair: Konstantin von Teuffel, Germany)

13:00 - 13:30: Heli Peltola (University of Joensuu, Finland), Sylvain Dupont, Veli-Pekka Ikonen, Hannu Väisänen, Ari Venäläinen, Seppo Kellomäki:
Integrated use of two dimensional airflow model Aquilon and mechanistic model HWIND for risk assessment of tree stands to wind damage

13:30 - 14:00: António Lopes (Universidade de Lisboa, Portugal), Marcelo Fragoso:
Tree damages in Lisbon during southern windstorms

14:00 - 14:30: Mart-Jan Schelhaas (Alterra, Wageningen, The Netherlands), Geerten Hengeveld, Zbigniew W. Kundzewicz:
Assessing risk and adaptation options to storms in European forestry

14:30 - 15:00: **Coffee break**

Silviculture, tree level management and harvest design to reduce wind damage II (chair: Kristina Blennow, Sweden)

15:00 - 15:30: Anne Oosterbaan (Alterra, Wageningen, The Netherlands):
Salvage decision scheme in The Netherlands

15:30 - 16:00: Amir Mosavi (University of Debrecen, Hungary):
Parametric modelling of trees and using integrated CAD/CFD tools: application to create a planting pattern for new forests

Post storm damage responses (chair: Christoph Kottmeier, Germany)

16:00 - 16:30: Jean-Claude Ruel (Laval University, Quebec, Canada), Alexis Achim, Raul Espinoza Herrera, Alain Cloutier:
Wood degradation after windthrow in a northern environment

16:30 - 17:00: Andrzej Wegiel (Poznan University of Life Sciences, Poland), Grzegorz Raczka, Pawel Strzelinski, Damian Sugiero:
Spatial analysis of Scots pine (Pinus sylvestris L.) stands' damages after catastrophic windstorms in years 2003-2007

17:00 - 17:30: Simon Riguelle (Public Service of Wallonia, Gembloux, Belgium), Jacques Hébert, Benoit Jourez:
A decision making tool to manage storm damage in Wallonia

17:30 - 18:00: Toshihiro Kitada (Toyohashi University of Technology, Toyohashi, Japan), Yohei Suzuki, Tomoyuki Katagiri:
Comprehensive evaluation of the effects of wet and dry deposition of various ionic species, atmospheric ozone, and mineral weathering on plant growth by using Plant Growth Stress Model: estimated growth of pine tree for hypothetical 100 years in Ijira lake area, Central Japan

Closing session

18:00: Closing session (Stephen J. Mitchell, Heli Peltola, Bodo Ruck)

Poster presentations in Freiburg from 13-15 October 2009:

P1: Hilppa Gregow (Finnish Meteorological Institute, Helsinki, Finland), Kimmo Ruosteenoja, Ari Venäläinen:
Analyses of the annual, winter time and extreme geostrophic wind speeds in northern Europe based on GCMs

P2: Woo-Sik Jung (Inje University, Gimhae, Korea), Jong-Kil Park, Hwa Woon Lee, Eun-Byul Kim, Hyo-Jin Choi:
Wind speed variation over the leeward region according to vegetation under the strong wind

P3: Karin Grebhan (Albert-Ludwigs-University of Freiburg, Germany), Dirk Schindler, Helmut Mayer:
GIS-based modeling for evaluation of wind damage probability in forests in southwest Germany

P4: Hannes Fugmann (Albert-Ludwigs-University of Freiburg, Germany), Dirk Schindler, Helmut Mayer:
A dynamic tree sway model

P5: Kajar Köster (Estonian University of Life Sciences, Tartu, Estonia), Kalev Jõgiste, Floor Vodde, Marek Metslaid:
Expansion of heavily damaged windthrow areas through tree mortality in surrounding areas

P6: Eva P. Roca Posado (Unidade de Xestión Forestal Sostible (UXFS), Universidade de Santiago de Compostela, Lugo, Spain), Juan G. Álvarez González, Alberto Rojo Alboreca:
Windstorm damage in coniferous forests in Galicia (NW Spain) under different thinning treatments

P7: Marcos Barrio-Anta (University of Oviedo, Spain), Felipe Crecente-Campo, Pedro Álvarez-Alvarez, Fernando Castedo-Dorado:
Inclusion of windthrow assessment in stand density management diagrams for even-aged stands

P8: Pat Pickett (Los Angeles, California, USA):
Digital video tracking imagery of tree movements in response to gusting airflow conditions

P9: Bernd Ahrends (Georg-August University of Göttingen, Germany), Martin Jansen, Oleg Panferov:
Effects of windthrow on drought risk in spruce and pine forest ecosystems under climate change conditions

P10: Harri Hautala (Finnish Forest Research Institute, Vantaa, Finland):
Effects of green tree retention on boreal forest understorey vegetation

P11: Osman Topaçoğlu (Kastamonu University, Turkey):
Wind disturbance in Karadere forest

P12: Farshad Yazdian (Cahools IAU University, Karaj, Iran):
The effect of wind exposure on beech trees canopy form and height in Caspian forests

P13: Jennifer C. Grace (Scion, Rotorua, New Zealand), Carolyn Andersen, Rod Brownlie, Marika Fritzsche:
Stem damage in radiata pine: observations with respect to site, silviculture and seedlot

2nd International Conference "Wind Effects on Trees"

Freiburg, Germany, 13-16 October 2009

Scientific Committee

Jürgen Bauhus, Freiburg, Germany
Yves Brunet, Villenave d'Omon, France
Barry Gardiner, Roslin, UK
Ulrich Kohnle, Freiburg, Germany
Christoph Kottmeier, Karlsruhe, Germany
Emmanuel de Langre, Palaiseau, France
Helmut Mayer, Freiburg, Germany (chair)
Stephen J. Mitchell, Vancouver, Canada
Heli Peltola, Joensuu, Finland
Bodo Ruck, Karlsruhe, Germany (co-chair)
Konstantin von Teuffel, Freiburg, Germany

Local Organising Committee

Christina Endler, Freiburg, Germany
Gerhard Fernbach, Freiburg, Germany
Karin Grebhan, Freiburg, Germany
Jutta Holst, Freiburg, Germany
Andrea Hug, Freiburg, Germany (co-chair)
Ulrich Kohnle, Freiburg, Germany
Kaisu Makkonen-Spiecker, Freiburg, Germany
Andreas Matzarakis, Freiburg, Germany
Helmut Mayer, Freiburg, Germany (chair)
Elli Mindnich, Freiburg, Germany
Dirk Redepenning, Freiburg, Germany
Dirk Schindler, Freiburg, Germany
Jochen Schönborn, Freiburg, Germany
student assistants, Freiburg, Germany

Berichte des Meteorologischen Institutes der Albert-Ludwigs-Universität Freiburg

Nr. 1: Fritsch, J.: Energiebilanz und Verdunstung eines bewaldeten Hanges. Juni 1998

Nr. 2: Gwehenberger, J.: Schadenpotential über den Ausbreitungspfad Atmosphäre bei Unfällen mit Tankfahrzeugen zum Transport von Benzin, Diesel, Heizöl oder Flüssiggas. August 1998

Nr. 3: Thiel, S.: Einfluß von Bewölkung auf die UV-Strahlung an der Erdoberfläche und ihre ökologische Bedeutung. August 1999

Nr. 4: Iziomon, M.G.: Characteristic variability, vertical profile and modelling of surface radiation budget in the southern Upper Rhine valley region. Juli 2000

Nr. 5: Mayer, H. (Hrsg.): Festschrift „Prof. Dr. Albrecht Kessler zum 70. Geburtstag". Oktober 2000

Nr. 6: Matzarakis, A.: Die thermische Komponente des Stadtklimas. Juli 2001*)

Nr. 7: Kirchgäßner, A.: Phänoklimatologie von Buchenwäldern im Südwesten der Schwäbischen Alb. Dezember 2001*)

Nr. 8: Haggagy, M.E.-N.A.: A sodar-based investigation of the atmospheric boundary layer. September 2003*)

Nr. 9: Rost, J.: Vergleichende Analyse der Energiebilanz zweier Untersuchungsflächen der Landnutzungen "Grasland" und „Wald" in der südlichen Oberrheinebene. Januar 2004*)

Nr. 10: Peck, A.K.: Hydrometeorologische und mikroklimatische Kennzeichen von Buchenwäldern. Juni 2004*)

Nr. 11: Schindler, D.: Characteristics of the atmospheric boundary layer over a Scots pine forest. Juni 2004*)

Nr. 12: Matzarakis, A., de Freitas, C.R., Scott, D. (Eds.): Advances in Tourism Climatology. November 2004*)

Nr. 13: Dostal, P.: Klimarekonstruktion der Regio TriRhena mit Hilfe von direkten und indirekten Daten vor der Instrumentenbeobachtung. Dezember 2004*)

Nr. 14: Imbery, F.: Langjährige Variabilität der aerodynamischen Oberflächenrauhigkeit und Energieflüsse eines Kiefernwaldes in der südlichen Oberrheinebene (Hartheim). Januar 2005*)

Nr. 15: Ali Toudert, F.: Dependence of outdoor thermal comfort on street design in hot and dry climate. November 2005*)

Nr. 16: Matzarakis, A., Mayer, H. (Hrsg.): Extended Abstracts zur 6. Fachtagung BIOMET des Fachausschusses Biometeorologie der Deutschen Meteorologischen Gesellschaft e.V.. März 2007*)

Nr. 17: Mayer, H. (Ed.): Celebrating the 50 years of the Meteorological Institute, Albert-Ludwigs-University of Freiburg, Germany. May 2008*)

Nr. 18: Mayer, H., Matzarakis, A. (Eds.): 5th Japanese-German Meeting on Urban Climatology. March 2009*)

Nr. 19: Mayer, H., Schindler, D. (Eds.): Proceedings of the 2nd International Conference „Wind Effects on Trees". October 2009*)

*) Report online available under:
http://www.meteo.uni-freiburg.de/forschung/publikationen/berichte/index_html